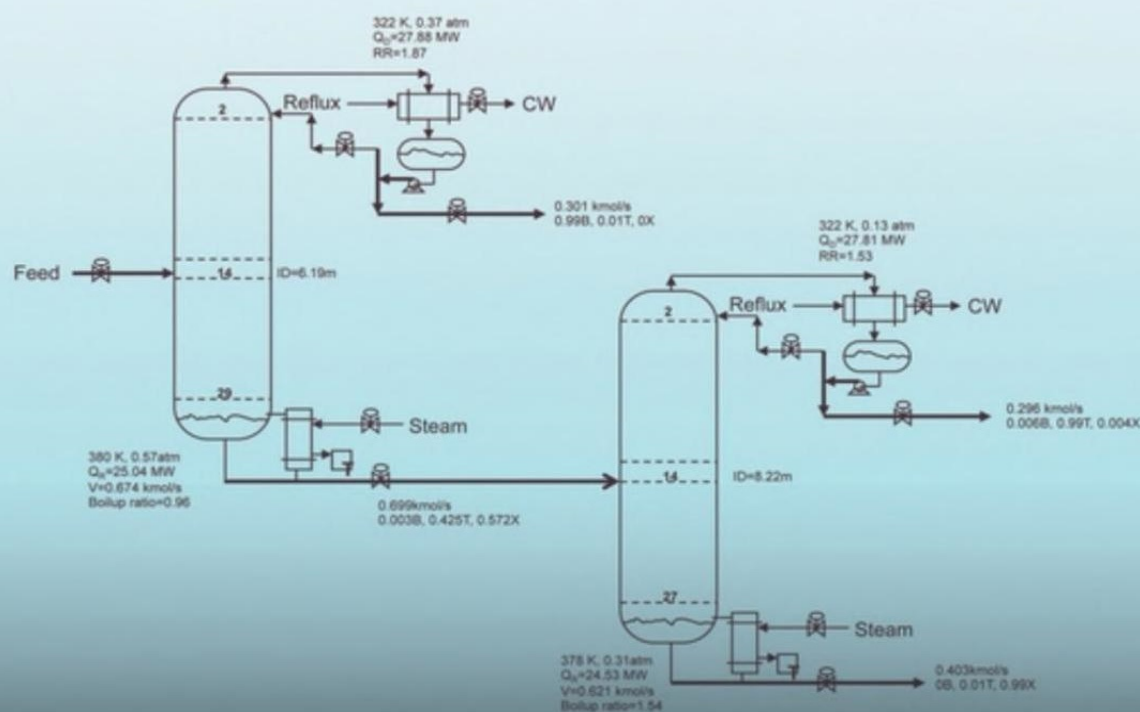


Second Edition

Distillation Design and Control Using AspenTM Simulation

William L. Luyben



AICHE

WILEY

DISTILLATION DESIGN
AND CONTROL USING
ASPENTM SIMULATION

DISTILLATION DESIGN AND CONTROL USING ASPENTM SIMULATION

Second Edition

WILLIAM L. LUYBEN
Lehigh University
Bethlehem, Pennsylvania

AICHE[®]

WILEY

Cover design: John Wiley & Sons, Inc.

Cover image: © William L. Luyben

Copyright © 2013 by John Wiley & Sons, Inc. All rights reserved.

Published by John Wiley & Sons, Inc., Hoboken, New Jersey.

Published simultaneously in Canada.

No part of this publication may be reproduced, stored in a retrieval system, or transmitted in any form or by any means, electronic, mechanical, photocopying, recording, scanning, or otherwise, except as permitted under Section 107 or 108 of the 1976 United States Copyright Act, without either the prior written permission of the Publisher, or authorization through payment of the appropriate per-copy fee to the Copyright Clearance Center, Inc., 222 Rosewood Drive, Danvers, MA 01923, (978) 750-8400, fax (978) 750-4470, or on the web at www.copyright.com. Requests to the Publisher for permission should be addressed to the Permissions Department, John Wiley & Sons, Inc., 111 River Street, Hoboken, NJ 07030, (201) 748-6011, fax (201) 748-6008, or online at <http://www.wiley.com/go/permission>.

Limit of Liability/Disclaimer of Warranty: While the publisher and author have used their best efforts in preparing this book, they make no representations or warranties with respect to the accuracy or completeness of the contents of this book and specifically disclaim any implied warranties of merchantability or fitness for a particular purpose. No warranty may be created or extended by sales representatives or written sales materials. The advice and strategies contained herein may not be suitable for your situation. You should consult with a professional where appropriate. Neither the publisher nor author shall be liable for any loss of profit or any other commercial damages, including but not limited to special, incidental, consequential, or other damages.

For general information on our other products and services or for technical support, please contact our Customer Care Department within the United States at (800) 762-2974, outside the United States at (317) 572-3993 or fax (317) 572-4002.

Wiley also publishes its books in a variety of electronic formats. Some content that appears in print may not be available in electronic formats. For more information about Wiley products, visit our web site at www.wiley.com.

Library of Congress Cataloging-in-Publication Data

Luyben, William L.

Distillation design and control using Aspen simulation / William L Luyben. – 2nd ed.

p. cm.

“AIChE.”

Includes index.

ISBN 978-1-118-41143-8 (cloth)

1. Distillation apparatus—Design and construction.
2. Chemical process control—Simulation methods.
3. Petroleum—Refining. I. American Institute of Chemical Engineers. II. Title.

TP159.D5L89 2013

660'.28425-dc23

2012030047

Printed in the United States of America

10 9 8 7 6 5 4 3 2 1

This book is dedicated to farmers all over the world.
No Farmers, No Food!

CONTENTS

PREFACE TO THE SECOND EDITION	xv
PREFACE TO THE FIRST EDITION	xvii
1 FUNDAMENTALS OF VAPOR–LIQUID–EQUILIBRIUM (VLE)	1
1.1 Vapor Pressure / 1	
1.2 Binary VLE Phase Diagrams / 3	
1.3 Physical Property Methods / 7	
1.4 Relative Volatility / 7	
1.5 Bubble Point Calculations / 8	
1.6 Ternary Diagrams / 9	
1.7 VLE Nonideality / 11	
1.8 Residue Curves for Ternary Systems / 15	
1.9 Distillation Boundaries / 22	
1.10 Conclusions / 25	
Reference / 27	
2 ANALYSIS OF DISTILLATION COLUMNS	29
2.1 Design Degrees of Freedom / 29	
2.2 Binary McCabe–Thiele Method / 30	
2.2.1 Operating Lines / 32	
2.2.2 q -Line / 33	
2.2.3 Stepping Off Trays / 35	
2.2.4 Effect of Parameters / 35	
2.2.5 Limiting Conditions / 36	

- 2.3 Approximate Multicomponent Methods / 36
 - 2.3.1 Fenske Equation for Minimum Number of Trays / 37
 - 2.3.2 Underwood Equations for Minimum Reflux Ratio / 37
- 2.4 Conclusions / 38

3 SETTING UP A STEADY-STATE SIMULATION 39

- 3.1 Configuring a New Simulation / 39
- 3.2 Specifying Chemical Components and Physical Properties / 46
- 3.3 Specifying Stream Properties / 51
- 3.4 Specifying Parameters of Equipment / 52
 - 3.4.1 Column C1 / 52
 - 3.4.2 Valves and Pumps / 55
- 3.5 Running the Simulation / 57
- 3.6 Using Design Spec/Vary Function / 58
- 3.7 Finding the Optimum Feed Tray and Minimum Conditions / 70
 - 3.7.1 Optimum Feed Tray / 70
 - 3.7.2 Minimum Reflux Ratio / 71
 - 3.7.3 Minimum Number of Trays / 71
- 3.8 Column Sizing / 72
 - 3.8.1 Length / 72
 - 3.8.2 Diameter / 72
- 3.9 Conceptual Design / 74
- 3.10 Conclusions / 80

4 DISTILLATION ECONOMIC OPTIMIZATION 81

- 4.1 Heuristic Optimization / 81
 - 4.1.1 Set Total Trays to Twice Minimum Number of Trays / 81
 - 4.1.2 Set Reflux Ratio to 1.2 Times Minimum Reflux Ratio / 83
- 4.2 Economic Basis / 83
- 4.3 Results / 85
- 4.4 Operating Optimization / 87
- 4.5 Optimum Pressure for Vacuum Columns / 92
- 4.6 Conclusions / 94

5 MORE COMPLEX DISTILLATION SYSTEMS 95

- 5.1 Extractive Distillation / 95
 - 5.1.1 Design / 99
 - 5.1.2 Simulation Issues / 101
- 5.2 Ethanol Dehydration / 105
 - 5.2.1 VLLE Behavior / 106

5.2.2	Process Flowsheet Simulation / 109	
5.2.3	Converging the Flowsheet / 112	
5.3	Pressure-Swing Azeotropic Distillation / 115	
5.4	Heat-Integrated Columns / 121	
5.4.1	Flowsheet / 121	
5.4.2	Converging for Neat Operation / 122	
5.5	Conclusions / 126	
6	STEADY-STATE CALCULATIONS FOR CONTROL STRUCTURE SELECTION	127
6.1	Control Structure Alternatives / 127	
6.1.1	Dual-Composition Control / 127	
6.1.2	Single-End Control / 128	
6.2	Feed Composition Sensitivity Analysis (ZSA) / 128	
6.3	Temperature Control Tray Selection / 129	
6.3.1	Summary of Methods / 130	
6.3.2	Binary Propane/Isobutane System / 131	
6.3.3	Ternary BTX System / 135	
6.3.4	Ternary Azeotropic System / 139	
6.4	Conclusions / 144	
	Reference / 144	
7	CONVERTING FROM STEADY-STATE TO DYNAMIC SIMULATION	145
7.1	Equipment Sizing / 146	
7.2	Exporting to Aspen Dynamics / 148	
7.3	Opening the Dynamic Simulation in Aspen Dynamics / 150	
7.4	Installing Basic Controllers / 152	
7.4.1	Reflux / 156	
7.4.2	Issues / 157	
7.5	Installing Temperature and Composition Controllers / 161	
7.5.1	Tray Temperature Control / 162	
7.5.2	Composition Control / 170	
7.5.3	Composition/Temperature Cascade Control / 170	
7.6	Performance Evaluation / 172	
7.6.1	Installing a Plot / 172	
7.6.2	Importing Dynamic Results into Matlab / 174	
7.6.3	Reboiler Heat Input to Feed Ratio / 176	
7.6.4	Comparison of Temperature Control with Cascade CC/TC / 181	
7.7	Conclusions / 184	

8 CONTROL OF MORE COMPLEX COLUMNS

185

- 8.1 Extractive Distillation Process / 185
 - 8.1.1 Design / 185
 - 8.1.2 Control Structure / 188
 - 8.1.3 Dynamic Performance / 191
- 8.2 Columns with Partial Condensers / 191
 - 8.2.1 Total Vapor Distillate / 192
 - 8.2.2 Both Vapor and Liquid Distillate Streams / 209
- 8.3 Control of Heat-Integrated Distillation Columns / 217
 - 8.3.1 Process Studied / 217
 - 8.3.2 Heat Integration Relationships / 218
 - 8.3.3 Control Structure / 222
 - 8.3.4 Dynamic Performance / 223
- 8.4 Control of Azeotropic Columns/Decanter System / 226
 - 8.4.1 Converting to Dynamics and Closing Recycle Loop / 227
 - 8.4.2 Installing the Control Structure / 228
 - 8.4.3 Performance / 233
 - 8.4.4 Numerical Integration Issues / 237
- 8.5 Unusual Control Structure / 238
 - 8.5.1 Process Studied / 239
 - 8.5.2 Economic Optimum Steady-State Design / 242
 - 8.5.3 Control Structure Selection / 243
 - 8.5.4 Dynamic Simulation Results / 248
 - 8.5.5 Alternative Control Structures / 248
 - 8.5.6 Conclusions / 254
- 8.6 Conclusions / 255
- References / 255

9 REACTIVE DISTILLATION

257

- 9.1 Introduction / 257
- 9.2 Types of Reactive Distillation Systems / 258
 - 9.2.1 Single-Feed Reactions / 259
 - 9.2.2 Irreversible Reaction with Heavy Product / 259
 - 9.2.3 Neat Operation Versus Use of Excess Reactant / 260
- 9.3 TAME Process Basics / 263
 - 9.3.1 Prereactor / 263
 - 9.3.2 Reactive Column C1 / 263
- 9.4 TAME Reaction Kinetics and VLE / 266
- 9.5 Plantwide Control Structure / 270
- 9.6 Conclusions / 274
- References / 274

10	CONTROL OF SIDESTREAM COLUMNS	275
10.1	Liquid Sidestream Column / 276	
10.1.1	Steady-State Design / 276	
10.1.2	Dynamic Control / 277	
10.2	Vapor Sidestream Column / 281	
10.2.1	Steady-State Design / 282	
10.2.2	Dynamic Control / 282	
10.3	Liquid Sidestream Column with Stripper / 286	
10.3.1	Steady-State Design / 286	
10.3.2	Dynamic Control / 288	
10.4	Vapor Sidestream Column with Rectifier / 292	
10.4.1	Steady-State Design / 292	
10.4.2	Dynamic Control / 293	
10.5	Sidestream Purge Column / 300	
10.5.1	Steady-State Design / 300	
10.5.2	Dynamic Control / 302	
10.6	Conclusions / 307	
11	CONTROL OF PETROLEUM FRACTIONATORS	309
11.1	Petroleum Fractions / 310	
11.2	Characterization Crude Oil / 314	
11.3	Steady-State Design of Preflash Column / 321	
11.4	Control of Preflash Column / 328	
11.5	Steady-State Design of Pipestill / 332	
11.5.1	Overview of Steady-State Design / 333	
11.5.2	Configuring the Pipestill in Aspen Plus / 335	
11.5.3	Effects of Design Parameters / 344	
11.6	Control of Pipestill / 346	
11.7	Conclusions / 354	
	References / 354	
12	DIVIDED-WALL (PETLYUK) COLUMNS	355
12.1	Introduction / 355	
12.2	Steady-State Design / 357	
12.2.1	<i>MultiFrac</i> Model / 357	
12.2.2	<i>RadFrac</i> Model / 366	
12.3	Control of the Divided-Wall Column / 369	
12.3.1	Control Structure / 369	
12.3.2	Implementation in Aspen Dynamics / 373	
12.3.3	Dynamic Results / 375	

- 12.4 Control of the Conventional Column Process / 380
 - 12.4.1 Control Structure / 380
 - 12.4.2 Dynamic Results and Comparisons / 381
- 12.5 Conclusions and Discussion / 383
- References / 384

13 DYNAMIC SAFETY ANALYSIS

385

- 13.1 Introduction / 385
- 13.2 Safety Scenarios / 385
- 13.3 Process Studied / 387
- 13.4 Basic *RadFrac* Models / 387
 - 13.4.1 Constant Duty Model / 387
 - 13.4.2 Constant Temperature Model / 388
 - 13.4.3 LMTD Model / 388
 - 13.4.4 Condensing or Evaporating Medium Models / 388
 - 13.4.5 Dynamic Model for Reboiler / 388
- 13.5 *RadFrac* Model with Explicit Heat-Exchanger Dynamics / 389
 - 13.5.1 Column / 389
 - 13.5.2 Condenser / 390
 - 13.5.3 Reflux Drum / 391
 - 13.5.4 Liquid Split / 391
 - 13.5.5 Reboiler / 391
- 13.6 Dynamic Simulations / 392
 - 13.6.1 Base Case Control Structure / 392
 - 13.6.2 Rigorous Case Control Structure / 393
- 13.7 Comparison of Dynamic Responses / 394
 - 13.7.1 Condenser Cooling Failure / 394
 - 13.7.2 Heat-Input Surge / 395
- 13.8 Other Issues / 397
- 13.9 Conclusions / 398
- Reference / 398

14 CARBON DIOXIDE CAPTURE

399

- 14.1 Carbon Dioxide Removal in Low-Pressure Air Combustion Power Plants / 400
 - 14.1.1 Process Design / 400
 - 14.1.2 Simulation Issues / 401
 - 14.1.3 Plantwide Control Structure / 404
 - 14.1.4 Dynamic Performance / 408
- 14.2 Carbon Dioxide Removal in High-Pressure IGCC Power Plants / 412

- 14.2.1 Design / 414
- 14.2.2 Plantwide Control Structure / 414
- 14.2.3 Dynamic Performance / 418
- 14.3 Conclusions / 420
- References / 421

15 DISTILLATION TURNDOWN

423

- 15.1 Introduction / 423
- 15.2 Control Problem / 424
 - 15.2.1 Two-Temperature Control / 425
 - 15.2.2 Valve-Position Control / 426
 - 15.2.3 Recycle Control / 427
- 15.3 Process Studied / 428
- 15.4 Dynamic Performance for Ramp Disturbances / 431
 - 15.4.1 Two-Temperature Control / 431
 - 15.4.2 VPC Control / 432
 - 15.4.3 Recycle Control / 433
 - 15.4.4 Comparison / 434
- 15.5 Dynamic Performance for Step Disturbances / 435
 - 15.5.1 Two-Temperature Control / 435
 - 15.5.2 VPC Control / 436
 - 15.5.3 Recycle Control / 436
- 15.6 Other Control Structures / 439
 - 15.6.1 No Temperature Control / 439
 - 15.6.2 Dual Temperature Control / 440
- 15.7 Conclusions / 442
- References / 442

16 PRESSURE-COMPENSATED TEMPERATURE CONTROL IN DISTILLATION COLUMNS

443

- 16.1 Introduction / 443
- 16.2 Numerical Example Studied / 445
- 16.3 Conventional Control Structure Selection / 446
- 16.4 Temperature/Pressure/Composition Relationships / 450
- 16.5 Implementation in Aspen Dynamics / 451
- 16.6 Comparison of Dynamic Results / 452
 - 16.6.1 Feed Flow Rate Disturbances / 452
 - 16.6.2 Pressure Disturbances / 453
- 16.7 Conclusions / 455
- References / 456

17	ETHANOL DEHYDRATION	457
17.1	Introduction / 457	
17.2	Optimization of the Beer Still (Preconcentrator) / 459	
17.3	Optimization of the Azeotropic and Recovery Columns / 460	
17.3.1	Optimum Feed Locations / 461	
17.3.2	Optimum Number of Stages / 462	
17.4	Optimization of the Entire Process / 462	
17.5	Cyclohexane Entrainer / 466	
17.6	Flowsheet Recycle Convergence / 466	
17.7	Conclusions / 467	
	References / 467	
18	EXTERNAL RESET FEEDBACK TO PREVENT RESET WINDUP	469
18.1	Introduction / 469	
18.2	External Reset Feedback Circuit Implementation / 471	
18.2.1	Generate the Error Signal / 472	
18.2.2	Multiply by Controller Gain / 472	
18.2.3	Add the Output of Lag / 472	
18.2.4	Select Lower Signal / 472	
18.2.5	Setting up the <i>Lag</i> Block / 472	
18.3	Flash Tank Example / 473	
18.3.1	Process and Normal Control Structure / 473	
18.3.2	Override Control Structure Without External Reset Feedback / 474	
18.3.3	Override Control Structure with External Reset Feedback / 476	
18.4	Distillation Column Example / 479	
18.4.1	Normal Control Structure / 479	
18.4.2	Normal and Override Controllers Without External Reset / 481	
18.4.3	Normal and Override Controllers with External Reset Feedback / 483	
18.5	Conclusions / 486	
	References / 486	
	INDEX	487

PREFACE TO THE SECOND EDITION

Distillation fundamentals do not change, nor does the importance of distillation in our energy-intensive society. What does change is the range of applications and methods of analysis that provide more insight and offer improvements in steady-state design and dynamic control. In the seven years since the first edition was published, a number of new concepts and applications have been developed and published in the literature.

Industrial applications of the divided-wall (Petlyuk) column have expanded, so a new chapter has been added that covers both the design and the control of these more complex coupled columns. The use of dynamic simulations to quantitatively explore the safety issues of rapid transient responses to major process upsets and failures is discussed in a new chapter. A more structured approach for selecting an appropriate control structure is outlined to help sort through the overwhelmingly large number of alternative structures. A simple distillation column has five factorial (120) alternative structures that need to be trimmed down to a workable number, so that their steady-state and dynamic performances can be compared.

Interest in carbon dioxide capture has become more widespread, so a chapter studying the design and control of the low-pressure amine absorber/stripper system and the high-pressure physical-absorption absorber/stripper system has been added. The capabilities and features in Aspen software have been updated. The importance of being able to operate columns over a wide ranges of throughputs has increased with the development of chemical plants that are coupled with power-generation processes or inherently intermittent “green” energy sources (solar and wind). A new chapter deals with column control structures that can effectively deal with these turndown issues.

I hope you find the new edition useful and understandable. The coverage is unapologetically simple and practical. Therefore, the material should have a good chance of actually being applied to real and important problems. Good luck in your distillation design and control careers. I think you will find it challenging but fun.

WILLIAM L. LUYBEN

PREFACE TO THE FIRST EDITION

The rapid run up in the price of crude oil in recent years and the resulting “sticker shock” at the gas pump have caused the scientific and engineering communities to finally understand that it is time for some reality checks on our priorities. Energy is the real problem that the world faces, and it will not be solved by the recent fads of biotechnology or nanotechnology. Energy consumption is the main producer of carbon dioxide, so it is directly linked with the problem of global warming.

A complete reassessment of our energy supply and consumption systems is required. Our terribly inefficient use of energy in all aspects of our modern society must be halted. We waste energy in our *transportation* system with poor-mileage SUVs and inadequate railroad systems. We waste energy in our *water* systems by using energy to produce potable water, and then flush most of it down the toilet. This loads up our *waste disposal* plants, which consume more energy. We waste energy in our *food* supply system by consuming large amounts of energy for fertilizer, tillage, transporting, and packaging our food for consumer convenience. The old farmer markets provided better food at lower cost and required much less energy.

One of the most important technologies in our energy-supply system is distillation. Essentially, all our transportation fuel goes through at least one distillation column on its way from crude oil to the gasoline pump. Large distillation columns called pipestills separate the crude into various petroleum fractions based on boiling points. Intermediate fractions go directly to gasoline. Heavy fractions are catalytically or thermally “cracked” to form more gasoline. Light fractions are combined to form more gasoline. Distillation is used in all of these operations.

Even when we begin to switch to renewable sources of energy, such as biomass, the most likely transportation fuel will be methanol. The most likely process is the partial oxidation of biomass to produce synthesis gas (a mixture of hydrogen, carbon monoxide, and carbon dioxide), and the subsequent reaction of these components to produce methanol and water. Distillation to separate methanol from water is an important part of this process. Distillation is also used to produce the oxygen used in the partial oxidation reactor.

Therefore, distillation is, and will remain in the twenty-first century, the premier separation method in the chemical and petroleum industries. Its importance is unquestionable in helping to provide food, heat, shelter, clothing, and transportation in our modern society. It is involved in supplying much of our energy needs. The distillation columns in operation around the world number in the tens of thousands.

The analysis, design, operation, control, and optimization of distillation columns have been extensively studied for almost a century. Until the advent of computers, hand calculations and graphical methods were developed and widely applied in these studies. Starting from about 1950, analog and digital computer simulations began to be used for solving many engineering problems. Distillation analysis involves iterative vapor-liquid phase equilibrium calculations and tray-to-tray component balances that are ideal for digital computation.

Initially, most engineers wrote their own programs to solve both the nonlinear algebraic equations that describe the steady-state operation of a distillation column and to numerically integrate the nonlinear ordinary differential equations that describe its dynamic behavior. Many chemical and petroleum companies developed their own in-house steady-state process-simulation programs in which distillation was an important unit operation. Commercial *steady-state* simulators took over about two decades ago and now dominate the field.

Commercial *dynamic* simulators were developed quite a bit later. They had to wait for advancements in computer technology to provide the very fast computers required. The current state-of-the-art is that both steady-state and dynamic simulations of distillation columns are widely used in industry and in universities.

My own technical experience has pretty much followed this history of distillation simulation. My practical experience started back in a high-school chemistry class in which we performed batch distillations. Next came an exposure to some distillation theory and running a pilot-scale batch distillation column as an undergraduate at Penn State, learning from Arthur Rose and “Black” Mike Cannon. Then, there were five years of industrial experience in Exxon refineries as a technical service engineer on pipestills, vacuum columns, light-ends units, and alkylation units, all of which used distillation extensively.

During this period, the only use of computers that I was aware of was for solving linear programming problems associated with refinery planning and scheduling. It was not until returning to graduate school in 1960 that I personally started to use analog and digital computers. Bob Pigford taught us how to program a Bendix G12 digital computer, which used paper tape and had such limited memory that programs were severely restricted in length and memory requirements. Dave Lamb taught us analog simulation. Jack Gerster taught us distillation practice.

Next, there were four years working in the Engineering Department of DuPont on process-control problems, many of which involved distillation columns. Both analog and digital simulations were heavily used. A wealth of knowledge was available from a stable of outstanding engineers: Page Buckley, Joe Coughlin, J. B. Jones, Neal O’Brien, and Tom Keane, to mention only a few.

Finally, there have been over 35 years of teaching and research at Lehigh in which many undergraduate and graduate students have used simulations of distillation columns in isolation and in plantwide environments to learn basic distillation principles and to develop effective control structures for a variety of distillation column configurations. Both home-grown and commercial simulators have been used in graduate research and in the undergraduate senior design course.

The purpose of this book is to try to capture some of this extensive experience with distillation design and control, so that it is available to students and young engineers when they face problems with distillation columns. This book covers much more than just the mechanics of using a simulator. It uses simulation to guide in developing the optimum economic steady-state design of distillation systems, using simple and practical approaches. Then, it uses simulation to develop effective control structures for dynamic control. Questions are addressed of whether to use single-end control or dual-composition control, where to locate temperature control trays, and how excess degrees of freedom should be fixed.

There is no claim that the material is all new. The steady-state methods are discussed in most design textbooks. Most of the dynamic material is scattered around in a number of papers and books. What is claimed is that this book pulls this material together in a coordinated easily accessible way. Another unique feature is the combination of design and control of distillation columns in a single book.

There are three steps in developing a process design. The first is conceptual design in which simple approximate methods are used to develop a preliminary flowsheet. This step for distillation systems is covered very thoroughly by Doherty and Malone (*Conceptual Design of Distillation Systems*, 2001, McGraw-Hill). The next step is preliminary design in which rigorous simulation methods are used to evaluate both steady-state and dynamic performance of the proposed flowsheet. The final step is detailed design in which the hardware is specified in great detail: types of trays, number of sieve tray holes, feed and reflux piping, pumps, heat-exchanger areas, valve sizes and so on. This book deals with the second stage, preliminary design.

The subject of distillation simulation is a very broad one, which would require many volumes to cover comprehensively. The resulting encyclopedic-like books would be too formidable for a beginning engineer to try to tackle. Therefore, this book is restricted in its scope to only those aspects that I have found to be the most fundamental and the most useful. Only continuous distillation columns are considered. The area of batch distillation is very extensive and should be dealt with in another book. Only staged columns are considered. They have been successfully applied for many years. Rate-based models are fundamentally more rigorous, but they require that more parameters be known or estimated.

Only rigorous simulations are used in this book. The book by Doherty and Malone is highly recommended for a detailed coverage of approximate methods for conceptual steady-state design of distillation systems.

I hope that the reader finds this book useful and readable. It is a labor of love that is aimed at taking some of the mystery and magic out of design and operating a distillation column.

W. L. L.

CHAPTER 1

FUNDAMENTALS OF VAPOR–LIQUID EQUILIBRIUM (VLE)

Distillation occupies a very important position in chemical engineering. Distillation and chemical reactors represent the backbone of what distinguishes chemical engineering from other engineering disciplines. Operations involving heat transfer and fluid mechanics are common to several disciplines. But distillation is uniquely under the purview of chemical engineers.

The basis of distillation is phase equilibrium—specifically, vapor–liquid equilibrium (VLE) and in some cases vapor–liquid–liquid equilibrium (VLLE). Distillation can only effect a separation among chemical components if the compositions of the vapor and liquid phases that are in phase equilibrium with each other are different. A reasonable understanding of VLE is essential for the analysis, design, and control of distillation columns.

The fundamentals of VLE are briefly reviewed in this chapter.

1.1 VAPOR PRESSURE

Vapor pressure is a physical property of a pure chemical component. It is the pressure that a pure component exerts at a given temperature when there are both liquid and vapor phases present. Laboratory vapor pressure data, usually generated by chemists, are available for most of the chemical components of importance in industry.

Vapor pressure depends *only* on temperature. It does not depend on composition because it is a pure component property. This dependence is normally a strong one, with an exponential increase in vapor pressure with increasing temperature. Figure 1.1 gives two typical vapor pressure curves, one for benzene and one for toluene. The natural log of the vapor pressures of the two components is plotted against the reciprocal of the absolute temperature. As temperature increases, we move to the left in the figure, which

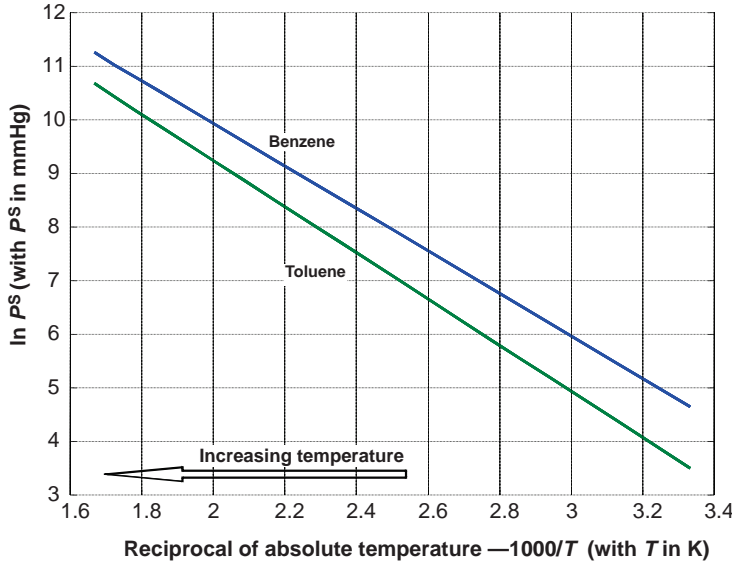


Figure 1.1 Vapor pressures of pure benzene and toluene.

means a higher vapor pressure. In this particular figure, the vapor pressure P^S of each component is given in units of mmHg. The temperature is given in kelvin.

Looking at a vertical constant-temperature line shows that benzene has a higher vapor pressure than toluene at a given temperature. Therefore, benzene is the “lighter” component from the standpoint of volatility (not density). Looking at a constant-pressure horizontal line shows that benzene boils at a lower temperature than toluene. Therefore, benzene is the “lower-boiling” component. Notice that the vapor pressure lines for benzene and toluene are fairly parallel. This means that the ratio of the vapor pressures does not change much with temperature (or pressure). As discussed in a later section, this means that the ease or difficulty of the benzene/toluene separation (the energy required to make a specified separation) does not change much with the operating pressure of the column. Other chemical components can have temperature dependences that are quite different.

If we have a vessel containing a mixture of these two components with liquid and vapor phases present, the vapor phase will contain a higher concentration of benzene than will the liquid phase. The reverse is true for the heavier, higher-boiling toluene. Therefore, benzene and toluene can be separated in a distillation column into an overhead distillate stream that is fairly pure benzene and a bottoms stream that is fairly pure toluene.

Equations can be fitted to the experimental vapor pressure data for each component using two, three, or more parameters. For example, the two-parameter version is

$$\ln P_j^S = C_j + D_j/T$$

The C_j and D_j are constants for each pure chemical component. Their numerical values depend on the units used for vapor pressure (mmHg, kPa, psia, atm, etc.) and on the units used for temperature (K or °R).

1.2 BINARY VLE PHASE DIAGRAMS

There are two types of VLE diagrams that are widely used to represent data for two-component (binary) systems. The first is a “temperature versus x and y ” diagram (T_{xy}). The x term represents the liquid composition, usually in terms of mole fraction. The y term represents the vapor composition. The second diagram is a plot of x versus y .

These types of diagrams are generated at a constant pressure. Because the pressure in a distillation column is relatively constant in most column (the exception is vacuum distillation in which the pressure at the top and bottom are significantly different in terms of absolute pressure level), a T_{xy} diagram and an xy diagram are convenient for the analysis of binary distillation systems.

Figure 1.2 gives the T_{xy} diagram for the benzene/toluene system at a pressure of 1 atm. The abscissa is the mole fraction of benzene. The ordinate is temperature. The lower curve is the “saturated liquid” line that gives the mole fraction of benzene in the liquid phase x . The upper curve is the “saturated vapor” line that gives the mole fraction of benzene in the vapor phase y . Drawing a horizontal line at some temperature and reading off the intersection of this line with the two curves give the compositions of the two phases. For example, at 370 K, the value of x is 0.375 mol fraction benzene, and the value of y is 0.586 mol fraction benzene. As expected, the vapor is richer in the lighter component.

At the leftmost point, we have pure toluene (0 mol fraction benzene), so the boiling point of toluene at 1 atm can be read from the diagram (384.7 K). At the rightmost point, we have pure benzene (1 mol fraction benzene), so the boiling point of benzene at 1 atm can be read from the diagram (353.0 K). The region between the curves is where there are two phases. The region above the saturated vapor curve is where there is only a single “superheated” vapor phase. The region below the saturated liquid curve is where there is only a single “subcooled” liquid phase.

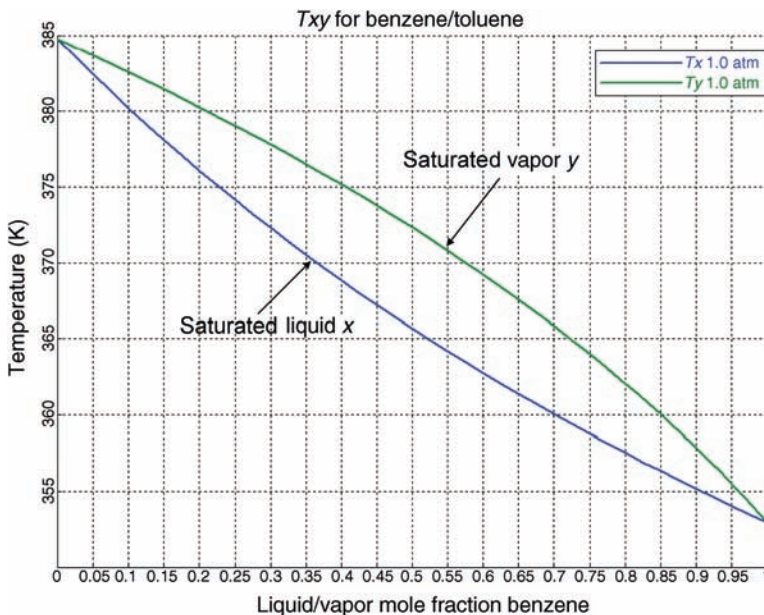


Figure 1.2 T_{xy} diagram for benzene and toluene at 1 atm.

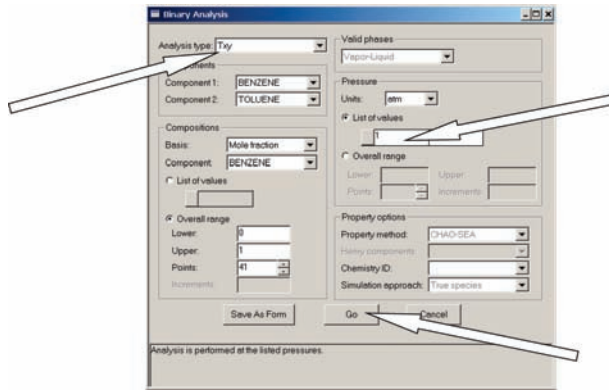


Figure 1.3 Specifying Txy diagram parameters.

The diagram is easily generated in Aspen Plus by going to *Tools* on the upper tool bar and selecting *Analysis*, *Property*, and *Binary*. The window shown in Figure 1.3 opens on which the type of diagram and the pressure are specified. Then click the *Go* button.

The pressure in the Txy diagram given in Figure 1.2 is 1 atm. Results at several pressures can also be generated as illustrated in Figure 1.4. The higher the pressure, the higher the temperature.

The other type of diagram, an xy diagram, is generated in Aspen Plus by clicking the *Plot Wizard* button at the bottom of the *Binary Analysis Results* window that also opens

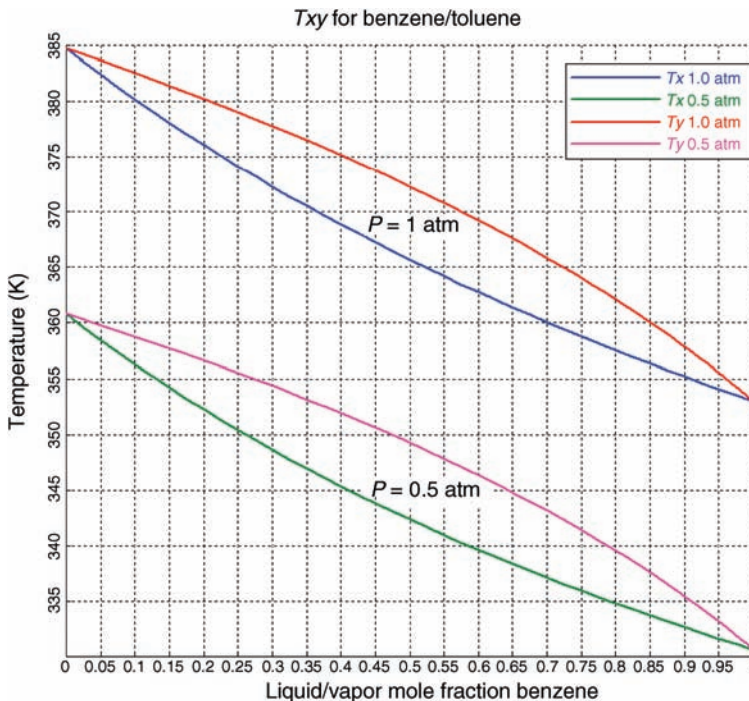


Figure 1.4 Txy diagrams at two pressures.

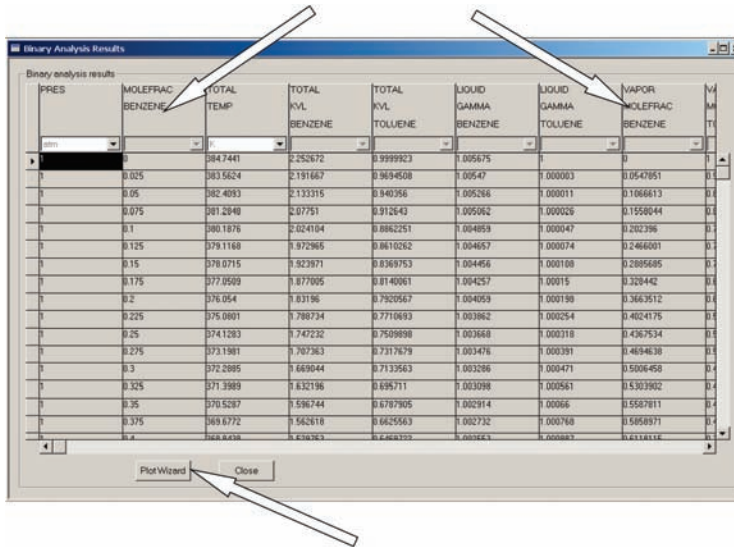


Figure 1.5 Using Plot Wizard to generate xy diagram.

when the Go button is clicked to generate the Txy diagram. As shown in Figure 1.5, this window also gives a table of detailed information. The window shown in Figure 1.6 opens, and xy picture is selected. Clicking the Next and Finish button generates the xy diagram shown in Figure 1.7. Figure 1.8 gives an xy diagram for the system propylene/propane. These components have boiling points that are quite close, which leads to a very difficult separation.

These diagrams provide valuable insight about the VLE of binary systems. They can be used for quantitative analysis of distillation columns, as we will demonstrate in Chapter 2. Three-component ternary systems can also be represented graphically, as discussed in Section 1.6.

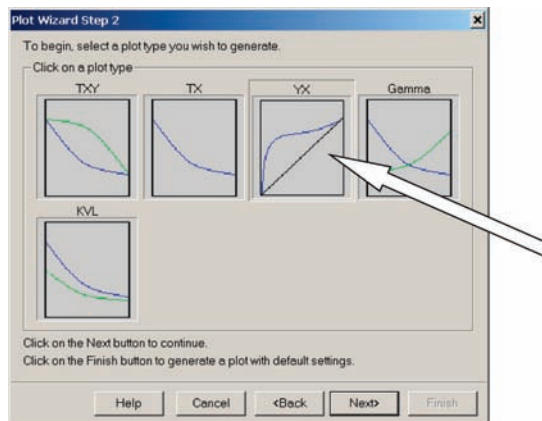


Figure 1.6 Using Plot Wizard to generate xy diagram.

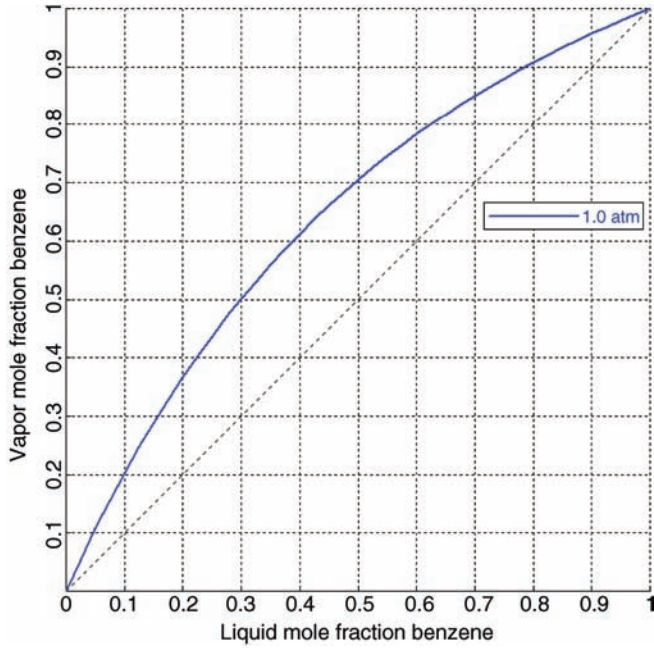


Figure 1.7 xy diagram for benzene/toluene.

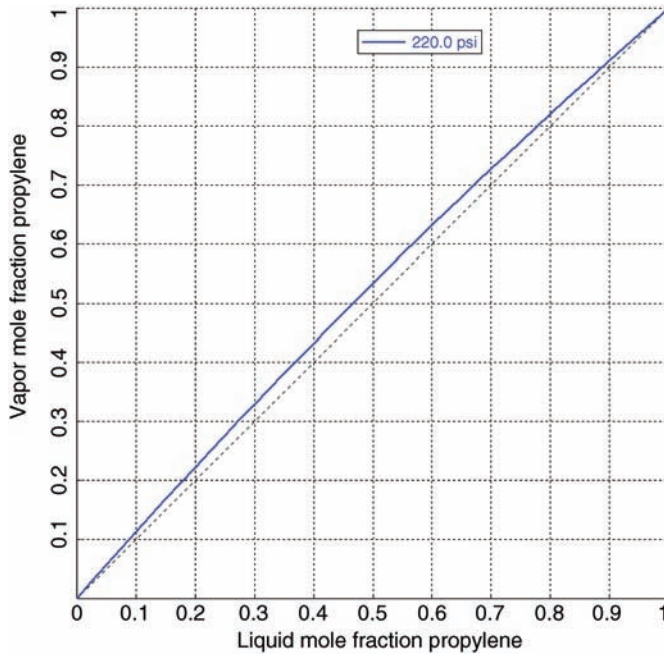


Figure 1.8 xy diagram for propylene/propane.

1.3 PHYSICAL PROPERTY METHODS

The observant reader may have noticed in Figure 1.3 that the physical property method specified for the VLE calculations in the benzene/toluene example was “Chao–Seader.” This method works well for most hydrocarbon systems.

One of the most important issues involved in distillation calculations is the selection of an appropriate physical property method that will accurately describe the phase equilibrium of the chemical component system. The Aspen Plus library has a large number of alternative methods. Some of the most commonly used methods are Chao–Seader, van Laar, Wilson, Unifac, and NRTL.

In most design situations, there is some type of data that can be used to select the most appropriate physical property method. Often VLE data can be found in the literature. The multivolume DECHEMA data books¹ provide an extensive source of data.

If operating data from a laboratory, pilot-plant, or plant column are available, it can be used to determine what physical property method fits the column data. There could be a problem in using column data because the tray efficiency is also not known, and the VLE parameters cannot be decoupled from the efficiency.

1.4 RELATIVE VOLATILITY

One of the most useful ways to represent VLE data is by the use of “relative volatility.” The definition of relative volatility is the ratio of the y/x values (vapor mole fraction over liquid mole fraction) of two components. For example, the relative volatility of component L with respect to component H is defined in the equation below.

$$\alpha_{LH} \equiv \frac{y_L/x_L}{y_H/x_H}$$

The larger the relative volatility, the easier the separation.

Relative volatilities can be applied to both binary and multicomponent systems. In the binary case, the relative volatility α between the light component and the heavy component can be used to give a simple relationship between the composition of the liquid phase (x is the mole fraction of the light component in the liquid phase) and the composition of the vapor phase (y is the mole fraction of the light component in the vapor phase).

$$y = \frac{\alpha x}{1 + (\alpha - 1)x}$$

Figure 1.9 gives xy curves for several value of α , assuming that α is constant over the entire composition space.

In the multicomponent case, a similar relationship can be derived. Suppose there are NC components. Component 1 is the lightest, component 2 is the next lightest, and so forth down to the heaviest of all the components, component H . We define the relative volatility of component j with respect to component H as α_j .

$$\alpha_j = \frac{y_j/x_j}{y_H/x_H}$$

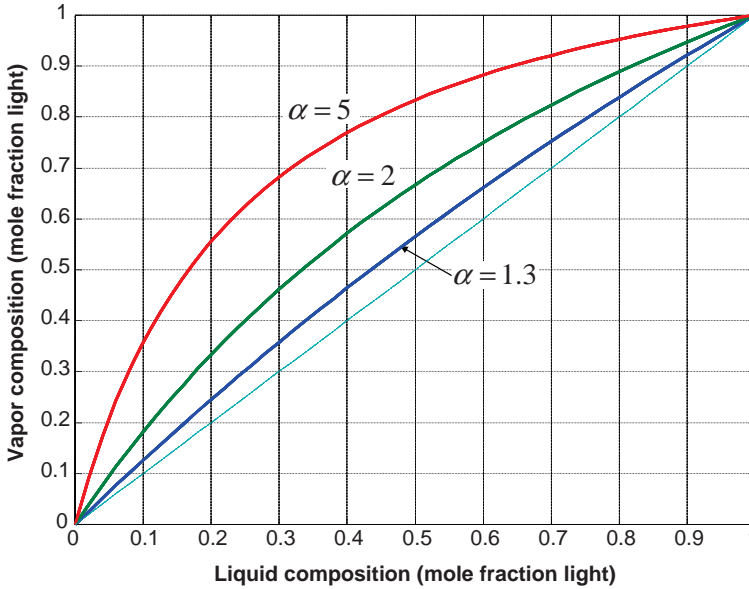


Figure 1.9 xy curves for relative volatilities of 1.3, 2, and 5.

Solving for y_j and summing all of the y 's (which must add to unity) give

$$y_j = \alpha_j x_j (y_H/x_H)$$

$$\sum_{j=1}^{NC} y_j = 1 = \sum_{j=1}^{NC} \alpha_j x_j (y_H/x_H)$$

$$1 = (y_H/x_H) \sum_{j=1}^{NC} \alpha_j x_j$$

Then solving for y_H/x_H and substituting this into the first equation above give

$$(y_H/x_H) = \frac{1}{\sum_{j=1}^{NC} \alpha_j x_j}$$

$$y_j = \frac{\alpha_j x_j}{\sum_{j=1}^{NC} \alpha_j x_j}$$

The last equation relates the vapor composition to the liquid composition for a constant relative volatility multicomponent system. Of course, if relative volatilities are not constant, this equation cannot be used. What is required is a “bubblepoint” calculation, which is discussed in Section 1.5.

1.5 BUBBLE POINT CALCULATIONS

The most common VLE problem is to calculate the temperature and vapor composition y_j that is in equilibrium with a liquid at a known total pressure of the system P and with a

known liquid composition (all of the x_j). At phase equilibrium, the “chemical potential” μ_j of each component in the liquid and vapor phases must be equal.

$$\mu_j^L = \mu_j^V$$

The liquid-phase chemical potential of component j can be expressed in terms of liquid mole fraction x_j , vapor pressure P_j^S , and activity coefficient γ_j .

$$\mu_j^L = x_j P_j^S \gamma_j$$

The vapor-phase chemical potential of component j can be expressed in terms of vapor mole fraction y_j , the total system pressure P , and fugacity coefficient σ_j .

$$\mu_j^V = y_j P \sigma_j$$

Therefore, the general relationship between vapor and liquid phases is

$$y_j P \sigma_j = x_j P_j^S \gamma_j$$

If the pressure of the system is not high, the fugacity coefficient is unity. If the liquid phase is “ideal” (no interaction between the molecules), the activity coefficient is unity. The latter situation is much less common than the former because components interact in liquid mixtures. They can either attract or repulse. Section 1.7 discusses nonideal systems in more detail.

Let us assume that the liquid and vapor phases are both ideal ($\gamma_j = 1$ and $\sigma_j = 1$). In this situation, the bubblepoint calculation involves an iterative calculation to find the temperature T that satisfies the equation

$$P = \sum_{j=1}^{NC} x_j P_j^S(T)$$

The total pressure P and all the x_j are known. In addition, equations for the vapor pressures of all components as functions of temperature T are known. The Newton–Raphson convergence method is convenient and efficient in this iterative calculation because an analytical derivative of the temperature-dependent vapor pressure functions P^S can be used.

1.6 TERNARY DIAGRAMS

Three-component systems can be represented in two-dimensional ternary diagrams. There are three components, but the sum of the mole fractions must add to unity. Therefore, specifying two mole fractions completely defines the composition.

A typical rectangular ternary diagram is given in Figure 1.10. The abscissa is the mole fraction of component 1. The ordinate is the mole fraction of component 2. Both of these dimensions run from 0 to 1. The three corners of the triangle represent the three pure components.

Since only two compositions define the composition of a stream, it can be located on this diagram by entering the appropriate coordinates. For example, Figure 1.10 shows the location of stream F that is a ternary mixture of 20 mol% n -butane (C4), 50 mol% n -pentane (C5), and 30 mol% n -hexane (C6).

One of the most useful and interesting aspects of ternary diagrams is the “ternary mixing rule.” This states that if two ternary streams are mixed together (one is stream D with composition x_{D1} and x_{D2} and the other is stream B with composition x_{B1} and x_{B2}), the

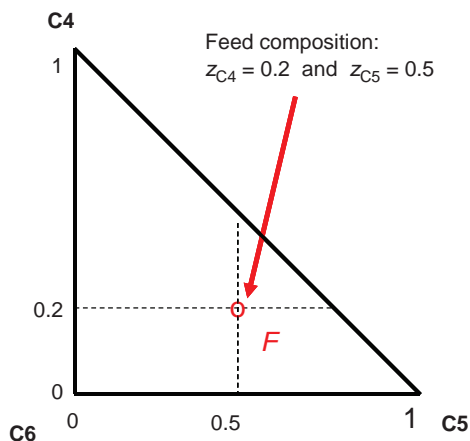


Figure 1.10 Ternary diagram.

mixture has a composition (z_1 and z_2) that lies on a *straight* line in x_1-x_2 ternary diagram that connects the x_D and x_B points.

Figure 1.11 illustrates the application of this mixing rule to a distillation column. Of course, a column *separates* instead of *mixes*, but the geometry is exactly the same. The two products D and B have compositions located at point ($x_{D1}-x_{D2}$) and point ($x_{B1}-x_{B2}$), respectively. The feed F has a composition located at point (z_1-z_2) that lies on a straight line joining D and B .

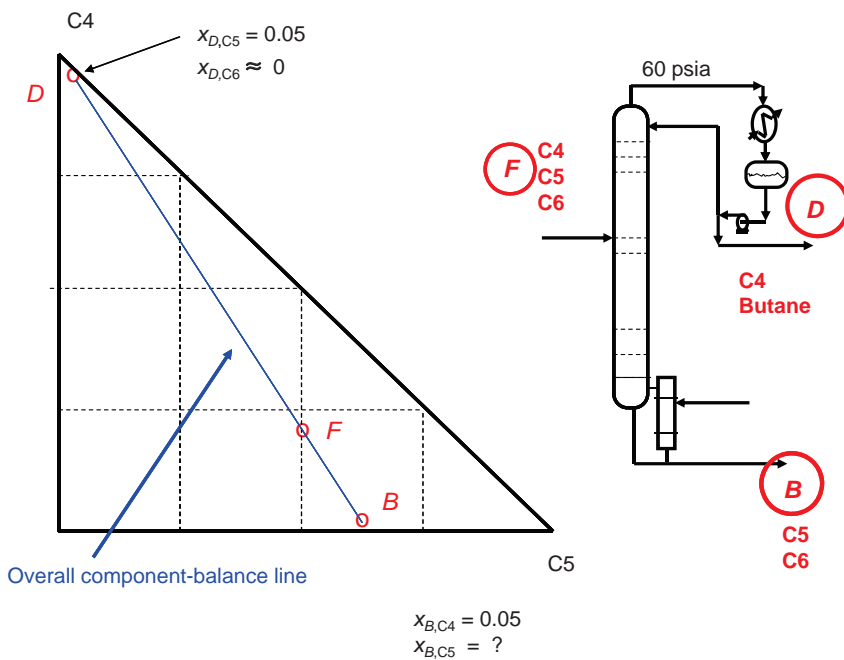


Figure 1.11 Ternary mixing rule.

This geometric relationship is derived from the overall molar balance and the two overall component balances around the column.

$$\begin{aligned}F &= D + B \\Fz_1 &= Dx_{D1} + Bx_{B1} \\Fz_2 &= Dx_{D2} + Bx_{B2}\end{aligned}$$

Substituting the first equation into the second and third gives

$$\begin{aligned}(D + B)z_1 &= Dx_{D1} + Bx_{B1} \\(D + B)z_2 &= Dx_{D2} + Bx_{B2}\end{aligned}$$

Rearranging these two equations to solve for the ratio of B over D gives

$$\begin{aligned}\frac{D}{B} &= \frac{(z_1 - x_{D1})}{(x_{B1} - z_1)} \\ \frac{D}{B} &= \frac{(z_2 - x_{D2})}{(x_{B2} - z_2)}\end{aligned}$$

Equating these two equations and rearranging gives

$$\begin{aligned}\frac{z_1 - x_{D1}}{x_{B1} - z_1} &= \frac{z_2 - x_{D2}}{x_{B2} - z_2} \\ \frac{x_{D1} - z_1}{z_2 - x_{D2}} &= \frac{z_1 - x_{B1}}{x_{B2} - z_2}\end{aligned}$$

Figure 1.12 shows how the ratios given above can be defined in terms of the tangents of the angles θ_1 and θ_2 . The conclusion is that the two angles must be equal, so the line between D and B must pass through F .

As we will see in subsequent chapters, this straight-line relationship is quite useful in representing what is going on in a ternary distillation system. This straight line is called the component-balance line.

1.7 VLE NONIDEALITY

Liquid-phase ideality (activity coefficients $\gamma_j = 1$) only occurs when the components are quite similar. The benzene/toluene system is a common example. As shown in Figure 1.5 in the sixth and seventh columns, the activity coefficients of both benzene and toluene are very close to unity.

However, if components are dissimilar, nonideal behavior occurs. Consider a mixture of methanol and water. Water is very polar. Methanol is polar on the “OH” end of the molecule, but the “CH₃” end is nonpolar. This results in some nonideality. Figure 1.13a gives the xy curve at 1 atm. Figure 1.13b gives a table showing how the activity coefficients of the two components vary over composition space. The Unifac physical property method is used. The γ values range up to 2.3 for methanol at the $x = 0$ limit and 1.66 for water at $x = 1$. A plot of the activity coefficients can be generated by selecting the *Gamma* picture when using the *Plot Wizard*. The resulting plot is given in Figure 1.13c.

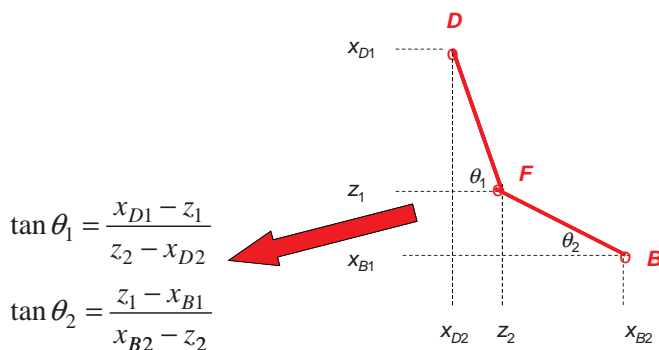


Figure 1.12 Proof of colinearity.

Now consider a mixture of ethanol and water. The “CH₃-CH₂” end of the ethanol molecule is more nonpolar than the “CH₃” end of methanol. We would expect the nonideality to be more pronounced, which is exactly what the *Txy* diagram, the activity coefficient results, and the *xy* diagram given in Figure 1.14 show.

Notice that the activity coefficient of ethanol at the $x = 0$ end (pure water) is very large ($\gamma_{\text{EtOH}} = 6.75$). Notice also that the *xy* curve shown in Figure 1.14c crosses the 45° line ($x = y$) at about 90 mol% ethanol. This indicates the presence of an “azeotrope.” Note also

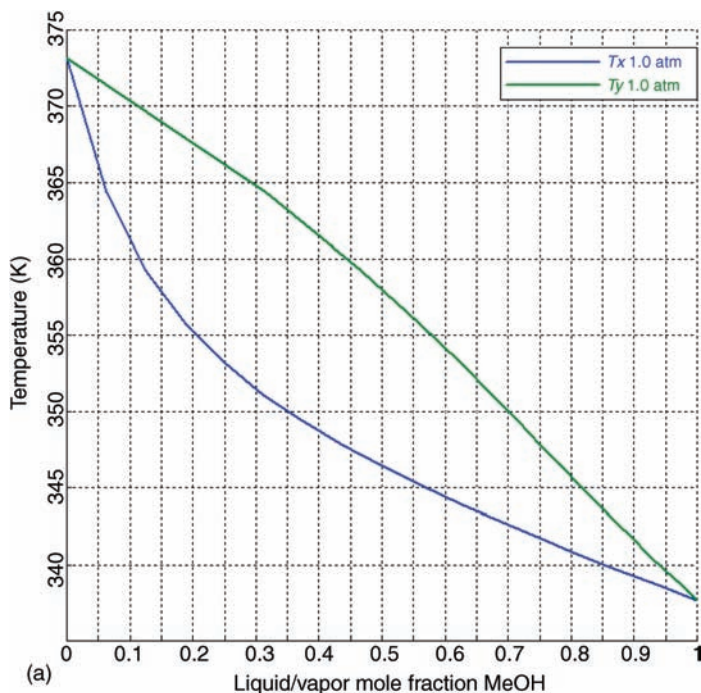


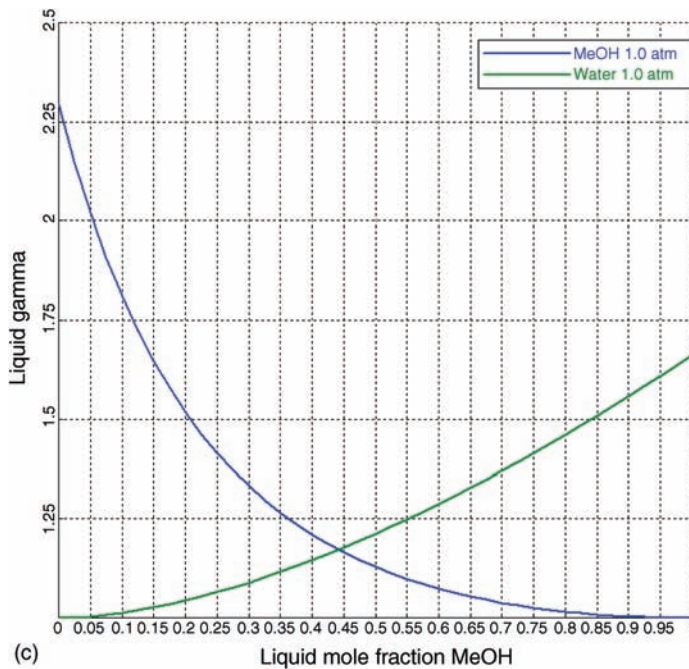
Figure 1.13 (a) *Txy* diagram for methanol/water. (b) Activity coefficients for methanol/water. (c) Activity coefficient plot for methanol/water.

Binary Analysis Results

Binary analysis results

Pressure	Molefrac MeOH	Total Temp	Total Vol MeOH	Total Vol Water	Liquid Gamma MeOH	Liquid Gamma Water	Vapor Molefrac MeOH	Vapor Molefrac Water
1	0	373.1675	7.740335	0.9999874	2.292559	0	0	0
1	0.0625	364.4015	6.643260	0.7364480	0.963214	0.804322	0.3152040	0.6047957
1	0.125	359.2501	5.741298	0.6084334	0.723613	0.618333	0.467590	0.532461
1	0.1875	356.7094	5.089333	0.5415125	0.547374	0.408593	0.5600963	0.4399937
1	0.25	353.1777	4.498813	0.5084891	0.415160	0.284555	0.6246248	0.3793391
1	0.3125	351.1955	4.150346	0.4754903	0.314360	0.195401	0.6744724	0.3295276
1	0.375	348.3501	3.809578	0.4649460	0.230537	0.130547	0.7152514	0.2942786
1	0.4375	347.8549	3.717998	0.4415318	0.175077	0.089971	0.7514485	0.2605681
1	0.5	348.4356	3.681811	0.4317911	0.132870	0.061164	0.7841888	0.2188812
1	0.5625	348.1601	3.427625	0.4248425	0.09178	0.04099	0.8142873	0.1887207
1	0.625	343.9502	3.240489	0.4150041	0.063149	0.027191	0.8403477	0.1573523
1	0.6875	342.8187	3.265091	0.4149424	0.041282	0.016323	0.8533338	0.1294441
1	0.75	341.2268	3.190336	0.4117060	0.024961	0.014393	0.8570506	0.1029444
1	0.8125	340.6716	3.136793	0.4081005	0.013338	0.012207	0.8242424	0.0707576
1	0.875	339.6497	3.084625	0.407549	0.006446	0.005072	0.8005888	0.0569432
1	0.9375	338.6559	3.03961	0.4081703	0.001349	0.001588	0.874814	0.025386
1	1	337.6848	0.9999999	0.4081123	0	0.002945	0	0

(b)



(c)

Figure 1.13 (Continued)

that the temperature at the azeotrope (351.0 K) is lower than the boiling point of ethanol (351.5 K).

An azeotrope is defined as a composition at which the liquid and vapor compositions are equal. Obviously when this occurs, there can be no change in the liquid and vapor compositions from tray to tray in a distillation column. Therefore, an azeotrope represents a “distillation boundary.”

Azeotropes occur in binary, ternary, and multicomponent systems. They can be “homogeneous” (single liquid phase) or “heterogeneous” (two liquid phases). They can be “minimum boiling” or “maximum boiling.” The ethanol/water azeotrope is a minimum-boiling homogeneous azeotrope.

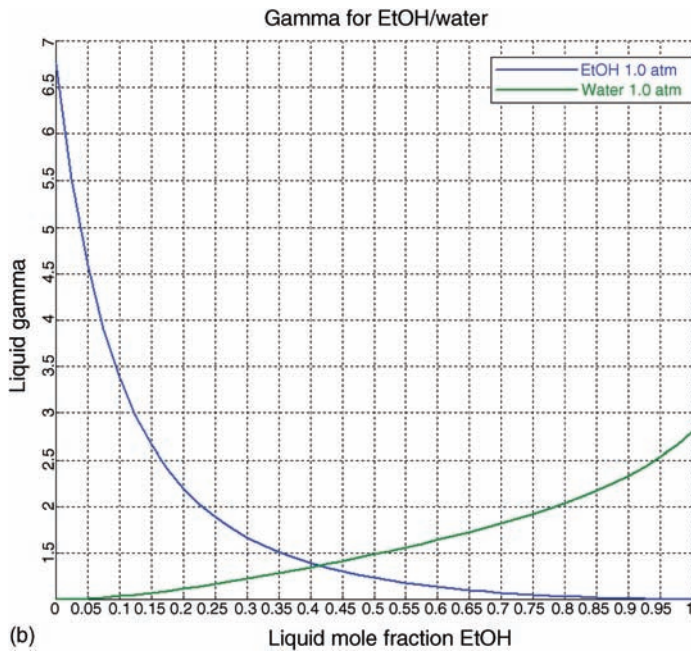
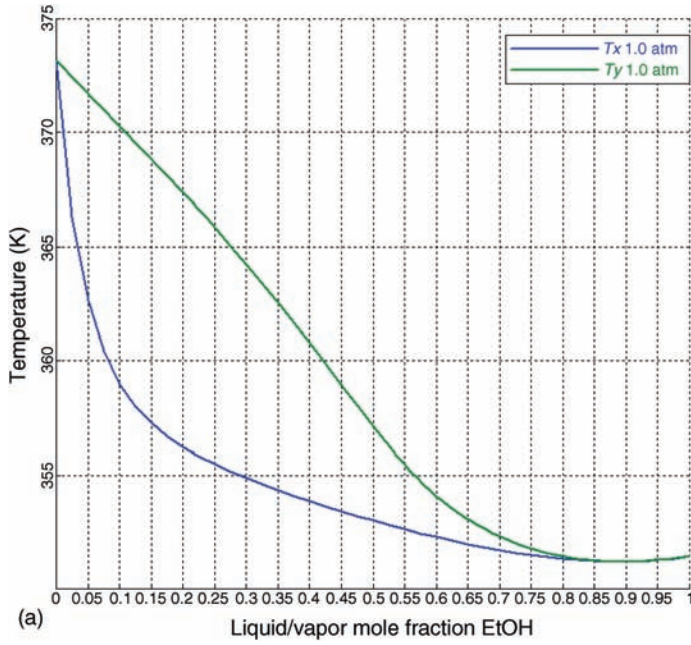


Figure 1.14 (a) Txy diagram for ethanol/water. (b) Activity coefficient plot for ethanol/water. (c) xy plot for ethanol/water.

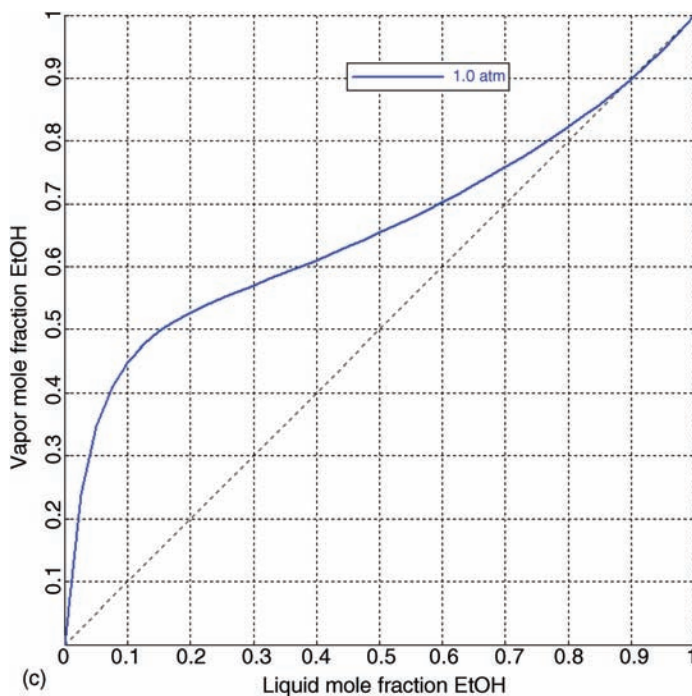


Figure 1.14 (Continued)

The software supplied in Aspen Plus provides a convenient method for calculating azeotropes. Go to *Tools* on the top tool bar, select *Conceptual Design* and *Azeotropic Search*. The window shown at the top of Figure 1.15 opens on which the components and pressure level are specified. The physical property package is set to be Uniquac. Clicking on *Azeotropes* opens the window shown at the bottom of Figure 1.15, which gives the calculated results: a homogeneous azeotrope at 78 °C (351 K) with composition 90.0 mol% ethanol.

Let us now study a system in which there is more dissimilarity of the molecules by looking at the *n*-butanol/water system. The normal boiling point of *n*-butanol is 398 K, and that of water is 373 K, so water is the low boiler in this system. The azeotrope search results are shown in Figure 1.16, and the *Txy* diagram is shown in Figure 1.17. Notice that “*Vap-Liq-Liq*” is selected in the “*Phases*” under the “*Property Model*.”

The liquid-phase nonideality is so large that a heterogeneous azeotrope is formed. The molecules are so dissimilar that two liquid phases are formed. The composition of the vapor is 75.17 mol% water at 1 atm. The compositions of the two liquid phases that are in equilibrium with this vapor are 43.86 and 98.05 mol% water, respectively.

1.8 RESIDUE CURVES FOR TERNARY SYSTEMS

Residue curve analysis is quite useful in studying ternary systems. A mixture with an initial composition $x_{1(0)}$ and $x_{2(0)}$ is placed in a container at some fixed pressure. A vapor stream is

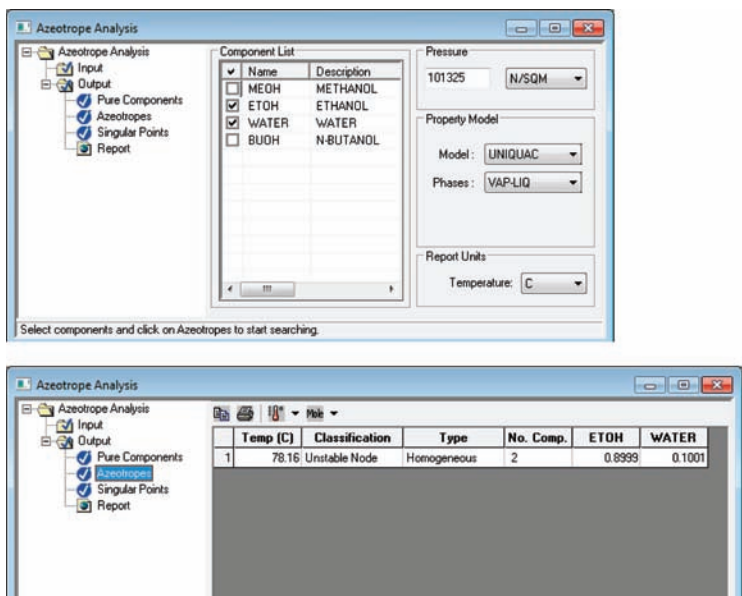


Figure 1.15 Azeotrope analysis: ethanol/water.

continuously removed, and the composition of the remaining liquid in the vessel is plotted on the ternary diagram.

Figure 1.18 gives an example of how the compositions of the liquid x_j and the vapor y_j change with time during this operation. The specific numerical example is a ternary mixture of components A , B , and C that have constant relative volatilities of $\alpha_A = 4$, $\alpha_B = 2$, and $\alpha_C = 1$. The initial composition of the liquid is $x_A = 0.5$ and $x_B = 0.25$. The initial

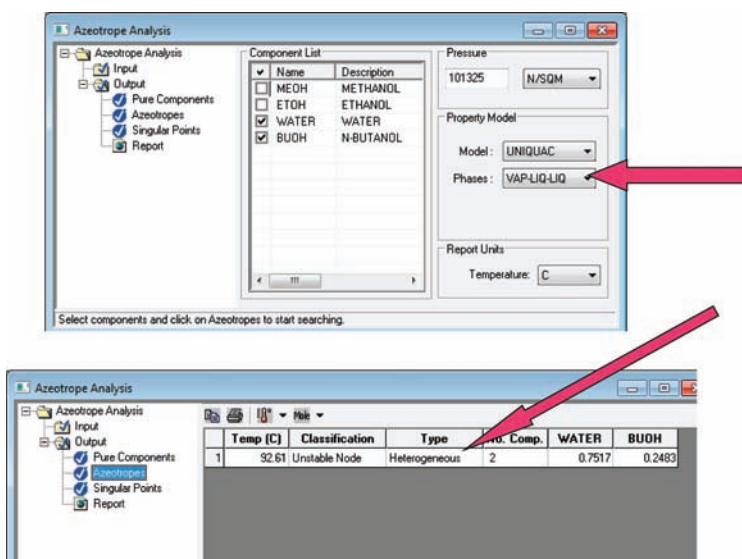


Figure 1.16 Azeotrope analysis: water/butanol.

Binary Analysis

Analysis type: Txy

Valid phases: Vapor-Liquid-Liquid

Components:
 Component 1: WATER
 Component 2: BUOH

Compositions:
 Basis: Mole fraction
 Component: WATER

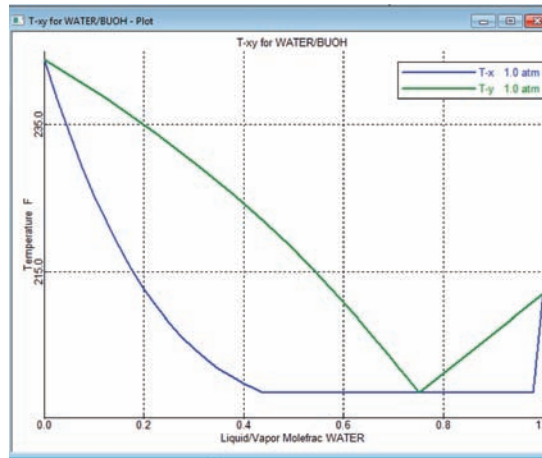
Pressure:
 Units: psia
 List of values: 14.69595

Property options:
 Property method: UNIQUAC
 Henry components:
 Chemistry ID:
 Simulation approach: True components

Save As Form Go Cancel

Analysis is performed at the listed pressures.

(a)



(b)

Figure 1.17 (a) Txy analysis: water/butanol. (b) Txy diagram: water/butanol.

amount of liquid is 100 mol, and vapor is withdrawn at a rate of 1 mol per unit of time. Notice that component A is quickly depleted from the liquid because it is the lightest component. The liquid concentration of component B actually increases for a while and then drops. Figure 1.19 plots the x_A and x_B trajectories for different initial conditions. These are the “residue curves” for this system.

Residue curves can be easily generated in Aspen Plus. Click on *Tools* in the upper tool bar in the Aspen Plus window and select *Conceptual Design* and *Ternary Maps*. This opens the window shown in Figure 1.20 on which the three components and pressure are selected. The numerical example is the ternary mixture of n -butane, n -pentane, and n -hexane. Clicking on *Ternary Plot* opens the window given in Figure 1.21. To generate a residue curve, right click the diagram and select *Add* and *Curve*. A cross-hair appears that can be

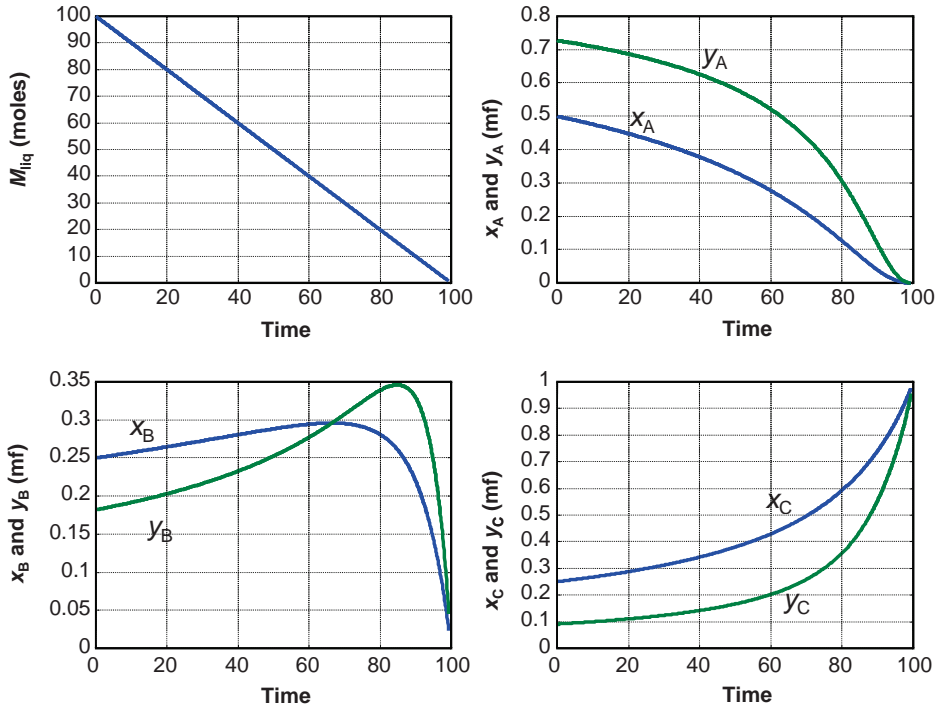


Figure 1.18 Generation of residue curves.

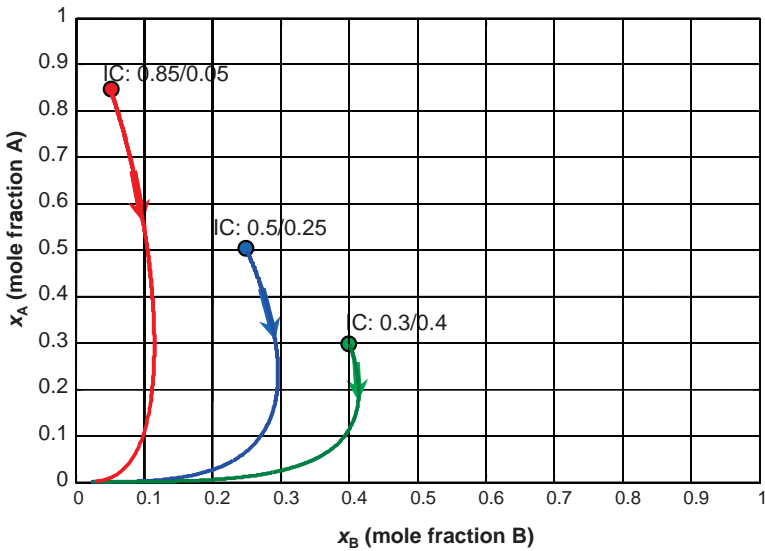


Figure 1.19 Residue curves starting from different initial conditions.

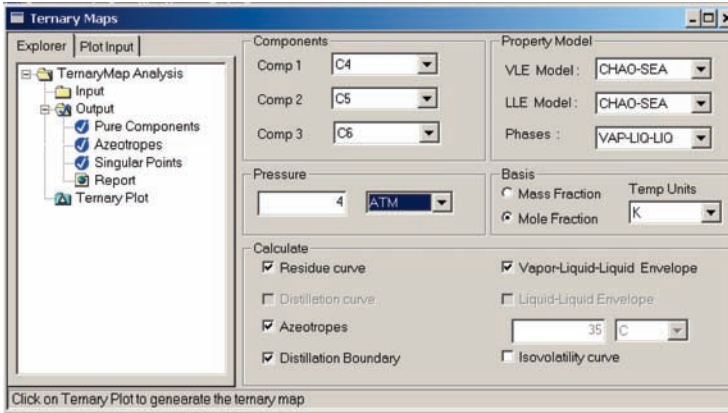


Figure 1.20 Setting up ternary maps.

moved to any location on the diagram. Clicking inserts a residue curve that passes through the selected point, as shown in Figure 1.22a. Repeating this procedure produces multiple residue curves shown in Figure 1.22b. Alternatively, the third button from the top on the right toolbar can be clicked. Then the cursor can be located at multiple points on the diagram, and right clicks will draw multiple residue curves.

Notice that all the residue curves start at the lightest component (C4) and move toward the heaviest component (C6). In this sense, they are similar to the compositions in a distillation column. The light components go out to the top, and the heavy components go out at the bottom. We will show below that this similarity proves to be useful for the analysis of distillation systems.

The generation of residue curves is described mathematically by a dynamic molar balance of the liquid in the vessel M_{liq} and two dynamic component balances for components A and B . The rate of vapor withdrawal is V (moles per time).

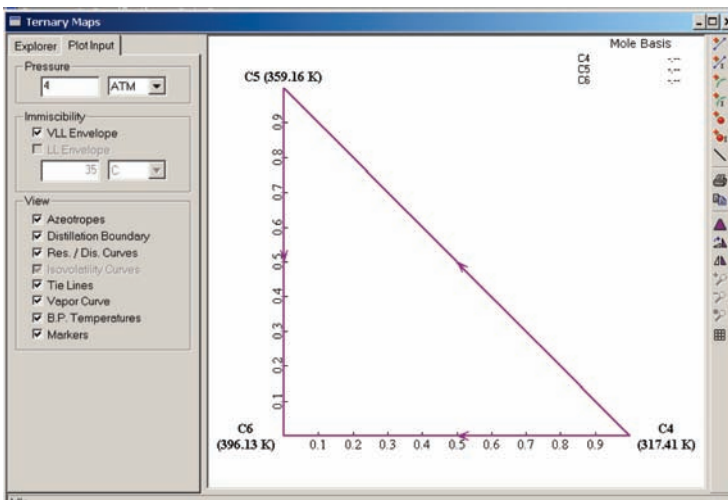
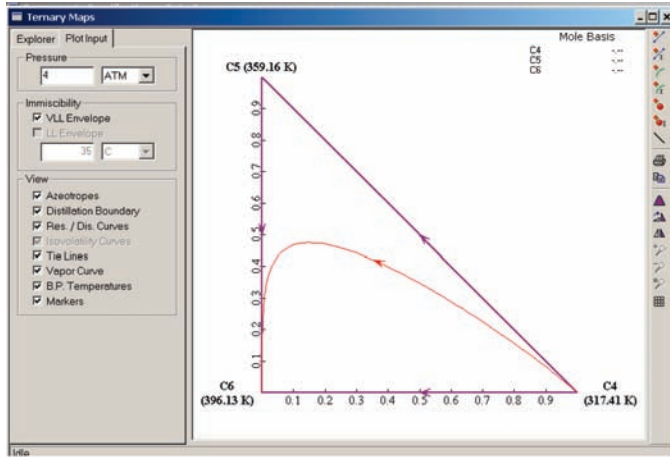
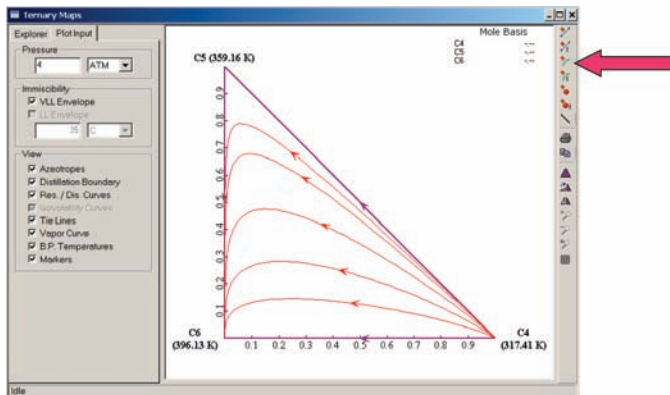


Figure 1.21 Ternary diagram for C4, C5, and C6.



(a)



(b)

Figure 1.22 (a) Adding a residue curve. (b) Several residue curves.

$$dM_{liq}/dt = -V$$

$$d(M_{liq}x_j)/dt = -Vy_j$$

Of course, the values of x_j and y_j are related by the VLE of the system. Expanding the second equation and substituting the first equation give

$$M_{liq}(dx_j/dt) + x_j(dM_{liq}/dt) = -Vy_j$$

$$M_{liq}(dx_j/dt) + x_j(-V) = -Vy_j$$

$$(M_{liq}/V)(dx_j/dt) = x_j - y_j$$

$$dx_j/d\theta = x_j - y_j$$

The parameter θ is a dimensionless time variable. The last equation models how compositions change during the generation of a residue curve. As we develop below, a

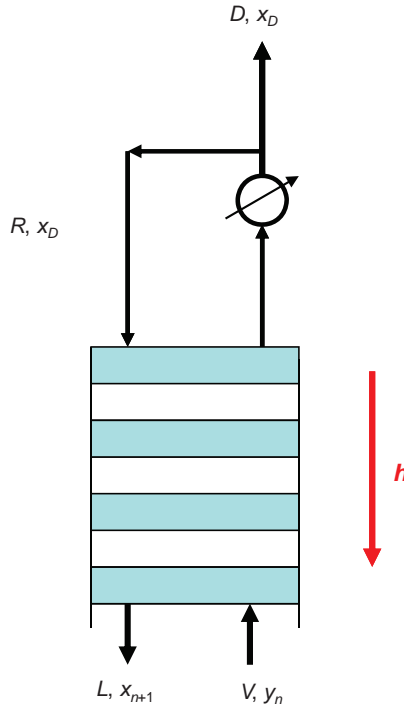


Figure 1.23 Distillation column.

similar equation describes the tray-to-tray liquid compositions in a distillation column under total reflux conditions. This relationship permits us to use residue curves to assess what separations are feasible or infeasible in a given system.

Consider the upper section of a distillation column shown in Figure 1.23. The column is cut at Tray n , at which the passing vapor and liquid streams have compositions y_{nj} and $x_{n+1,j}$ and flow rates are V_n and L_{n+1} . The distillate flow rate and composition are D and x_{Dj} , respectively. The steady-state component balance is

$$V_n y_{nj} = L_{n+1} x_{n+1,j} + D x_{Dj}$$

Under total reflux conditions, D is equal to zero and L_{n+1} is equal to V_n . Therefore, y_{nj} is equal to $x_{n+1,j}$.

Let us define a continuous variable h as the distance from the top of the column down to any tray. The discrete changes in liquid composition from tray to tray can be approximated by the differential equation

$$\frac{dx_j}{dh} \approx x_{nj} - x_{n+1,j}$$

At total reflux, this equation becomes

$$\frac{dx_j}{dh} = x_{nj} - y_{nj}$$

Notice that this is the same equation as developed for residue curves.

The significance of this similarity is that the residue curves approximate the column profiles. Therefore, a feasible separation in a column must satisfy two conditions

1. The distillate compositions x_{Dj} and the bottoms compositions x_{Bj} must lie near a residue curve.
2. They must lie on a straight line through the feed composition point z_j .

We will use these principles in Chapters 2 and 5 for analyzing both simple and complex distillation systems.

1.9 DISTILLATION BOUNDARIES

The existence of azeotropes can introduce limits on the ability to separate components using distillation. These limitations are called distillation boundaries. They separate regions of feasible separations. Feed streams with compositions located in one region can produce certain products, while feed compositions in other regions will produce other products (different compositions of the distillate and bottoms streams).

To illustrate this phenomenon, let us start with a simple binary mixture. If there are no azeotropes, the xy diagram shows the VLE curve entirely above the 45° line, as shown in left graph in Figure 1.24. However, if there is a homogeneous minimum-boiling azeotrope as shown in Figure 1.25a, there is a distillation boundary at the azeotropic composition. The figure on the right shows that if the feed composition z_1 is lower than the azeotrope, the bottoms product will be mostly the *heavy-key* component, and the distillate will have a composition slightly lower than the azeotrope. On the other hand, if the feed composition is higher than the azeotrope (Fig. 1.25b), the bottoms product will be mostly the *light-key* component, and the distillate will have a composition slightly higher than the azeotrope.

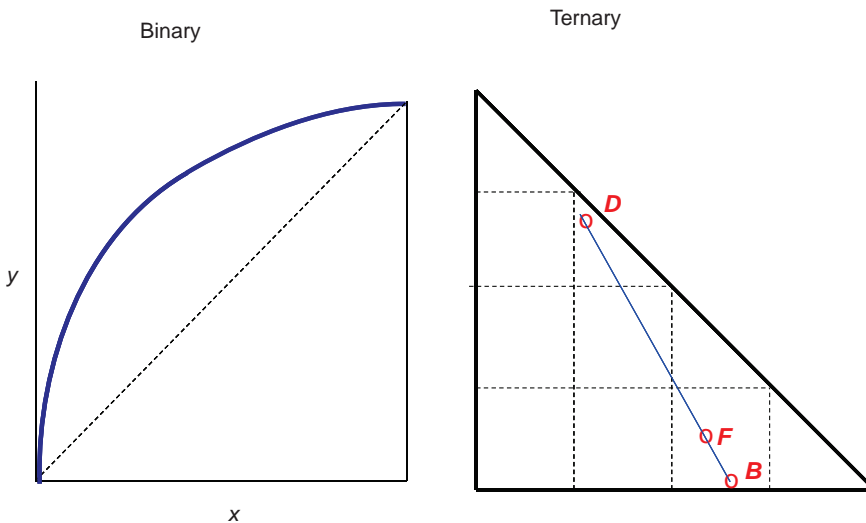


Figure 1.24 No distillation boundaries in ideal systems.

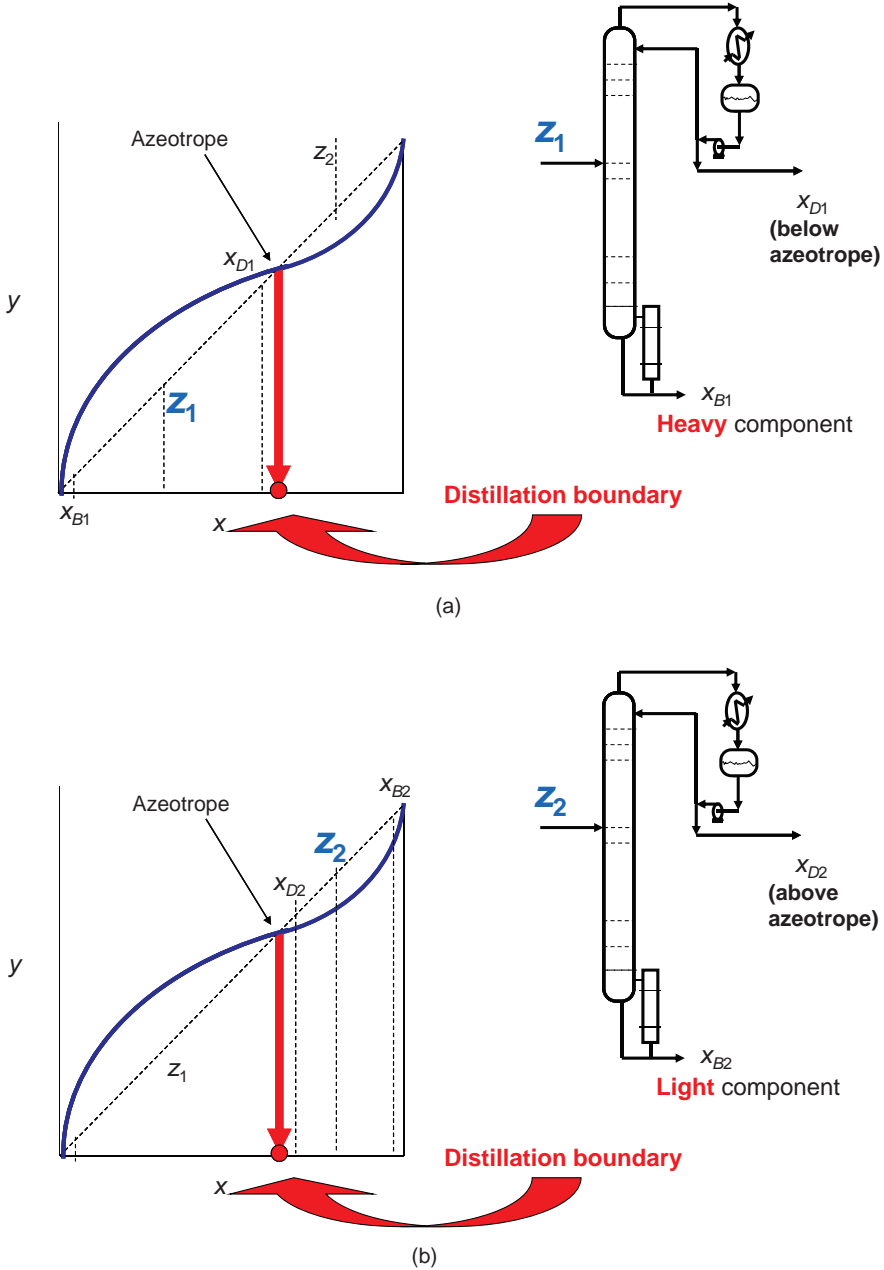


Figure 1.25 Distillation boundary in binary nonideal systems. (a) Feed composition z_1 less than azeotrope. (b) Feed composition z_2 greater than azeotrope.

Now, let us consider a ternary system. The ternary diagram of an ideal system shown in the right graph in Figure 1.24 displays no distillation boundaries. However, Figure 1.26 gives the ternary diagram for a nonideal system with two binary azeotropes. One is the A/B azeotrope and the other is the A/C azeotrope. A curve connecting the two azeotropes

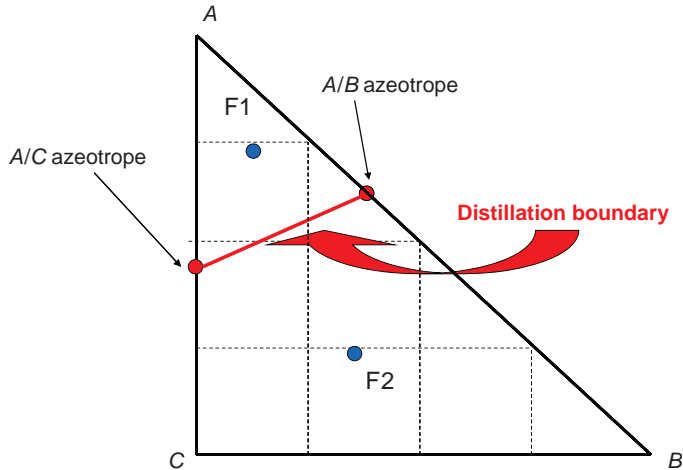


Figure 1.26 Distillation boundaries in ternary systems.

represents a distillation boundary. There are two regions in the ternary space. A feed stream located in the upper regions (F1) can produce products that lie only in this upper region. A feed stream located in the lower regions (F2) can produce products that lie only in this lower region.

The ternary system of methyl acetate, methanol, and water illustrates the occurrence of a distillation boundary. Figures 1.27 and 1.28 give the binary azeotropes of the system at 20 psia using NRTL physical properties. Figure 1.29 shows the ternary diagram with a distillation boundary.

A more complex system is shown in Figures 1.30 and 1.31. Ethanol, water, and benzene display three binary azeotropes and one ternary azeotrope. The resulting ternary diagram (Fig. 1.31) has three distillation boundaries that separate the ternary space into three regions.

We return to this complex system in Chapter 5 and develop a separation scheme for producing high-purity ethanol (upper corner in Fig. 1.31).

NRTL physical properties

Boiling points at 20 psia: MeOAc = 330.2 K
 MeOH = 337.7 K
 H₂O = 373.2 K

Binary azeotropes:

MeAc/MeOH: 64.5 mol% MeAc at 326.8 K
 MeOAc/H₂O: 95 mol% MeOAc at 330.1 K

Figure 1.27 Methyl acetate/methanol/water ternary.

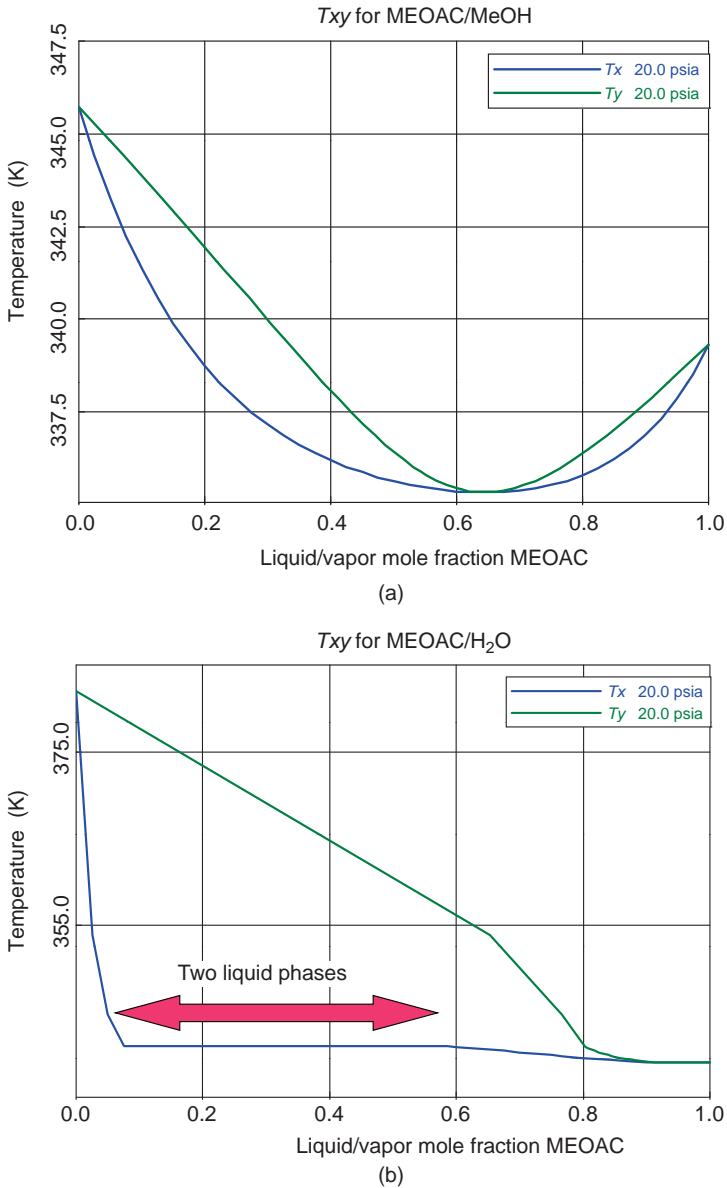


Figure 1.28 Binary azeotropes (NRTL). (a) Methyl acetate/methanol. (b) Methyl acetate/water.

1.10 CONCLUSIONS

The basics of vapor–liquid phase equilibrium have been reviewed in this chapter. A good understanding of VLE is indispensable in the design and control of distillation systems. These basics will be used throughout this book.

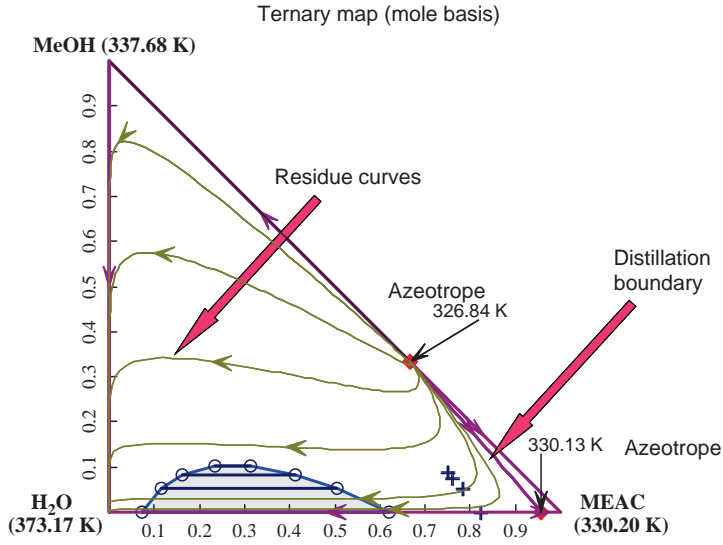


Figure 1.29 Methyl acetate/methanol/water ternary diagram.

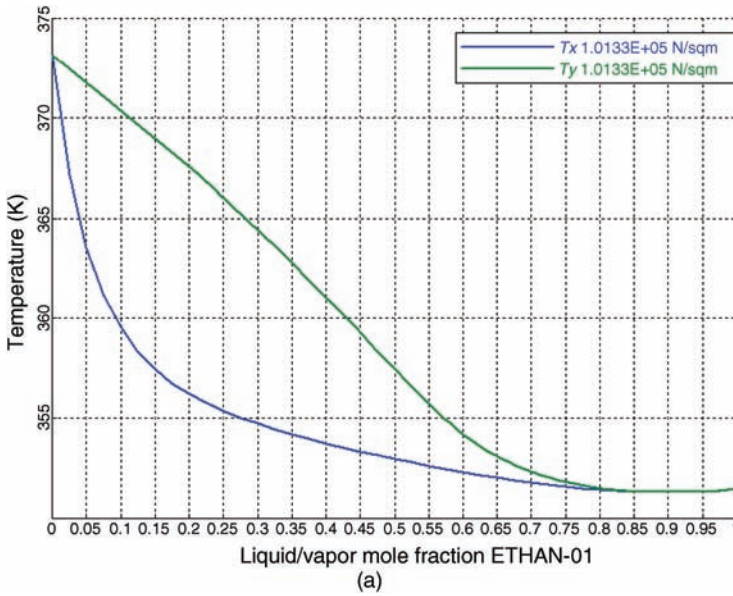


Figure 1.30 (a) T_{xy} diagram for ethanol/water. (b) T_{xy} diagram for ethanol/benzene.

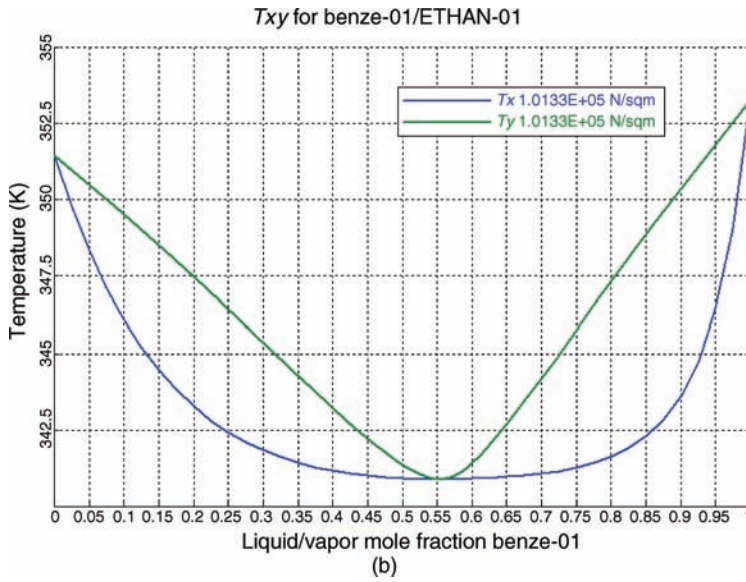


Figure 1.30 (Continued)

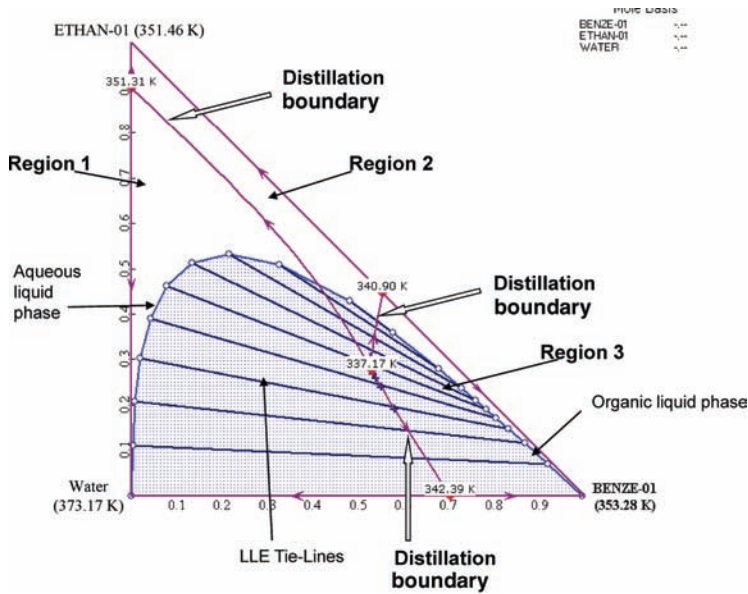


Figure 1.31 Ternary diagram.

REFERENCE

1. J. Gmehling et al., *Vapor-Liquid Equilibrium Data Collection*, DECHEMA, Frankfurt/Main, 1977.

CHAPTER 2

ANALYSIS OF DISTILLATION COLUMNS

The major emphasis of this book is the use of rigorous steady-state and dynamic simulation for the design and control of distillation columns. However, there are several simple approximate methods that provide significant insight into how the various design and operating parameters impact separation. Some of these methods employ graphical techniques that give visual pictures of the effects of parameters. Although some of the methods are limited to binary systems, the relationships can be extended to multicomponent systems.

2.1 DESIGN DEGREES OF FREEDOM

The design of a distillation column involves many parameters: product compositions, product flow rates, operating pressure, total number of trays, feed-tray location, reflux ratio, reboiler heat input, condenser heat removal, column diameter, and column height. Not all of these variables are independent, so a “degrees of freedom” analysis is useful in pinning down exactly how many independent variables can (and must) be specified to completely define the system.

A rigorous mathematical degrees of freedom analysis involves counting the number of variables in the system and subtracting the number of equations that describe the system. For a multicomponent, multistage column, this can involve hundreds, if not thousands, of variables and equations. Any error in counting is grossly amplified because we are taking the difference between two very large numbers. A simple intuitive approach is used below.

The normal situation in distillation design is that the feed conditions are given: flow rate F (mol/h), composition z_j (mole fraction component j), temperature T_F , and pressure P_F . The desired compositions of the product streams are also typically known. We consider a two-product column, so that the normal specifications are to set the heavy-key impurity in the distillate $x_{D,HK}$, and the light-key impurity in the bottoms $x_{B,LK}$. These specifications apply in binary and multicomponent systems.

The design problem is to establish the operating pressure P , the total number of trays N_T , and the feed-tray location N_F that produces the desired product purities. All other parameters are then fixed. Therefore, the number of design degrees of freedom is *five*: $x_{D,HK}$, $x_{B,LK}$, P , N_T , and N_F . Therefore, if the desired product purities and the pressure are given, there are *two* degrees of freedom.

Just to emphasize this point, the five variables that could be specified might be the distillate flow rate D , reflux ratio $RR = R/D$, P , N_T , and N_F . In this case, the product compositions cannot be specified but depend on the distillate flow rate and reflux ratio selected.

The steps in the design procedure will be illustrated in subsequent chapters. Our purpose in this chapter is to discuss some of the ways to establish reasonable values of some of the parameters, such as the number of stages or the reflux ratio.

2.2 BINARY MCCABE–THIELE METHOD

The McCabe–Thiele method is a graphical approach that shows very nicely in pictorial form the effects of vapor–liquid equilibrium (VLE), reflux ratio, and number of trays. It is limited to binary systems, but the effects of parameters can be extended to multicomponent systems. The basic effects can be summarized

1. The easier the separation, the fewer trays required and the lower the required reflux ratio (lower energy consumption).
2. The higher the desired product purities, the more trays required. But the required reflux ratio does not increase significantly as product purities increase.
3. There is an engineering trade-off between the number of trays and the reflux ratio. An infinite number of columns can be designed that produce exactly the same products, but have different heights, different diameters, and different energy consumptions. Selecting the optimum column involves issues of both steady-state economics and dynamic controllability.
4. There are minimum values of the number trays (N_{\min}) and the reflux ratio (RR_{\min}) that are required for a given separation.

All of these items can be visually demonstrated using the McCabe–Thiele method.

The distillation column considered is shown in Figure 2.1 with the various flows and composition indicated. We assume that the feed molar flow rate F and composition z are given. If the product compositions are specified, the molar flow rates of the two products D and B can be immediately calculated from the overall total molar balance and the overall component balance on the light component.

$$\begin{aligned} F &= D + B \\ zF &= Dx_D + Bx_B \\ \Rightarrow D &= F[(z - x_B)/(x_D - x_B)] \end{aligned}$$

For the moment, let us assume that the pressure has been specified, so the VLE is fixed. Let us also assume that the reflux ratio has been specified, so the reflux flow rate can be calculated $R = (RR)(D)$. The “equimolal overflow” assumption is usually made in the McCabe–Thiele method. The liquid and vapor flow rates are assumed to be constant in a given section of the column. For example, the liquid flow rate in the rectifying section L_R is equal to the reflux

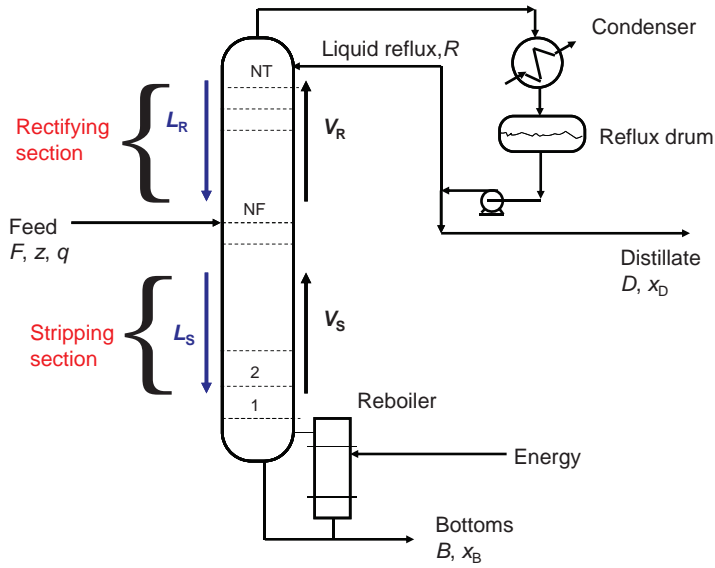


Figure 2.1 McCabe–Thiele method: distillation column.

flow rate R . From an overall balance around the top of the column, the vapor flow rate in the rectifying section V_R is equal to the reflux plus the distillate ($V_R = R + D$).

The method uses an xy diagram whose coordinates are the mole fraction of the light component in the liquid x and the mole fraction of the light component in the vapor phase y . The VLE curve is plotted for the selected pressure. The 45° line is plotted. The specified product compositions x_D and x_B are located on the 45° line, as shown in Figure 2.2.

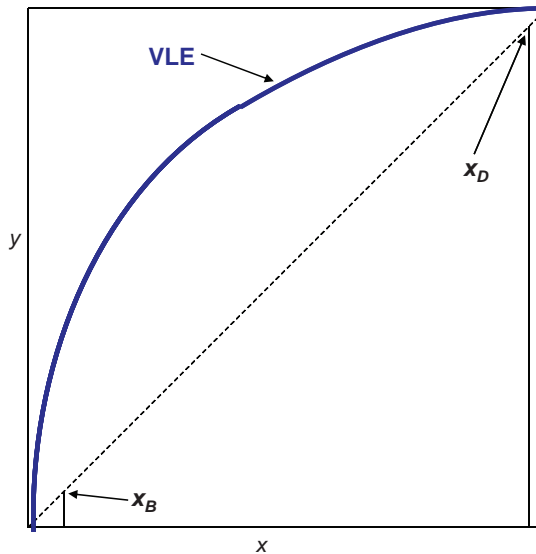


Figure 2.2 McCabe–Thiele method: locate products and VLE.

2.2.1 Operating Lines

Next the rectifying operating line (ROL) is drawn. This is a straight line with a slope equal to the ratio of the liquid and vapor flow rates in the rectifying section.

$$\text{Slope ROL} = L_R/V_R = R/(R + D) = RR/(1 + RR)$$

The line intersects the 45° line at the distillate composition x_D , so it is easy to construct (see Fig. 2.3). The proof of this construction can be derived by looking at the top of the column, as shown in Figure 2.4.

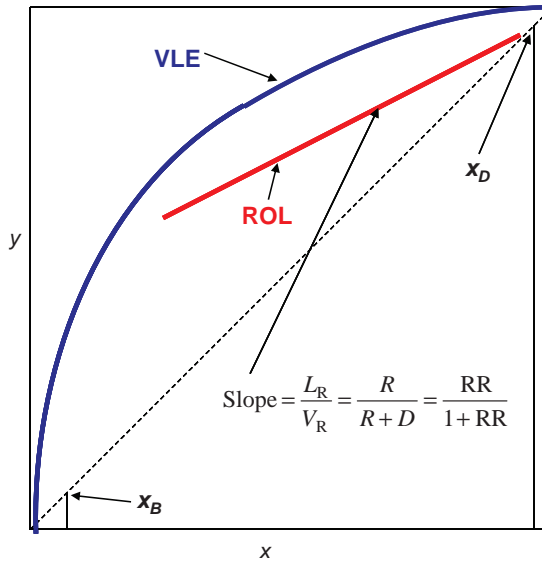


Figure 2.3 McCabe–Thiele method: draw operating lines.

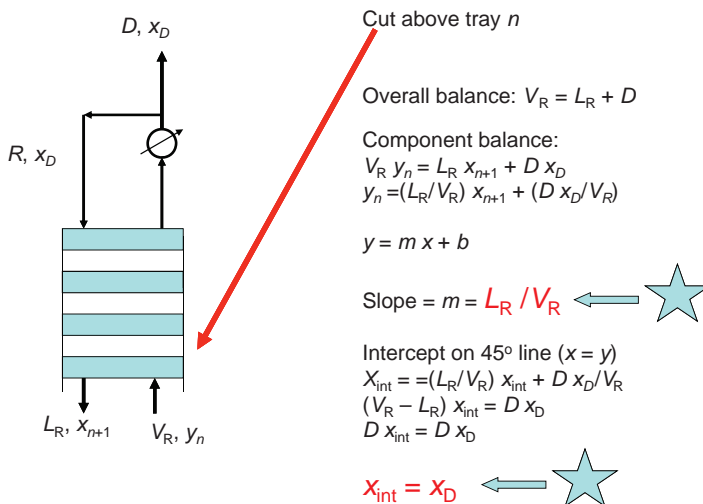


Figure 2.4 ROL construction.

The liquid and vapor flow rates in the stripping section (L_S and V_S) can be calculated if the thermal condition of the feed is known. Since the temperature, pressure, and composition of the feed are given, the fraction of the feed that is liquid can be calculated from an isothermal flash calculation. This fraction is defined as the variable “ q .” Knowing q , the liquid and vapor flow rates in the stripping section can be calculated. If the feed is saturated liquid, q is 1. If the feed is saturated vapor, q is 0.

$$q = (L_S - L_R)/F$$

$$\Rightarrow L_S = qF + L_R$$

$$V_S = L_S - B$$

The stripping operating line can be drawn. It is a straight line with slope L_S/V_S that intersects the 45° line at the bottoms composition x_B . The proof of this construction can be derived by looking at the bottom of the column, as shown in Figure 2.5. Figure 2.6 shows the two operating lines.

2.2.2 q -Line

There is a relationship between the intersection point of the two operating lines and feed conditions. As shown in Figure 2.7, a straight line can be drawn from the location of the feed composition z on the 45° line to this intersection point. As we will prove below, the slope of this line is only a function of the thermal condition of the feed, which is defined in the parameter q . The slope is $-q/(1 - q)$. This makes the construction of the McCabe–Thiele diagram very simple.

1. Locate the three compositions on the 45° line (z , x_D , and x_B)
2. Draw the ROL from the x_D point with a slope of $RR/(1 + RR)$.
3. Draw the q line from the z point with a slope of $-q/(1 - q)$.
4. Draw the SOL from the x_B point to the intersection of the q line and the ROL.

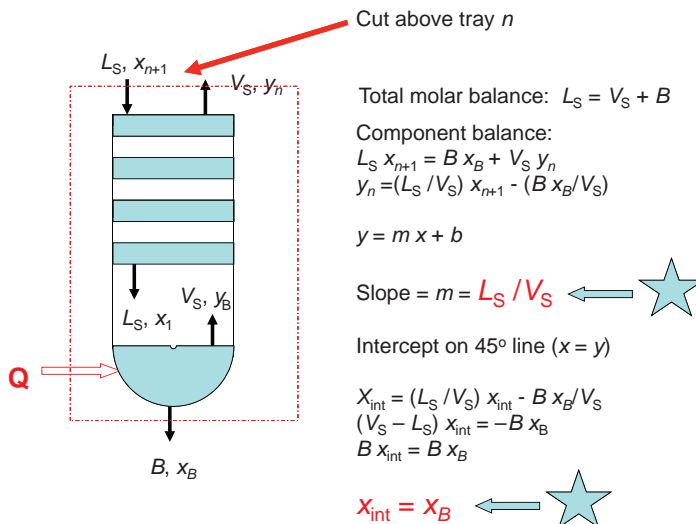


Figure 2.5 SOL construction.

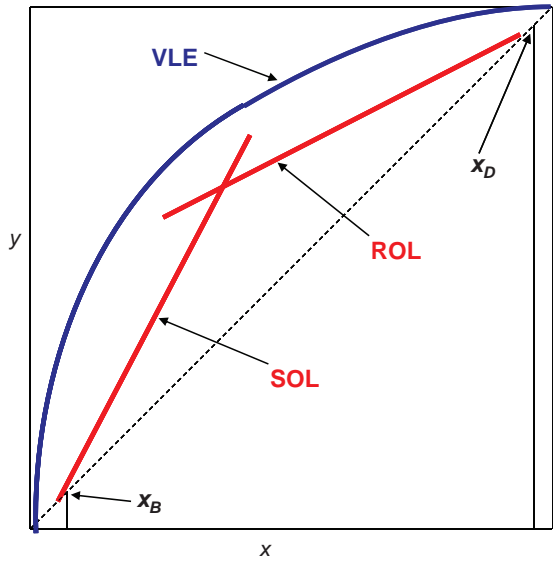


Figure 2.6 Operating lines.

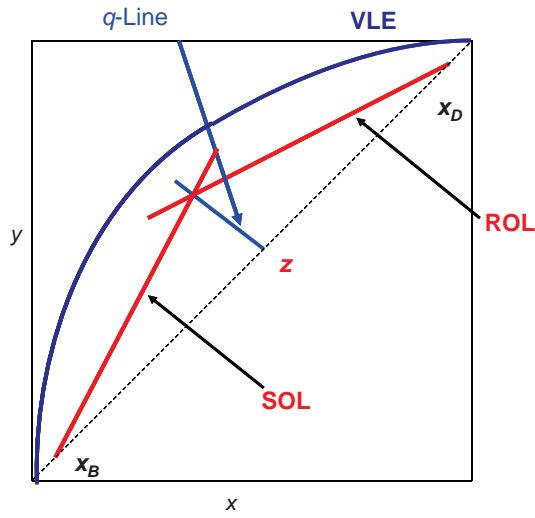


Figure 2.7 *q*-Line.

The equations of the rectifying and stripping operating lines are given below in terms of the point of intersection of the two lines at y_{int} and x_{int} .

$$\text{ROL} : y_{int} = (L_R/V_R)x_{int} + Dx_D/V_R$$

$$\text{SOL} : y_{int} = (L_S/V_S)x_{int} - Bx_B/V_S$$

Subtracting the two equations gives

$$(V_R - V_S)y_{\text{int}} = (L_R - L_S)x_{\text{int}} + (Dx_D + Bx_B)$$

The last term on the right is just Fz . Using the definition of q leads to

$$\begin{aligned}(V_R - V_S) &= (1 - q)F \\ (L_R - L_S) &= -qF\end{aligned}$$

Substituting these relationships into the previous equation gives

$$\begin{aligned}(1 - q)Fy_{\text{int}} &= -qFx_{\text{int}} + Fz \\ y_{\text{int}} &= (-q/(1 - q))x_{\text{int}} + (z/(1 - q))\end{aligned}$$

This is the equation of a straight line with slope $-q/(1 - q)$. The q -line is vertical for saturated liquid feed ($q = 1$), and it is horizontal for saturated vapor feed ($q = 0$). On the 45° line, x_{int} is equal to y_{int} . Define this as x_{45} .

$$\begin{aligned}(1 - q)x_{45} &= -qx_{45} + z \\ x_{45} &= z\end{aligned}$$

Thus, the q -line intersects the 45° line at the feed composition z .

2.2.3 Stepping Off Trays

The number of trays is determined by moving vertically from the x_B point on the 45° line to the VLE line. This is the composition of the vapor y_B , leaving the partial reboiler. Then, we move horizontally over to the SOL. This step represents the partial reboiler. The value of x on the SOL is the composition of liquid x_1 , leaving Tray 1 (if we are numbering from the bottom of the column up). This stepping is repeated, moving vertically to y_1 and horizontally to x_2 . Stepping continues until we cross the intersection of the operating lines. This is the feed tray. Then the horizontal line is extended to the ROL. Continuing to step until the x_D value is crossed gives the total number of trays.

2.2.4 Effect of Parameters

We know enough now about the McCabe–Thiele diagram to make several observations, which can be applied to any distillation system, not just a binary separation.

1. The farther the VLE curve is from the 45° line, the smaller the slope of the rectifying operation line. This means a smaller reflux ratio and therefore lower energy consumption. A “fat” VLE curve corresponds to large relative volatilities and an easy separation.
2. The easier the separation, the fewer trays it takes to make a given separation.
3. The higher the product purities, the more trays it takes to make a given separation.
4. Increasing product purities does not have a big effect on the required reflux ratio.

5. Increasing the liquid-to-vapor ratio in a section of a column increases the separation that occurs in that section.
6. These effects apply to all types of separations and distillation columns.

2.2.5 Limiting Conditions

We need to discuss some of the limiting conditions in distillation systems. The minimum number of trays for a specified separation corresponds to total reflux operation. If the column is run under total reflux conditions, the distillate flow rate is zero. Therefore, the reflux ratio is infinite, and the slope of the operating lines is unity. This is the 45° line. Thus, the minimum number of trays can be determined by simply stepping up between the 45° line and the VLE curve (see Fig. 2.8).

The minimum reflux ratio for a specified separation corresponds to having an infinite number of trays. This usually occurs when the intersection of the operating lines and the q -line occurs exactly on the VLE curve. This is a “pinch” condition. It would take an infinite number of trays to move past this point. This is illustrated in Figure 2.9. The minimum reflux ratio is calculated from the slope of this limiting operating line.

2.3 APPROXIMATE MULTICOMPONENT METHODS

Many years before the availability of computers for rigorous analysis, several simple approximate methods were developed for analyzing multicomponent systems. These methods are still quite useful for getting quick estimates of the size of a column (number of trays) and the energy consumption (reflux ratios and the corresponding vapor boilup and reboiler heat input).

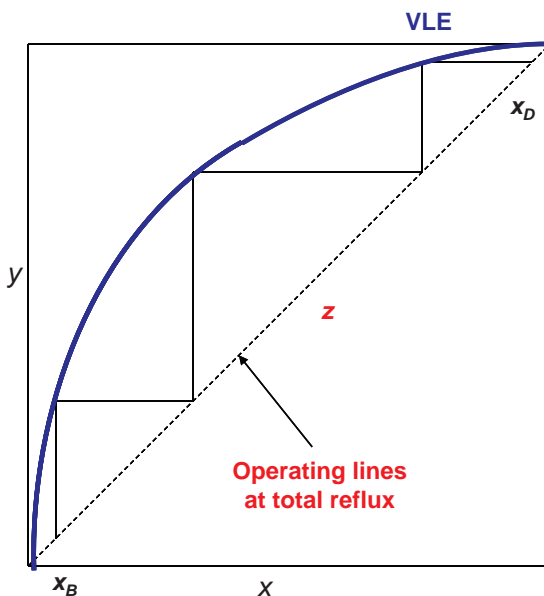


Figure 2.8 Minimum number of trays.

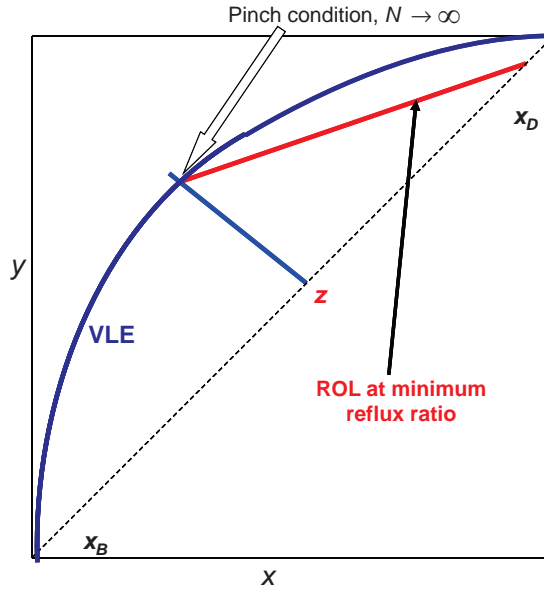


Figure 2.9 Minimum reflux ratio.

2.3.1 Fenske Equation for Minimum Number of Trays

The minimum number of trays corresponds to total reflux operation (an infinite reflux ratio). The Fenske equation relates the compositions at the two end of a column to the number of stages in the column under this limiting condition.

$$N_{\min} + 1 = \frac{\log \left[\left(x_{D,LK} / x_{D,HK} \right) \left(x_{B,HK} / x_{B,LK} \right) \right]}{\log(\alpha_{LK,HK})}$$

where N_{\min} is the minimum number of stages, $x_{D,LK}$ is the mole fraction of the light-key component at the top of the column, $x_{D,HK}$ is the mole fraction of the heavy-key component at the top of the column, $x_{B,HK}$ is the mole fraction of the heavy-key component at the bottom of the column, $x_{B,LK}$ is the mole fraction of the light-key component at the bottom of the column, and $\alpha_{LK,HK}$ is the relative volatility between the LK and HK components.

This equation is applicable to multicomponent systems, but it assumes a constant relative volatility between the two components considered.

An example of the use of the Fenske equation is given in Chapter 4. Results of this approximate method will be compared with the results found from rigorous simulation.

2.3.2 Underwood Equations for Minimum Reflux Ratio

The Underwood equations can be used to calculate the minimum reflux ratio in a multicomponent system if the relative volatilities of the components are constant. There are two equations.

$$\sum_{j=1}^{NC} \frac{\alpha_j z_j}{\alpha_j - \theta} = 1 - q$$

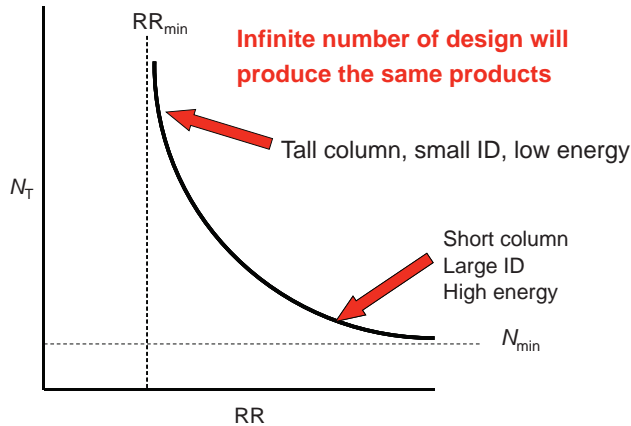


Figure 2.10 Trade-off between reflux ratio and number of trays.

$$\sum_{j=1}^{NC} \frac{\alpha_j x_{Dj}}{\alpha_j - \theta} = 1 + RR_{\min}$$

The feed composition z_j (mole fractions $j = 1, NC$), the desired distillate composition x_{Dj} ($j = 1, NC$), and the feed thermal condition q are specified. The relative volatilities α_j ($j = 1, NC$) of the multicomponent mixture are known.

The first equation contains one unknown parameter θ . However, expanding the summation of NC terms and multiplying through all the denominator terms ($\alpha_j - \theta$) give a polynomial in θ whose order is NC . Therefore, there are NC roots of this polynomial. One of these roots lies between the two relative volatility values α_{LK} and α_{HK} . This is found using some iterative solution method. It is substituted into the second equation, which can then be solved explicitly for the minimum reflux ratio.

An example of the use of the Underwood equations is given in Chapter 4. The results of this approximate method will be compared with the results found from rigorous simulation.

2.4 CONCLUSIONS

Several methods for analyzing distillation columns have been presented in this chapter. Graphical methods provide valuable insight into how various parameters affect separations in distillation.

Some of the general relationships that hold for both binary and multicomponent distillation columns are as follows

1. There is a trade-off between energy and number of trays required to make a specified separation, as illustrated in Figure 2.10.
2. Lower relative volatilities make separation more difficult and require more trays or higher reflux ratios.
3. Higher product purities require more trays but not higher reflux ratios.

CHAPTER 3

SETTING UP A STEADY-STATE SIMULATION

In this chapter we begin at the beginning. We take a simple binary separation and go through all the details of setting up a simulation of this system in Aspen Plus using the rigorous distillation column simulator *RadFrac*.

All the pieces of a distillation column will be specified (column, control valves, and pumps) so that we can perform a dynamic simulation after the steady-state simulation is completed. If we were only interested in a steady-state simulation, pumps and control valves would not have to be included in the flowsheet. However, if we want the capability to do “simultaneous design” (steady-state and dynamic), these items must be included to permit a “pressure-driven” dynamic simulation.

3.1 CONFIGURING A NEW SIMULATION

Open up a blank flowsheet by going to *Start* and *Programs* and then clicking sequentially on *Aspen Tech*, *Process Modeling V7.3*, *Aspen Plus*, and *Aspen Plus User Interface*. The window shown in Figure 3.1 opens up. Selecting the *Blank Simulation* button and clicking *OK* opens up the blank flowsheet shown in Figure 3.2. The page tabs along the bottom let us choose what unit operations to place on the flowsheet. We are going to need a distillation column, two pumps, and three control valves.

Clicking the *Columns* page tab and clicking the arrow just to the right of *RadFrac* opens the window shown in Figure 3.3, which contains several types of columns: full columns, strippers (with a reboiler but no condenser), rectifiers (with a condenser but no reboiler), absorbers (with neither) and so on. Click the full column button on the top row, second from the left, and move the cursor to the blank flowsheet. The cursor becomes a cross. If we click on the flowsheet, a column icon appears, as shown in Figure 3.4.

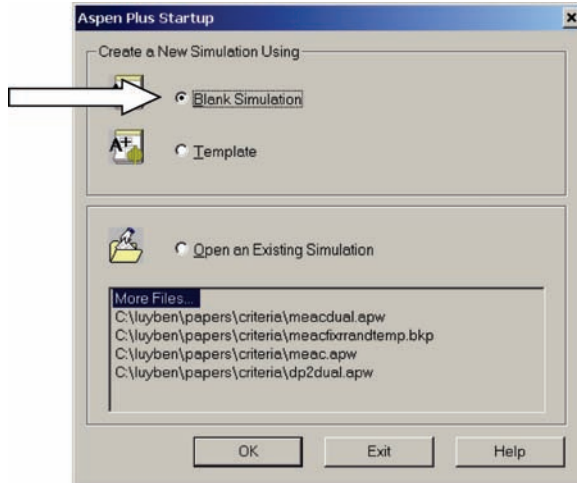


Figure 3.1 Aspen Plus startup.

To add the pumps and control valves to the flowsheet, click the page tab on the bottom of the window labeled *Pressure Changers*. This opens the window shown in Figure 3.5a on which we can select the *Pump* button or the *Valve* button. Clicking the arrow just to the right of the *Valve* button lets us select a valve icon (Fig. 3.5b). Move the cursor to the flowsheet and paste a valve to the left of the column (Fig. 3.5c). The cursor remains a cross on the flowsheet, and we can paste as many additional valves as needed. Two more are inserted to the right of the column in Figure 3.5d. In a similar way, we click the *Pump* button, select an icon and paste two pumps on the flowsheet as shown in Figure 3.6.

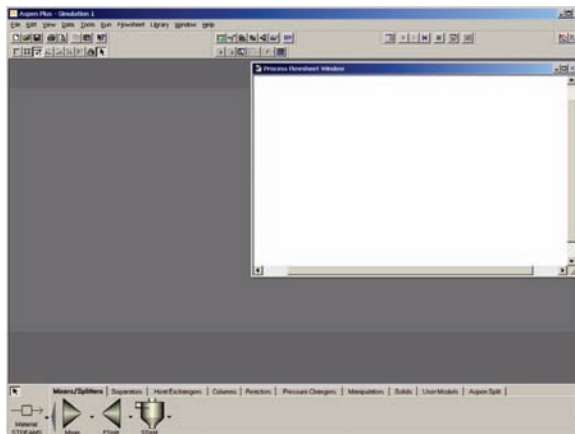


Figure 3.2 Blank flowsheet.

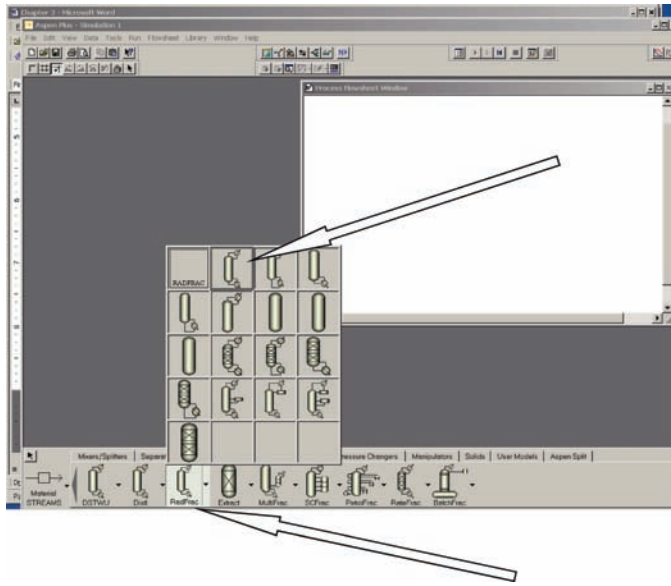


Figure 3.3 Selecting type of column.

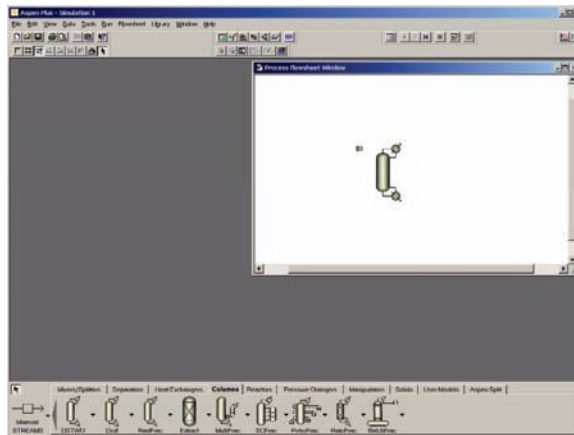


Figure 3.4 Paste the column icon on the flowsheet.

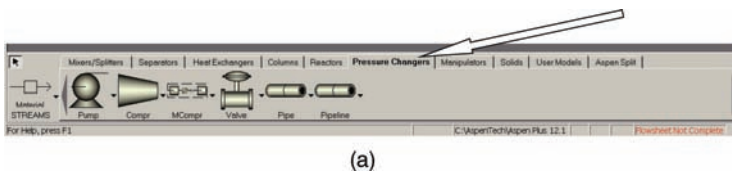
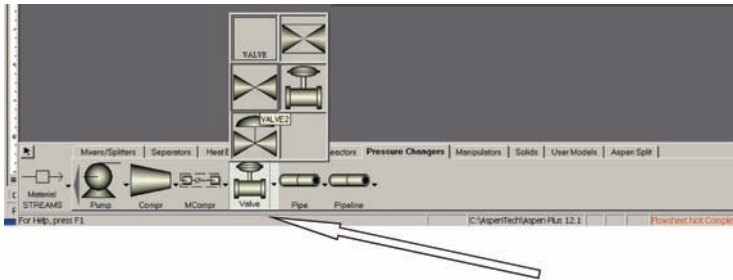
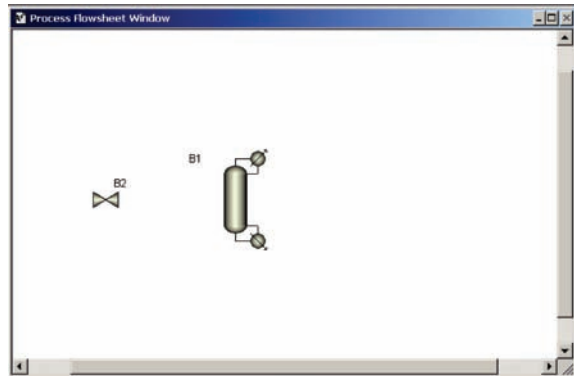


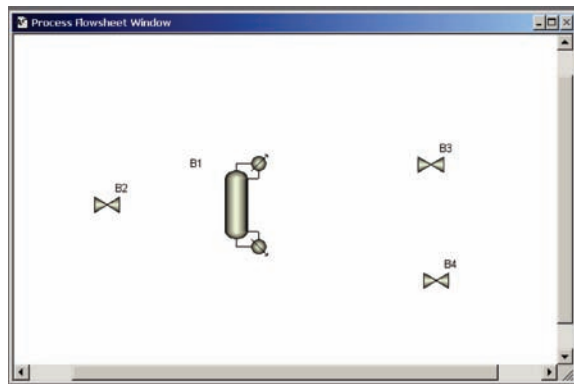
Figure 3.5 (a) Pressure changers. (b) Selecting a valve icon. (c) Paste valve on flowsheet. (d) Flowsheet with three valves added.



(b)



(c)



(d)

Figure 3.5 (Continued)

The next job is to add streams to connect all the pieces in the flowsheet. This is achieved by moving the cursor all the way to the left at the bottom of the window and clicking the *Material STREAMS* button as shown in Figure 3.7. Click the *Material* button and move the cursor to the flowsheet. A number of arrows appear (Fig. 3.8) that show all the possible places where a material stream can be located as an input stream or an output stream from each of the units. Place the cursor on one arrow and left click. Then place the cursor on a second arrow where you want to connect the stream and click. Figure 3.9 shows a stream

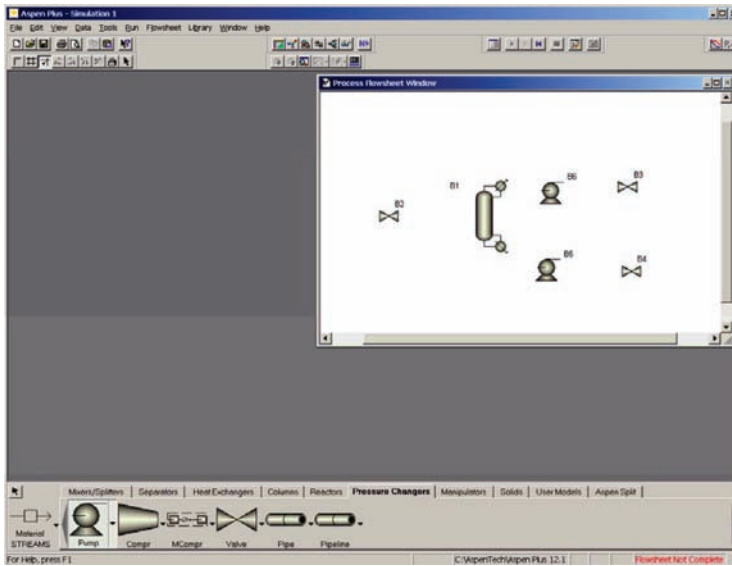


Figure 3.6 Flowsheet with two pumps inserted.

“1” that connects valve block *B2* with column block *B1*. To connect a stream to the inlet red arrow and then click on the flowsheet to the left of the valve (Fig. 3.10). This inserts stream “2.”

All the other material streams are connected in a similar manner as shown in Figure 3.11. Notice that the stream “3” from the top of the column has been connected at

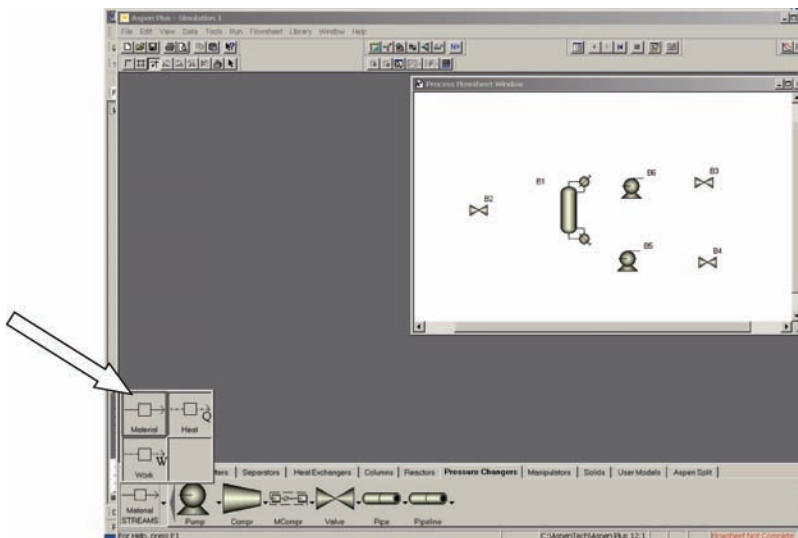


Figure 3.7 Adding streams to flowsheet.

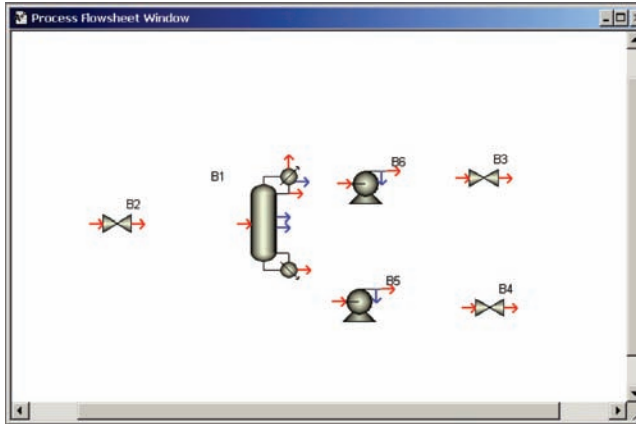


Figure 3.8 Flowsheet with possible connections displayed.

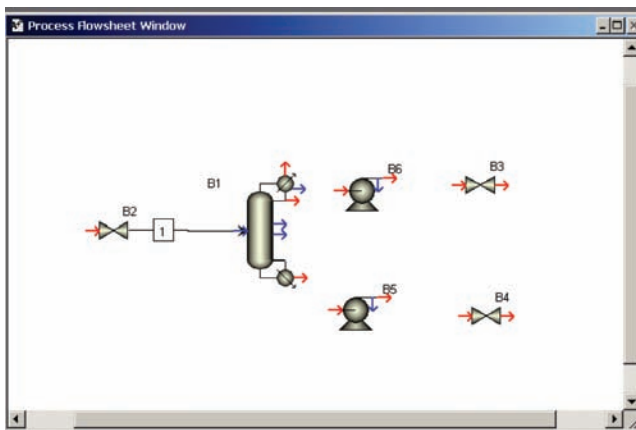


Figure 3.9 Connecting a valve to the column.

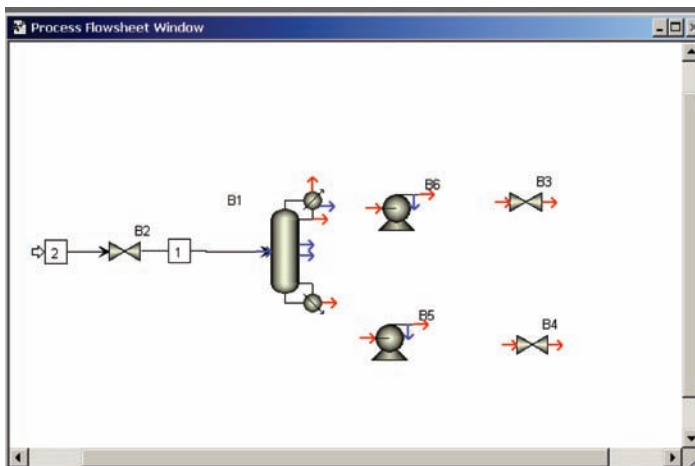


Figure 3.10 Connecting stream to inlet valve.

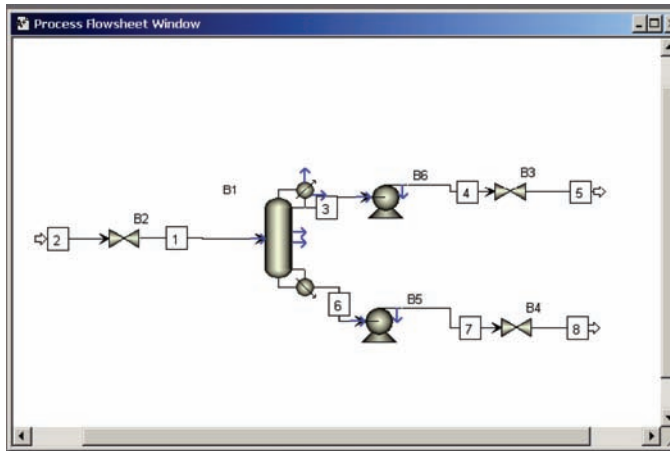


Figure 3.11 Flowsheet with all streams attached.

the arrow that is below the condenser symbol. This gives a liquid distillate product. If the stream had been connected to the arrow coming out the top of the condenser, the distillate is a vapor and the condenser is a partial condenser. When you are finished adding streams and units, click the arrow that is immediately above the *Material STREAMS* block at the bottom left of the window. This is the *Cancel Insert Mode* button.

At this point, the flowsheet has been configured. It is a good idea to rename the various pieces of equipment and the streams, so that it is easy to keep track of what each is. To rename a block, left click its icon and right click to get a drop-down menu. Selecting *Rename* gives the window shown in Figure 3.12. Type in the desired new name. The same procedure is used to rename streams. Figure 3.13 gives the flowsheet with all blocks and streams renamed to correspond to conventional distillation terminology. The feed stream is *F1*, the distillate stream is *D1*, and the bottoms stream is *B1*. Notice that the pumps and valves have been renamed for easy association with this column *C1*. Some logical scheme for renaming units and streams is essential in a large plantwide simulation with many units and streams.

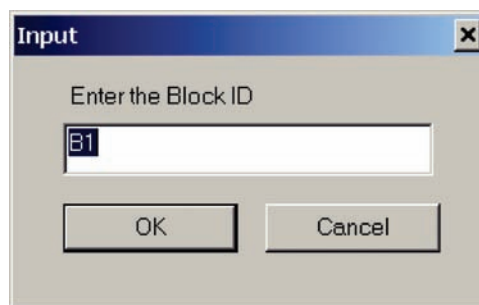


Figure 3.12 Renaming a block.

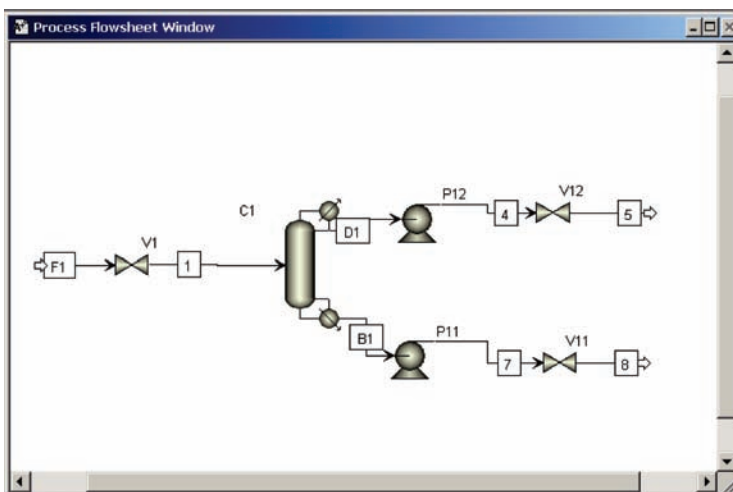


Figure 3.13 Renamed flowsheet.

3.2 SPECIFYING CHEMICAL COMPONENTS AND PHYSICAL PROPERTIES

The structure of the flowsheet is now completely specified. Next, we must define the chemical components involved in the separation and specify what physical property package is to be used. Chapter 1 discussed many aspects of choosing a physical property relationships, so that an accurate representation of reality is used.

A simple binary separation of propane from isobutane is used in the numerical example considered in this chapter. The VLE relationships for most hydrocarbon systems are well handled by the Chao–Seader correlation, so we select that package.

To start specifying chemical components, go to the tool bar at the top of the window and click the fourth item from the left *Data*. Select the top item *Setup*. This opens the *Data Brower* window shown in Figure 3.14. This is the window that is used to look at all aspects of the simulation. It is used to define components, set physical properties, specify the parameters of the equipment (e.g., the number of stages in the column and the pressure), and specify properties of various streams (e.g., flow rate, composition, temperature, and pressure).

A couple of preliminary items should be done first. In the middle of the window, there are two boxes in which we can specify the units to be used in the simulation. Figure 3.15 shows the standard three alternatives: *ENG* (English engineering), *MET* (metric), and *SI* (Système International). We will use SI units in most of the examples in this book because of the increasing importance of our global economy. However, we will make one departure from regular SI units. In the SI system, pressures are in pascals (N/m^2), which are quite inconvenient for most chemical processes because typical pressures are very large numbers in pascals ($1 \text{ atm} = 101,325 \text{ Pa}$). Therefore, we will use pressures in atmosphere in most of the examples. However, make sure that you select the correct units when you enter data.

The second preliminary item is to indicate what properties we want to see for all the streams. The defaults do not include compositions in mole fractions, which are very useful

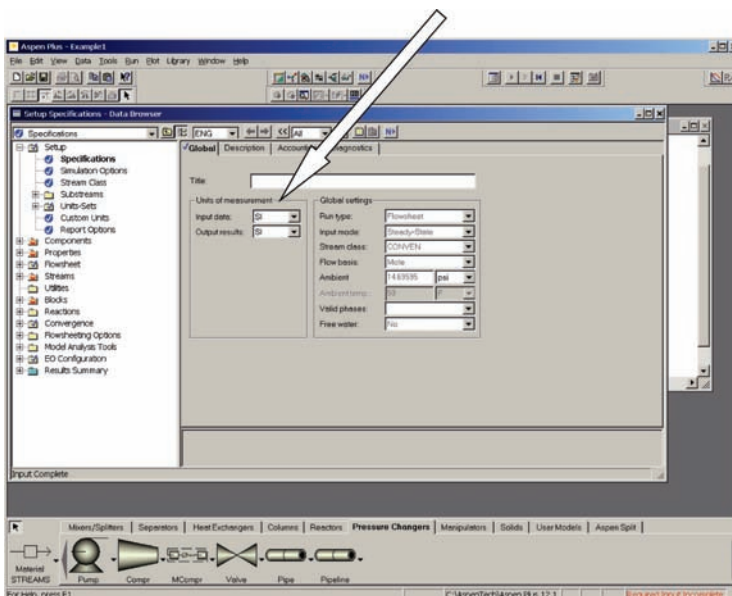


Figure 3.14 Data browser window.

in distillation calculations. To include mole fractions in the list of stream properties, click on the last item on the *Setup* list at the left of the window, which is labeled *Report Options*. This opens the window shown in Figure 3.16a. Click the page tab labeled *Stream*. This opens the window shown in Figure 3.16b. Select *Mole* under the *Fraction basis* column in the middle of the window.

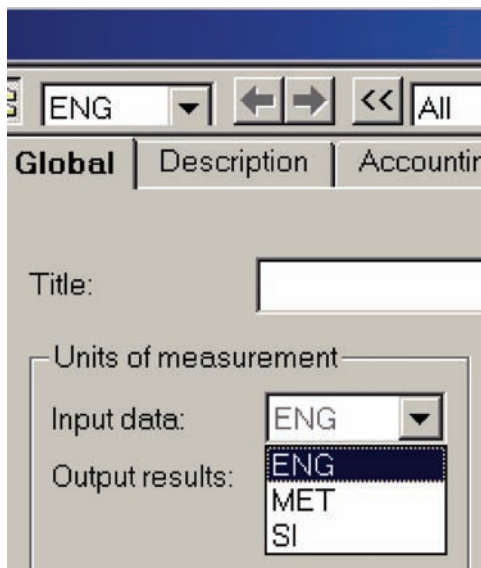


Figure 3.15 Selecting units.

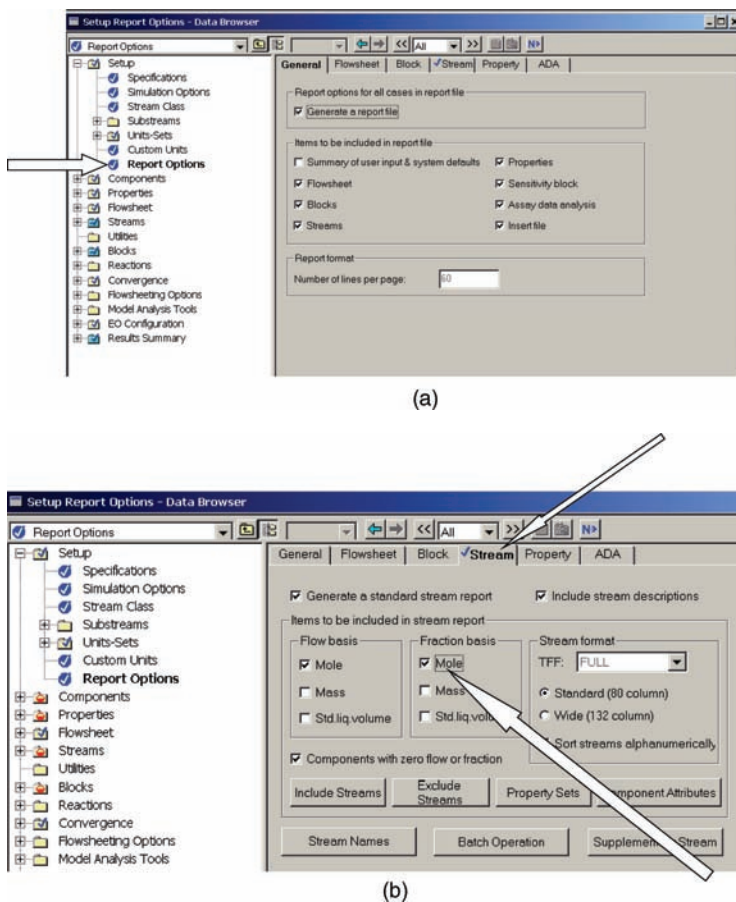


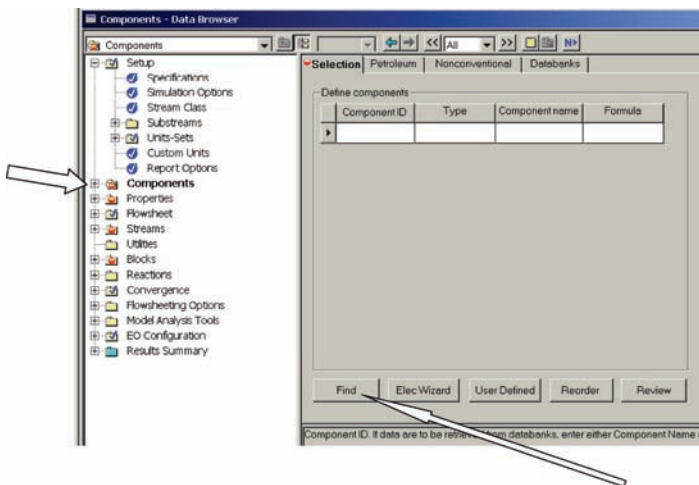
Figure 3.16 (a) Modifying reported stream properties. (b) Specifying mole fractions.

With these book-keeping issues out of the way, we can select the chemical components by clicking *Components* on the left of the *Data Browser* window. This opens the window shown in Figure 3.17a. Clicking the *Find* button near the bottom of the window opens another window shown in Figure 3.17b. Type in *propane* and click *Find now*.

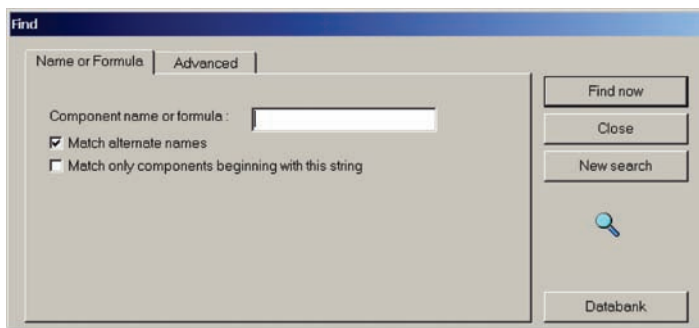
A list of components is opened at the bottom of the window (Fig. 3.18). Click *PROPANE* and click the *Add* button at the bottom of the window. Repeat for *ISOBUTANE* and click *Close*.

The two components have now been selected (Fig. 3.19). It is often desirable to change the name of a component. For example, suppose we want to use “C3” for propane and “IC4” for isobutane. This can be accomplished by highlighting the name listed under *Component ID* and typing the desired name. Click anywhere on the window, and the message shown in Figure 3.20 will appear. Click *Rename*. Repeat for isobutane.

Now, we are ready to select a physical property package. Click *Properties* and *Specifications* on the left side of the window. Figure 3.21 shows the window that opens. Under *Property methods & models* click the arrow on the right of *Base method*. A long



(a)



(b)

Figure 3.17 (a) Specifying chemical components. (b) Finding components.

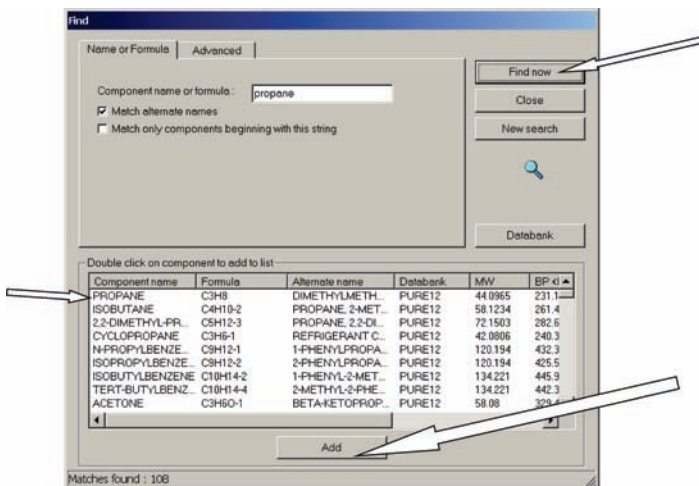


Figure 3.18 Selecting components.

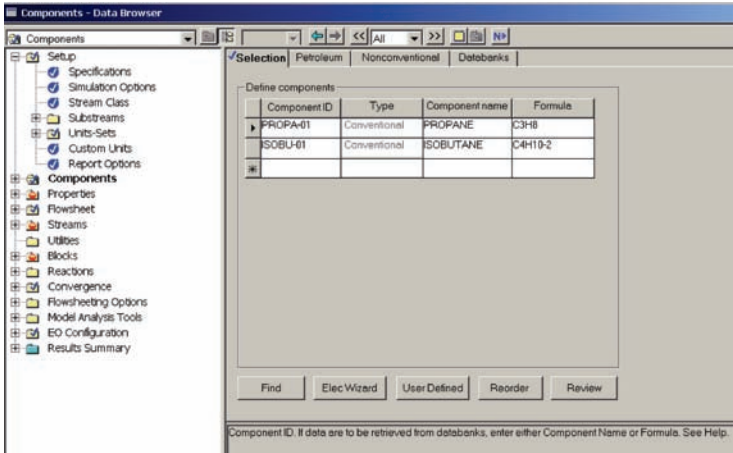


Figure 3.19 Two components selected.

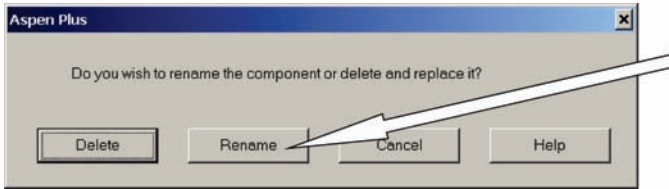


Figure 3.20 Message to rename.

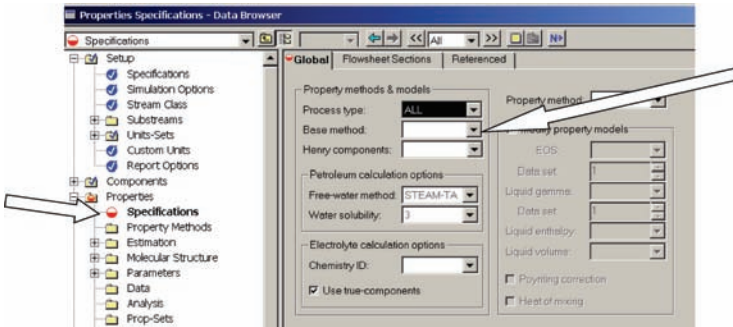


Figure 3.21 Specifying physical properties.

list of alternatives is listed as shown in Figure 3.22. Scroll down and select *CHAO-SEAD*.

It should be noted that different physical property packages can be used in different unit operations in a flowsheet. For example, we may be simulating a distillation column and a decanter. The best VLE package should be used in the column, and the best LLE package should be used in the decanter.

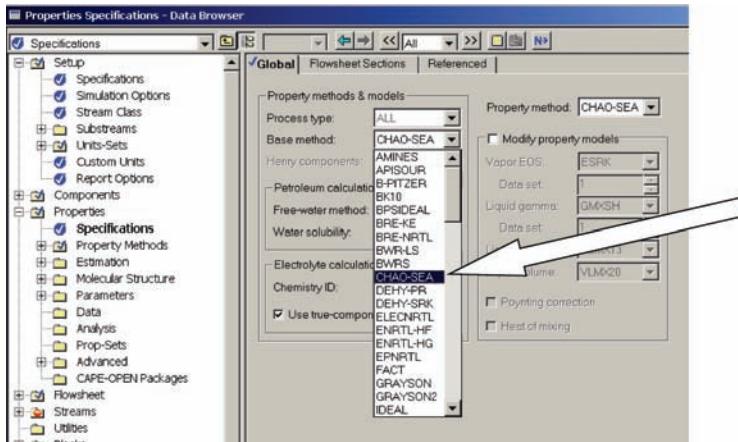


Figure 3.22 Specify base method.

3.3 SPECIFYING STREAM PROPERTIES

The input streams to the process must be specified. In this example, there is only one input stream, the feed stream *F1*. The flow rate, composition, temperature, and pressure of this stream must be specified. Clicking *Streams* and *F1* and then *Input* opens the window shown in Figure 3.23.

In distillation calculations, molar flow rates and compositions are usually employed. Let us assume that the feed flow rate is 1 kmol/s and the feed temperature is 322 K (120 °F). These are entered in the middle of the window. The feed composition is 40 mol% propane and 60 mol% isobutane. The composition can be entered in terms of mole or mass fractions, or it can be entered in terms of molar or mass flow rates. In our example, we use the drop-down arrow to change to *Mole-Frac* and enter the appropriate values (see Figure 3.24).

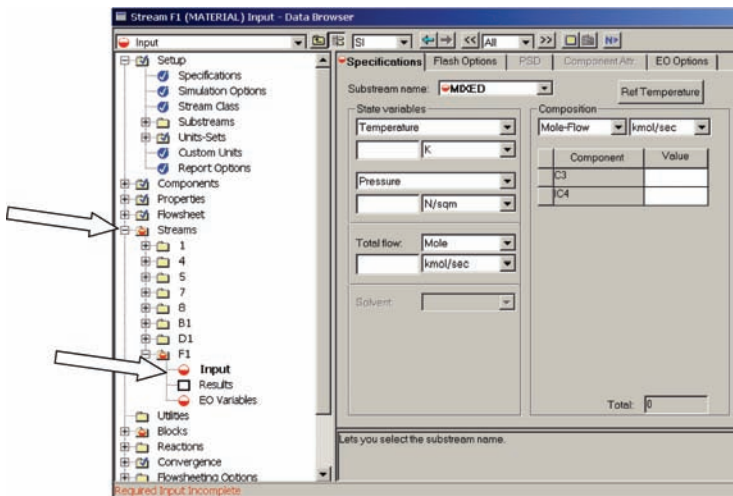


Figure 3.23 Input stream data.

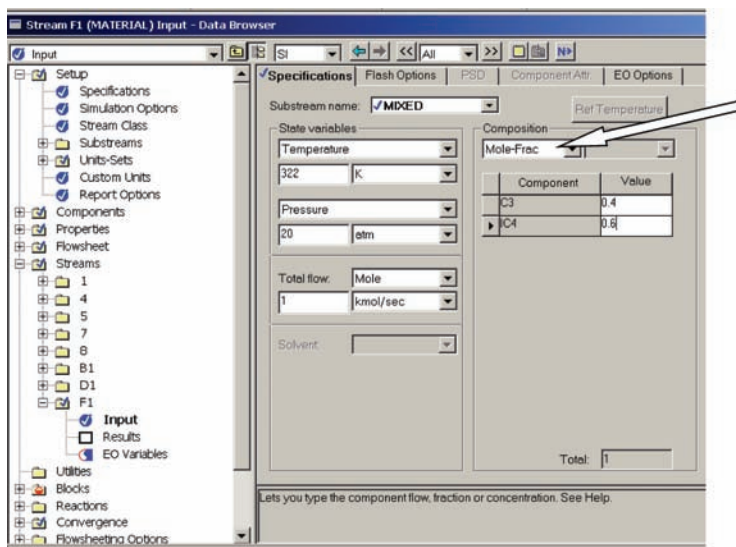


Figure 3.24 Feed input conditions.

The specification of the feed pressure takes a little thought. We will discuss the selection of column pressure in more detail later in this chapter. We know that the distillate product is propane. We will want to use cooling water in the condenser because it is an inexpensive heat sink compared with refrigeration. Cooling water is typically available at about 305 K. A reasonable temperature difference for heat transfer in the condenser is 20 K. Therefore, reflux drum temperature will be about 325 K. The vapor pressure of propane at 325 K is about 14 atm (206 psia). Therefore, the column will have a pressure at the feed tray of something a little higher than 14 atm.

In addition, we need to allow for some pressure drop over the control valve on the feed stream. More will be said about the subject of selecting control valve pressure drops later in this book. For the moment, let us assume that we need a 5 atm pressure drop. Thus, the feed pressure should be set at about 20 atm. Be careful to specify “atm” instead of the default “N/m²” for the pressure units. The final conditions of the feed are shown in Figure 3.24.

3.4 SPECIFYING PARAMETERS OF EQUIPMENT

The parameters for all the equipment must be specified. Clicking on *Blocks* on the left side of the *Data Browser* window produces a list of all the blocks that must be handled. Any block with a red color is not completely specified. The column is the most complex and has the most parameters to fix. Hence, we will start with the column C1.

3.4.1 Column C1

Clicking on the block labeled C1 opens a window with a long list of items. The top sub-item is labeled *Setup*. Clicking it opens the window shown in Figure 3.25. There are several page

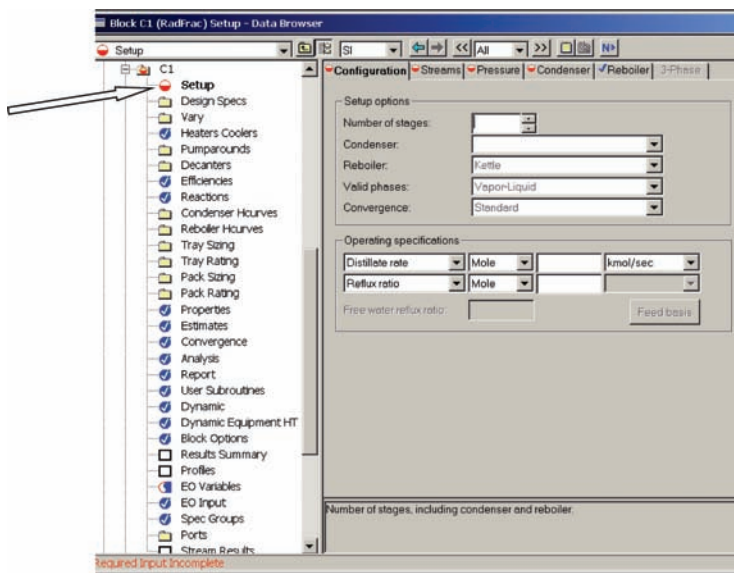


Figure 3.25 Column C1.

tabs. The first is *Configuration* on which the number of total stages, the type of condenser, the type of reboiler, the numerical convergence method, and two other variables are specified. We consider each of these below.

1. *Number of stages*: The rigorous way to select the number of stages is to perform an economic optimization. We discuss this in detail in Chapter 4. For the moment, let us select a column with 32 stages. Aspen uses the tray numbering convention of defining the reflux drum as Stage 1. The top tray is Stage 2 and so forth on down the column. The base of the column in this example is Stage 32. Therefore, this column has 30 trays.
2. *Condenser*: Use the drop-down menu to select *Total*. If the distillate is removed as a vapor, *Partial-Vapor* should be selected.
3. *Reboiler*: Both the kettle and thermosyphon reboilers are partial reboilers (the vapor from the reboiler is in equilibrium with the liquid bottoms product withdrawn), so it does not matter which you select.
4. *Convergence*: The *Standard* method works well in hydrocarbon systems. Alternative methods must be used in highly nonideal systems. Examples in latter chapters will illustrate this.
5. *Operating specifications*: As discussed in Chapter 2, a distillation column has two degrees of freedom once the feed, pressure, number of trays, and feed tray location have been fixed. There are several alternative ways to select these two degrees of freedom as shown in Figure 3.26. At this stage in our simulation, the usual approach is to fix the distillate flow rate and the reflux ratio. Later, once we obtain a converged solution, we will change the specified variable, so that the product specifications are met. For now, let us fix the distillate flow rate at 0.4 kmol/s, because we know that this is the molar flow rate of propane in the feed. In addition, let us select a reflux ratio of 2

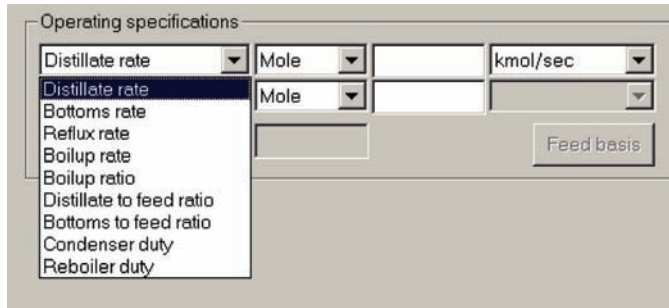


Figure 3.26 Alternative choices of operating specifications.

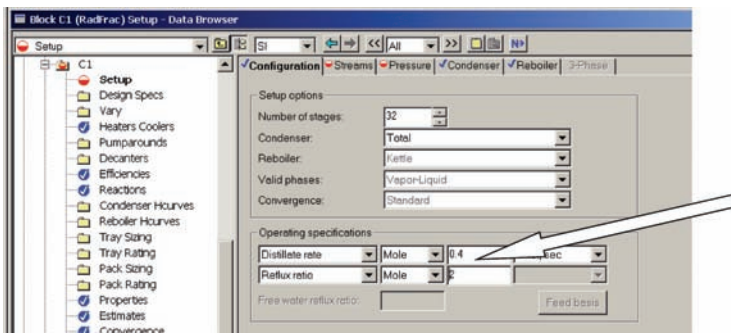


Figure 3.27 Configuration page with all data.

because the propane/isobutane separation is neither very difficult nor is it very easy. Figure 3.27 shows the *Configuration* page with all this data inserted. Notice, that the red dot on the C1 block becomes a blue check mark when all the required input data have been provided.

Now click the *Streams* page tab. A window opens on which the location of the feed tray must be given. For the moment, we set this in the middle of the column on Stage 16 (see Figure 3.28). Later, we will come back to this question and determine the “optimum” feed tray location by finding the tray that minimizes reboiler heat input.



Figure 3.28 Specifying the feed stage.

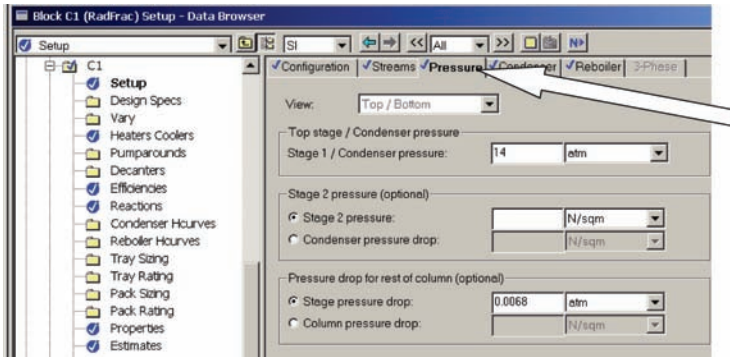


Figure 3.29 Specifying pressure and tray pressure drop.

The last page tab is *Pressure*. Clicking it opens the window shown in Figure 3.29 in which we specify the pressure in the reflux drum (condenser) and the pressure drop through each of the trays in the column. As discussed above, we set the reflux drum pressure at 14 atm (be careful to change from “N/m²”). A reasonable tray pressure drop is about 0.0068 atm per tray (0.1 psi per tray). All the items in the C1 block are now blue, so the column is completely specified. Next, the design parameters of all the valves and pumps must be specified.

3.4.2 Valves and Pumps

We assume that both pumps generate a pressure difference of 6 atm between suction and discharge. Click *Setup* under pump P11 and enter this data. Figure 3.30 shows the input

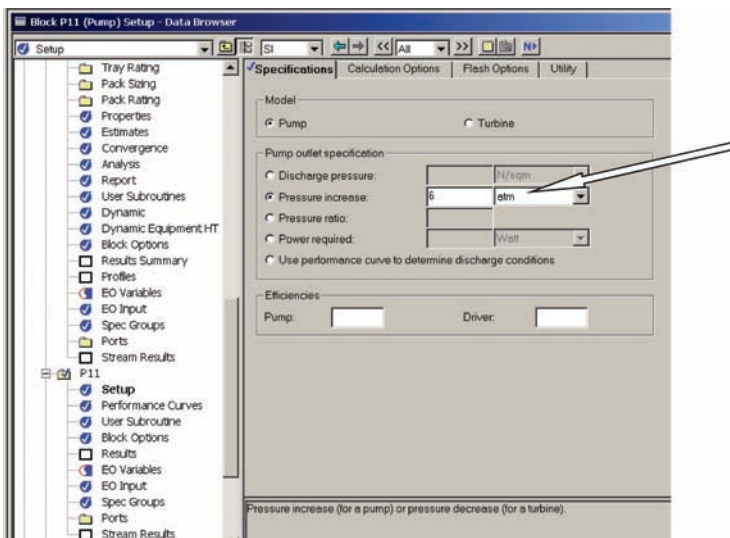


Figure 3.30 Pump P1 specifications.

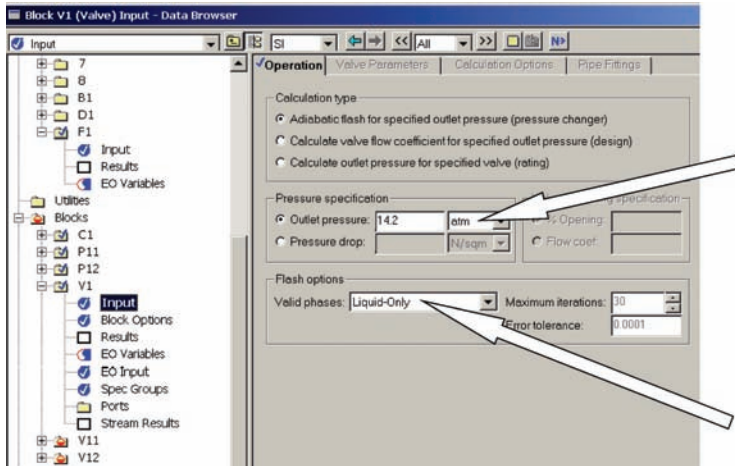


Figure 3.31 Valve V1 specifications.

form for pump P11 with the *Pressure increase* button selected and 6 atm pump head entered. Pump P12 is handled in the same way.

The pressure at the exit of the feed valve (V1) must be equal to the pressure on the feed tray (Stage 16). We do not know exactly what this is at this point, but we guess it to be about 14.2 atm. Clicking *Setup* for the V1 block opens the window shown in Figure 3.31. The outlet pressure is set at 14.2 atm. We will come back and adjust this pressure after the flowsheet has been converged and when we know exactly what the pressure on the feed tray is.

Notice that under the *Flash options*, the *Valid phases* has been set to *Liquid-Only*. This is not necessary for a steady-state simulation, but it will become useful when we move into dynamic simulation in Chapter 7. The other two control valves are each given a pressure drop of 3 atm, as shown in Figure 3.32, and the *Flash options* for *Valid phases* are set to *Liquid-Only*.

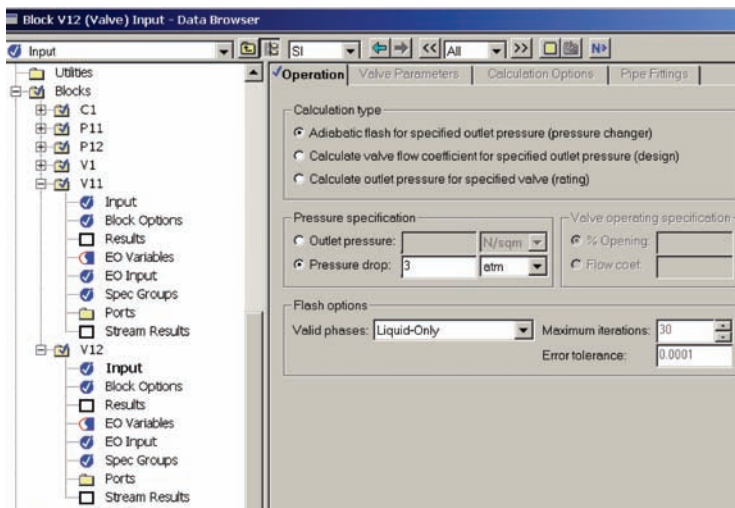


Figure 3.32 Valves V11 and V12 specifications.

The flowsheet is fully specified at this point. All the read buttons are blue, and we are ready to run the simulation.

3.5 RUNNING THE SIMULATION

The blue “N” button (stands for “Next”) at the top of the *Data Browser* window on the far right is clicked to run the simulation. If there is any information that is needed, the program will go to that location on the window and display a red symbol. If everything is ready to calculate, the message shown in Figure 3.33 will appear, and you should click *OK*. The *Control Panel* window shown in Figure 3.34 opens and indicates that the column was successfully converged. It took four iterations to converge the column.

Now, we want to look at the compositions of the product streams leaving the column to see if they satisfy their desired purities. We assume that the specification of the heavy impurity in the distillate (isobutane = *iC4*) is 2 mol% and that of the light impurity in the bottoms (propane = C3) is 1 mol%. To look at the properties of these streams, we open the C1 block in the *Data Browser* window and click the item *Stream Results*, which is at the very bottom of the list.

There are three streams in the table shown in Figure 3.35. Stream 1 is the feed inlet to the column. Stream *D1* is the liquid distillate leaving the reflux drum. Stream *B1* is the liquid bottoms leaving the base of the column. We can see that there is about 12 mol% *iC4* in the distillate and 8 mol% C3 in the bottoms. The purities are too low, so we need to increase the reflux ratio or add more stages to get a better separation.

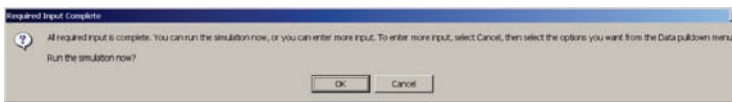


Figure 3.33 Ready to run message.

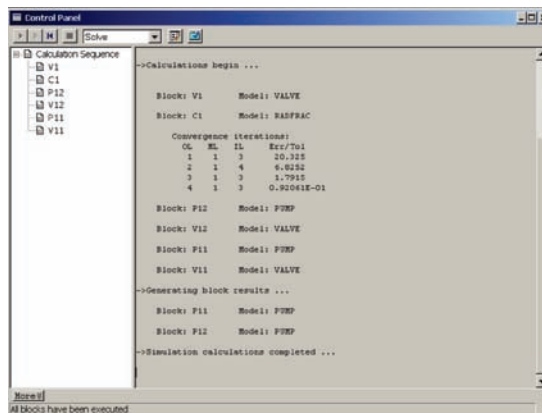


Figure 3.34 Control panel.

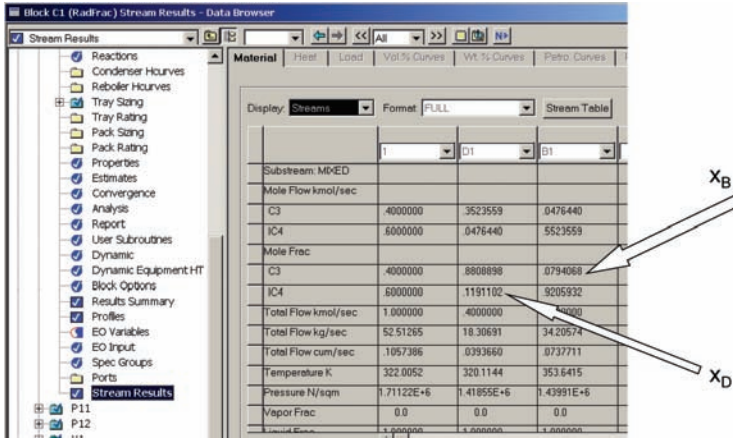


Figure 3.35 Stream results for column with RR = 2.

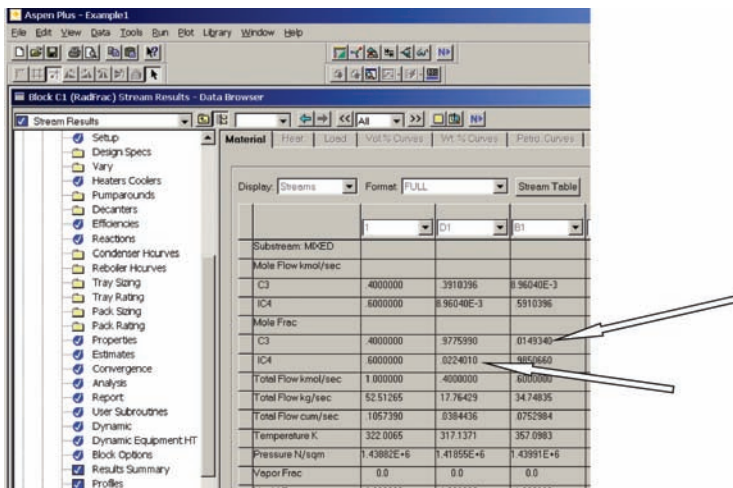


Figure 3.36 Stream results for column with RR = 3.

If we go back to *Setup* in the C1 block, change the reflux ratio to 3, and click the *N* button, the simulation converges with the results shown in Figure 3.36. The distillate impurity has decreased to about 2 mol% *iC4*, and the bottoms now has about 1.5 mol% C3. So we are getting pretty close to the desired purities. We could continue to manually change the reflux ratio and the distillate flow rate to attempt to achieve the desired product purities by trial and error. However, there is a much easier way, as discussed in the next section.

3.6 USING DESIGN SPEC/VARY FUNCTION

The specifications for product impurities are 1 mol% propane in the bottoms and 2 mol% isobutane in the distillate. To achieve these precise specifications, Aspen Plus uses the “Design Spec/Vary” function. A desired value of some “controlled” variable is specified,

and the variable to be manipulated is specified. The simulation attempts to adjust the manipulated variable in such a way that the specified value of the controlled variable is achieved.

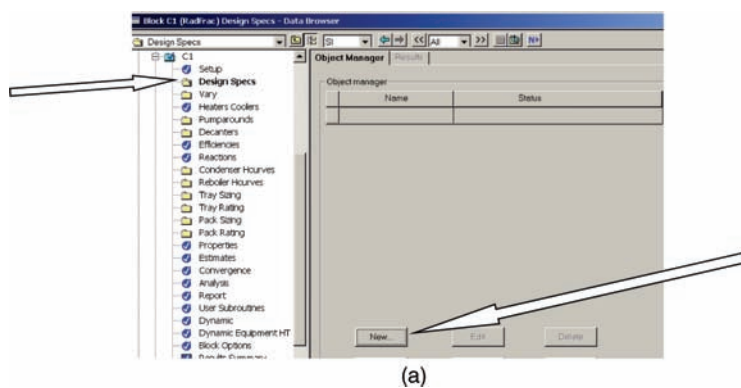
In the example under study, we want to find the values of distillate flow rate and reflux ratio that drive the distillate composition to 2 mol% isobutane and the bottoms composition to 1 mol% propane.

A word of caution might be useful at this point. The solution of a large set of simultaneous nonlinear algebraic equations is very difficult. There is no guarantee that a solution will be found because of numerical problems. In addition, if good engineering judgment is not used in selecting the target values, there may be no physically realizable solution. For example, if the specified number of stages is less than the minimum required for the specified separation, there is no value of the adjusted variable that can produce the desired result.

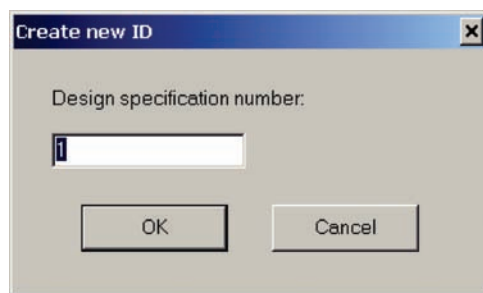
Another possible complication is multiplicity. Because the equations are nonlinear, there may be multiple solutions. Sometimes, the program will converge to one solution, and at other times, it will converge to another solution, depending on the initial conditions.

It is usually a good idea to start by converging only one variable at a time instead of trying to handle several simultaneously. In our example, we will converge the distillate specification first by adjusting distillate flow rate. Then, with this specification active, we will converge the bottoms specification by adjusting the reflux ratio. The order of this sequential approach is deliberately selected to use distillate first because the effect of distillate flow rate on compositions throughout the column is much larger than the effect of reflux ratio.

To set up the Design Spec/Vary function, click on *Design Spec* under the C1 block in the *Data Browser* window. The window shown in Figure 3.37a opens up. Clicking the *New* button opens the window shown in Figure 3.37b. Click *OK* and another window

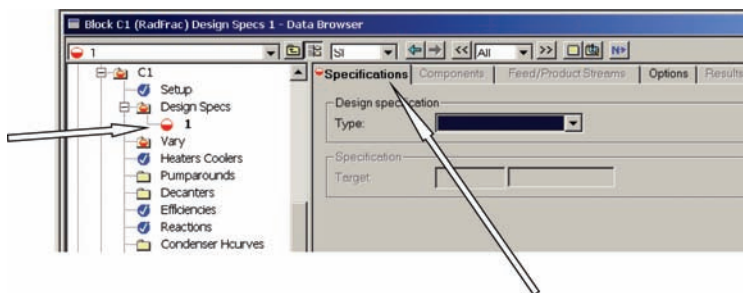


(a)

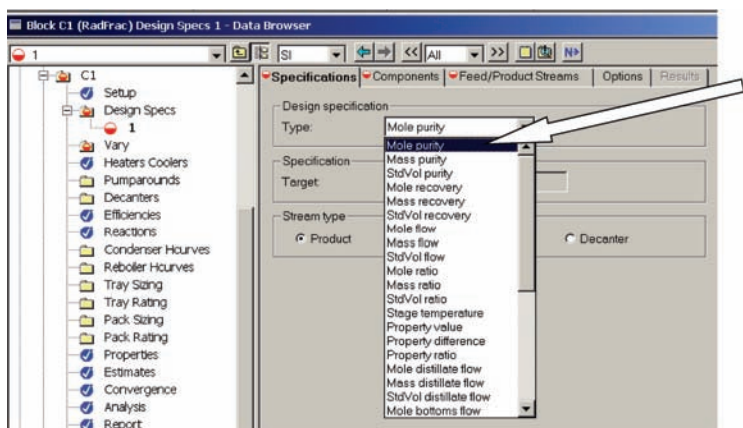


(b)

Figure 3.37 (a) Setting up the Design Spec. (b) Set Design Spec number.



(a)



(b)

Figure 3.38 (a) Specifying the controlled variable. (b) Select type of variable.

opens (Fig. 3.38a), which has several page tabs. On the first one, *Specifications*, you can specify the type of variable and what its desired value is. Clicking the drop-down menu under *Design specification* and *Type* opens a long list of possible types of specifications (Fig. 3.38b). Select *mole purity*. Go down to *Target* and type in “0.02.” This is the desired mole fraction of isobutane in the distillate.

Then, click the second page tab *Components*. Click the “IC4” in the left column under *Available* components. Clicking the “>” button moves IC4 over to the right *Selected components* column (Fig. 3.39b). Click the third page tab *Feed/Product Streams*, select “D1” in the left column and click the “>” button to move it to the right column. The Design Spec is now completed. Notice that the number “1” in Figure 3.39c is blue.

Now, we must specify what variable to adjust. Clicking the *Vary* under the C1 block opens the window shown in Figure 3.40a. Clicking the *New* button and specifying the number to be “1” opens the window shown in Figure 3.40b on which the manipulated variable is defined.

Opening the drop-down menu under *Adjusted variable* and *Type* produces a long list of possible variables. We select *Distillate rate*, which opens several boxes (Fig. 3.40c), in which the range of changes in the distillate flow rate can be restricted. We set the lower bound at 0.2 and the upper bound at 0.6 kmol/s.

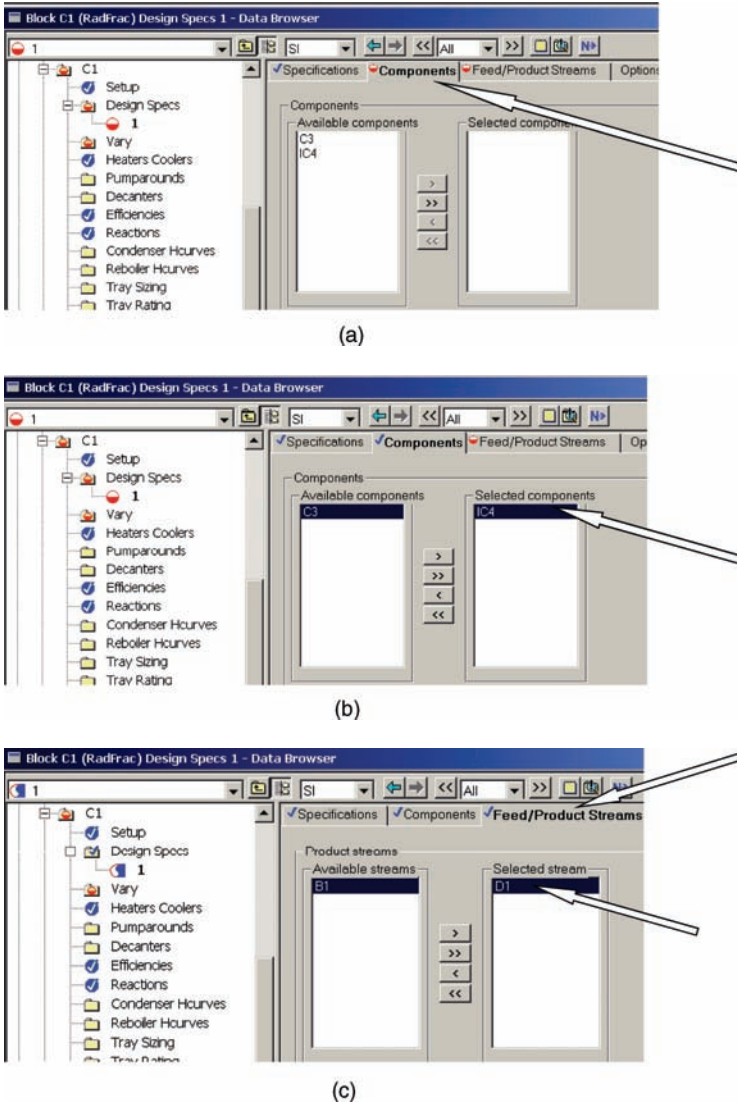
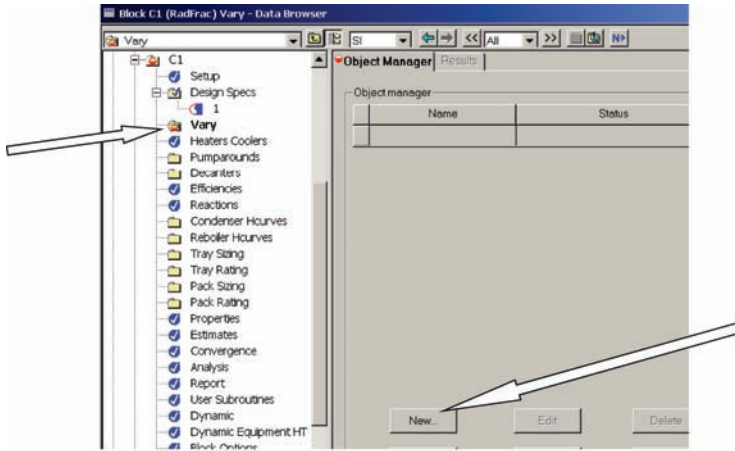
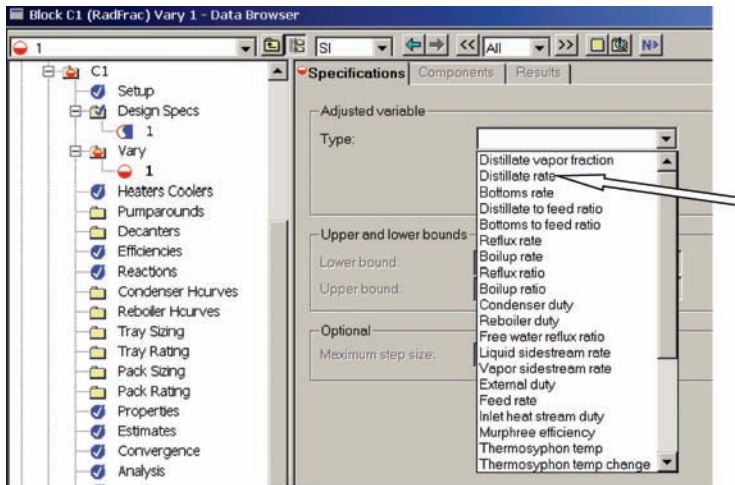


Figure 3.39 (a) Select components. (b) Select IC4. (c) Specify stream.

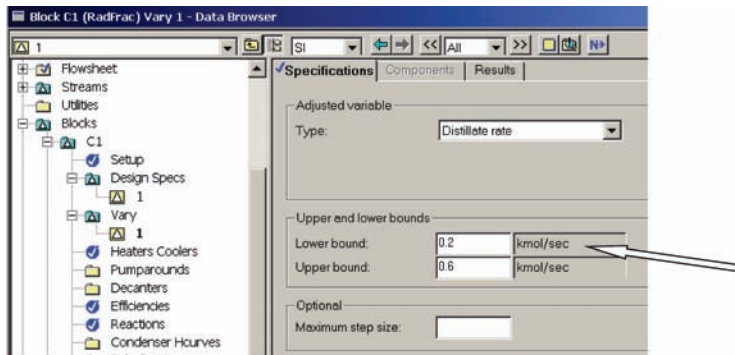
Notice that all the items in the *Data Browser* window are blue, so the simulation is ready to run. We click the blue *N* button and run the program. The *Control Panel* window opens and tells us that it has taken three iterations to converge (Fig. 3.41). Going down to *Stream Results* at the bottom of the list under the C1 block lets us look at the new values of the stream properties. Figure 3.42 shows that mole fraction of IC4 in D1 is 0.01999713, which is within the error tolerance of the 0.02 mol fraction desired. Notice that the flow rate of D1 has changed to 0.39753743 kmol/s.



(a)



(b)



(c)

Figure 3.40 (a) Opening the vary. (b) Defining manipulated variable. (c) Setting limits on distillate flow rate.

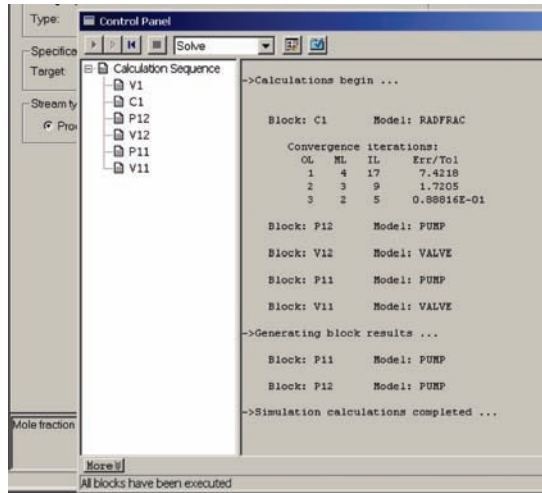
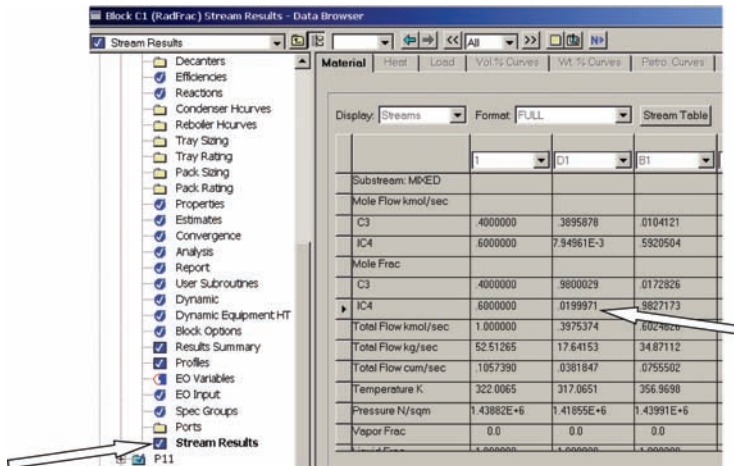
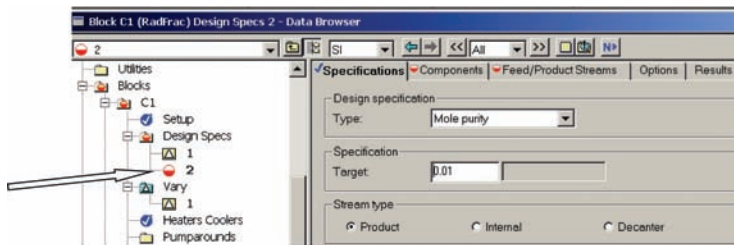


Figure 3.41 Control panel.

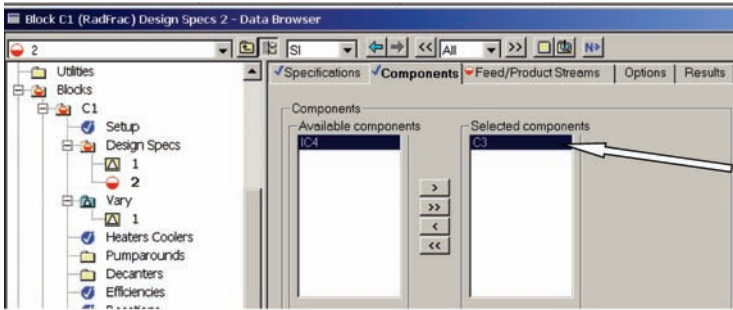


(a)

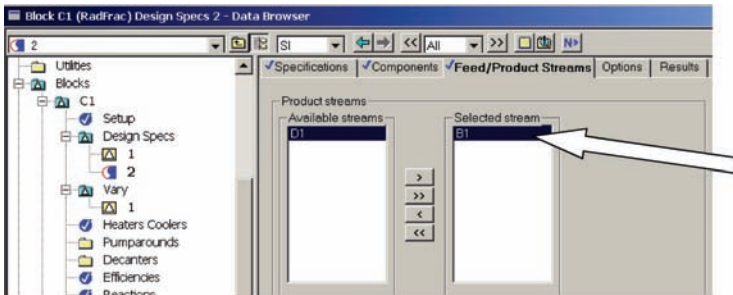


(b)

Figure 3.42 (a) New stream results. (b) Setting up second Design Spec. (c) Selecting propane. (d) Selecting bottoms.



(c)



(d)

Figure 3.42 (Continued)

The second Design Spec/Vary is set up in the same way. Clicking *Design Spec* opens a window on which you specify a new Design Spec “2”. Then, the mole purity of the bottoms *B1* is specified to be 0.01 mol fraction propane. See Figure 3.42 for the three steps on the three-page tabs.

Next, a second *Vary* “2” is set up as shown in Figure 3.43 with reflux ratio selected. The upper and lower bounds are set at 1 and 5, respectively, because we know a reflux ratio of about 3 gives results that are close to the desired.

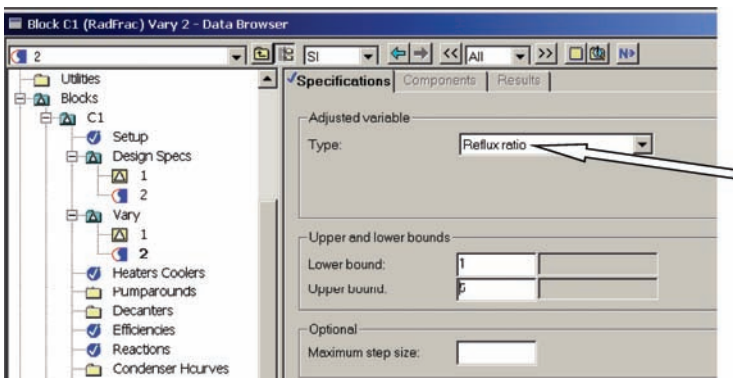


Figure 3.43 Set up second vary.

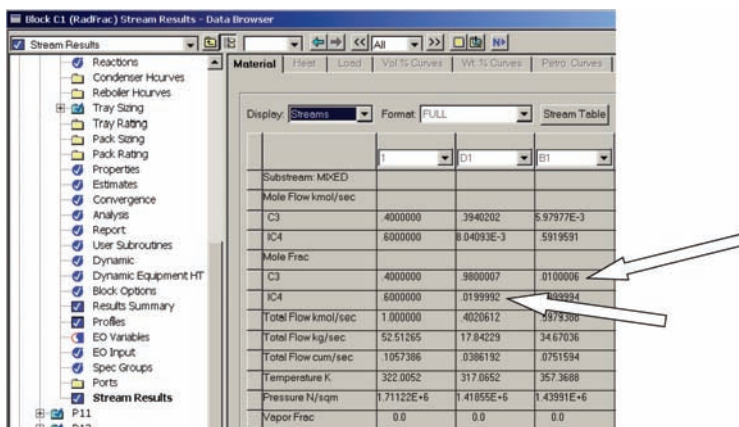


Figure 3.44 Stream results.

Everything is ready to run again. Clicking the blue *N* button executes the program. The simulation converges in three iterations.

Figure 3.44 shows the new stream results. The mole fraction of *iC4* in the distillate is 0.0200027, and the mole fraction of the *C3* in the bottoms is 0.0100008. Both are now very close to their specified values. Of course, the distillate flow rate and the reflux ratio have been changed to produce the desired product purities. The stream results show that the flow rate of *D1* is 0.4021 kmol/s. To find out what the reflux ratio is, click on *Results Summary* under the *C1* block. The window shown in Figure 3.45 opens on which the conditions at the top of the column are given. The reflux ratio is 3.095.

The other important pieces of information in the window are the condenser heat removal (−22.29 MW) and the reflux drum temperature (317.06 K) at 14 atm pressure, which we specified. If you recall, we guessed that a pressure of 14 atm would give us a reflux drum temperature of about 325 K, so cooling water could be used in the condenser. To attain the desired 325 K, the pressure should be increased a little. If we rerun the simulation with a pressure of 16.8 atm, the reflux drum temperature is 325.06 K.

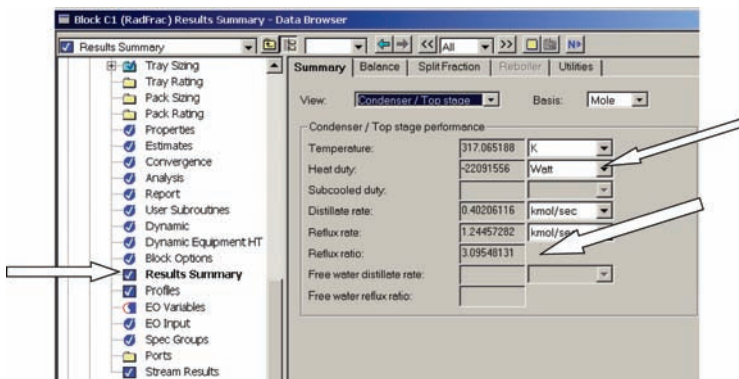


Figure 3.45 Results for top of column at 14 atm pressure.

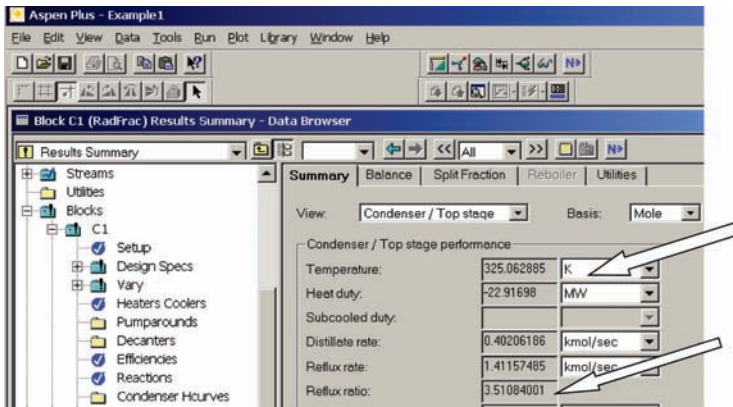


Figure 3.46 Results for top of column at 16.8 atm pressure.

Of course, at this new pressure, the required reflux ratio changes. It increases from 3.095 to 3.511 (see Fig. 3.46). This shows the adverse effect of pressure on relative volatilities that occurs in most hydrocarbon systems. The column should be operated at as low pressure as possible to save energy.

To find the conditions at the base of the column, we use the drop-down menu that is next to *View* on the *Results Summary* window and select *Reboiler/Column base*. Figure 3.47 shows the information obtained. The most important piece of information is the reboiler heat input 27.409 MW.

The base temperature is 366.11 K. This will dictate the pressure of the steam used in the reboiler. A reasonable differential temperature is 40 K, which corresponds to a saturated steam pressure of about 3 atm at 406 K. Thus, if steam is available in the plant at about 6 atm, it can be used to supply the heat required in the reboiler, assuming a 3 atm pressure drop over the steam control valve.

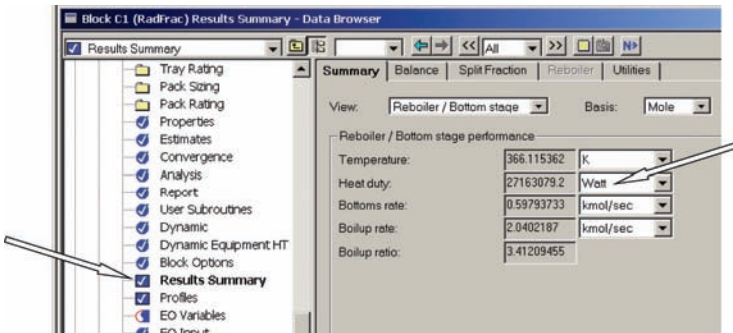


Figure 3.47 Results for base of column at 16.8 atm pressure.

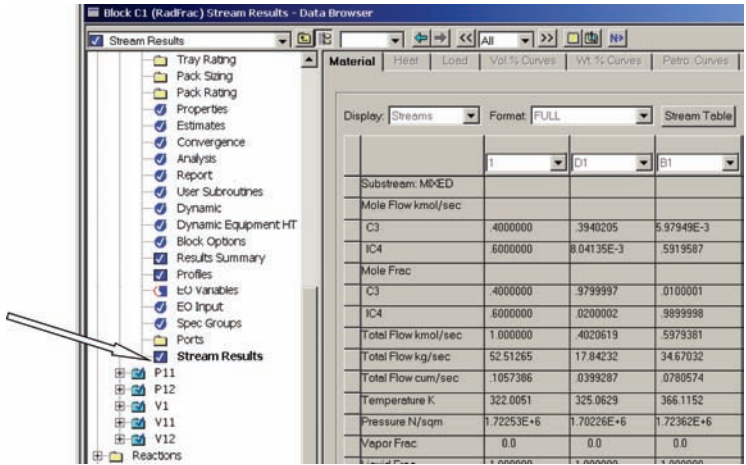


Figure 3.48 Stream properties at 16.8 atm pressure.

The stream conditions at 16.8 atm column pressure are shown in Figure 3.48. The column temperature and composition profiles can be obtained by selecting *Profiles* in the C1 block. The window that opens is shown in Figure 3.49. There are several page tabs. The first *TPQF* gives the temperature and pressure on each stage. Selecting the second page tab *Compositions* opens the window shown in Figure 3.50, in which *Liquid* has been selected from the drop-down menu in the *View* box.

Using the “Plot Wizard” makes generating plots of these profiles quite easy. Click on *Plot* at the top tool bar of the Aspen Plus simulation window. Then click *Plot Wizard*. This

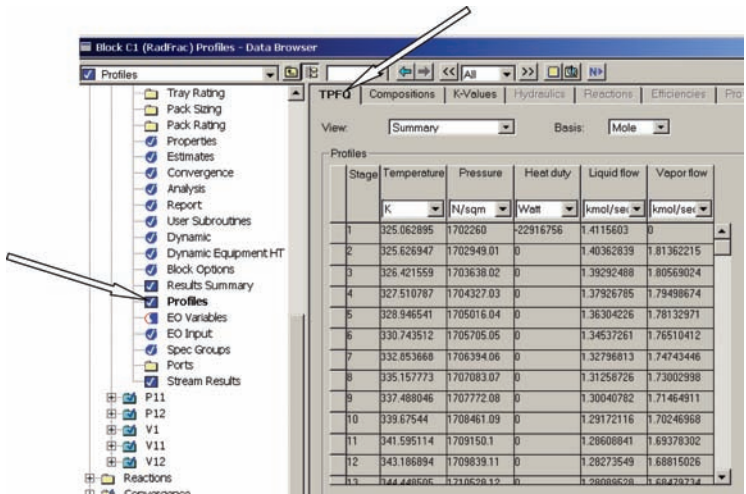


Figure 3.49 Temperature and pressure profiles.

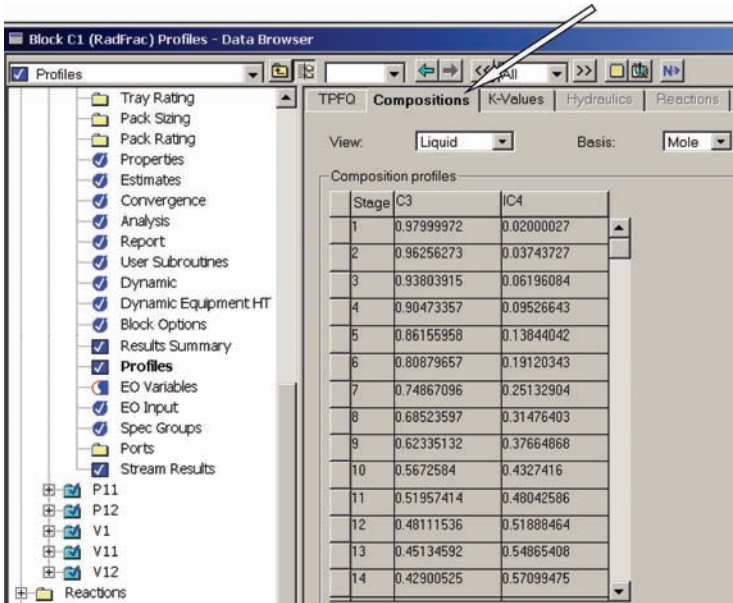


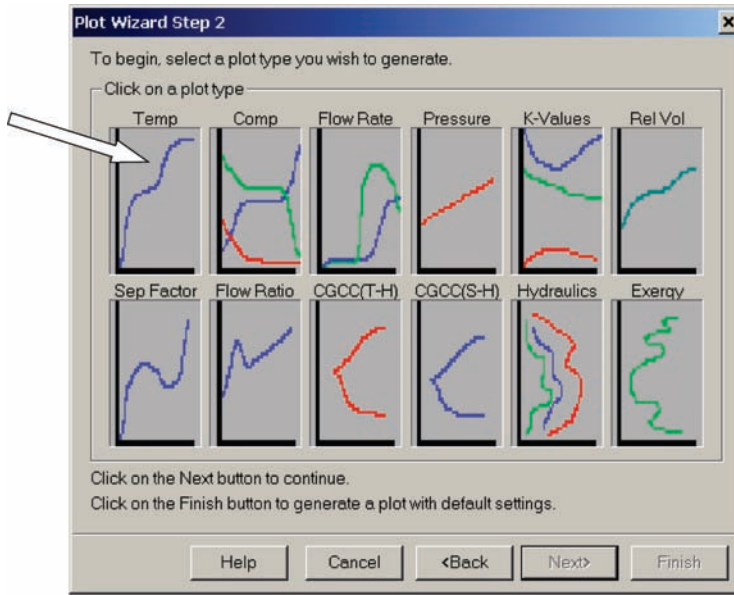
Figure 3.50 Composition profiles.

opens the window shown in Figure 3.51a . Clicking *Next* opens the window shown in Figure 3.51b. Clicking on the upper left picture labeled “Temp” produces the temperature profile plot given in Figure 3.51c. Clicking on the picture labeled “Comp” and then clicking *Next* opens the window on which you can select what components to plot and what phase (liquid or vapor compositions). Figure 3.52a shows the selections, and Figure 3.52b gives the composition profile.

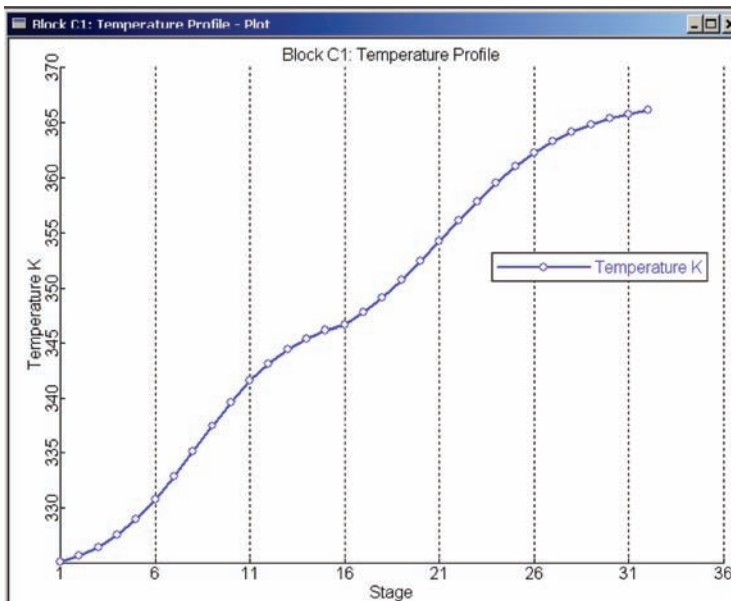


(a)

Figure 3.51 (a) Plot Wizard. (b) Select type of plot. (c) Temperature profile.

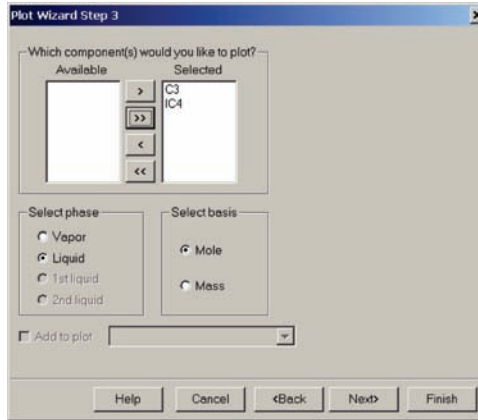


(b)

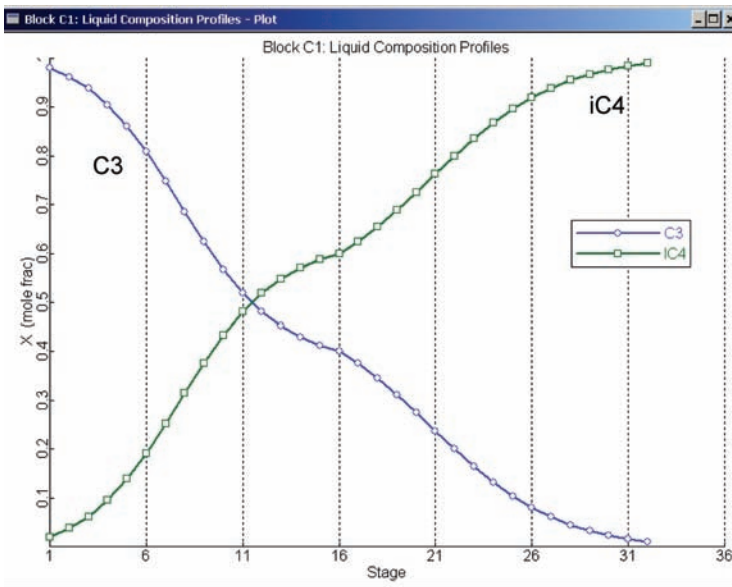


(c)

Figure 3.51 (Continued)



(a)



(b)

Figure 3.52 (a) Selecting components. (b) Liquid composition profile.

3.7 FINDING THE OPTIMUM FEED TRAY AND MINIMUM CONDITIONS

Now that the pressure has been determined and the product specifications attained, we need to go back and find the “optimum” feed tray. In addition, the minimum reflux ratio and the minimum number of trays can be determined. These will be useful for heuristic optimization, which is discussed in detail in Chapter 4.

3.7.1 Optimum Feed Tray

In most distillation columns, the major operating cost is reboiler energy consumption. Of course, if refrigeration was used in the condenser, this heat removal expense would also be

TABLE 3.1 Effect of Feed Stage on Reboiler Heat Input

Feed Stage Number	Reboiler Heat Input (MW)	Condenser Heat Removal (MW)	Reflux Ratio
12	27.94	23.45	3.616
13	27.39	22.90	3.508
14	27.17	22.68	3.463
15	27.18	22.64	3.465
16	27.41	22.92	3511

quite large. For our propane/isobutane example, the pressure was deliberately set so that cooling water could be used in the condenser. Therefore, reboiler heat input is the quantity that should be minimized.

The simulation is run using different feed stages. The purities of both products are held constant. The feed stage that minimizes reboiler heat input is the optimum. Table 3.1 gives the results of these calculations. Feeding on Stage 14 gives the minimum energy consumption.

3.7.2 Minimum Reflux Ratio

The simulation can be used to find the minimum reflux ratio by increasing the number stages until there is no further reduction in the reflux ratio. Product purities are held constant. It is assumed that the feed stage is a fixed ratio of the total number of stages. Results are given in Table 3.2 and show that the minimum reflux ratio is about 2.9.

3.7.3 Minimum Number of Trays

The simulation can also be run to find the minimum number of trays by decreasing the number of stages until the required reflux ratio becomes very large. Product purities are held constant. It is assumed that the feed stage is a fixed ratio of the total number of stages. Results are given in Table 3.3 and show that the minimum number of stages is 15.

TABLE 3.2 Minimum Reflux Ratio

Total Stages	Feed Stage	Reflux Ratio
32	14	3.463
48	21	2.959
64	28	2.912
96	42	2.908

TABLE 3.3 Minimum Number of Stages

Total Stages	Feed Stage	Reflux Ratio
32	14	3.463
22	10	6.021
20	9	8.100
18	8	13.56
17	8	20.59
16	7	21.35
15	7	160.8

3.8 COLUMN SIZING

The last topic to discuss in this chapter before going into economic optimization of column design is how to determine the diameter and length of the vessel.

3.8.1 Length

Calculating the height of the column is fairly easy if the number of trays is given. The typical distance between trays (tray spacing) is 0.61 m (2 ft). If there are N_T stages, the number of trays is $N_T - 2$ (one stage for the reflux drum and one for the reboiler).

In addition to the trays, some space is needed at the top where the reflux piping enters the vessel and at the feed tray for feed distribution piping. More significantly, space is needed at the base to satisfy two requirements. First, liquid holdup is needed for surge capacity. Second, the liquid height in the base of the column must be high enough above the elevation of the bottoms pump to provide the necessary NPSH requirements for this pump.

Therefore, a design heuristic is to provide an additional 20% more height than that required for just the trays. Therefore, the length of the vessel can be estimated from the following equation.

$$L = 1.2(0.61)(N_T - 2)$$

3.8.2 Diameter

The diameter of a distillation column is determined by the maximum vapor velocity. If this velocity is exceeded, the column liquid and vapor hydraulics will fail and the column will flood. Reliable correlations are available to determine this maximum vapor velocity.

As the vapor flow rates change from tray to tray in a nonequimolar overflow system, the tray with the highest vapor velocity will set the minimum column diameter. Knowing the vapor mass flow rate and the vapor density, the volumetric flow rate of the vapor can be calculated. Then, knowing the maximum allowable velocity, the cross-sectional area of the column can be calculated.

Aspen Plus has an easy-to-use tray sizing capability. Click the item *Tray Sizing* under the C1 block, and then click *New* and *OK* for the identification number. A window will open on which the column sections to be sized, and the type of tray can be entered. Figure 3.53a shows the parameter values used in the example. The stages run from Stage 2 (the top tray) to Stage 31 (the bottom tray). Sieve trays are specified.

The simulation must be run by clicking the *N* button. Then the page tab *Results* is clicked (see Fig. 3.53b), and the column diameter is seen to be 7.75 m. This is a very large distillation column, and therefore a single liquid pass would produce very large liquid gradients across the tray and liquid heights over the weir. A column this large would use at least two-pass trays. Changing the number of passes to two on the *Specifications* page tab produces a large change in the calculated diameter, dropping it from 7.73 to 5.91 m.

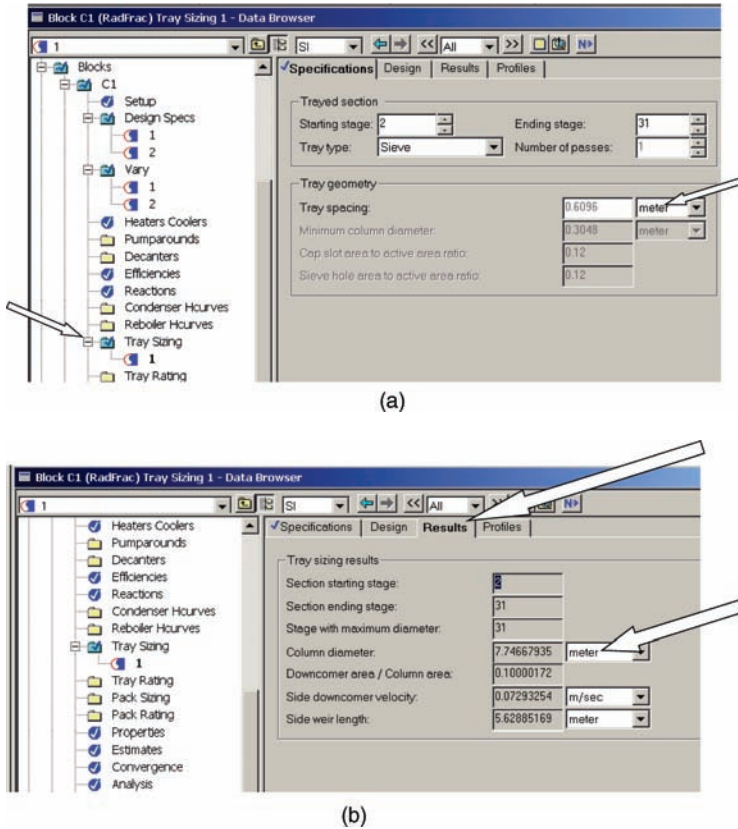


Figure 3.53 (a) Tray sizing setup. (b) Tray sizing results with single pass trays.

The diameter given by Aspen Plus can be checked by using the approximate heuristic that the “F factor” should be equal to 1 (in English Engineering units).

$$F \text{ factor} = V_{\max} \sqrt{\rho_V}$$

where V_{\max} is the maximum vapor velocity in units of ft/s and ρ_V is the vapor density in units of lb/ft³.

All the detailed information about the vapor and liquid flows throughout the column can be accessed by clicking the item *Report* under the C1 block and under *Property Options*, checking the box in front of *Include hydraulic parameters*. Then, after the program is run, click the item *Profiles* and the *Hydraulics* page tab. The window that opens gives lots of information about liquid and vapor rates and properties, as shown in Figure 3.54.

The maximum vapor volumetric flow rate is 9.23 ft³/s and occurs on Stage 32. The vapor density on this stage is 2.82 lb/ft³. Using an F factor of 1, the maximum velocity is 0.595 ft/s, which give a cross-sectional area of 155 ft². This corresponds to a diameter of 14.0 ft or 4.28 m, which is somewhat lower than the Aspen Plus result (5.91 m).

In either case, this is a very large distillation column, and as we will see in the next chapter, it is very expensive to buy.

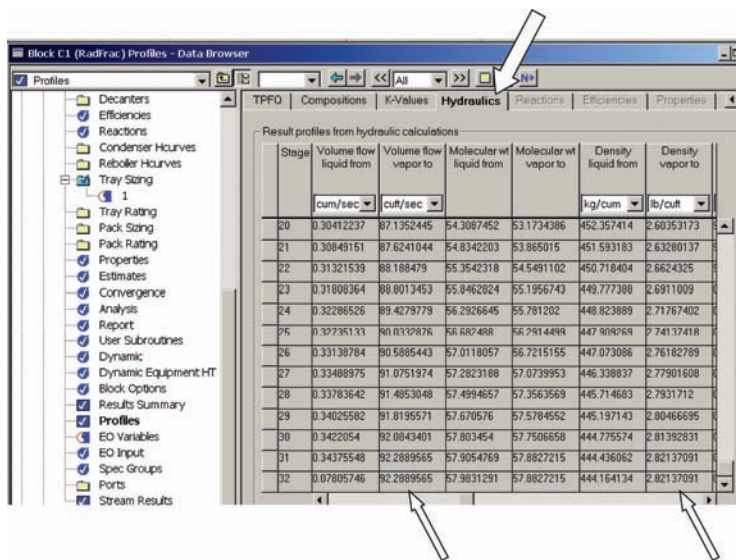


Figure 3.54 Hydraulic results.

3.9 CONCEPTUAL DESIGN

The steady-state simulation of distillation columns in Aspen Plus discussed in previous sections took a “rating” approach to the problem. Specific values for the total number of trays and the feed-tray location were selected, and the required reflux ratio and reboiler duty were determined for this specific configuration, subjected to attaining the desired product specifications. Then, economics must be used to find what the optimum tray configuration is.

Aspen Plus provides feature called *Conceptual Design* that offers another approach to the problem (a “design” approach). In this method, the product specifications are set at both ends of the column, as is a reflux ratio. Then, the program performs tray-to-tray calculations, both up and down the column, creating composition profiles for both the rectifying and stripping sections. If these two composition profile intersect, the reflux ratio selected is above the minimum, and the number of trays in both sections is now known. The method is applicable to ternary systems with a single feed stream.

A numerical example is given in this section to illustrate the use of *Conceptual Design*. The ternary mixture of *n*-butane, *n*-pentane, and *n*-hexane is separated at 4 atm pressure, using Chao–Seader physical properties. Click on *Library* on the tool bar at the top of the window and select *References*. The window shown in Figure 3.55 opens, and the box to the left of *Conceptual Design* is clicked. A new page tab called *ConceptualDesign* is added at the bottom right of the window (Fig. 3.56). Clicking the page tab opens a *ConSep* icon (Fig. 3.57), which is clicked and a column icon is dropped onto the flowsheet (Fig. 3.58). Feed, distillate and bottoms streams are added in the normal way (Fig. 3.59). The feed stream is specified to be 100 kmol/h with a composition of 30 mol% *n*-butane, 30 mol% *n*-pentane, and 40 mol% *n*-hexane (Fig. 3.60).

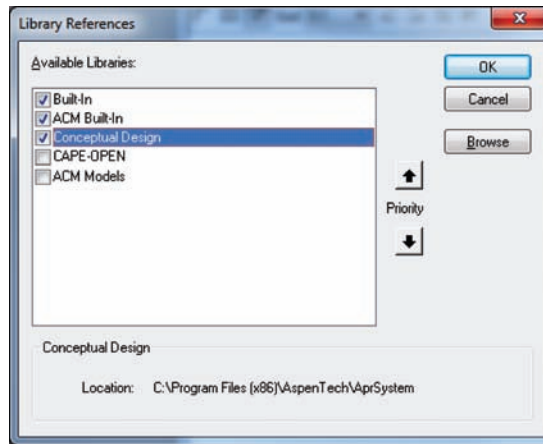


Figure 3.55 Opening view of conceptual design.

Clicking the *N* button causes the simulation to run. A new file is shown at the bottom of the monitor, which opens the window shown in Figure 3.61 when clicked. The information about the components, pressure, and physical property package are entered. The *Design* option under the *Mode* item is selected (Figure 3.62).

Then, the *Specifications* item is clicked, which opens the window shown in Figure 3.63. The specifications for the product purities are selected. Note that only three product compositions can be set. We want to achieve a separation between *nC4* and *nC5*, so these are the light and heavy key components. A 1 mol% *nC5* impurity in the distillate and a 1 mol% *nC4* impurity in the bottoms are selected. The third specification is to have a very

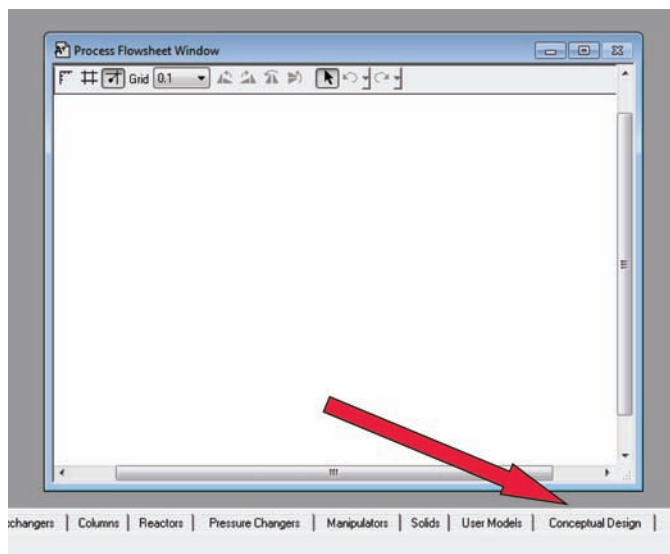


Figure 3.56 Conceptual design page tab.

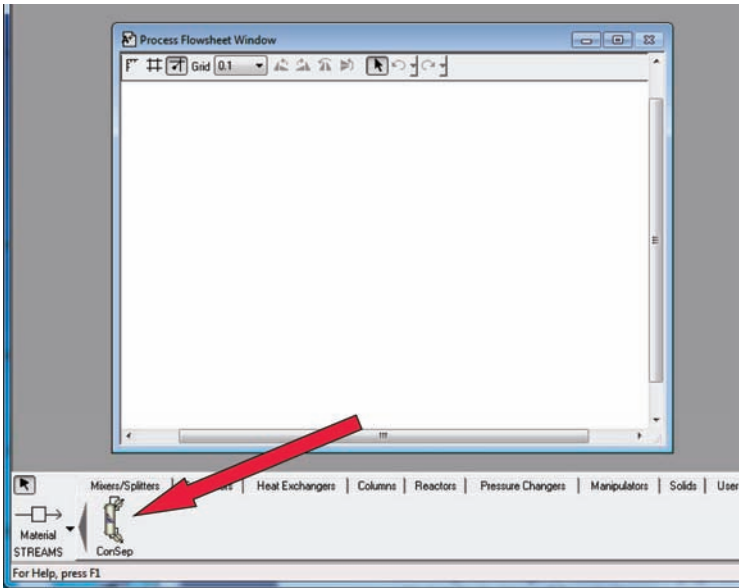


Figure 3.57 Conceptual design icon.

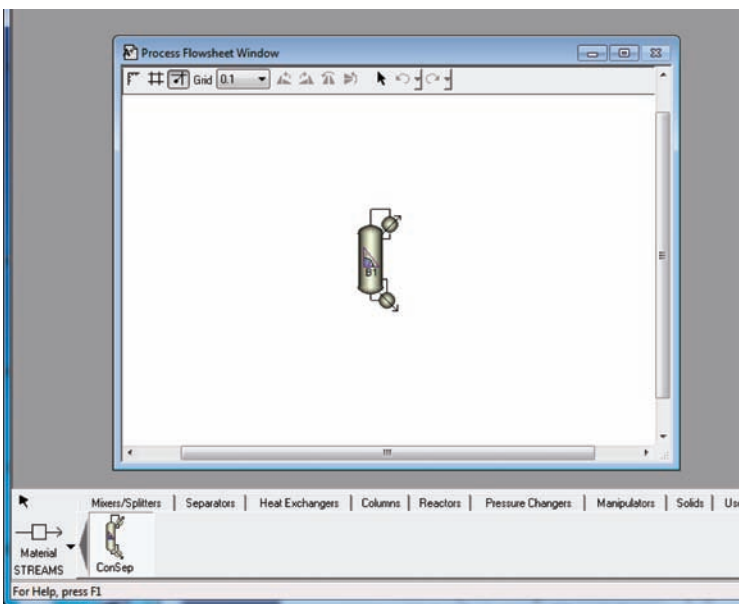


Figure 3.58 Dropping ConSep icon on flowsheet.

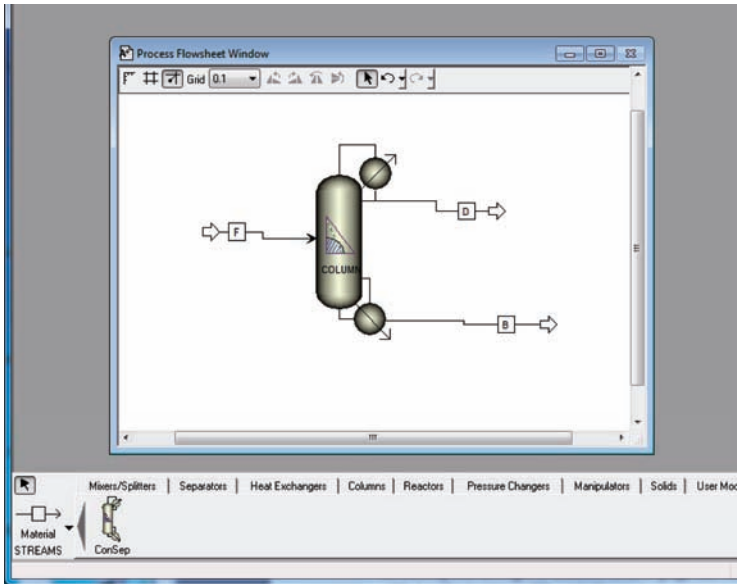


Figure 3.59 Adding streams and renaming.

The screenshot shows a software window titled "Stream F (MATERIAL) Input - Data Browser". The window is divided into a left sidebar with a tree view and a main right pane. The tree view includes categories like "Specifications", "Simulation Options", "Stream Class", "Substreams", "Costing Options", "Stream Price", "Units-Sets", "Custom Units", "Report Options", "Components", "Properties", "Flowsheet", "Streams", "Input", "Results", "EO Variables", "Custom Stream Resul", "Blocks", and "Utilities". The main pane is titled "Specifications" and contains the following fields and tables:

- Substream name: MIXED
- State variables:
 - Temperature: 50 C
 - Pressure: 4 atm
 - Total flow: 100 kmol/hr
 - Solvent: (empty)
- Composition table:

Component	Value
NC4	0.3
NC5	0.3
NC6	0.4
Total	1

At the bottom of the main pane, there is a text box that says "Lets you select the substream name."

Figure 3.60 Specifying feed.

small amount of the heavier-than-heavy key $nC6$ in the distillate (0.01 mol%). A tentative guess of the reflux ratio is made ($RR = 3$).

Finally, the *Calculate* button at the far right of the tool bar is clicked. The window shown in Figure 3.64 opens. The straight composition line between the distillate D and the bottoms B is shown running through the feed F . There are two composition trajectories, one for the stripping section (starting at B) and one for the rectifying section (starting at D).

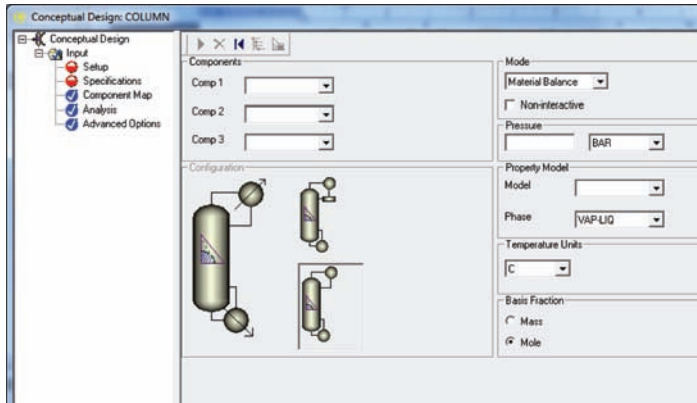


Figure 3.61 Conceptual design input.

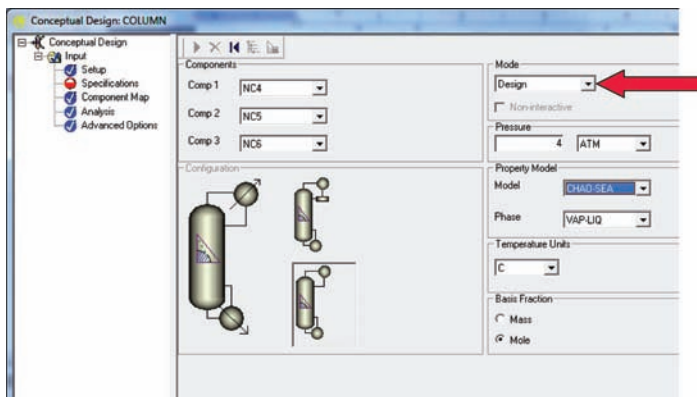


Figure 3.62 Conceptual design setup.

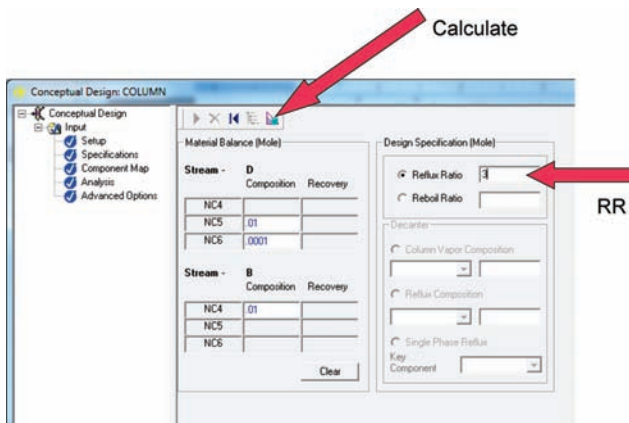
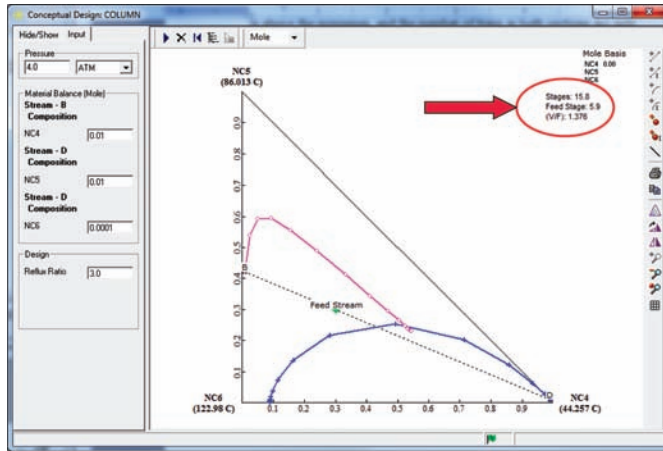
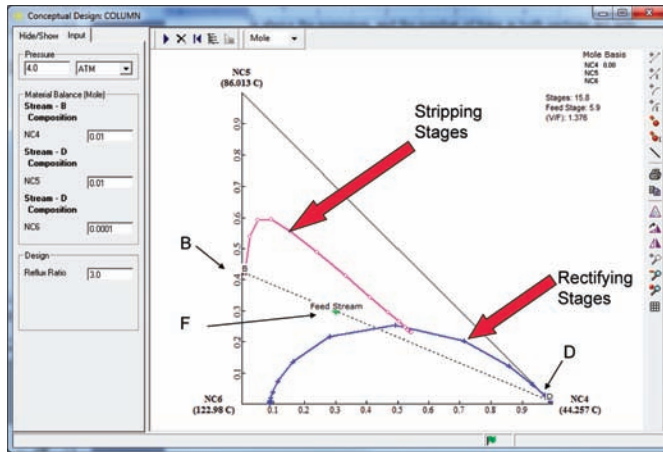


Figure 3.63 Conceptual design specifications.



(a)



(b)

Figure 3.64 (a) Conceptual design ternary diagram. (b) Streams and tray composition profiles.

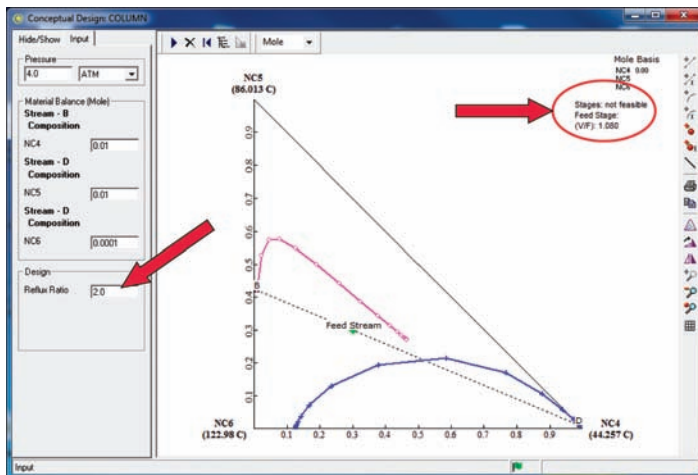


Figure 3.65 Infeasible separation with reflux ratio of 2.

Because these trajectories intersect, the selected reflux ratio is above the minimum. In the upper right corner, the design of the column is shown to be 15.8 stages with a feed stage of 5.9.

As the reflux ratio is reduced, the number of stages increases. Reflux ratios < 2.64 give a message that the separation is infeasible. Figure 3.65 illustrates this situation for a reflux ratio of 2.

3.10 CONCLUSIONS

All the details of setting up and running a steady-state simulation of a simple distillation column have been presented in this chapter. These methods are applied to a variety of columns in later chapters.

CHAPTER 4

DISTILLATION ECONOMIC OPTIMIZATION

In Chapter 3, we studied how to design a distillation column, given the feed conditions, the desired product specifications, and the total number of stages. The calculated design parameters included the operating pressure of the column, the reboiler and condenser heat duties, and the length and diameter of the column vessel.

In this chapter, the steady-state economic optimization of a distillation column design is discussed. Basically, we need to find the optimum number of total stages. There are some simple approaches, and there are more rigorous approaches. The simple methods use heuristics such as setting the total number of trays equal to twice the minimum. The rigorous methods look at how the capital and energy costs change with the number of trays and find the configuration of stages (total and feed stage) that gives the minimum total annual cost (TAC).

4.1 HEURISTIC OPTIMIZATION

There are two widely used heuristics for optimum distillation design. We will discuss both of them in this section and compare the designs that result from applying each. It should be emphasized that they cannot *both* be used simultaneously for rigorous design because fixing one of the two completely specifies the design of the column.

4.1.1 Set Total Trays to Twice Minimum Number of Trays

We discussed using the Fenske equation to find the minimum number of trays in Chapter 2 for constant relative volatility systems. We found the minimum number of trays more rigorously in Chapter 3 by using the simulator to find the number of stages where the

required reflux ratio became very large. In the numerical example, the minimum number of trays is 15. Taking twice this number and adding two stages for the reflux drum and reboiler give a 32-stage column, which is the column we designed in Chapter 3. Remember that the reflux drum (condenser) is denoted as Stage 1 in Aspen notation.

It is interesting to compare this rigorous number with the approximate prediction of the Fenske equation for the same system. The first issue is to find an appropriate value for the relative volatility for the propane/isobutane system at the operating pressure of the column (16.8 atm). The usual approach is to find the relative volatility at the temperature in the top of the column (Stage 2 temperature is 325.6 K) and at the temperature in the reboiler (Stage 32 temperature is 366.1 K).

By definition, relative volatility α_{LH} is the ratio of the vapor and liquid compositions of component L divided by the same ratio of component H. The propane and isobutane compositions on the top tray (Stage 2) can be seen in the item *Profiles* under the column C1 block in the *Data Browser* window.

$$\text{Propane : } \quad x = 0.96256322 \quad y = 0.98$$

Of course, in this binary system, the isobutane compositions are simply 1 minus the propane mole fractions. Therefore, the relative volatility between propane and isobutane on the top tray is

$$\alpha = \frac{y_{C3}/x_{C3}}{y_{iC4}/x_{iC4}} = \frac{0.98/0.96356322}{(1 - 0.98)/(1 - 0.96356322)} = 1.8529$$

Repeating this calculation for conditions in the reboiler gives

$$\text{Propane : } \quad x = 0.01 \quad y = 0.01715812$$

$$\alpha = \frac{y_{C3}/x_{C3}}{y_{iC4}/x_{iC4}} = \frac{0.01715812/0.01}{(1 - 0.01715812)/(1 - 0.01)} = 1.7633$$

The geometric average of these relative volatilities is

$$\alpha_{\text{average}} = \sqrt{(1.8529)(1.7633)} = 1.8076$$

The distillate and bottoms propane compositions are $x_D = 0.98$ and $x_B = 0.01$. Substituting these values in the Fenske equation gives the minimum number of trays N_{\min} .

$$\begin{aligned} N_{\min} + 1 &= \frac{\log[(x_D/(1 - x_D))((1 - x_B)/x_B)]}{\log(\alpha_{\text{average}})} \\ &= \frac{\log[(0.98/(1 - 0.98))((1 - 0.01)/0.01)]}{\log(1.8076)} = 14.34 \end{aligned}$$

Therefore, the minimum number of trays is 13.43, which is close to that found from the simulation (15). Using this heuristic would lead us to set the actual number of trays equal to two times 15 = 30. This would give 32 stages.

4.1.2 Set Reflux Ratio to 1.2 Times Minimum Reflux Ratio

The other common distillation economic heuristic is to select a reflux ratio that is 20% larger than the minimum reflux ratio. The minimum reflux ratio found in Chapter 3 from the simulation was 2.9. Multiplying this by 1.2 gives an actual reflux ratio of 3.48. This is very close to the reflux ratio (3.49) we found was necessary in Chapter 3 for a 32-stage column.

It is interesting to compare the minimum reflux ratio found in the rigorous simulation with the approximate prediction from the Underwood equations. These equations are derived assuming constant relative volatilities. As we have seen in Section 4.1.1, the relative volatility between propane and isobutane is almost constant. It varies from 1.85 to 1.76. Therefore, the Underwood equations should predict the minimum reflux ratio quite well.

As discussed in Chapter 2, there are two equations. The first is solved for a parameter θ that is one of the roots of this equation.

$$\sum_{j=1}^{\text{NC}} \frac{\alpha_j z_j}{\alpha_j - \theta} = 1 - q$$

where NC is the number of components, α_j is the relative volatility of component j , and q is the thermal condition of the feed ($q = 1$ for saturated liquid feed, $q = 0$ for saturated vapor feed).

Applying this to the binary propane/isobutane system for saturated liquid feed with composition of 40 mol% propane and using the average relative volatility of 1.8076 for propane and 1 for isobutane give

$$\begin{aligned} \sum_{j=1}^{\text{NC}} \frac{\alpha_j z_j}{\alpha_j - \theta} &= \frac{(1.8076)(0.40)}{1.8076 - \theta} + \frac{(1)(0.60)}{1 - \theta} = 1 - 1 \\ 0.72304(1 - \theta) + (0.6)(1.8076 - \theta) &= 0 \\ \theta &= 1.3662 \end{aligned}$$

This value of θ is substituted into the second Underwood equation, using the distillate composition $x_D = 0.98$ mol fraction propane.

$$\begin{aligned} \sum_{j=1}^{\text{NC}} \frac{\alpha_j x_{Dj}}{\alpha_j - \theta} &= 1 + \text{RR}_{\min} \\ \frac{(1.8076)(0.98)}{1.8076 - 1.3662} + \frac{(1)(0.02)}{1 - 1.3662} &= 1 + \text{RR}_{\min} \\ \text{RR}_{\min} &= 2.959 \end{aligned}$$

As expected, this is very close to the 2.9 value found in the simulation.

4.2 ECONOMIC BASIS

Equations to calculate the capital cost of all the equipment and the energy cost of the heat added to the reboiler are needed to perform economic optimization calculations. The major pieces of equipment in a distillation column are the column vessel (of length L and diameter D , both with units of meters) and the two heat exchangers (reboiler and

condenser with heat-transfer areas A_R and A_C , respectively, with units of m^2). Smaller items such as pumps, valves, and the reflux drum are usually not significant at the conceptual design stage. The cost of the trays themselves is usually small compared with the vessel and heat exchangers unless expensive internals are used such as structured packing. Table 4.1 gives the economic parameter values and the sizing relationships and parameters used.

The sizing of the column vessel has been discussed in Chapter 3. The condenser and reboiler heat duties are determined in the simulation, but we need to have an overall heat-transfer coefficient and a differential temperature-driving force in each heat exchanger to be able to calculate the required area. The values of these parameters given in Table 4.1 are typical of condensing and boiling hydrocarbon systems. Notice that the overall heat-transfer coefficient of the condenser is larger than that of the reboiler. Reboilers have a higher tendency to foul because of the higher temperature (more coking or polymerization) and because any heavy material in the feed drops to the bottom of the column.

There are a variety of objective functions that are used for economic optimization. Some are quite elegant and incorporate the concept of the “time value of money.” Examples are “net-present-value” and “discounted cash flow.” These methods are preferred by business majors, accountants, and economists because they are more accurate measures of profitability over an extended time period. However, a lot of assumptions must be made in applying these methods, and the accuracy of these assumptions is usually quite limited. The prediction of future sales, prices of raw materials and products, and construction schedule is usually a guessing game made by marketing and business managers whose track record for predicting the future is almost as poor as the weather man.

TABLE 4.1 Basis of Economics

Condensers
Heat-transfer coefficient = 0.852 kW/(K m ²)
Typical differential temperature = 13.9 K
Capital cost = 7296 (area) ^{0.65} Area in m ²
Reboilers
Heat-transfer coefficient = 0.568 kW/(K m ²)
Typical differential temperature = 34.8 K
Capital cost = 7296 (area) ^{0.65} Area in m ²
Column vessel capital cost = 17,640 (D) ^{1.066} (L) ^{0.802}
Diameter and length in meters
Energy costs
LP steam (6 bar, 87 psia, 160 °C, 433 K, 320 °F) = \$7.78/GJ
MP steam (11 bar, 160 psia, 184 °C, 457 K, 363 °F) = \$8.22/GJ
HP steam (42 bar, 611 psia, 254 °C, 527 K, 490 °F) = \$9.88/GJ
Electricity = \$16.8/GJ
Refrigeration
Chilled water at 5 °C, returned at 15 °C = \$4.43/GJ
Refrigerant at -20 °C = \$7.89/GJ
Refrigerant at -50 °C = \$13.11/GJ
TAC = $\frac{\text{capital cost}}{\text{payback period}} + \text{energy cost}$
Payback period = 3 years

Therefore, the use of some simple economic objective function usually serves the purpose of optimizing a distillation column design. We will use the TAC. As shown in Table 4.1, this measure incorporates both energy cost and the annual cost of capital. The units of TAC are \$/year. The units of capital investment are \$. The units of annual cost of capital are \$/year, and it is obtained by dividing the cost of capital by a suitable payback period.

The typical temperature differentials shown in Table 4.1 are only approximate and should be used with some caution. More rigorous temperature differentials can be determined by specifying in more detail the temperatures of the utility. The process temperatures are known from the simulation. For example, supposed cooling water is used in the condenser with an inlet temperature of 90 °F and an outlet temperature of 110 °F. A log-mean temperature differential can be calculated from the known reflux-drum temperature. In the reboiler, the base temperature is known. If the heat source is steam, the saturation temperature of the condensing steam inside the reboiler is used to calculate the differential temperature-driving force. Remember that the steam pressure in the reboiler is less than the supply pressure because of the pressure drop over the control valve. Therefore, if the temperature in the base of the column is 366 K (see the depropanizer example in Chapter 3) and a 35 K differential is specified, the saturated steam temperature in the steam side of the reboiler should be 401 K, which corresponds to a pressure of 2.52 atm. Thus, typical low-pressure steam at 6 bar could be used with plenty of control-valve pressure drop. Table 4.1 gives typical costs of various sources of heat and refrigeration.

The cost of energy varies quite a bit from plant to plant. In some locations, energy sources are plentiful and inexpensive. For example, in Saudi Arabia, gas coming from an oil well is sometimes simply flared (burned). In other locations, fuel is quite expensive because it must be transported long distances. For example, in Japan, some of the natural gas is shipped in from Indonesia on liquefied natural gas (LNG) tankers, which are very expensive. Therefore, energy costs depend on location. The recent drastic drop in natural gas prices in the United States due to increased production from Marcellus shale has lowered (temporarily at least) energy costs.

4.3 RESULTS

The equations to calculate the capital cost of all the equipment and the energy cost of the energy are given in the Matlab program shown in Table 4.2. The numerical example is for the 32-stage column studied in Chapter 3.

Table 4.3 gives results for a range of values for the total number of stages. The 32-stage case is shown in the second column. The capital cost of the column shell, which is 5.91 m in diameter and $1.2(0.61)(30) = 22$ m in length, is \$1,400,000. The capital cost of the two large heat exchangers at \$1,790,000 is more than the vessel. The TAC is \$5,090,000 per year. Notice that most of this is energy (\$4,030,000 per year).

The other columns in Table 4.3 give results for columns with other total stages. If the number of stages is reduced to 24, which gives a shorter column, reboiler heat input increases. This increases column diameter and heat-exchanger areas. This results in an increase in both capital and energy costs.

If the number of stages is increased, the column becomes taller, but its diameter becomes smaller because reboiler heat input decreases. This decreases heat-exchanger costs and energy costs. However, the cost of the vessel increases because it is taller.

TABLE 4.2 Matlab Program to Evaluate Economics

```

% Program "economics.m"
% Economics for distillation column example 1 (depropanizer)
% Given Qr, Qc, and number of trays, calculate TAC
% For standard column
% Using SI units (m, K, and MW) U units kW/K/m^2
% Cost of energy = $4.7/GJ
ur = 0.568; uc = 0.852; dtr = 34.8; dtc = 13.9; cost energy = 4.7;
% 32 stage column
nt = 30; d = 5.91; qr = 27.17; qc = 22.68;
l = nt*2*1.2/3.281;
Shell = 17640*(d^1.066)*(l^0.802);
ar = qr*1000/(dtr*ur); ac = qc*1000/(dtc*uc);
hx = 7296*(ar^0.65 + ac^0.65);
Energy = qr*cost energy*3600*24*365/1000;
Capital = shell + hx;
TAC = energy + capital/3;
nt + 2, ac, ar, shell, hx, energy, capital, TAC;

```

TABLE 4.3 Rigorous Optimization Results

Stages	24	32	36	42	44	48
N_F	10	14	16	18	19	21
D (m)	6.82	5.91	5.77	5.67	5.65	5.63
Q_C (MW)	39.0	22.7	21.4	20.5	20.3	20.1
RR	5.10	3.46	3.21	3.04	3.00	2.96
Q_R (MW)	35.5	27.2	25.9	25.0	24.8	24.6
A_C (m ²)	3280	1910	1800	1730	1710	1700
A_R (m ²)	1800	1370	1310	1260	1260	1240
Shell (10 ⁶ \$)	1.27	1.40	1.50	1.68	1.74	1.87
HX (10 ⁶ \$)	2.36	1.79	1.73	1.69	1.68	1.67
Energy (10 ⁶ /year)	5.26	4.03	3.84	3.71	3.68	3.65
Capital (10 ⁶ \$)	3.62	3.18	3.23	3.37	3.42	3.53
TAC (10 ⁶ \$/year)	6.46	5.09	4.92	4.83	4.82	4.83

Hence, the effect of increasing the number of stages is to increase the capital cost of the shell and to decrease the capital cost of the heat exchangers and energy costs. As more and more stages are added, the incremental decrease in reboiler heat input gets smaller and smaller. The cost of the shell continues to increase (to the 0.802 power as shown in Table 4.1). Figure 4.1 shows how the variables change with the number of stages.

The TAC reaches a minimum of \$4,823,000 per year for a column with 44 stages. Thus, in this numerical case, the optimum ratio of the actual number of trays to the minimum is $42/15 = 2.8$ instead of the heuristic 2. The reflux ratio is 3 at the optimum 44-stage design, which gives a ratio of actual to minimum of $3/2.9 = 1.04$ instead of the heuristic 1.2.

These differences may seem quite large and indicate that the heuristics are not very good. However, good engineers always build in some safety factors in their designs. Building a column that is larger in diameter and has more heat-exchanger area than the real economic optimum is good conservative engineering. The number of trays in a column can

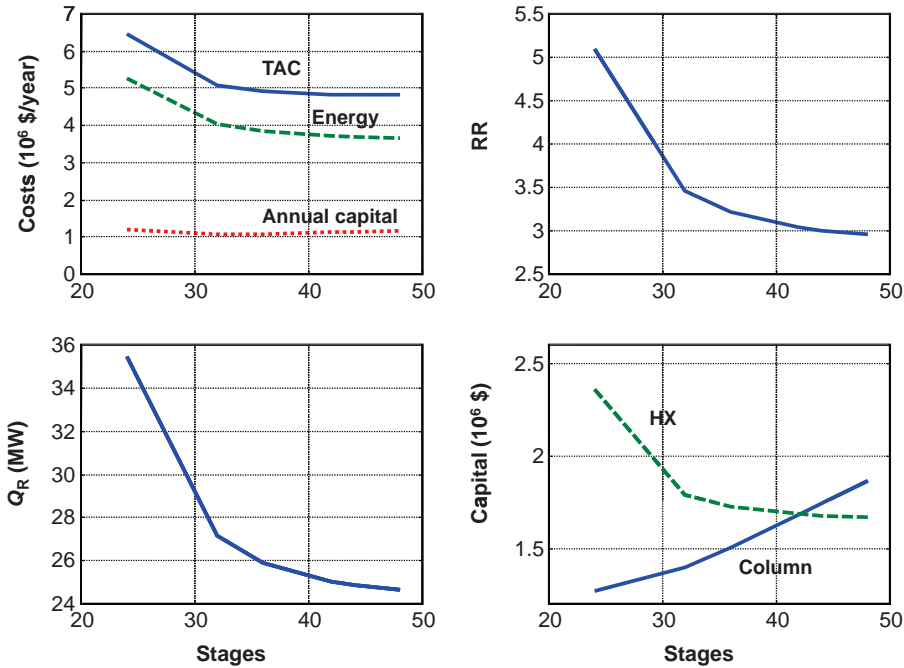


Figure 4.1 Propane/isobutane example.

sometimes be increased by going to smaller tray spacing or installing more efficient contacting devices. However, changing the diameter requires a completely new vessel. Therefore, the heuristics give a pretty good design.

It should also be noted that the optimum is quite flat. The TAC only decreases from 5.09 to $4.82 \cdot 10^6$ \$/year as the number of stages is increased from the heuristic 34 stages to the optimum 44 stages. This is only 5%.

If the cost of energy is reduced, the optimum number of stages becomes smaller. Using an energy cost of half that assumed above, the optimum number of stages is 42 instead of 44, and the TAC drops to \$2,980,000 per year from \$4,823,000. It is clear that energy costs dominate the design of distillation columns.

Stainless steel is used in the cost estimates given in Table 4.1. If the materials of construction were more exotic, the optimum number of stages would decrease.

4.4 OPERATING OPTIMIZATION

In the discussion up to this point, we have been considering the “design problem”, that is, finding the optimum number of stages. A second type of optimization problem of equal importance is the “rating problem,” that is, finding the optimum operating conditions for a given column with a fixed number of stages.

There are several types of rating problems. One of the most common is finding the product purities that maximize profit. In the design problem considered in previous sections, we assume the product purities were given. In many columns, the purity of one product may be fixed by a maximum impurity specification, but the other product has

no set purity. For example, suppose the propane product is more valuable than the isobutane, and it has a maximum impurity specification of 2 mol% isobutane. We know that distillate flow rate should be maximized and that as much isobutane as possible should be included in this stream, up to the impurity constraint. This can be achieved by minimizing the concentration of propane that is lost in the bottoms. However, reducing x_B requires an increase in reboiler heat input, which increases energy cost. Therefore, there is some value of x_B that maximizes profit. The optimization must take into account the value of the propane product compared with the bottoms and the cost of energy.

The steady-state simulator can be used to find this optimum operating condition. The distillate composition is held constant using a Design Spec/Vary. A value of the bottoms composition is specified in a second Design Spec/Vary, and the simulation is run to find the corresponding reboiler heat input, the distillate flow rate, and the bottoms flow rate. The profit is calculated for this value of x_B by multiplying the price of each product (\$/kg) by its mass flow rate (kg/s), multiplying the price of the feed by its mass flow rate and multiplying the reboiler heat input (MW) by the cost of energy (\$/(MW s)). Profit (\$/s) is defined as the income from the two products minus the cost of the feed minus energy cost. Then, a new value of bottoms composition is specified and the calculations are repeated.

Figure 4.2 shows the results of these calculations using the following parameter values

1. Value of distillate = 0.528 \$/kg
2. Value of bottoms = 0.264 \$/kg
3. Cost of feed = 0.264 \$/kg
4. Cost of energy = \$ 4.7/10⁶ kJ

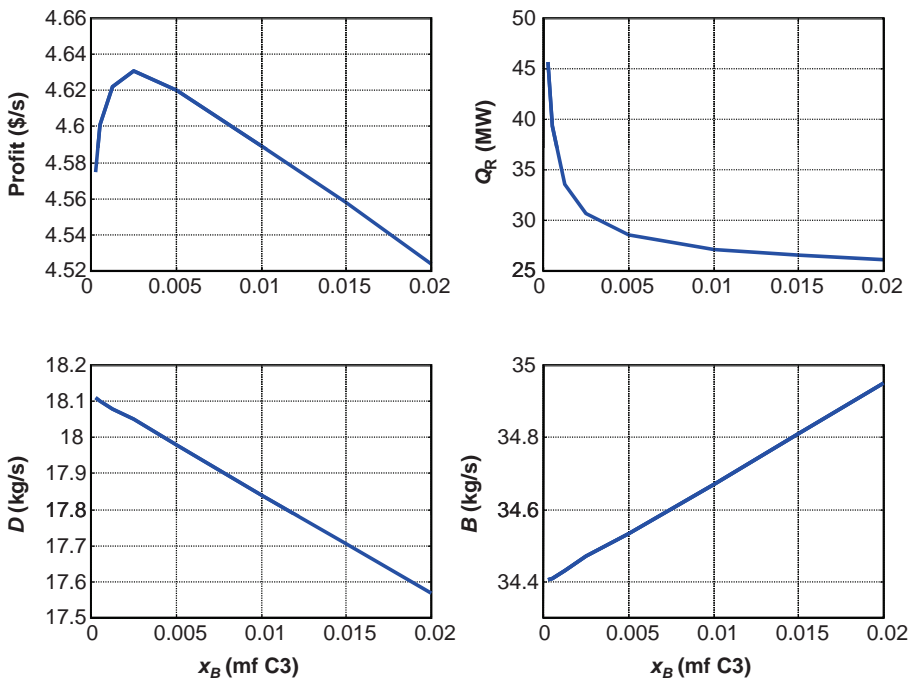


Figure 4.2 Optimum bottoms purity.

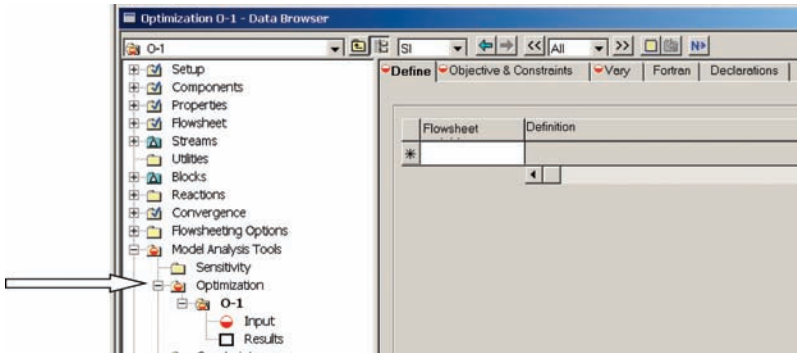


Figure 4.3 Setting up optimization.

As the bottoms composition decreases, the reboiler heat input and the distillate flow rate increase. There is a rapid rise in reboiler heat input below 0.2 mol% propane. The maximum profit is obtained with a bottoms composition of 0.25 mol% propane.

This type of optimization is a “nonlinear programming” (NLP) problem, which can be performed automatically in Aspen Plus. Click *Model Analysis Tools* on the *Data Browser* window and select *Optimization*. Click the *New* button and then *OK* to create an ID. The window shown in Figure 4.3 opens, which has a number of page tabs.

On the *Define* page, the variables to be used in calculating the profit are defined. Type a variable name under the *Flowsheet* label. Figure 4.4 shows that several variables have been entered. The mass flow rates of feed, distillate, and bottoms are FW, DW, and BW in kg/s. Reboiler heat input is Q_R in watts.

Placing the cursor on one of the lines and clicking the *Edit* button open the windows shown in Figure 4.5 on which the information about that variable is specified. For example,

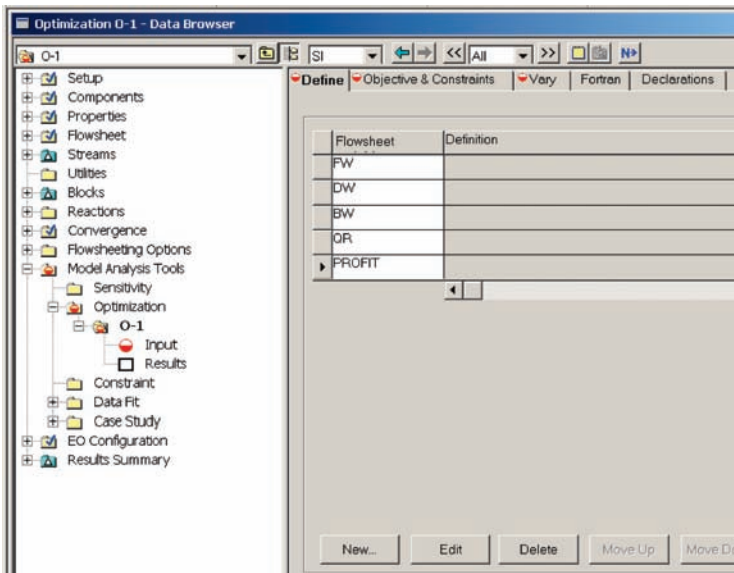
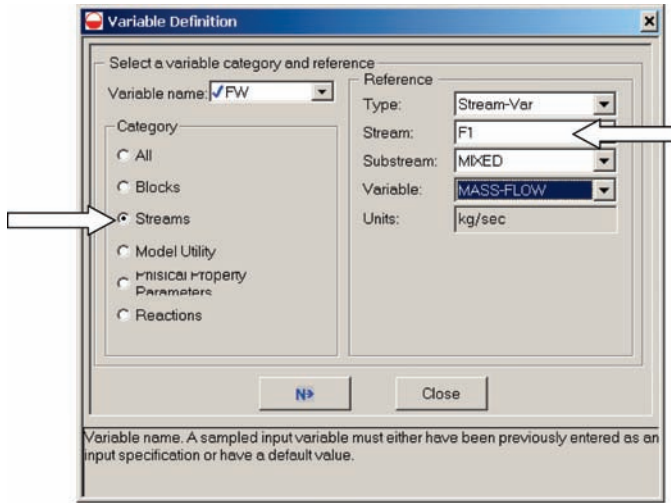
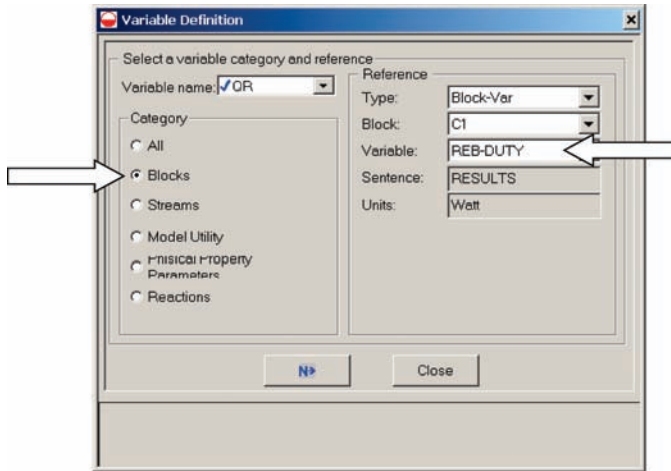


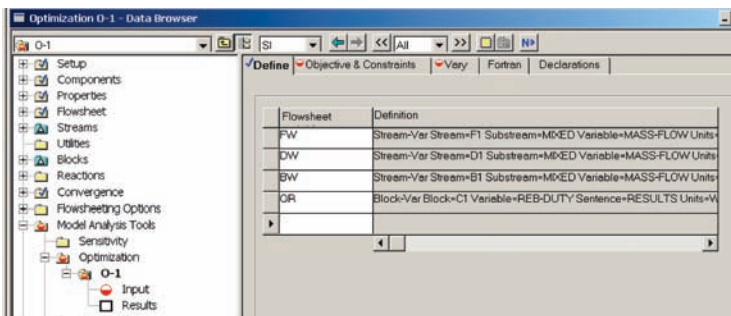
Figure 4.4 Define variables.



(a)



(b)



(c)

Figure 4.5 (a) Editing stream variables. (b) Editing block variable. (c) All variables specified.

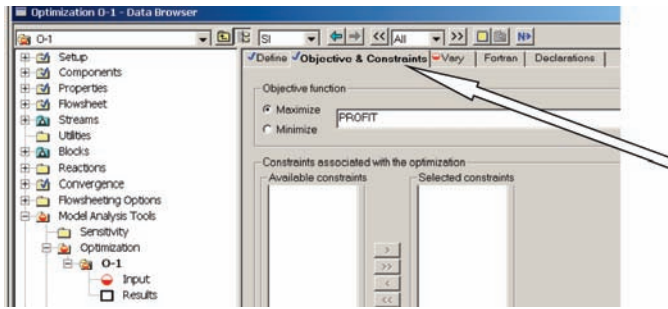


Figure 4.6 Defining the objective function.

FW is edited in Figure 4.5a. Under the *Category* heading, *Stream* is selected. Under the *Reference* heading, the type is *Stream-Var*, the stream is *F1*, and the variable is *Mass-Flow*.

Figure 4.5b shows the editing for the reboiler heat input. Since it is in the C1 block, *Block* under the *Category* heading is selected. Figure 4.5c shows that all variables have been defined. Clicking the *Objectives & Constraints* page tab opens the window shown in Figure 4.6 on which *PROFIT* is specified to be maximized. This variable is defined by clicking the *FORTRAN* page tab and entering the equation for profit as shown in Figure 4.7.

$$\text{PROFIT} = \text{DW} * 0.528 + \text{BW} * 0.264 - \text{FW} * 0.264 - \text{QR} * 4.7e - 9$$

Selecting the final page tab *Vary* opens the window shown in Figure 4.8 in which the variable to be manipulated is defined. The distillate composition is being held constant by manipulating distillate flow using a *Design Spec/Vary*. The variable selected to vary in order to find the maximum profit is the reflux ratio. When the window first opens, the box to the right of *Variable number* is blank. Right clicking opens a little window with *Create* that can be selected. Then, the variable *MOLE-RR* is selected in block C1, and limits on its possible range are inserted.

The optimizer is now ready to run. Clicking the *N* button executes the program. The *Control Panel* window (Fig. 4.9) shows that the optimizing algorithm is *SQP* (sequential quadratic programming) and it took four iterations to find the maximum profit. The

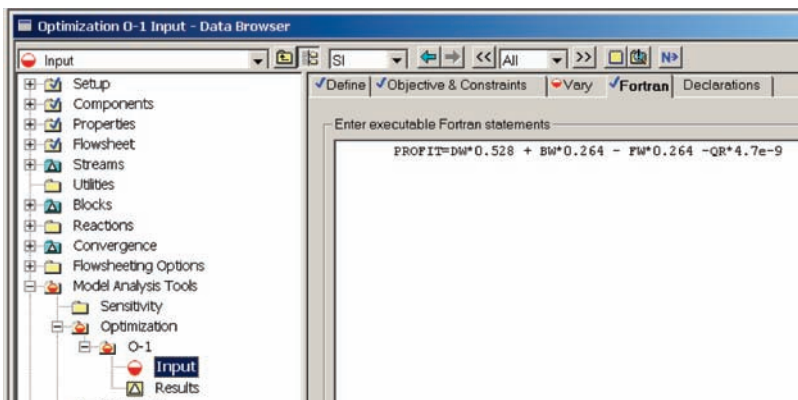


Figure 4.7 Equation for profit.



Figure 4.8 Specifying reflux ratio to vary.

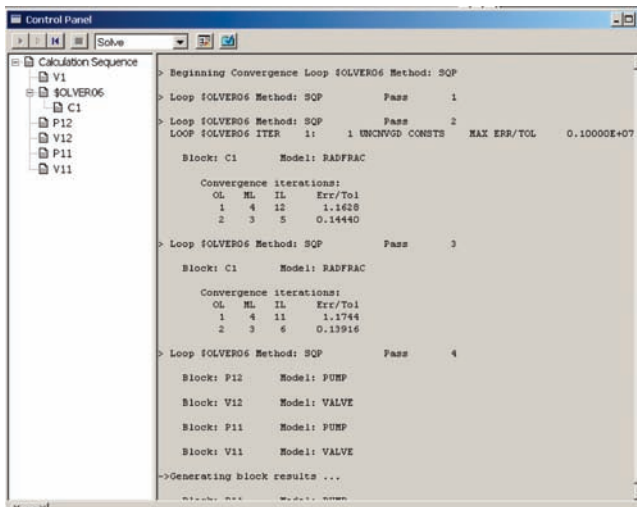


Figure 4.9 Control panel results.

resulting values of the variables can be seen by clicking *Results* (see Figure 4.10) and by looking at the stream results in the C1 block.

The optimum value of bottoms composition is 0.2246 mol% propane, which gives distillate and bottoms flow rates of 18.05 and 34.46 kg/s, respectively. The reboiler heat input is 27.17 MW. The profit is \$4.637/s.

4.5 OPTIMUM PRESSURE FOR VACUUM COLUMNS

Many separations are favored by lower temperatures, so conventional distillation wisdom recommends operating at the lowest pressure permitted by the use of cooling water in the condenser. Therefore, many columns are designed for 120 °F reflux-drum temperatures. If the components going overhead in the distillate are fairly high boiling, the column could operate under vacuum conditions.

Variable	Initial value	Final value	Units
FW	52.512648	52.512648	KG/SEC
DW	18.0527529	18.0527529	KG/SEC
BW	34.4598951	34.4598951	KG/SEC
DR	31050874.6	31050874.6	WATT

Figure 4.10 NLP optimization results.

Energy would be saved and a lower-temperature less-expensive heat source could be used as pressure is lowered. However, there are competing effects that must be considered. Vapor density decreases as pressure is lowered, so the diameter of the column increases, which increases capital cost. In addition, the lower pressure means lower reflux-drum temperature, which decreases the heat-transfer differential temperature-driving forces in the condenser. This results in more heat-transfer area being required, which increases capital cost. Therefore, an economic analysis is required to find the best balance between these effects.

To illustrate the problem, a column from the MMH (2-methoxy-2-methylheptane) process is considered. This process involves the reaction of methanol with 2-methyl-1-heptene (MH) to form MMH. The distillate is mostly MH with a small amount of methanol. The normal boiling point of MH is 392.2 K, so operation at vacuum conditions is possible if there is an advantage to do so. Operating at 0.6 atm gives a base temperature of 420 K, which requires *medium-pressure* steam (457 K at \$8.22/GJ). The reboiler energy at 0.6 atm is 0.9793 MW. The diameter of the column is 1.929 m.

Running at 0.4 atm reduces the base temperature to 410 K, which permits the use of *low-pressure* steam (433 K at \$7.78/GJ). In addition, the reboiler energy requirement drops to 0.9147 MW. However, the diameter of the column increases to 2.044 m because of the lower vapor density at the lower pressure. This increases the capital cost of the vessel. In addition, the required condenser area increases rapidly as pressure is reduced because of the smaller temperature differential driving force. This also increases capital costs. Table 4.4 gives results over a range of pressures for Column C2. Operation at 0.4 atm gives the smallest TAC.

TABLE 4.4 Effect of Pressure

Column C2 pressure (atm)	0.2	0.3	0.4	0.5	0.6
Q_R (MW)	0.8432	0.8799	0.9147	0.9475	0.9793
T_R (K)	399	405	410	416	420
Q_C (MW)	2.655	2.599	2.558	2.527	2.527
T_C (K)	339	350	358	365	365
A_C (m ²)	163.7	101.5	78.45	65.79	57.82
Diameter (m)	2.484	2.217	2.044	1.929	1.929
Capital (10 ⁶ \$)	0.9818	0.851	0.7792	0.7336	0.7066
Energy (10 ⁶ \$/year)	0.2069 (LP)	0.2159 (LP)	0.2244 (LP)	0.2456 (MP)	0.2539 (MP)
TAC (10 ⁶ \$/year)	0.5342	0.4995	0.4842	0.4902	0.4894

4.6 CONCLUSIONS

Several types of distillation optimizations have been considered in this chapter. The approaches presented are simple and practical. There are many advanced techniques in the optimization area that are beyond the scope of this book.

CHAPTER 5

MORE COMPLEX DISTILLATION SYSTEMS

In the example distillation system considered in Chapters 3 and 4, we studied the binary propane/isobutane separation in a single distillation column. This is a fairly ideal system from the standpoint of vapor–liquid equilibrium (VLE), and it has only two components, a single feed and two product streams. In this chapter, we will show that the steady-state simulation methods can be extended to multicomponent nonideal systems and to more complex column configurations.

Many chemical systems exhibit nonideal vapor–liquid behavior in which azeotropes produce distillation boundaries that necessitate the use of more complex distillation configurations to achieve a separation. The use of ternary diagrams provides very useful insight into the design of these complex systems. There are several methods for handling azeotropes. Three examples are discussed in this chapter: extractive distillation, heterogeneous azeotropic distillation, and pressure-swing azeotropic distillation. The final complex example studied in this chapter is heat-integrated distillation, in which the pressures and temperatures in two columns are adjusted so that the condenser of a high-temperature column can be used as the reboiler in a low-temperature column. This configuration is called “multieffect distillation.”

5.1 EXTRACTIVE DISTILLATION

An example of extractive distillation is the separation a binary mixture of acetone and methanol. These two components form a binary homogeneous minimum-boiling azeotrope. The normal boiling points of acetone and methanol are 329 and 338 K, respectively, so acetone is the light-key component. The boiling point of the azeotrope (328 K) is lower than the boiling point of the pure light component. The composition of the acetone/methanol

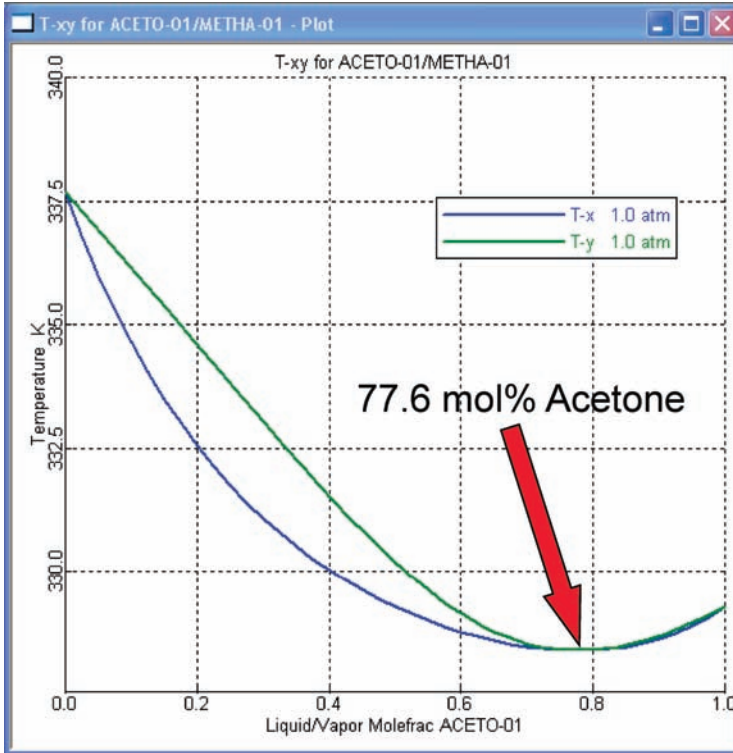


Figure 5.1 Txy diagram for acetone/methanol at 1 atm.

azeotrope is 77.6 mol% acetone at atmospheric pressure, as shown in the Txy diagram given in Figure 5.1.

The components can be separated by using a two-column extractive distillation system and an extractive solvent that alters the phase equilibrium. The fresh feed of acetone and methanol is fed into the first column near the middle. An appropriate solvent, which is less volatile than the two key components, is fed near the top of this extractive column. Depending on the properties of the solvent, one of the key components is preferentially absorbed in the solvent and leaves in the bottoms stream. The other component goes overhead as a high-purity product. The bottoms stream is fed to a solvent recovery column that removes the solvent from the bottom for recycling back to the extractive column. The distillate is a high-purity product stream of the other key component. Figure 5.2 gives the flowsheet of a typical two-column extractive distillation system with solvent recycle.

In the numerical example studied in this section, the solvent is dimethyl sulfoxide (DMSO) whose boiling point (465 K) is much higher than either of the key components. It preferentially attracts methanol, so the bottoms from the extractive column is essentially a binary mixture of methanol and DMSO with a very small amount of impurity acetone.

Figure 5.3 gives the ternary diagram for the system. The acetone/methanol binary azeotrope is shown on the ordinate axis. The residue curves originate from this minimum-boiling azeotrope and move to the heaviest component DMSO corner. Figure 5.4 shows the location of the distillate (D) and bottoms (B) products. The straight “component-balance

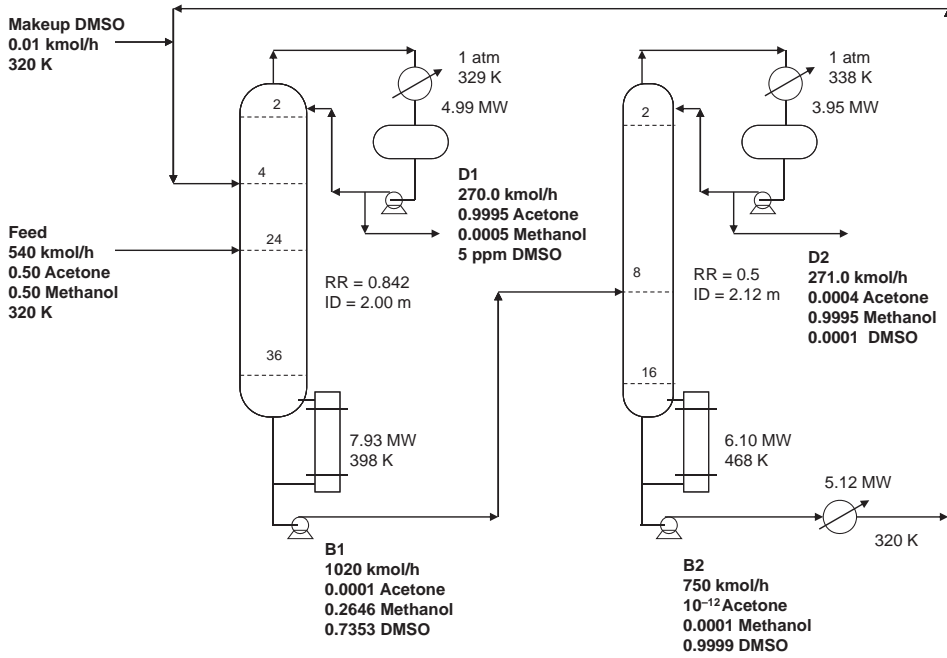


Figure 5.2 Acetone/methanol extractive distillation with DMSO solvent.

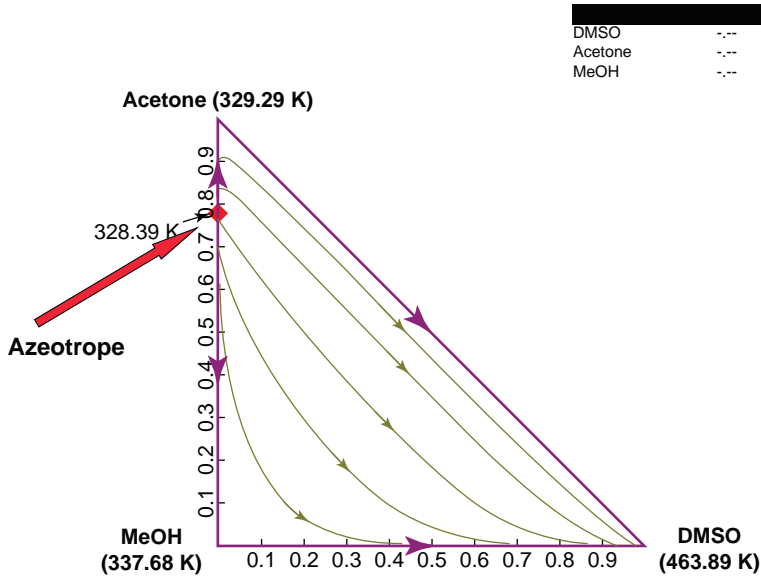


Figure 5.3 Acetone/methanol/DMSO diagram.

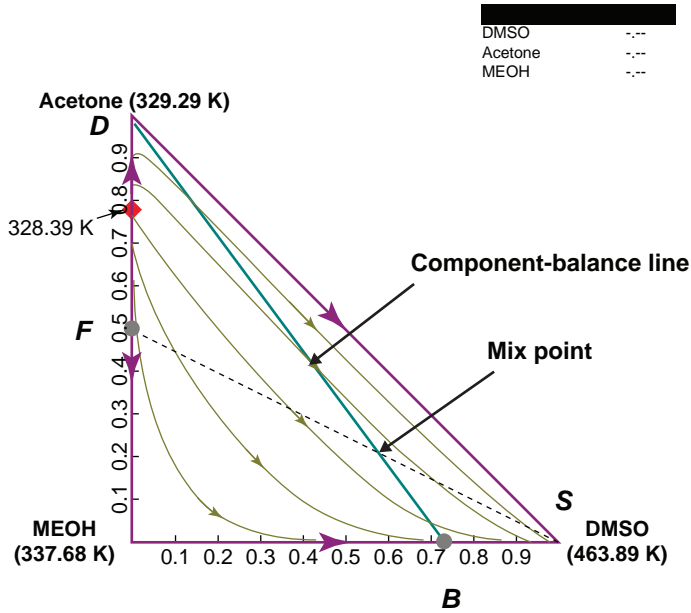


Figure 5.4 Ternary diagram with feed and product points.

line” passes through the “mix” point, which is the molar composition average of the fresh binary feed (*F*) and the solvent (*S*) with their respective flow rates.

Figure 5.5 gives the *Txy* diagram for methanol/DMSO, which indicates an easy separation in the solvent recovery column. As shown in Figure 5.2, the column only requires 17 stages and runs with a low reflux ratio (RR=0.5). The Uniquac physical property package in Aspen Plus is used.

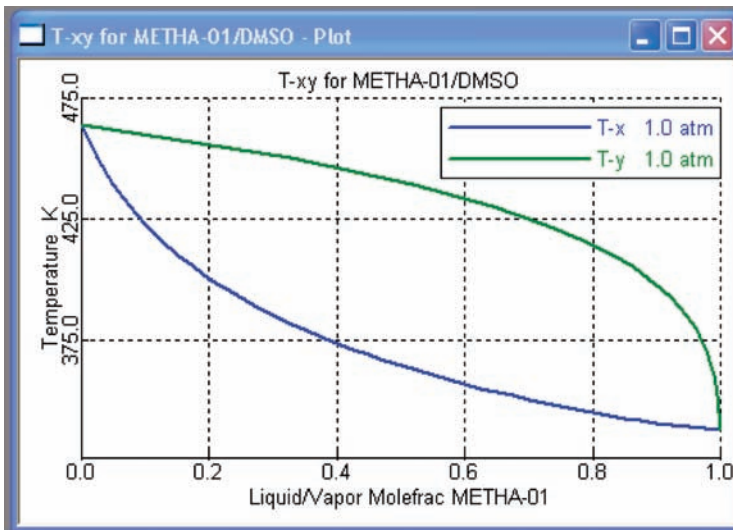


Figure 5.5 *Txy* diagram for methanol with DMSO.

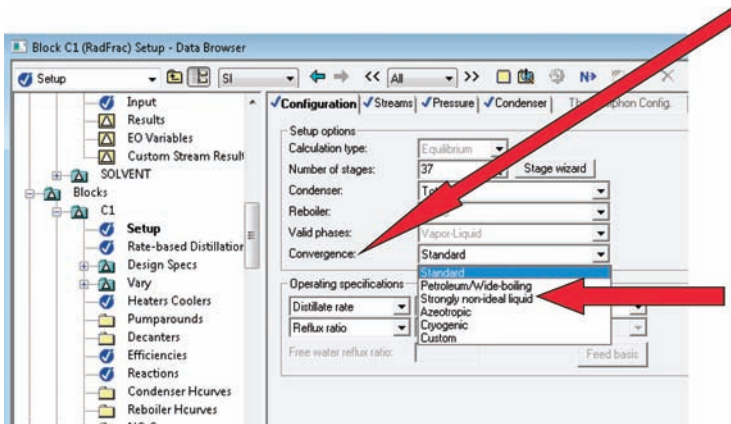


Figure 5.6 Selecting nonideal convergence method.

The phase equilibrium is far from ideal in this system, so it may be necessary to use an alternative convergence method in the columns. Figure 5.6 shows that the “Standard” convergence method can be changed to “Azeotropic” or “Strongly nonideal liquid” to improve convergence. Another adjustment that is often necessary is to change the maximum number of iterations. The default is 25. This can be increased by clicking the *Convergence* item under the column block (see Fig. 5.7) and entering a larger number.

5.1.1 Design

The design of an extractive distillation system with azeotropes is more complex than a single column with ideal VLE. The extractive system has an additional degree of freedom, the solvent-to-feed ratio. Obviously if no solvent is used, the separation is unattainable because of the azeotrope. If a very large amount of solvent is used, the sizes of the columns and their energy consumptions are very large. Therefore, we must find the solvent-to-feed ratio (S/F) that is just large enough to achieve the desired purity. Solvent flow rate affects

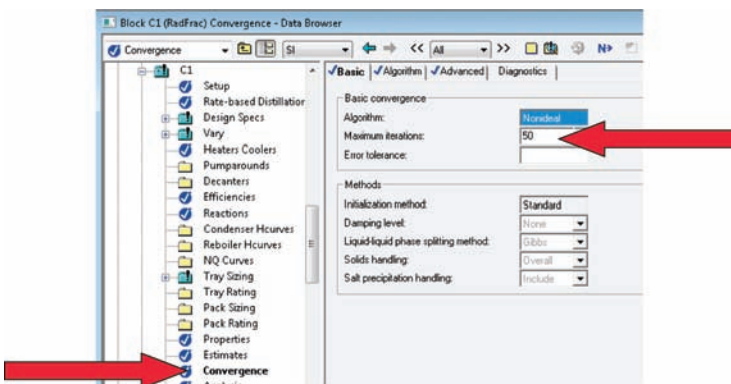


Figure 5.7 Setting number of iterations.

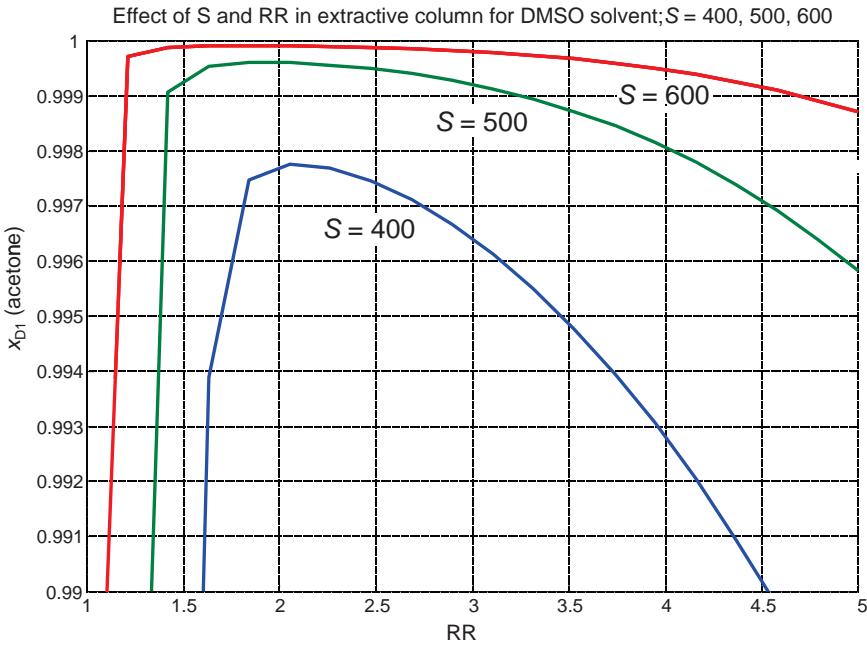


Figure 5.8 Effect of RR and solvent on acetone product purity with DMSO solvent.

the purity of the distillate product from the extractive column. Figure 5.8 gives results for the system studied. More solvent flow rate reduces the impurity of methanol in the distillate, which is supposed to be high-purity acetone. So the S/F ratio that satisfies the distillate specification must be selected.

Notice that there is a very interesting nonmonotonic effect of reflux ratio on the curves shown in Figure 5.8. Too little or too much reflux adversely affects product purity. This behavior is not seen in regular distillation in which increasing reflux ratio always increases product purity. This phenomenon in extractive distillation is easily explained. If too little reflux is used, more of the heavy solvent goes overhead and lowers distillate acetone purity. If too much reflux is used, the acetone-rich reflux dilutes the concentration of DMSO inside the column, which lets more methanol go overhead. These effects are illustrated in Figure 5.9. These results are generated holding a bottoms composition in the extractive column of 0.01 mol% acetone so that the desired high purity of the methanol leaving in the distillate of the solvent recovery column can be attained. Any acetone that enters the second column must go overhead and nothing can be done in the second column to affect distillate purity in terms of acetone.

So there are two vital design parameters that must be determined in extractive distillation: the solvent-to-feed ratio and the reflux ratio. The three graphs given in Figures 5.8 and 5.9 show the effects of solvent-to-feed ratio and reflux ratio on the composition of the distillate from the extractive column: solvent impurity (DMSO), heavy-key impurity (methanol), and light-key purity (acetone). They provide the basis for designing an extractive distillation system.

In the numerical example, the feed is 540 kmol/h of 50/50 mol% acetone/methanol. Both columns operate at atmospheric pressure, which is high enough to permit the use of

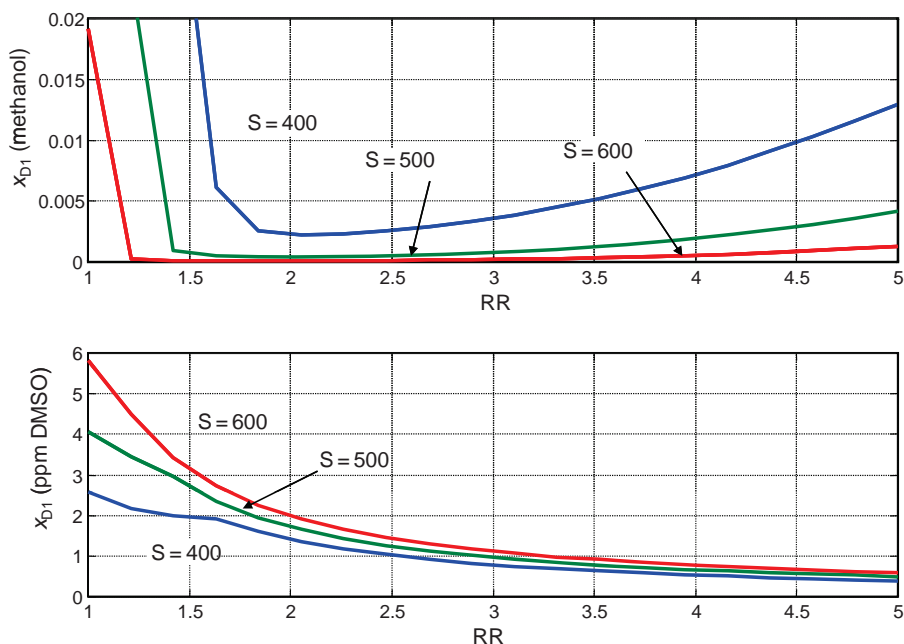


Figure 5.9 Effect of RR and S on impurities in acetone product with DMSO solvent.

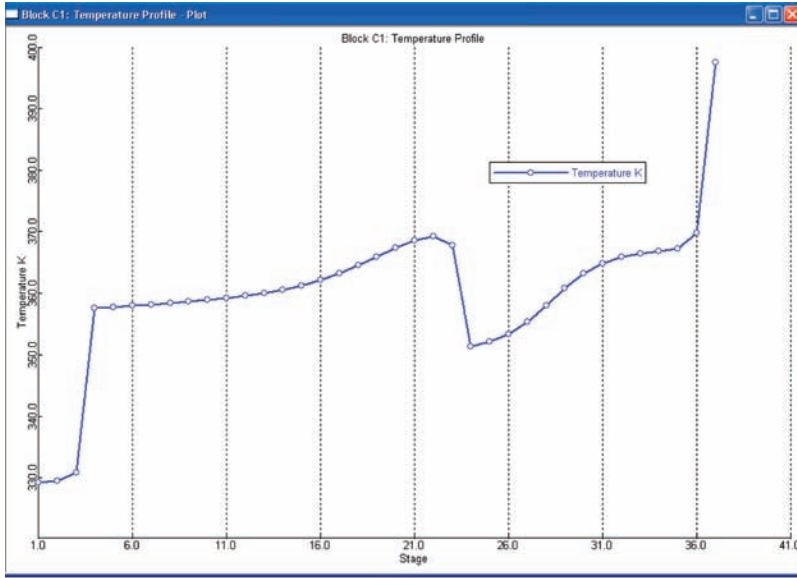
cooling water in the condensers. The Aspen “*Design Spec/Vary*” feature is used to drive overhead and bottoms compositions to their desired values by manipulating distillate flow rate and reflux ratio. Solvent flow rate is fixed at a level high enough to achieve the specified product purities.

The acetone product and the methanol product are specified to be 99.95 mol% pure. Figure 5.8 shows that this high-purity acetone can be achieved if the solvent flow rate is >500 kmol/h. The solvent rate used in flowsheet shown in Figure 5.2 is 750 kmol/h, which gives a S/F ratio of 1.39. Figure 5.10 gives temperature and composition profiles for both columns. The shape of the temperature profile in the extractive column is quite unusual. It is not obvious what stage to use for temperature control. We return to this issue in the development of a control structure for this system later in this book.

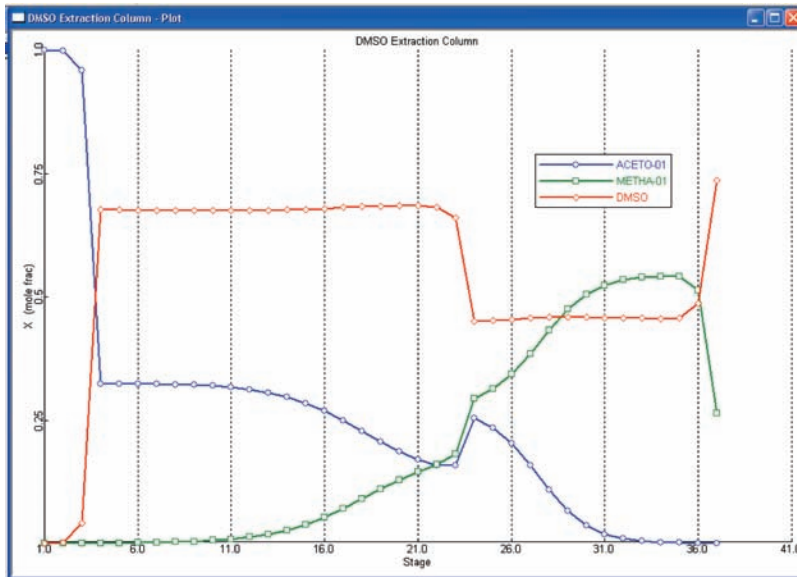
5.1.2 Simulation Issues

The simple single column considered in Chapter 2 had no recycle streams since there was only a single unit. In this extractive distillation column, the design of the first column depends on the bottoms from the second column. Therefore, we must worry about converging this recycle loop.

A simple approach to this problem is to set up the flowsheet without the recycle connect. This is called “tearing” the recycle (see Fig. 5.11). We do not know exactly what the bottoms from the methanol column will be nor do we know exactly how much makeup DMSO will be required to make up for the very small losses in the product streams. However, in this particular system, we can get a fairly accurate estimate of how much DMSO is lost in the two product streams. The flowsheet shown in Figure 5.2 shows about

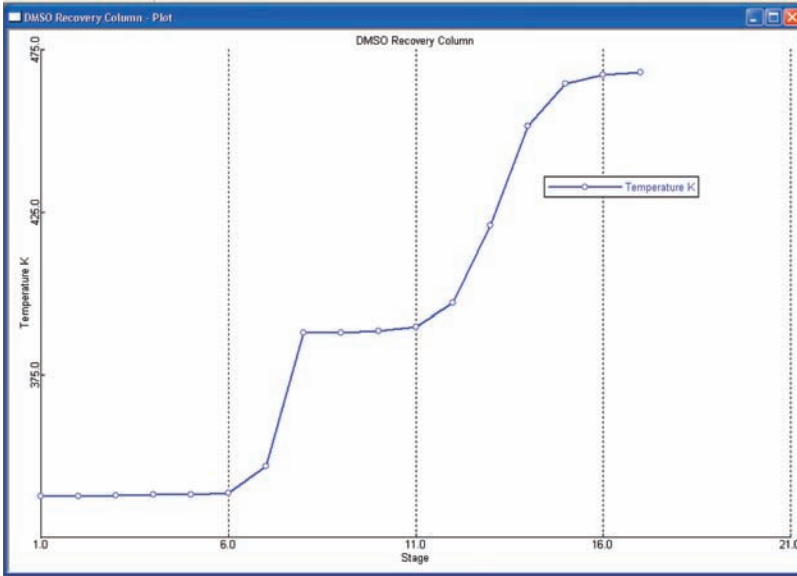


(a)

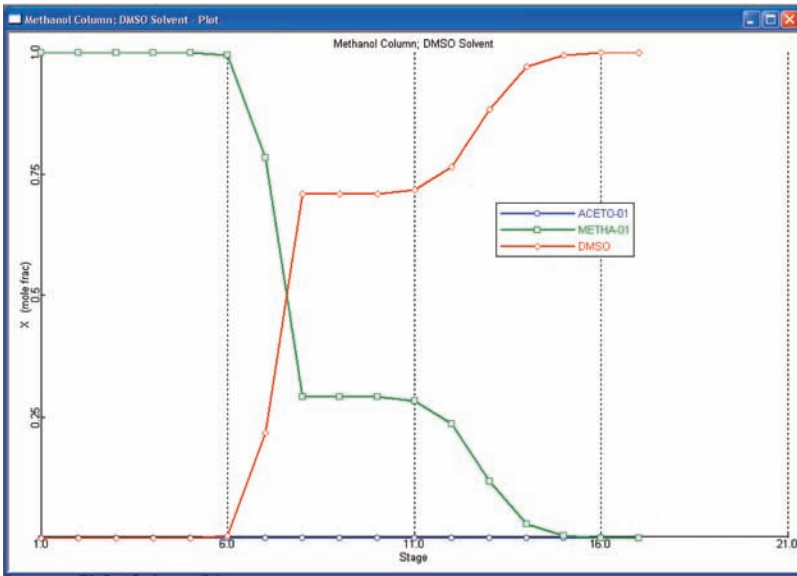


(b)

Figure 5.10 (a) Extractive column temperature profile: DMSO solvent. (b) Extractive column composition profiles: DMSO solvent. (c) Methanol column temperature profile: DMSO solvent. (d) Methanol column composition profiles: DMSO solvent.



(c)



(d)

Figure 5.10 (Continued)

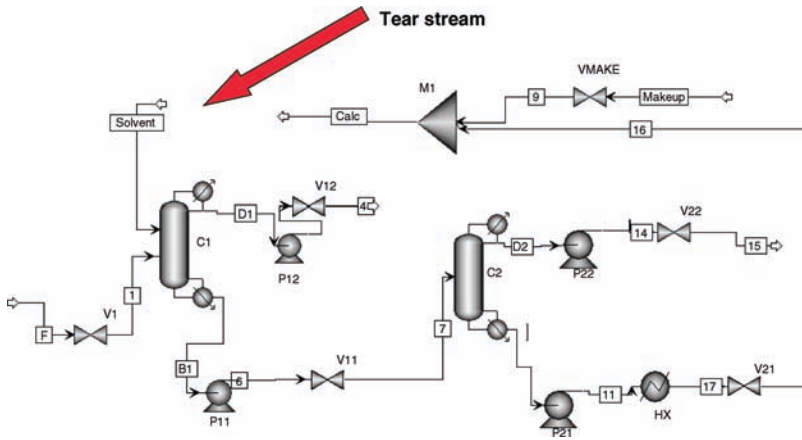


Figure 5.11 Solvent stream torn.

0.00275 kmol/h of DMSO impurity in the distillate of the extractive column and 3.64×10^{-14} kmol/h of DMSO in the distillate of the solvent recovery column. So we specify a makeup flow rate of 0.00275 kmol/h.

Then the “CALC” stream in Figure 5.11 is deleted, and the source of the “SOLVENT” stream is reconnected to the output of the mixer “M1” as shown in Figure 5.12. Before clicking the N button, go to the *Convergence* item in the Data Browser (see Fig. 5.13) and select the “SOLVENT” stream as a *Tear* stream. The system converges in two iterations using the default Wegstein convergence method.

Converging the recycle in this system is easy. In general, this will not be true. The heterogeneous azeotropic system studied in the next section illustrates some of these difficulties. A more robust method for converging recycle will be discussed.

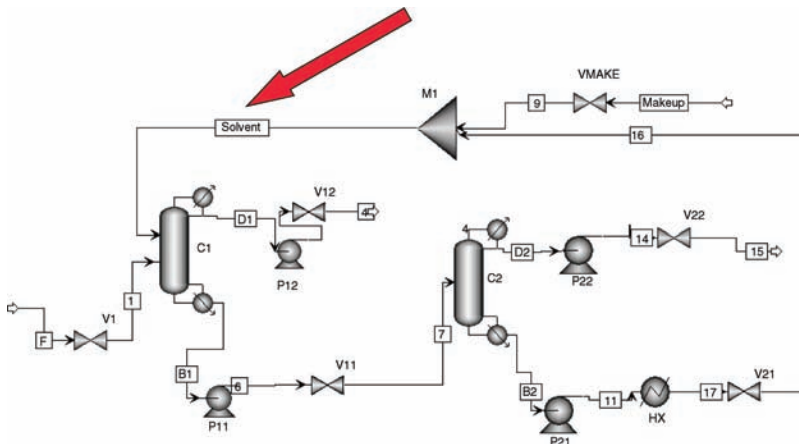


Figure 5.12 Solvent stream connected.

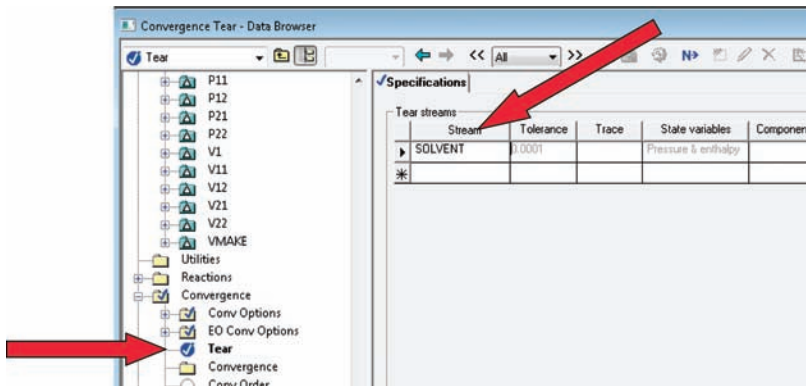


Figure 5.13 Tear stream defined.

5.2 ETHANOL DEHYDRATION

For our second nonideal system, we look at a process that has extremely nonideal VLE behavior and has a complex flowsheet. The components involved are ethanol, water, and benzene. Ethanol and water at atmospheric pressure form a minimum-boiling homogeneous azeotrope at 351 K of composition 90 mol% ethanol. Much more complexity is introduced by the benzene/water system, which forms two liquid phases with partial miscibility. The flowsheet contains two distillation columns and a decanter. There are two recycle streams, which create very difficult convergence problems as we will see. So this complex example is a challenging simulation case.

The origins of the example go back over a century when a process to produce high-purity ethanol was needed. Ethanol is widely produced in fermentation processes. A typical mixture from a fermentation process has very low ethanol concentrations (4–6 mol%). If this mixture is fed to a distillation column operating at atmospheric pressure, high-purity water can be produced out at the bottom, but the ethanol purity of the distillate cannot exceed 90 mol% because of the azeotrope.

Some ingenious engineers came up with the idea of running the fermentation liquid through a conventional “preconcentrator” distillation column that takes most of the water out at the bottom and produces a distillate that is perhaps 84 mol% ethanol and 16 mol% water. This binary stream is then fed into a second distillation column. A reflux stream that contains a high concentration (80 mol%) of benzene is fed to the top of this column. The benzene serves as a “light entrainer” that goes overhead and preferentially takes water with it because the large dissimilarity between water and benzene makes the water very volatile. The ethanol goes out at the bottom of this column, despite the fact that water is the “heavier” key component (normal boiling point of ethanol is 351.5 K whereas that of water is 373.2 K).

The overhead vapor is a ternary mixture of all three components. When it is condensed, the repulsion between the water molecules and the organic benzene molecules is so great that two liquid phases form. The reflux drum becomes a decanter. The lighter organic liquid phase is pumped back to the column as organic reflux. The heavier aqueous phase contains significant amounts of ethanol and benzene, so it is fed to a second distillation column in which the water is removed in the bottoms stream. The distillate stream is recycled back to the first column. Figure 5.14 gives the flowsheet of the process with the azeotropic column C1, the decanter and the column C2.

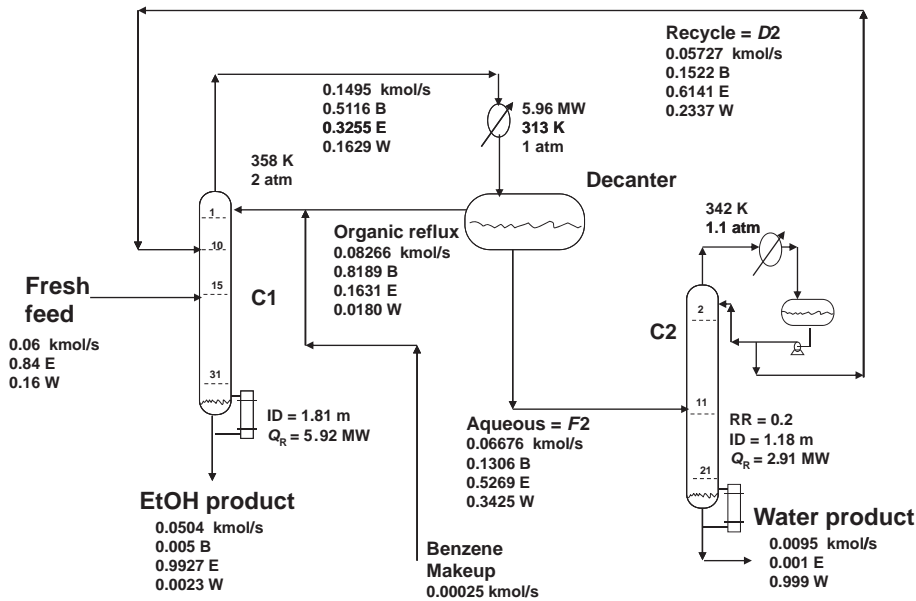


Figure 5.14 Flowsheet of heterogeneous azeotropic process.

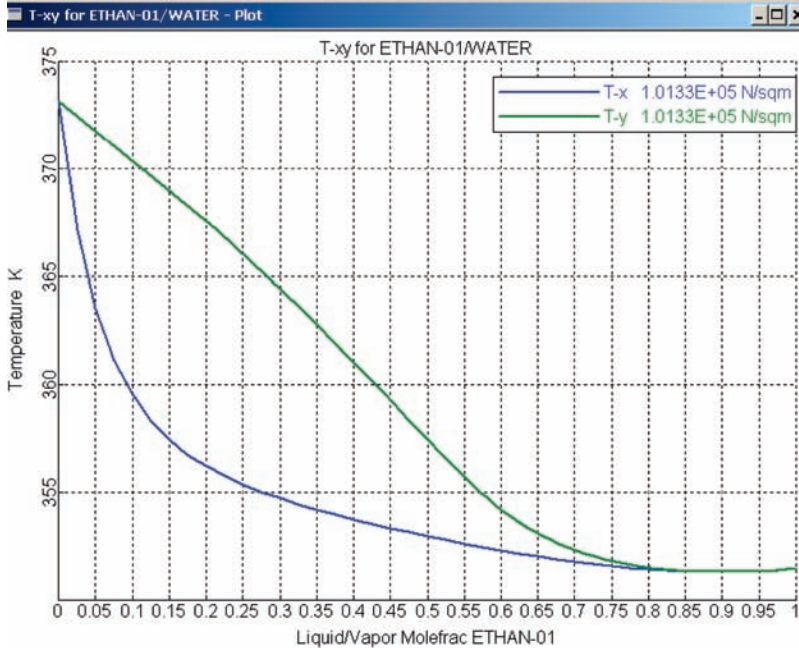
The first item to explore is the complex vapor–liquid–liquid equilibrium (VLLE) of this heterogeneous vapor–liquid–liquid system.

5.2.1 VLLE Behavior

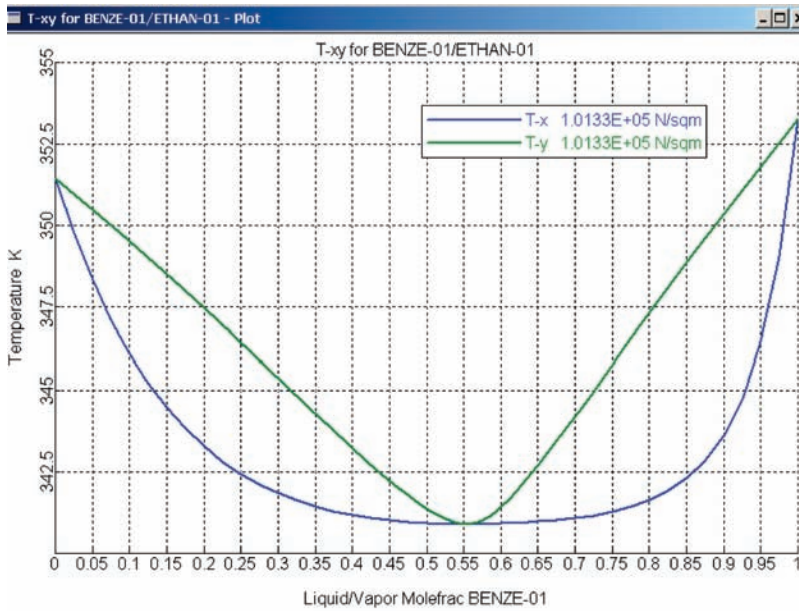
The phase equilibrium is described by the Uniquac physical property package. Two binary T_{xy} diagrams are given in Figure 5.15a and b. The two homogeneous minimum-boiling azeotropes are clearly shown. The ternary diagram (Fig. 5.16) is generated using Aspen *Conceptual Design* as described earlier in Chapter 1. A large part of the composition space has two liquid phases. The liquid–liquid equilibrium tie-lines are shown. The aqueous phase is on the left and the organic phase is on the right.

Figure 5.17 gives the report of all of the azeotropes in this very nonideal VLLE system. Notice that the ternary azeotrope is heterogeneous and has the lowest boiling point (337.17 K) of any of the azeotropes and the pure components. This means that the overhead vapor from the first column will have a composition that is similar to this azeotrope. Notice also that the diagram is split up into three regions by the distillation boundaries that connect the four azeotropes. As you recall from Chapter 1, these boundaries limit the separation that is attainable in a single column. The bottoms and distillate points must lie in the same region.

It may be useful at this point to locate on the ternary diagram several points (see Fig. 5.18), so that we can get a preliminary feel for the design problem we are facing. The feed has a composition 0/84/16 mol% benzene, ethanol, water (B/E/W). So the F point is located on the ordinate axis in region labeled Region 1 in Figure 5.16. One of the desired products is very pure water, which is located at the bottom left corner in Region 1. However, the other desired product is very pure ethanol, which is located at the top corner in Region 2. This is on the other side of a distillation boundary, so the separation cannot be achieved in a single simple distillation column. The decanter and the second column are



(a)



(b)

Figure 5.15 (a) Txy diagram for ethanol/water. (b) Txy diagram for ethanol/benzene.

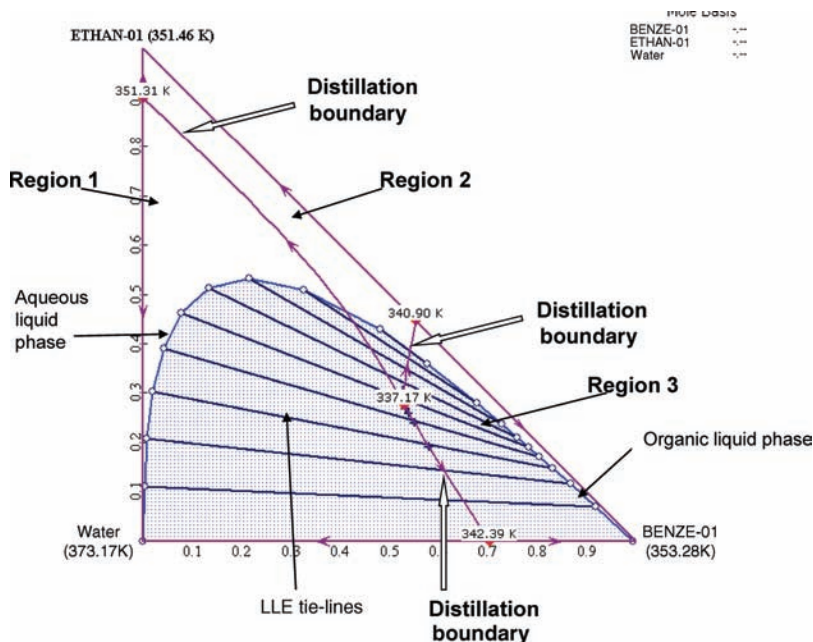


Figure 5.16 Ternary diagram.

01	Number Of Components: 2 Homogeneous		Temperature 340.90 K Classification: Saddle	
		MOLE BASIS	MASS BASIS	
	BENZE-01	0.5543	0.6783	
	ETHAN-01	0.4457	0.3217	

02	Number Of Components: 3 Heterogeneous		Temperature 337.17 K Classification: Unstable Node	
		MOLE BASIS	MASS BASIS	
	BENZE-01	0.5306	0.7194	
	ETHAN-01	0.2749	0.2198	
	WATER	0.1945	0.0608	

03	Number Of Components: 2 Heterogeneous		Temperature 342.39 K Classification: Saddle	
		MOLE BASIS	MASS BASIS	
	BENZE-01	0.7024	0.9110	
	WATER	0.2976	0.0890	

04	Number Of Components: 2 Homogeneous		Temperature 351.31 K Classification: Saddle	
		MOLE BASIS	MASS BASIS	
	ETHAN-01	0.8999	0.9583	
	WATER	0.1001	0.0417	

Figure 5.17 Report of azeotropes.

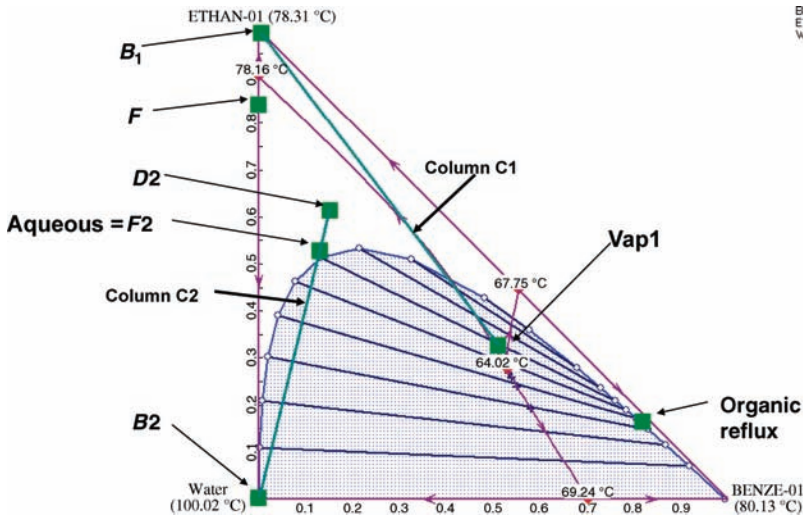


Figure 5.18 Ternary diagram with streams located.

added so that the distillation boundary can be crossed. Column C1 has three feed streams (the binary fresh feed F , organic reflux and distillate from Column C2). These are all combined to produce a “mix point” that is in (or near) Region 2 in the ternary diagram.

Now that the complexity of the VLLE is apparent, let us develop a simulation of a flowsheet to produce high-purity ethanol and water. The flowsheet will have two distillation columns and a decanter. There are two recycle streams back to the first column: organic phase from the decanter and distillate from the second column.

5.2.2 Process Flowsheet Simulation

The first column does not have a condenser, so the appropriate “stripper” icon is selected from the many possible types under *RadFrac*, as shown in Figure 5.19. The three streams fed to this column are added with control valves. The stream *Feed* is specified to be 0.06 kmol/s with a composition of 84 mol% ethanol. The other two streams fed to column C1 are unknown. We must make some reasonable guesses of what the flow rates and the compositions of the organic reflux and the recycle from the top of the second column will be.

One way to estimate these compositions is to recognize that the overhead vapor from the first column will have a composition that is close to the ternary azeotrope: 53.06/27.49/19.45 mol% (B/E/W). We set up a simulation with a stream with this composition feeding a decanter operating at 313 K. The predicted compositions of the organic and aqueous liquid phases are

Composition (mol%)	Organic	Aqueous
Benzene	84.35	7.24
Ethanol	14.14	47.04
Water	1.51	45.72

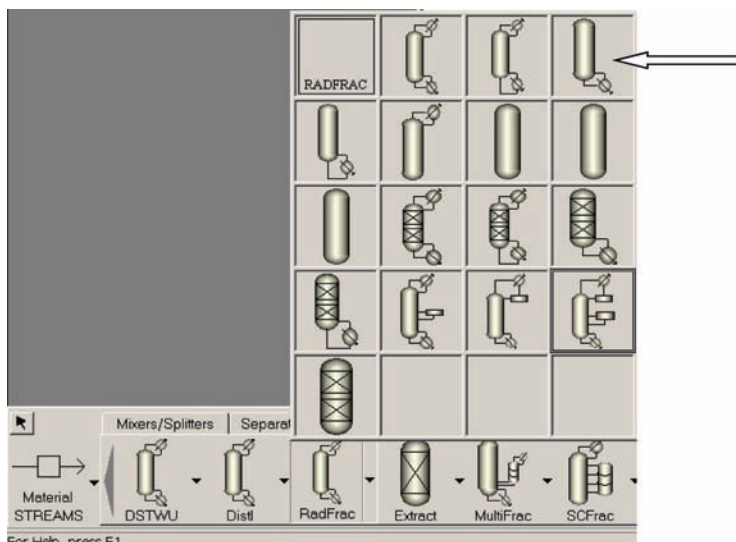


Figure 5.19 Selecting a stripper column.

The composition of the organic reflux should be close to the composition of the organic liquid phase. The composition of the feed to the second column should be close to the composition of the aqueous liquid phase. As essentially all the water in the feed comes out at the bottom of the second column at a high purity, the amount of water removed from the feed is only $(0.06 \text{ kmol/s})(0.16) = 0.0096 \text{ kmol of water/s}$. Therefore, as a first estimate, we can use the composition of the aqueous liquid phase for a guess of the recycle composition.

The next issue is guessing the flow rates of the reflux and the recycle. One brute-force way to do this is to guess a recycle flow rate and then find the flow rate of organic reflux to column C1 that is required to keep water from leaving in the bottoms. When this is achieved, the resulting aqueous phase is fed to the second column, and the calculated distillate $D2$ is compared with the guessed value of recycle (both in flow rate and composition). The composition of the organic phase from the decanter is also compared with the guessed composition. Compositions are adjusted and a new guess of the recycle is made.

The simulation of the first column is extremely tricky, as we demonstrate below. A very small change in the organic reflux can produce a drastic change in the product compositions. Multiple steady states also occur: the same reflux flow rate can give two different column profiles and product compositions.

The number of stages in column C1 is set at 31. Notice that because there is no condenser, the top tray is Stage 1. Organic reflux is fed at the top. Recycle is fed at Stage 10. Fresh feed is fed at Stage 15. Column pressure is set at 2 atm because we need a control valve on the overhead vapor line.

The vapor from column C1 goes through a valve V12 and to a heat exchanger HX . The conditions specified in HX block on the *Input* item (Fig. 5.20) are the exit temperature of 313 K and a 0.1 atm pressure drop (entering a negative number for *Pressure* means a pressure drop).

A decanter is then inserted on the flowsheet by clicking on *Separator* at the bottom of the window and selecting *Decanter*, as shown in Figure 5.21a. The operation of the

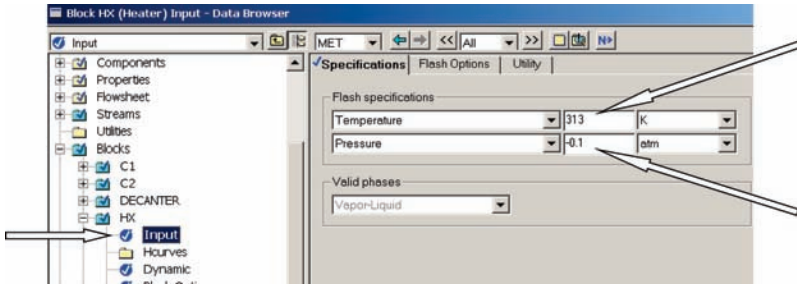
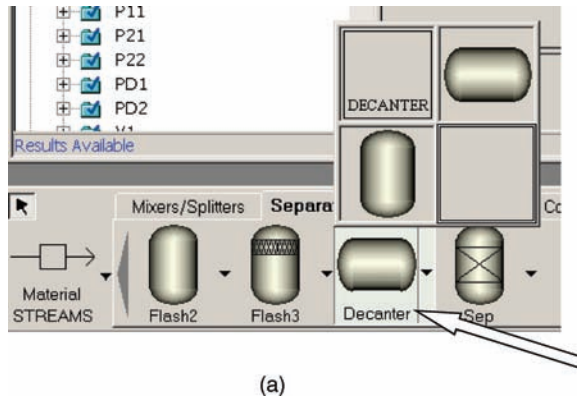
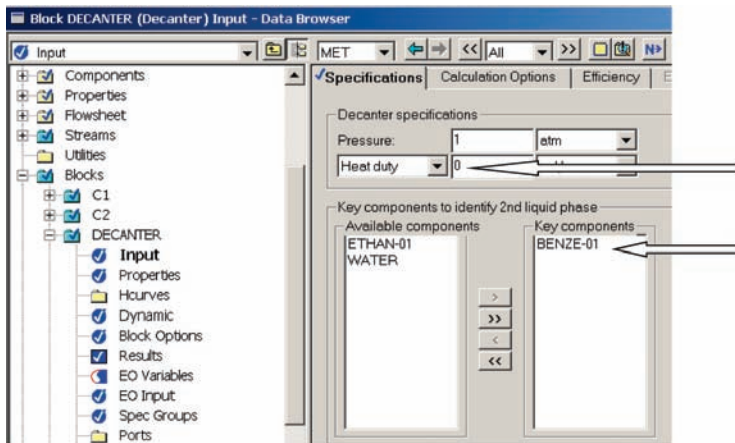


Figure 5.20 Heat exchanger specifications.



(a)



(b)

Figure 5.21 (a) Inserting a decanter. (b) Specifying conditions in the decanter.

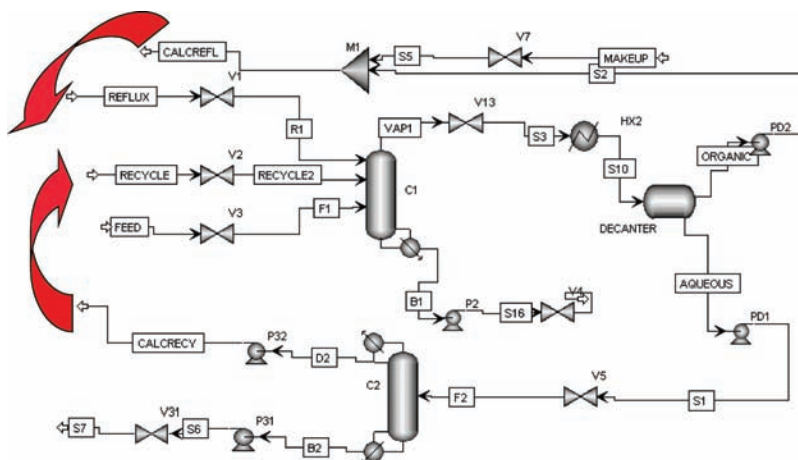


Figure 5.22 Full flowsheet with recycles torn.

decanter is specified by clicking the *Input* item under the Decanter block. The pressure is set at 1 atm and adiabatic operation is selected (heat duty is zero as shown in Fig. 5.21b). Under the item *Key components to identify second liquid phase*, the benzene component is specified by moving benzene into the right *Key components* window (see Fig. 5.21b).

A very small amount of benzene will be lost in the two product streams, so a small makeup stream of fresh benzene is added to the organic phase from the decanter before it is fed to the first column as reflux.

Finally, a second column C2 is added in the normal way. A 22-stage column is specified with feed on Stage 11 and operating at 1 atm. The final flowsheet with all the pumps and valves installed is shown in Figure 5.22. Note that neither of the recycles streams is connected. The two streams that we have made some initial guesses of flow rates and compositions are “REFLUX” and “RECYCLE.” The two streams that have been calculated and should be approximately the same as these two are “ORGREF” and “D2CALC.”

5.2.3 Converging the Flowsheet

The fresh feed is 0.06 kmol/s with a composition of 84 mol% ethanol and 16 mol% water. Essentially, all the ethanol must come out in the bottoms *B1* from the first column. So in the setup of this column, a bottoms flow rate is fixed at $(0.06)(0.84) = 0.0504$ kmol/s. This column only has one degree of freedom because it has no condenser or internal reflux. The organic reflux will eventually be adjusted to achieve the desired purity of the ethanol bottoms product (99.92 mol% ethanol). Note that both benzene and water can appear in the bottoms as impurities.

Similarly, essentially all the water must come out in the bottoms *B2* of the second column. So in the setup of this column, the bottoms is fixed at $(0.06)(0.14) = 0.0096$ kmol/s. Initially, the reflux ratio is fixed at 2 as the other degree of freedom. This will be adjusted later to achieve the desired purity of the water product (99.9 mol% water).

The first guesses of the compositions of the recycle and reflux are inserted in the *Input* of these streams. First guesses of reflux and recycle flow rates are made of 0.12 and 0.06 kmol/s, respectively. The simulation is run giving a bottoms composition of 21 mol% benzene and 7×10^{-4} mol% water in the first column. The water is driven overhead, but there is too much

TABLE 5.1 Effect of Changing Reflux Flow Rate

Reflux (kmol/s)	Bottoms Composition (mol% B)	Bottoms Composition (mol% W)	Notes
0.12	20.9	7×10^{-4}	–
0.10	10.1	8×10^{-3}	–
0.09	4.70	0.04	–
0.08	3×10^{-17}	43.6	Jump to high water B1
0.09	3×10^{-17}	43.9	–
0.10	3×10^{-17}	43.8	–
0.11	15.5	2×10^{-3}	Jump back to low water B1

benzene in the bottoms because the organic reflux flow rate is too large. Reflux flow rate is reduced from 0.12 to 0.1 to 0.09 kmol/s (as shown in Table 5.1), which reduces the benzene impurity in the bottoms. However, when the reflux flow rate is reduced to 0.08 kmol/s, there is a drastic change in the bottoms composition. Now the water is not driven out in the overhead. It comes out in the bottoms because there is not enough benzene to entrain the water overhead.

Now if the reflux is increased back to 0.09 kmol/s, the column does not converge to the same steady state that it had previously at this flow rate. The flow rate must be increased to about 0.11 kmol/s to reestablish the desired low water content in the bottoms. This multiple steady-state phenomenon is one of the severe complexities that simulations of distillation columns experience when highly nonideal VLE relationships are involved.

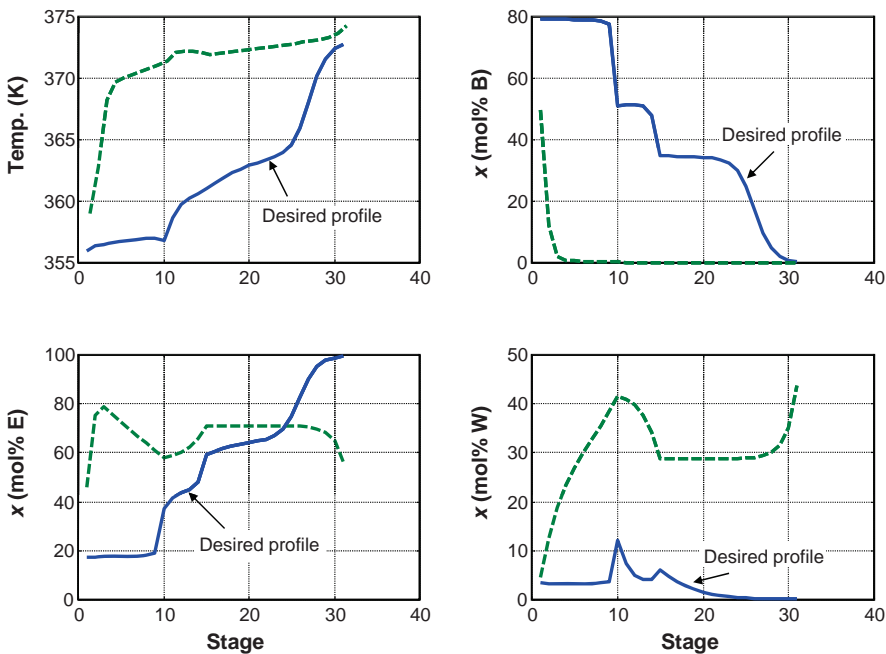


Figure 5.23 Multiple steady states.

Figure 5.23 compares temperature and composition profiles at two different steady states. The reflux flow rate is 0.082 kmol/s in both cases. The fresh feed and recycle are identical. The bottoms flow rate is the same. However, the bottoms composition is drastically different.

Obviously, the steady state indicated by the solid lines in Figure 5.23 is the desired one. The bottoms purity with this steady state is 99.27 mol% ethanol. The impurities are 0.50 mol% benzene and 0.23 mol% water. Getting the simulation to converge to this steady state is quite difficult.

The calculated compositions of the reflux and recycle are compared with the guessed values. The reflux composition is quite close: 84.4/14.0/1.6 mol% B/E/W calculated versus 84.4/14.1/1.5 mol% assumed. The recycle composition is somewhat different: 4.7/41.6/53.7 mol% calculated versus 7.2/47.1/45.7 mol% assumed. Changing these compositions to the calculated values and rerunning the program give a new *B1* composition of 0.926/98.92/0.157 mol% B/E/W. The calculated flow rate of the distillate *D2* under these conditions is 0.0704 kmol/s versus the 0.06 kmol/s assumed.

Now that we have some reasonable guesses for the values of the recycle streams, the *Design Spec/Vary* capability can be used to drive the compositions of the two product streams to their desired values. The key feature in the first column is to keep enough benzene in the column to entrain out the water so the bottoms is high-purity ethanol. On the other hand, if too much benzene reflux is fed to the column, it will go out the bottom and drive the bottoms off-specification. A *Design Spec/Vary* is set up to maintain the benzene composition of the bottoms at 0.5 mol% by manipulating the “REFLUX” stream, which is considered a *Feed rate* on the list of choices given in the *Vary, Specifications, Adjusted variable, and Type*.

The initial guessed value of the reflux ratio in the second column was 2. The bottoms purity was very high. The reflux ratio was reduced to about $RR = 0.2$ without affecting the bottoms purity significantly. A second *Design Spec/Vary* is set to maintain the ethanol composition of the bottoms of the second column at 0.1 mol% by varying the bottoms flow rate *B2*.

Several runs are made, in which the guessed compositions of the reflux and the recycle are compared with those of the calculated organic stream from the decanter and the distillate *D3* from the second column. When these variables are fairly close, the recycle/*D2* loop is closed. The procedure for doing this involves three steps

1. Delete the stream labeled “D2CALC” in Figure 5.22.
2. Click the stream labeled “REYCLE” and reconnect it to the valve labeled “V2.”
3. Go down near the bottom of the list of item on the *Data Browser* window and click *Convergence* and then *Tear*. This opens the window shown in Figure 5.24 on which the drop-down menu is used to select *RECYCLE*.

When the program is rerun, it converges to the values shown on the flowsheet given in Figure 5.14. Figure 5.18 gives the ternary diagram with the locations of all the streams marked.

In theory, the next and final step is to close the organic reflux loop. The stream labeled “ORGREF” is deleted, the stream “REFLUX” connected to the summer “M1” and “REFLUX” is defined as a *TEAR* stream. Unfortunately, this loop does not converge even though the initial values of the guessed and calculated values are very close in both composition and flow rate. An alternative way to converge this system using dynamic simulation will be discussed in Chapter 8 after we have discussed the details of dynamic simulation.

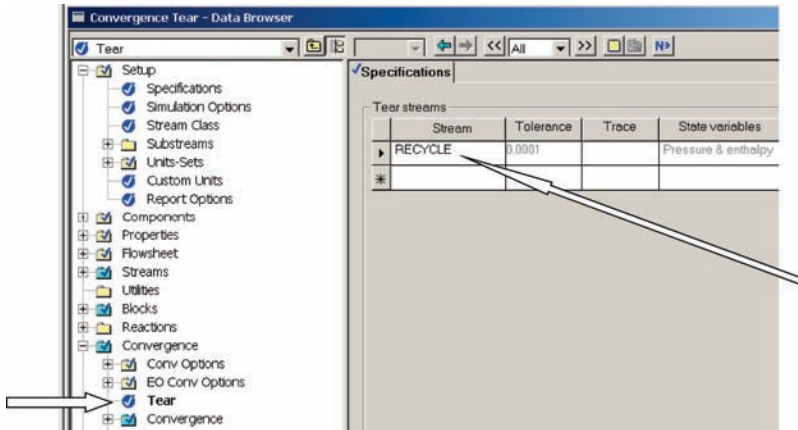


Figure 5.24 Specifying tear stream.

5.3 PRESSURE-SWING AZEOTROPIC DISTILLATION

The two azeotropic separation methods considered in Sections 5.1 and 5.2 required the addition of a third component to alter the vapor–liquid equilibrium. Another factor that sometime affects the phase equilibrium is pressure. If the composition of a binary azeotrope is a strong function of pressure, a two-column process can be used to achieve separation without adding a third component, which is desirable because small levels of impurity of this third component in the product streams are unavoidable. The two columns operate at different pressures, so the azeotropic compositions are different.

Pressure-swing azeotropic distillation can be applied in both minimum-boiling and maximum-boiling systems. With minimum-boiling azeotropes, the *distillate* streams have compositions close to the azeotropic composition at the corresponding pressure. The bottoms streams are the high-purity products of the light- and heavy-key components. Figure 5.25 shows the flowsheet for this type of system. With maximum-boiling azeotropes, the *bottoms* streams have compositions close to the azeotropic composition at the corresponding pressure. The distillate streams are the high-purity products of the light and heavy-key components.

Let us consider the minimum-boiling acetone/methanol separation discussed in Section 5.1, where extractive distillation was used. The first thing to find out is the pressure dependence of the azeotrope. Figure 5.26 gives Txy diagrams at two pressures: 1 and 10 atm. The azeotropic compositions are 77.6 and 37.5 mol% acetone at these two pressures. This significant shift indicates that pressure swing should be feasible.

Figure 5.27 gives xy curves at pressures of 1 and 10 atm. The compositions of the various streams are indicated (all in mole fractions of acetone). The feed composition is $z = 0.5$, and the feed is fed into the low-pressure column. The bottoms composition is $x_{B1} = 0.005$ (this is the methanol product stream). The distillate composition is selected to be $x_{D1} = 0.74$, which is slightly less than the 1 atm azeotropic composition ($y_{AZ,1} = 0.776$). The distillate from the low-pressure column is fed to the high-pressure column. The bottoms composition in the high-pressure column is $x_{B2} = 0.994$ (this is the acetone product stream). The distillate composition is selected to be $x_{D2} = 0.40$, which is slightly

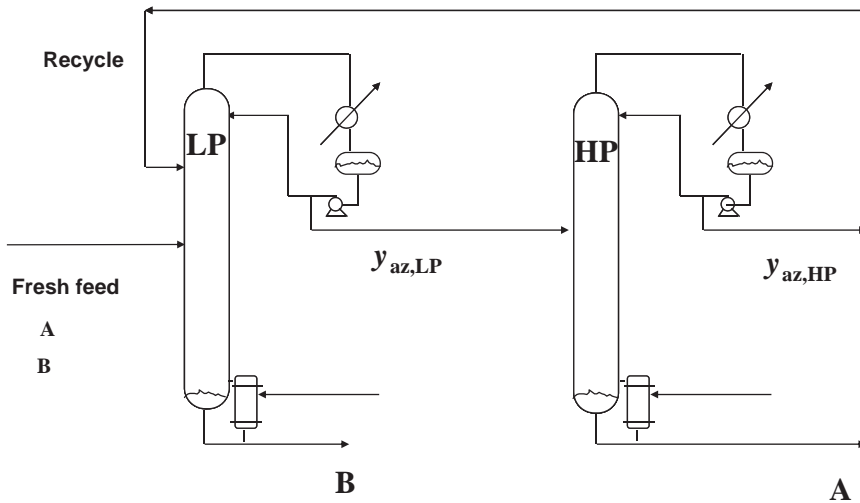


Figure 5.25 Pressure-swing azeotropic distillation flowsheet: minimum-boiling azeotrope.

greater than the 10 atm azeotropic composition ($y_{AZ,10} = 0.375$). The distillate from the high-pressure column is recycled back to the low-pressure column. Figure 5.28 shows the flowsheet of this process.

The two bottoms specifications are the required product purities. The two distillate compositions are design optimization variables to be established by economics. As the distillate specifications get closer and closer to the corresponding azeotropic compositions, the separations in each column become more difficult and more trays are required (higher capital investment). However, the flow rates of the recycle stream $D1$ and $D2$ decrease as the difference between the two distillate compositions increases, so energy consumption

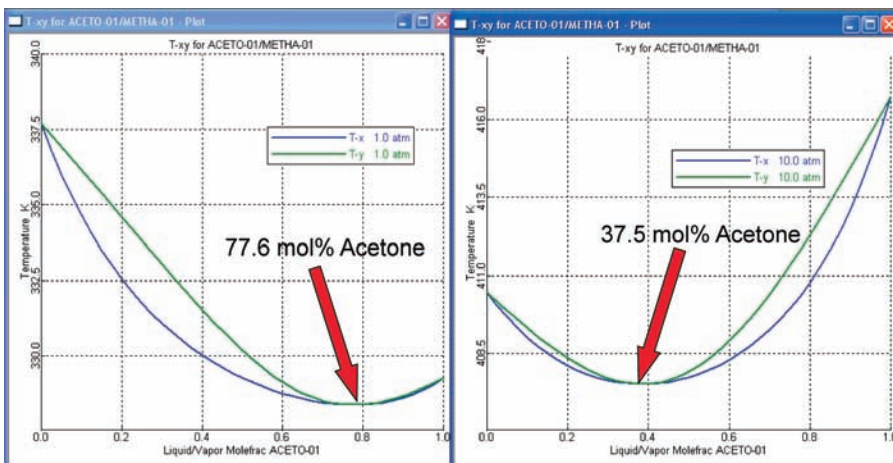


Figure 5.26 Txy diagrams for acetone/methanol at 1 and 10 atm.

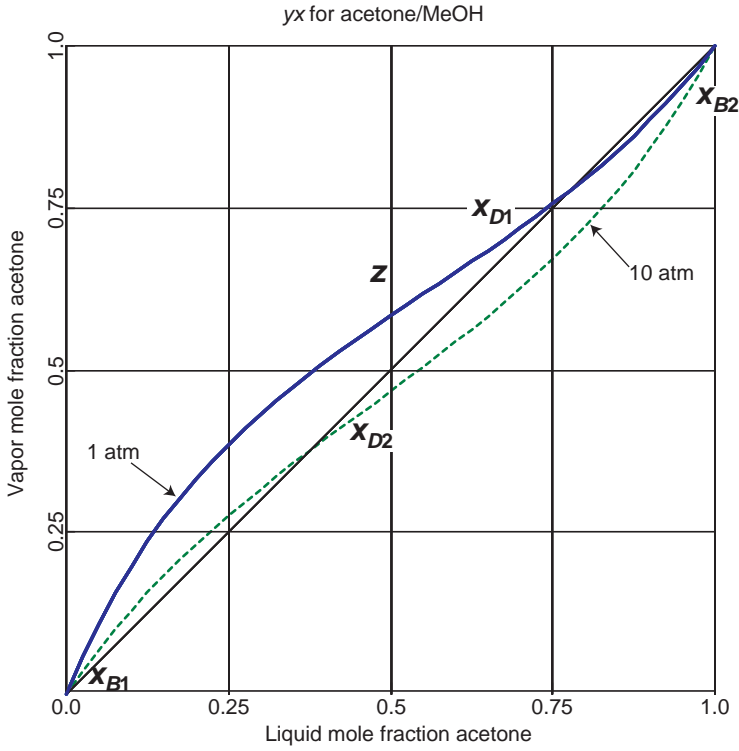


Figure 5.27 Pressure-swing azeotropic distillation xy diagram.

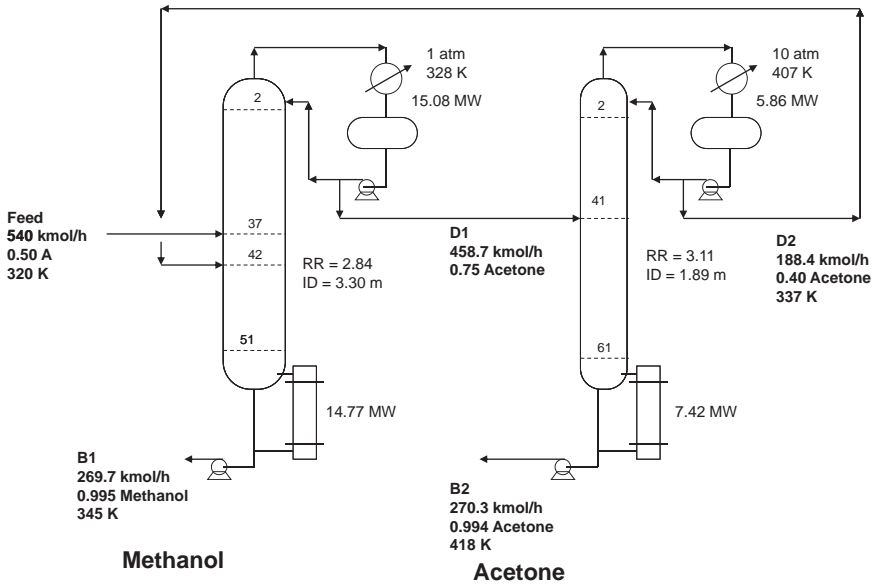


Figure 5.28 Flowsheet for pressure-swing distillation: acetone/methanol.

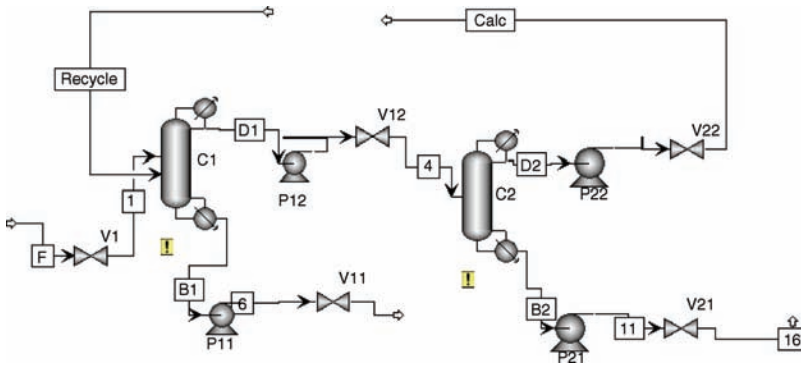


Figure 5.29 Recycle not closed.

decreases. A total-annual-cost analysis, as discussed in Chapter 3 is required to find the optimum trade-off.

The only complication in setting up the pressure-swing distillation simulation is the recycle stream of the high-pressure distillate back to the low-pressure column. One approach is to make a guess of the conditions of this second feed to the low-pressure column and then set up the both columns sequentially, starting with the low-pressure column with its two design specification ($x_{B1} = 0.005$ and $x_{D1} = 0.74$) and then moving to the high-pressure column with its two design specification ($x_{B2} = 0.994$ and $x_{D2} = 0.40$). Figure 5.29 shows the Aspen Plus process flow diagram with the recycle torn. Then the “CALC” stream is deleted, the source of the “RECYCLE” stream is selected as the output of valve “V22” and a *Tear* is defined as “RECYCLE.”

However, some simple total molar and component balances for this binary system can be used to obtain precisely the flow rates of all the distillate and product streams since we have specified the compositions of all four streams.

Overall balances

$$\begin{aligned}
 F &= B1 + B2 \\
 zF &= B1x_{B1} + B2x_{B2}
 \end{aligned}$$

Solving for the two bottoms product flow rates gives

$$\begin{aligned}
 B2 &= \frac{F(z - x_{B1})}{x_{B2} - x_{B1}} \\
 B1 &= F - B2
 \end{aligned}$$

Balances around low-pressure column

$$\begin{aligned}
 F + D2 &= B1 + D1 \\
 zF + D2x_{D2} &= B1x_{B1} + D1x_{D1}
 \end{aligned}$$

Solving for the two distillate flow rates gives

$$D1 = \frac{F(z - x_{D2}) + B1(x_{D2} - x_{B1})}{x_{D1} - x_{D2}}$$

$$D2 = B1 + D1 - F_2$$

Therefore, the convergence of the recycle loop is simple because the flow rate and composition of the recycle stream $D2$ are known exactly. Remember, however, that the number of trays in each column and feed locations must be such that the specified stream compositions are achievable with finite reflux ratios.

Figures 5.30 and 5.31 give temperature and composition profiles in the two columns. Notice that the temperature in the condenser of the high-pressure column is 407 K and the condenser heat duty is 5.86 MW (see Fig. 5.28). The temperature in the base of the low-pressure column is 345 K and the reboiler duty is 14.77 MW. This 62 K temperature differential indicates that these two columns could be heat-integrated: the condenser of the high-pressure column serving as a reboiler in the low-pressure column. Since the heat duties are not equal, an additional steam-heated reboiler would be needed in the low-pressure column. An example of heat integration is presented in Section 5.4.

It is interesting to compare the extractive-distillation flowsheet with the pressure-swing flowsheet for the acetone/methanol separation. Figure 5.2 can be compared with Figure 5.28. The economics of pressure swing look significantly worse (larger columns and more energy consumption). However, remember that both the acetone and the methanol products are contaminated in the extractive distillation process with small concentrations of the solvent, which may be a problem in some applications.

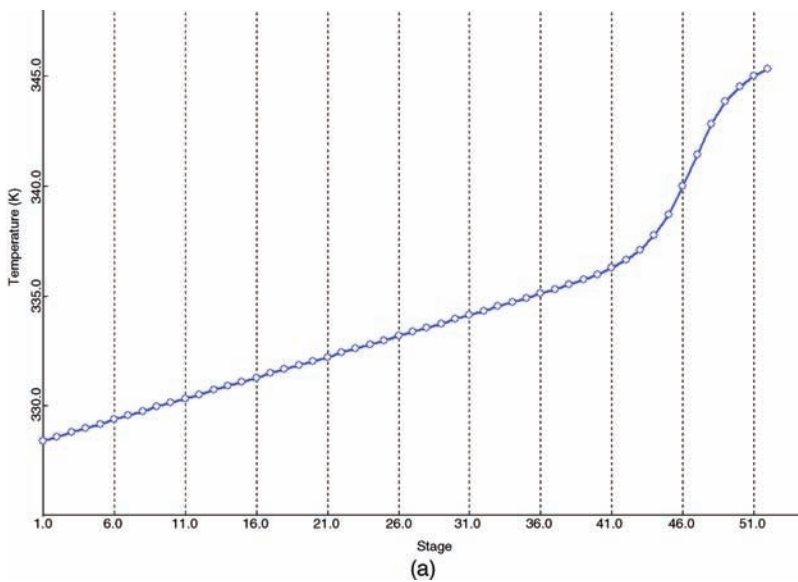


Figure 5.30 (a) Low-pressure column temperature profile. (b) Low-pressure column composition profiles.

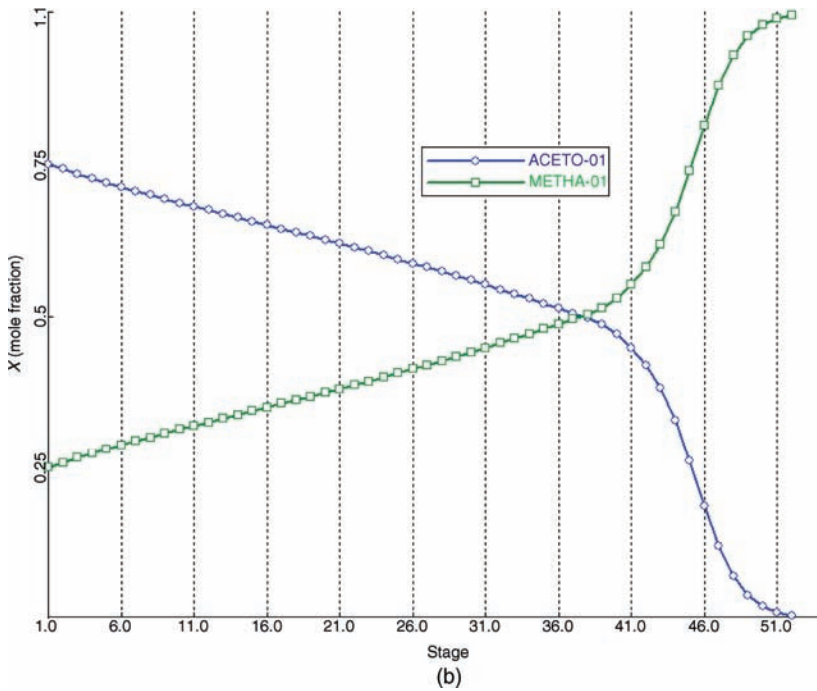


Figure 5.30 (Continued)

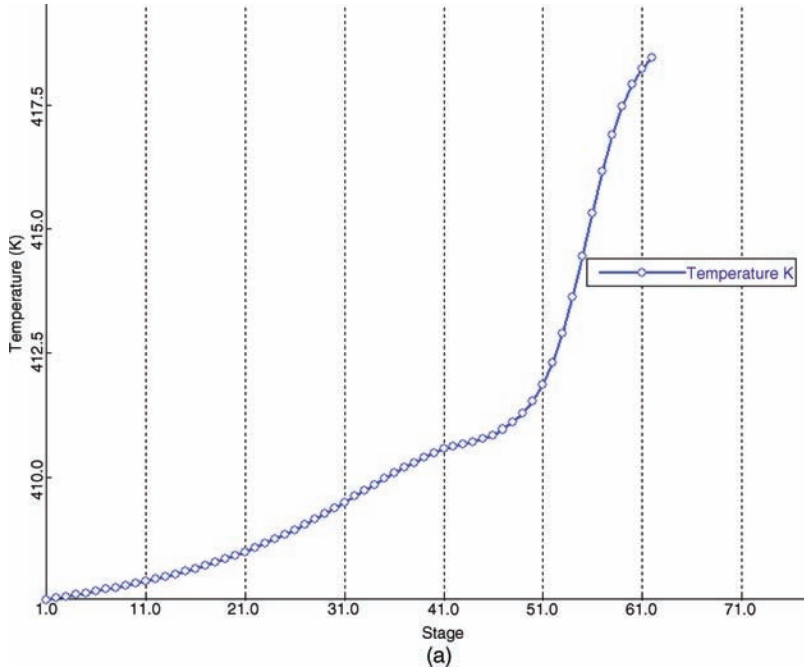


Figure 5.31 (a) High-pressure column temperature profile. (b) High-pressure column composition profiles.

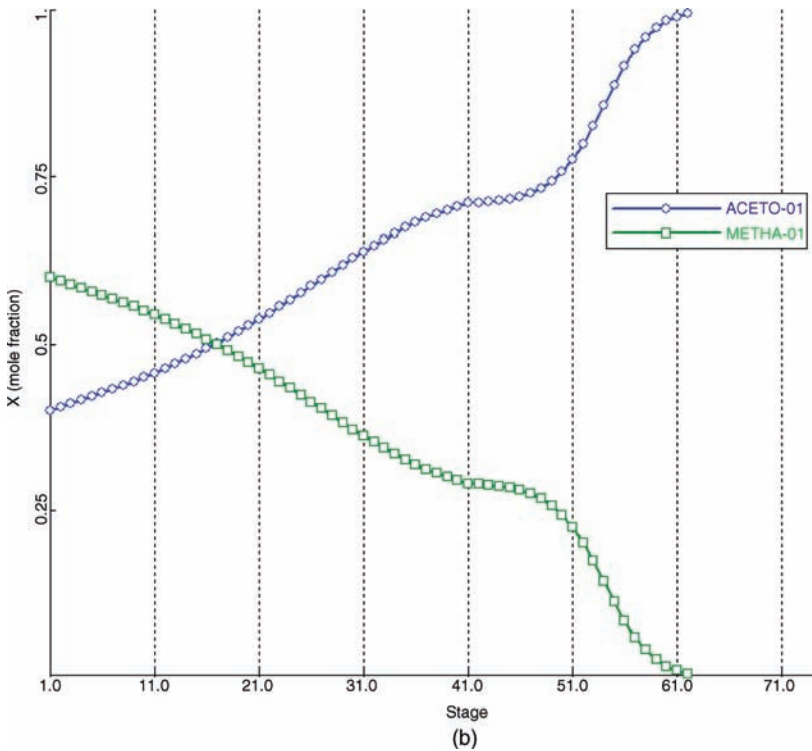


Figure 5.31 (Continued)

5.4 HEAT-INTEGRATED COLUMNS

The last example discussed in this chapter has fairly simple phase equilibrium but has a complex process structure. Two columns are operated at two different pressures so that the condenser for the high-pressure (high-temperature) column can be used as the reboiler in the low-pressure (low-temperature) column.

5.4.1 Flowsheet

Figure 5.32 gives the conceptual flowsheet. The specific system used as an example is methanol/water. Product specifications are 99.9 mol% methanol in the distillate streams (there is one from each column) and 99.9 mol% water in the two bottoms streams. The fresh feed is 1 kmol/s with a composition of 60 mol% methanol and 40 mol% water. The feed is split between the two columns, so that the system operates “neat,” that is, the condenser heat removal in the high-pressure column is exactly equal to the reboiler heat input in the low-pressure column. Each column has 32 stages and is fed on the stage that minimizes reboiler heat input.

To achieve the required temperature differential driving force in the condenser/reboiler, the pressures in the two columns must be appropriately selected. The low-pressure column C1 operates at a pressure of 0.6 atm (vacuum conditions, 456 mmHg) that gives a reflux

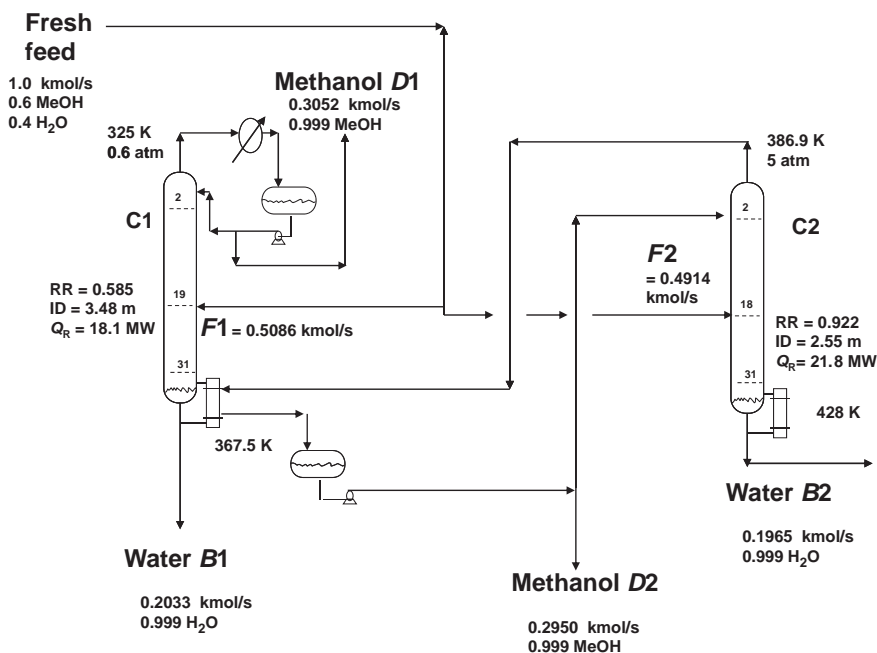


Figure 5.32 Heat-integrated columns.

drum temperature of 326 K, so cooling water can be used. The pressure drop per tray is assumed to be 0.0068 atm (0.1 psi). The base temperature of C1 is 367 K.

A reasonable differential temperature-driving force is about 20 K. If the ΔT is too small, the heat-transfer area of the condenser/reboiler heat exchanger becomes quite large. The pressure in the second column is adjusted to give a reflux drum temperature of $367 + 20 = 387$ K. The pressure in C2 is 5 atm. The base temperature in C2 at this pressure is 428 K, which will determine the pressure of the steam used in this reboiler.

5.4.2 Converging for Neat Operation

Initially, the total feed is split equally between the two columns. This is achieved in the *Splitter* labeled “T1” on the flowsheet shown in Figure 5.33. Two *Design Spec/Vary* are set up in each column to adjust distillate flow rate and reflux ratio to attain the 99.9 mol% product purities of all four streams. The optimum feed tray location is determined by finding the feed stage that minimizes reboiler heat input. In column C1, it is Stage 19. In column C2, it is Stage 18.

Under these conditions, the resulting reboiler heat input in the low-pressure column C1 is 17.91 MW. The resulting condenser heat removal in the high-pressure column C2 is 18.62 MW. These are very close, but if the system is to be operated “neat” (no auxiliary reboilers or condensers), these heat duties must match exactly.

One way to do this is to manually adjust the feed split in “T1” until Q_{R1} is equal to Q_{C2} . This can be automated by going to *Flow Sheet Options* on the *Data Browser* window and selecting *Design Spec*. This is similar to the *Design Spec/Vary* in the column blocks,

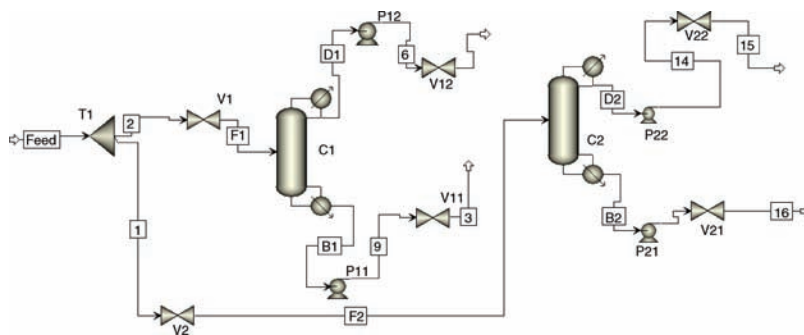


Figure 5.33 Aspen Plus flowsheet.

but now variables from any block can be used. Figure 5.34a shows the window that opens after *New* and *OK* is clicked. On the first page tab *Define* we enter two variables $QR1$ and $QC2$, and click on *Edit* to define what they are. Figure 5.34b shows how the $QR1$ is defined.

On the *Spec* page tab (Fig. 5.34c) a parameter “DELTAQ” is specified with the desired value *Target* and *Tolerance*. Clicking the *Vary* page tab opens the window shown in Figure 5.35. The “T1” block is selected and the variable is *Flow/Frac*. The *ID1* is set at “2” because the flow rate of the stream “2” leaving the splitter is the first variable and is the one specified.

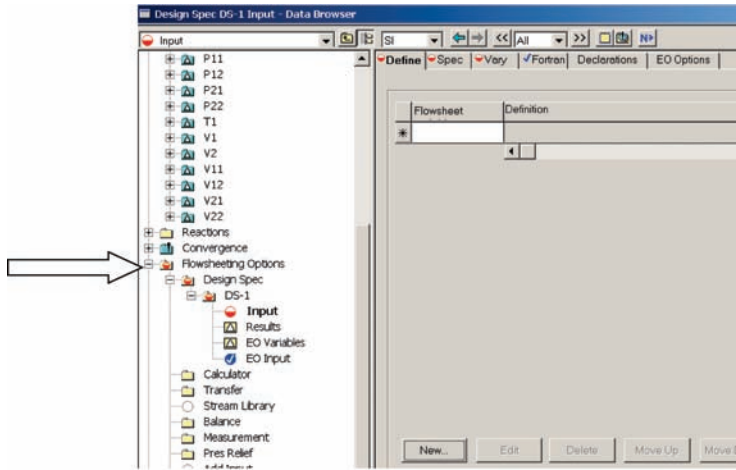
The final item is to define DELTAQ on the *Fortran* page tab (see Fig. 5.36). Remember that the convention in Aspen Plus is that heat addition is a positive number and heat removal is a negative number. Therefore, we want the sum of Q_{R1} and Q_{C2} (in watts) to be small. Running the program yields a feed split with 0.5086 kmol/s fed to the low-pressure column C1 and 0.4914 kmol/s fed to the high-pressure column C2. The heat duty in the condenser/reboiler is 18.10 MW as shown in Figure 5.37, which is obtained by selecting *Results* under the *DS-I* design spec. The final flowsheet conditions are given in Figure 5.32.

The last item of interest is to compare the energy and capital costs of this heat-integrated two-column system with those of a single column making exactly the same separation. This single column is the same as the low-pressure column in terms of operating pressure, but its energy consumption, column diameter, and heat exchanger areas will be larger.

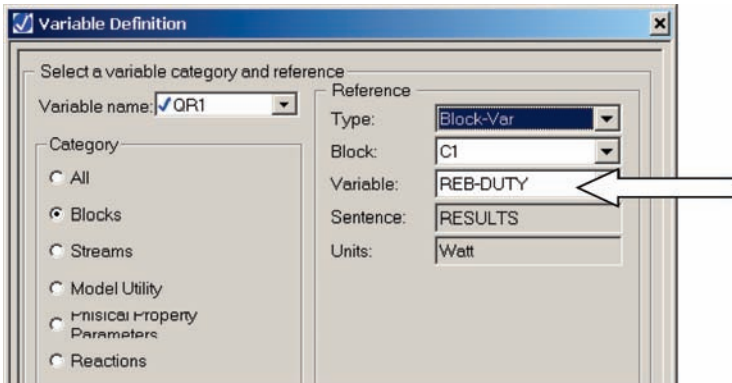
The comparison of the two alternative designs is given in Table 5.2. The energy consumption is reduced from 35.58 MW in a single column to 21.81 MW in the high-pressure column of the heat-integrated design. This cuts energy cost from \$2,640,000 per year to \$1,610,000 per year. The same value of energy is used in both cases. However, high-pressure steam is needed in the heat-integrated design because the base temperature is 428 K compared with 367 K in the single column. Using a 34.8 K temperature difference between the column base temperatures and the condensing steam temperature in the reboiler and a 4 atm pressure drop over the steam valve, give supply steam pressures of 6.8 and 17 atm, respectively, for the two processes. The difference in the cost of these two steam supplies would reduce the energy savings.

Total capital investment is also reduced. This is somewhat counterintuitive because one column with two heat exchangers would be expected to be less expensive than two columns with three exchangers. However, the column diameters and the heat-exchanger areas are smaller in the heat-integrated design.

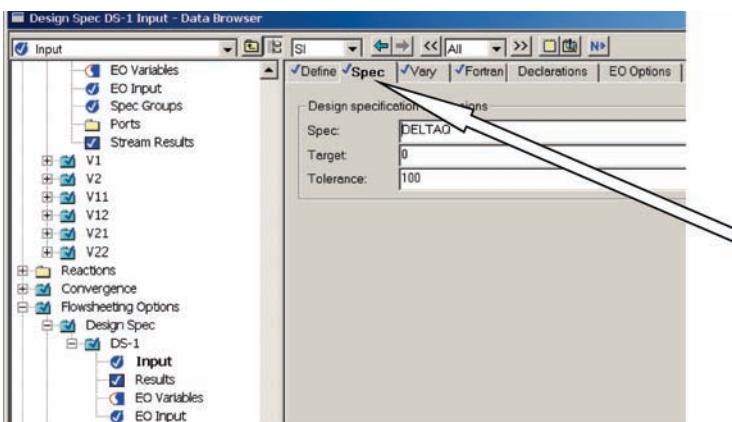
An additional aspect of this heat-integration simulation is the calculation of the heat-transfer rate in the condenser/reboiler heat exchanger. In this steady-state simulation, we



(a)



(b)



(c)

Figure 5.34 (a) Setting up design spec. (b) Defining variables. (c) Setting specification.

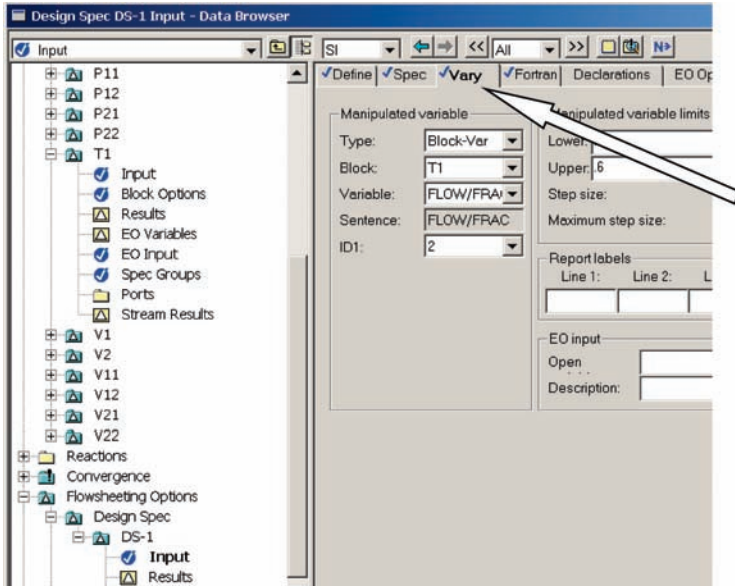


Figure 5.35 Selecting manipulated variable.

have specified that the condenser heat removal in the first column is equal to the reboiler heat input in the second column. This satisfies the first law of thermodynamics. The area of the condenser/reboiler is then calculated based on the heat duty, the differential temperature-driving force (the temperature in the reflux drum of the high-pressure column minus the temperature in the base of the low-pressure column) and an overall heat-transfer coefficient. In a dynamic simulation this area is fixed. The heat-transfer rate will change

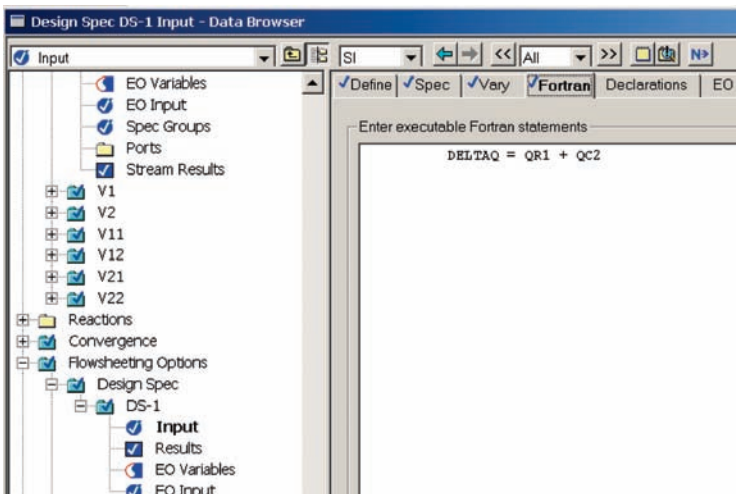


Figure 5.36 Defining DELTAQ.

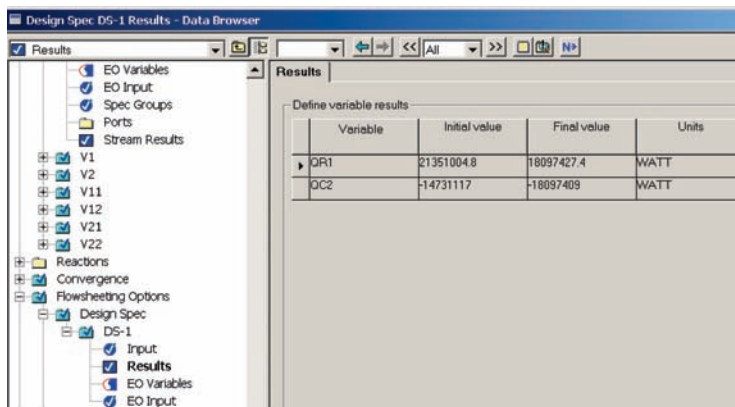


Figure 5.37 Results of design spec.

TABLE 5.2 Comparison of Single and Heat-Integrated Columns

	Single	Low Pressure	High Pressure
Stages	32	32	32
N_F	19	19	18
D (m)	4.93	3.48	2.55
Q_C (MW)	34.29	17.44	–
RR	0.585	0.585	0.922
Q_R (MW)	35.58	–	21.81
A_C (m ²)	2890	1433	251
A_R (m ²)	1797	–	161
Shell (10 ⁶ \$)	1.15	0.794	0.255
HX (10 ⁶ \$)	2.25	0.822	0.692
Energy (10 ⁶ \$/year)	2.64	–	1.62
Capital (10 ⁶ \$)	3.40	1.62	1.26
TAC (10 ⁶ \$/year)	3.77	–	2.58

dynamically as the two temperatures change. So in the dynamic simulation the heat-transfer rates in the two column must be calculated from $Q = UA(T_{D1} - T_{B2})$, so that the second law of thermodynamics is satisfied. This can be achieved by using *Flowsheet Equations* in Aspen Dynamics, which will be discussed in later chapters.

5.5 CONCLUSIONS

The complex nonideal distillation columns considered in this chapter provide good examples of the difficulties and capabilities of using simulation in distillation systems for steady-state design. Now we are ready to move to an equally important phase of design in which the dynamics and control of the column or systems of columns and other units are considered. “Simultaneous design” involves both steady-state and dynamic aspects of the process.

CHAPTER 6

STEADY-STATE CALCULATIONS FOR CONTROL STRUCTURE SELECTION

Before we get into the details of converting a steady-state simulation into a dynamic one, it might make sense to discuss some important steady-state calculations that are frequently performed to aid in the selection of a practical effective control structure for a distillation column.

6.1 CONTROL STRUCTURE ALTERNATIVES

6.1.1 Dual-Composition Control

The majority of distillation columns are designed to attain a specified separation between the two key components. The two steady-state design degrees of freedom are usually specified to be the impurity of the heavy-key component in the distillate and the impurity of the light-key component in the bottoms. Therefore, in the operation and control of a distillation column, the “ideal” control structure would measure the compositions of the two products and manipulate two input variables (e.g., reflux flow rate and reboiler heat input) to maintain the desired amounts of the key-component impurities in the two product streams.

However, very few distillation columns use this ideal “dual-composition” control structure. There are a number of practical reasons for this. Composition analyzers are often expensive to purchase and have high maintenance costs. Their reliability is sometimes inadequate for on-line continuous control. They also introduce deadtime into the control loop if chromatographic methods are used.

In addition, it is often possible to achieve very effective control without using direct composition measurements and without controlling both products. “Single-end” control structures are widely used because of their simplicity and effectiveness.

6.1.2 Single-End Control

In “single-end” control structures, only one composition or one temperature is controlled. The remaining control degree of freedom is selected to provide the least amount of product quality variability. For example, a constant reflux ratio RR can be maintained or the reflux-to-feed ratio R/F can be fixed. The control engineer must find out whether this more simple approach will provide effective control of the compositions of both product streams. One approach to this problem is to use steady-state simulations to see how much the reflux ratio and the reflux flow rate must change to maintain the specified impurity levels in both product streams (heavy-key impurity in the distillate $x_{D(\text{HK})}$ and light-key impurity in the bottoms $x_{B(\text{LK})}$) when changes in *feed composition* occur. The procedure is called “feed composition sensitivity analysis.”

6.2 FEED COMPOSITION SENSITIVITY ANALYSIS (ZSA)

In the steady-state design using Aspen Plus, two *Design Spec/Vary* functions are typically used to manipulate the flow rates of reflux and distillate to achieve the specified purities (or impurities) of the two products. These calculations are done at the design feed composition and the design feed flow rate.

If we change the design feed flow rate, all the column internal and external flow rates and heat-exchanger duties simply scale directly with the feed flow rate. In addition, the resulting temperature and compositions profiles are exactly the same at any flow rate. This occurs because the column pressure and tray pressure drops are specified in the design program and do not change with flow rates. Therefore, in theory, any control structure that incorporates any flow ratio (reflux-to-feed, reflux-to-distillate, etc.) will drive the column to the desired product compositions (at steady state) for feed flow rate disturbances.

However, the flow ratios usually have to change, as do the temperature and composition profiles, when feed compositions change. Therefore, the disturbance that must be examined is feed composition.

The procedure is as follows:

1. Set up the steady-state simulation at design feed composition with the two *Design Spec/Vary* functions active. Record the required reflux ratio RR and reflux-to-feed ratio R/F.
2. Run several cases in which the feed compositions of the light and heavy-key components are varied over a realistic range around the design feed compositions.
3. Record the new required RR and R/F at each of these feed compositions.
4. If there are significant changes in both of these ratios, single-end control will probably be ineffective. Because the flow ratios have to change, the control structure must be capable of changing both manipulated variables (reflux and reboiler duty). This implies that “two-end control” is required. The structure could control two compositions, two temperatures or one composition and one temperature. This decision depends on the shape of the temperature profile, which we explore in Section 6.3.
5. If there are only small changes in one of the ratios, a single-end control structure with this ratio fixed may provide effective disturbance rejection in the face of both feed composition and feed flow rate disturbances.

TABLE 6.1 Feed Composition Sensitivity Results

Z_{C3}	Z_{iC4}	R/F	% Change from Design	RR	% Change from Design
0.30	0.39	0.9560	-0.57	3.163	+33.8
0.35	0.34	0.9643	+0.29	2.721	+15/1
0.40	0.29	0.9615	0	2.364	0
0.45	0.24	0.9477	-1.43	2.065	-12.7
0.50	0.19	0.9208	-4.23	1.800	-23.9

The results from a distillation column with a five-component hydrocarbon feed mixture are given in Table 6.1. The feed flow rate is 100 kmol/h, and the design feed composition is 1 mol% ethane (C2), 40 mol% propane (C3), 29 mol% isobutane (*i*C4), 29 mol% normal butane (*n*C4), and 1 mol% isopentane (*i*C5). The operating objective is to separate the light-key component propane from the heavy-key component isobutane. Of course, the heavier than heavy-key components *n*C4 and *i*C5 go out the bottom with the *i*C4. The lighter than light-key component C2 goes out the top with the propane. Column pressure is set at 16 atm to give a reflux-drum temperature of 320 K so that cooling water can be used in the condenser. The column has 37 stages and is fed on Stage 18. Distillate impurity is specified to be 2 mol% *i*C4. Bottoms impurity is specified to be 2 mol% C3. The reflux ratio required to achieve these purities is 2.364.

Table 6.1 gives results of the feed sensitivity analysis. They clearly show that in this system the required changes in reflux are very small. Therefore, a single-end control structure with a reflux-to-feed ratio has a good chance of providing effective control of both product purities.

A further comment relating to feed flow rate changes should be made. As stated above, in the *design* of the column the pressures on the trays are specified and are normally not changed at different throughputs. In the steady-state simulator Aspen Plus, tray pressure drops are specified. In this situation all the flow ratios are independent of throughput. However, in an operating column and in Aspen Dynamic simulations, tray pressure drops vary with vapor and liquid flow rates. Therefore, the pressures on the trays change with throughput. The consequence of this is that holding a constant RR or a constant R/F may not bring the product compositions back precisely to their design values when throughput changes occur. This subtlety should be kept in mind in design control systems. In columns where pressure changes are significant (vacuum columns), measurements of both temperature and pressure are sometimes required to maintain product purities for both feed flow rate and feed composition disturbances. Pressure changes can also be significant in heat-integrated columns and columns that are operated to always be at minimum pressure to conserve energy. Chapter 16 discusses the use of pressure-compensated temperature control for columns in which pressure changes have significant effects.

6.3 TEMPERATURE CONTROL TRAY SELECTION

If tray temperatures are to be used, the issue is the selection the best tray on which temperature should be held constant. This problem has been discussed in the distillation literature for over a half century, and several alternative methods have been proposed. All of these methods use steady-state simulations to assess some aspect of performance, given

a certain control structure. We will review these alternative methods and illustrate their effectiveness for several systems.

It is important to note that all of these methods use only steady-state information, so steady-state process simulators such as Aspen Plus can be easily used to perform the calculations. The methods all require that various variables are held constant, while other variables change. For example, two product compositions can be held constant, or a tray temperature and reflux flow rate may be held constant. The “Design Spec/Vary” feature in Aspen Plus is used to achieve the fixing of the desired independent variables and the calculation of all the remaining dependent variables.

6.3.1 Summary of Methods

Slope Criterion: Select the Tray Where There Are Large Changes in Temperature from Tray to Tray. This is by far the easiest and most often applied method. The temperature profile at design conditions is plotted, and the “slope” of profile is examined to find the tray where this slope is the largest. Large changes in temperature from tray to tray indicate a region where compositions of important components are changing. Maintaining a tray temperature at this location should hold the composition profile in the column and prevent light components from dropping out the bottom and heavy components from escaping out the top.

Sensitivity Criterion: Find the Tray Where There Is the Largest Change in Temperature for a Change in the Manipulated Variable. A very small change (0.1% of the design value) is made in one of the manipulated variables (e.g., reflux flow rate). The resulting changes in the temperatures of all the trays are examined to see which tray has the largest change in temperature. The procedure is repeated for the other manipulated variable (e.g., reboiler heat input). Dividing the change in the tray temperature by the change in the manipulated variable gives the open-loop steady-state gain between temperature on that tray and each manipulated variable. The tray with the largest temperature change is the most “sensitive” and is selected to be controlled. A large gain indicates that the temperature on that tray can be effectively controlled by the corresponding manipulated variable. A small gain indicates that valve saturation can easily occur and the operability region could be limited.

SVD Criterion: Use Singular Value Decomposition Analysis. Singular value decomposition (SVD) of the steady-state gain matrix is thoroughly treated by Moore.¹

The steady-state gains between all the tray temperatures and the two manipulated variables are calculated as described in the previous section. A gain matrix K is formed, which has N_T rows (the number of trays) and two columns (the number of manipulated variables). This matrix is decomposed using standard SVD programs (e.g., the “*svd*” function in Matlab) into three matrices: $K = U\sigma V^T$. The two U vectors are plotted against tray number. The tray or trays with the largest magnitudes of U indicate locations in the column that can be most effectively controlled. The σ matrix is a 2×2 diagonal matrix whose elements are the “singular values.” The ratio of the larger to the smaller is the “condition number,” which can be used to assess the feasibility of dual-temperature control. A large condition number (or small minimum singular value) indicates a system

that is difficult to control. The controller is the inverse of the plant gain matrix, and a singular value of zero means the matrix is “singular” and cannot be inverted.

Invariant Temperature Criterion: With Both the Distillate and Bottoms Purities Fixed, Change the Feed Composition Over the Expected Range of Values. Select the Tray Where the Temperature Does Not Change as Feed Composition Changes. The difficulty with this method is that there may be no constant-temperature tray for all feed compositions changes. This is particularly true in multicomponent systems where the amounts of the nonkey components can vary and significantly affect tray temperatures, especially near the two ends of the column.

Minimum Product Variability Criterion: Choose the Tray that Produces the Smallest Changes in Product Purities When it is Held Constant in the Face of Feed Composition Disturbances. Several candidate tray locations are selected. The temperature on one specific tray is fixed, and a second control degree of freedom is fixed such as reflux ratio or reflux flow rate. Then the feed composition is changed over the expected range of values, and the resulting product compositions are calculated. The procedure is repeated for several control tray locations. The tray is selected that produces the smallest changes in product purities when it is held constant in the face of feed composition disturbances.

We have described five criteria that are the most frequently used. Sometimes these criteria recommend the same control tray location. In other cases, they recommend different control tray locations. In the next sections, we apply these criteria to several typical industrial distillation systems to assess their relative effectiveness.

6.3.2 Binary Propane/Isobutane System

The first separation system examined is a binary mixture of propane and isobutane. The feed flow rate is 1 kmol/s and the design feed composition is 40 mol% propane. We use the conventional notation that the composition of the feed is z , the composition of the distillate is x_D and the composition of the bottoms is x_B (all in mole fraction propane). Column pressure is set at 13.5 atm so that cooling water can be used in the condenser (reflux drum temperature is 315 K). The column has 37 stages and is fed on Stage 16, using Aspen notation of numbering stages from the reflux drum down the column.

Distillate purity is specified to be 98 mol% propane. Bottoms impurity is specified to be 2 mol% propane. The reflux ratio required to achieve these purities is 1.08.

Slope Criterion. The upper graph in Figure 6.1 gives the temperature profile at design conditions. The lower graph shows the differences between the temperatures on adjacent trays. The location of the tray with the largest slope is Stage 8. There is another tray (Stage 29) that has a slope that is almost as large. We will compare the use of both of these later in this section.

Sensitivity Criterion. The upper graph in Figure 6.2 gives the open-loop gains between tray temperatures and the two manipulated variables reflux R and reboiler heat input Q_R . The solid lines are for reflux flow rate changes, and the dashed lines are for reboiler heat input changes. Very small increases from the steady-state values (+0.1 %) of the two inputs are used. As expected, the gains between the tray temperatures and reflux are negative, and they are positive for heat input.

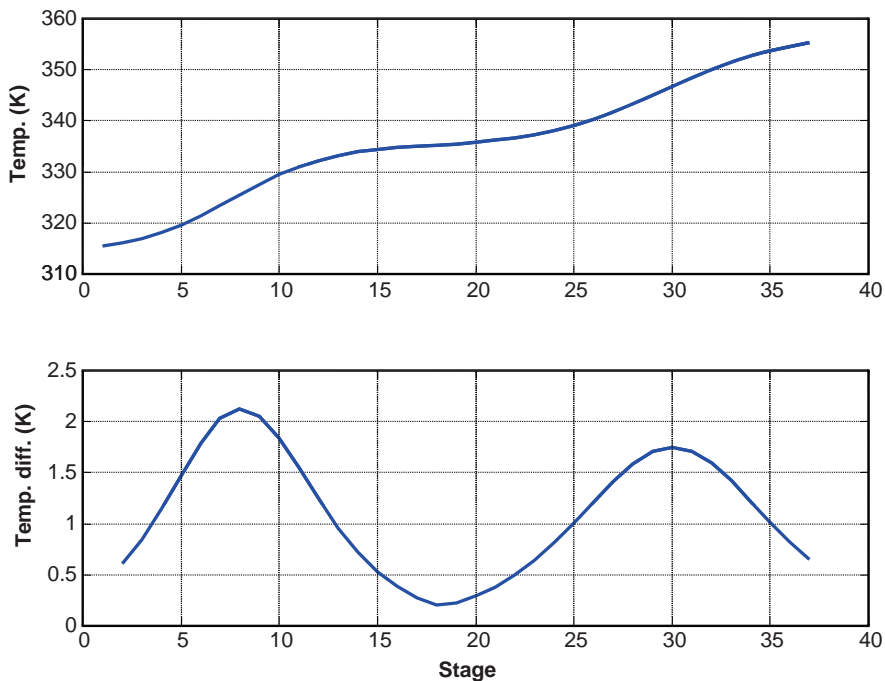


Figure 6.1 Propane/isobutane: temperature profile and slope.

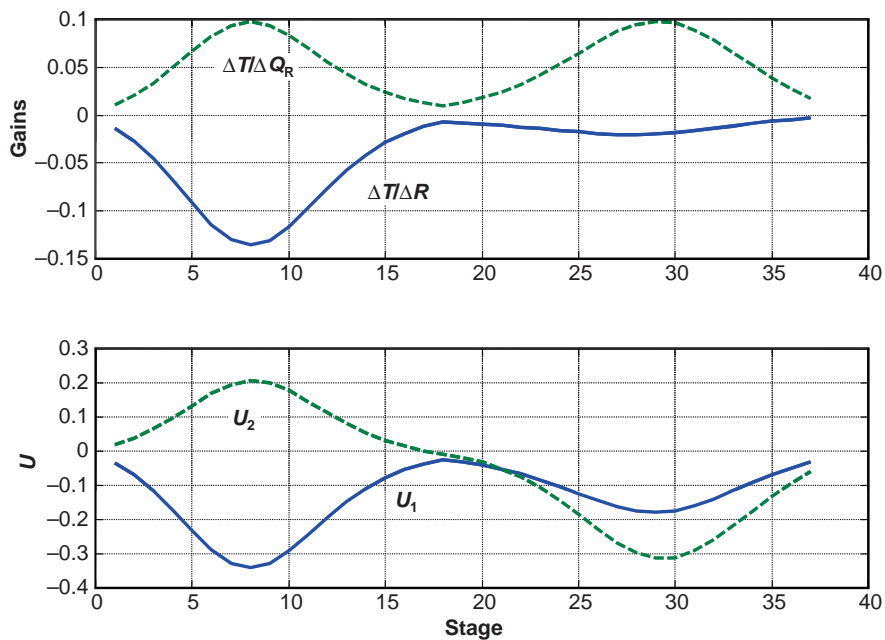


Figure 6.2 Propane/isobutane: sensitivity and SVD analysis.

These curves show that Stage 8 is sensitive to changes in reflux and both Stages 8 and 29 are sensitive to changes in heat input. Therefore, Stage 8 can be controlled using either reflux or heat input, while Stage 29 can be controlled by only heat input.

It should be remembered that these are steady-state results and tell us nothing about dynamics. Temperatures on all trays in the column are quickly affected by changes in heat input, so pairing heat input with any tray temperature is dynamically feasible. However, a change in reflux flow rate takes a significant time to affect temperatures on trays near the bottom of the column because of liquid hydraulic lags (3–6 s per tray). Therefore, poor control can be expected when reflux is paired with a tray temperature significantly down from the top of the column.

SVD Criterion. The lower graph in Figure 6.2 gives the U_1 and U_2 values from SVD analysis. The first is the solid line and is associated with reflux. The second is the dashed line and is associated with heat input.

The SVD results are similar to the sensitivity results. They suggest that Stage 8 can be controlled by reflux and Stage 29 by heat input. The singular values of the steady-state gain matrix are $\sigma_1 = 0.479$ and $\sigma_2 = 0.166$, which gives a condition number $CN = \sigma_1/\sigma_2 = 2.88$. This indicates that the two temperatures are fairly independent, so a dual-temperature control scheme should be feasible, at least from a steady-state point of view.

Invariant Temperature Criterion. Figure 6.3 gives the changes in the temperature profiles for two feed compositions on either side of the steady-state value (40 mol% propane). The solid lines are for 35 mol% propane, and the dashed lines are for 45 mol% propane in the feed. The product distillate and bottoms compositions are fixed at 98 and 2 mol%, respectively, for both feed compositions.

As expected in a binary constant-pressure system, fixing the composition fixes the temperature. So the temperatures at the top and at the bottom do not change. In theory,

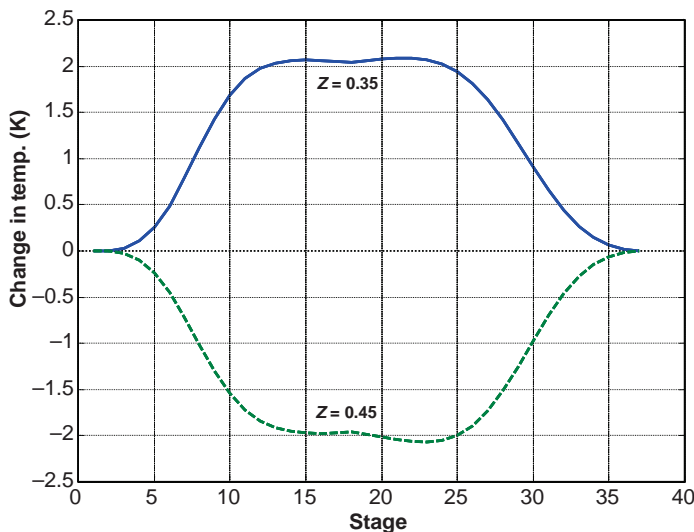


Figure 6.3 Propane/isobutane: changes in temperature profile for feed composition changes with product purities fixed.

these end temperature could controlled to achieve constant product purities. In practice, however, small amounts of other components or changes in pressure can make the use of temperatures at the very ends of the column ineffective. This will be demonstrated later when multicomponent systems are considered.

Minimum Product Variability Criterion. Figure 6.4 shows how product purities change when the temperature on a specific tray is held constant and feed composition

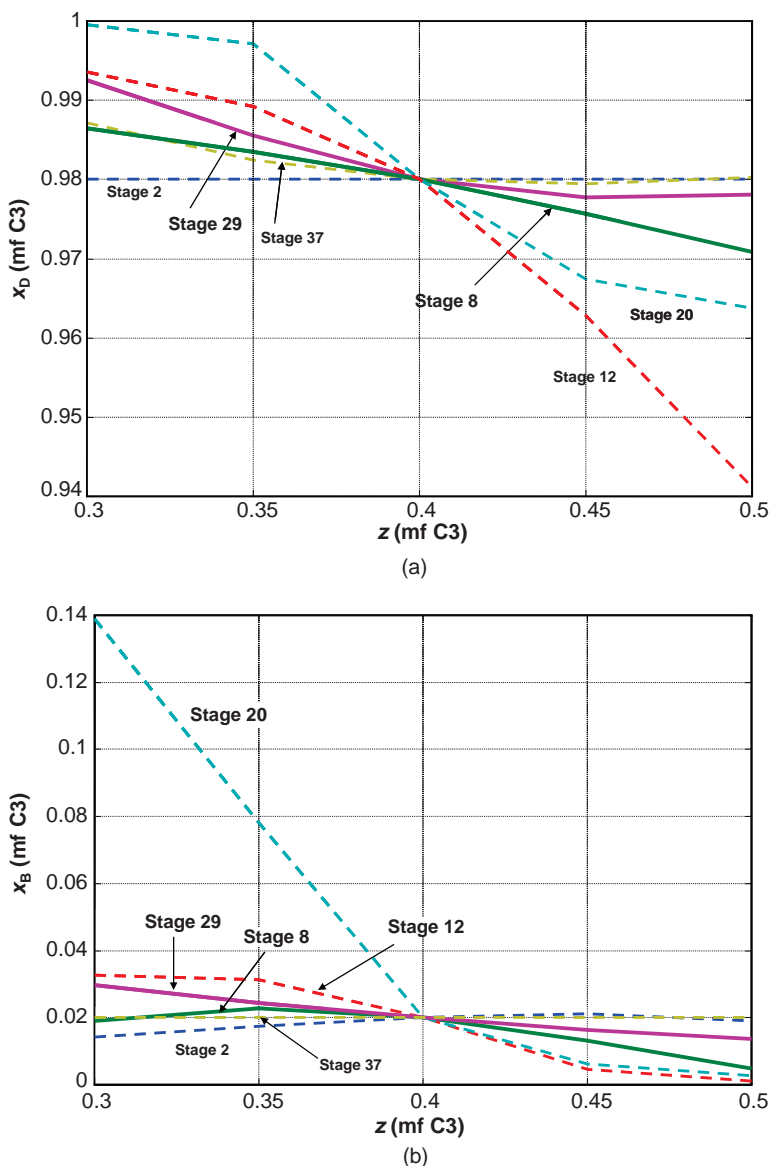


Figure 6.4 (a) Propane/isobutane: distillate purity for feed composition changes with fixed reflux and stage temperature. (b) Propane/isobutane: bottoms impurity for feed composition changes with fixed reflux and stage temperature.

TABLE 6.2 Effect of Feed Composition on Required Reflux Flow Rate and Reflux Ratio for Constant Product Purities

System	Product Purities or Impurities (mol%)	Z (mol%)	Reflux Flow Rate (kmol/s)	Reflux Ratio
D/P	98/2	35 C3	1.0736	3.1233
		40 C3	1.0797	2.7276
		45 C3	1.0798	2.4106
BTX	0.1/0.1	25 B	0.5607	2.247
		30 B	0.5715	1.908
		35 B	0.5830	1.667
MeAc	0.1/0.1	25 MeAc	0.3091	0.6730
		30 MeAc	0.3642	0.7323
		33 MeAc	0.4436	0.8618

changes. The second control degree of freedom that is fixed in this figure is the reflux flow rate.

The justification for choosing constant reflux as opposed to constant reflux ratio is given in the feed composition sensitivity analysis shown in the top three rows of Table 6.2. As the results in Table 6.2 clearly show, the required changes in reflux flow rate are much smaller than the required changes in the reflux ratio.

So the reflux flow rate is fixed at 1.0797 kmol/s in Figure 6.4, and the temperature on one stage is held constant (Stage 2, 8, 12, 20, 29, or 37). The abscissa in the plots are the mole fraction of propane in the feed. The ordinates are the purity of the distillate x_D and the impurity of the bottoms x_B .

These results display some counter-intuitive results. Controlling the temperature on Stage 8 near the top of the column does a better job in maintaining bottoms purity than does controlling Stage 29 near the bottom. The bottoms impurity is held quite close to or under the desired 2 mol% propane. On the other hand, controlling the temperature on Stage 29 near the bottom of the column does a better job of maintaining the purity of the distillate at or above the desired 98 mol% propane. Conventional wisdom says that a tray located nearer the product stream should hold its purity more constant.

These results indicate that either Stage 8 or Stage 29 do a fairly good job in maintaining product purities in this binary system when single-end temperature control is used. If dual-temperature control was used and the temperatures at the two ends of the column were controlled, product compositions would be held exactly at their desired values under steady-state conditions if pressure changes do not occur.

6.3.3 Ternary BTX System

The next separation system examined is a ternary mixture of benzene, toluene, and *o*-xylene. The feed flow rate is 1 kmol/s, and the design feed composition is 30 mol% benzene, 30 mol% toluene, and 40 mol% *o*-xylene. The operating objective is to separate the light-key component benzene from the heavy-key component toluene. Of course, the heavier than heavy-key component *o*-xylene goes out the bottom with the toluene. Column pressure is set at 1 atm. The column has 32 stages and is fed on Stage 16. Distillate impurity is specified to be 0.1 mol% toluene. Bottoms impurity is specified to be 0.1 mol% benzene. The reflux ratio required to achieve these purities is 1.908.

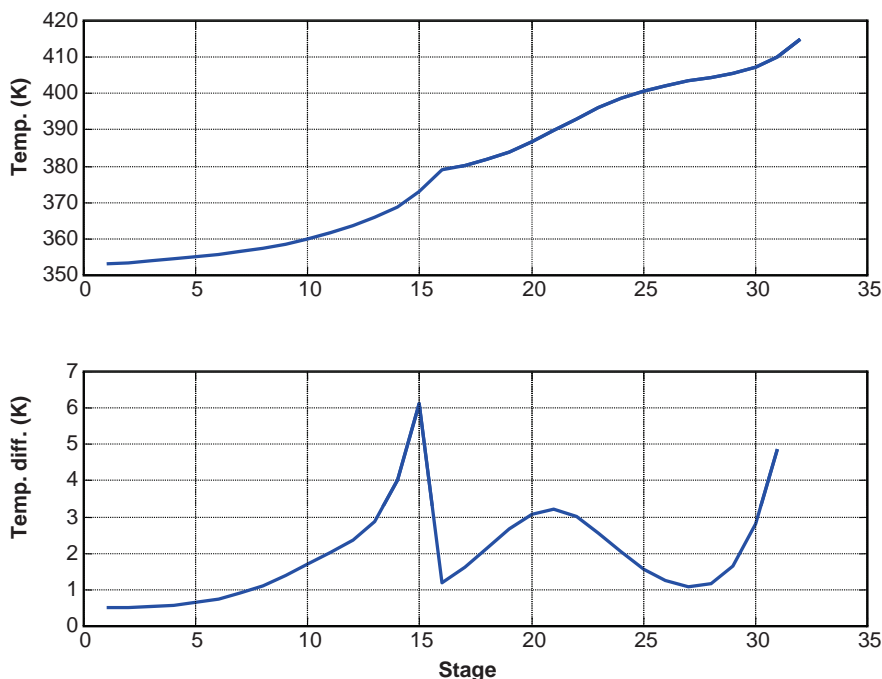


Figure 6.5 BTX: temperature profile and slope.

Slope Criterion. The upper graph in Figure 6.5 gives the temperature profile at design conditions. The lower graph shows the difference between the temperatures on adjacent trays. There is large change right at the feed stage. Because of the introduction of the feed, this is not a good location for temperature control. There is also a large change in temperature near the bottom of the column, which is due to the buildup of the heavier than heavy-key component *o*-xylene. This is also not a good location for temperature control since we are trying to infer the compositions of benzene and toluene. The slope analysis suggests the use of Stage 21 for temperature control.

Sensitivity Criterion. The upper graph in Figure 6.6 gives the open-loop steady-state gains between tray temperatures and the two manipulated variables. These curves show that Stage 21 is sensitive to changes in heat input and Stage 22 is sensitive to changes in reflux.

SVD Criterion. The lower graph in Figure 6.6 gives the U_1 and U_2 values from SVD analysis. The first is the solid line and is associated with reflux. The second is the dashed line and is associated with heat input.

The SVD results are similar to the sensitivity results. They indicate that Stage 21 can be controlled by reflux and Stage 23 by heat input. The singular values of the steady-state gain matrix are $\sigma_1 = 9.14$ and $\sigma_2 = 0.518$, which gives a condition number $CN = \sigma_1/\sigma_2 = 17.6$. This indicates that the two temperatures are not nearly as independent as in the propane/isobutane system, so a dual-temperature control scheme may not be as

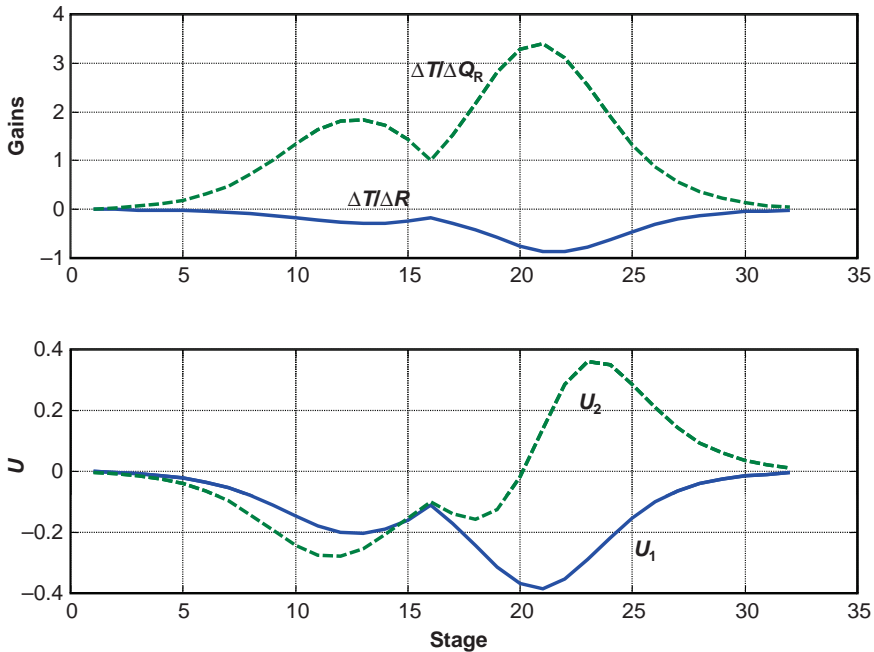


Figure 6.6 BTX: sensitivity and SVD analysis.

effective. This makes sense because Stages 21 and 23 are too close together to be independent.

Invariant Temperature Criterion. Figure 6.7 gives the changes in the temperature profiles for three different feed compositions in the ternary system. The design feed composition is 30/30/40 mol% benzene/toluene/xylene (BTX). The impurities in the bottoms and in the distillate are kept constant at 0.1 mol% benzene and 0.1 mol% toluene, respectively. The solid lines are for 25/35/40 mol% BTX feed composition. The dashed lines are for 35/25/40 mol% BTX feed composition. The dotted lines are for 25/25/50 mol% BTX feed composition.

For changes in the benzene/toluene ratio in the feed, the results show that the temperature on Stage 27 does not change for constant product impurities. So if this is the type of feed composition disturbance expected, controlling Stage 27 should provide effective control.

However, for the change in the xylene concentration of the feed, Stage 27 changes almost 3 K.

Minimum Product Variability Criterion. Figure 6.8 shows how product impurities change when the temperature on a specific tray is held constant and feed composition changes. The second control degree of freedom that is fixed in this figure is the reflux flow rate.

The justification for choosing constant reflux as opposed to constant reflux ratio is given in the middle three rows of Table 6.2. The required changes in reflux flow rate are

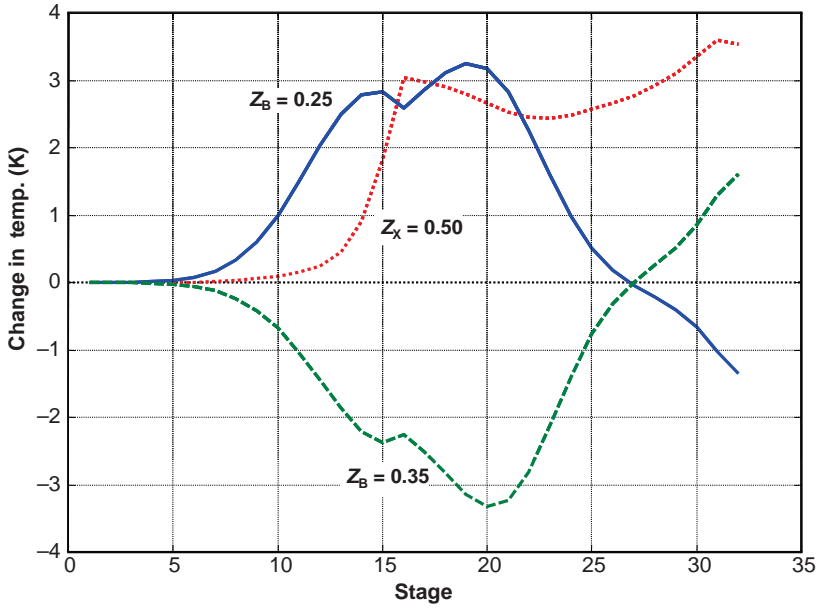


Figure 6.7 BTX: changes in temperature profile for benzene and xylene feed composition changes with product purities fixed.

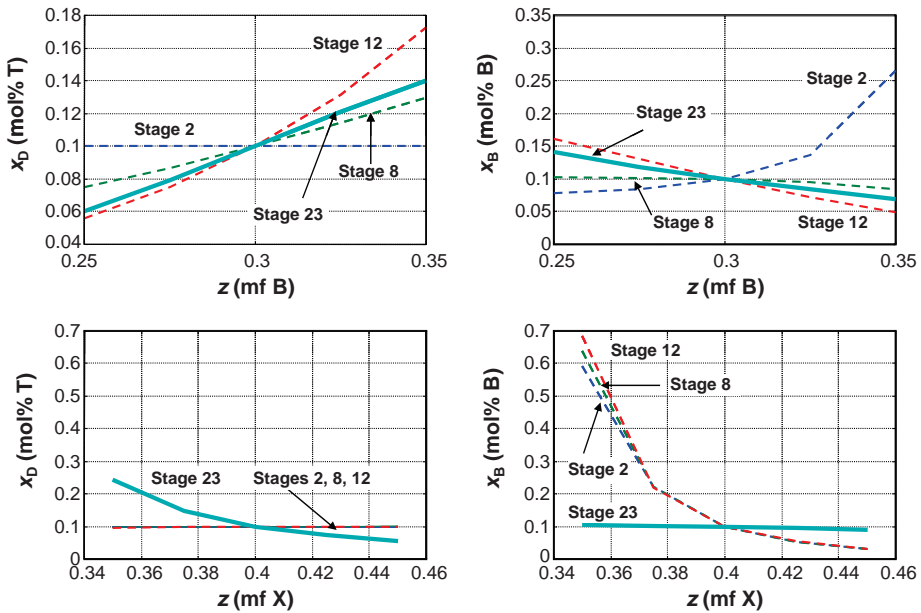


Figure 6.8 BTX: product purities for benzene and xylene feed composition changes with fixed reflux and stage temperature.

much smaller than the required changes in the reflux ratio in the BTX system. The reflux flow rate is fixed at 0.5715 kmol/s.

Figure 6.8 give results for changes in feed composition when the temperature on Stage 2, 8, 12, or 23 is held. The upper graphs are for changes in the mole fraction of benzene in the feed. The xylene mole fraction is fixed at 0.4, so the toluene composition in the feed changes inversely with the benzene composition. For this type of disturbance, holding Stage 23 constant produces less variability in both product purities.

The lower graphs in Figure 6.8 show that holding Stage 23 temperature for changes in the xylene composition of the feed is also effective. However, lowering the xylene in the feed strongly affects distillate purity.

These results indicate the problems with the invariant-temperature criteria. Effectiveness is strongly dependent on what components in the feed change.

6.3.4 Ternary Azeotropic System

Up to this point we have looked at systems with fairly ideal vapor–liquid equilibrium behavior. The last separation system examined is a highly nonideal ternary system of methyl acetate (MeAc), methanol (MeOH), and water. Methyl acetate and methanol form a homogeneous minimum-boiling azeotrope at 1.1 atm with a composition of 66.4 mol% methyl acetate and a temperature of 329 K. This means that the overhead product from the distillation column cannot have a composition greater than this azeotropic composition.

The design objectives are to produce a distillate product with 0.1 mol% water and a bottoms product with 0.1 mol% methyl acetate. The feed flow rate is 1 kmol/s, and the design feed composition is 30 mol% methyl acetate, 50 mol% methanol and 20 mol% water. Column pressure is set at 1.1 atm. The column has 42 stages and is fed on Stage 36 (the stage that minimizes reboiler heat input at design feed composition). The reflux ratio required to achieve the specified purities is 0.7323.

Slope Criterion. The upper graph in Figure 6.9 gives the temperature profile at design conditions. The lower graph shows the differences between the temperatures on adjacent trays. The largest change occurs on Stage 37. There is also a large change in temperature at the very bottom of the column that is due to the buildup of the heaviest component water.

Sensitivity Criterion. The upper graph in Figure 6.10 gives the open-loop gains between tray temperatures and the two manipulated variables. These curves show that Stage 38 is sensitive to changes in heat input and Stage 27 is sensitive to changes in reflux.

SVD Criterion. The lower graph in Figure 6.10 gives the U_1 and U_2 values from the SVD analysis. The results indicate that Stage 38 can be controlled by either reflux or reboiler heat input. There is a second smaller peak in U_2 at about Stage 28 that could be controlled by heat input. The singular values of the steady-state gain matrix are $\sigma_1 = 0.5965$ and $\sigma_2 = 0.0855$, which gives a condition number $CN = \sigma_1/\sigma_2 = 6.98$.

Invariant Temperature Criterion. Figure 6.11 gives the changes in the temperature profiles for three different feed compositions. The design feed composition is 30/50/20 mol% MeAc/MeOH/H₂O. The impurities in the bottoms and in the distillate are kept constant at 0.1 mol% MeAc and 0.1 mol% H₂O, respectively. The solid line is for a feed composition in

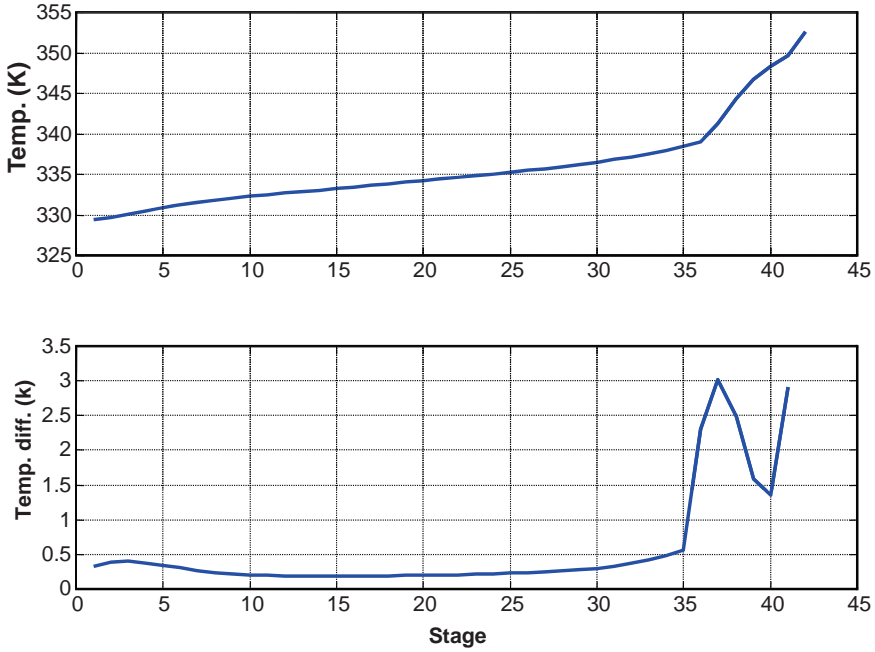


Figure 6.9 MeAc/MeOH/H₂O: temperature profile and slope.

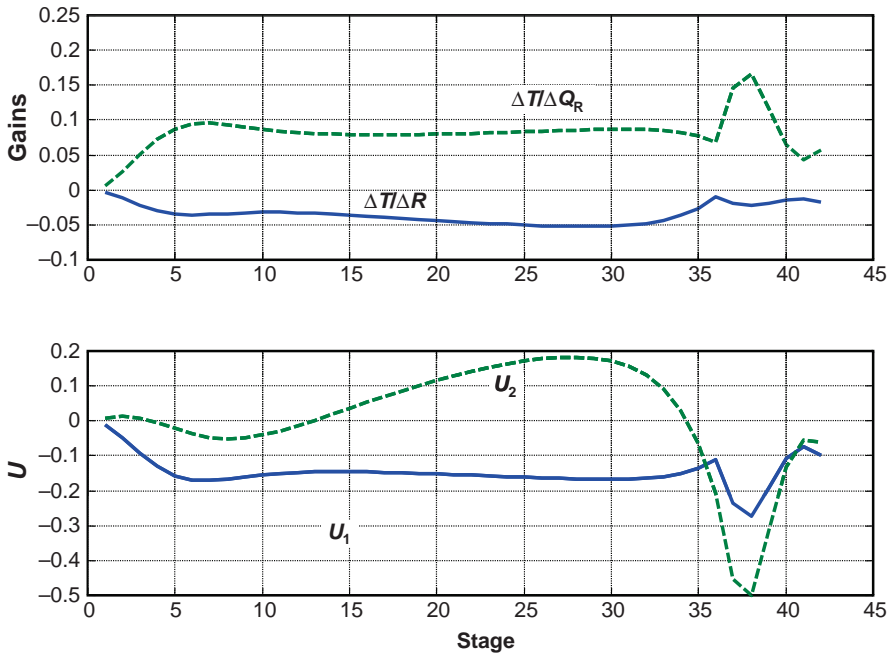


Figure 6.10 MeAc/MeOH/H₂O: sensitivity and SVD analysis.

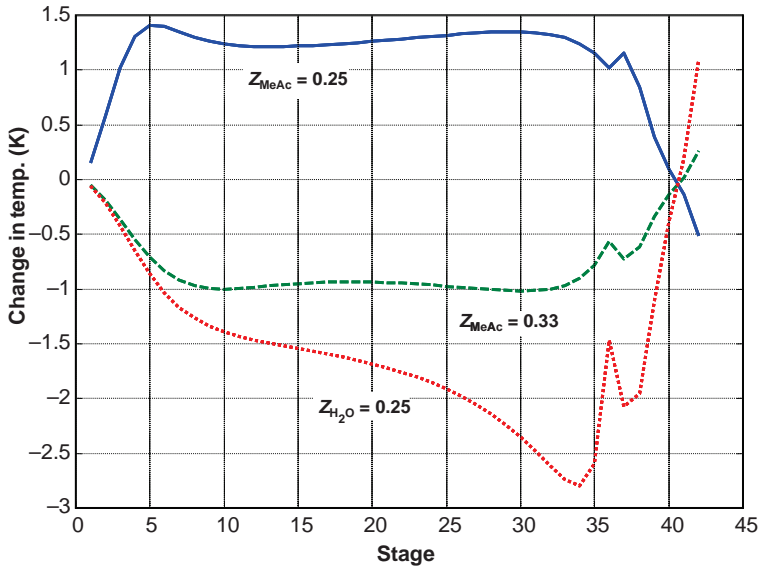


Figure 6.11 MeAc/MeOH/H₂O: changes in temperature profile for MeAc and water feed composition changes with product purities fixed.

which the MeAc composition is decreased from 30 to 25 mol% and the MeOH composition increased from 50 to 55 mol%. The dashed line is for a feed composition in which the MeAc composition is increased from 30 to 33 mol% and the MeOH composition decreased from 50 to 47 mol%. The dotted line is for a feed composition in which the H₂O composition is increased from 20 to 25 mol% and the MeOH composition decreased from 50 to 45 mol%.

Results indicate that the temperature on Stage 41 does not change for constant product impurities for all of these feed composition disturbances. So there is a conflict between the SVD and the invariant-temperature criteria. One recommends Stage 38, while the other recommends Stage 41.

Minimum Product Variability Criterion. Figure 6.12 shows how product impurities change for two different temperature control trays as feed composition changes. In the first case, the temperature of Stage 38 is fixed at 344.28 K. In the second case, the temperature of Stage 41 is fixed at 349.71 K.

The other control degree of freedom that is fixed in this figure is the *reflux ratio*. Unlike the other systems studied, the bottom three rows of Table 6.2 show that the required changes in reflux ratio are smaller than the required changes in the reflux flow rate in this multicomponent, nonideal system. The reflux ratio is fixed at 0.732.

Figure 6.12a give results for changes in the MeAc composition of the feed. The control tray recommended by SVD (Stage 38) does a better job in holding distillate close to its specified value of 0.1 mol%. The changes in the bottoms composition are about the same for both Stage 38 and Stage 41, but in the opposite direction.

Figure 6.12b give results for changes in the water composition of the feed. Controlling the temperature on Stage 38 keeps both products closer to their specification than when Stage 41 is controlled.

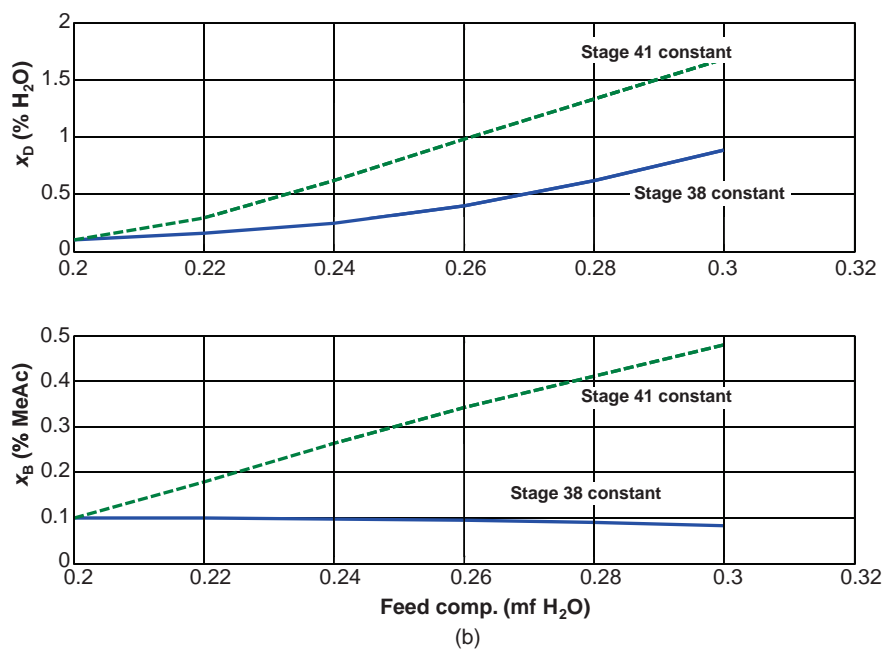
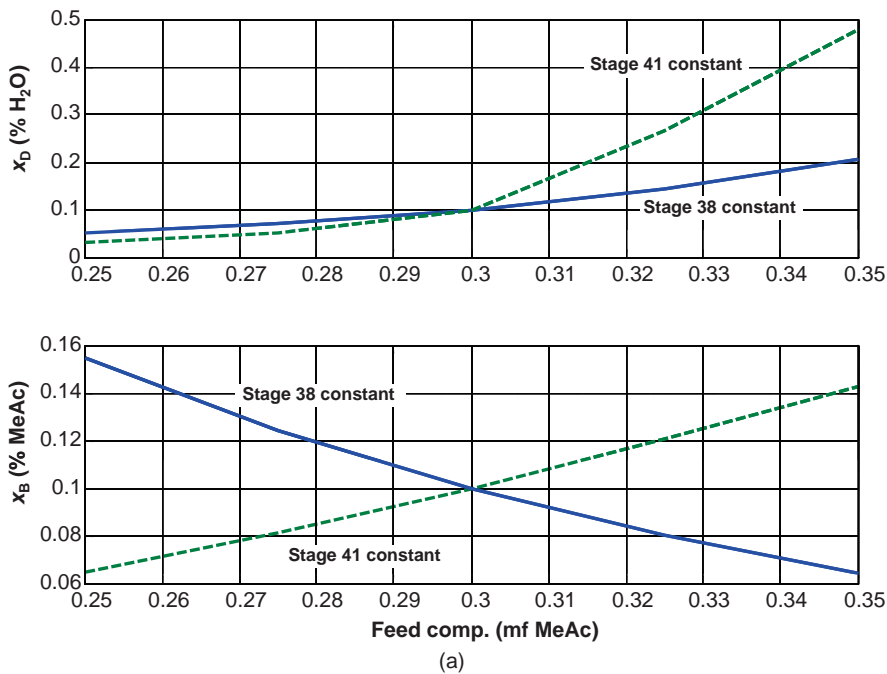


Figure 6.12 (a) MeAc/MeOH/H₂O: changes in product impurities for MeAc feed composition changes with fixed reflux ratio and stage temperature. (b) MeAc/MeOH/H₂O: changes in product impurities for water feed composition changes with fixed reflux ratio and stage temperature.

Closed-loop Multiplicity. One of the interesting features of nonlinear systems is the possible appearance of multiple steady states. Most researchers have explored open-loop multiplicity. We found that closed-loop multiplicity occurs in the methyl acetate/methanol/water system.

The two product impurity levels are fixed at their specified values, and feed composition is varied over a range of values. The required reflux flow rate and reflux ratio are calculated for each case. Figure 6.13 shows what happens when we start with a feed composition of 30/50/20 mol% MeAc/MeOH/H₂O. The reflux ratio is 0.732 and the reflux flow rate is 0.364 kmol/s with this feed composition. As the feed composition is increased, the required reflux and reflux ratio increase. At a feed composition of 33/47/20 mol% MeAc/MeOH/H₂O, the reflux ratio is 0.862 and the reflux flow rate is 0.444 kmol/s. This is labeled “Profile 1” in Figure 6.13.

However, if the feed composition is changed to 34/46/20 mol% MeAc/MeOH/H₂O, there is a huge increase in the required reflux ratio to 1.94 and the reflux flow rate to 0.991 kmol/s. Further increases in MeAc in the feed continue to increase RR and *R*.

Now if the feed composition is reduced back to 33/47/20 mol% MeAc/MeOH/H₂O (labeled “Profile 2”), the reflux ratio does not return to 0.862 but only changes to 1.87. Similarly, the reflux flow rate does not return to 0.444 kmol/s but changes to 0.925 kmol/s. The reflux ratios and reflux flow rates remain high until the feed composition drops to about 30/50/20 mol%, at which point the required RR and *R* drop back to their original levels.

Figure 6.14 gives the composition and temperature profiles of the two steady states. Both have the same feed composition: 33/47/20 mol% MeAc/MeOH/H₂O. Both have the same impurities in the two product streams. But they have different composition and temperature profiles, and they have greatly different reflux ratios and reflux flow rates.

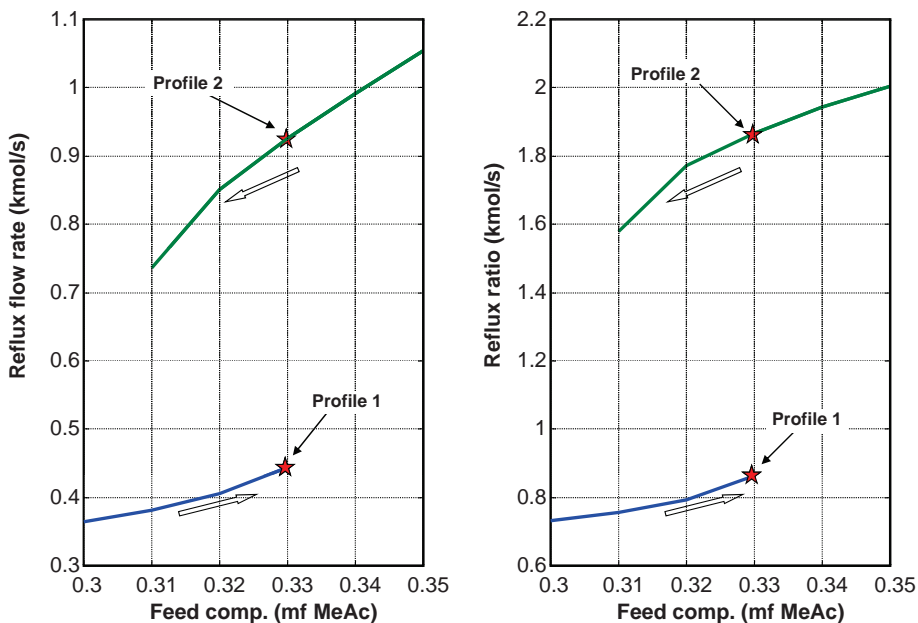


Figure 6.13 MeAc/MeOH/H₂O: closed-loop multiplicity.

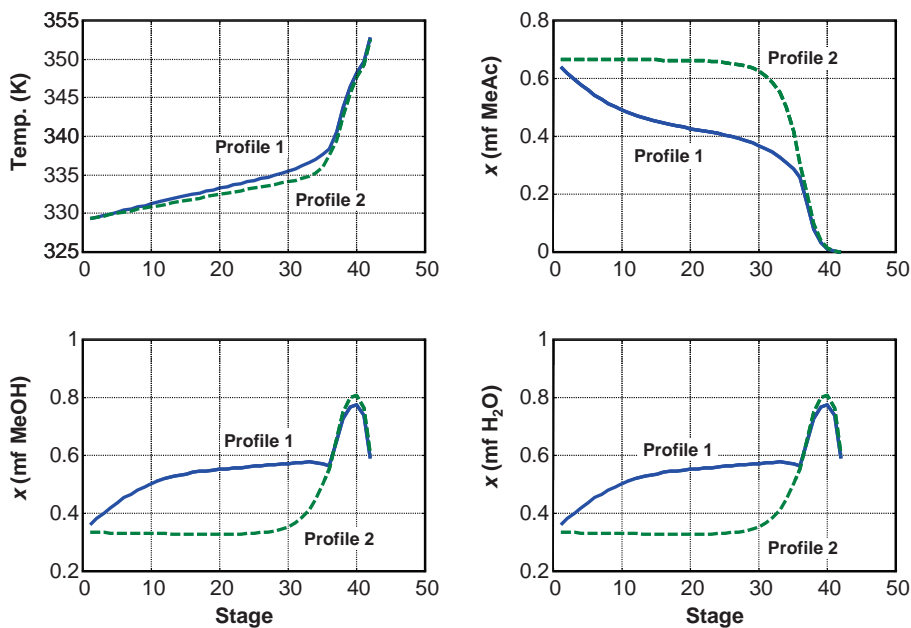


Figure 6.14 MeAc/MeOH/H₂O: profiles at two different steady states.

6.4 CONCLUSIONS

In this chapter, we have illustrated how steady-state calculations can be used to provide guidance in the selection of effective control structures for distillation columns.

REFERENCE

1. C. F. Moore, Selection of controlled and manipulated variables, Chapter 8 in *Practical Distillation Control*, Van Nostrand Reinhold, 1992.

CONVERTING FROM STEADY-STATE TO DYNAMIC SIMULATION

We are now ready to get into the details of converting a steady-state simulation into a dynamic one. Basically, the additional information that must be provided is the physical sizes of the various pieces of equipment.

It is important to remember that pumps and control valve have already been installed in the steady-state simulation. These are not necessary for steady-state simulations in Aspen Plus, which is a “flow-driven” simulation. Streams in Aspen Plus can flow from a vessel at low pressure into a vessel at high pressure (water can flow uphill). Obviously, this is not reality, and we want our dynamic control studies to reflect reality. Therefore, pumps, compressors, and control valves are vital for a realistic dynamic simulation. Pressure drops through heat exchangers must also be incorporated. Providing sufficient pressure drop over a control valve at design conditions with the valve at some fraction opening (typically 50%) is crucial for dynamic controllability. If valve pressure drop is too small, changing the valve opening from 50 to 100% will, in piping systems with other equipment taking pressure drops, result in only a fairly small increase in flow rate. If a valve saturates, controllability is lost.

It is important when specifying the control valves to select the correct valid phase. If the stream is all liquid, select *Liquid-Only* in the *Valid Phases* under *Flash options* on the *Operation* page tab of the valve block. If the stream is all vapor, select *Vapor-Only*. Some valves have both phases (particularly when the inlet is liquid at its bubble point temperature and pressure, which means flashing occurs when the pressure decreases as the fluid flows through the valve) and *Vapor-Liquid* should be selected. Numerical problems can occur in Aspen Dynamics if these valid phases are not correct.

The propane/isobutane column developed in Chapter 3 is used in this chapter as a numerical example. The control valves all have pressure drops of about 3 atm. The column

as 32 stages, is fed on Stage 14, operates at 16.8 atm and produces distillate and bottoms products with impurity levels of 2 mol% isobutane and 1 mol% propane, respectively.

7.1 EQUIPMENT SIZING

The dynamic response of a flow system depends on the flow rate and the volume. For a given flow rate, the smaller the volume, the faster the transient response.

The procedure for sizing the distillation column shell (diameter and height) has already been discussed in Chapter 3. The only remaining issues are the sizes of the reflux drum and the column base. A commonly used heuristic is to set these holdups such that there are 5 min of liquid holdup when the vessel is 50% full, based on the *total* liquid entering or leaving the vessel. For the reflux drum, this is the sum of the liquid distillate and the reflux. For the column base, it is the liquid entering the reboiler from the bottom tray.

These volumetric liquid flow rates can be found by clicking on *Profiles* under the block C1 and then opening the *Hydraulics* page tab. Figure 7.1 shows the window that opens on which the volumetric liquid flow rate for the reflux drum (Stage 1) is given as 0.1782 m³/s. Scrolling down to the bottom tray (Stage 31) gives a volumetric liquid flow rate of 0.3438 m³/s. The total volume of the reflux drum should be 0.1782(60)(10) = 106.9 m³ and that of the column base 0.3438(60)(10) = 206.3 m³. Assuming a length to diameter ratio of two, the diameters and lengths can be calculated.

$$\text{Volume} = \frac{\pi D^2}{4} (2D)$$

The diameter of the reflux drum is 4.08 m and its length is 8.16 m. The column base (or reboiler or “sump”) has a diameter of 5.08 m and a length of 10.16 m.

The values are entered by clicking the *Dynamics* button on the top toolbar (see Fig. 7.2). If this button is not displayed, click the *View* button, then *Toolbar* and check the *Dynamics*

Stage	Temperature liquid from	Temperature vapor to	Mass flow liquid from	Mass flow vapor to	Volume flow liquid from	Volume flow vapor to
	K	K	kg/sec	kg/sec	cum/sec	cum/sec
1	325.062886	325.626931	79.6300297	79.6300297	0.17820154	2.15465763
2	325.626931	326.41917	61.7791152	79.6214374	0.13808464	2.14846053
3	326.41917	327.501948	61.7805846	79.6229067	0.13785861	2.14083596
4	327.501948	328.925276	61.8100485	79.6523707	0.13763178	2.13204887
5	328.925276	330.702512	61.895741	79.7380632	0.13747747	2.12279459
6	330.702512	332.785899	62.0720935	79.9144157	0.13750009	2.11411135
7	332.785899	335.058705	62.3673861	80.2097083	0.13780378	2.1070404
8	335.058705	337.357283	62.7873503	80.6296726	0.13844272	2.10220285
9	337.357283	339.516701	63.3060909	81.1484131	0.13938533	2.09959173
10	339.516701	341.414672	63.8729448	81.7152671	0.14052185	2.09870549
11	341.414672	342.991565	64.4312658	82.2735881	0.14171069	2.09886435
12	342.991565	344.244191	64.9364211	82.7787433	0.14282931	2.09947507
13	344.244191	345.205932	65.3639534	83.2062757	0.14380183	

Figure 7.1 Hydraulics page tab.

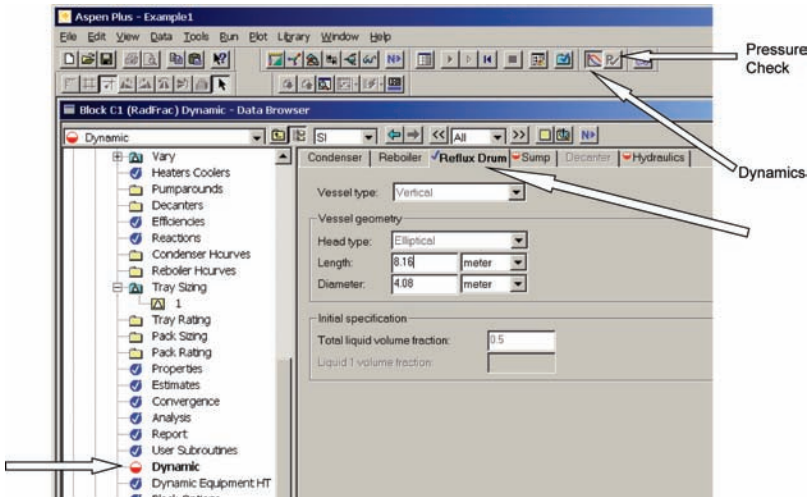


Figure 7.2 Dynamics button.

box. The window that opens has several page tabs. On the *Reflux Drum* page tab, the appropriate diameter and length are entered. The same is done on the *Sump* page tab.

Finally, the *Hydraulics* page tab is clicked, and the window shown in Figure 7.3 opens, on which stage numbers (2 through 31) and the column diameter (5.91 m) are entered. The default values of weir height and tray spacing are 0.05 and 0.6096 m, respectively.

At this point all equipment has been sized. There remain two items to take care of. The pressure of the feed stream leaving valve V1 must be exactly equal to the pressure on the stage where it is fed. The pressure on Stage 14 is found by looking in *Profiles* (1709839.11 N/m²). The outlet pressure of valve V1 is set equal to this value, and the simulation is run again. The last thing to do is to click the *Pressure Checker* button, which is just to the right of the *Dynamics* button on the top toolbar (see Fig. 7.2). If the plumbing has been correctly specified, the window shown in Figure 7.4 appears. We are ready to go to Aspen Dynamics.

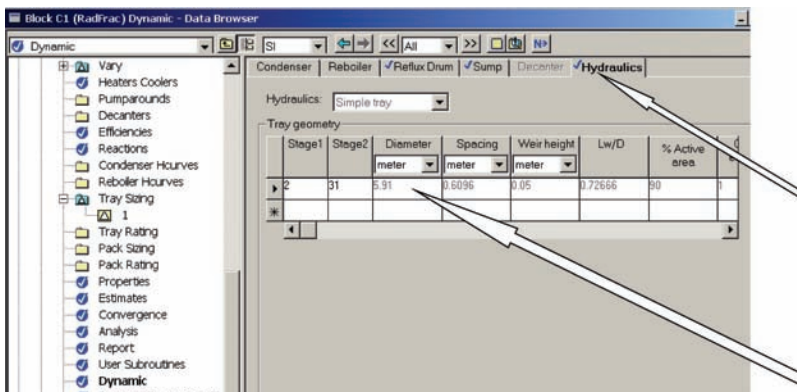


Figure 7.3 Specifying diameter and weir height.



Figure 7.4 Pressure check.

7.2 EXPORTING TO ASPEN DYNAMICS

Aspen Dynamics uses the steady-state information generated in Aspen Plus, but the two simulators are different programs with different files. The Aspen Plus file is *filename.apwz*, and there is also a backup file *filename.bkp*, which is generated. The latter file can be used to upgrade to newer versions of Aspen Plus.

The information from Aspen Plus is “exported” into Aspen Dynamics by generating two additional files. The first is a *filename.dynf* file, which is used in Aspen Dynamics and is modified to incorporate controllers, plots and other features. The second file is a *filenamedyn.appdf* file that contains all the physical property information to be used in Aspen Dynamics.

In the propane/isobutane column example, the Aspen Plus files are called *Example1.apwz* and *Example1.bkp*. The files generated and used in Aspen Dynamics are *Example1.dynf* and *Example1dyn.appdf*. Both of these files are needed to run the simulation in Aspen Dynamics.

The procedure for “exporting” is to click on *File* at the top left corner of the Aspen Plus window and select *Export*. The window shown in Figure 7.5 opens and the drop-down menu is used to select *P-driven Dyn Simulation*, which is the 12th item on the list. Then the *Save* button is clicked. Make sure you know the location where you are saving the file.

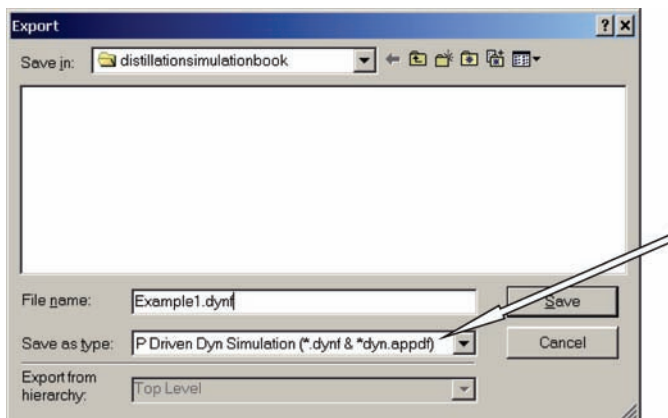
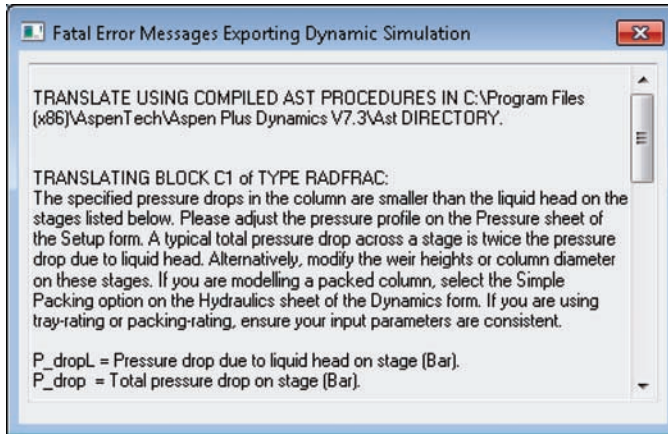
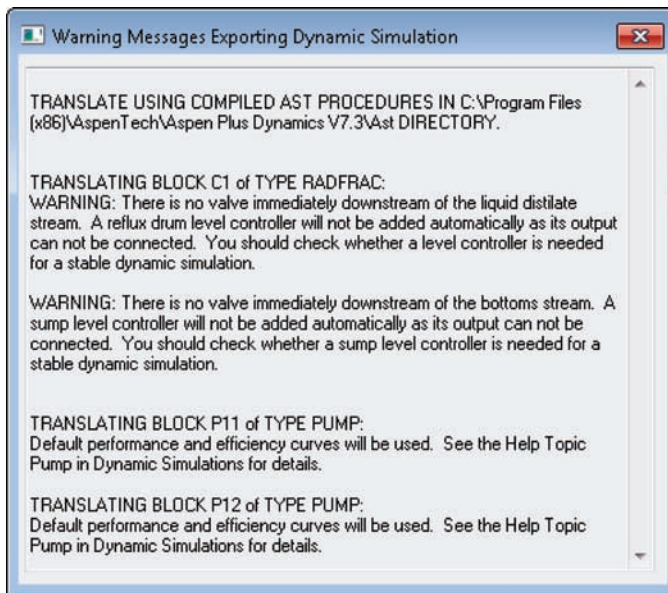


Figure 7.5 Exporting.



(a)



(b)

Figure 7.6 (a) Error message. (b) Warning message.

An error appears (Fig. 7.6a) that informs us that the specified pressure drop (0.0068 atm) is too small for the given weir height and vapor rates. Aspen Dynamics calculates tray pressure drops rigorously, and they change with vapor and liquid rates.

We have two alternatives: increase the specified pressure drop or decrease the weir height. The latter has no effect on the steady-state solution, so we go back to *Dynamics* under the C1 block, select the *Hydraulics* page tab and change the weir height from 0.05 to 0.025 m. Running the program again, pressure checking, and “Exporting” again cause the window shown in Figure 7.6b to open. These messages just remind us that level controllers should be installed once we get into Aspen Dynamics and typical pump curves are

used in the pumps. The “export” is successful, and we are ready to go into Aspen Dynamics.

7.3 OPENING THE DYNAMIC SIMULATION IN ASPEN DYNAMICS

Go to the location where you have saved the files and open the *Example1.dynf* file. The screen that opens contains several windows (see Fig. 7.7).

The *Process Flowsheet Window* is where the control structure will be developed. The *Simulation Messages* window is where the progress of the simulation is shown and simulation time is displayed. The window in the upper left corner *Exploring* is where various types of controllers, control signals, and other elements can be found to “drag and drop” onto the flowsheet.

The very first thing to do with any newly imported file is to make an “Initialization” run to make sure everything is running. At the very top of the screen there is a little window that says *Dynamic*. Clicking the arrow to the right, opens the drop-down menu shown in Figure 7.8a. Select *Initialization* and click the *Run* button, which is just to the right. If everything is set up correctly, the window shown in Figure 7.8b opens.

The next thing to do is to make sure the integrator is working correctly. This is done by changing from *Initialization* back to *Dynamic* and clicking the *Run* button again. The *Simulation Messages* window at the bottom of the screen should start displaying advancing simulation time. An example is shown in Figure 7.8c. Notice the green block at the bottom of the screen. If something is wrong, this block will turn red and you will not be able to run. The run is stopped by clicking the *Pause* button, which is the second button to the right of the *Run* button.

The initial flowsheet has some default controllers already installed. In this simple, single-column process there is only one default controller, the pressure controller. It is

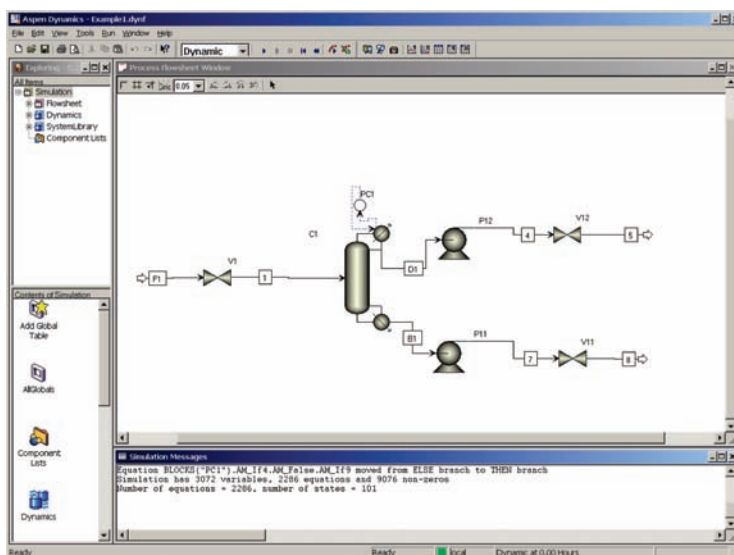


Figure 7.7 Initial screen in Aspen Dynamics.

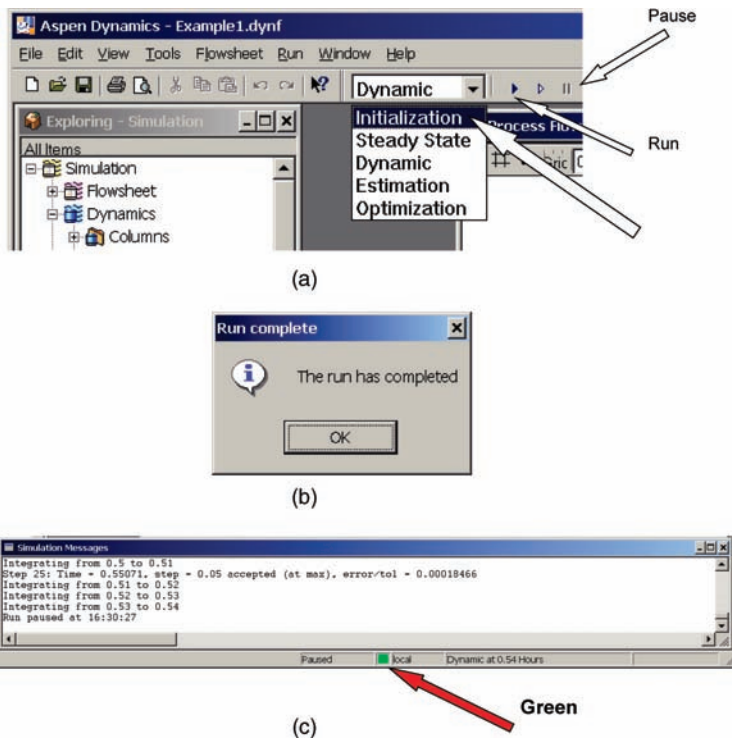


Figure 7.8 (a) Selecting initialization. (b) Initialization run successful. (c) Making dynamic run.

configured to measure condenser pressure and manipulate condenser heat removal. The action of the controller, the range of the pressure transmitter, the maximum heat-removal rate, and the controller tuning constants are all set up at some nominal values. We will come back and look at these later. But this indicates the number of items that must be specified for each new controller that we add to the flowsheet. At a minimum, four additional controllers must be added to achieve effective operation of the column.

1. Reflux drum level controller
2. Base level controller
3. Feed flow controller
4. Tray temperature controller (TC)

There are four remaining *manipulated* variables (distillate flow rate, bottoms flow rate, reboiler duty, and feed flow rate) to control these four *controlled* variables. The issue of pairing which manipulated variable with which controlled variable is called control structure selection. A variety of different types of control structures will be discussed in this and subsequent chapters.

We have not listed reflux in the list above because the default configuration in Aspen Dynamics is to fix the *mass* flow rate of the reflux. We will discuss how this setup can be changed later in this chapter.

7.4 INSTALLING BASIC CONTROLLERS

Let us go through the details of installing a level controller on the base of the column. There are several ways to select control elements and drop them on the *Process Flowsheet Window*.

In older versions of Aspen Dynamics, the user would go to the *Exploring* window, click on *Dynamics* under *Libraries* and *Simulation* and select *Control Models*. A long list of alternative controller types and dynamic elements is displayed, as shown in Figure 7.9a. We will use several of these extensively: *Dead_time*, *Lag_1*, *Multiply*, and *PIDIncr*.

In the present version 7.3, all the elements can be shown on a palette at the base of the window as shown in Figure 7.9b by clicking *View* at the top of the window and clicking the box next to *Model Libraries*. Elements can be easily dropped onto the PFD. Control signals can be added by clicking the box on the left side.

To install a controller, click the *PIDIncr* icon, move the cursor to the flowsheet window and drop the controller at the desired location (see Fig. 7.10). The controller can be

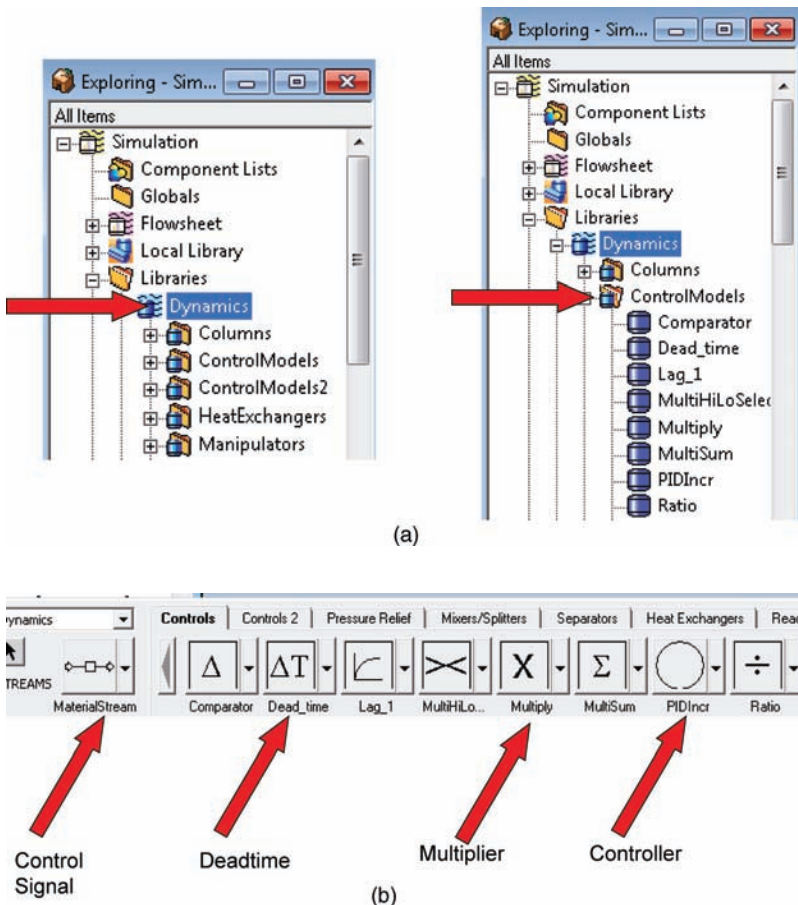


Figure 7.9 (a) Control models. (b) Control model panels.

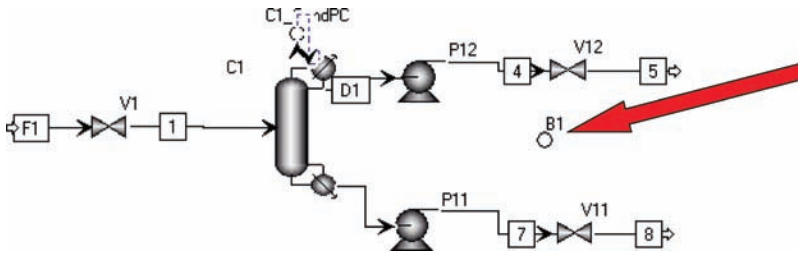


Figure 7.10 Controller placed on flowsheet.

renamed by clicking the circle, right clicking, selecting *Rename block*, and typing in the desired label “LC11.”

Now the control signals must be connected. The process variable (PV) signal is the variable to be controlled. For this level controller, it is the liquid level on the last stage of the column (Stage 32). We click the box on the left side of the control palette, as shown in Figure 7.11a. Click the *Control Signal* and move the cursor to the flowsheet. A number of blue arrows show up that indicate where a control signal can be placed (Fig. 7.11b). Placing the cursor on the arrow coming out of the reboiler and releasing the mouse button, opens the window shown in Figure 7.12a on which we can scroll down to the very bottom and select *Sump Level*. Alternatively (and equivalently) we can scroll down to Stage 32 and select *Level*, as shown in Figure 7.12b.

Clicking *OK* connects the control signal line to the column base and lets us connect the other end to the controller (see Fig. 7.13a). Clicking on the blue arrow on the left side of the controller opens the window shown in Figure 7.13b on which we select *LC11.PV*. Clicking *OK* completes the control signal connection between the column base level and the controller.

The next step is to connect a control signal from the controller to the valve V11 on the bottoms stream. The cursor is placed on the arrow exiting the controller and the window shown in Figure 7.14a opens. We select the *LC11.OP* and click *OK*. Then the line is connected to the valve. The final LC11 loop is shown in Figure 7.14b.

To set up the controller, double click on the “LC11” icon on the flowsheet. The controller faceplate shown at the top of Figure 7.15a opens. Controller faceplates are where we keep track of what is going on in the dynamic simulation, where we set controller parameters, where we switch from manual to automatic control, where we change SPs, and so on. The very first thing to do is to click the *Configure* button. This opens the window shown at the bottom of Figure 7.15a. Then click on the *Initialize Values* button at the bottom of this window. As shown in Figure 7.15b, this provides the steady-state values of the base level (6.35 m) and the control valve opening (*Initial output = 50%*).

The action of the controller should be *Direct* because if the level increases, the signal to the valve should increase ($PV\uparrow, OP\uparrow$) to remove more bottoms. In some columns, base level is controlled by manipulating a valve in the feed to the column. In that control structure, the base level controller action should be *Reverse*.

As we want proportional-only control, the controller gain is set equal to 2 and the integral time is set at a very large number (9999 min shown in Fig. 7.15b).

Next, the *Ranges* page tab is clicked, which opens the window shown in Figure 7.16. The default value for the level transmitter range is 0–12.7 m. The default value of the

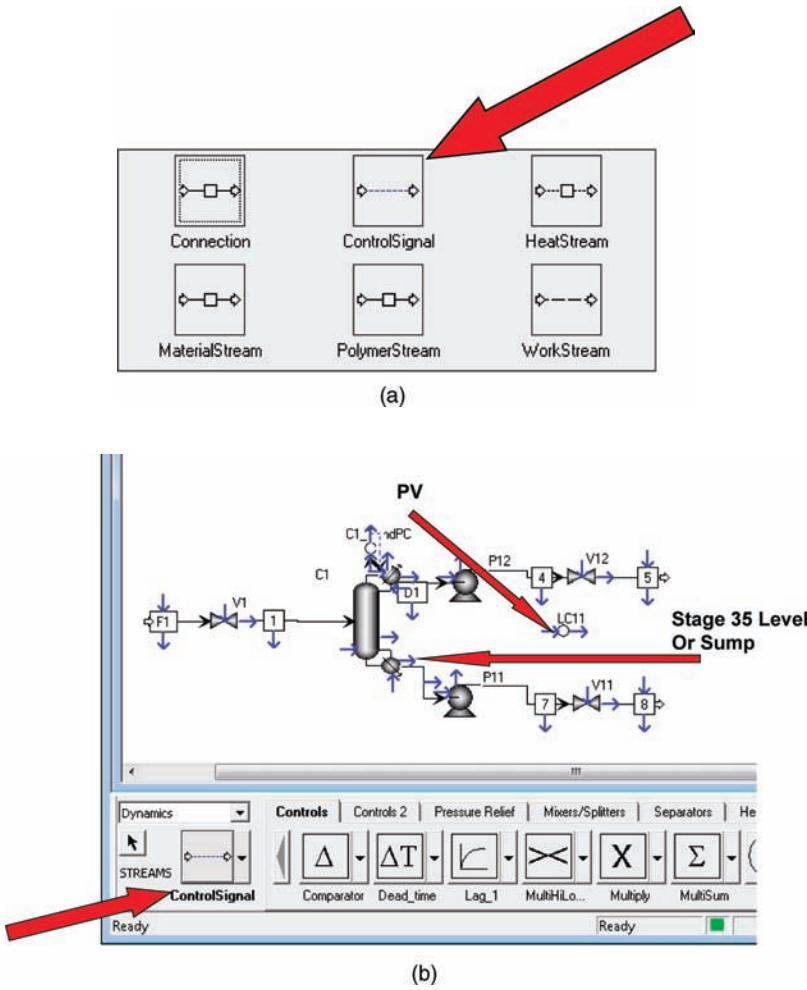


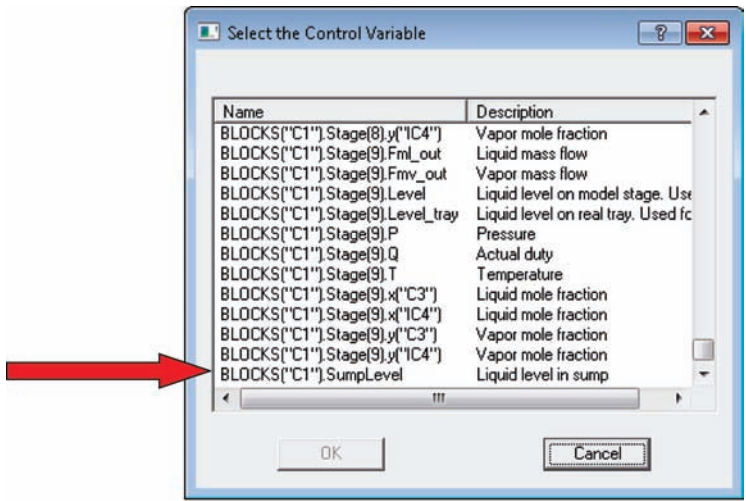
Figure 7.11 (a) Selecting control signal. (b) Attaching control signal.

controller output range is 0–100%. Both of these are what we want, so they require no changes. The *Configure* window is then closed.

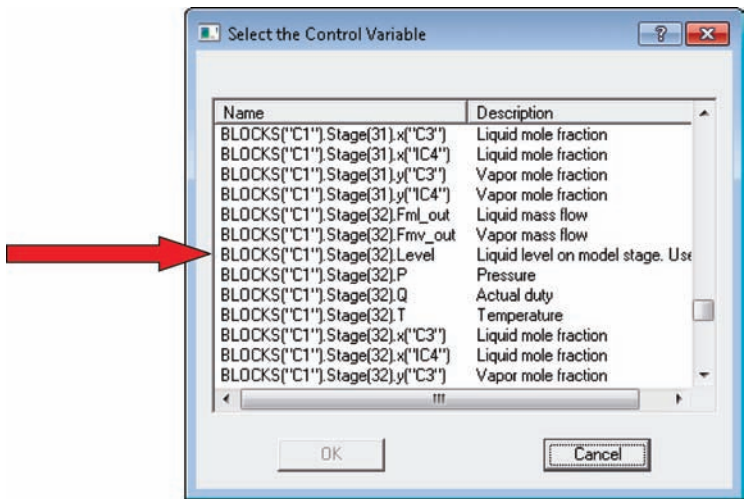
The faceplate is located at some convenient spot in the window where we can keep an eye on what is going on with this level loop. Remember there will eventually be five controller faceplates.

Let us look in detail at the faceplate. As shown in Figure 7.17, there are six important buttons at the top. The first button on the left is the *Auto* button, the second is *Manual* and the third is *Cascade*. When the *Auto* button is pushed the controller changes the *OP* signal automatically based on the current values of the set point (*SP*) and the *PV*. The value of the *SP* can be changed by double clicking on the number in the box to the right of *SP*, typing in the desired number and hitting *Enter* on the keyboard.

When the *Manual* button is pushed, you can manually set the *OP* signal. This is done by double clicking on the number in the box to the right of *OP*, typing in the desired number and hitting *Enter* on the keyboard. When the *Cascade* button is pushed, the controller



(a)



(b)

Figure 7.12 (a) Selecting sump level. (b) Selecting stage 32 level.

receives its set point signal from some other control element. We will illustrate this later in this chapter. The other buttons on the faceplate will be discussed later.

Now would be a good time to check out the pressure controller, which was automatically set up when we started Aspen Dynamics. Figure 7.18a shows the faceplate (which appears after double clicking the icon on the flowsheet) and clicking the *Configure* page tab. The default controller tuning constants are a gain of 20 and an integral time of 12 min. These work pretty well in most column simulations. Note that the controller output is *not* a “% of scale” signal sent to a valve. It is a heat-removal rate in the condenser. As a result, the controller is set up to be reverse acting: when pressure goes up, the controller output signal goes down causing more heat to be removed. The reason for this action becomes clear when we look at the *Ranges* page tab shown in Figure 7.18b. Notice that the range of the

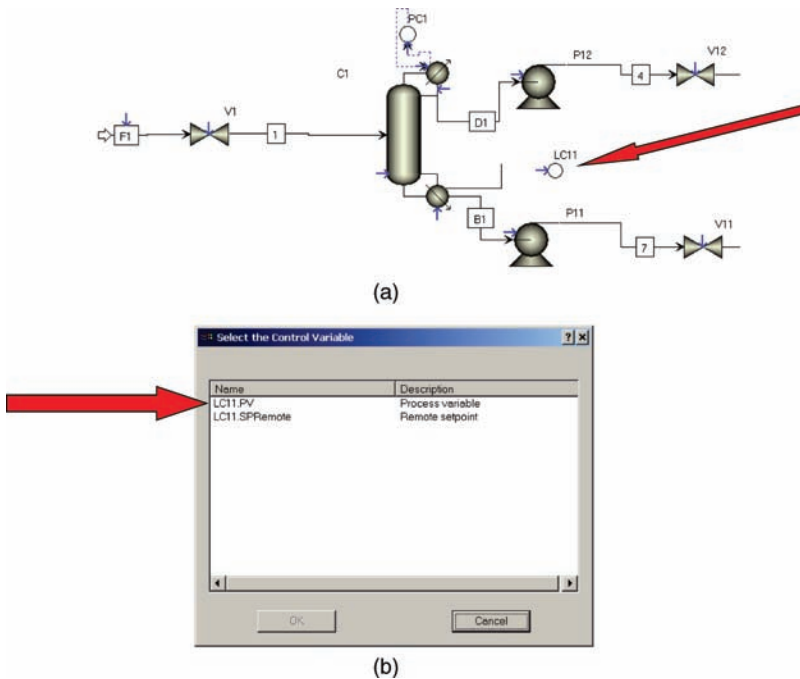


Figure 7.13 (a) Control signal attached to reboiler. (b) Attaching to controller.

controller output is from a minimum of $-45,347,000$ W to a maximum of 0 W. This is to conform with the Aspen convention that heat removal is negative.

In my experience the only modification that sometimes needs to be made to the pressure controller is to change to a more convenient pressure transmitter range. For example, in this column the operating pressure is 16.8 atm. We might change the pressure transmitter range to 14–19 atm from the very wide range used in the default setup. Of course, the gain should be correspondingly reduced.

The second-level controller LC12 for the reflux drum is installed and connected in the same way. The *PV* signal comes from the level on Stage 1. The *OP* goes to valve V12. A direct-acting proportional-only controller is specified.

The final basic controller we need to set up is a flow controller on the feed. A controller is placed on the flowsheet. Its *PV* signal is the molar flow rate of the feed stream *F1*. Its *OP* signal goes to valve V1. After opening the *Tuning* page tab and clicking the *Initialize Values* button, the controller is set up to be *Reverse* acting, and conventional flow controller tuning is used ($K_C = 0.5$ and integral time = 0.3 min), as shown in Figure 7.19. The most common error in setting up a flow controller is to forget to specify *Reverse* action.

The flowsheet now has four controller face plates displayed, as shown in Figure 7.20. We have one more controller to add, a temperature controller that holds the temperature on a selected tray by adjusting the reboiler heat input.

7.4.1 Reflux

It is important to clarify what is happening to the reflux flow. The column icon does not show the plumbing details of a reflux drum, pump, and reflux valve. As mentioned earlier,

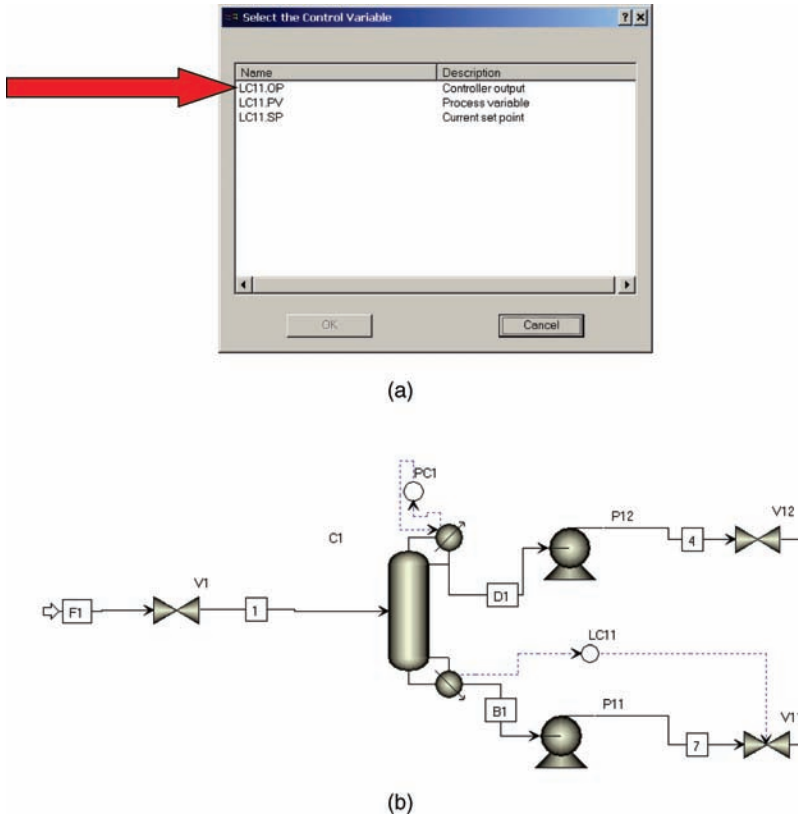


Figure 7.14 (a) Selecting OP signal. (b) Final loop with signal connected.

the default condition in Aspen Dynamics is that the *mass* flow rate of reflux is constant, unless otherwise adjusted. For example, if we wanted to control reflux drum level with reflux flow rate, the level controller *OP* signal would be connected to the column and the *Reflux.FmR* would be selected. The second common application is when we want to ratio the reflux flow rate to the feed flow rate. We will illustrate these by examples in this and later chapters.

7.4.2 Issues

A word of caution is appropriate at this point. During the initialization of controllers sometimes quirky things occur. There are some bugs in Aspen Dynamics that sometimes set the *OP* signal at the wrong initial value (e.g., at 100 instead of 50%) or the *PV* at a value not equal to the steady-state value. To get around these problems, switch the controller to manual, type in the correct *OP* value and run the simulation for a while. Then switch the controller to automatic and run out to a steady state.

Another bit of advice is to run the simulation for a short period of time after each controller has been added to make sure everything is set up okay and there are no errors. If you add several controllers and then find out the simulation will not run, you don't know where the error was made. A final suggested "good practices" is to adhere to Silebi's first

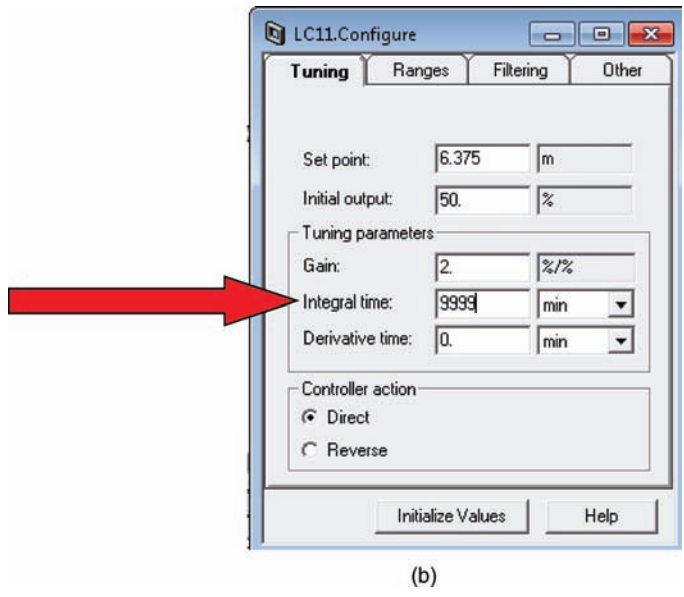
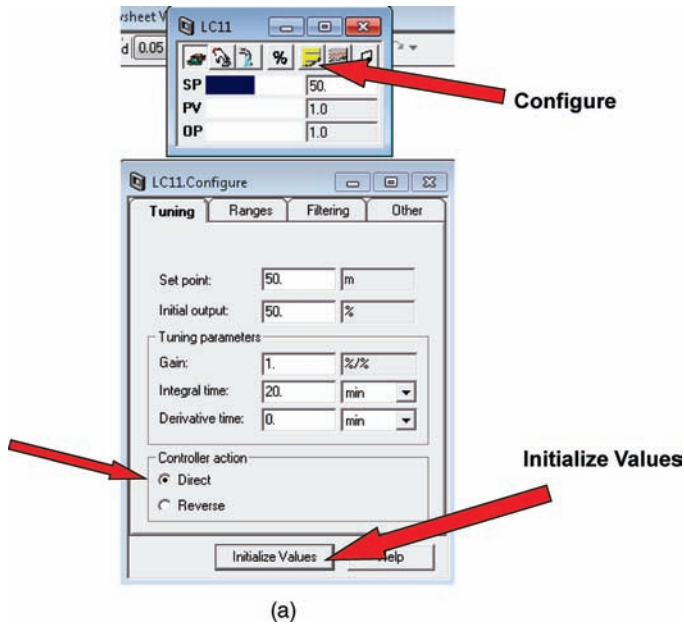


Figure 7.15 (a) Initial controller faceplate and initialize. (b) Proportional level control tuning.

law of Aspen simulation: “save early and save often.” The software shuts every once in a while, and you will lose all your work since the last time you saved the file.

While we are on the subject of running, once the simulation runs out in time and converges to a steady state, the file should be saved as an initial condition from which disturbances and alternative control structures can be started for evaluation. We want to

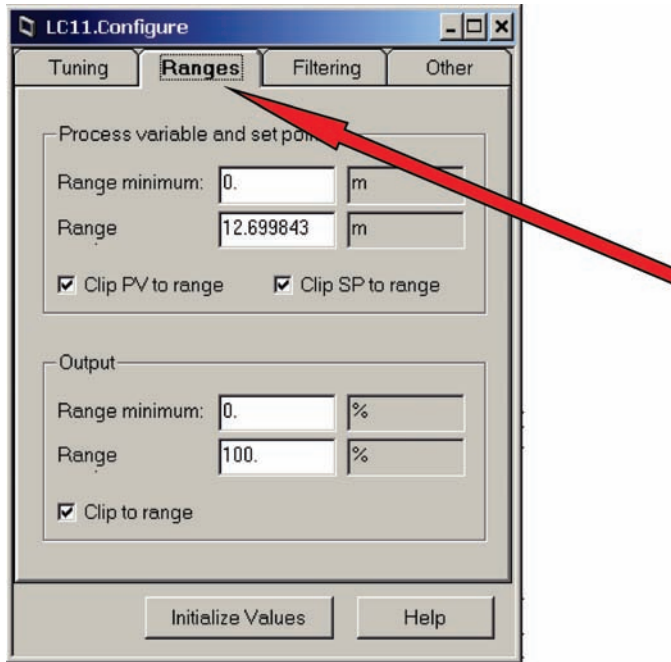


Figure 7.16 Ranges page tab.

save the file with time set equal to zero so that it can be used to establish initial conditions for new runs. To do this, make an *Initialization* run and then switch to *Dynamic* (but do not run). Click the *Rewind* button, which is the fifth one from the right on the upper tool bar (see Fig. 7.20). A window opens (Fig. 7.21) on which you can select the *Initialization Run* as the *Select rewind snapshot* and then save the simulation file. Note that time is now set to zero. You can then “rewind” to these conditions whenever you want to start again at this steady state.

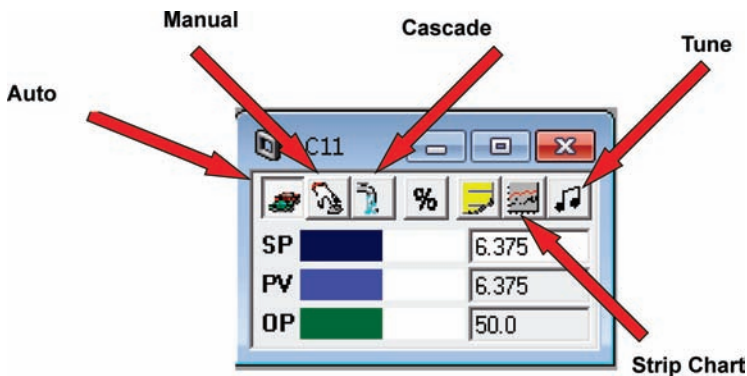
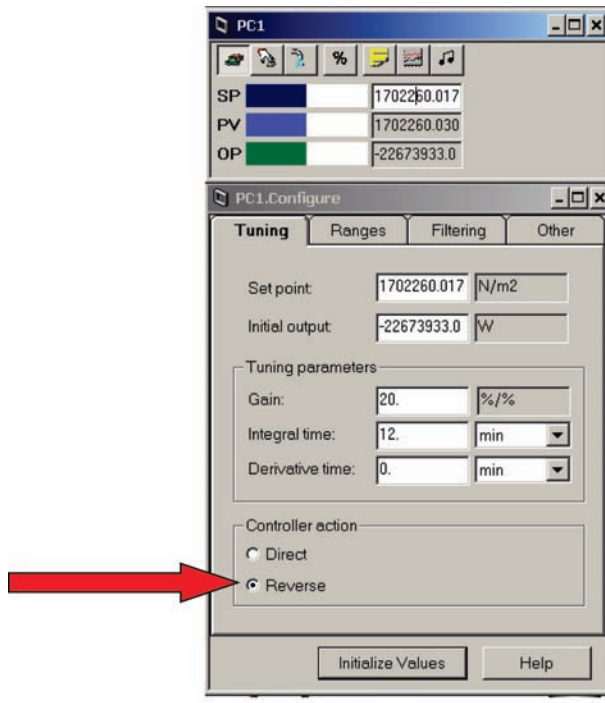
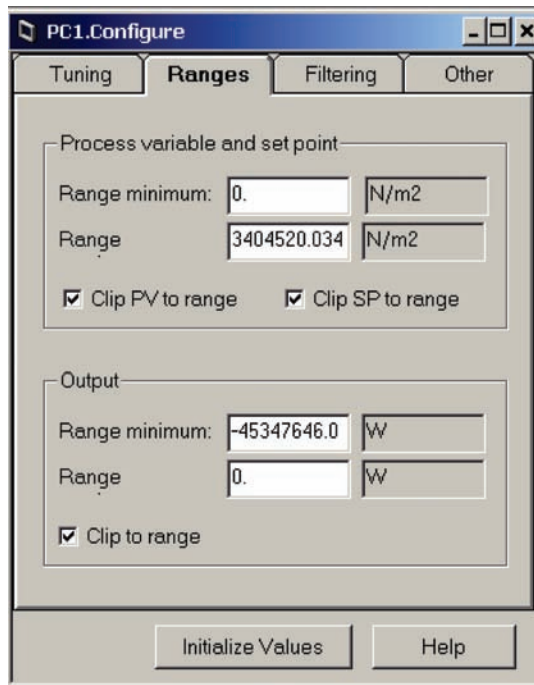


Figure 7.17 Faceplate details.



(a)



(b)

Figure 7.18 (a) Pressure controller. (b) Ranges page tab.

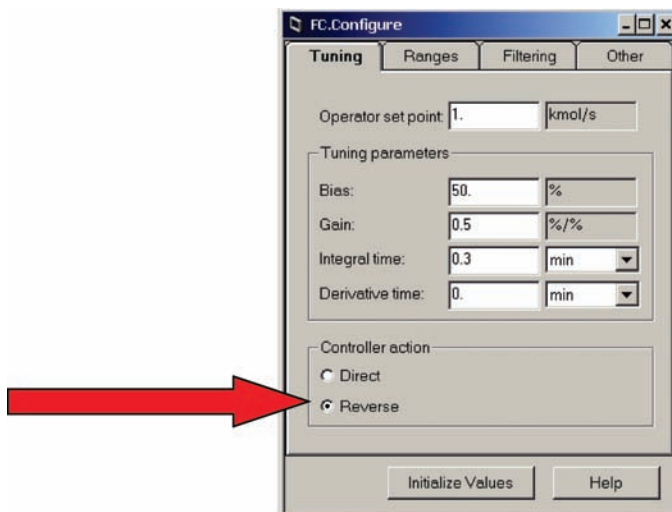


Figure 7.19 Flow controller setup.

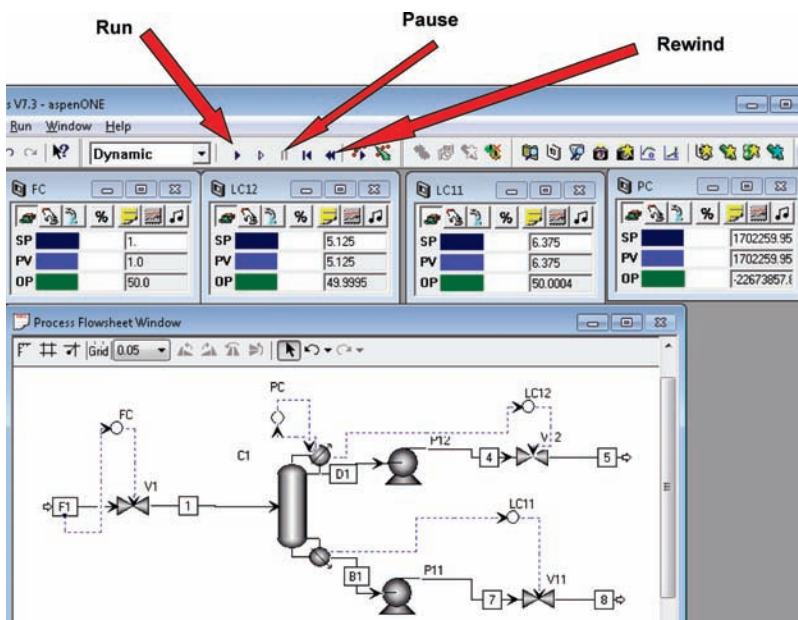


Figure 7.20 Running, pausing, and rewinding.

7.5 INSTALLING TEMPERATURE AND COMPOSITION CONTROLLERS

Installing temperature and composition controllers is somewhat more involved than installing level and flow controllers because of three issues. First, we need to include additional dynamic elements in the loop. Temperature and composition measurements

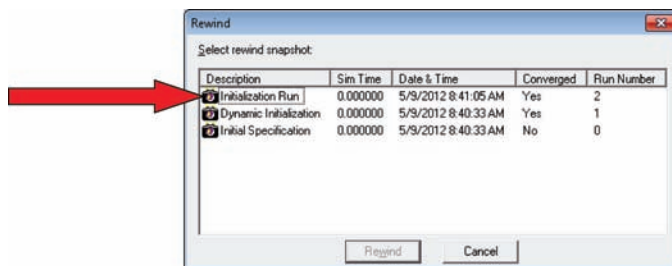


Figure 7.21 Rewinding the snapshot.

have significant inherent dynamic lags and deadtimes. These should be incorporated in the control loop. This is necessary so that we use realistic controller tuning constants and do not predict dynamic performance that is better than the performance achievable in a real plant installation.

Second, the tuning of temperature and composition controllers is more involved than simply using heuristics as is done in the case of flow and level controllers. Some convenient and effective tuning procedure is required. One of the best methods is to run a relay-feedback test to find the ultimate gain and ultimate frequency. This test is incorporated into Aspen Dynamics and is very easy to run. Knowing the ultimate gain and period, some standard tuning rules can be applied. The conservative Tyreus–Luyben tuning settings work well for distillation columns in which aggressive responses are undesirable because they could cause column flooding or dumping due to hydraulic limitations.

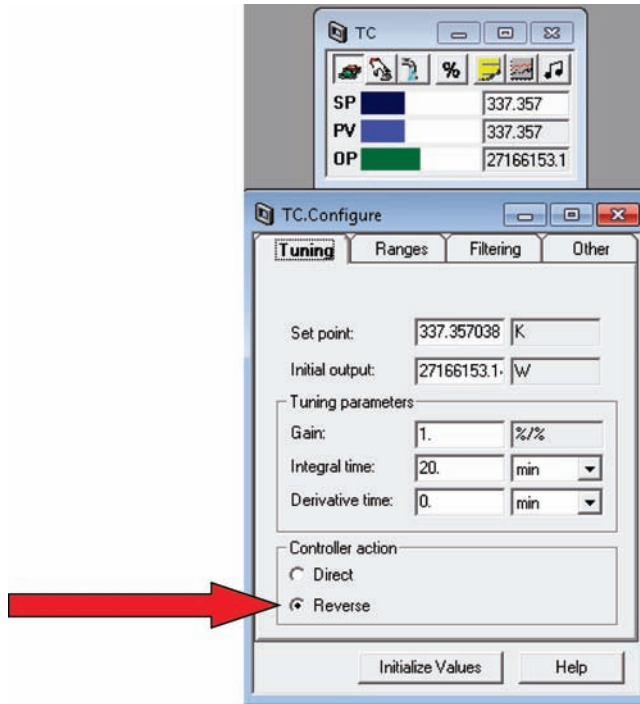
Third, the appropriate location for the temperature or composition sensor may not be obvious. Some method for making a good selection must be used. As discussed in Chapter 6, there are several ways to approach this problem. These include looking at the shape of the temperature profile in the column, calculating steady-state gains and using SVD analysis.

7.5.1 Tray Temperature Control

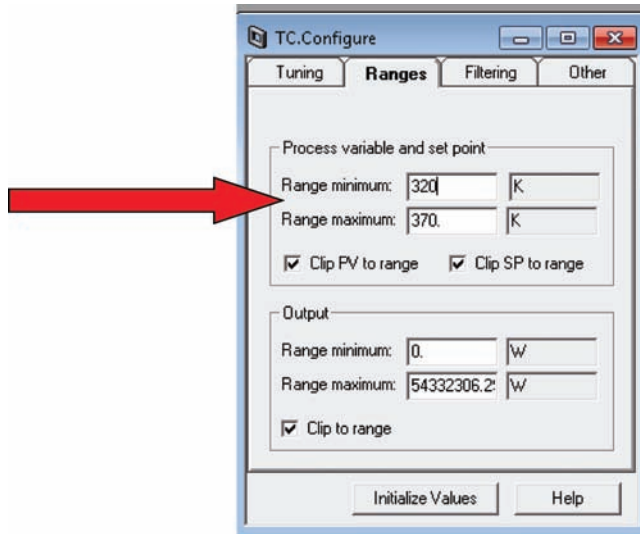
Let us first discuss using a temperature controller to maintain a tray temperature in the column. Looking at the temperature profile in Aspen Plus, we see that Stage 9 displays a fairly steep slope. Its temperature is 337.36 K.

A controller is installed on the flowsheet in the normal way. The *PV* is selected to be the temperature on Stage 9. The *OP* is selected to be the reboiler heat input Q_{RebR} . Figure 7.22a shows the controller faceplate and the *Tuning* page tab after the *Initialize Values* button has been clicked. The normal controller output is 27,166,000 W. The controller action should be set at *Reverse* because if the tray temperature is going up, the reboiler heat input should be decreased. It is convenient to change the range of the temperature transmitter from the default 273–401 K to a more convenient and narrower range 320–370 K, as shown on the *Ranges* page tab in Figure 7.22b.

The program is run to make sure everything works okay without a lag or a deadtime in the loop. Now we back up and insert a deadtime element on the flowsheet between the column and the temperature controller. The reason for installing the controller initially without the deadtime element is to avoid initialization problems that sometime crop up if you attempt to install the deadtime and the controller all in one shot.



(a)



(b)

Figure 7.22 (a) Initial installation of temperature controller. (b) Ranges page tab.

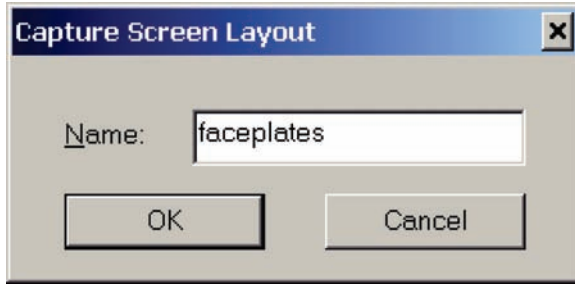


Figure 7.23 Saving screen layout.

Capture Screen Layout. Before we proceed, it might be wise to save some of the work. Since a fair amount of time has been spent in setting up the faceplates and arranging them on the screen, we can avoid having to do this again by clicking on *Tools* in the toolbar at the top of the screen and selecting *Capture screen layout*. The window shown in Figure 7.23 opens on which we enter an appropriate name. When the program is restarted, the screen layout can be reinstalled by going to the *Exploring* window, clicking *Flowsheet*, and double clicking on the icon in the lower *Flowsheet Contents* window with the name you provided.

Install Deadtime. Now let us install the deadtime element. The control signal line from Stage 9 temperature is selected. Right clicking, selecting *Reconnect Destination* and placing the icon on the arrow pointing to the deadtime icon connect the input to the deadtime. A new control signal is inserted between the deadtime and the controller. The deadtime icon then is selected. Right clicking, selecting *Forms* from the drop-down list and selecting *All Variables* open the window shown in Figure 7.24a. The *DeadTime* value is initially 0 min. Notice that the *Input* and *Output* values are set at a default number, not the actual 337.36 K value. A deadtime of 1 min is entered, and performing an *Initialization run*

	Value
ComponentList	Type1
DeadTime	0.0
Input_	274.15
Output_	274.15
TimeScaler	3600.0

(a)

	Value	Spec	Units
ComponentList	Type1		
DeadTime	1.0	Fixed	min
Input_	337.358	Free	K
Output_	337.358	Free	K
TimeScaler	3600.0		

(b)

Figure 7.24 (a) Deadtime all variables table. (b) After initialization run.

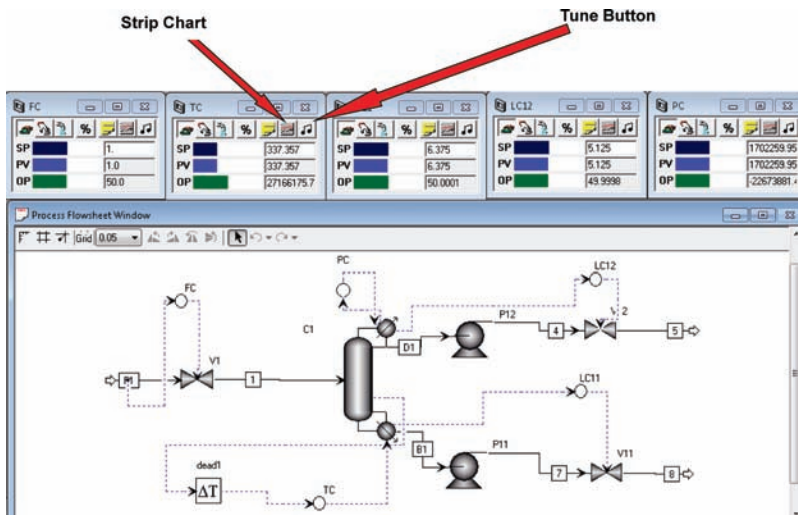
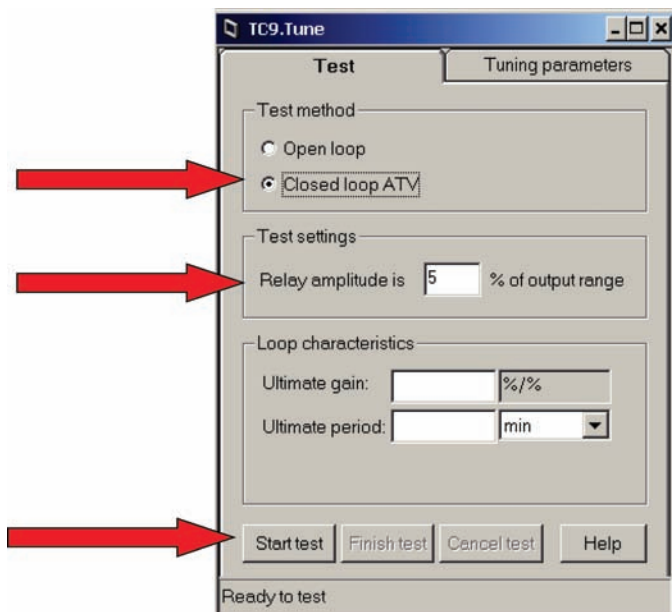


Figure 7.25 Flowsheet with controller faceplate.

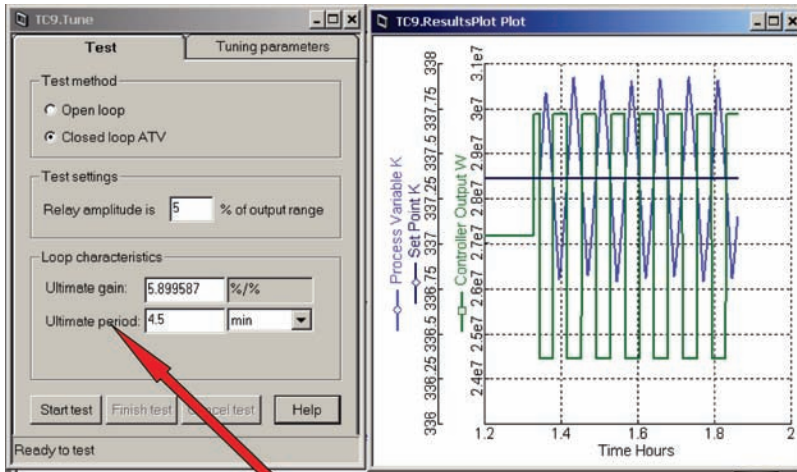
fills in the correct values, as shown in Figure 7.24b. The final flowsheet and controller faceplates are shown in Figure 7.25.

Relay-Feedback Test. Everything is ready for the relay-feedback test. Clicking the *Tune* button on the far right at the top of the controller faceplates (see Fig. 7.25) opens the window shown in Figure 7.26a. We specify a *Closed loop ATV* as

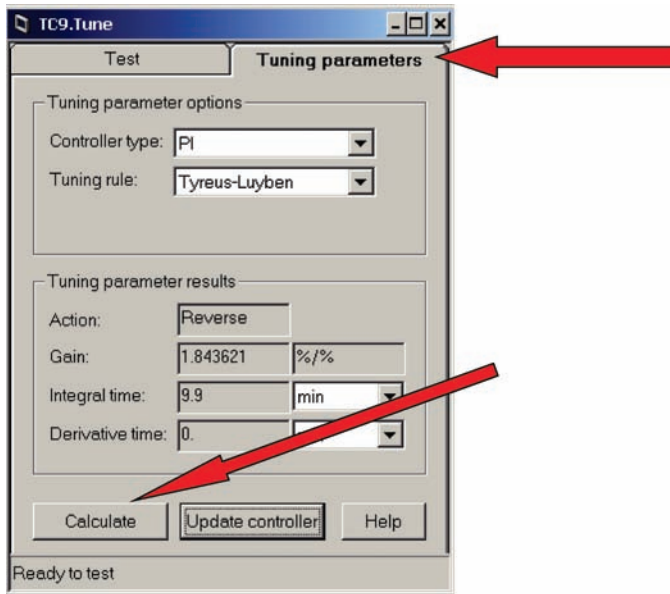


(a)

Figure 7.26 (a) Setting up the relay-feedback test. (b) Relay-feedback test results. (c) Calculated controller settings.



(b)



(c)

Figure 7.26 (Continued)

the *Test method*. The default value of the *Relay output amplitude* is 5%, which is usually good. For a very nonlinear column, the amplitude may have to be reduced.

To start the test, click the *Run* button at the top of the screen and click the *Start test* button on the *Tune* window. To be able to see the dynamic responses, click the *Plot* button at the top of the controller faceplate.

After several (5–6) cycles have occurred, pause the run and click the *Finish test* button. Figure 7.26b gives results. The predicted ultimate gain is 5.9 and the ultimate period is 4.5 min.

The timescale in Figure 7.26b is fairly small. To get good-looking plots, the plot time interval must be reduced from the default value of 0.01 h. Aspen Dynamics calls this parameter *Communication Time*, and it can be accessed by going to top toolbar in the Aspen Dynamics window and selecting *Run* and *Run Options*. A window opens on which *Communication Time* can be set. A value of 0.0005 h was used to get the plots shown in Figure 7.26b. This parameter does not affect the results of a dynamic simulation, except for slowing it down somewhat. It only affects the appearance of plots.

Finally, the *Tuning parameters* page tab is clicked, the *Tyreus–Luyben Tuning rule* is selected and the *Calculate* button is pushed (see Fig. 7.26c). The resulting controller settings are gain $K_C = 1.84$ and integral time $\tau_I = 9.9$ min. The Tyreus–Luyben tuning formula are

$$\begin{aligned}K_C &= K_U/3.2 \\ \tau_I &= 2.2 P_U\end{aligned}$$

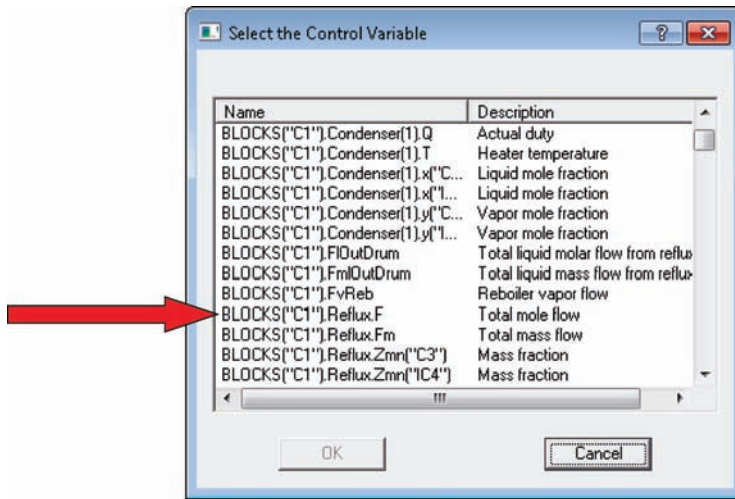
These are loaded into the controller by clicking the *Update controller* button. Run the simulation out in time for a while to see how well these settings work in terms of bringing the column to steady state. In the next section, we will subject the column to disturbances and evaluate the performance of several control structures. Once steady state is achieved, follow the normal procedure of making an initialization run, rewinding and saving.

Reflux-to-Feed Ratio. Before we illustrate the use of a composition controller, it might be instructive to show how a reflux-to-feed ratio structure is set up. Remember in Chapter 5, steady-state calculations indicated that the R/F ratio scheme should do a pretty good job of maintaining product purities in the propane/isobutane system in the face of feed composition disturbances and, of course, feed flow rate changes.

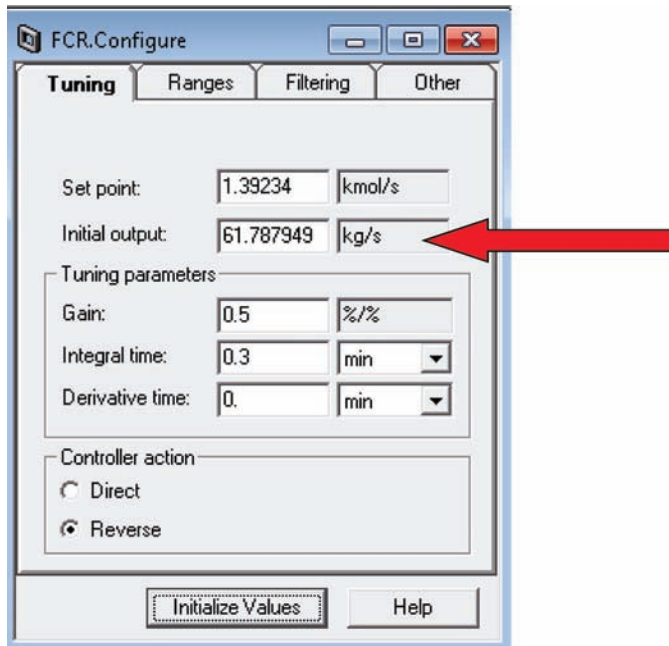
The obvious way to implement this ratio is to simply use a multiplier block whose first input signal is feed flow rate, whose second input is the desired R/F ratio and whose output set the reflux flow rate. However, Aspen Dynamics has the strange limitation that the reflux flow rate sent to the column block is a *mass* flow rate. However, the R/F ratio determined in the feed composition sensitivity analysis is a *molar* flow rate ratio.

A work-around to this problem is to first install a reflux flow controller whose *PV* and *SP* signals are the molar flow rate of the reflux stream and whose *OP* signal is the mass flow rate of the reflux stream. Figure 7.27a shows the window that opens when we place a control signal on a blue arrow on the column block, click and scroll down to find the molar flow rate of the reflux (*F* not *Fm*). This is selected as the *PV* signal to the flow controller *FCR*. The *OP* signal from the controller is connected to the column block and the mass flow rate of reflux is selected. Figure 7.27b shows the configuration after an initialization run has been made and the standard flow controller action (reverse) and tuning constants have been inserted. Note that the *PV* and *SP* are in molar units, and the *OP* is in mass units.

Finally, a control signal is connected from the molar flow rate of the feed (1 kmol/s) to one of the inputs of the multiplier block. The second input is specified to be the desired molar ratio of R/F (1.392) (see Fig. 7.28). The output of the multiplier is connected to the reflux flow controller as the *SP* signal. The reflux flow controller is then put on “cascade” getting its *SP* signal from the output of the multiplier.



(a)



(b)

Figure 7.27 (a) Select molar flow rate of reflux. (b) Reflux flow controller.

The flowsheet and controller faceplates are shown in Figure 7.29a and b. We will compare the performance of this control structure with some alternatives later in this chapter. First we want to illustrate the use of a composition controller.

Reflux Ratio. Although we are on the subject of setting up ratios, now is a good time to discuss installing a reflux ratio control configuration. There are two alternative schemes.

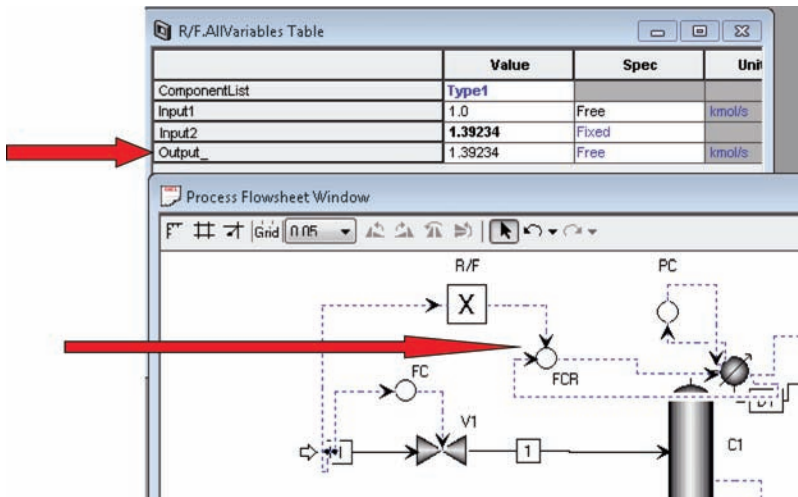


Figure 7.28 Multiplier output signal is SP of reflux flow controller.

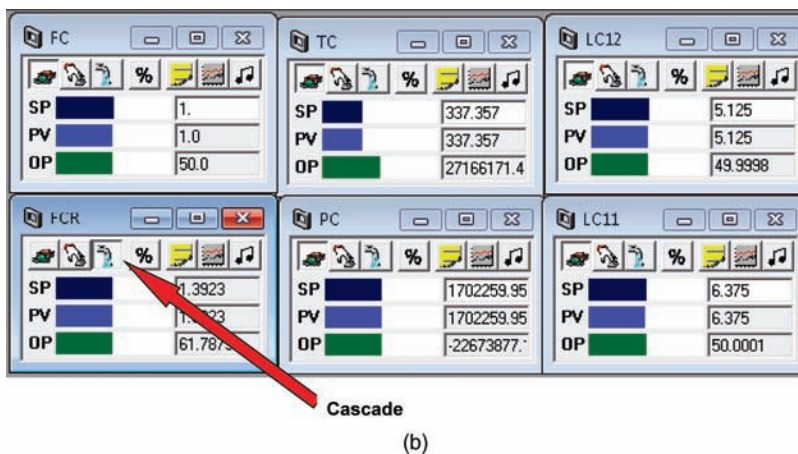
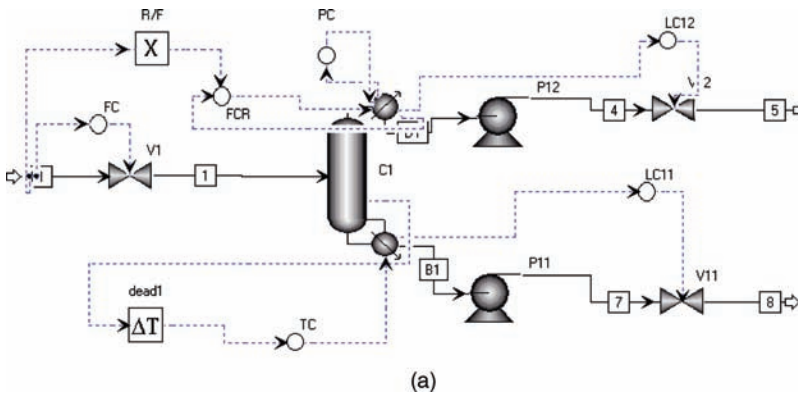


Figure 7.29 (a) Flowsheet with R/F structure. (b) Faceplates with R/F structure.

The choice of which to use depends on the column reflux ratio. Conventional distillation wisdom recommends that columns with reflux ratios less than about 3 can use a control structure in which reflux-drum level is controlled by manipulating the distillate flow rate. However, columns with higher reflux ratios should control reflux-drum level with reflux flow rate. The logic here is to avoid saturation of the control valve.

The low reflux ratio case is pretty straightforward. The distillate flow rate is measure and the flow signal is sent to a multiplier whose other input is the desire reflux ratio. The output of the multiplier sets the reflux flow rate.

In the high reflux ratio case, the reflux flow rate is set by the level controller. The reflux flow rate is measured and sent to a multiplier whose other input is the reciprocal of the desired reflux ratio (D/R). The output signal from the multiplier goes to the SP of a distillate flow controller, which is on “cascade.” A common simulation error is to send the output signal of the multiplier directly to a control valve. This is an obvious and serious error, but is one that is often made. These control configurations will be used in examples in later chapters.

7.5.2 Composition Control

We want to compare tray temperature control with two types of composition control. In both, the composition of the distillate propane product is measured directly and controlled at 2 mol% isobutane impurity. The first type is “direct composition control” in which a single PI controller is used with reboiler heat input manipulated. The second type uses a cascade composition-to-temperature control structure.

Composition measurement typically has larger deadtime and lags than temperature control. We assume a 3 min deadtime in the composition measurement.

First, we add a *PIDIncr* controller to the flowsheet and make the appropriate connections and do not use a deadtime. It will be added later. The controller should be *Reverse* because the *PV* is the mole fraction isobutane impurity in the distillate stream and the *OP* is reboiler heat input. If too much isobutane is going overhead in the distillate, the reboiler heat input should be reduced. A composition transmitter range 0–0.05 mol fraction isobutane is used, as shown in Figure 7.30.

After the simulation is run, a 3 min deadtime is inserted. *Initialization* and *Dynamic* runs are made to converge to steady-state conditions. Then a relay-feedback test is run. Results are shown in Figure 7.31. Notice that the timescale on the plot is much different than for the temperature controller. The ultimate gain is 0.547 and the ultimate period is 33.6 min. The Tyreus–Luyben settings are calculated and inserted in the composition controller. The flowsheet is given in Figure 7.32.

7.5.3 Composition/Temperature Cascade Control

Temperature control has the advantage of being fast, but it may not hold the product purity constant. Composition control is slow, but it will drive the product purity to the desired value. The next control structure studied is a cascade combination of composition and temperature control that achieves both fast control and the maintenance of product purity.

The tray temperature controller is the secondary (slave) controller. It is set up in exactly the same way as we did in the previous section. It looks at tray temperature (Stage 9) and manipulates reboiler heat input. However, its SP is not fixed. The SP signal is the output signal of the composition controller, which is the primary (master) controller.

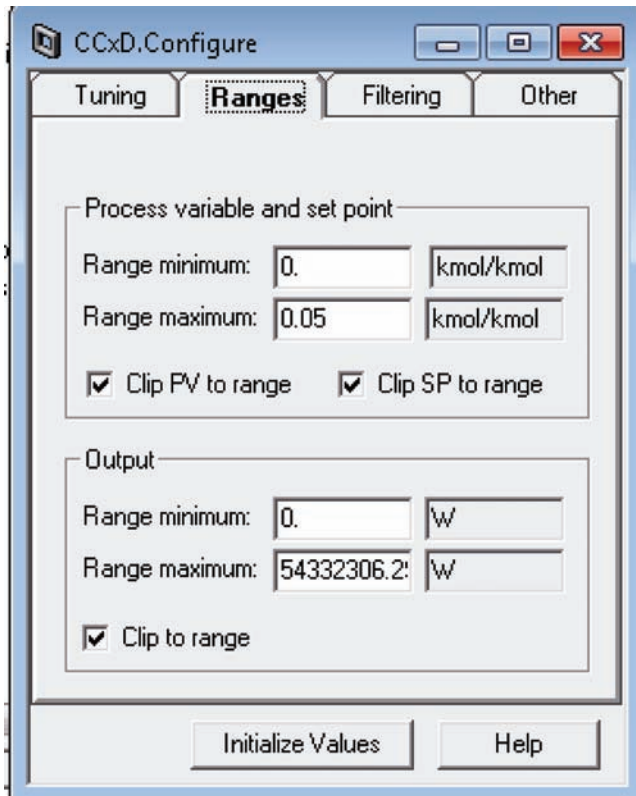


Figure 7.30 Ranges page tab for x_D composition controller.

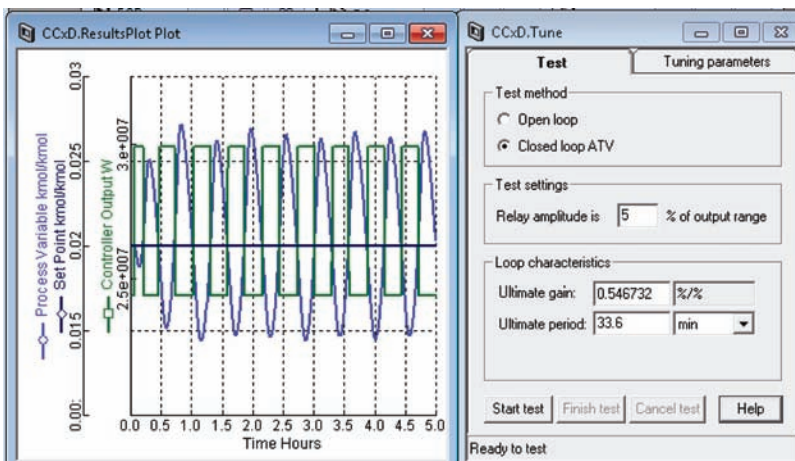


Figure 7.31 Relay-feedback test.

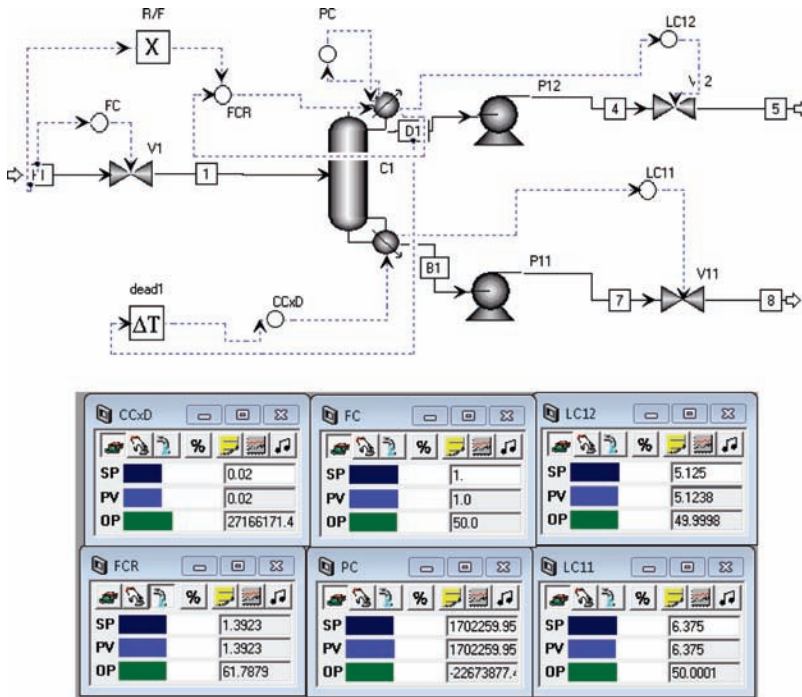


Figure 7.32 Flowsheet with CC.

The tuning of the secondary temperature controller remains unchanged. The primary composition controller must be retuned as its output signal is now a temperature SP. With the temperature controller on cascade, the relay-feedback test is run on the composition controller. The ultimate gain and ultimate period found from the new tuning test are 0.98 and 15.9 min. These should be compared with the direct composition results of 0.58 and 32.4 min. We can see immediately that a higher gain and smaller integral time result, which means tighter control with the cascade control (CC) structure. Figure 7.33 shows the CC structure and controller faceplates. Note that the TC temperature controller is “on cascade” (its SP signal is the output signal of the composition controller).

7.6 PERFORMANCE EVALUATION

We want to see how well the three alternative control structures developed above perform in the face of disturbances, that is, how close to the desired values of temperature and composition are these variables maintained, both at steady state and dynamically. A disturbance is made and the transient responses are plotted.

7.6.1 Installing a Plot

To see what is going on, the first thing to do is to set up a plot or a strip chart. This will show how the variables of interest change dynamically with time. To open a plot, go to *Tools* on the top tool bar, click *New Form* and a *Plot*. A window opens as shown at the top

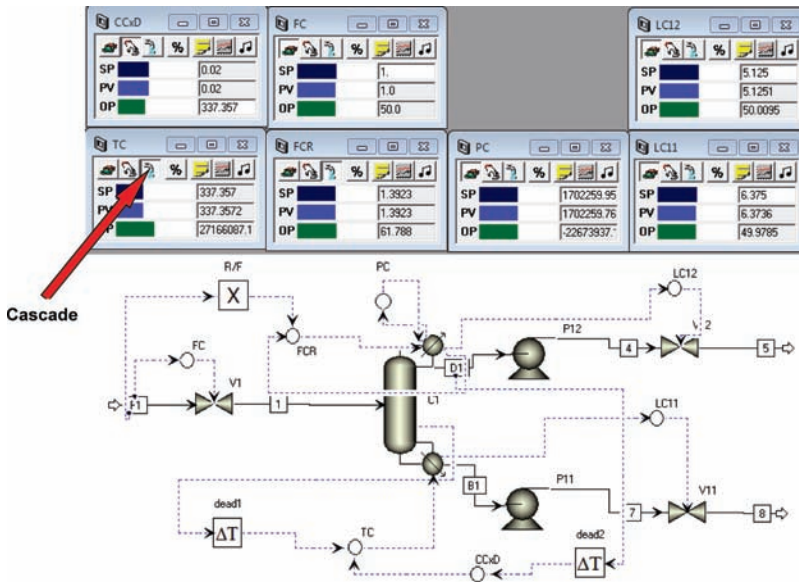


Figure 7.33 Flowsheet with CC/TC cascade.

of Figure 7.34. Enter a name for the plot (“results”) and click OK. A plot window opens, as shown at the bottom of Figure 7.34. A number of variables will be plotted: flow rates of the feed, distillate, bottoms, and reflux; Stage 7 temperature; reboiler heat input; distillate impurity (*mf* isobutane), and bottoms impurity (*mf* propane). We “drag-and-drop” each one of these variables onto the plot window.

For example, if we want to plot the molar flow rate of the feed *F1*, we click the icon of the *F1* stream, right click and select *Forms* and then *Results*. Double clicking on the icon does the same thing. The window shown on the left in Figure 7.35 opens. Place the cursor at the *F* line in this table and click once. Then click again and holding the left mouse key down, drag it to the plot and release. As shown in plot window on the right, the molar flow rate of stream *F1* has been added to the plot.

This procedure is repeated for each variable. Now we need to define the scales of each variable, simplify the labels and make other “beautification” changes to the plot. This is done by right click on the plot and selecting *Properties*. The window shown in Figure 7.36a opens, which contains a number of page tabs. On the *Axis Map* page tab, click the box *One for Each* to get different scales for each variable, as shown in Figure 7.36b.

This is all that is really necessary for plotting since we will be using other more suitable plotting software to show the dynamic results in a compact and effective fashion. However, you can make changes to the plot to make it look nicer if you want. To get fixed scales (instead of scales that change during the dynamic run), go to the *Axis* page tab, uncheck the box to the left of *Reset axis range to data* for each of the variables, and define minimum and maximum values for each. If you want to remove a variable from the plot, go to the *Variable* page tab, highlight the variable you wish to remove and click the *Remove* button as shown in Figure 7.37.

Figure 7.38 illustrates the type of plot that results from making a dynamic run. At time equal 0.5 h, the SP of the feed flow controller is changed from 1 to 1.2 kmol/s. To pause the simulation at some point in time, go to the top toolbar and click *Run* and then *Pause At*,

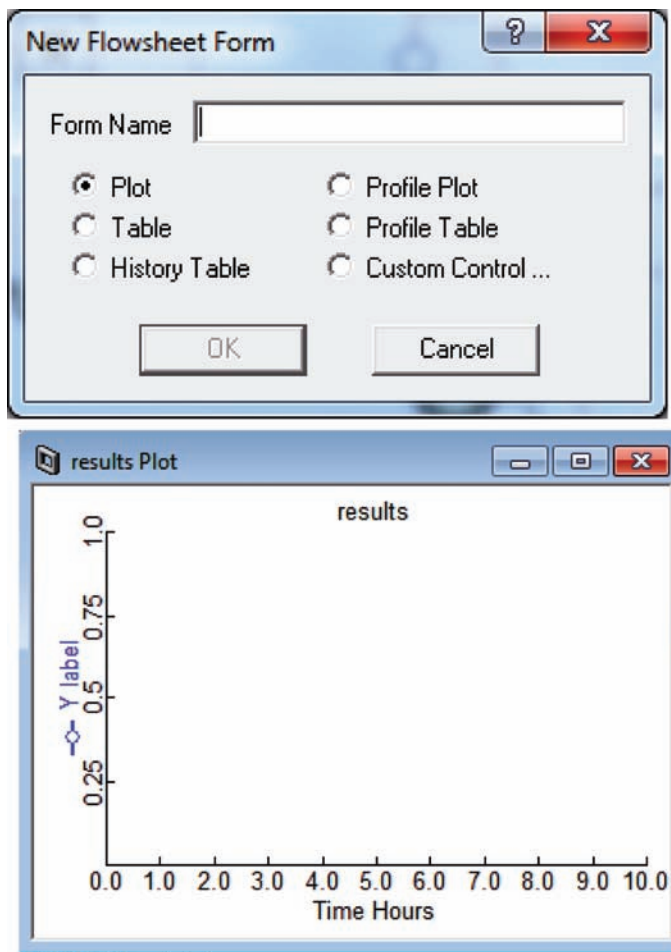


Figure 7.34 Opening plot.

which opens the window shown in Figure 7.39. The dynamic results shown in Figure 7.37 are when the plain temperature controller is manipulating reboiler duty and the reflux-to-feed ratio is installed. The disturbance is a 20% increase in feed flow rate. These results will be compared with those produced by other control structures in the next section. First we need to be able to improve our plotting capability.

7.6.2 Importing Dynamic Results into Matlab

Although these Aspen Dynamics plot are useful to see what is going on during each run, they have a fixed structure (multiple variables per plot), and they do not permit comparisons of results from different runs. Fortunately, this is easily handled by storing the data in a file and then producing your own plots using your favorite plotting software. To store the data after a run has completed, right click the plot and select *Show as History*. Figure 7.40 shows the resulting table, which can be copied and pasted into a file such as *Notepad*.

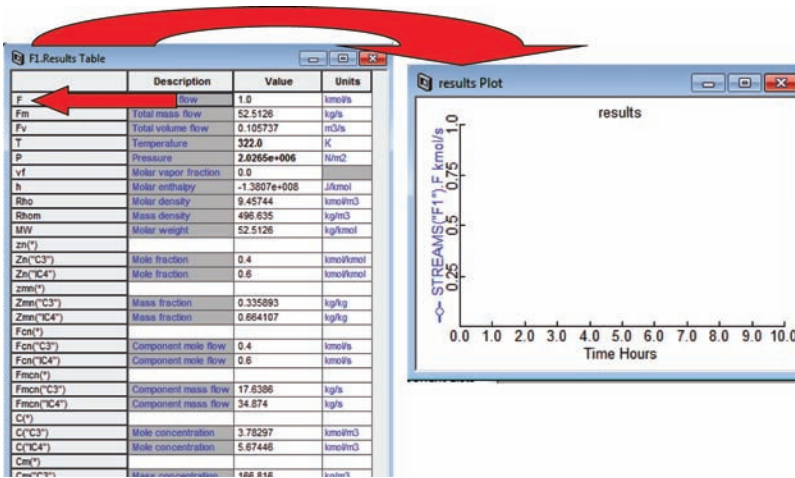
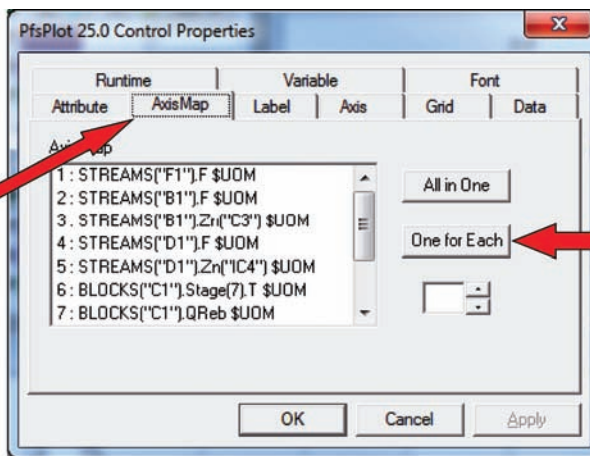


Figure 7.35 Drag and drop from F1 results table.

There are numerous plotting software packages available, but I strongly recommend the use of *Matlab*. It permits multiple plots of several of the important variables for direct comparisons. Figure 7.41 shows a Matlab program for making the plots given in Figure 7.42. Each of the files is loaded into Matlab and the appropriate subplots are defined and plotted.

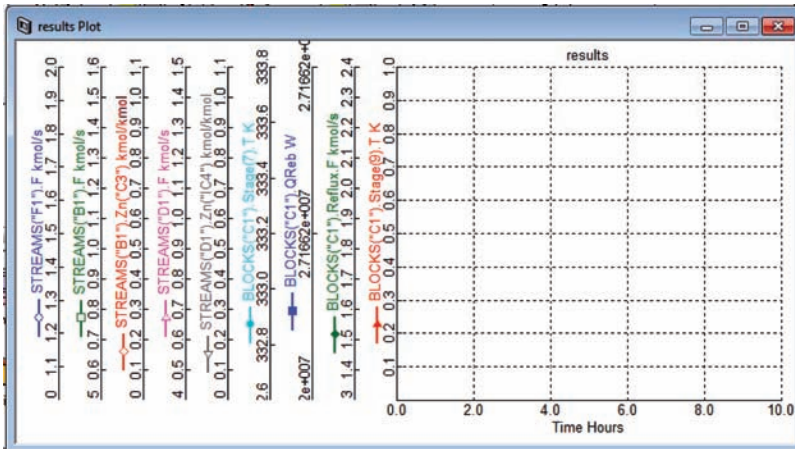
At this point I find it convenient to copy the Matlab figure (go to *Edit and Copy Figure*) and paste it into *Powerpoint*. Then click on the picture and go up to the Powerpoint toolbar and click *Ungroup* (see Figure 7.43a). A message will appear asking whether you want to convert to a Powerpoint drawing object (Fig. 7.43b). After this is okayed, click on *Ungroup* again until all the elements in the picture have been selected (Fig. 7.43c).

Now you can change text fonts and sizes, line types and thicknesses, add new text, add any desired symbols, and so on. The use of block arrows is very effective in highlighting



(a)

Figure 7.36 (a) Axis map. (b) One axis for each variable.



(b)

Figure 7.36 (Continued)

important regions of the dynamic plots. Figure 7.44 gives the final edited plot for both positive and negative 20% changes in feed flow rate.

Note the block arrows in Figure 7.44 pointing to the transient disturbances in Stage 9 temperature and also in the product purities. These can be reduced by the use of some feed-forward control, as discussed in the following section.

7.6.3 Reboiler Heat Input to Feed Ratio

The results shown in Figure 7.44 show fairly large transient disturbances in both temperature and compositions for feed flow rate disturbances. The change in feed flow rate enters the column and must impact the control tray temperature before any corrective action in reboiler heat input occurs.

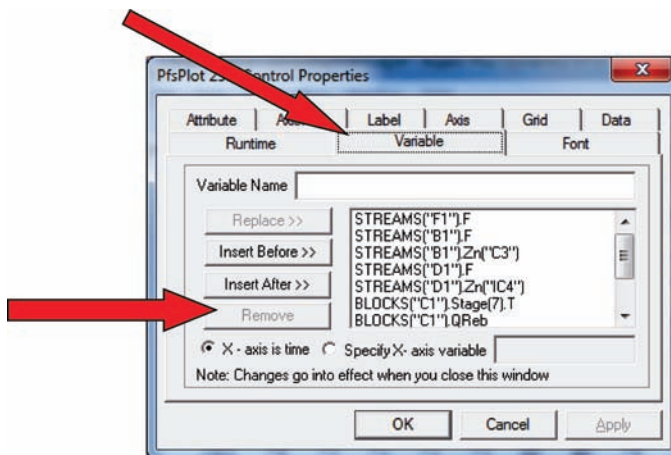


Figure 7.37 Remove variable.

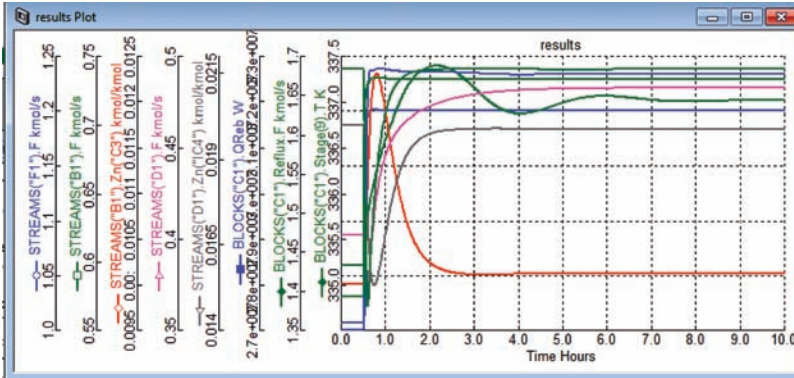


Figure 7.38 Plot for +20% feed flow: TC.

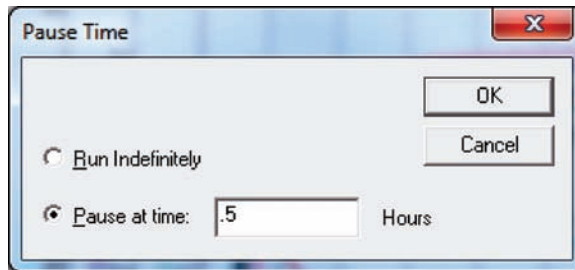


Figure 7.39 Pause window.

The dynamics can be greatly improved by using a feed-forward ratio scheme to anticipates that reboiler duty must be changed when feed flow rate changes occurs. The control structure is similar to the reflux-to-feed ratio discussed above. However, there are two differences.

Time Hours	STREAMS('F1')F kmol/s	STREAMS('B1')F kmol/s	STREAMS('B1')Zn('C3') kmol/kmol	STREAMS('D1')F kmol/s	STREAMS('D1')Zn('C4') kmol/kmol
0.0	1.0	0.597802	0.0100044	0.402103	0.020001
0.01	1.0	0.597801	0.0100043	0.402102	0.020001
0.02	1.0	0.597801	0.0100042	0.402101	0.020001
0.03	1.0	0.597801	0.0100042	0.4021	0.020001
0.04	1.0	0.597801	0.0100041	0.4021	0.020001
0.05	1.0	0.597801	0.010004	0.402099	0.020001
0.06	1.0	0.597801	0.0100039	0.402098	0.020001
0.07	1.0	0.597801	0.0100039	0.402098	0.020001
0.08	1.0	0.597801	0.0100038	0.402097	0.020001
0.09	1.0	0.597801	0.0100037	0.402096	0.020001
0.1	1.0	0.597802	0.0100037	0.402096	0.020001
0.11	1.0	0.597803	0.0100036	0.402095	0.020000
0.12	1.0	0.597804	0.0100036	0.402094	0.020000
0.13	1.0	0.597805	0.0100035	0.402094	0.020000
0.14	1.0	0.597806	0.0100034	0.402093	0.020000
0.15	1.0	0.597807	0.0100034	0.402092	0.020000
0.16	1.0	0.597808	0.0100033	0.402092	0.020000
0.17	1.0	0.597808	0.0100033	0.402091	0.020000
0.18	1.0	0.597809	0.0100032	0.40209	0.020000
0.19	1.0	0.59781	0.0100032	0.402089	0.020000

Figure 7.40 Show as history table.

```

1  % Program "tcplot.m"
2  clear
3  % 20% increase in feed
4  load tcplus.txt;
5  t=tcplus(:,1);f=tcplus(:,2);t9=tcplus(:,9);
6  xb=tcplus(:,4)*100;xd=tcplus(:,6)*100;qr=tcplus(:,7)*1e-6;
7  r=tcplus(:,8);b=tcplus(:,3);d=tcplus(:,5);
8  % 20% decrease in feed
9  load tcminus.txt;
10 t2=tcminus(:,1);f2=tcminus(:,2);t92=tcminus(:,9);
11 xb2=tcminus(:,4)*100;xd2=tcminus(:,6)*100;qr2=tcminus(:,7)*1e-6;
12 r2=tcminus(:,8);b2=tcminus(:,3);d2=tcminus(:,5);
13
14 clf
15 subplot(3,2,1)
16 plot(t,f,t2,f2,'--');grid;ylabel('F (kmol/s)');
17 title('TC Control; 20% Feed Disturbances');
18 subplot(3,2,2)
19 plot(t,r,t2,r2,'--');grid;ylabel('R (kmol/s)');
20
21 subplot(3,2,3)
22 plot(t,xb,t2,xb2,'--');grid;ylabel('xB (%C3)');
23 subplot(3,2,4)
24 plot(t,xd,t2,xd2,'--');grid;ylabel('xD (%iC4)');
25 subplot(3,2,5)
26 plot(t,t9,t2,t92,'--');grid;ylabel('T9 (K)');xlabel('Time (h)');
27 subplot(3,2,6)
28 plot(t,qr,t2,qr2,'--');grid;ylabel('QR (MW)');xlabel('Time (h)');
29
30

```

Figure 7.41 Matlab program.

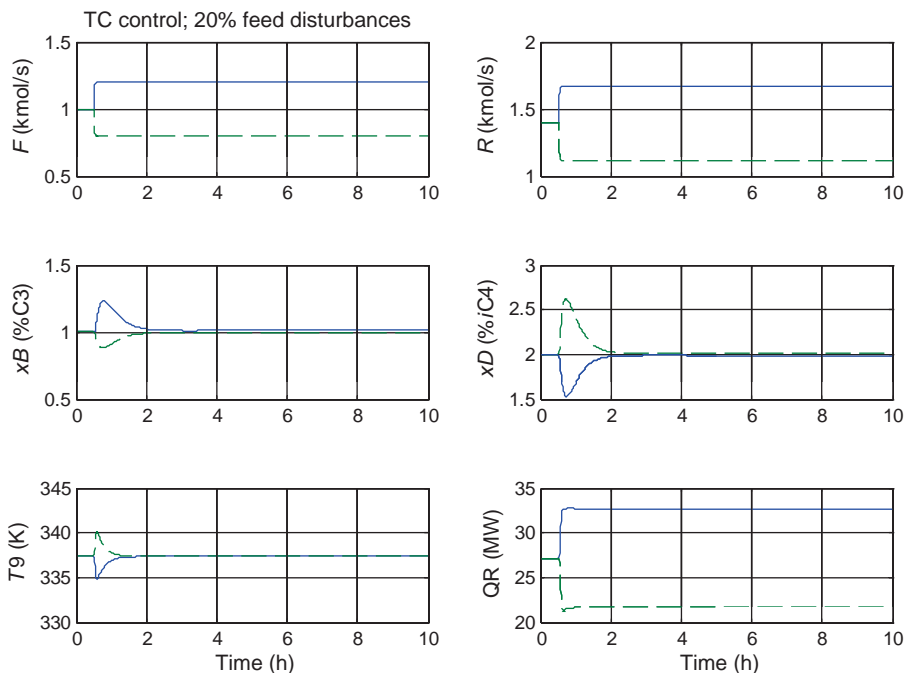


Figure 7.42 Matlab plots.

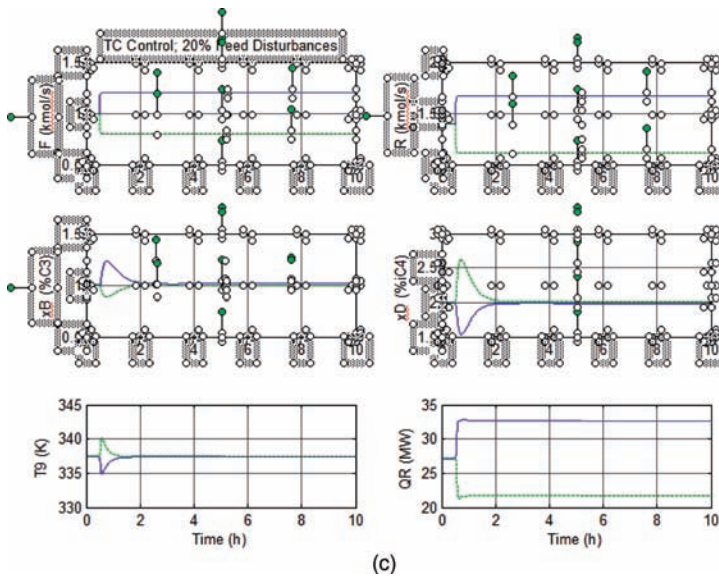
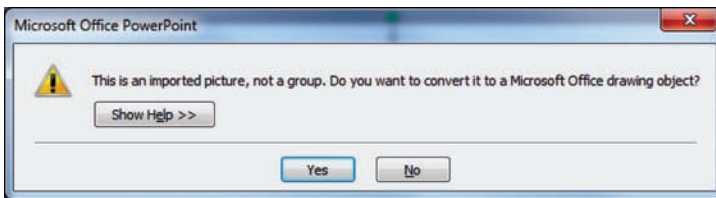
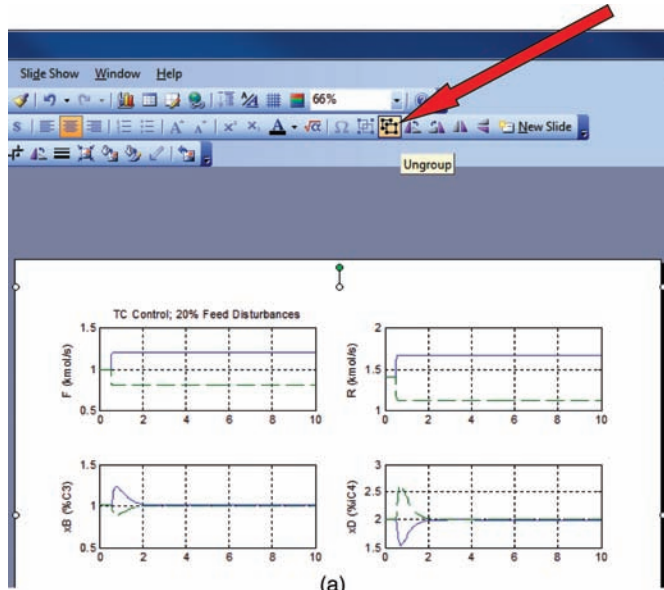


Figure 7.43 (a) Ungroup in Powerpoint. (b) Convert to Microsoft drawing. (c) Ungroup all elements.

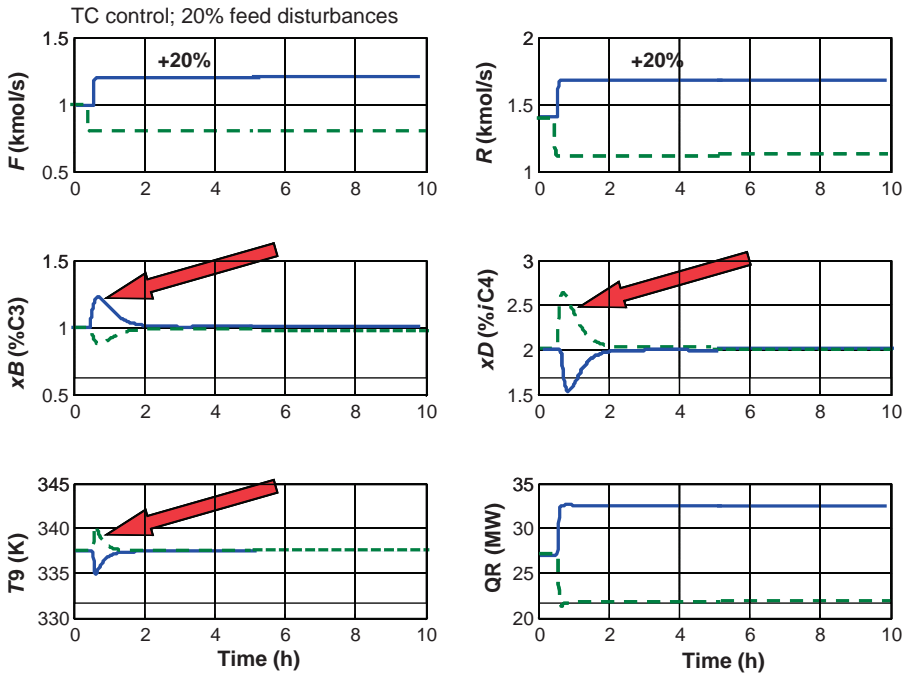


Figure 7.44 Plot edited in Powerpoint.

First the QR/F ratio is used in conjunction with the temperature controller. A multiplier is setup with one input being the feed flow rate and the other input a QR/F ratio that is the output signal of the temperature controller. So the control structure is a combined feed-forward/feedback system.

The second difference is the issue of units. In the R/F ratio, the units of both flow rates are the same (kmol/h or lb/h), so the ratio is independent of the units involved. In the QR/F ratio, the units must be in “GJ/kmol” because Aspen Dynamics always uses metric units in its calculations. So if we are using Btu/h for reboiler heat input and lb/h for flow rates, we must convert these into GJ/h and kmol/h to calculate the multiplier constant.

Figure 7.45 shows the *All Variables* view of the multiplier QR/F . The first input is the molar flow rate of the feed. The second input is the output signal from the temperature controller. The output signal is the reboiler heat input. Notice that the unit displayed are the units being used in the simulation (kmol/s and W), but the ratio is given in GJ/kmol.

$$\frac{97.799 \text{ GJ/h}}{3600 \text{ kmol/h}} = 0.02717$$

The final control structure is shown in Figure 7.46. Both the R/F and the QR/F ratios are installed. Of course the temperature controller must be retuned. Relay-feedback testing and Tyreus–Luyben tuning give $K_C = 1.96$ and $\tau_1 = 11.9$ min. The composition controller also must be retuned but changes only slightly.

The improvement in the dynamic performance of the temperature controller when the QR/F ratio is used is demonstrated in Figure 7.47 for 20% increase in feed flow rate. The

ComponentList	Value	Spec	Units
Input1	1.0	Free	kmol/s
Input2	0.02717	Free	
Output	2.717e+007	Free	W

Figure 7.45 Multiplier for QR/F ratio.

solid lines are without the QR/F ratio and the dashed lines are with it in service. The peak magnitudes of the disturbances are greatly reduced.

7.6.4 Comparison of Temperature Control with Cascade CC/TC

Runs are made to compare the dynamic and steady-state performance of the two alternative control structures (temperature control and cascade composition/temperature control) with the R/F and QR/F ratio installed. The column is subjected to disturbances in feed flow rate and then feed composition.

Figure 7.48 gives results for a 20% increase in feed flow rate. Both control structures provide stable base-level regulatory control. The temperature controller brings the Stage 9 temperature back to a fixed SP. The distillate *i*C4 impurity comes to a new steady state that is slightly below the 2 mol% specification. The bottoms C3 impurity moves to a new steady state that is slightly above the 1 mol% specification.

In the CC structure, the *x*D composition controller increases the SP of the temperature controller by a very small amount, but enough to drive the distillate composition to 2 mol% *i*C4. The bottoms composition ends up closer to the 1 mol% C3 specification because of the

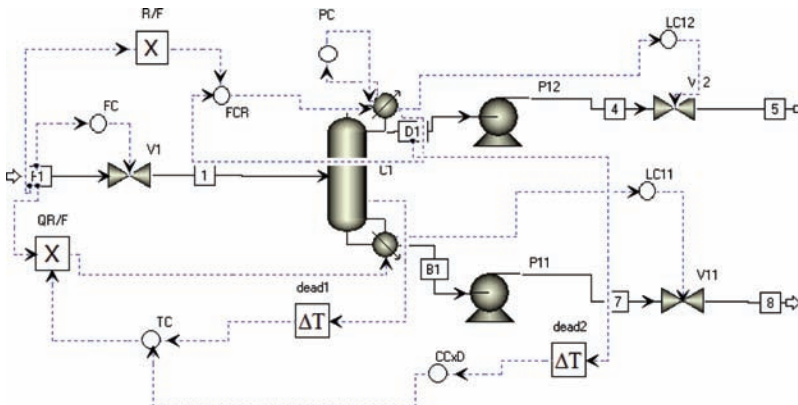


Figure 7.46 Cascade CC/TC with QR/F ratio.

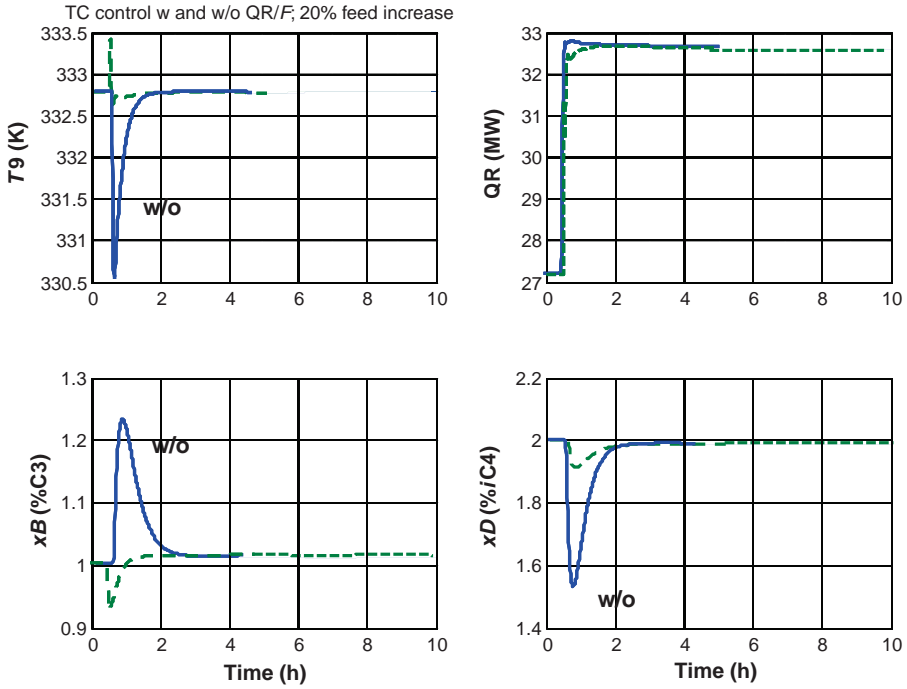


Figure 7.47 TC with and without QR/F ratio.

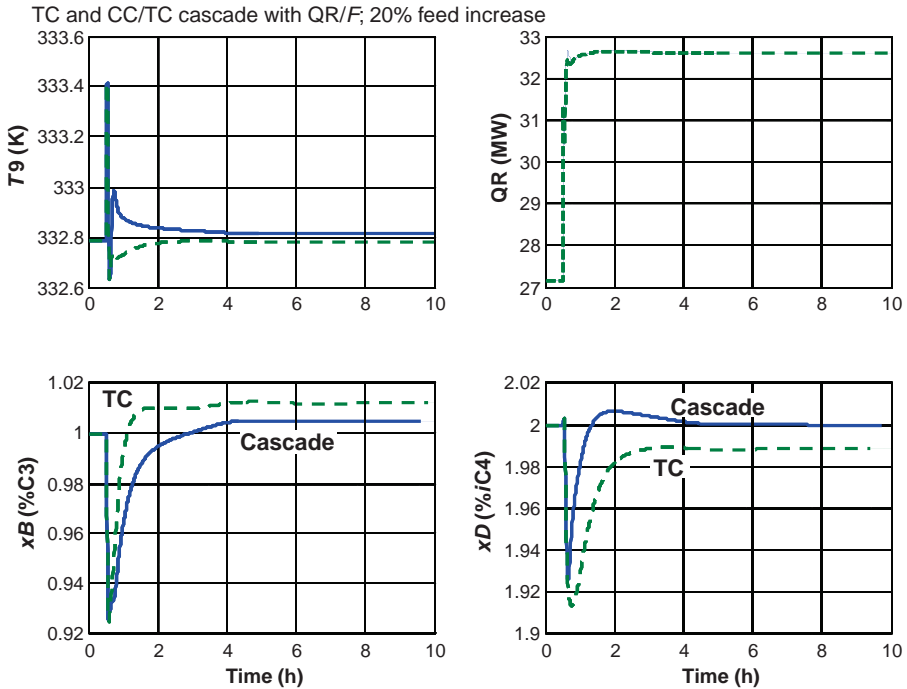


Figure 7.48 Comparison of TC and cascade: 20% increase in feed.

	Description	Value	Units	Spec
FR	Specified total molar flow	1.0	kmo/s	Free
FmR	Specified total mass flow	52.5126	kg/s	Free
FvR	Specified total volume flow	0.105737	m3/s	Free
T	Temperature	322.0	K	Fixed
P	Pressure	2.0265e+006	N/m2	Fixed
vR	Specified molar vapor fraction	-0.375767		Free
ZR(*)				
ZR('C3')	Specified mole fraction	0.4		
ZR('C4')	Specified mole fraction	0.6	kmo/kmol	Fixed
ZmR(*)				
ZmR('C3')	Specified mass fraction	0.335893	kg/kg	Free
ZmR('C4')	Specified mass fraction	0.664107	kg/kg	Free

Figure 7.49 Manipulate composition of feed.

higher Stage 9 temperature. Feed flow rate changes are pretty well handled by both control structures.

To make changes in feed composition, the *F1* stream icon is highlighted and right clicked. Then selecting *Forms* and *Manipulate* opens the window shown in Figure 7.49 on which the mole fractions of propane and isobutane are changed from 0.40/0.60 to 0.50/0.50. Figure 7.50 gives a direct comparison of TC with CC (CC/TC). The TC structure brings the temperature on Stage 9 back to a constant SP of 337.4 K. Both distillate and bottoms impurities change significantly with impurity levels increasing or decreasing by almost a factor of two. The distillate impurity climbs from the desired 2 mol% isobutane level to almost 3 mol%. The bottoms stream becomes overly pure.

Using the CC/TC cascade control structure, the distillate purity is maintained. The SP of the temperature controller is decreased by the composition controller down to 335.2 K so

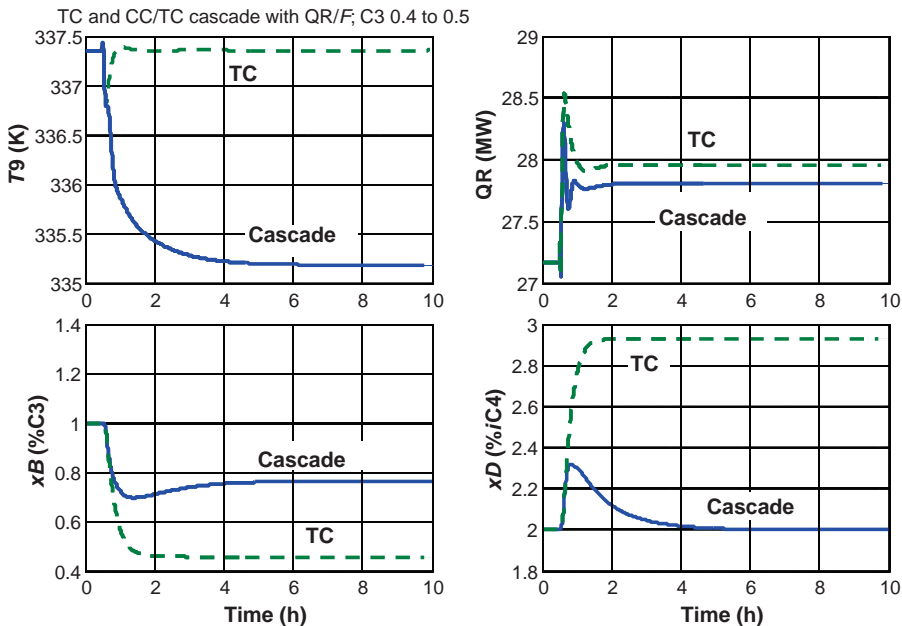


Figure 7.50 Feed composition 0.4–0.5 mf C3.

drive the distillate impurity back to 2 mol% isobutane. Bottoms impurity does not change as much as with only temperature control.

7.7 CONCLUSIONS

A very full bag of distillation dynamic simulation techniques has been developed and demonstrated in this chapter. The example considered is a simple binary ideal vapor–liquid equilibrium (VLE) column. As the remaining chapters in this book demonstrate, these techniques can be readily extended to much more complex flowsheets and phase equilibrium.

Methods for setting up and evaluating many of the control structures required for distillation control have been demonstrated, including several important ratio structures.

CHAPTER 8

CONTROL OF MORE COMPLEX COLUMNS

In this chapter, we apply the techniques learned in Chapter 7 for the simple binary column to more complex phase equilibria and more complex distillation flowsheets.

8.1 EXTRACTIVE DISTILLATION PROCESS

The steady-state design of a two-column extractive distillation system was developed in Chapter 5. Now, we want to design an effective control structure for this system. The process has two distillation columns, and a plantwide control structure must be developed that accounts for the interaction between the columns and for the solvent recycle.

8.1.1 Design

Figure 8.1 gives the flowsheet of process (Figure 5.1). The 540 kmol/h of fresh feed is a binary mixture of acetone and methanol, which is fed on Stage 24 of a 37-stage column operating at 1 atm. The DMSO solvent is fed on Stage 4 at a flow rate of 271 kmol/h. High-purity acetone (99.95 mol%) is the distillate product of the extractive column. The reflux ratio (RR) is 0.842.

The bottoms of the extractive column has a very small impurity of acetone (0.01 mol%), so it is essentially a binary mixture of methanol and DMSO. The bottoms stream is fed to the 17-stage solvent-recovery column on Stage 8. The pressure is 1 atm, and the reflux ratio is 0.5. The distillate product is high-purity (99.95 mol%) methanol. The bottoms is recycled back to the extractive column as high-purity (99.99 mol%) DMSO solvent.

Figures 8.2 and 8.3 give the temperature and composition profiles for the two columns. Notice the very large changes in temperatures in the solvent-recovery column, which is due

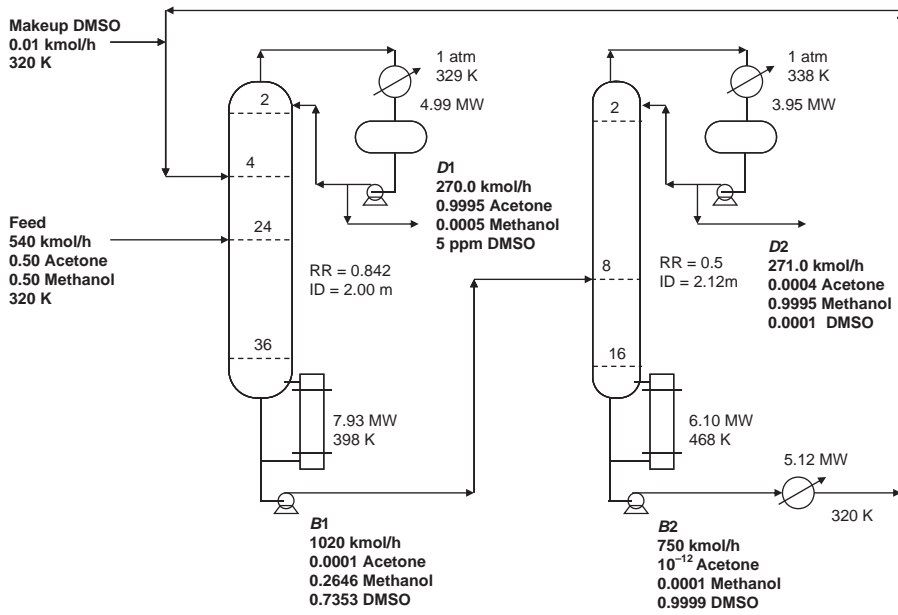
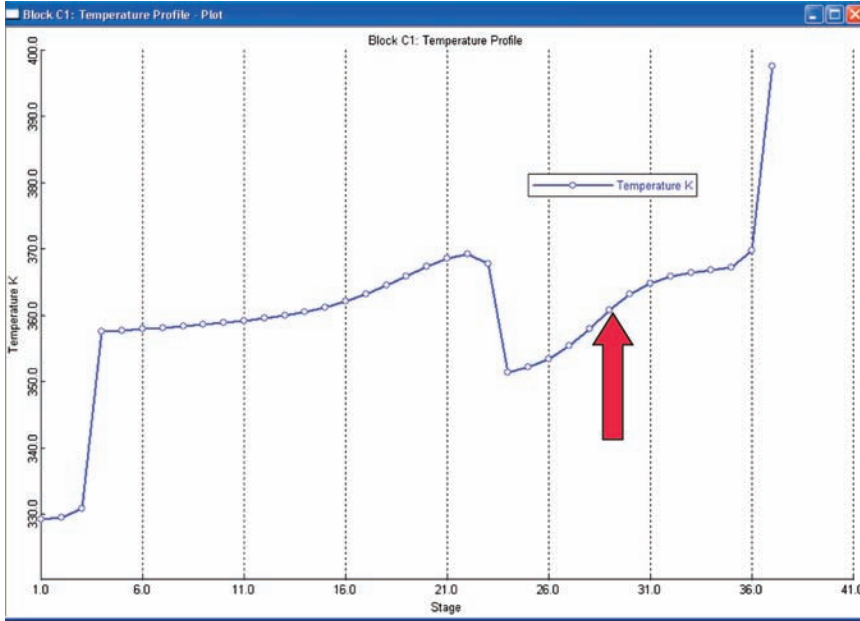


Figure 8.1 Acetone/methanol extractive distillation with DMSO solvent.



(a)

Figure 8.2 (a) Extractive column temperature profile: DMSO solvent. (b) Extractive column composition profiles: DMSO solvent.

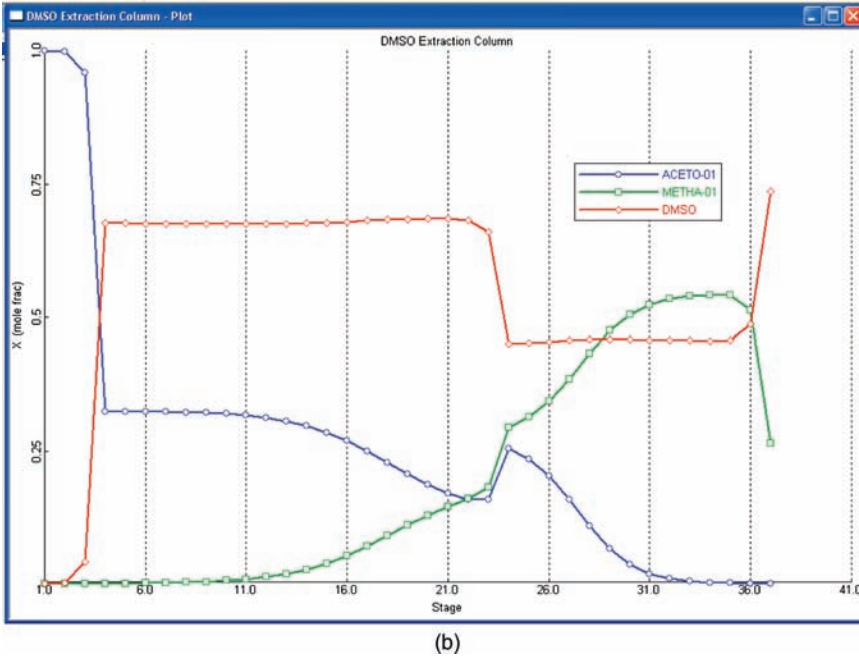


Figure 8.2 (Continued)

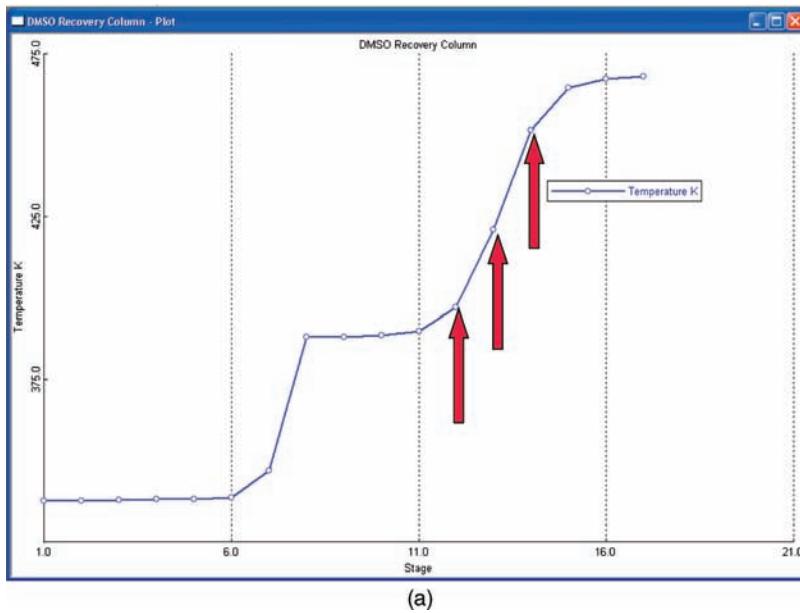
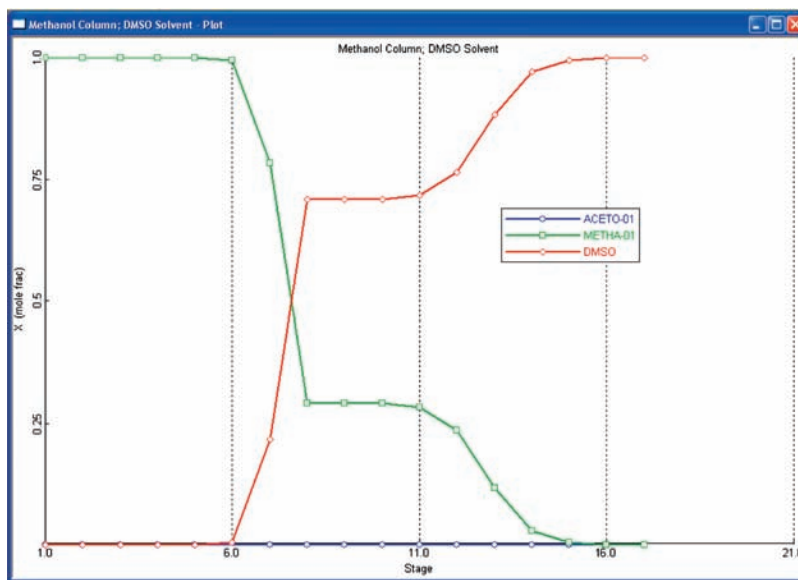


Figure 8.3 (a) Methanol column temperature profile: DMSO solvent. (b) Methanol column composition profiles: DMSO solvent.



(b)

Figure 8.3 (Continued)

to the large difference in the boiling points between methanol (338 K) and DMSO (465 K). This will have an impact on the control structure selected for this column. We will use simple single-end temperature control in each column.

8.1.2 Control Structure

The temperature on Stage 29 in the extractive column (360.9 K) is selected. As shown in Figure 8.2a, this is *not* where the temperature is changing most rapidly, which at the very base of the column because of the increase of the DMSO concentration relative to the methanol (Fig. 8.2b). There is a reasonable change in temperature from tray-to-tray at Stage 29, and this is where the acetone composition is decreasing rapidly. Because we want to keep acetone from dropping out of the bottom, Stage 29 is a good location to control.

If a single tray temperature were selected in the solvent-recovery column, the sharp temperature profile would produce a very large process gain (a small change in reboiler heat input produces a large change in tray temperature at the location of the steep temperature profile). The resulting controller would have a very small gain because of closed-loop stability constraints. The response of the column to load disturbances is likely to be poor (large deviations in temperatures and product purities). Therefore, an *average temperature* is often used in this situation with a very steep temperature profile. We measure the temperatures on three trays: Stage 12 at 401 K, Stage 13 at 430 K, and Stage 14 at 457 K. Figure 8.4 shows the variables in each of the control devices used to implement this average temperature control in Aspen Dynamics. Remember that Aspen Dynamics uses metric unit, so the output signals of the first two summers are in °C, even though we are using temperatures in kelvin.

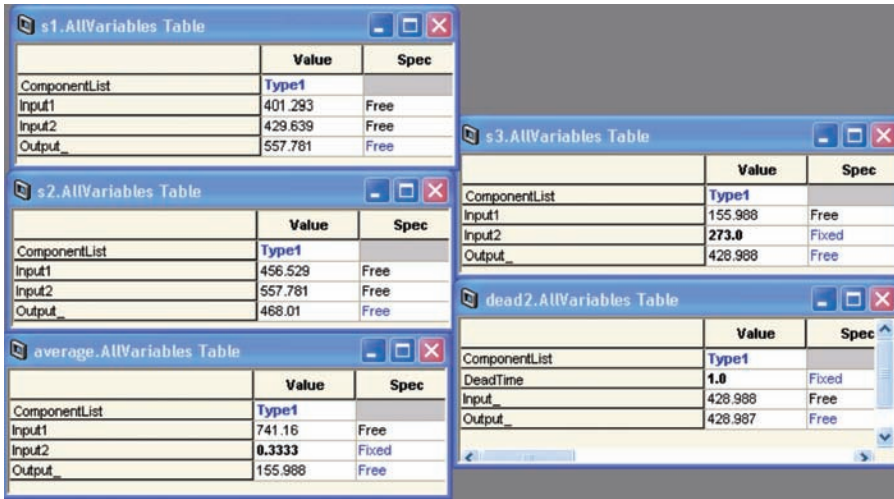


Figure 8.4 Average temperature control.

Figure 8.5a shows the plant-wide control structure for both columns. The first two summer blocks add the three-stage temperatures. The multiplier block “average” multiplies by 0.3333. The last summer block adds the constant “273” to convert the signals back to K from the metric units ($^{\circ}\text{C}$) used in Aspen Dynamics. The average temperature is 429 K, which is the set point of the “TC2” controller shown on the faceplates in Figure 8.5b. Note that the solvent flow controller is on cascade because the solvent flow rate is ratioed to the flow rate of the fresh feed.

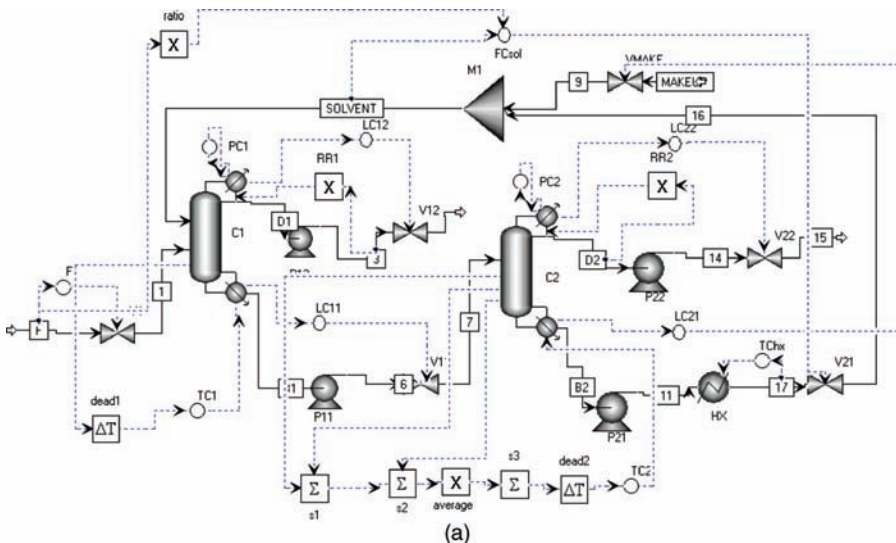


Figure 8.5 (a) Extractive distillation control structure. (b) Controller faceplates.

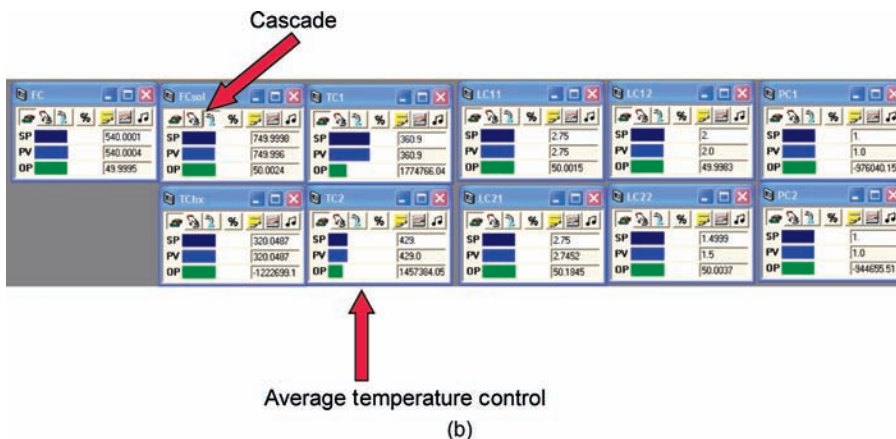


Figure 8.5 (Continued)

Other features of the control structure are

1. Fresh feed is flow controlled.
2. Column pressures are controlled by condenser duty.
3. Reflux-drum levels are controlled by distillate flow rates. Note that both columns have small RRs.

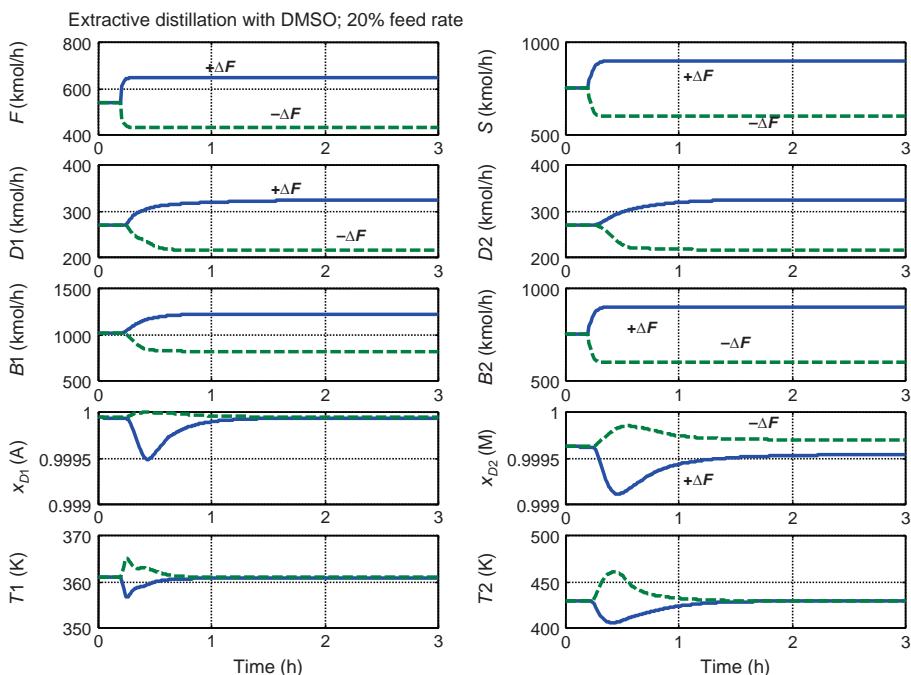


Figure 8.6 20% feed flow rate disturbances.

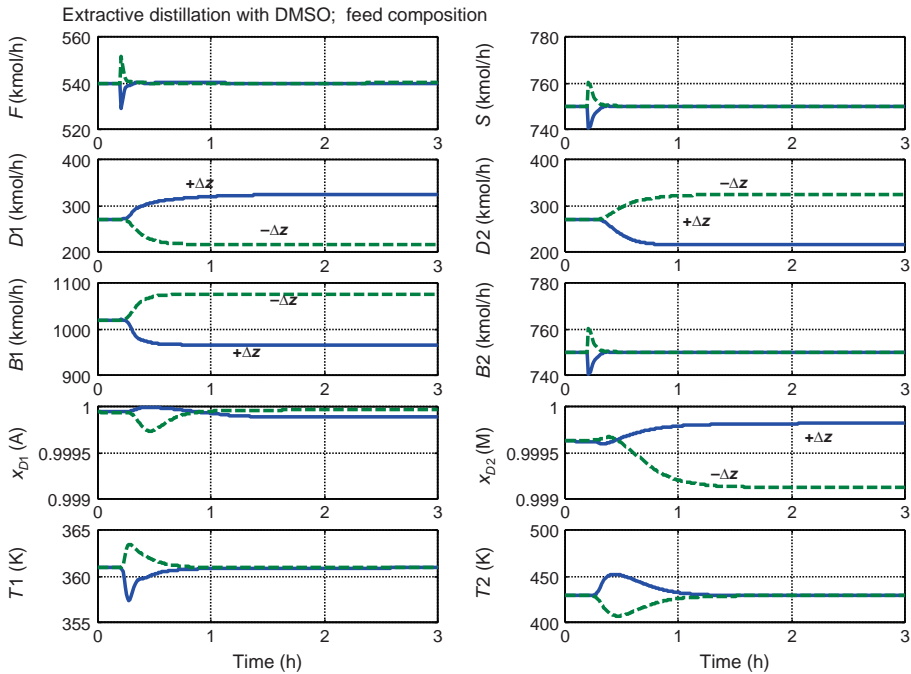


Figure 8.7 Feed-composition disturbances.

4. Reflux ratios are controlled by measuring distillate flow rates, sending this signal into a multiplier whose other input is the design RR and whose output sets the mass flow rate of the reflux. Note that *mass* units can be used here because the distillate and the reflux have the same composition.
5. Bottoms level in the extractive column is controlled by bottoms flow rate.
6. Bottoms level in the solvent-recovery column is controlled (loosely) by the flow rate of the solvent makeup. Very little solvent is lost, so the base level will float up and down with throughput. Sufficient surge volume must be provided in the base of this column to handle these dynamic transients.

8.1.3 Dynamic Performance

The responses of the DMSO system to large 20% increases and decreases in feed flow rate are shown in Figure 8.6. Responses for feed composition are shown in Figure 8.7. Product purities ($x_{D1(A)}$ and $x_{D2(M)}$) are held quite close to their specifications, which are quite high (99.95 mol%). The control structure provides effective regulatory control. It takes about 1 h to come to a new steady state.

8.2 COLUMNS WITH PARTIAL CONDENSERS

All of the distillation columns considered up to this point in this book have used total condensers, that is, the distillate product is a liquid. However, many industrial columns

have partial condensers in which some or all of the distillate product is removed as a vapor stream. In this section, we look at two different situations. In the first, the distillate is completely vapor. The only liquid condensed in the reflux drum is that used for refluxing back to the column. The other situation is when there are two distillate streams, one vapor and one liquid. This is commonly employed when there are very light components in the feed to the column that would require a high column pressure and low condenser temperature to completely condense these very volatile components. The use of a partial condenser can avoid the use of costly refrigeration in the condenser.

The important difference between the two cases is that in the second case the objective is to condense as much as possible, subject to heat-transfer temperature limitations. This means running with maximum cooling water.

8.2.1 Total Vapor Distillate

The control of partial condenser columns is more complex than total condenser columns because of the interaction among the pressure, reflux-drum level, and tray-temperature control loops. Both pressure and level in the reflux drum need to be controlled, and there are several manipulated variables available. The obvious are reflux flow, distillate flow, and condenser heat removal, but even reboiler heat input can be used. In this section, we explore three alternative control structures for this type of system, under two different design conditions: (1) a large vapor distillate flow rate (moderate RR) and (2) a very small vapor distillate flow rate (high RR).

As the dynamic simulation results will show, the preferred control structure depends on the control objectives of the entire process. For example, when the distillate goes to a downstream unit and large variability in its flow rate is undesirable, the control structure should control pressure with condenser heat removal, control level with reflux, and maintain a constant RR.

Process Studied. The numerical example used in this section with an all-vapor distillate stream is a depropanizer with a feed that contains a small amount of ethane, but is mostly propane, isobutane, and *n*-butane. Two cases are considered. The first has a feed composition that is 2 mol% ethane and 40 mol% propane, so the distillate flow rate is large and the RR is moderate ($RR = 2.6$). In the second case, the propane in the feed is only 4 mol% (with 0.02 mol% ethane), which gives a small vapor distillate flow rate and a large reflux ratio ($RR = 20$). Table 8.1 gives design parameters for the two cases. The Chao-Seader physical properties are used.

Design specifications are 1 mol% isobutane impurity in the distillate and 0.5 mol% propane impurity in the bottoms. The column contains 30 trays (32 stages) and is fed in the middle.

If the column is designed with a vapor distillate product, the column operates with a reflux drum pressure of 210 psia, which gives a reflux drum temperature of 110 °F and permits the use of cooling water in the condenser. If a total condenser were used, the column pressure would have to be 230 psia to give a reflux drum temperature of 110 °F. Of course, higher ethane concentrations in the feed would increase the difference between the operating pressures of total and partial condenser columns.

The major difference between the two cases is the distillate flow rate: 42.15 lb mol/h in the first case and only 3.76 lb mol/h in the second. The small vapor flow rate in the latter case corresponds to a volumetric flow rate of only 1.44 ft³/min. Considering the total volume of the 30-tray column (41.8 ft³) and the volume of vapor in the half-full reflux drum

TABLE 8.1 Design Parameters for Two Cases

		High Distillate; Low RR	Low Distillate; High RR
Reflux ratio		2.63	20.3
Flows (lb mol/h)	<i>D</i>	42.15	3.76
	<i>B</i>	57.85	96.24
	<i>F</i>	100	100
	<i>R</i>	111	76.1
Compositions (mf C2/C3)	<i>Z</i>	0.02/0.40	0.0002/0.04
	(mf <i>i</i> C4)	x_D	0.01
	(mf C3)	x_B	0.005
Pressure (psia)		210	210
Temperatures (°F)	Reflux drum	110	110
	Base	196	197
Heat duty (10 ⁶ Btu/h)	Condenser	0.641	0.440
	Reboiler	1.04	0.742
Diameter (ft)		1.6	1.5
Total stages		32	32

(9.5 ft³), the overall pressure time constant of the process is 36 min. This indicates that control of pressure using the small vapor distillate flow will be difficult and slow. The dynamic results given in a later section confirm this expected performance.

The diameters of the columns for the two cases are 1.6 and 1.5 ft, respectively. The reflux drum and base dimensions were sized to give 10 min holdups.

Alternative Control Structures. Three alternative control structures are studied. In the first two, pressure is controlled by manipulating the flow rate of the vapor distillate stream from the reflux drum. This is the conventional configuration that is recommended in most papers and books. In the third, control structure, pressure is controlled by condenser heat removal.

Fundamentals. Conventional single-end control is used in all configuration since dual-composition control is rarely used with this propane/butane separation. The temperature on a tray in the rectifying section of the column, where the temperature changes from tray-to-tray are large, is controlled by manipulating reboiler heat input. The steady-state design shows a temperature on Stage 8 of 128 °F in the large distillate case and 155 °F in the small distillate case. Figure 8.8 gives the temperature profiles for the two design cases.

The tray temperature controllers are tuned by inserting a 1 min deadtime in the loop and using the relay-feedback test to determine the ultimate gain and ultimate frequency. Then, the Tyreus–Luyben settings are used. Table 8.2 gives the tuning constants.

Note that these tuning constants are different for the two design cases because of the different vapor distillate flow rates. Note also that the tuning constants are different for some of the different control structures because the effect of reboiler heat input (or the equivalent vapor flow rate to the condenser) on pressure is different depending on what manipulated variable is used to control pressure. Proportional level controllers are used with gains of 2. The default pressure controller tuning constants from Aspen Dynamics are used.

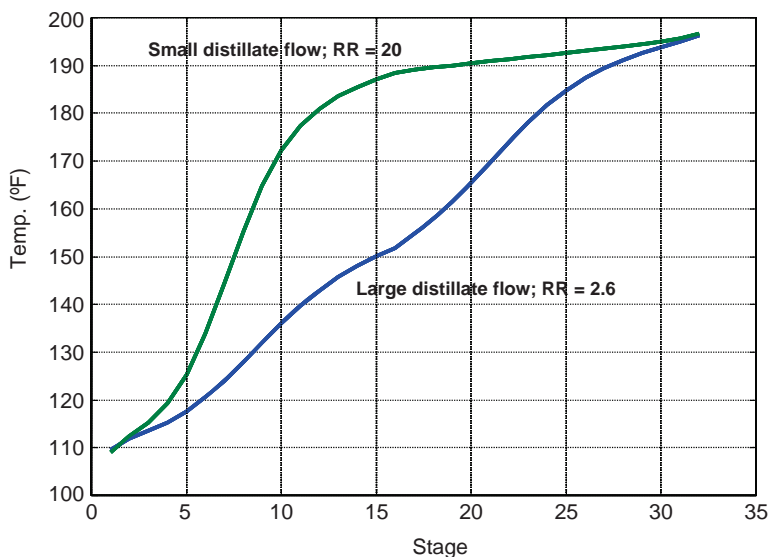


Figure 8.8 Temperature profiles.

Control Structure CS1. Figure 8.9a shows the control structure that is probably most commonly used for distillation columns with partial condensers. The main features of this structure are pressure controlled by manipulating vapor distillate flow rate and reflux drum level controlled by manipulating condenser heat removal. Reflux flow rate is fixed or ratioed to feed.

The interaction between the level and pressure loops is present because any disturbance that affects either loop will propagate to the other loop. For example, suppose the feed-composition changes and more ethane enters the column. The temperature in the reflux drum will drop and the rate of heat transfer in the condenser will decrease for a fixed flow rate of cooling water. The rate of condensation will decrease. Pressure will *increase*, so the pressure controller will increase the distillate flow rate. The drop in condensation will also *decrease* the reflux drum level. When the level controller increases cooling water flow rate

TABLE 8.2 Temperature Controller Tuning Constants

Control Structure		Large Distillate, Moderate RR	Small Distillate, Large RR
CS1/CS2	K_u	4.8	8.1
	P_u (min)	5.1	4.2
	K_C	1.6	2.5
	τ_I (min)	11	9.2
CS3	K_u	3.6	2.8
	P_u (min)	4.2	5.4
	K_C	1.1	0.86
	τ_I (min)	9.2	12

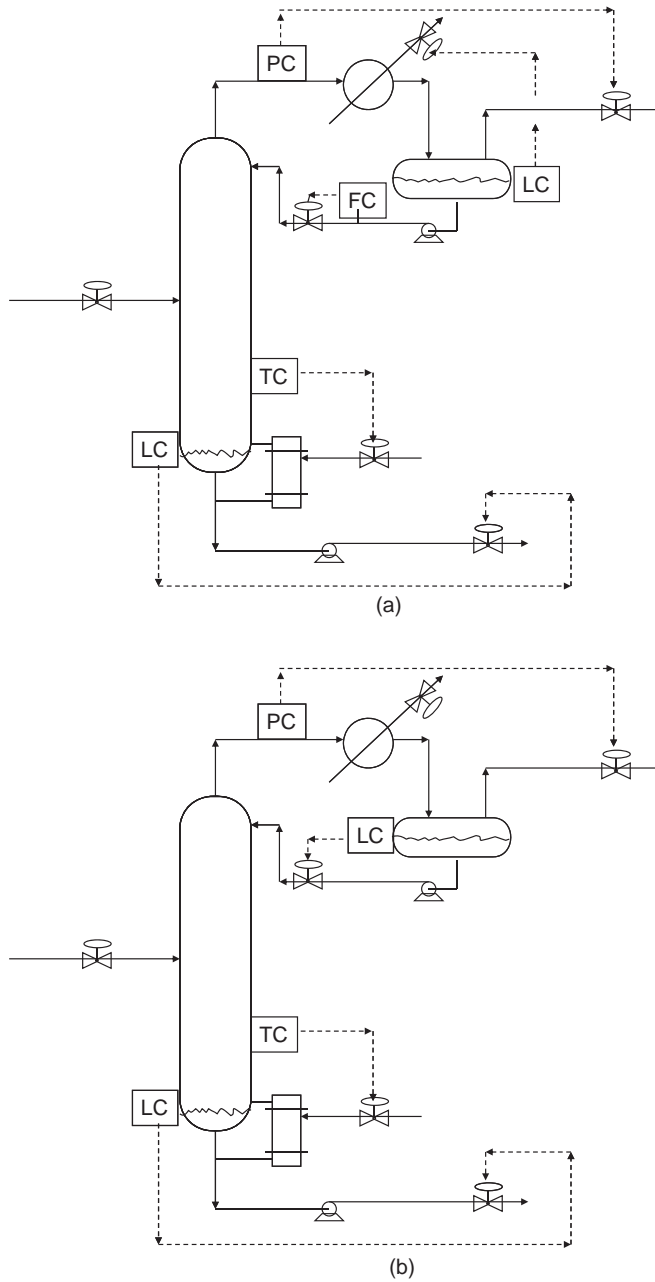


Figure 8.9 (a) CS1 (R fixed). (b) CS2 (Q_c fixed). (c) CS3 (RR fixed).

to increase the level, pressure will decrease. This interaction can cause the pressure controller and the level controller to start fighting each other.

One of the fundamental concepts in distillation control is to prevent rapid changes in pressure. If pressure *increases* too quickly, vapor rates through the trays decrease, which

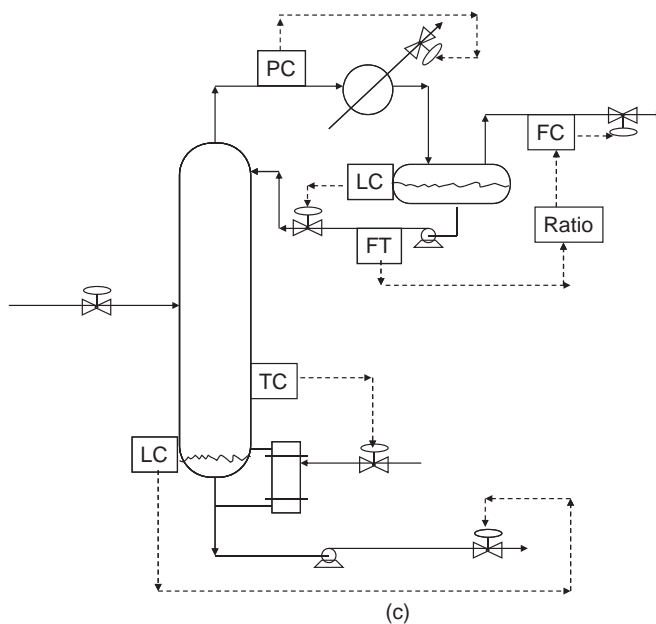


Figure 8.9 (Continued)

can cause weeping and dumping. If pressure *decreases* too rapidly, vapor rates increase due to flashing, which can cause flooding. Therefore, fairly tight pressure control is required. This leads to large and rapid changes in the vapor distillate flow rate when it is used to control pressure. If the distillate is fed to a downstream unit, these large flow rate changes represent severe disturbances.

One of the main advantages of the CS1 structure is that the constant reflux flow rate establishes steady liquid flow rates down through the trays of the column. Changing vapor rates can be achieved fairly rapidly (20–30 s). Changing liquid rates takes much longer because of the hydraulic lags introduced by weirs and baffles. The rule of thumb is about 3–6 s per tray. So in a 30-tray column, it will take 2–3 min for a change in reflux flow to work its way down to the base of the column.

Control Structure CS2. Figure 8.9b presents an alternative control structure in which the condenser heat removal is fixed instead of fixing the reflux flow rate. Because pressure is controlled by manipulating the flow rate of vapor distillate, this structure has the same problem of distillate flow rate variability to a downstream unit.

This structure does not keep reflux flow rate constant, so internal liquid rates can fluctuate, which can lead to poor hydraulic performance.

Some distillation columns with partial condensers are constructed with the condenser installed at the top of the column inside the shell. There is usually no reflux drum. Vapor flows upward through the tubes of the condenser. The condensate liquid flows downward and drops into a liquid distributor above the top tray. These “dephlegmator” systems are frequently used when very toxic or dangerous chemicals are involved because it avoids potential leak problems with pumps and extra vessels and fittings.

In this type of system, there are only two manipulated variables: vapor distillate leaving the top of the condenser and condenser heat removal. The absence of a reflux drum means that there is no surge capacity to attenuate disturbances. As a result, these systems have very poor dynamic disturbance behavior and should be avoided if possible.

A viable alternative is to place a large total trap-out tray below the condenser that can serve as an internal reflux drum. Liquid reflux can be taken from this trap-out tray and fed to the top tray through a control valve. This modified system requires additional column height, which means higher capital investment. But its dynamic controllability is much better.

Control Structure CS3. Figure 8.9c shows the third alternative control structure studied. Now condenser heat removal is used to control pressure, and reflux is used to control level.

Since the distillate flow rate cannot be held constant, the control scheme must permit it to change. This is achieved in this control structure by ratioing of the distillate flow rate to the reflux flow rate.

Of course maintaining a constant reflux ratio may or may not be the best structure to handle feed-composition changes when single-end control is used in a distillation column. To answer this question, the curves shown in Figure 8.10 are generated by varying the feed composition (in terms of the light and heavy key components) while maintaining the purities at both ends of the column. The required changes in the reflux and RR are plotted in terms of ratios to their design values at the design feed composition (40 and 4 mol% propane, respectively, for the two cases).

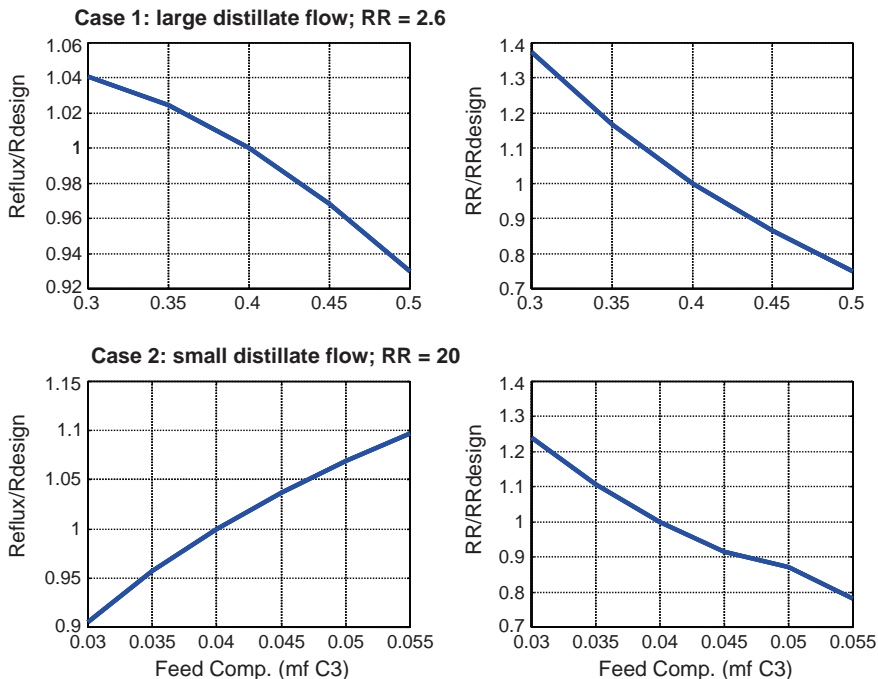


Figure 8.10 Required changes in R and RR .

The required changes in the reflux flow rate are less than those required in the RR. Therefore, a fixed reflux-to-feed structure should do a better job in maintaining, at steady state, the desired product purities than a fixed RR structure for this column.

Control structure CS3 may have a steady-state disadvantage, but it may provide dynamic advantages because of less variability in the vapor distillate flow rate. The dynamic simulation results presented in the next section illustrate these effects.

Dynamic Performance. The three control structures are simulated in Aspen Dynamics, controllers are tuned, and feed flow rate disturbances are imposed on the system. At time equal to 0.2 h, the feed flow rate is increased from 100 to 120 lb mol/h. At time equal to 4 h, the feed is dropped to 80 lb mol/h. Finally, at time equal to 7 h, the feed is increased to 120 lb mol/h. These very large disturbances are handled with different degrees of effectiveness by the three control structures.

Control Structure CS1. Figure 8.11 gives results using control structure CS1. Reflux is ratioed to the feed flow rate, pressure is controlled by distillate flow rate, and reflux-drum level is controlled by condenser heat removal.

Figure 8.11a gives dynamic responses for the large distillate, low RR case. This control structure produces very large changes in the distillate flow rate as well as fairly large deviations in pressure. When feed is increased and reflux is increased, the level starts to drop, which increases condenser heat removal. Note that heat removal is shown as a negative number, using Aspen notation, so the lower the curve of Q_C , the more heat removal. This tends to reduce pressure. However, at the same time, the temperature controller sees a drop in

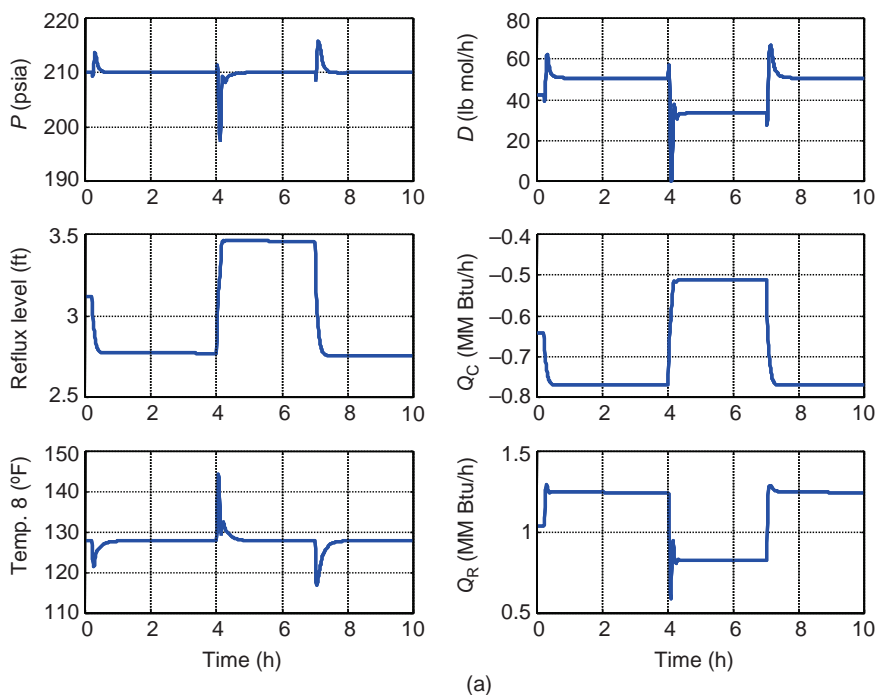


Figure 8.11 (a) Responses for large distillate case (CS1). (b) Responses for small distillate case (CS1).

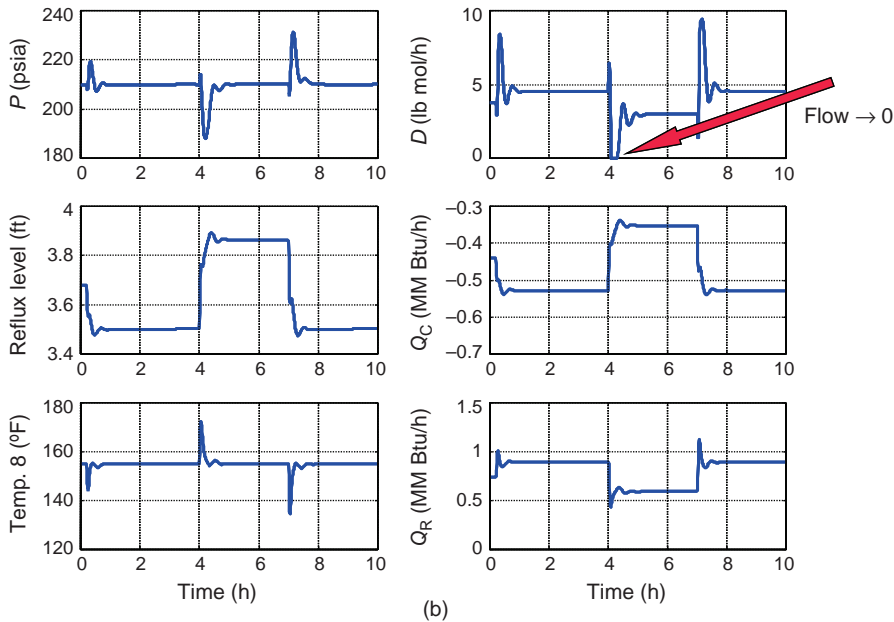


Figure 8.11 (Continued)

Stage 8 temperature caused by the increase in feed flow rate, so it increases reboiler heat input. The net effect is a small initial drop in pressure followed by a large increase.

The disturbance that produces the largest deviations is the 50% step decrease from 120–80 lb mol/h in feed flow rate at time equal 4 h. It produces a drop in pressure of over 10 psi and an increase in temperature of about 15 °F. The distillate flow rate goes all the way to zero, which would make life very difficult for a downstream unit.

Figure 8.11b gives dynamic responses for the small-distillate, high RR case. The changes in the distillate flow rate are even larger (on a percentage basis). In fact, the distillate is completely shut off for about 20 min following the large drop in feed flow rate at time equal to 4 h. The deviations in pressure are much larger than those seen in the previous case.

These results show that this control structure has poor dynamic performance, particularly when the distillate is fed to a downstream unit.

Control Structure CS2. Figure 8.12 gives results using control structure CS2. Condenser heat removal is fixed, pressure is controlled by distillate flow rate, and reflux-drum level is controlled by reflux. Figure 8.12a is for the large distillate case, and Figure 8.12b is for the small distillate case.

The deviations in pressure are much less than with the previous control structure because condenser heat removal is constant and does not contribute to the changes in pressure. The variability in the flow rate of the vapor distillate is also significantly reduced. This is true for both the large and small distillate flow rate cases.

Therefore, from the perspective of plantwide control, this structure is dynamically better than the previous.

Control Structure CS3. Figure 8.13 gives results using control structure CS3. Pressure is controlled by condenser heat removal, reflux-drum level is controlled by reflux, and distillate

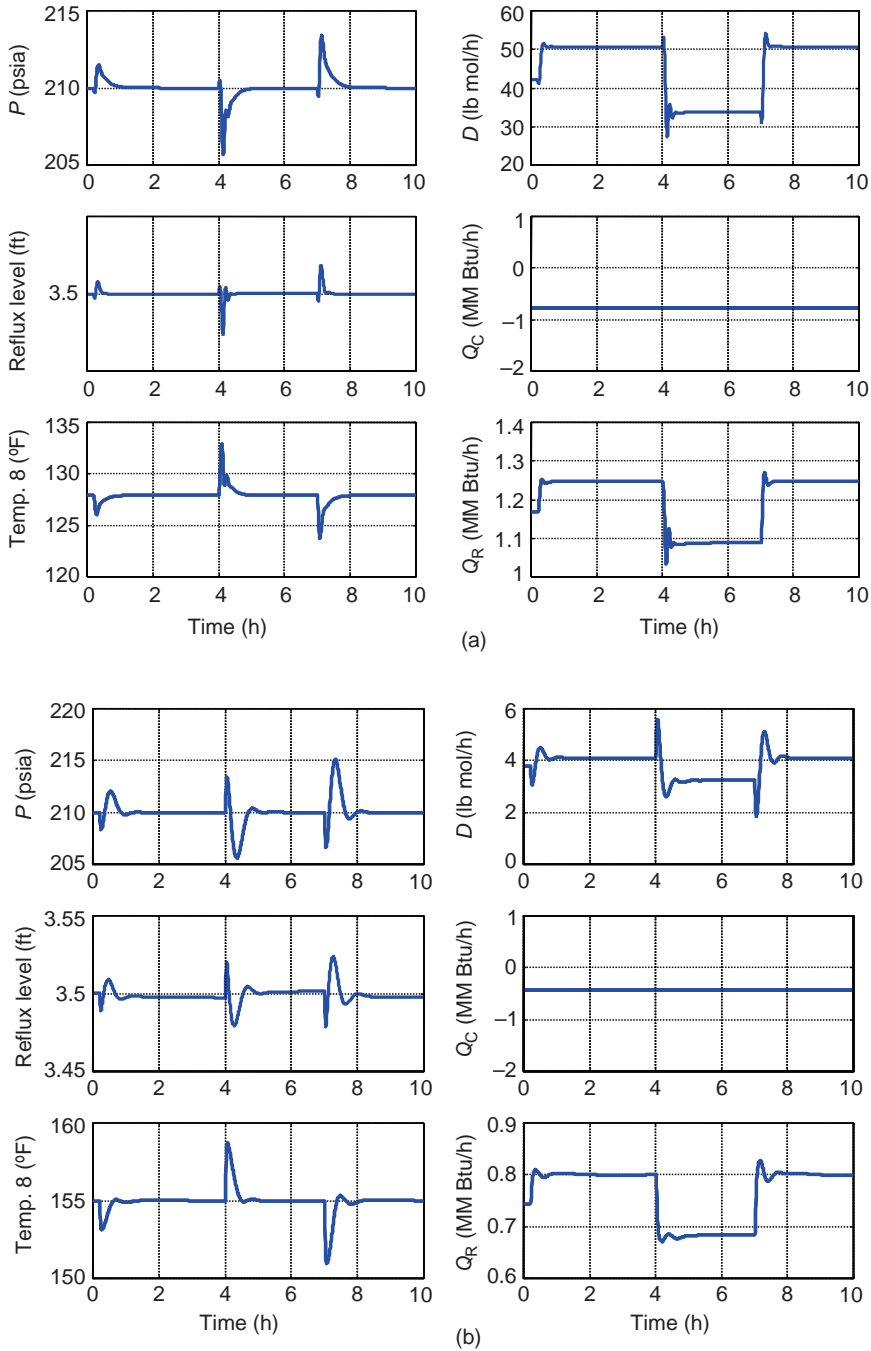


Figure 8.12 (a) Responses for large distillate case (CS2). (b) Responses for small distillate case (CS2).

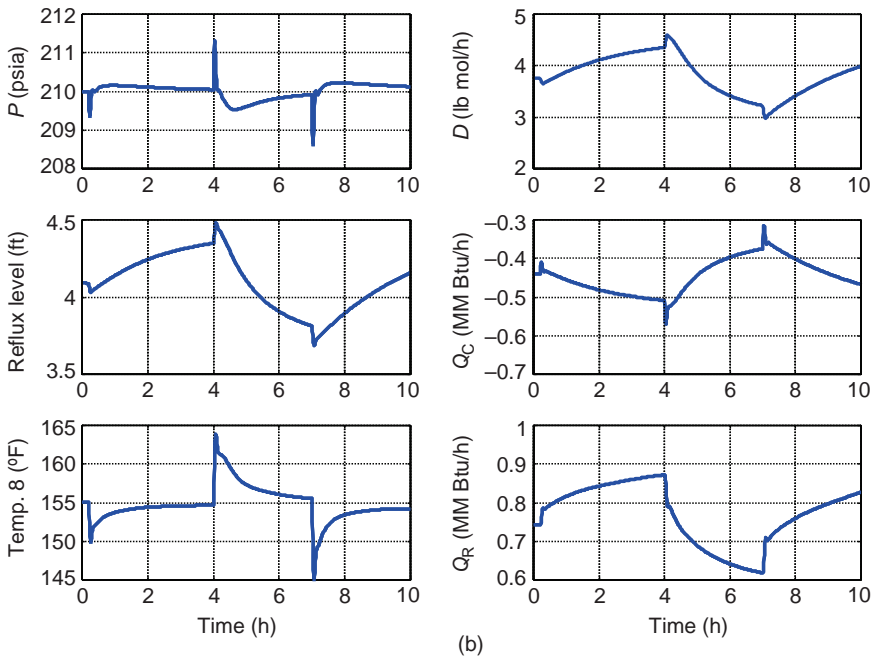
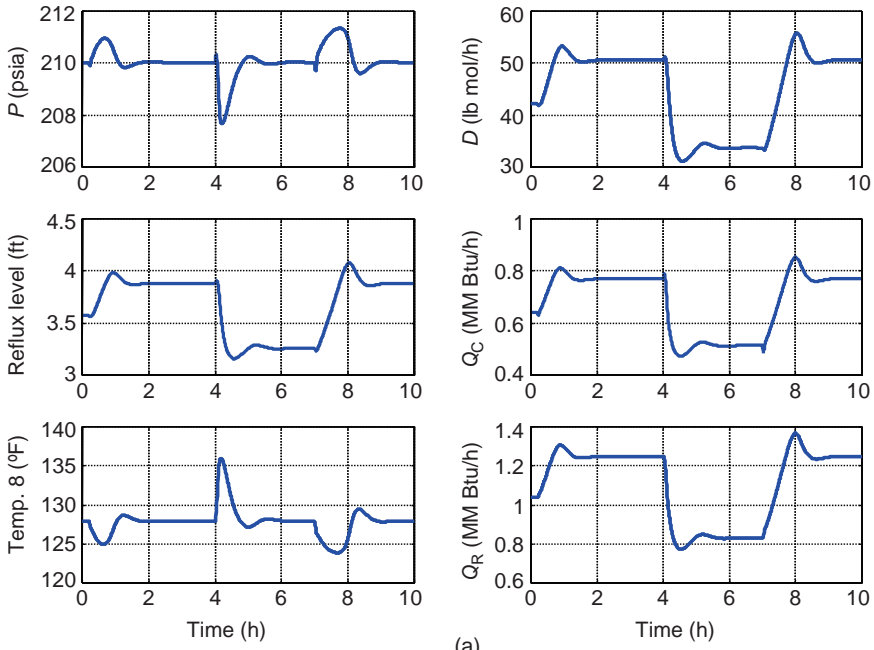


Figure 8.13 (a) Responses for large distillate case (CS3). (b) Responses for small distillate case (CS3).

flow rate is ratioed to the reflux flow rate. Figure 8.13a is for the large distillate case, and Figure 8.13b is for the small distillate case.

The deviations in pressure are even smaller than in either of the previous control structures. In addition, the changes in the vapor distillate flow rate are more gradual.

However, notice that Stage 8 temperature takes longer to return to the set point value, and the changes in reboiler heat input are larger. This occurs because both the distillate and the reflux flow rates change for a change in feed flow rate, which necessitates larger changes in vapor boilup.

Thus, this control structure is better from a plantwide control perspective, but it may not be as good from an individual column control perspective.

Comparisons. Figure 8.14 provides direct comparisons among the three alternative control structures for the two cases. The solid lines are the small distillate case, and the dashed lines are the large distillate case.

Figure 8.14a shows how pressure responds to the three disturbances with the three control structures. Figure 8.14b shows the responses in the distillate flow rate. Figure 8.14c gives the responses in Stage 8 temperatures.

These results illustrate the important conclusion that control structure CS3 provides smaller and more gradual changes in the vapor distillate flow rate, which would be desirable from a plantwide control perspective if this stream is fed to a downstream process.

Product Composition Performance. The results presented up to this point have only looked at flows, levels, pressures, and tray temperatures. The effects of control

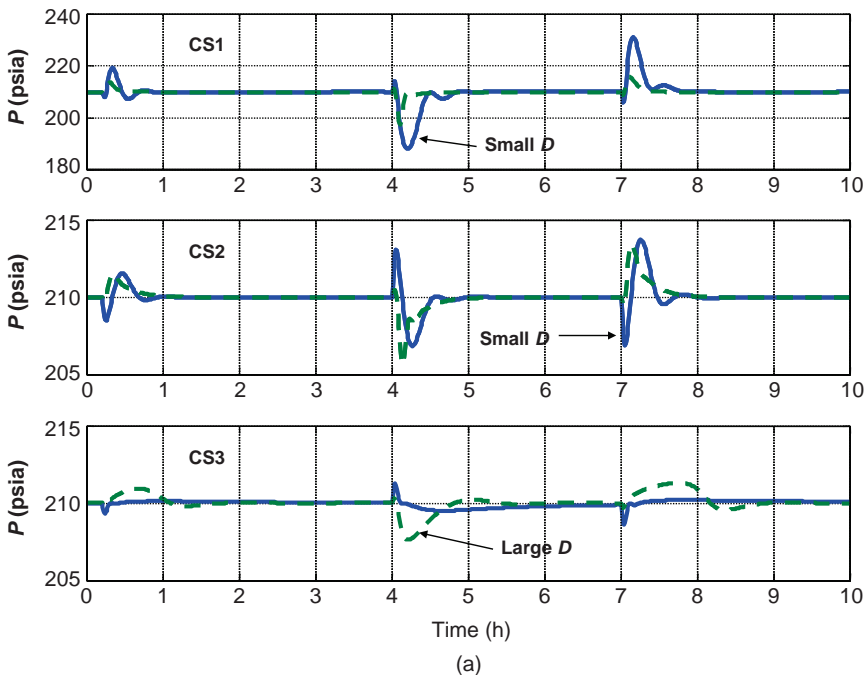


Figure 8.14 (a) Pressure responses. (b) Distillate flow rate responses. (c) Tray temperature responses.

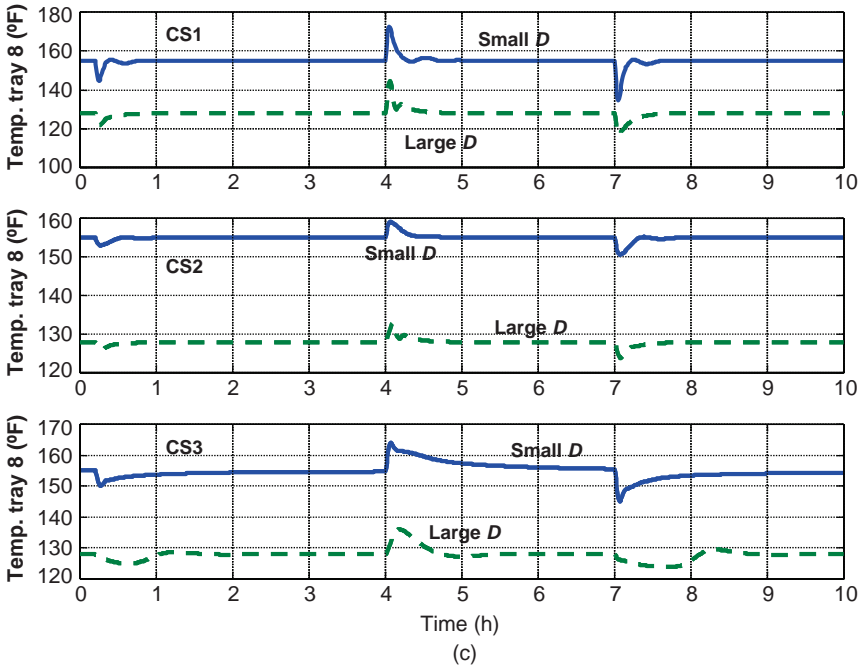
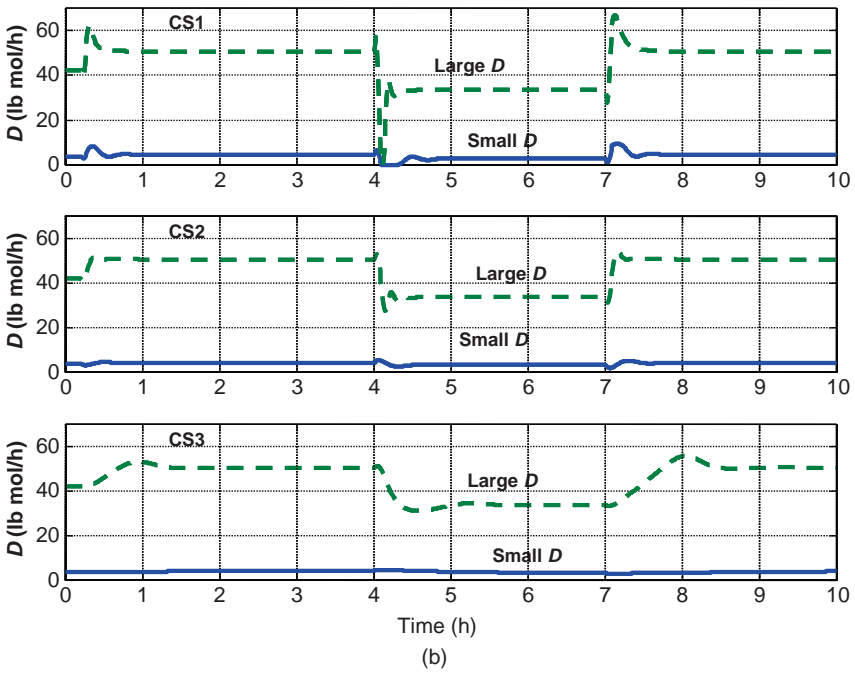


Figure 8.14 (Continued)

structure and steady-state distillate flow rate have been examined for disturbances in feed flow rate. We have not looked at feed-composition disturbances.

The job of the column is to achieve the desired product purities in the face of disturbances. Recall that the design specifications are 1 mol% *i*C4 in the distillate and 0.5 mol% C3 in the bottoms. We are using single-end control with a temperature on a tray in the column controlled by manipulating reboiler heat input. The other degree of freedom is held constant and depends on the control structure. In CS1, it is the reflux-to-feed ratio, and in CS3, it is the RR. In control structure CS2, the other degree of freedom is a fixed condenser heat removal.

Feed Flow Rate Changes. Both CS1 and CS3 structures should handle feed rate changes, at least from a steady-state standpoint, that is, product compositions should come back to their design values for feed rate changes. This is expected because we are maintaining flow ratios. Dynamically, the product compositions will not be constant, as the results in Figure 8.15 illustrate. The two left graphs show how the impurities in the bottoms ($x_{B,C3}$) and in the distillate ($x_{D,iC4}$) vary during the feed flow rate disturbances described earlier. Results are given for the large distillate design case for all three structures.

Control structures CS1 and CS3 drive both product compositions back close to the desired values at the new steady state. There are significant dynamic departures, particularly in the bottoms composition when using CS3. Consider the effect of the large increase in feed flow rate at time equal to 7 h. There is a dynamic 10-fold increase in the impurity of propane in the bottoms at about 7.5 h. This occurs because the increase in feed flow rate brings more light material into the column that affects bottoms composition quickly before the corresponding drop in Stage 8 temperature can increase reboiler heat input to compensate for the increase in feed flow rate. Remember that the feed is liquid, so it affects the bottoms much more quickly and drastically than the distillate. In addition, there

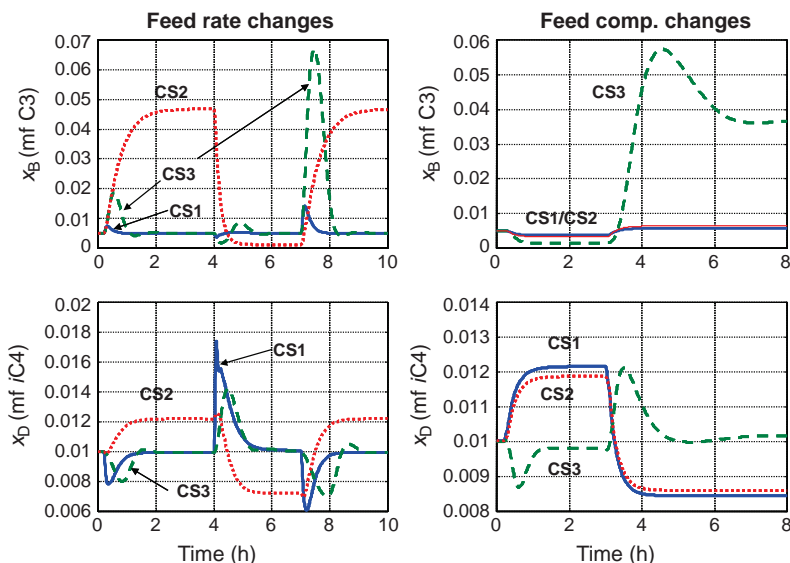


Figure 8.15 Product composition responses.

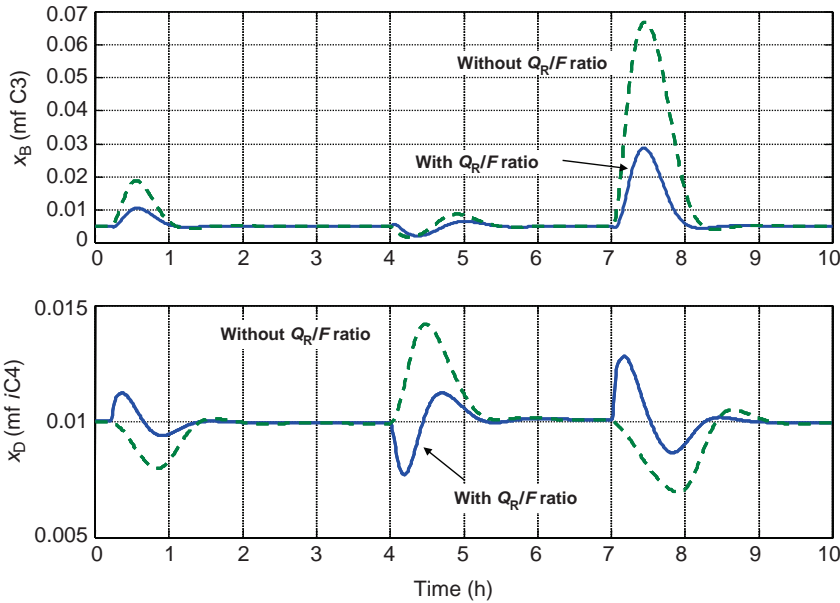


Figure 8.16 CS3: Feed rate disturbances with and without Q_R/F ratio.

is a 1 min deadtime in the temperature loop. Also, keep in mind that the tray selected is in the rectifying section above the feed tray.

This same problem exists in the other control structures, but in CS1, the increase in feed flow rate is accompanied by an immediate increase in reflux flow rate. This quickly affects Stage 8 temperature, and reboiler heat input increases in time to limit the peak in the propane impurity in the bottoms to about 1.5 mol%.

The CS3 control structure with its fixed condenser heat removal does not return the product purities to their desired values for feed flow rate changes.

Obviously, all three of these control structures could be improved by using feedforward control. In CS1 and CS3, the reboiler heat input could be ratioed to the feed flow rate (with the ratio reset by the temperature controller), and in CS3, the condenser heat removal could be ratioed to the feed flow rate. Figure 8.16 illustrates that the improvement of the Q_R -to- F ratio provides for CS3 with the large distillate case.

The solid lines are with the ratio and the dashed lines are without. The worst-case peak in the propane impurity in the bottoms ($x_{B,C3}$) is reduced for about 6.6 mol% to <3 mol%. This is still very large compared with the specification of 0.5 mol%, but keep in mind that the disturbance is very large, a 50% step increase in feed flow rate, which is probably much larger than that to which an industrial column would typically be subjected.

Feed-Composition Changes. Perhaps of more importance are the performances of the three alternative control structures to disturbances in feed compositions because feed forward is seldom an option to handle these disturbances. The right two graphs in Figure 8.15 compare the three alternative control structures for two-step changes in feed composition. At time equal to 0.2 h, the feed composition is changed from 40 to 45 mol% propane and from 30 to 25 mol% isobutane. Then, at time equal 3 h, the feed composition is changed from 45 to 36 mol% propane and from 25 to 34 mol% isobutane.

The performances of structures CS1 and CS2 are quite similar because in both the reflux flow rate is essentially constant because feed composition is changing. There is some steady-state deviation from the desired product purities. Increasing propane content in the feed with a fixed Stage 8 temperature produces (somewhat counter intuitively) a higher level of isobutane impurity in the distillate and a lower level of propane impurity in the bottoms.

The response of structure CS3 shows some important results, both steady state and dynamic. From the analysis discussed earlier and presented in Figure 8.10, we would expect that the constant RR strategy used in CS3 would not handle feed-composition changes as well as the constant reflux flow rate strategies of the other two structures, at least from a steady-state point of view. Figure 8.10 shows that a slightly higher than design reflux flow rate (4% higher for the high distillate case and 10% for the low distillate case) would give on-specification product purities over the range of feed composition. To achieve the same product purities with a constant RR strategy would require operating with 35% and 24% higher RRs than the values at the design feed composition for the two cases. Thus, it is no surprise that CS3, with its RR fixed at the design value, does not do as good a job in maintaining product purities for feed-composition disturbances.

The results in Figure 8.15 show that an increase in propane concentration in the feed produces only a small steady-state shift in distillate purity when CS3 is used, which is less than that produced by the other two control structures. However, the change in the bottoms purity is larger than that produced by the other structures. The same occurs for a decrease in feed propane composition.

The results shown in Figure 8.10 are for the case when both distillate and bottoms purities are maintained. The results in Figure 8.15 reveal an asymmetric behavior in which distillate purity changes little but bottoms purity changes drastically. One of the fundamental reasons for this is our selection of a rectifying section tray to control. Had we selected a tray in the stripping section, bottoms purity would be better maintained at the expense of larger changes in distillate purity. These results suggest that the method for selecting the control tray temperature depends on which product is more important.

Of course, this problem of steady-state shift in product purity for feed-composition changes could be solved by using a cascade composition/temperature-control structure. Keep in mind, however, that the RR would have to be fixed at the highest value needed to handle the range of feed compositions.

The results shown above are for the high distillate case. Similar results were obtained for the small distillate case. However, the dynamics for the feed-composition disturbances is much slower because the changes made in the propane concentration of the feed are much smaller (changed from 4 to 5 mol% C3).

Dual-Composition Control. The control structures studied up to this point all use single-end inferential control. A single-tray temperature is controlled with the objective of maintaining a temperature profile in the column that we hope will hold product purities close to their specifications. This goal was achieved with varying degrees of success, depending on the control structure used and the disturbance. If tight product composition control is required, a dual-composition control structure can be used. However, it requires two on-line composition analyzers, which are expensive and require high maintenance.

To illustrate the improvement in control that is achieved by using dual-composition control, the CS3 control structure is augmented by two composition controllers, one controlling propane impurity in the bottoms (CCxB) and the second controlling isobutane

Setting up the multiplier for the reboiler heat input to feed ratio requires the use of metric units: flows in kmol/h and heat in GJ/h. Thus, the steady-state value of the second input to the multiplier, which is the temperature-controller output signal, is calculated

$$\frac{QR(\text{GJ/h})}{F(\text{kmol/h})} = \frac{(1.038 \times 10^6 \text{ Btu/h})(1.055 \text{ GJ}/10^6 \text{ Btu/h})}{(100 \text{ lb mol/h})(0.454 \text{ kmol/h})} = 0.0241$$

Figure 8.17b shows the controller faceplates. Notice that the flow controller on the vapor distillate (FCD) has a remote set point (on “cascade”) coming from a multiplier (“ratio”) whose two inputs are the reflux flow rate and the CCxD controller output signal. The temperature controller is also on “cascade” with its set point coming from the CCxB controller.

Figure 8.18 demonstrates the effectiveness of this dual-composition control structure. Figure 8.18a shows how product purities vary in the face of the same scenario of feed flow rate disturbances and feed-composition disturbances previously used. A comparison of these results with the CS3 results given in Figure 8.15 reveals a very significant reduction in product quality variability, both dynamically and at steady state. Both products are returned to the specifications, even for feed-composition disturbances.

Figure 8.18b shows the changes in other key variables. The solid lines are for feed flow rate disturbances. The dashed lines are for feed-composition disturbances. Notice that the CCxB composition-controller changes the set point temperature for the feed-composition disturbances, shifting it lower than the design 128 °F for higher propane compositions in the feed and higher for the lower propane compositions in the feed. Likewise, the RR is

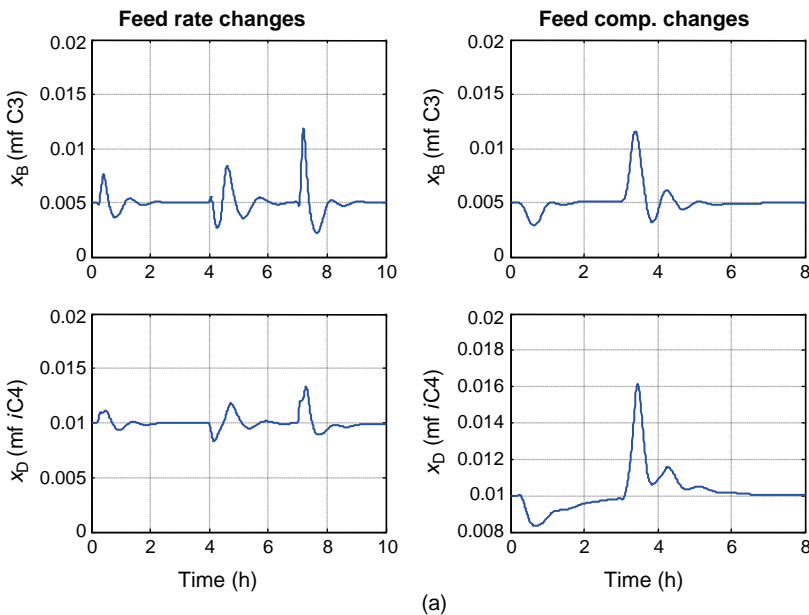


Figure 8.18 (a) Dual-composition control: product purities. (b) Dual-composition control: flows and temperatures.

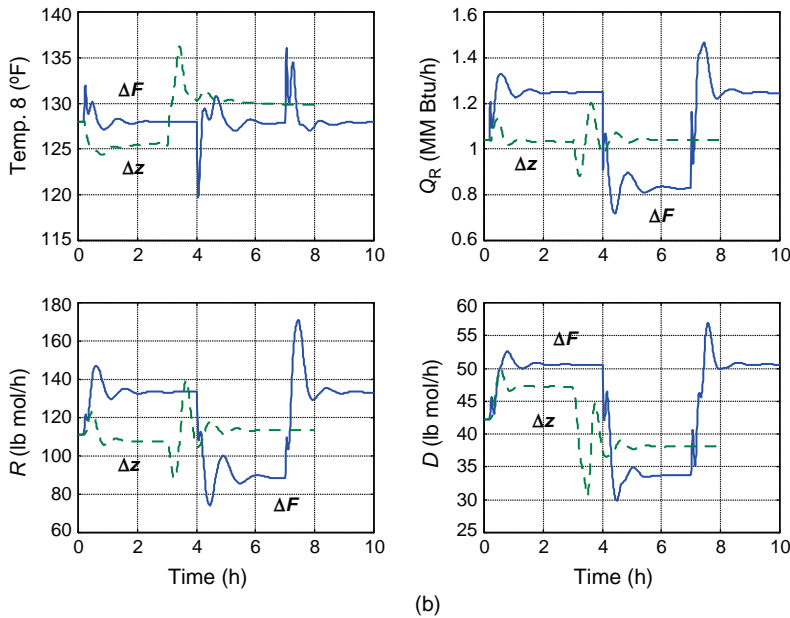


Figure 8.18 (Continued)

adjusted by the CCxD controller from its design value of 2.63, so that the distillate purity is maintained for feed-composition disturbances.

The variability in the vapor distillate flow rate is still much less than with the other control structures, so even with dual-composition control, the downstream unit is not subjected to large and rapid disturbances.

These results illustrate the improvement in dynamic and steady-state performance that is achievable with conventional PI control structures through the use of ratio and cascade control schemes. Of course, on-line composition measurements are required for dual-composition control.

Conclusions. This process provides an interesting and important example of the conflicts between individual unit performance and plantwide performance. Considering only the column in isolation, control structure CS1 gives the best results in terms of product purities for disturbances in both feed flow rate and feed composition. However, this control structure produces large and rapid changes in the vapor distillate flow rate, which could seriously degrade the performance of downstream units. Control structure CS3 provides more gradual changes in the distillate flow rate, but it does not hold product purities as close to their specifications as control structure CS1 does in the face of feed-composition disturbances.

Modifying the CS3 structure by the addition of dual-composition control provides effective product quality control with essentially the same low variability in distillate flow rate.

8.2.2 Both Vapor and Liquid Distillate Streams

Distillation columns frequently produce both vapor and liquid distillate product streams from the reflux drum when the feed stream contains small amounts of light components

that would require high pressures or low temperatures if a total condenser were used to completely condense the overhead product. Because removing heat using cooling water in the condenser is much less expensive than using refrigeration, many columns are designed to operate with reflux-drum temperatures of about 120 °F, so that cooling water at 90 °F can be used. Fixing reflux-drum temperature and selecting a reasonable pressure determines the split between the amount of vapor product and the amount of liquid product.

In the operation of these systems, we usually want to condense as much as possible, so as to minimize compression costs of dealing with the vapor product. Therefore, the flow rate of cooling water should be maximized. This section demonstrates a realistic way to model a partial-condenser distillation system with both vapor and liquid distillate streams using Aspen simulation.

With a reflux-drum design temperatures set at 120 °F, the required pressure depends on the composition of the overhead and whether the distillate product is removed as a liquid or as a vapor. In the former case, the reflux drum would operate at the bubblepoint pressure at 120 °F. In the latter case, the reflux drum would operate at the dewpoint pressure at 120 °F. There is no difference in these pressures if the overhead is a single pure component. If the overhead is a mixture of chemical components, the bubblepoint pressure is larger than the dewpoint pressure. If the volatilities of the components are quite different, running with a total condenser (bubblepoint pressure) can require a much higher pressure than running with a partial condenser. This is true even if some of the distillate product is taken off as liquid and some is taken off as vapor.

A very frequently encountered situation is when the feed to the column contains a small amount of a very light component in addition to the light and heavy key components. Trying to totally condense the overhead mixture of the lighter-than-light key and light key components could require a very high pressure for a fixed 120 °F reflux-drum temperature. A good example of this situation is in the methanol process where the feed to the distillation column comes from a flash tank that is operating at high pressure with a gas recycle stream containing large amounts of light components (hydrogen, carbon monoxide, and carbon dioxide). Small amounts of these light components will be present in the flash tank liquid and fed to the column. Trying to totally condense the overhead (a mixture of these light components and methanol) would require either a high pressure or a very low temperature (refrigeration). The solution to the problem is to take a small vapor stream from the top of the reflux drum in addition to taking a liquid distillate, which is mostly methanol. Some methanol will be lost in the vapor stream, but the small vapor stream can be compressed and recycled back to the reaction section of the process if the economics justify the additional capital and operating expenses.

The normal distillation column with either a liquid or a vapor distillate product (but not both) has two steady-state design degrees of freedom once feed conditions, column pressure, total trays, and feed location are fixed. Distillate flow rate and RR are usually manipulated to achieve two product-composition specifications (the heavy-key impurity in the distillate and the light-key impurity in the bottoms).

A distillation column that is designed to produce both a liquid distillate stream and a vapor distillate stream from the reflux drum has an additional design degree of freedom. This is usually specified to be the reflux-drum temperature. Under these conditions, the split between the flow rates of the vapor and liquid distillates is fixed. The condenser heat duty is also fixed. Specifying a reasonable design minimum temperature differential temperature (at the either the cold or the hot end of the condenser), and a reasonable overall heat-transfer coefficient fixes the heat-transfer area. This also fixes the required flow rate of

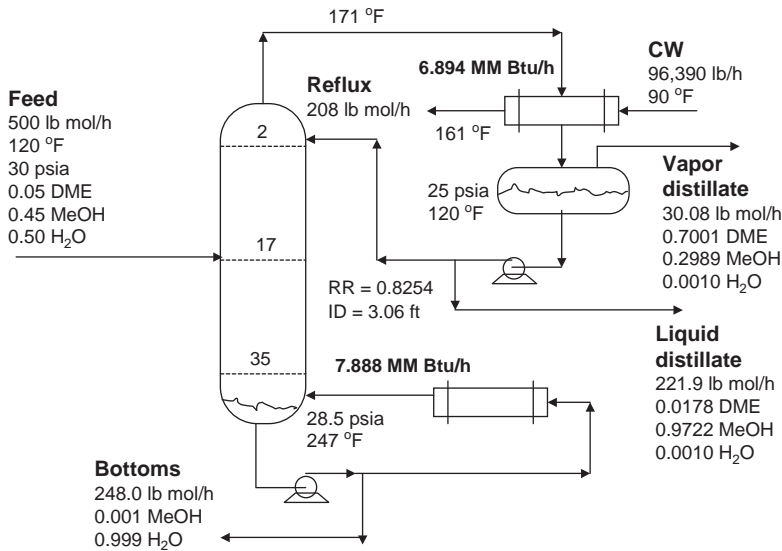


Figure 8.19 Column flowsheet: DME/methanol/water at 25 psia.

the cooling water because both the inlet and exit cooling water temperatures are known. All these sizing calculations are performed at the design stage to select the correct equipment (column and heat exchangers).

Once the column is built and the condenser area is fixed, the normal operating objective is to minimize the vapor flow rate by maximizing condenser heat removal. This is achieved by maximizing cooling water flow rate.

Process Studied. The numerical example considered has 500 lb mol/h of feed that is a ternary mixture of 5 mol% dimethyl ether (DME), 45 mol% methanol, and 50 mol% water. The DME is a lighter-than-light key component that is mostly removed in a vapor stream from the top of the reflux drum. Most of the light-key component methanol comes off in the liquid distillate, and most of the heavy-key component water leaves in the bottoms.

Figure 8.19 shows the flowsheet. The column has 36 stages (Stage 1 is the reflux drum and Stage 36 is the base). Feed is introduced on Stage 17. The reflux-drum pressure is set at 25 psia and the reflux-drum temperature is 120 °F. A tray pressure drop of 0.1 psi per stage is assumed. NRTL physical properties are used in the Aspen simulations.

There are three design degrees of freedom in this partial condenser column. They are selected to be 0.1 mol% water in the *liquid* distillate, 0.1 mol% methanol in the bottoms, and 120 °F reflux-drum temperature. The resulting small vapor distillate flow rate is 30.08 lb mol/h, and the larger liquid distillate flow rate is 221.9 lb mol/h. Column diameter is 3.06 ft, and the reflux flow rate is 208 lb mol/h.

The heat-removal rate in the condenser is 6.894×10^6 Btu/h, which requires 96,390 lb/h of 90 °F cooling water. Notice that the temperature of the overhead vapor from the column is 171 °F, which is much higher than the reflux-drum temperature. This occurs because of the large difference between the boiling points of DME (−12.7 °F) and methanol (148.5 °F) and the 25 psia operating pressure. The condenser is designed for a

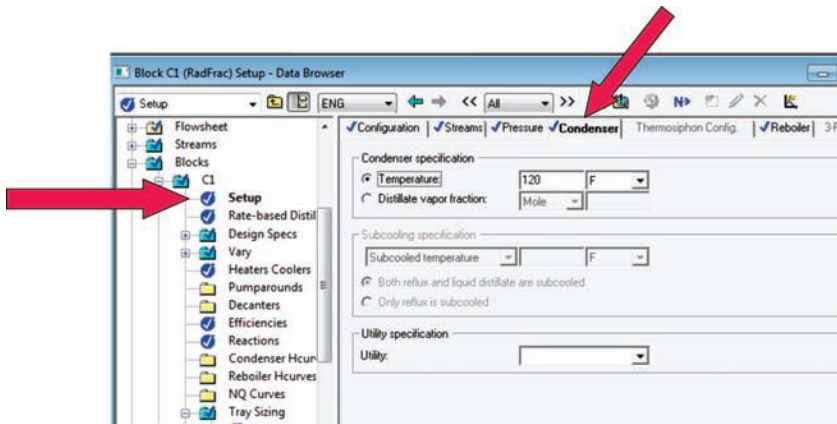


Figure 8.20 Fix partial condenser temperature.

10 °F approach, so the cooling-water exit temperature is 161 °F. In some plant cooling-water systems, the cooling-water chemistry imposes a limit on the permitted change in the cooling-water temperature (20–30 °F). In this situation, the design approach temperature would be increased, which would require a higher flow rate of cooling water and a smaller area condenser.

Steady-State Design. The feed conditions, the pressure, the total stages, and the feed stage are specified in the steady-state design using Aspen Plus (version 7.3). Two Aspen *Design Spec/Vary* functions are set up to achieve the desired product specifications of 0.001 mol fraction water in the liquid distillate and 0.001 mol fraction methanol in the bottoms.

Figure 8.20 shows how the third specification is fixed in Aspen Plus. Under the C1 column block, the *Setup* item is selected and the *Condenser* page tab is opened. The condenser specification is selected to be a fixed temperature (120 °F).

In preparation for exporting into dynamics, the reflux drum and the column base are both sized in the normal way to provide 5 min of liquid holdup when half full. The column diameter is determined from the *Tray Sizing* item in the column block.

The Aspen Plus default dynamic conditions for the reboiler and condenser are *Constant duty*. When the Aspen Plus file is exported into Aspen Dynamics, the heat duty in the condenser will be fixed. It can be manipulated to control some variable, usually pressure.

However, there are other options for setting up the condenser, which can be used to obtain more realistic models. Figure 8.21 shows that clicking the drop-down arrow on the right of the *Heat transfer option* gives several options. The *Constant duty* option is the default and produces a dynamic model in which condenser heat removal is the manipulated variable.

The *Constant temperature* option assumes that the temperature of the cooling medium is the same at all axial positions in the condenser. This situation can be used when the cooling medium is a liquid that is being vaporized in the condenser by the heat of condensation of the process vapor stream. The medium could be a vaporizing refrigerant in low-temperature columns or vaporizing boiler feed water to generate steam in high-

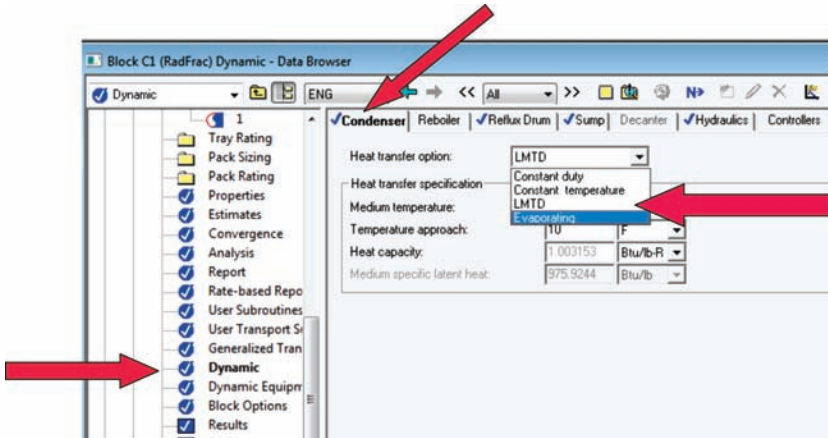


Figure 8.21 Select LMTD dynamic model in partial condenser.

temperature columns. The *Constant temperature* option produces a dynamic model in which the temperature of the cooling medium is the manipulated variable.

The *Evaporating* option is similar to the *Constant temperature* option, except that the flow rate of the cooling medium is the manipulated variable.

The most realistic option for partial condenser modeling is the *LMTD* option. The cooling medium is a liquid that enters a counter-current heat exchanger at a specified inlet temperature. The minimum approach differential temperature is specified. The process inlet and outlet temperatures are known, so the log-mean temperature differential driving force is known. With the known condenser duty, the required product of the overall heat-transfer coefficient and the condenser heat-transfer area (UA) is calculated. The required flow rate of the cooling medium can also be calculated.

The *LMTD* option produces a dynamic model in which the flow rate of the cooling medium is the manipulated variable. This is the model that will realistically provide prediction of how the partial condenser system responds to disturbances.

Dynamic Simulation. Two files were exported into Aspen Dynamics with the two alternative condenser models (*Constant duty* and *LMTD*). Three cases were explored. The *Constant duty* model was used in the first two cases, and the *LMTD* model was used in the third.

In the first case (constant QC), the condenser duty was held constant. In the second case (constant TC), the reflux-drum temperature was controlled by manipulating condenser heat duty. In the third case (constant CW), the flow rate of cooling water was held constant (using the *LMTD* model). Disturbances in the flow rate and composition of the feed to the column were made.

In all cases, the basic control structure used the following conventional control loops. The only difference among the cases was how the condenser heat duty was determined.

1. Feed was flow controlled.
2. Pressure was controlled by manipulating the flow rate of the vapor distillate.

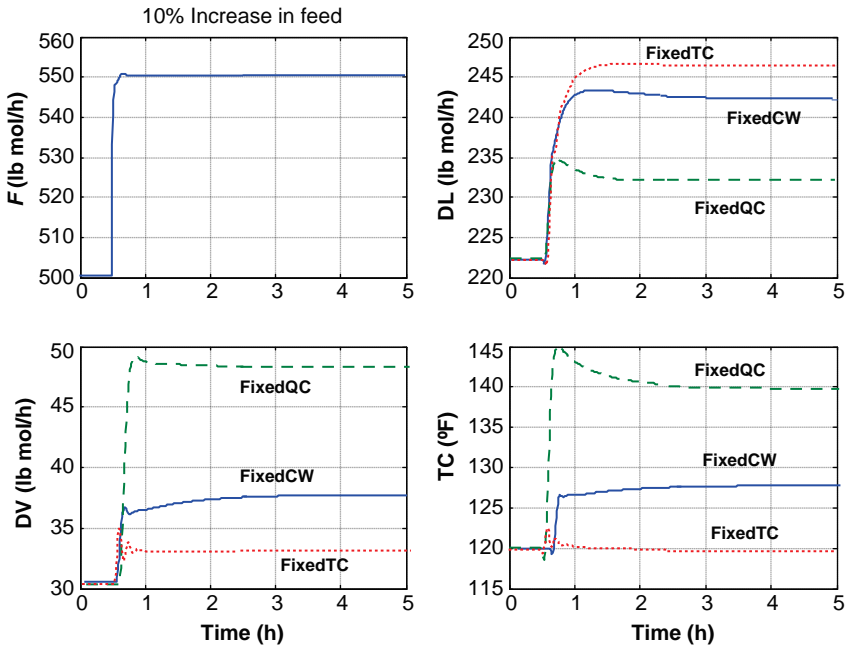


Figure 8.22 Throughput increase.

3. Base level was controlled by manipulating bottoms flow rate.
4. Reflux-drum level was controlled by manipulating liquid distillate flow rate.
5. Reflux flow rate was fixed.
6. The temperature on Stage 33 was controlled by manipulating reboiler heat input.

Figures 8.22 and 8.23 show the responses of the process to 10% disturbances in feed flow rate. The solid lines are when the flow rate of cooling water is fixed. The dashed lines are when the condenser duty is fixed. The dotted lines are when the temperature of the reflux drum is controlled.

In Figure 8.22, feed flow rate is increased to 10%. If condenser duty is fixed (fixed QC), no additional heat transfer occurs in the condenser, so there are large increases in the flow rate of the vapor distillate (DV) and in the reflux-drum temperature. These responses are unrealistic because the increase in the flow rate of the overhead vapor into the condenser should change the condenser heat-transfer rate.

If the reflux-drum temperature is fixed (fixed TC) by varying condenser duty (using a temperature controller), the increases in the flow rates of the vapor and distillate are about proportional to the increase in feed flow rate. But these responses are also unrealistic because the increase in condenser duty would require a proportional increase in the differential temperature driving force that could only be attained by a large increase in the flow rate of the coolant.

The realistic situation is when the cooling water flow rate is fixed (at its maximum because we are trying to minimize the flow rate of the vapor distillate). Flow rate is the only

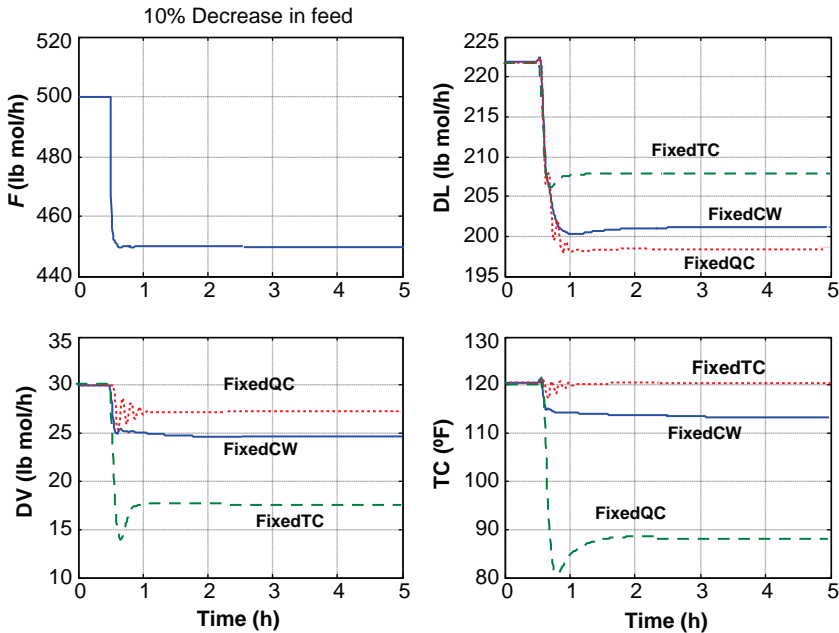


Figure 8.23 Throughput decrease.

true manipulated variable. The fixed CW responses show a reflux-drum temperature that increases slightly and a slightly larger ratio of vapor-to-liquid flow rates.

Figure 8.23 gives results for a 10% decrease in feed flow rate. Results are the opposite of those shown for an increase. Unrealistic responses are shown for the fixed QC and the fixed TC cases. Notice that the fixed QC case requires a reflux-drum temperature (TC shown in the bottom right graph in Figure 8.23) that is lower than the temperature of the available cooling water.

Figures 8.24 and 8.25 give responses for feed-composition disturbances with the three alternative condenser models. In Figure 8.24, the DME concentration in the feed is increased from 5 to 7.5 mol% (with a corresponding decrease in methanol). The flow rate of the vapor distillate DV increases in all cases as expected, but the fixed QC model gives a smaller increase in DV accompanied by an unrealistically large decrease in reflux-drum temperature down to 101 °F. The DME impurity in the liquid distillate $x_D(\text{DME})$ shows a large increase.

Decreasing the DME concentration in the feed has the opposite effects, as shown in Figure 8.25. The fixed QC model predicts less change in the flow rate of the vapor distillate and a high reflux-drum temperature. The most realistic predictions are those given by the fixed CW model.

Three different distillation condenser models have been compared for columns producing both vapor and liquid distillate streams. When the objective is to minimize the flow rate of the vapor, we should try to condense as much of the overhead vapor as possible. The realistic means for accomplishing this objective is to maximize the flow rate of the cooling medium. Therefore, the model that assumes a fixed flow rate of cooling water gives the most realistic predictions of performance to disturbances.

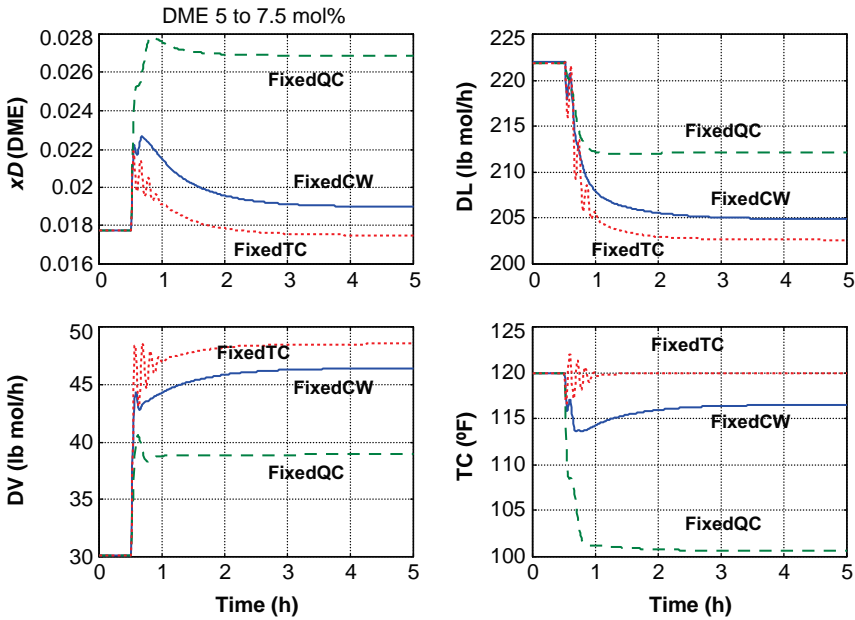


Figure 8.24 Increase in DME in feed.

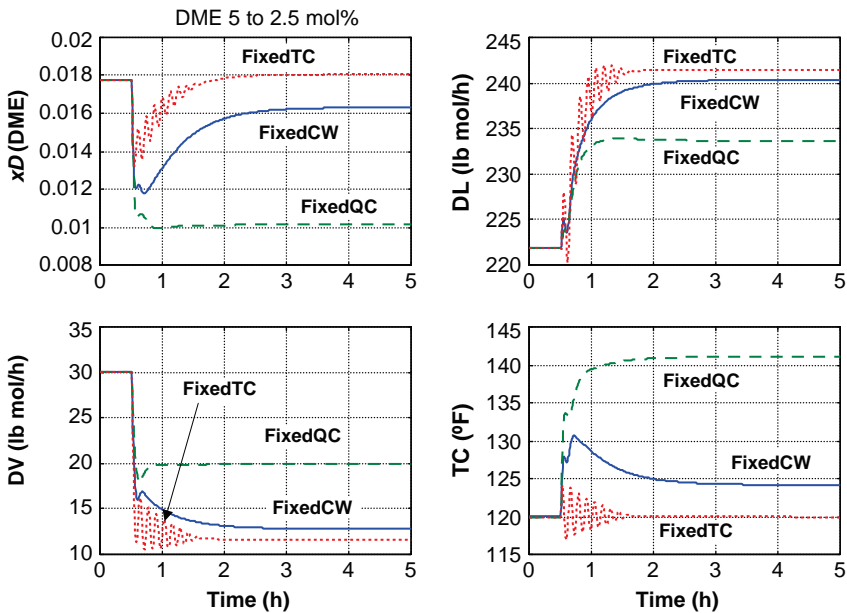


Figure 8.25 Decrease in DME in feed.

8.3 CONTROL OF HEAT-INTEGRATED DISTILLATION COLUMNS

In Chapter 5, the steady-state simulation of a two-column heat-integrated distillation system was developed in which the total feed was split between the two columns. The two columns are designed to run “neat,” so all the energy released in the condenser of the high-pressure column is used in the reboiler of the low-pressure column. In the steady-state design, this balance was achieved by using a *Design Spec* under *Flowsheeting Options* that splits the total feed between the two columns such that the two heat duties are equal.

Now, we want to look at the dynamics of this complex flowsheet. There are three major issues that must be addressed in designing a control system for a heat-integrated column process that is operating under “neat” conditions. Auxiliary reboilers or auxiliary condensers are not used to balance the vapor boilup needed at the base of the low-pressure column with vapor condensation needed at the top of the high-pressure column.

1. Just as in the steady-state design situation, the heat duties must be equal (with opposite sign) at every point in time.
2. Unlike in the design situation, the heat duty must be calculated at each point in time from the current value of the differential temperature driving force between the temperature in the reflux drum at the top of the high-pressure column and the temperature in the base of the low-pressure column. The overall heat-transfer coefficient U and the heat-transfer area A have been fixed in the steady-state design, and these constants are used in the dynamic simulation to calculate the heat-transfer rate at each point in time. These two temperatures will change because of dynamic changes in compositions and, more importantly, because of dynamic changes in pressure. The pressure of the high-pressure column will not be controlled. It will float up and down to achieve the required high-pressure column reflux-drum temperature to produce the required heat-transfer rate.
3. There is only one reboiler duty to manipulate, and only one variable can be controlled by this input. As discussed later, we will use a control structure in which a tray temperature in the high-pressure column is controlled by manipulating the heat input to the reboiler in the high-pressure column (the only steam-heated reboiler). Then, we will vary the feed split (the fraction of the total feed fed to the low-pressure column) to control a temperature on a tray in the low-pressure column.

8.3.1 Process Studied

The heat-integrated process considered in Chapter 5 was simplified in order to clearly convey the design issues. The number of trays used in each column was made the same (32 stages). This means that the design is not the economic optimum. Because the separation is more difficult at higher pressures, the high-pressure column should use more trays than the low-pressure column. Note that the RR in the high-pressure column from Chapter 5 was 0.585, and the RR in the high-pressure column was much higher at 0.922.

In order to study a more realistic case, the optimum economic design presented almost 40 years ago in a pioneering paper is used as a numerical example in this chapter.¹

The optimum design is shown in Figure 8.26. The low-pressure column has 33 stages and operates at 17 psia. The high-pressure column has 63 stages and operates at 100 psia.

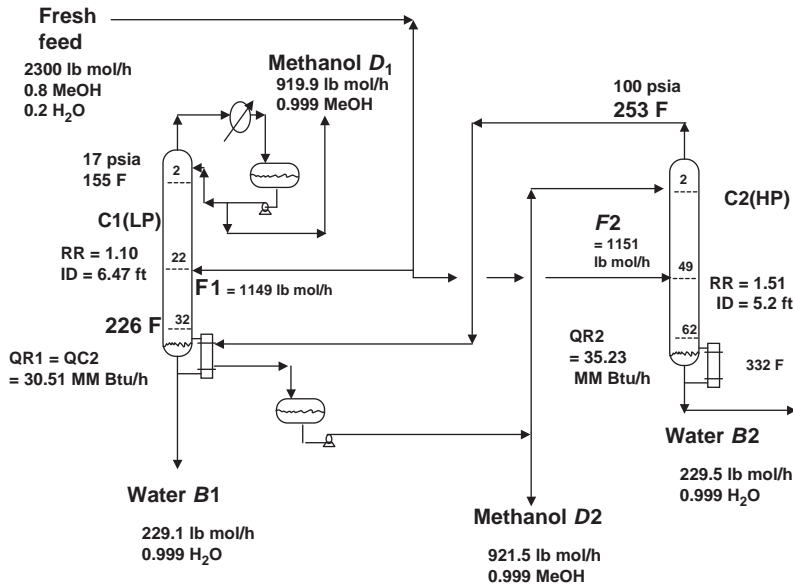


Figure 8.26 Heat-integrated columns.

The resulting temperatures in the high-pressure reflux drum (253 °F) and in the base of the low-pressure column (226 °F) give a reasonable differential temperature-driving force. The heat duty in the condenser/reboiler heat exchanger is 30.51×10^6 Btu/h, which requires $A = 8170 \text{ ft}^2$ of heat-transfer area if an overall heat-transfer coefficient of $U = 150 \text{ Btu}/(\text{h ft}^2 \text{ } ^\circ\text{F})$ is assumed. These values of U and A are calculated at the design stage and are subsequently fixed in the dynamic simulation. The heat-transfer rate can only change by changing the differential temperature-driving force (the difference between the top temperature in the high-pressure column and the base temperature of the low-pressure column).

The total feed of 2300 lb mol/h of a binary mixture of 80 mol% methanol and 20 mol% water is split between the two columns to exactly balance the heat duties in high-pressure column condenser (QC_{HP}) and the low-pressure reboiler (QR_{LP}). Both columns produce 99.9 mol% methanol distillate streams and 99.9 mol% water bottoms streams. The required reflux ratios are 1.1 and 1.5 in the low- and high-pressure columns, respectively. Column diameters are 6.5 and 5.2 ft in the low- and high-pressure columns, respectively. Temperature profiles are given in Figure 8.27. The NRTL physical properties are used in the Aspen simulations.

8.3.2 Heat Integration Relationships

There are two relationships that must hold in the dynamic simulation at each point in time

$$QR_{LP} = UA(T_{R,HP} - T_{B,LP})$$

$$QC_{HP} = -QR_{LP}$$

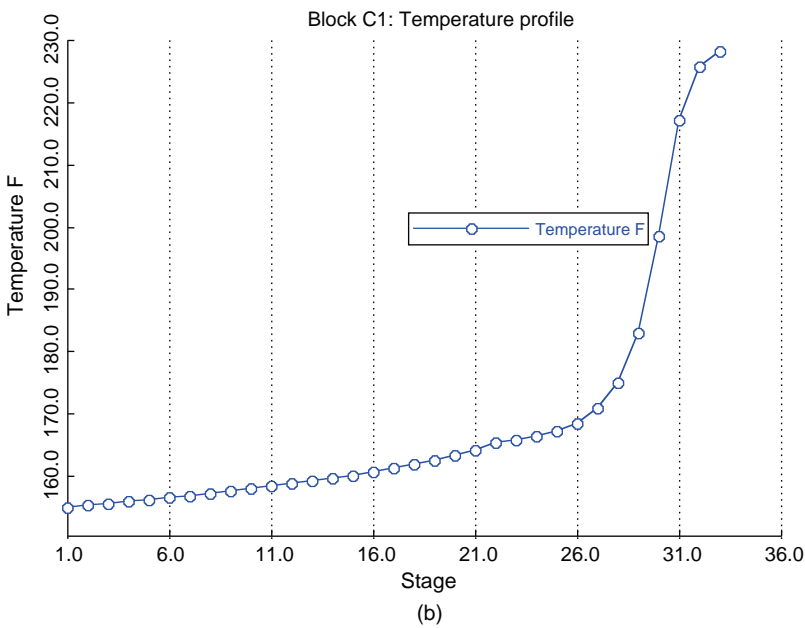
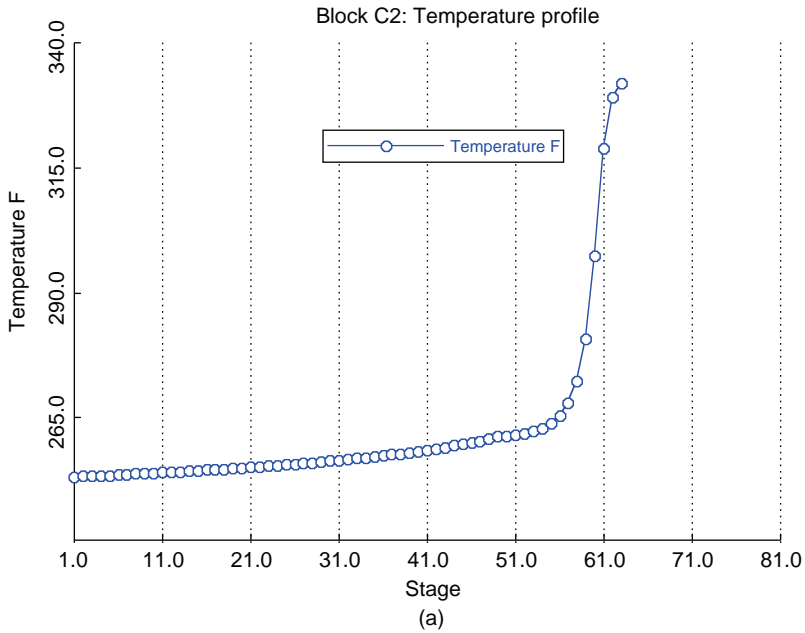


Figure 8.27 (a) HP column temperature profile. (b) LP column temperature profile.

These are implemented in Aspen Dynamics by using *Flowsheet Equations*. Figure 8.28a shows the window that opens when *Flowsheet* is clicked in the *Exploring-Simulation* window. The parallel bars labeled “*Flowsheet*” are clicked and the *Constraint-Flowsheet* window shown in Figure 8.28b opens. The two required equations are entered using

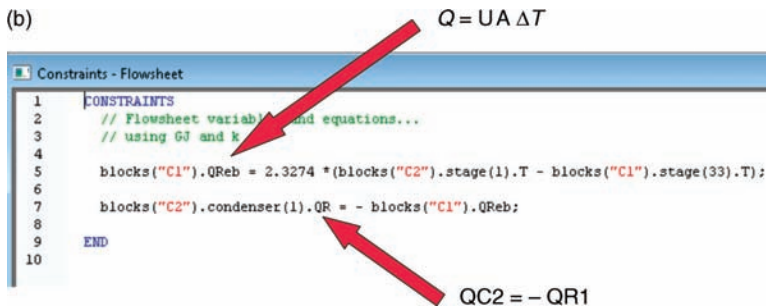
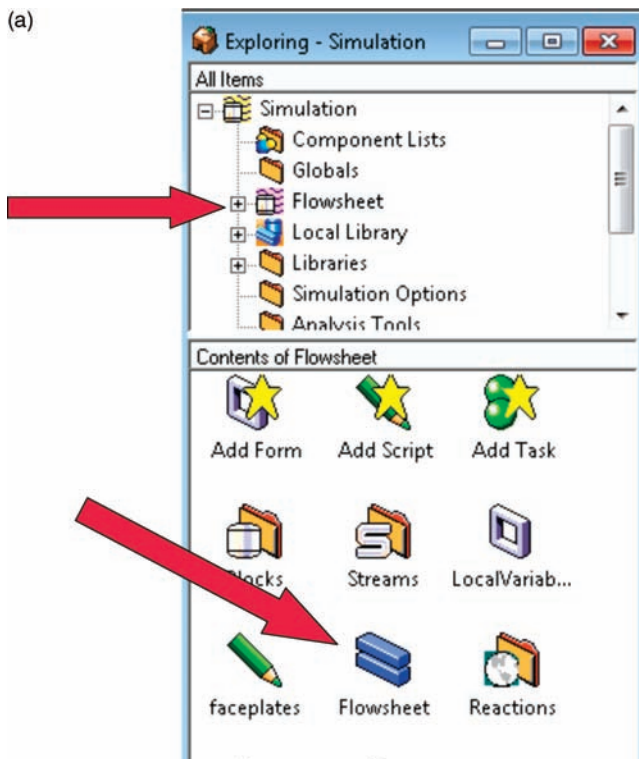


Figure 8.28 (a) Flowsheet equations. (b) Flowsheet equations.

precisely the proper Aspen Dynamics syntax.

```
blocks("C1").QReb =
2.3274*(blocks("C2").stage(1).T-blocks("C1").stage(33).T);
blocks("C2").condenser.QR = blocks("C1").QReb;
```

Remember to end each equation with a semicolon.

It is important to remember that Aspen Dynamics uses metric units (heat duties in GJ/h and temperatures in °C), despite the fact that English engineering units are being

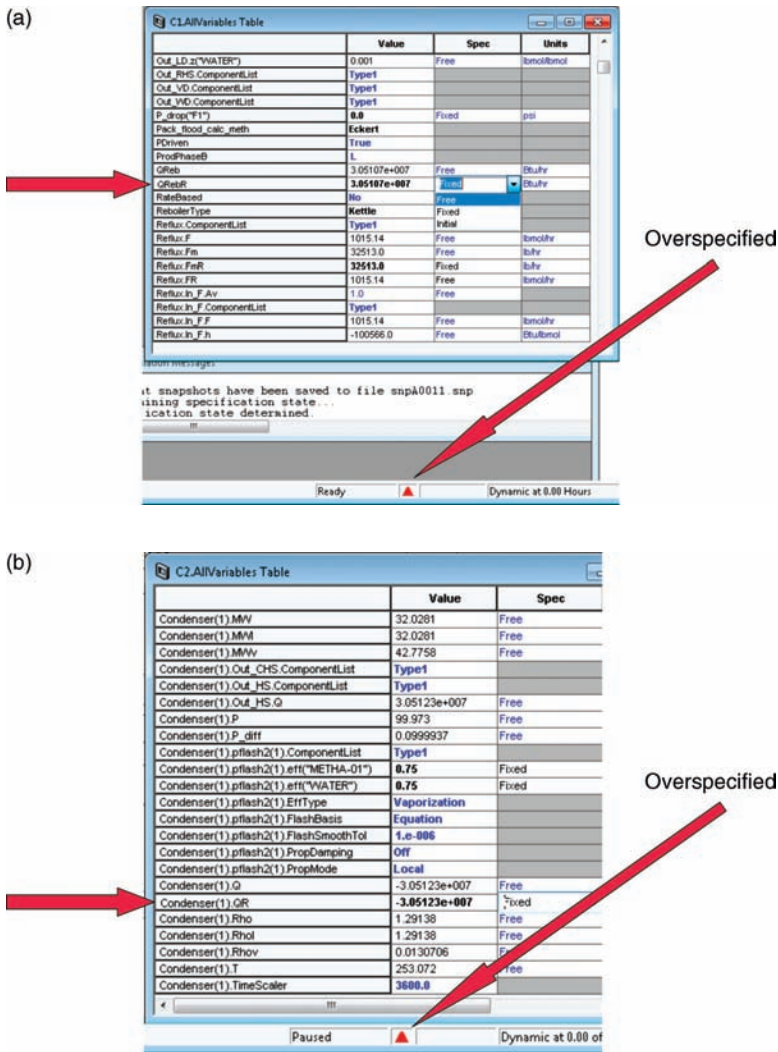


Figure 8.29 (a) Making QRebR in LP column “free.” (b) Making condenser (1)QR in HP column “free.”

used in this example. The constant “2.3274” in the first equation is the value of UA expressed in GJ/(h K), which is calculated from 32.196 GJ/h (30.51×10^6 Btu/h) and 13.83 °C (24.9 °F).

Right click the window and select *Compile* to implement these relationships. At this point, a red button appears at the bottom of the screen, as shown in Figure 8.29a, and the simulation will not run. Clicking this button gives a message that the simulation is overspecified (too many “fixed” variables). We must change the low-pressure reboiler duty (QRebR in the column C1 block) and the high-pressure condenser duty (Condenser(1).QR

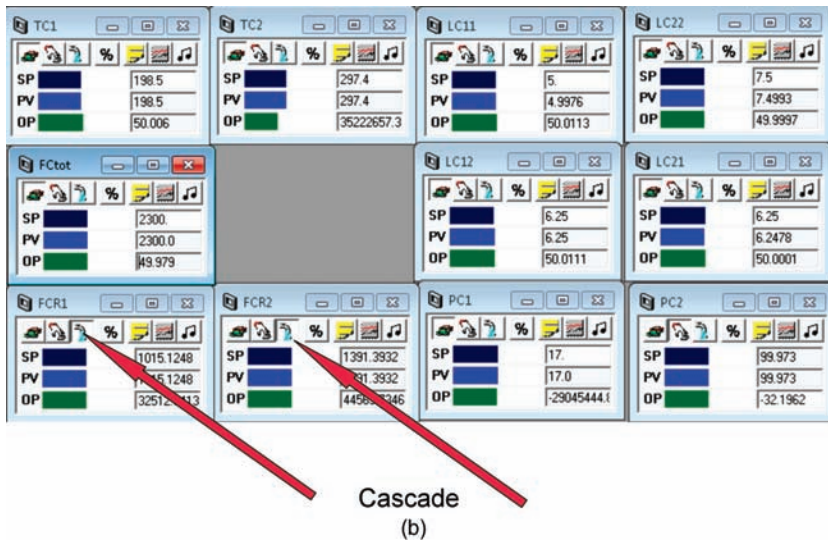
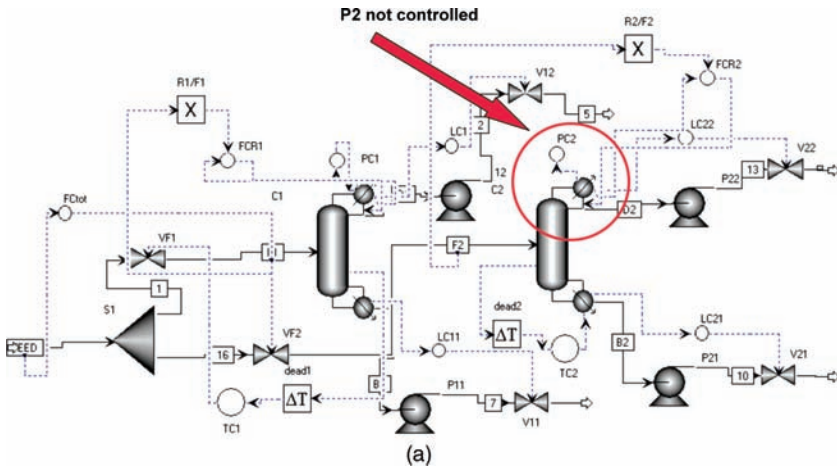


Figure 8.30 (a) Control structure. (b) Controller faceplates.

in the column C2 block) from “Fixed” to “Free” as shown in Figure 8.29a and b. Now, the red button turns green and the dynamic simulation will run.

8.3.3 Control Structure

Figure 8.30 shows the initial control structure developed for the two-column process. The loops are listed below. Note that the pressure in the high-pressure column is *not* controlled.

1. Total feed is controlled by manipulating the valve in the feed line to the high-pressure column.

2. The temperature on Stage 60 in the high-pressure column is controlled by manipulating reboiler duty in the high-pressure column.
3. The temperature on Stage 30 in the low-pressure column is controlled by manipulating the valve in the feed line to the low-pressure column.
4. Molar reflux-to-feed ratios are implemented on both columns. Note the molar reflux flow controllers on cascade with set points coming from multipliers ($R1/F1 = 0.8834$ in the low-pressure column and $R2/F2 = 1.209$ in the high-pressure column).
5. Pressure in the low-pressure column is controlled by condenser heat removal.
6. Reflux-drum levels are controlled by manipulating distillate flow rates.
7. Base levels are controlled by manipulating bottoms flow rates.

Clearly, the key control loops are the two temperature controllers. Temperature control by manipulating reboiler duty in the high-pressure column is conventional. Relay-feedback testing and Tyreus–Luyben tuning give $K_C = 0.157$ and $\tau_I = 10.6$ min for a temperature transmitter range of 250–350 °F and an output maximum of 94.8×10^6 Btu/h. The TC2 controller is reverse acting.

In the low-pressure column, a direct acting temperature controller is used to manipulate feed to the column. Clearly, the two temperature controllers are interacting because vapor flow rates affect both columns, as do changes in feed flow rates. The tuning strategy used was to tune the TC2 controller in the high-pressure column first with the TC1 controller in the low-pressure column on manual (fixed feed flow rates to each column). Then the TC1 controller was tuned with the TC2 controller on automatic.

Relay-feedback testing and Tyreus–Luyben tuning TC1 give $K_C = 0.0917$ and $\tau_I = 54.1$ min for a temperature transmitter range of 150–250 °F and an output range of 0–100% valve opening. Deadtimes of 1 min are inserted in both temperature controllers to account for temperature measurement lags. Figure 8.30b shows the controller faceplates.

The heat-integrated process provides an excellent example of the power and usefulness of dynamic simulation of distillation column systems. Alternative control structures can be easily and quickly evaluated.

8.3.4 Dynamic Performance

The process is subjected to step changes in the set point of the total feed flow controller at time equal 0.5 h. Figure 8.31 gives results of a fairly small 5% increase. The solid lines are for the low-pressure column variables, and the dashed lines are for the high-pressure column variables.

There is an immediate large change in the feed $F2$ to the high-pressure column, which results in a sharp drop in the purity of the bottoms of this column (lowest left graph in Figure 8.31). The large transient deviation is clearly undesirable and is a result of the large increase in feed to the high-pressure column. The feed to the low-pressure column eventually also increases but only after the temperature controller detects the increase in Stage 30 temperature due to the increase in the vapor boilup in both columns caused by the temperature controller in the high-pressure column seeing a drop in temperature.

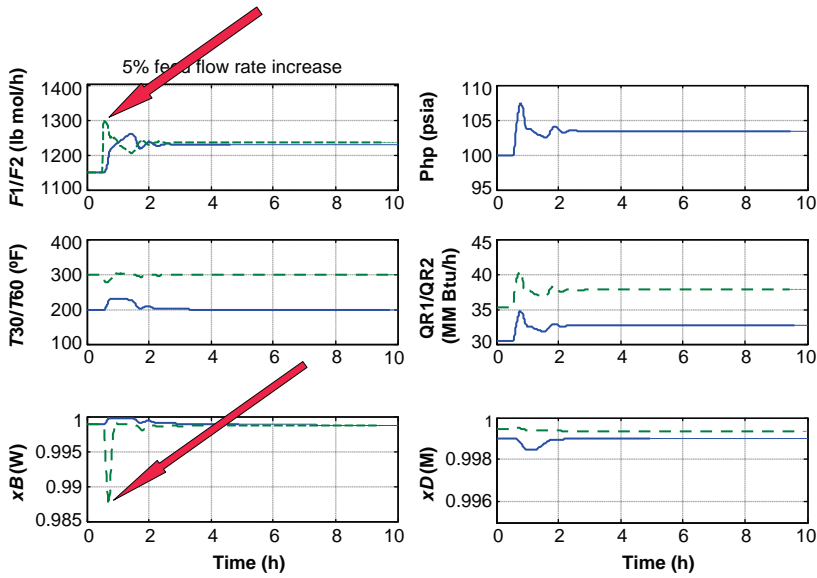


Figure 8.31 Five percent increase in feed.

The transient response can be improved by distributing the load disturbance between the two feed streams. Figure 8.32 shows one method for implementing such a structure. A flow controller FCF1 is installed on the feed to the low-pressure column and put on cascade with a set point signal coming from a multiplier with two inputs. The first is the flow rate $F2$ of the feed to the high-pressure column. The second input is the desired ratio of $F1$ to $F2$. This ratio is changed by the temperature controller TC1 in the low-pressure column. Thus, both feed are changed initially in unison.

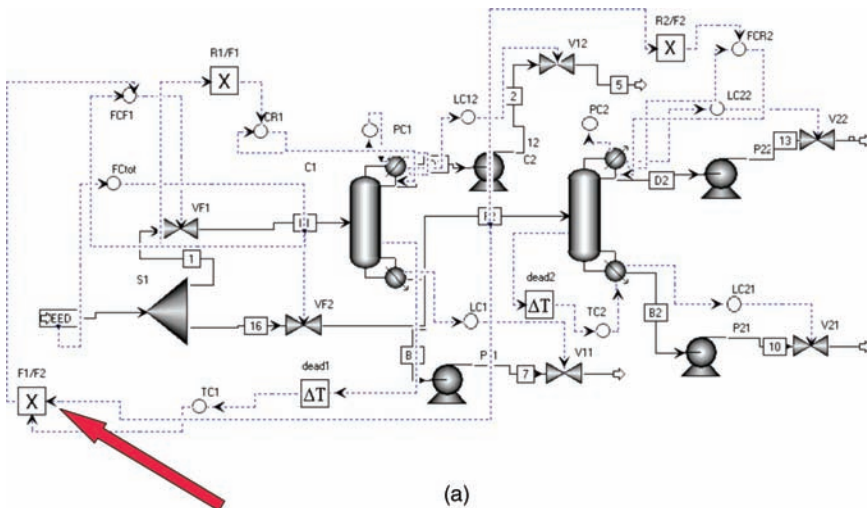


Figure 8.32 (a) Control structure with $F1/F2$ ratio. (b) Controller faceplates.

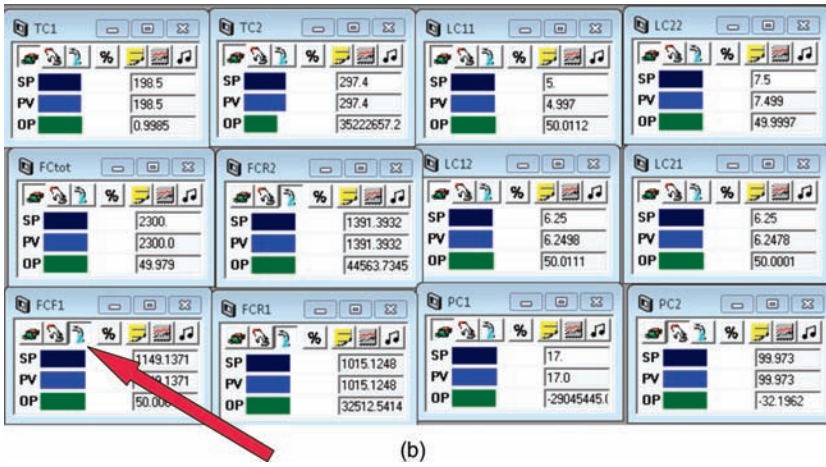


Figure 8.32 (Continued)

Retuning of the TC1 controller is required, yielding $K_C = 0.118$ and $\tau_I = 51.5$ min. Figure 8.33 shows that the transient deviations in bottoms purity are greatly reduced. Of course, if a larger disturbance is made (10% in Fig. 8.34) the transient deviation increases.

Figure 8.35 illustrates that feed-composition disturbances are also well handled. The methanol composition in the feed is increased from 80 to 85 mol%, with a corresponding reduction in water composition. The compositions of all four product streams remain very close to their specifications.

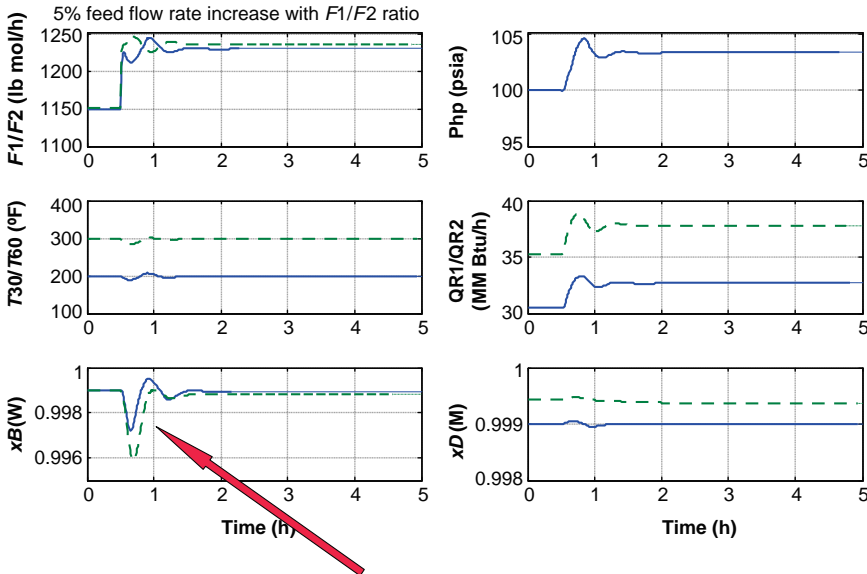


Figure 8.33 Five percent increase in feed with $F1/F2$ ratio.

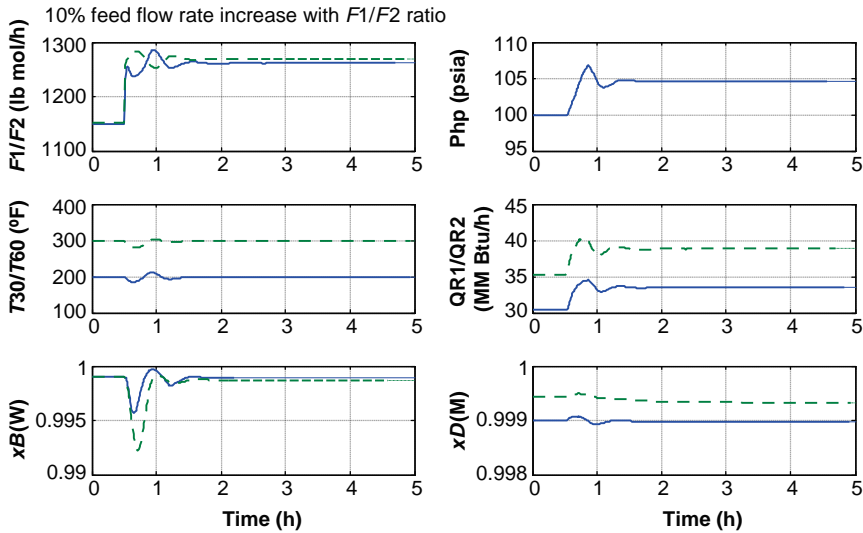


Figure 8.34 Ten percent increase in feed with $F1/F2$ ratio.

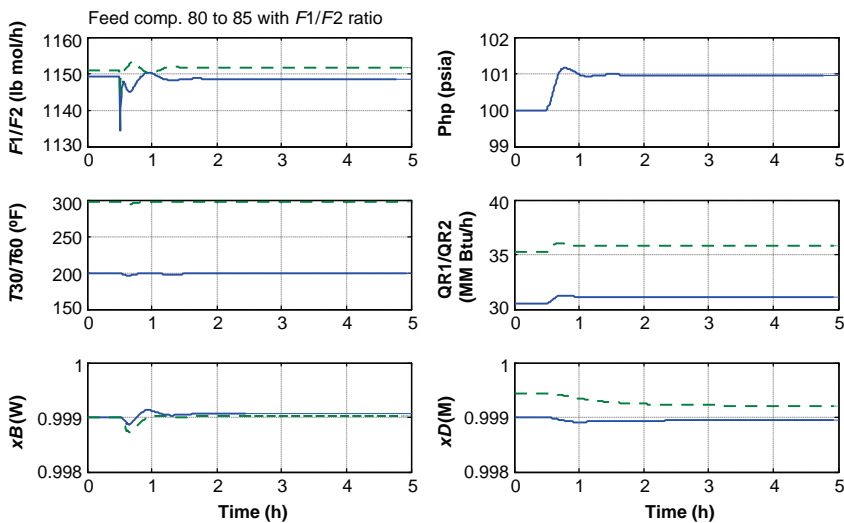


Figure 8.35 Feed composition 80–85 mol% methanol.

8.4 CONTROL OF AZEOTROPIC COLUMNS/DECANTER SYSTEM

In Chapter 5, the steady-state design of a heterogeneous azeotropic distillation process for the dehydration of ethanol using benzene as a light entrainer was studied. The process consisted of two distillation columns, one decanter and two recycle streams. One of the recycle streams was successfully closed, but the second would not converge using steady-state Aspen Plus.

In this section, we demonstrate how this second recycle loop can be successfully converged in Aspen Dynamics. A plantwide control structure is developed and its

effectiveness evaluated. A counter-intuitive reverse-acting aqueous/organic interface-level control loop is shown to be required for stable operation when the “Decanter” model is used. However, when the “Flash3” model is used, a conventional direct-acting aqueous level controller works as we would expect.

8.4.1 Converting to Dynamics and Closing Recycle Loop

The usual base and reflux drum-sizing procedure gives column base diameters of 1.76 and 0.855 m, respectively, in columns C1 and C2. Assuming an aspect ratio (L/D) of 2 gives the lengths. There is no reflux drum in the first column. The decanter is sized to provide 20 min of holdup based on the total liquid entering in the two liquid phases (aqueous and organic). The resulting decanter has a diameter of 2 m and a length of 4 m. Horizontal orientation is specified to aid in the phase separation. Figure 8.36a shows the Aspen Plus flowsheet with

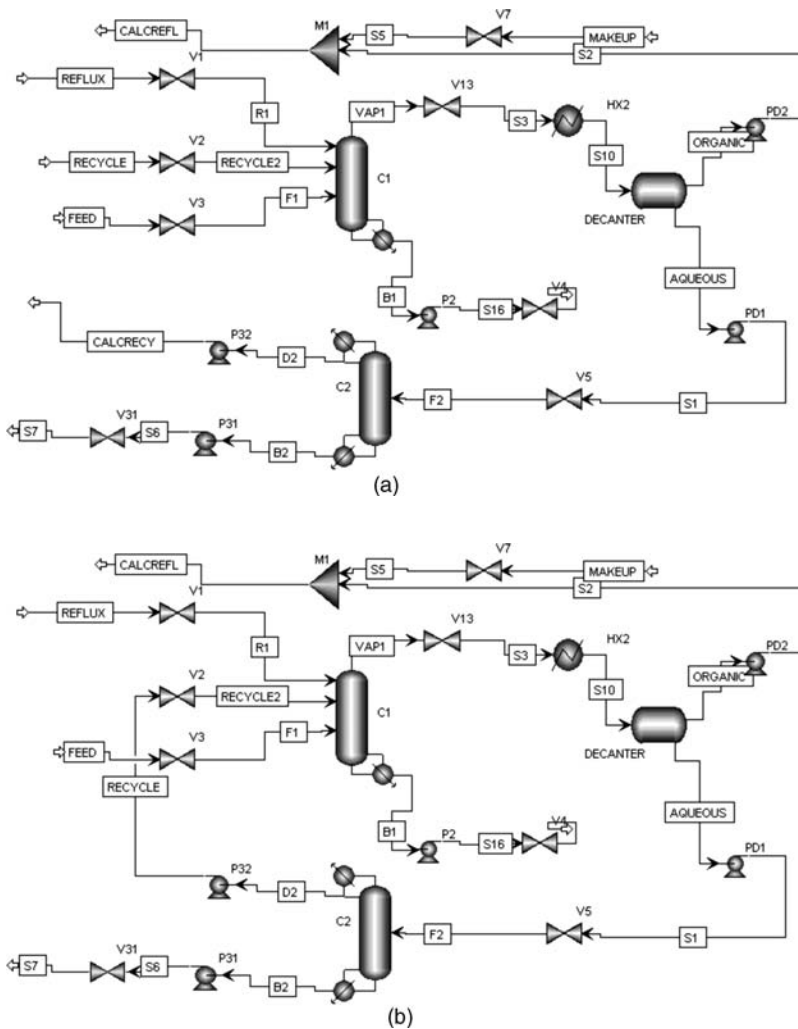


Figure 8.36 (a) Aspen Plus PFD with recycle loop open. (b) Aspen Plus PFD with recycle loop closed.

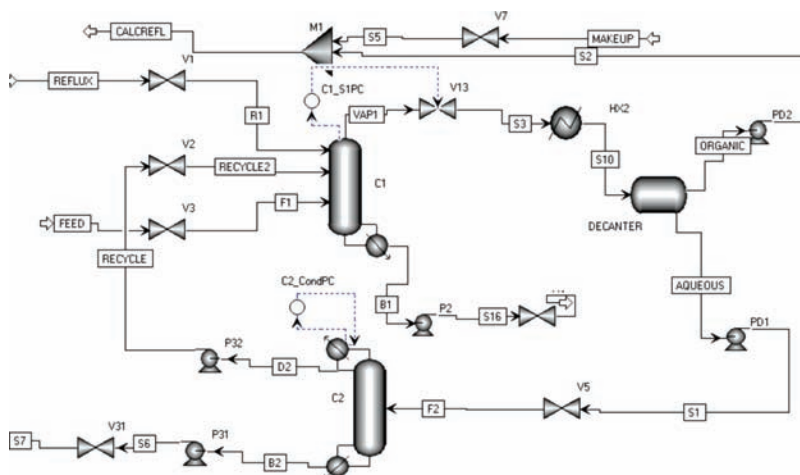


Figure 8.37 Initial flowsheet in Aspen Dynamics.

both recycle open (“torn”). Figure 8.36b shows the flowsheet with the recycle of distillate *D2* from column *C2* connected to column *C1*.

With the equipment sized and the flowsheet pressure checked, it is exported into Aspen Dynamics. Figure 8.37 shows the initial flowsheet that opens in Aspen Dynamics. Pressure controllers are already installed on each column. In column *C1*, pressure is held by manipulating the position of valve *V13* in the overhead vapor line upstream of the condenser. Note that the Reflux recycle loop is not closed.

Now, we are ready to close the organic reflux loop. The stream “CALCREFL” is deleted from the flowsheet. The “REFLUX” stream is selected and right clicked. Selecting *Reconnect Source*, this stream is attached to the mixer “M1.” The little red light appears at the bottom of the window, as shown in Figure 8.38a. Placing the cursor on the button opens a message that the simulation is overspecified by two variables. We must change the temperature and the pressure of the reflux stream from *Fixed* to *Free*. The green light appears at the bottom, indicating the simulation is now “square” (as many variables as equations, i.e. zero degrees of freedom). An *Initialization* run and a *Dynamics* run are made to check that the integrator is working okay with both recycle streams connected.

After all the controllers have been added, the simulation is run out in time until there are no changes in all variables. The final converged flowsheet variables are shown in Figure 8.38b.

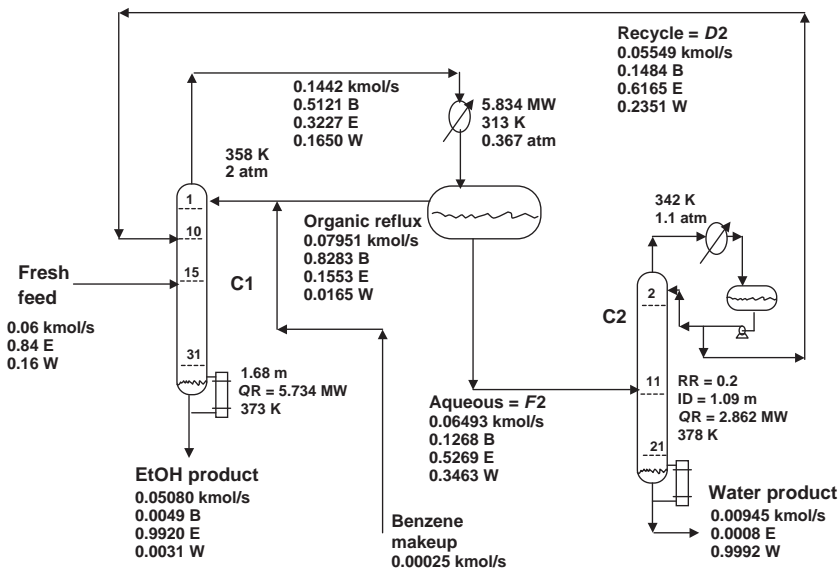
8.4.2 Installing the Control Structure

The controllers are now added in the usual way. Base levels are held by bottoms flow rates. Reflux drum level in column *C2* is held by the distillate flow rate (the RECYCLE stream back to column *C1*).

Temperatures. The most important loop is temperature control in column *C1*. Figure 8.39a shows that Stage 28 in the stripping section is the only location with a significant break. In the first edition of this book, the control structure used had this temperature controlled by manipulating organic reflux. However, the liquid hydraulic lags

	Value	Spec
Out_P.hrev	5.e+007	Free
Out_P.P	506625.0	Free
Out_P.Slip	1.0	Free
Out_P.T	313.0	Free
Out_P.Trev	298.15	Free
Out_P.V	0.05	Free
Out_P.z("BENZE-01")	0.82	Free
Out_P.z("ETHAN-01")	0.16	Free
Out_P.z("WATER")	0.02	Free
Out_P.Zrev("BENZE-01")	0.333333	Free
Out_P.Zrev("ETHAN-01")	0.333333	Free
Out_P.Zrev("WATER")	0.333333	Free
P	506625.0	Fixed
PassThrough	Normal	
PDriven	True	
Rho	11.8802	Free
Rhom	1000.0	Free
SComps	{}	
SensorActive	No	
SolidsPresent	No	
Solvent		
StreamClass	CONVEN	
T	313.0	Fixed
TearStream	False	

(a)



(b)

Figure 8.38 (a) Change P and T of REFLUX from “Fixed” to “Free.” (b) Steady state from Dynamic simulation.

result in slow temperature control (the temperature controller integral time with this pairing is 44 min). Here we use a more effective structure in which Stage 28 temperature is controlled by manipulating reboiler duty QR1 in the first column. Tuning of this loop gives a much smaller integral time (9.2 min) and therefore better load disturbance rejection.

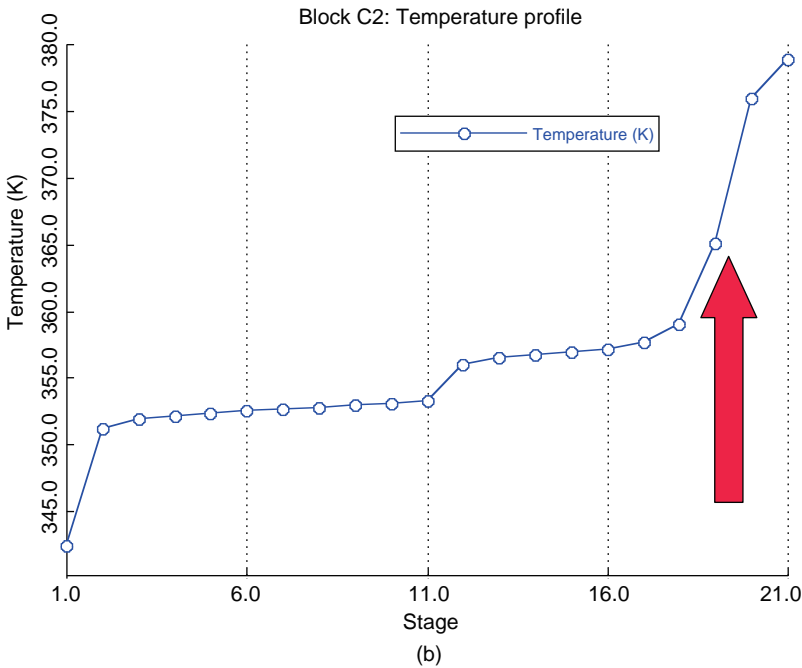
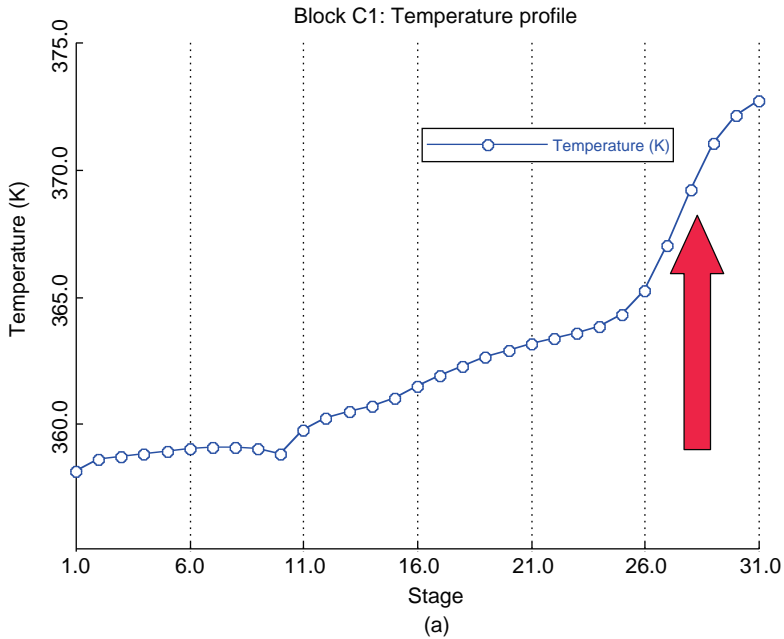


Figure 8.39 (a) C1 temperature profile. (b) C2 temperature profile.

The tray with the sharpest temperature change in column C2 is Stage 19 (365.1 K at steady state) as shown in Figure 8.39b. The temperature controller TC2 manipulates reboiler heat input. A third temperature controller is added on the heat exchanger before the decanter to control the temperature of the stream entering the decanter at 313 K.

Deadtimes of 1 min are included in both column temperature controllers, and relay-feedback tests are run to find the controller settings. In TC1, they are $K_C=0.98$ and $\tau_1=9.2$ min (using a temperature range of 300–400 K and an output range of 0–27.8 MW). In TC2, the controller settings are $K_C=0.84$ and $\tau_1=10.6$ min (using a temperature range of 300–400 K and an output range of 0–9.26 MW).

Organic Reflux. Another very important variable is the flow rate of organic reflux to the top of column C1. If there is too little benzene, water will drop out to the bottom. If there is too much benzene in the column, benzene will drop out to the bottom. The amount of benzene required depends on the feed flow rate and also on the flow rate of recycle from column C2 back to column C1. The control structure selected adds these two flow rates and sends this signal to a multiplier whose other input is the ratio of organic reflux flow rate at design to the sum of the design feed and recycle flow rates (molar flow rates are used in this example). The output of the multiplier adjusts the set point of a flow controller on the organic reflux. The entire control structure is shown in Figure 8.40a.

Decanter Levels. The control of the two liquid inventories in the decanter is critical. Because only a very small amount of benzene is lost, the organic level basically floats up and down as changes occur in the reflux flow rate. An organic phase-level controller adjusts the benzene make-up stream, but it is so small that the level changes are significant. This does not hurt anything as long as the decanter does not overflow or the organic level is lost.

The control of the aqueous level would appear to be straight forward. A level controller would manipulate the valve “V5.” Conventional logic says that this controller should be *Direct* acting. If the level goes up, the flow rate of the aqueous stream should be increased and more fed to column C2. Very surprisingly, this set-up was found to *not* work. The

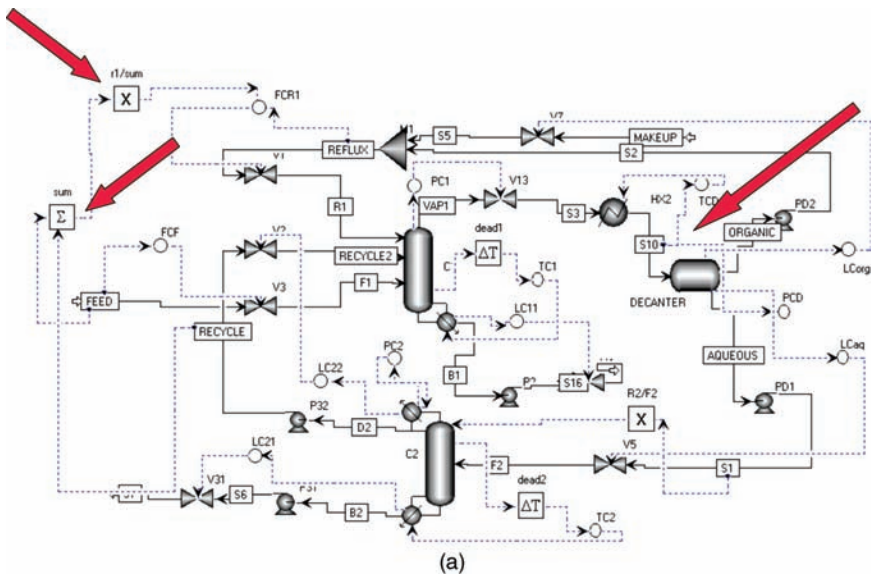


Figure 8.40 (a) Control structure with decanter model. (b) Control structure with Flash3 model. (c) Controller faceplates with Flash3 model.

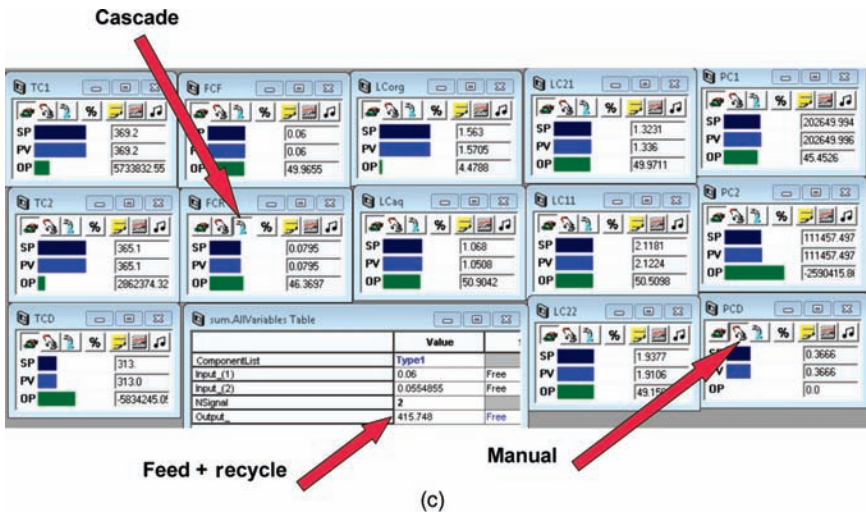
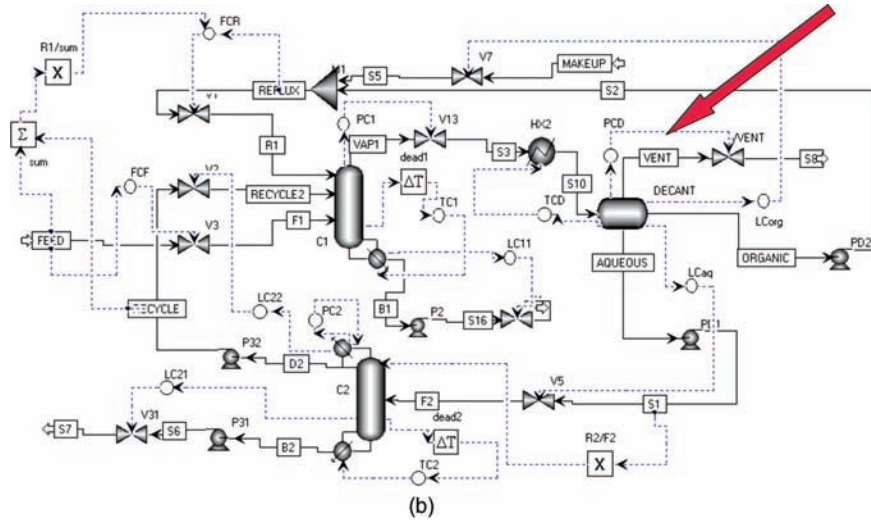


Figure 8.40 (Continued)

system shut down. However, making the controller *Reverse* acting produce a stable control structure. We demonstrate this in the next section.

Decanter Models in Aspen. Up to this point, we have been using the “Decanter” model in the simulations. It assumes that there are only two phases, both liquid, and that the decanter pressure is fixed at the specified design value (pressure does not change with temperature or composition). These assumptions do not reflect reality but appear to suffice for steady-state design. In a real decanter, there is a vapor space above the two liquid phases, and pressure will vary with compositions and temperatures unless an inert gas is used to keep a constant pressure *via* a vent-bleed split-ranged valve setup.

Aspen has another model that is more realistic, the *Flash3* model under *Separators*. This model has two liquid outlet streams and a vapor outlet stream.

An alternative simulation was developed using the *Flash3* model, as shown in Figure 8.40b after exporting and installing a control structure. In Aspen Plus, a vapor line with a valve is added. The decanter is specified to be adiabatic and at a fixed pressure (0.6 atm). The temperature specified in the upstream condenser “HX2” is adjusted to 320 K to give a very small vapor flow rate (3% of the feed). After the file is exported, a pressure controller is inserted on the decanter, but it is put on manual and the vapor valve is closed. Now decanter pressure varies with temperature and composition. Its steady-state value is 0.366 atm with the decanter temperature controller set point at 313 K so that a direct comparison with the previous case can be studied.

Figure 8.40c shows the controller faceplate with the *Flash3* model. Note that the flow rates used in the summer are molar, and the organic reflux flow controller is on cascade.

8.4.3 Performance

The first thing to show is that a *direct-acting* aqueous level controller does not work when the simple *Decanter* model is used. Figure 8.41a shows what happens when feed flow rate is increased to 5% at time equal to 0.5 h.

The bottom right plot shows the instantaneous increase in the flow rate of the organic reflux because it is ratioed to the sum of the feed and the recycle streams. The aqueous level goes down, and the direct-acting controller decreases the aqueous flow rate. The reduced feed to column C2 reduces its distillate flow rate *D2*, which is the recycle stream to column C1. This reduces the organic reflux flow rate even more through the action of the summer. Eventually, in about 3.5 h, the organic level exceeds the high limit and the simulation shuts down (liquid is vented from the decanter).

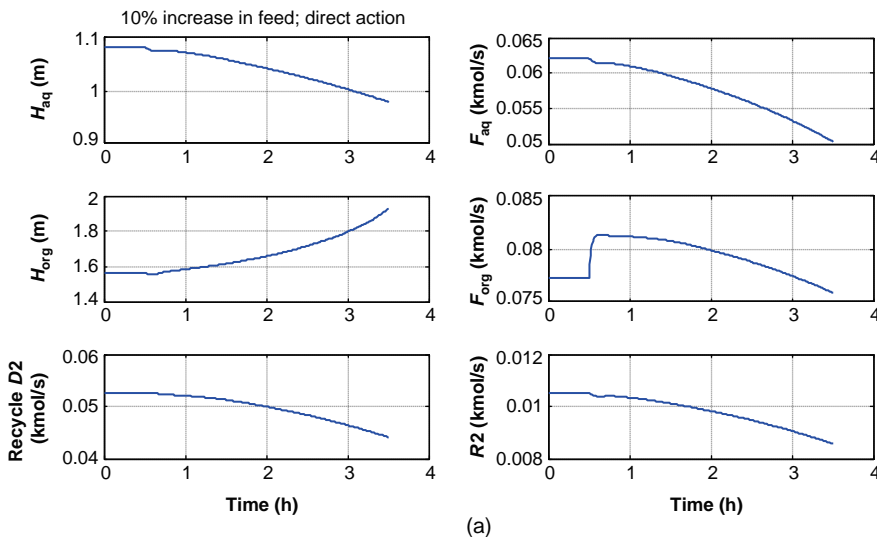


Figure 8.41 (a) Direct-acting aqueous-level controller: 10% increase in feed flow rate. (b) Reverse-acting aqueous-level controller: 10% increase in feed flow rate. (c) *Flash3* model: direct-acting aqueous-level controller: 10% increase in feed flow rate.

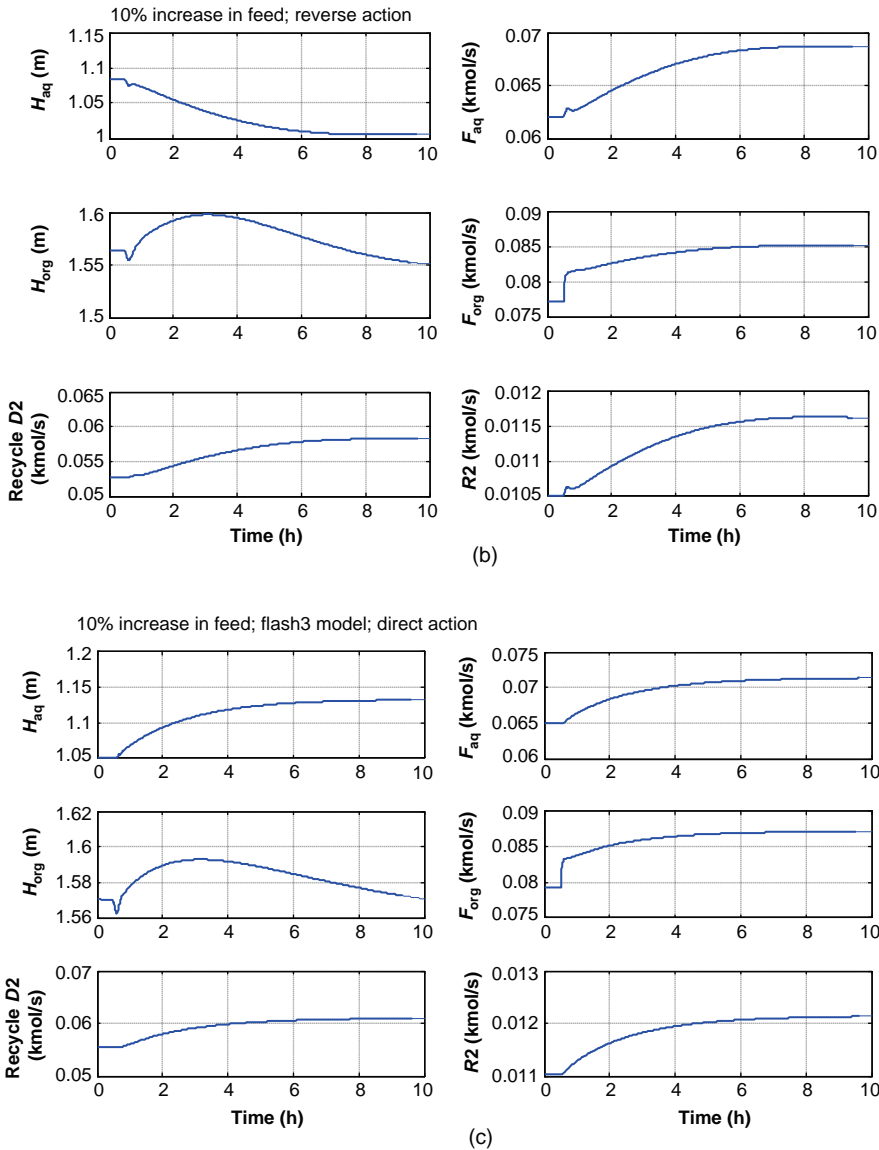


Figure 8.41 (Continued)

Figure 8.41b gives results when the aqueous level controller is switched to *reverse* action. As the aqueous level drops, the flow rate of the aqueous stream increases. The larger feed to column C2 results in an increase in the rate of the recycle, which increases the organic reflux even more (F_{org} in the middle right graph in Fig. 8.41b). Thus, the organic level does not continue to climb. It increases for a while but drops down to a steady-state level.

Figure 8.41c gives results when the *Flash3* decanter model is used with a *direct-acting* aqueous-level controller. A comparison of the upper left graphs in Figure 8.41b (*Decanter*

model) and Figure 8.41c (*Flash3* model) reveal the basic difference between these two models. The 10% increase in feed to the process causes the aqueous level to go down in the former case, while in the latter case, it increases, which makes sense physically. Why the *Decanter* model behaves in this way is unclear. Other workers have not reported this problem. Chien et al.² apparently did not see this problem in the isopropanol/water/cyclohexane heterogeneous azeotropic distillation process.

Figure 8.42 shows the responses of the system with the *Flash3* decanter using a direct-acting aqueous-level controller. Figure 8.42a is for positive and negative 20% step changes

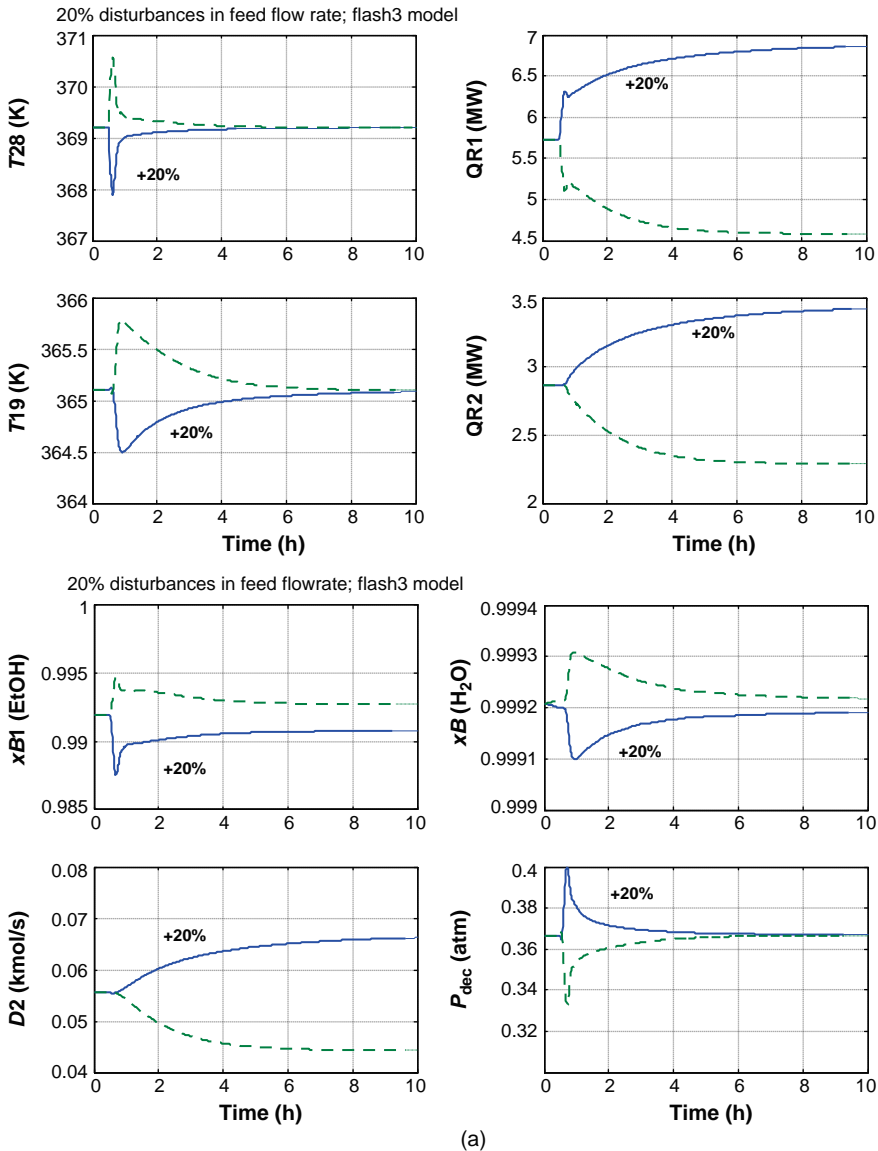


Figure 8.42 (a) 20% feed flow rate disturbances. (b) Feed-composition disturbances.

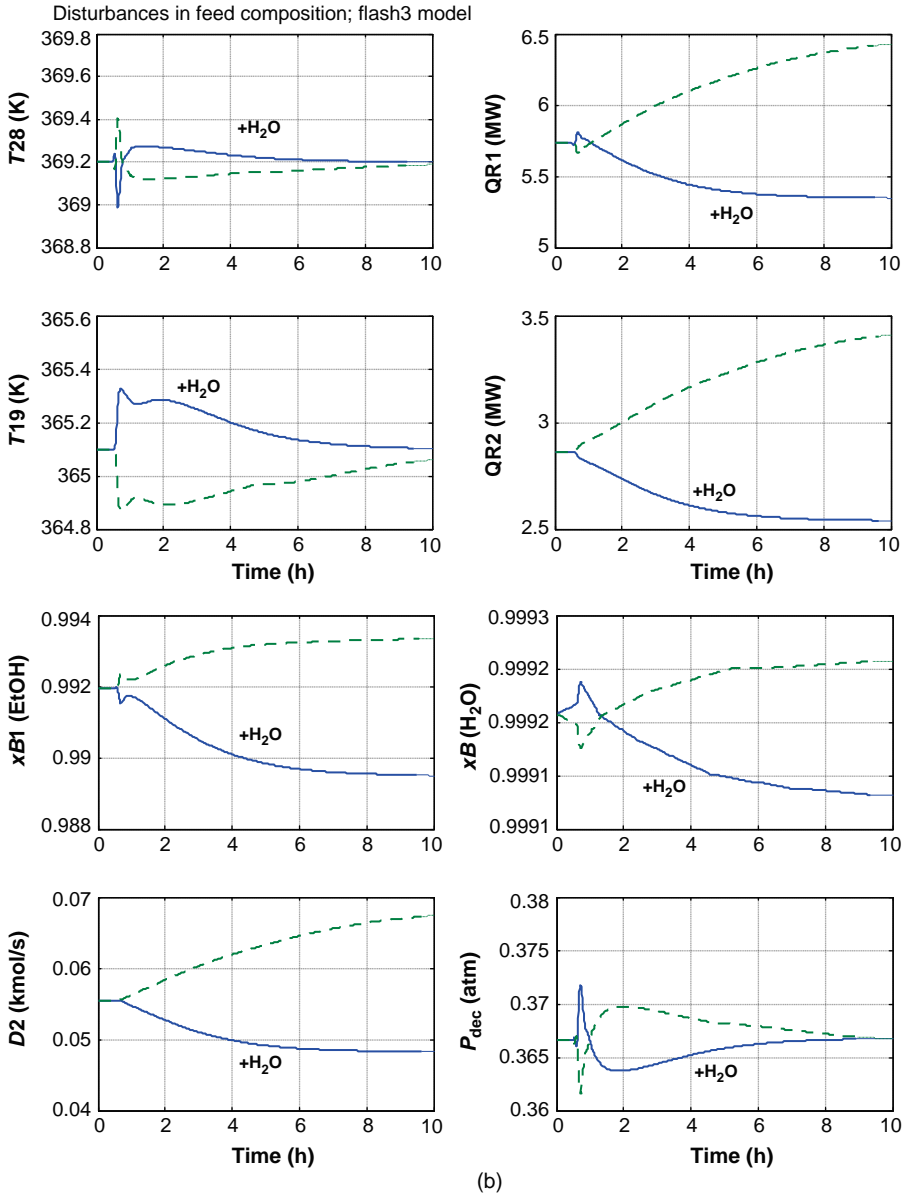


Figure 8.42 (Continued)

in the set point of the feed flow controller. Stable regulatory control of the highly nonideal distillation system is achieved. Both the ethanol and the water products are kept close to their desired purity levels.

Figure 8.42b gives responses to changes in feed composition from 16 to 20 mol% water, and from 16 to 12 mol% water, with the corresponding changes in ethanol. Both the ethanol and the water products are kept close to their desired purity levels. More water

in the feed requires less reboiler heat input to both reboilers because the recycle flow rate $D2$ is smaller.

8.4.4 Numerical Integration Issues

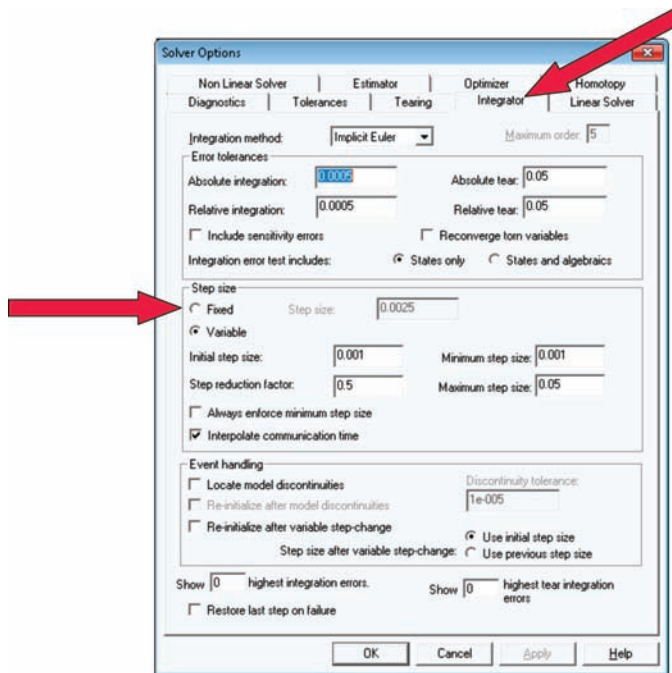
During the development of several simulation studies using the current Aspen Version 7.3, a strange low-amplitude oscillation has been experienced, which is not affected by controller tuning. The solution to the problem was found to be a modification in the integrator.

The default numerical integration algorithm uses a variable step size. Switching to a fixed step size eliminated the oscillation problem. To achieve this, go to *Run* on the upper toolbar in Aspen Dynamics, select *Solver Options* and click the *Integrator* page tab. The window shown in Figure 8.43a opens on which the step size can be changed to *Fixed*.

The problem is illustrated in Figure 8.43b where the temperature on Stage 28 in Column C1 is plotted. The step size is specified to be *Fixed*, and a 10% increase in feed flow rate is made at time equal to 0.5 h. At time equal to 2 h, the simulation is paused and the step size is changed to *Variable*. An oscillation occurs until the step size is changed back to *Fixed* at time equal to 7 h.

Aspen users should be aware of this problem.

The heterogeneous azeotropic distillation process provides an excellent example of the utility of distillation simulation to both design and control of a very complex nonideal system.



(a)

Figure 8.43 (a) Setting integrator step size. (b) Effect of integrator step.

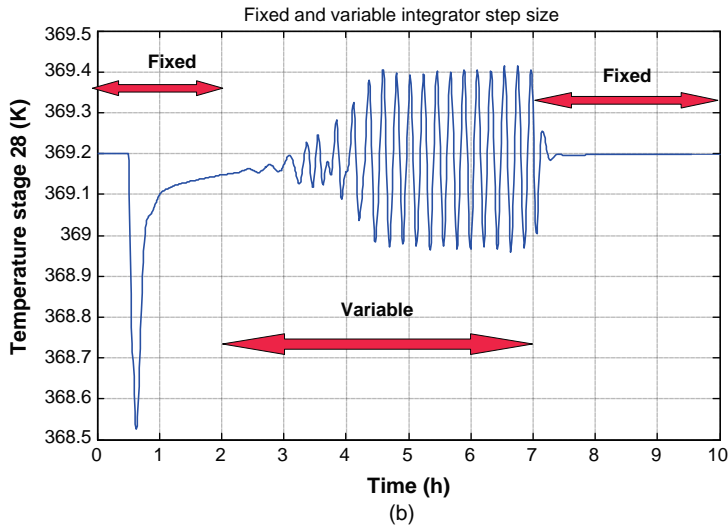


Figure 8.43 (Continued)

8.5 UNUSUAL CONTROL STRUCTURE

In the last three chapters, we have developed a number of conventional control structures: dual-composition, single-end with RR, single-end with reflux-to-feed, tray temperature control, and so on. Structures with steam-to-feed ratios have also been demonstrated to reduce transient disturbances. Four out of the six control degrees of freedom (six available valves) are used to control the four variables of throughput, pressure, reflux-drum level, and base level. Throughput is normally controlled by the feed valve. In “on-demand” control structures, throughput is set by the flow rate of one of the product streams. Pressure is typically controlled by condenser heat removal. Base liquid level is normally controlled by bottoms flow rate.

The structure of the reflux-drum level loop depends on the reflux ratio. Distillation wisdom recommends that reflux-drum level should be controlled by manipulating reflux flow rate in high RR columns ($RR > 3$). So reflux-drum level is sometimes controlled by manipulating distillate flow rate and sometimes controlled by manipulating reflux flow rate. In the latter structure, the flow rate of the distillate must be varied in some way. It cannot be fixed because this violates the first law of distillation control.

The flow rate of a product stream cannot be fixed and still control a composition (or temperature) in the column because the overall material balance has a dominant effect on compositions.

Only in a purge column (a very small stream is removed to get rid of an inert component) can a product stream be fixed (or ratioed to feed flow rate). The distillate stream can be manipulated to control a composition (or temperature), or it could be manipulated to maintain a RR. In this structure, the reflux flow rate is measured, the flow signal is sent to a multiplier, and the output signal of the multiplier is the set point of a distillate flow controller.

The other two control degrees of freedoms are typically reboiler duty and reflux flow rate (or distillate flow rate in high RR columns). Reboiler heat input is an effective

manipulated variable because changes in vapor flow rates occur quickly in all sections of the column. So reboiler duty can be used to control a temperature (or composition) on any tray in the column.

Reflux, on the other hand, can only be used to control a temperature in the upper section of the column. The hydraulic lags of liquid flowing down the column from tray-to-tray are typically 3–6 s per tray. Thus, attempting to control a temperature 40 trays down in the column will introduce a 2–4 min lag in the loop, which will adversely affect load rejection performance.

There are a host of conventional control structures, and the best choice depends on a number of factors, some of which we have already discussed: the shape of the temperature profile and the sensitivity of the several flow ratios to feed composition. Economics obviously have an impact, mostly in terms of energy consumption versus control structure complexity. The control structure that minimizes energy is dual-composition control. But it is more complex than a simple single-end control structure. Therefore, we must evaluate how much money is lost by using a more simple structure. In areas of the world where energy is inexpensive, both the optimum design and the appropriate control structure are different than in areas with expensive energy.

Some of the most used control structures are as follows:

1. Control two compositions (impurity of heavy-key component in the distillate and impurity of light-key component in the bottoms).
2. Control two tray temperatures (requires two breaks in the temperature profile).
3. Control one tray temperature and one composition (if there is only one break in the temperature profile).
4. Control one temperature and fix the reflux-to-feed ratio.
5. Control one temperature and fix the RR.

Complications arise when the column has a large RR and, at the same time, the feed-composition sensitivity analysis suggests the use of a reflux-to-feed ratio. Distillation control wisdom suggests that reflux flow rate should be used to control reflux-drum level, but this is in conflict with the desire to use the R/F structure. In this section, we suggest a control structure that handles this situation.

8.5.1 Process Studied

A specific numerical example is used as representing a typical situation. High RR columns are frequently encountered in distillation column systems. Difficult separations (low relative volatilities) require many trays and high reflux ratios. Another common situation is when there is a small amount of the light key component entering in the feed. The distillate flow rate will be small, resulting in a high RR. Removal of small amounts of impurities is often achieved using distillation, and all these columns exhibit high RR.

The distillation column studied is based on a system that presents challenging design problems because of the severe nonlinearity of the phase equilibrium. The ternary system is water, acetic acid, and formic acid. The physical property package UNIQ-HOC is used in the Aspen simulations, which accounts for the dimerization of acetic acid in the vapor phase.

As shown in Figure 8.44, the predicted ternary phase equilibria at 1 atm show three homogeneous azeotropes. Two are binary (water/formic acid and water/acetic acid) and

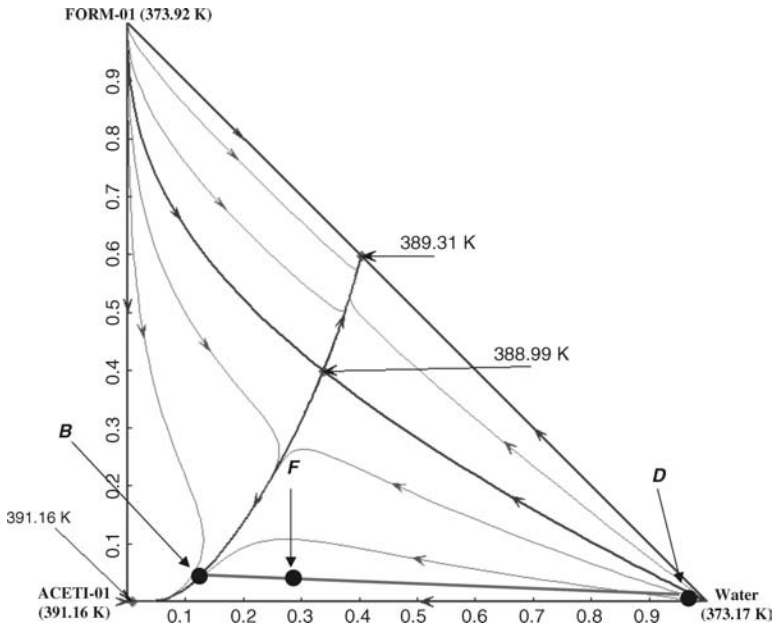


Figure 8.44 Ternary diagram.

one is ternary. Note that water and formic acid have almost identical normal boiling points (373 and 374 K, respectively) and form a maximum-boiling azeotrope at 389 K, as shown in the T_{xy} diagram in Figure 8.45a. The other binary T_{xy} diagrams are given in Figure 8.45b and c. The prediction of a water/acetic acid azeotrope is suspect because

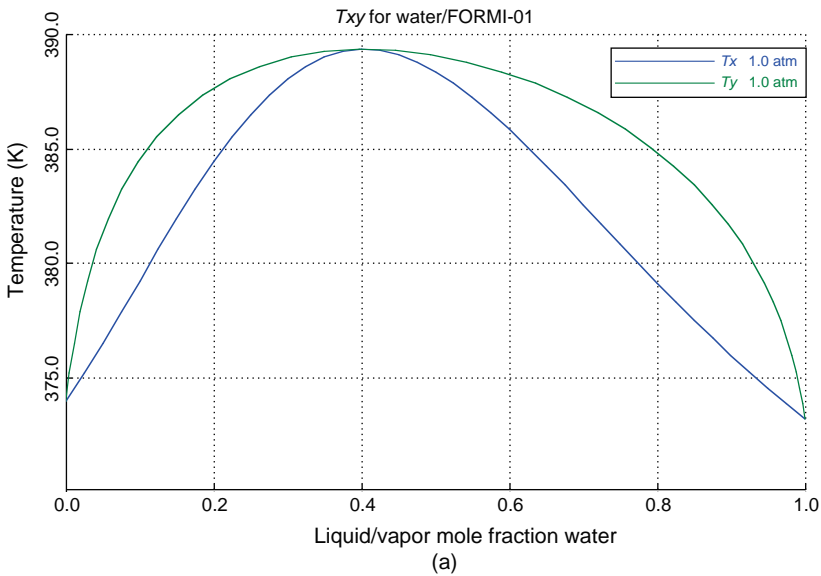


Figure 8.45 (a) Water/formic acid T_{xy} diagram. (b) Water/acetic acid T_{xy} diagram. (c) Acetic acid/formic acid T_{xy} diagram.

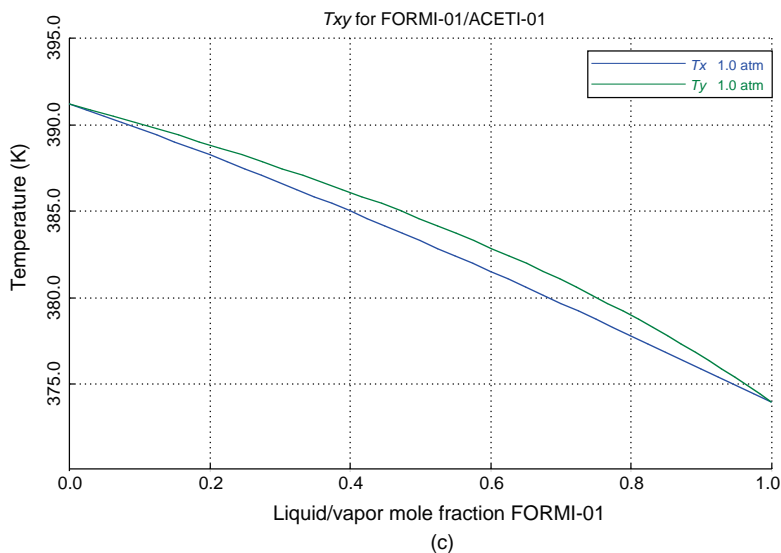
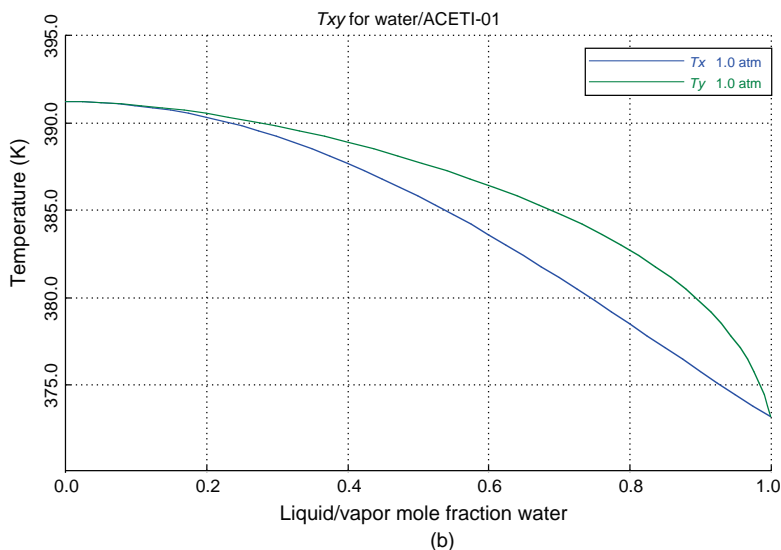


Figure 8.45 (Continued)

this system is known to only produce a tight pinch at high acetic-acid concentrations. However, this inaccuracy should not affect the results of the simulation because the column operates at high water concentrations.

The ternary diagram shows four regions separated by distillation boundaries (dark lines). The locations of the feed, distillate, and bottoms points used in the example are indicated in Figure 8.44. They all lie in the lower region of the diagram. The objective is to produce high-purity water in the distillate (99.5 mol% water). The feed composition is 28.63 mol% water, 5.37 mol% formic acid, and 66.00 mol% acetic acid. A feed flow rate of 100 kmol/h is used. Feed temperature is 390 K. Figure 8.46 shows the flowsheet with

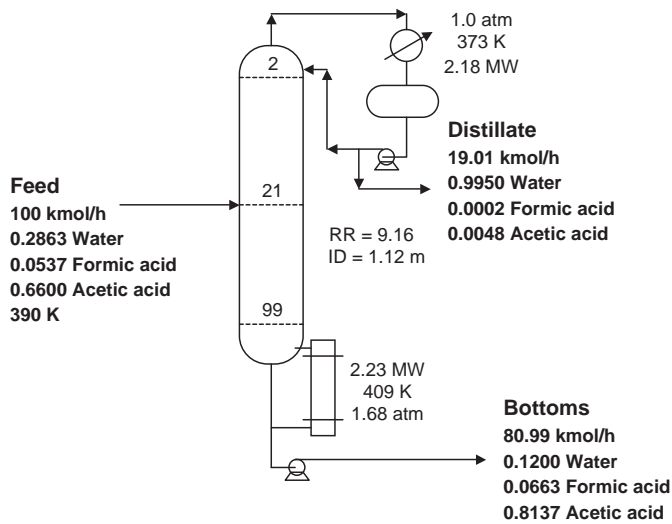


Figure 8.46 Flowsheet.

design and operating variables for the economic optimum column, as discussed in the next section. A 0.1 psi tray pressure drop is assumed, which gives a base pressure of 1.68 atm with a reflux drum pressure of 1 atm.

Notice that the column has a large number of trays and a high reflux ratio because of the difficult separation involved. The high reflux ratio is the feature that leads to the control structure dilemma of wanting to control reflux-drum level with reflux but also wanting a reflux-to-feed control structure.

8.5.2 Economic Optimum Steady-State Design

The economic design objective is to minimize total annual cost, given feed conditions, and desired product specifications. The two product specifications are 99.5 mol% water in the distillate and 12 mol% water in the bottoms. The Aspen *Design Spec/Vary* feature is used to attain these specifications by varying the distillate flow rate and the reflux ratio. The Aspen *Tray Sizing* feature is used to determine the diameter of the column. A tray spacing of 2 ft is used to determine column height.

The economic parameters and sizing relationships given in Chapter 4 are used to determine heat-exchanger areas (reboiler and condenser), capital investment, and energy cost. Total annual cost (TAC) takes the total capital investment, divides by a payback period (3 years), and adds the annual cost of reboiler energy.

Table 8.3 gives results for columns over a range of total number of stages. Energy cost decreases monotonically as more trays are used. Capital cost also initially decreases as more trays are used because of the reductions in column diameter and heat-exchanger areas. However, capital investment begins to increase as the number of stages rises above 80 because of the increase in column height.

The minimum TAC case shown in Table 8.3 is the 120-stage column. However, the reduction in TAC between this case and the 100-stage column is <1%. Therefore, the 100-stage column is used in the control study discussed in the next section.

TABLE 8.3 Optimization Cases

Total Stages	60	80	100	120
Optimum feed stage	17	14	21	55
Diameter (m)	1.82	1.23	1.12	1.06
QC (MW)	5.24	2.52	2.02	2.02
QR (MW)	5.27	2.57	2.23	2.08
Area condenser (m ²)	97.4	46.9	37.5	37.5
Area reboiler (m ²)	266	130	112	105
Capital costs				
Shell (K \$)	673	563	612	672
Heat exchangers (K \$)	418	261	234	227
Total capital (K \$)	1091	823	846	899
Energy (K \$/year)	782	389	331	308
TAC (K \$/year)	1.145	654.6	612.0	607.4

8.5.3 Control Structure Selection

Evaluation of R/F and RR Structures. The first thing to do is to explore the effect of feed composition on the required changes in reflux-to-feed and reflux ratio while holding the two products at their specified values. The specifications are 99.5 mol% water purity in the distillate and 12 mol% water impurity in the bottoms.

Table 8.4 gives results for reflux-to-feed ratio and reflux ratio over a range of feed compositions. The concentration of water in the feed is increased and decreased 4 mol% around the design value of 28.63 mol%. The concentration of acetic acid is decreased and increased in the opposite direction. The concentration of formic acid is kept constant at 5.37 mol%. Feed flow rate is constant at 100 kmol/h.

Table 8.4 shows that there are monotonic decreases in both the reflux flow rate and the reflux ratio as the concentration of water in the feed increases and the concentration of acetic acid decreases. The distillate flow rate naturally increases as more water comes in with the feed. The fairly small decrease in reflux flow rate and the increase in distillate result in large decreases in the reflux ratio.

These results clearly display a strong preference for a constant R/F ratio structure. The reflux-to-feed ratio only changes about 10% over the entire range of feed compositions, while the reflux ratio changes over 60%.

But the reflux ratio is quite high (RR = 9.16 at design). The reflux-drum level should be controlled by reflux flow rate when the reflux ratio is this large, which would preclude the use of the reflux-to-feed control structure. In the following section, a control structure that permits the use of the R/F scheme is developed.

It should be emphasized that the analysis discussed in this section considers only steady-state effects. Dynamics are not considered. However, just because a control structure looks

TABLE 8.4 Effect of Feed Composition on R/F and RR

	zW	zAA	R/F	RR
Design }	0.2663	0.6800	1.785	10.67
	0.2863	0.6600	1.732	9.114
	0.3263	0.6200	1.655	7.018

good from a steady-state perspective, there is no guarantee that the control structure will be dynamically effective. An interesting example of this is presented in a later section. The reflux ratio control structure is demonstrated to unstable in this distillation system.

Control Structure Holding Reflux-Drum Level with Reboiler Heat Input. The liquid level in the reflux drum is directly affected by three variables: distillate flow rate, reflux flow rate, and condenser duty. Condenser duty affects the amount of liquid entering the reflux drum due to condensation of the vapor coming overhead from the column. Either distillate or reflux is conventionally used for reflux-drum level control. Condenser duty is occasionally used to control reflux-drum level in columns with partial condensers in which pressure is controlled by the flow rate of the vapor distillate product.

However, if condenser duty is being used to control pressure, reboiler heat input will also *indirectly* affect liquid level in the reflux drum. A change in vapor generation in the reboiler changes column pressure, which causes the pressure controller to change the condenser heat removal. Therefore, it is feasible to control reflux-drum liquid level with reboiler heat input. This configuration permits the use of the R/F structure.

Conventionally, reboiler duty is used to control a tray temperature in a single-end structure, so if reboiler duty is used in the level loop, another manipulated variable must be used for temperature control. The obvious choice is the flow rate of the distillate.

Changing distillate flow rate has no *direct* effect on temperatures in the column. Reflux and vapor boilup are the inputs that change temperatures (and compositions) inside the vessel. However, the distillate flow rate changes the level in the reflux drum, which results in a change in vapor rate when the level loop is on automatic. So the level loop is “nested” inside the temperature loop in this structure. The level loop must be on automatic for the temperature control loop to be effective.

As previously discussed, there are limitations in the use of manipulating reflux (or distillate) for the control of internal tray temperatures due to liquid hydraulic lags. Attempting to control a temperature in the stripping section using reflux (or distillate) would result in poor control.

Fortunately, the appropriate temperature in our case is near the top of the column, as we will discuss in the next section. Thus, manipulating distillate to control a tray temperature provides an effective control. A temperature break near the top of the column is observed in many systems in which there is only a small amount of the light key component in the feed (which leads to a high reflux ratio).

Temperature Control Tray Selection. There are a number of methods for selecting the best tray for temperature control. The easiest and most frequently used is to simply look at the temperature profile and select a tray where temperatures are changing significantly from tray-to-tray.

Figure 8.47a gives the temperature profile of the column studied. There is only one location (near the top) where the temperature profile exhibits a break. We select Stage 3 for temperature control by manipulating distillate flow rate.

Notice that the temperature profile through most of the column is almost linear. This is due to the effect of pressure. Temperature increases as we move down the column because of both compositions of the less-volatile components and pressure increase. Attempting to control a temperature in the stripping section could yield poor control because the temperature is more affected by pressure changes than by composition changes.

Figure 8.47b gives the composition profiles. The only location in the column where compositions are changing significantly from tray-to-tray is in the top 10 stages.

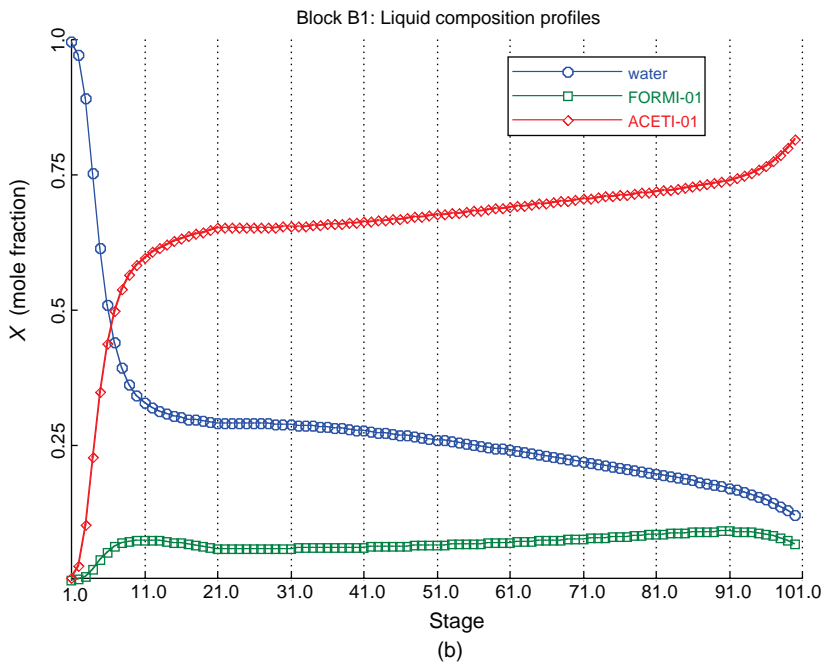
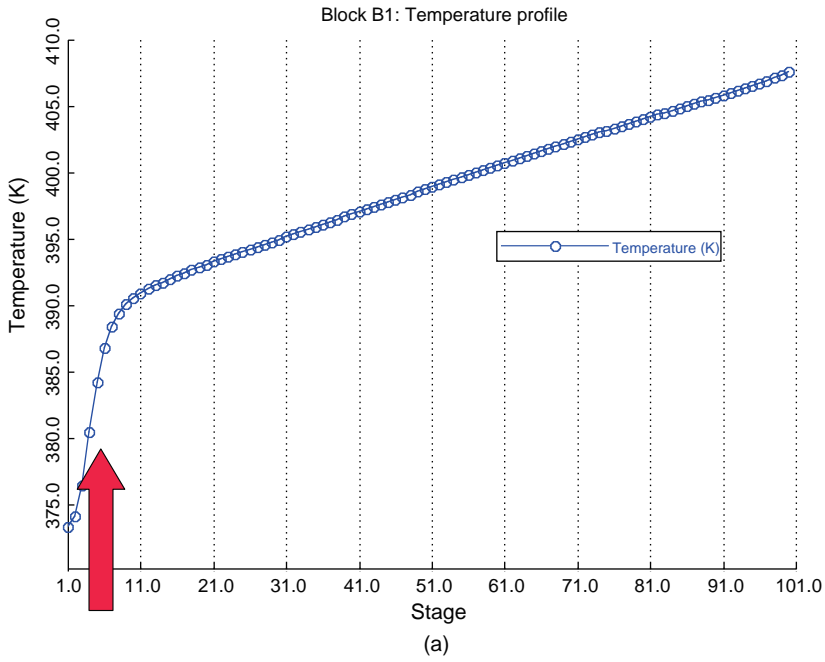


Figure 8.47 (a) Temperature profile. (b) Composition profiles.

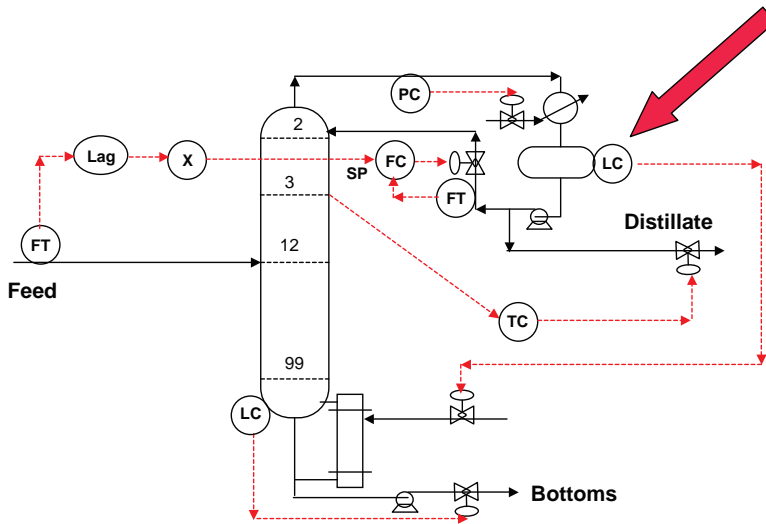


Figure 8.48 Proposed control structure.

Proposed Unusual Control Structure. Figure 8.48 shows the control structure proposed for achieving the objective of using the R/F structure in a high reflux ratio column. The details of the individual loops are listed below

1. Feed is flow controlled.
2. Reflux is flow controlled with the set point of the reflux flow controller coming from a multiplier whose input signal is the feed flow rate and whose output signal is the reflux set point.
3. Column pressure is controlled by manipulating condenser heat removal.
4. Stage 3 temperature is controlled by manipulating distillate flow rate.
5. Base liquid level is controlled by manipulating bottoms flow rate.
6. Reflux-drum liquid level is controlled by manipulating reboiler heat input.

This last loop is the unusual element in the control structure. The tuning of most conventional level loops is simple because we use a proportional controller with a gain of 2. The level loop in the proposed structure is not conventional. In this application, we want fairly tight level control because the distillate/temperature loop depends on the vapor/level loop. In addition, the dynamics of the vapor/level loop contain some dynamic lags because the pressure loop is involved, that is, increasing reboiler heat input increases pressure, and the pressure controller increases condenser heat removal, which affects reflux-drum level.

Notice that the R/F loop contains a dynamic lag. The feed flow rate signal passes through a first-order lag of 5 min, so that the changes in reflux are not instantaneous with changes in feed flow rate. This provides dynamic compensation in this “feed forward” ratio loop, so that the dynamic effect of a change in feed flow is a better match in time with the dynamic effect of a change in reflux. If the reflux changed instantaneously for changes in feed flow rate, the reflux-drum level would be immediately affected, which would immediately change the reboiler heat input. This would affect Stage 3 temperature before

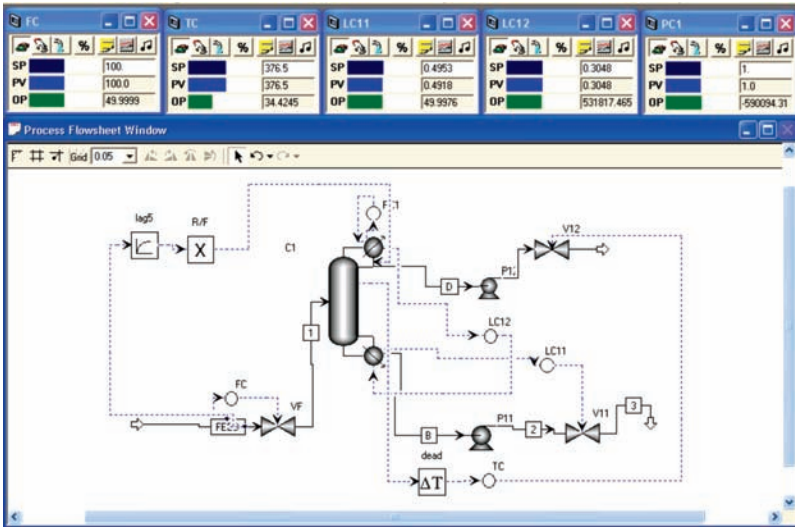


Figure 8.49 Aspen Dynamics PFD and controller faceplates.

the effect of the change in feed flow rate begins to change it. Therefore, the temperature loop would be unintentionally disturbed. Delaying the feed flow rate signal avoids this dynamic timing problem.

Figure 8.49 shows the Aspen Dynamics process flow diagram that implements the control structure. The controller faceplates are also shown. Notice that the output signal of the reflux-drum level controller LC12 is the reboiler heat input (in cal/s).

Controller Tuning. The reflux drum and column base are sized to provide 5 min of holdup when at 50% level. The base level control is proportional only with $K_C = 2$. The column pressure controller used Aspen default tuning of $K_C = 20$ and $\tau_I = 12$ min.

Since the reflux-drum level loop is nested inside the temperature loop, the level loop is tuned first. A relay-feedback test and Tyreus–Luyben tuning rules give the results shown in Table 8.5. Notice that the gain and integral times are very much different than a conventional level control loop. The integral time is about 8 min and the gain is only 0.3.

Then, the Stage 3 temperature loop is tuned with the level loop on automatic. A deadtime of 1 min is used in the loop to simulate the temperature measurement lags (Table 8.5). Notice

TABLE 8.5 Controller Parameters

	Reflux-Drum Level LC12	Pressure PC	Temperature Stage 3 TC	Base Level LC11	Feed Flow Rate FC
SP	0.3048 m	1 atm	376.5 K	0.495 m	100 kmol/h
Transmitter range	0–0.6 m	0–2 atm	300–400 K	0–1 m	0–200 kmol/h
OP	531.8 kcal/s	–590 kcal/s	34.4%	50%	50%
OP range	0–1000 kcal/s	0–1000 kcal/s	0–100%	0–100%	0–100%
Deadtime	–	–	1 min	–	–
K_C	0.31	2	63	2	0.5
τ_I (min)	7.9	20	6.6	9999	0.3

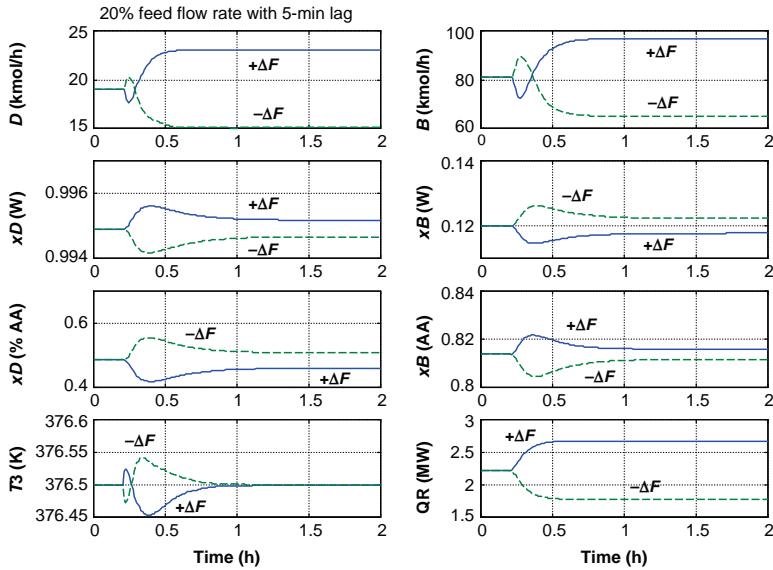


Figure 8.50 20% increase in feed flow rate.

that the controller gain in this loop is quite large, indicating that tight temperature control should be possible. The results presented in the next section confirm this prediction.

8.5.4 Dynamic Simulation Results

Large disturbances in both feed flow rate and feed composition were imposed on the system to test its ability to maintain stable regulatory control and to hold product streams near their desired specifications.

Figure 8.50 gives responses to 20% increases and decreases in the set point of the feed flow controller. The solid lines are increases and the dashed lines are decreases. Stable control is obtained with transients settling out in about an hour. Stage 3 temperature is tightly controlled by manipulating distillate flow rate. Bottoms water composition remains quite close to the desired 12 mol% specification. Distillate water purity remains quite close to the desired 99.5 mol% specification.

Figure 8.51 gives responses to increases and decreases in the composition of water in the feed. The solid lines are for changes from 28.63 to 32.63 mol% water with a corresponding reduction in acetic-acid concentration. The dashed lines are for changes from 28.63 to 24.63 mol% water with a corresponding increase in acetic-acid concentration. Stable control is obtained with transient settling out in about 2 h. Increasing feed water concentration produces more distillate and less bottoms. Stage 3 temperature is tightly controlled by manipulating distillate flow rate. Bottoms and distillate compositions remains quite close to their desired specifications.

8.5.5 Alternative Control Structures

In this section, comparisons of the proposed unusual control structure with three more conventional control structures are presented.

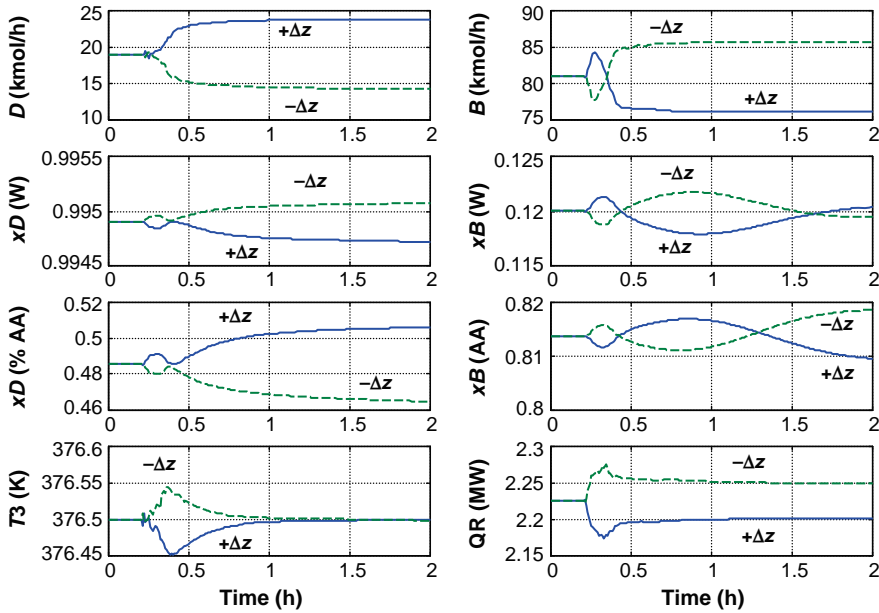


Figure 8.51 Feed-composition disturbances.

Conventional Structure. If we ignore conventional distillation wisdom, reflux-drum level can be controlled by manipulating the small distillate flow rate using a proportional controller with $K_C = 2$. The reflux-to-feed ratio is fixed, and Stage 3 temperature is controlled by manipulating reboiler heat input. The temperature loop is tuned in the normal way. The resulting controller settings are $K_C = 3.8$ and $\tau_1 = 8$ min when the temperature transmitter range is 350–450 K and the controller output range is 0–530 kcal/s.

Results are shown in Figure 8.52 for increases in feed flow rate. Figure 8.52a compares the proposed “unusual” structure (solid lines) with the “conventional” structure (dashed lines) for a 20% increase in feed flow rate. The transient swings in the distillate flow rate are much larger when the conventional structure is used, which would result in larger disturbances to a downstream process. In addition, the dynamic variation in Stage 3 temperature is much larger, which produces larger variability in the purity of the distillate product stream.

In Figure 8.52b, a 40% increase in feed is introduced. This large disturbance causes the distillate valve to go completely closed for several minutes when the conventional structure is used, but this large disturbance is easily handled by the unusual structure.

Reflux Ratio Structure. If we ignore the results of the analysis that shows that the R/F structure can handle feed-composition disturbances better than the RR structure, we can set up another conventional control structure in which reflux-drum level is controlled by reflux flow rate, Stage 3 temperature is controlled by reboiler heat input, and distillate flow rate is ratioed to reflux flow rate. This structure is commonly used in many distillation systems and would be expected to provide stable regulatory control but result in more deviation of product purities for feed-composition disturbances.

The reflux-drum level controller is proportional with $K_C = 2$. The tuning of the temperature controller is essentially the same as in the previous structure. The reflux flow rate is

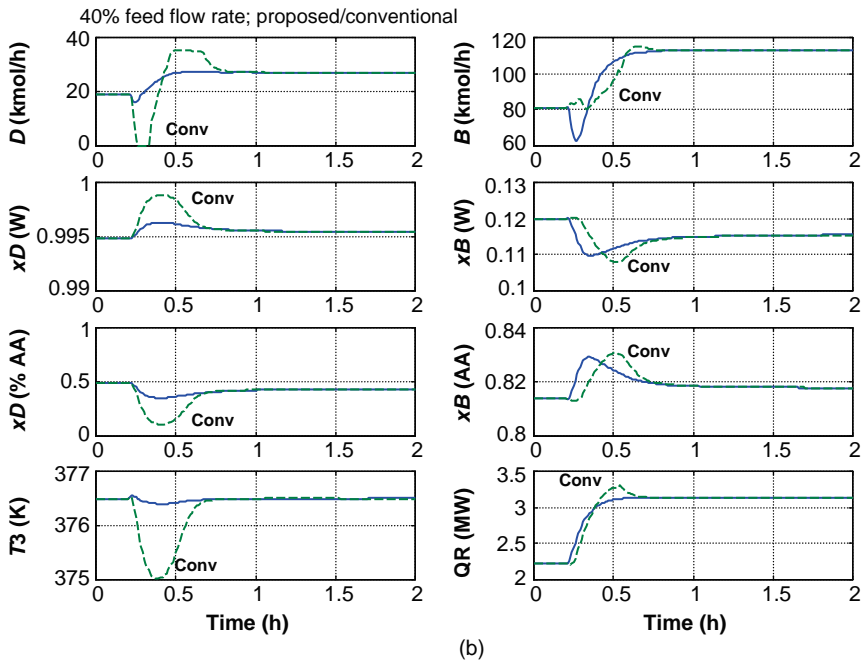
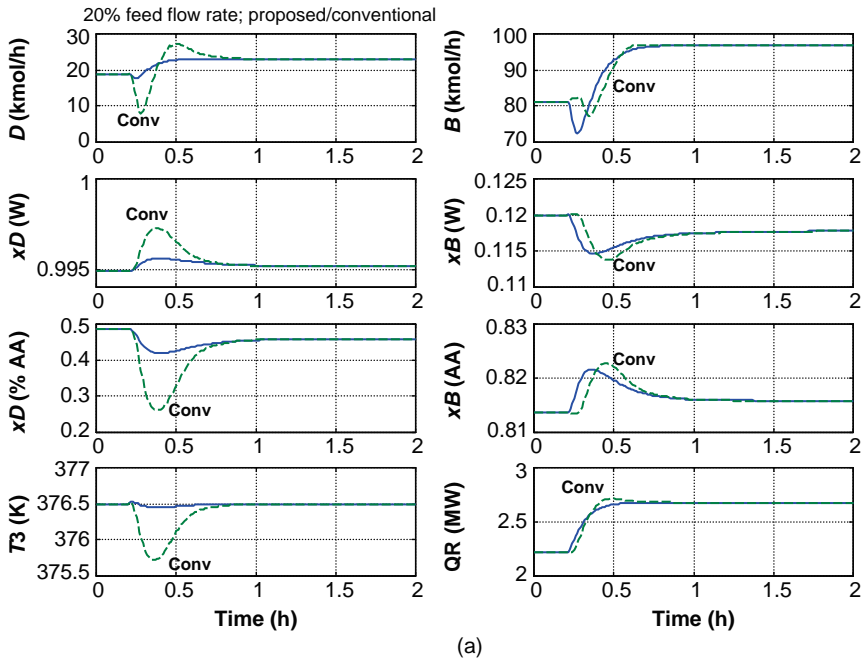


Figure 8.52 (a) Conventional structure: 20% feed flow rate disturbances. (b) Conventional structure: 40% feed flow rate disturbances.

measured and sent to a multiplier whose constant is the reciprocal of the desired reflux ratio. The output signal of the multiplier is the set point of the distillate flow controller.

This structure was tested and gave unexpected results. Figure 8.53a shows what happens when all controllers are on automatic and no disturbance is introduced. Everything runs along for about 20 h, but then a small *decrease* in Stage 3 temperature occurs. This increases the reboiler heat input, which increases the reflux-drum level. This increases the reflux and distillate flow rates. The temperature then undergoes a large *increase*, which produces an extreme drop in reboiler heat input and cuts reflux and distillate flow rates. The system shuts down after about 30 h.

These simulation results indicate that the reflux-ratio structure in this column produces a “closed-loop” unstable system. The reason for this unexpected behavior appears to be the competing effects of changes in reflux and changes in distillate. Increasing reflux *decreases* temperatures. Increasing distillate *increases* temperatures.

Since changing distillate flow rate is affecting the material balance around the column, it has a much larger effect on column temperatures than changes in reflux flow rate. Distillate flow rate changes the feed split, while reflux flow rate changes affect fractionation. Temperatures are much more sensitive to the former variable than to the latter. Figure 8.53b gives the response for a small 5% increase in feed flow rate. The system saturates and shuts down in about 10 h.

The proposed control structure does not have these problems because the distillate is manipulated to control temperature with the reflux-drum level controlled by reboiler heat input. The effects of distillate flow rate and reboiler heat input do not conflict. Increasing distillate flow rate increases column temperatures because of material balance adjustment. The resulting decrease in reflux-drum level causes the level controller to increase reboiler heat input, which also increases column temperatures. Thus, the effects of these two variables do not conflict. If two input variables have opposite effects, the result can be inverse response, which may explain the dynamic problems found in this RR control structure for this particular highly nonlinear column.

Valve Position Control Structure. Hori and Skogestad³ proposed another alternative structure that is similar to valve position controller (VPC). The idea is to slowly adjust the distillate flow rate to drive the reflux flow rate back to a value that corresponds to the desired reflux-to-feed ratio.

Dynamically, reflux flow rate controls reflux-drum level, and Stage 3 temperature is controlled by reboiler heat input. The signal from the feed flow transmitter is sent to a multiplier whose constant is the desired reflux-to-feed ratio. The output signal from the multiplier is the desired reflux flow rate and is the set point signal of a VPC controller, which is basically a reflux flow controller. The output signal of this controller positions the control valve on the distillate line.

Hori and Skogestad give some limited qualitative guidance on how to tune the controllers involved in this structure. They say that the reflux-drum level loop should be “fast” and the VPC controller should be “slow.” A number of simulations were run trying different tuning constants. The gain of the proportional level controller was set at $K_C = 2$ for “fast” level control. We started with a low gain of 1 and a large integral time ($\tau_I = 20$ min) in the VPC controller. The responses were oscillatory, as shown in Figure 8.54a. The disturbance is a 20% increase in feed flow rate. Reducing the gain made things worse, which is counter intuitive. Figure 8.54b shows that using a gain of 4 eliminates the oscillations.

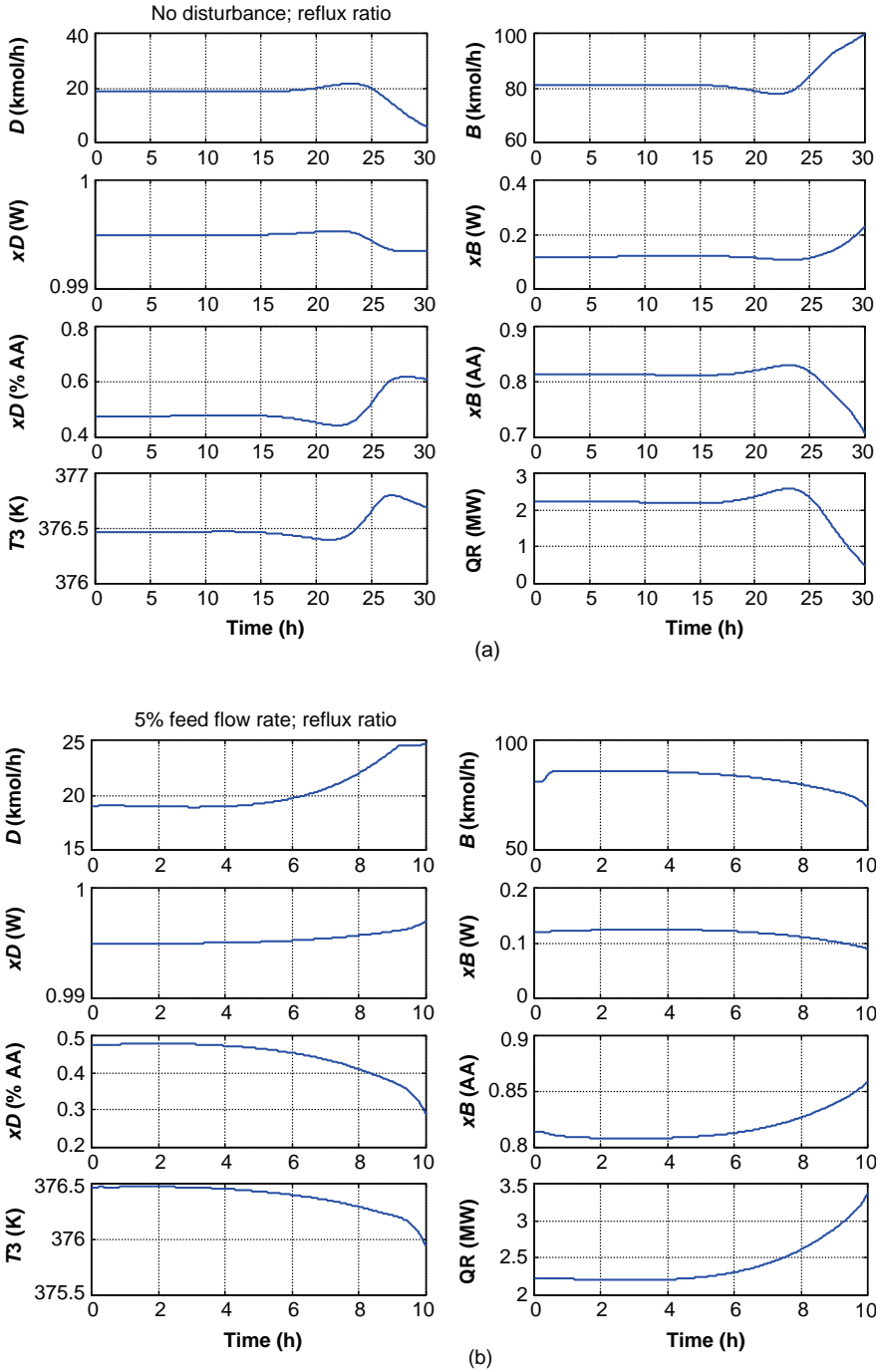


Figure 8.53 (a) Reflux ratio structure: no disturbance. (b) Reflux ratio structure: 5% increase in feed flow rate.

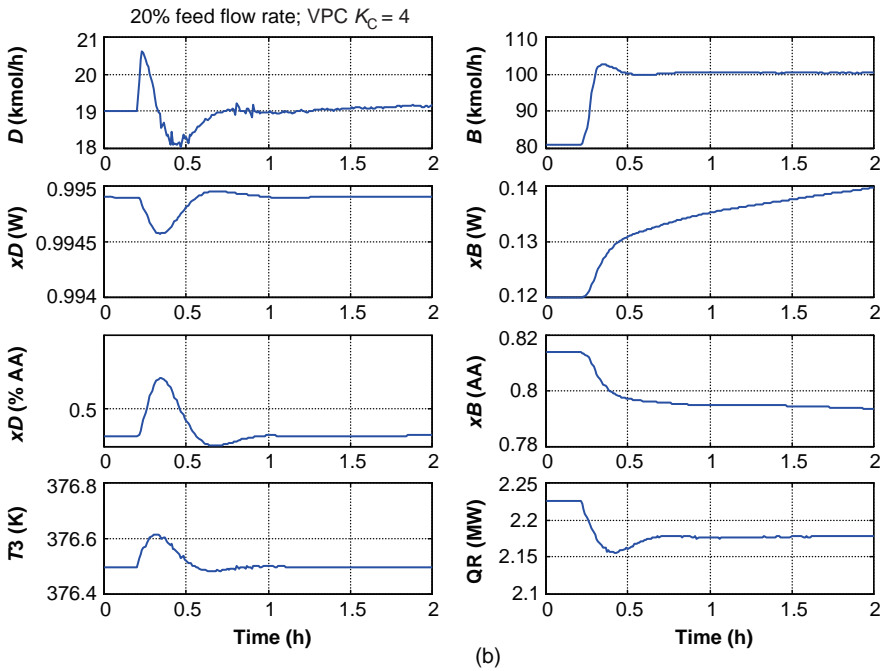
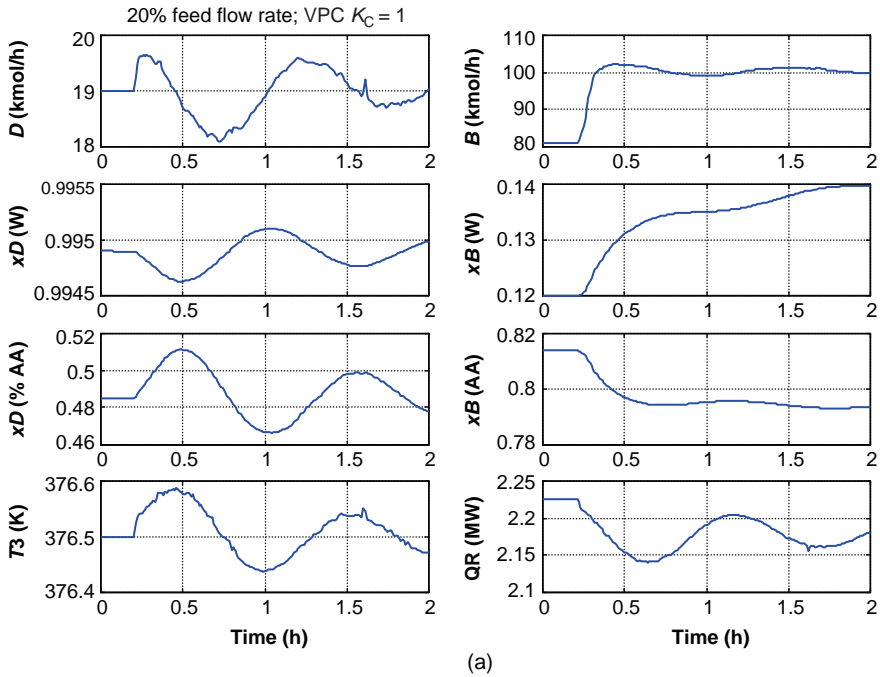


Figure 8.54 (a) VPC: $K_C = 1$. (b) VPC: $K_C = 4$.

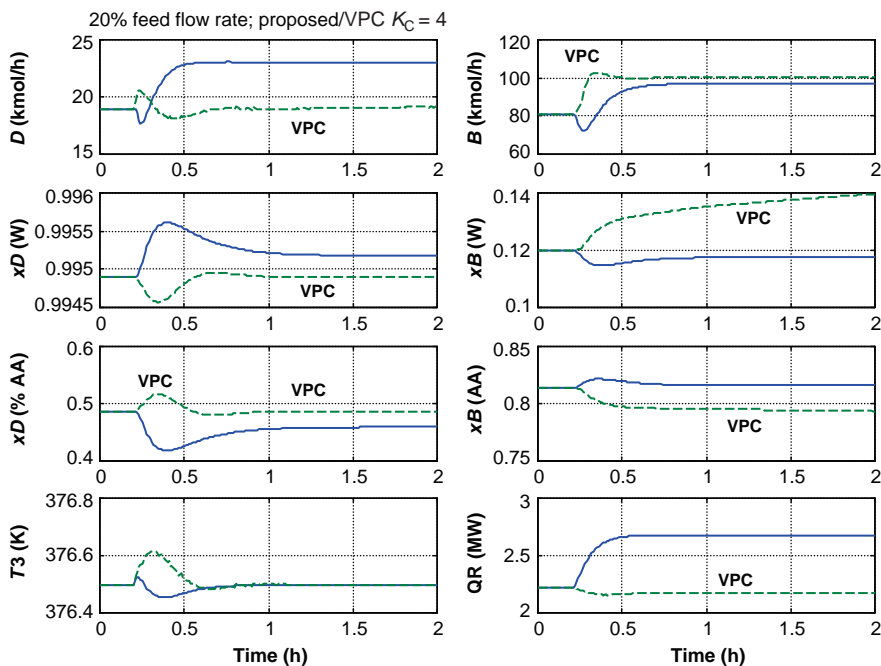


Figure 8.55 Comparison of proposed structure with VPC: $K_C = 4$.

However, the bottoms purity drifts far away from its specification. Distillate flow rate ends up at about its original value, which means that the increase in feed flow all goes out the bottom of the column. Reboiler heat input actually decreases instead of increasing as it should for an increase in feed flow rate.

Figure 8.55 provides a direct comparison between the VPC structure and the proposed structure. The latter is much superior. Product purities are held near their specifications. Changes in distillate and bottoms flow rates are gradual, so downstream units are not disturbed.

8.5.6 Conclusions

An unconventional control structure has been shown to provide effective control in the situation where reflux ratio is large and a reflux-to-feed ratio is preferred in a single-end control structure. The reflux-drum level is controlled by reboiler heat input. The condenser heat-removal loop controlling pressure must be on automatic for this structure to work because reflux-drum level is not directly affected by reboiler heat input.

The structure handles large disturbances in both feed composition and feed flow rate. Its performance is much better than those of other conventional control structures.

8.6 CONCLUSIONS

Several complex distillation systems have been examined in this chapter. The complexity can arise in either the vapor–liquid equilibrium or in the configuration of multiple interconnected units. Conventional and not-so-conventional control structures have been applied.

REFERENCES

1. B. D. Tyreus and W. L. Luyben, Two columns cheaper than one, *Hydrocarbon Process.* 93–96 (1975).
2. I. L. Chien, K. L. Zeng, and H. Y. Chao, Dynamics and control of a complete heterogeneous azeotropic distillation column system, *Ind. Eng. Chem. Res.* **43**, 2160–2174 (2004).
3. E. S. Hori and S. Skogestad, Selection of control structure and temperature location for two-product distillation columns, *Chem. Eng. Res. Des. Trans. IChemE, Part A* **85** (A3), 293–306 (2007).

CHAPTER 9

REACTIVE DISTILLATION

9.1 INTRODUCTION

Reactive distillation columns incorporate both phase separation and chemical reaction in a single unit. In some systems, they have economic advantages over conventional reactor/separation/recycle flowsheets, particularly for reversible reactions in which chemical equilibrium constraints limit conversion in a conventional reactor. Because both reaction and separation occur in a single vessel operating at some pressure, the temperatures of reaction and separation are not independent. Therefore, reactive distillation is limited to systems in which the temperatures conducive for reaction are compatible with temperatures conducive for vapor–liquid separation.

Pressure in conventional distillation design is usually set by a minimum temperature in the reflux drum (so that cooling water can be used) or a maximum temperature in the reboiler (to prevent fouling or thermal decomposition). Establishing the optimum pressure in a reactive distillation column is more complex because of the interplay between reaction and phase separation. Most vapor–liquid equilibrium (VLE) relationships show an increase in volatility with decreasing temperature. On the other hand, reaction rates decrease with decreasing temperature. If the reaction is exothermic, the chemical equilibrium constant increases with decreasing temperature. Therefore, low operating pressure/temperature that makes the phase separation easier may require lots of catalyst or liquid tray holdup to compensate for the low reaction rates.

In conventional distillation design, tray holdup has no effect on steady-state compositions. In reactive distillation, tray holdup (or amount of catalyst) has a profound effect on conversion, product compositions, and column composition profiles. Therefore, in addition to the normal design parameters of reflux ratio, number of trays, feed tray location, and pressure, reactive distillation columns have the additional design parameter of tray holdup.

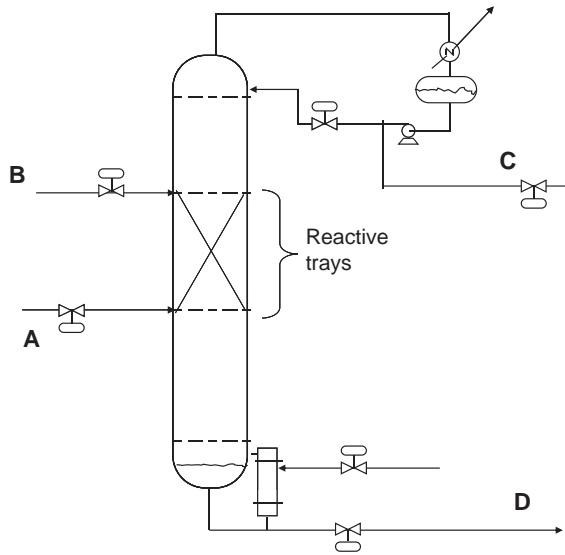


Figure 9.1 Ideal reactive distillation.

If there are two reactant feed streams, an additional design parameter is the location of the second feed.

Reactive distillation is usually applied to systems in which the relative volatilities of the reactants and products are such that the products can be fairly easily removed from the reaction mixture while keeping the reactants inside the column. For example, consider the classical reactive distillation system with reactants A and B reacting to form products C and D in a reversible reaction



For reactive distillation to be effective, the volatilities of the products C and D should be greater or less than the volatilities of the reactants A and B. Suppose the volatilities are

$$\alpha_C > \alpha_A > \alpha_B > \alpha_D$$

Reactant A would be fed into the lower section of a reactive column and rise upward. Reactant B would be fed into the upper section and flow downward. As the components react, product C would be distilled out of the top of the column and product D would be withdrawn out of the bottom. The reactants can be retained inside the column by vapor boilup and reflux while the products are removed. Figure 9.1 illustrates this ideal case.

In this chapter, we present a brief overview of reactive distillation and illustrate its application in a numerical example. A much more thorough treatment of reactive distillation is available in the book *Reactive Distillation Design and Control*.¹

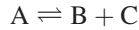
9.2 TYPES OF REACTIVE DISTILLATION SYSTEMS

There are many types of reactive distillation systems because there are several types of reactions that are carried out in reactive columns. There are also several types of process

structures that are used, some with recycle of an excess reactant and others without any reactant recycle.

9.2.1 Single-Feed Reactions

Reactions with a single reactant producing two products are easy to design and control because there is no need to balance the stoichiometry



There is only one reactant that is fed to the column. The two products are removed out of the two ends of the column. Olefin metathesis is an example of this type of reactive distillation column. Figure 9.2 illustrates this system and gives an effective control scheme. A C5 olefin reacts to form a light C4 olefin, which is removed in the distillate, and a heavy C6 olefin, which is removed in the bottoms. The two temperature controllers are used to maintain conversion and product quality. The production rate is set by a feed flow controller.

9.2.2 Irreversible Reaction with Heavy Product

The ethylene glycol reactive distillation system is an example of a reactive distillation system with two reactants that are consumed in a fast and irreversible reaction

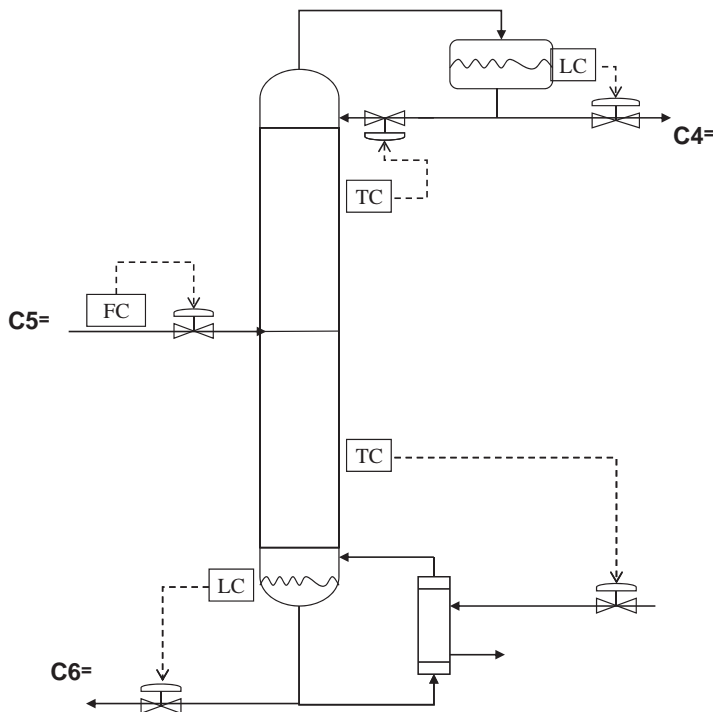


Figure 9.2 Olefin metathesis.

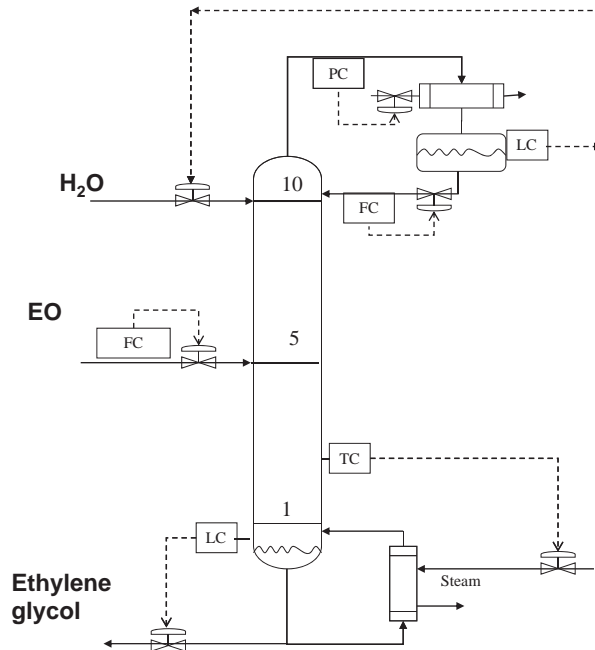


Figure 9.3 Ethylene glycol.

Figure 9.3 shows the system and an effective control structure. Ethylene oxide is very volatile, and ethylene glycol is very heavy. Thus, the product is removed from the bottom of the column. The ethylene oxide concentrates in the top of the column. *No* distillate product is removed. The water feed is introduced to hold the liquid level in the reflux drum. This level loop achieves the necessary balancing of the reaction stoichiometry by adjusting the makeup water flow rate to exactly match the water consumption by reaction with ethylene oxide. Production rate is set by flow controlling the ethylene oxide.

9.2.3 Neat Operation Versus Use of Excess Reactant

If the reaction involves two reactant feed streams, two basic flowsheets are used. Consider the reaction $A + B \rightleftharpoons C + D$. One way to design the process is to feed an excess of one of the reactants into the reactive distillation column along with the other reactant. Figure 9.4 shows a system in which an excess of reactant B is fed. In most cases this excess must be recovered. A second distillation column is used in Figure 9.4 to achieve this recovery. The fresh feed of reactant B is mixed with the recycle of B coming from the recovery column.

The control of this system is fairly easy. The total flow is controlled by manipulating the fresh feed of B. The fresh feed of reactant A sets the production rate, and the set point of the total B flow controller is ratioed to the flow rate of A. The control scheme features reflux ratio control and temperature controllers in both columns.

The alternative flowsheet uses just one column and is more economical, but it presents a much more difficult control problem. The operation is “neat,” that is, the amounts of the two reactants fed are exactly balanced so as to satisfy the reaction stoichiometry. Figure 9.5

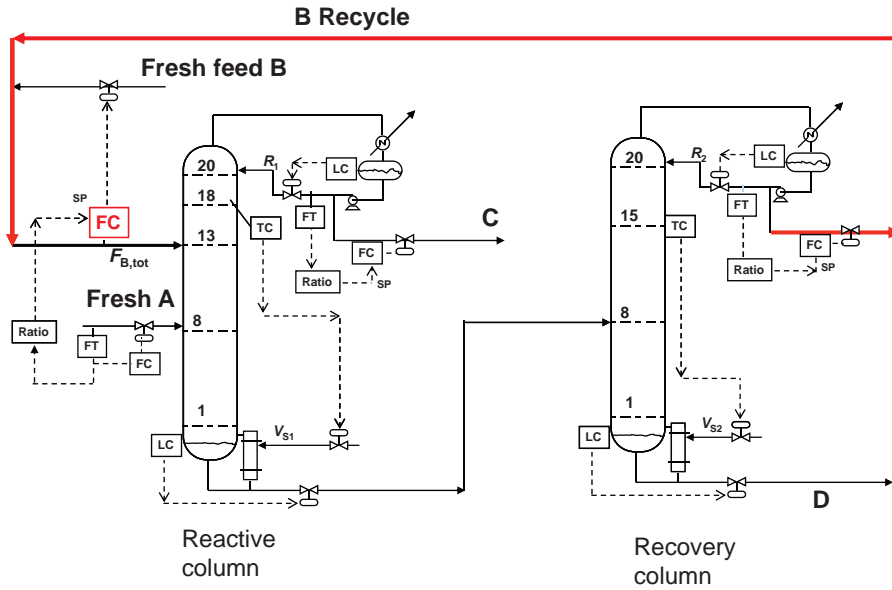


Figure 9.4 Excess of reactant B.

illustrates the system for the case when the reaction produces two products ($A + B \rightleftharpoons C + D$), which go out of the two ends of the column. The two temperature controllers achieve the balancing of the reactants. With two products, the column temperature information can be used to detect if more or less of each reactant should

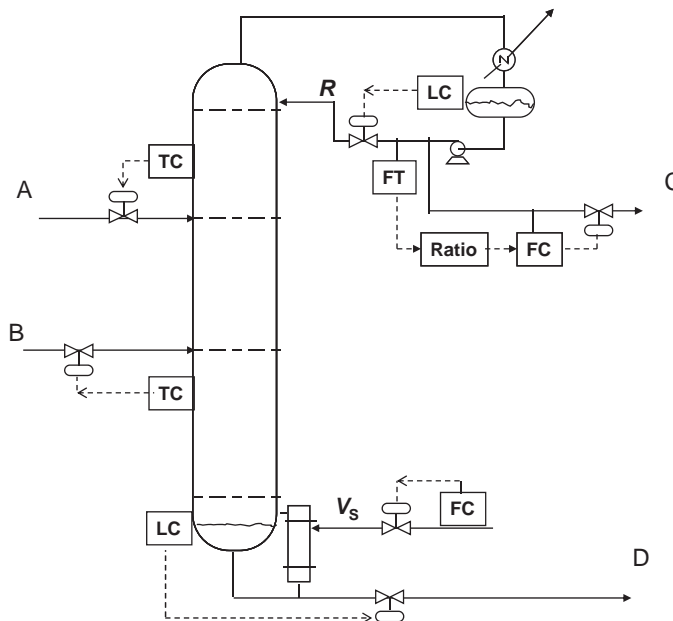


Figure 9.5 Neat operation (two products).

be fed. The production of methyl acetate and water from methanol and acetic acid is an example of this type of reactive distillation system.

A commonly made mistake in these two-reactant feed systems is to assume that a control structure with one feed ratioed to the other will provide effective control. This scheme does not work because of inaccuracies in flow measurements and changes in feed compositions. Remember in neat operation the reactants must be balanced down to the last molecule. This can only be achieved by using some sort of feedback information from the process that indicates a buildup or depletion of reactant.

However, consider the case when there is only one product: the reaction $A + B \rightleftharpoons C$. Now the column temperature information is not rich enough to use to balance the stoichiometry. This means that the measurement and control of an internal column composition must be used in this neat operation. An example of this type of system is shown in Figure 9.6. The production of ethyl *tert*-butyl ether (ETBE) from ethanol and isobutene produces a heavy product, which goes out of the bottom of the column. The C4 feed stream contains inert components in addition to isobutene. These inerts go out of the top of the column. The production rate is set by the flow controller on the isobutene feed stream. The ethanol concentration on a suitable tray in the column is maintained by manipulating the ethanol fresh feed. Reboiler heat input controls a tray temperature in the stripping section to maintain ETBE product quality.

The *tert*-amyl methyl ether (TAME) reactive distillation system considered in Section 9.3 has similar chemistry (two reactants and only one product), and an internal composition controller is required to balance the reaction stoichiometry. There is a recycle stream of one

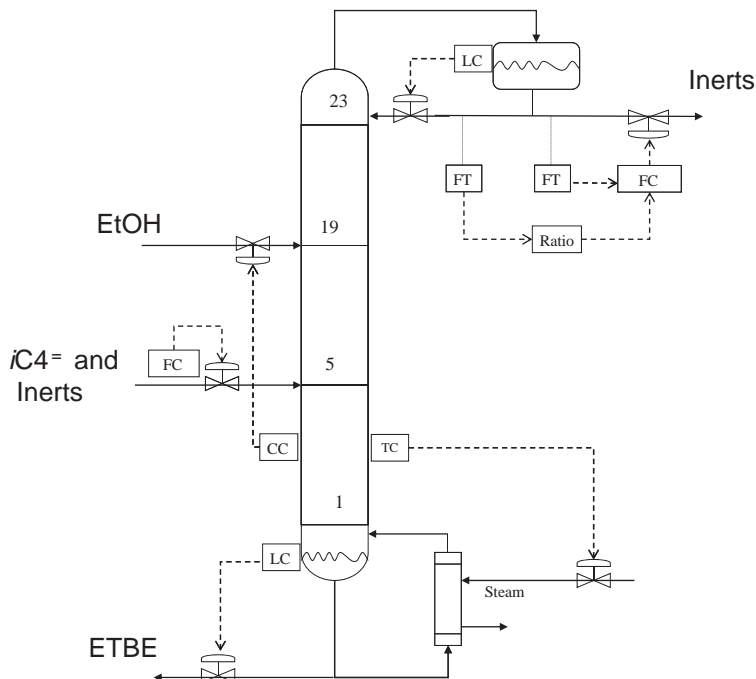


Figure 9.6 ETBE reactive distillation.

of the reactants in the TAME system, but this occurs because of the existence of azeotropes that carry some of this reactant out of the column with the inerts present in the olefin feed.

9.3 TAME PROCESS BASICS

In this section, we study the simulation and control of the TAME process as a typical example of a reactive distillation system. There are two feed streams: one is methanol and the second is a mixture of reactants and inert components.

The C5 feed stream to the TAME process contains about 24 mol% reactive isoamylenes: 2-methyl-1-butene (2M1B) and 2-methyl-2-butene (2M2B). The remaining components are pentanes and pentenes (largely isopentane, *i*C5), which are inert in the TAME reaction. TAME is the highest boiling component, so it leaves in the bottoms stream from the reactive distillation column. The lighter C5s leave in the distillate stream along with a significant amount of methanol.

Methanol forms minimum boiling azeotropes with many of the C5s. The reactive column operates at 4 bar, which is the optimum pressure that balances the temperature requirements for reaction with those for vapor–liquid separation. At this pressure, isopentane and methanol form an azeotrope at 339 K that contains 26 mol% methanol. Therefore, the distillate from the reactive column contains a significant amount of methanol that must be recovered.

Since the *i*C5/methanol azeotrope is pressure sensitive (79 mol% *i*C5 at 10 bar and 67 mol% *i*C5 at 4 bar), it is possible to use a pressure-swing process with two distillation columns, operating at two different pressures, to separate methanol from the C5 components. An alternative separation process for this system is extractive distillation, which is studied in this chapter.

Figure 9.7 gives the flowsheet of the process. There is a prereactor upstream of the reactive distillation column C1. The flowsheet contains three distillation columns (one reactive) and there are two recycle streams (methanol and water). The design of the prereactor and reactive column is based on the study of Subawalla and Fair.²

9.3.1 Prereactor

The prereactor is a cooled liquid-phase tubular reactor containing 9544 kg of catalyst. The C5 fresh feed (1040 kmol/h) and 313 kmol/h of methanol are fed to the reactor.

9.3.2 Reactive Column C1

The reactor effluent is fed into a 35-stage reactive distillation column (C1) on Stage 28. Catalyst is present on Stages 7–23. The reactor effluent is fed five trays below the reactive zone. A methanol stream is fed at the bottom of the reactive zone (Stage 23). The flow rate of the methanol fed to the reactive column is 235 kmol/h.

Figure 9.8 gives composition and temperature profiles in the reactive column C1. The reflux ratio is 4, which gives a bottoms purity of 99.2 mol% TAME and a distillate impurity of 0.1 ppm TAME. Reboiler heat input and condenser heat removal are 38.2 and 39 MW, respectively. The operating pressure is 4 bar. The column diameter is 5.5 m. The overall conversion of 2M1B and 2M2B in the C5 fresh feed is 92.4%. Table 9.1 gives stream information for the prereactor and column C1.

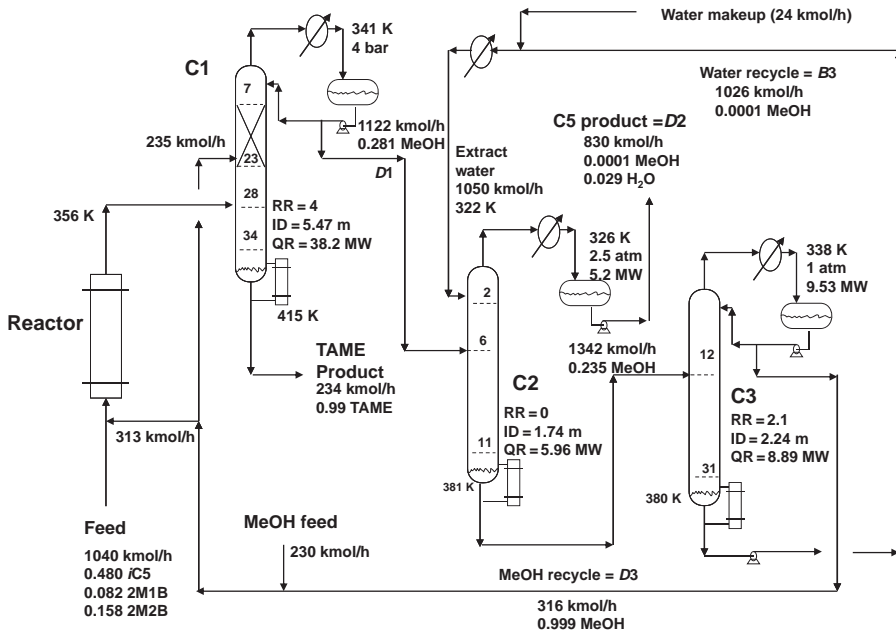


Figure 9.7 TAME process with extractive-distillation methanol recovery.

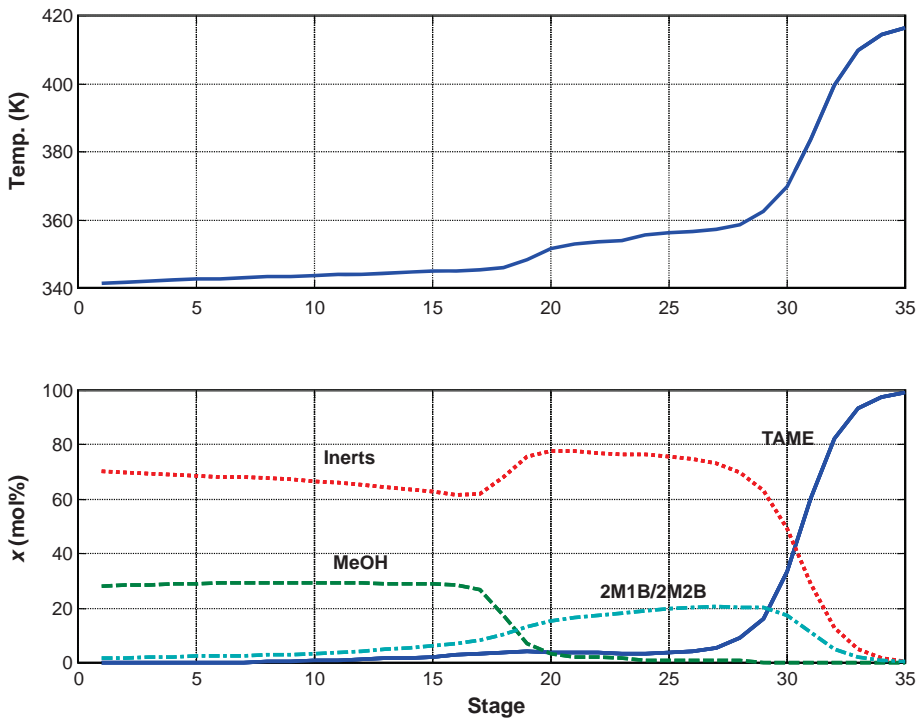


Figure 9.8 C1 temperature and composition profiles.

TABLE 9.1 Stream Information for Prereactor and Column C1

	Fresh Methanol (kmol/h)	Feed (kmol/h)	MeOH Reactor (kmol/h)	Reactor Effluent (kmol/h)	MeOH C1 (kmol/h)	<i>B</i> 1 (kmol/h)	<i>D</i> 1 (kmol/h)
MeOH	230	–	313	188	235	–	316
2M1B	–	85.6	–	13.7	–	0.01	3.31
2M2B	–	165	–	112	–	0.60	14.1
TAME	–	–	–	125	–	232	–
<i>n</i> C5	–	88.4	–	88.4	–	0.22	88.2
<i>i</i> C5	–	501	–	501	–	0.17	501
1-Pentene	–	38.1	–	38.1	–	0.18	37.9
2-Pentene	–	162	–	162	–	0.76	161
Total	230	1040	313	1228	235	234	1122
<i>T</i> (K)	325	343	351	355	351	415	341
<i>P</i> (atm)	17	10	7	6	4	4.29	3.95

The distillate *D*1 has a methanol composition (28 mol% methanol) that is near the azeotrope at 4 bar. It is fed at a rate of 1122 kmol/h to Stage 6 of a 12-stage extraction column. Water is fed on the top tray at a rate of 1050 kmol/h and a temperature of 322 K, which is achieved by using a cooler (heat removal 1.24 MW). The column is a simple stripper with no reflux. The column operates at 2.5 atm so that cooling water can be used in the condenser (reflux drum temperature is 326 K). Reboiler heat input is 5.96 MW. The overhead vapor is condensed and is the C5 product stream.

This column is designed by specifying a very small loss of methanol in the overhead vapor (0.01% of methanol fed to the column) and finding the minimum flow rate of extraction water that achieves this specification. Using more than 10 trays or using reflux did not affect the recovery of methanol.

The bottoms is essentially a binary methanol/water (23.5 mol% methanol), which is fed to a 32-stage column operating at atmospheric pressure. The number of trays in the second column was optimized by determining the total annual cost of columns over a range of tray numbers. Reboiler heat input and condenser heat removal are 8.89 and 9.53 MW, respectively. The column diameter is 2.24 m.

A reflux ratio of 2.1 produces 316 kmol/h of high-purity methanol in the distillate (99.9 mol% MeOH) and 1026 kmol/h of high-purity water in the bottoms (99.9 mol% H₂O). The methanol is combined with 230 kmol/h of fresh methanol feed, and the total is split between the methanol feed streams to the prereactor and to the reactive column. The water is combined with a small water makeup stream, cooled, and recycled back to the extractive column C2.

Some makeup water is needed because a small amount of water goes overhead in the vapor from column C2 (2.9 mol% water). The solubility of water in pentanes is quite small, so the reflux drum of column C2 would form two liquid phases (not shown in Fig. 9.1). The aqueous phase would be 19.9 kmol/h and 99.9 mol% water. The organic phase would be 809 kmol/h and 0.5 mol% water. Table 9.2 gives stream information around columns C2 and C3.

The convergence of the steady-state flowsheet was unsuccessful, so it was converged in the dynamic simulation, using the methods discussed in Chapter 8.

TABLE 9.2 Stream Information for Columns C2 and C3

	B2 (kmol/h)	D2 (kmol/h)	B3 (kmol/h)	D3 (kmol/h)	Water Makeup (kmol/h)	Extract Water to C2 (kmol/h)
MeOH	316	0.03	1.03	315	—	—
2M1B	—	3.31	—	—	—	—
2M2B	—	14.1	—	—	—	—
TAME	—	—	—	—	—	—
nC5	—	88.4	—	—	—	—
iC5	—	501	—	—	—	—
1-Pentene	—	38.0	—	—	—	—
2-Pentene	—	161	—	—	—	—
Water	1025	—	1026	0.32	24	1050
Total	230	830	1027	315	24	1050
T (K)	325	326	379	338	325	322
P (atm)	17	2.5	1.2	1.0	7	2.5

9.4 TAME REACTION KINETICS AND VLE

The liquid-phase reversible reactions considered are



The kinetics for the forward and reverse reactions are given in Table 9.3. These reaction rates are given in units of $\text{kmol}/(\text{s kg}_{\text{cat}})$ and are converted to units of $\text{kmol}/(\text{s}/\text{m}^3)$ by using a catalyst bulk density of $900 \text{ kg}/\text{m}^3$. The concentration units in the reaction rates are in mole fractions. The reactive stages in the column each contain 1100 kg of catalyst. This corresponds to 1.22 m^3 on each tray, which gives a weir height of 0.055 m for a reactive column with a diameter of 5.5 m.

The reactions and all the kinetic parameters must be set up in Aspen Plus. In the *Exploring* window, click on *Reactions* and on the second *Reactions*. Right click and select *New*. This opens the window shown in Figure 9.9a on which the type of reaction selected is *REAC-DIST*. Then click on the new reaction *R-1*, which opens the window shown in Figure 9.9b on which *Kinetic* is selected.

Clicking *OK* opens the window shown in Figure 9.9c on which reactant and product components are selected. The reactant coefficients are negative and the product coefficients are positive. The *Exponent* is the power-law exponent used in the reaction rate expression. Make sure to select *Kinetic* in the upper right corner.

TABLE 9.3 Reaction Kinetics

Reaction	A_F (kmol/(s/kg))	E_F (kJ/mol)	A_R (kmol/(s/kg))	E_R (kJ/mol)	ΔH_{RX} (kJ/mol)
R1	1.3263×10^8	76.103737	2.3535×10^{11}	110.540899	-34.44
R2	1.3718×10^{11}	98.2302176	1.5414×10^{14}	124.993965	-26.76
R3	2.7187×10^{10}	96.5226384	4.2933×10^{10}	104.196053	-7.67

Enter ID:
R-1

Select type:
REAC-DIST
POWERLAW
REAC-DIST
USER
USERACM

Cancel

(a)

Choose reaction type:
 Kinetic/Equilibrium/Conversion
 Salt precipitation

Reaction No.:
1

OK Cancel

(b)

Reaction No.: 1

Reaction type: Kinetic

Reactants			Products		
Component	Coefficient	Exponent	Component	Coefficient	Exponent
2MTB	-1	1	TAME	1	1
MECH	-1	1			
*					

Close

Lets you type the positive stoichiometric coefficient for the reactant component.

(c)

Figure 9.9 (a) Create new reaction. (b) Select reaction type. (c) Input reactants and products.

The procedure is repeated for the three forward reactions and for the three reverse reactions. These are shown in Figure 9.10. All of this input is done on the *Stoichiometry* page tab. Clicking the *Kinetic* page tab and selecting one of the six reactions opens the window shown in Figure 9.11a on which all the kinetic parameters are entered for that

Pxn No.	Reaction type	Stoichiometry
1	Kinetic	2M1B + MEOH → TAME
2	Kinetic	TAME → 2M1B + MEOH
3	Kinetic	2M2B + MEOH → TAME
4	Kinetic	TAME → 2M2B + MEOH
5	Kinetic	2M1B → 2M2B
6	Kinetic	2M2B → 2M1B

Figure 9.10 Six reactions specified.

reaction. Remember to select *Liquid* for the reacting phase and *mole fraction* for the concentration basis (see Fig. 9.11b).

Concentrations in mole fractions are used in the kinetics of the TAME reactions. Aspen accepts other concentrations units such as molarity, partial pressure and activity (called *mole gamma*).

Use built-in Power Law
 Use user kinetic subroutine

1) 2M1B + MEOH → TAME

Reacting phase: Liquid

Power Law kinetic expression
 $r = k(T/T_0)^n e^{-(E/R)[1/T-1/T_0]}$

k: 1.1939E+11
 n: 0
 E: 76103.7 kJ/kmol
 T₀: K
 [C] basis: Mole fraction

Edit reactions

(a)

Figure 9.11 (a) Kinetic parameters. (b) Specify concentration basis and reactive phase.

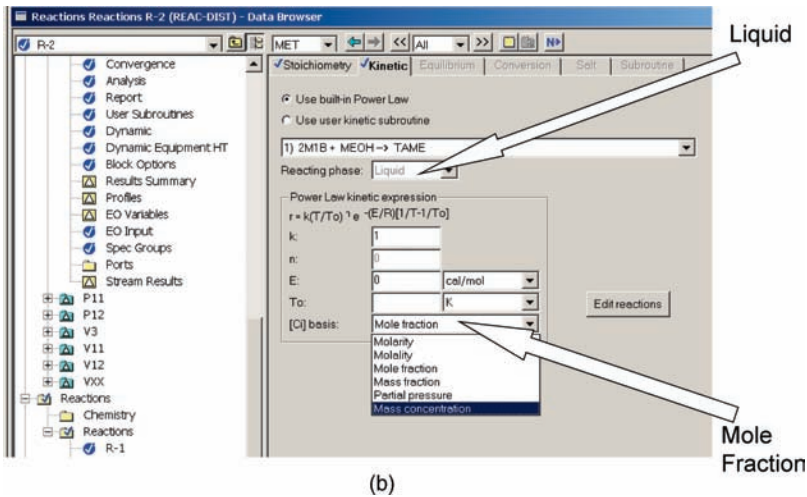


Figure 9.11 (Continued)

Now the reactions have been set up. Go to the C1 block and click *Reactions*. On the *Specifications* page tab, enter the starting and ending stages on which the reaction occurs and select the reaction *R-1*. Note that *R-1* is a set of six reactions. Clicking the *Holdups* page tab opens the window shown in Figure 9.12b in which the molar or volumetric holdups on each of the reactive trays are entered. The reactive liquid volume on each tray is set at 1.22 m^3 , which corresponds to a liquid of 0.055 m for a reactive column with a diameter of 5.5 m .

It is important to note that the diameter of the column is not known initially because this depends on vapor velocities that are unknown until the column is converged to the desired specifications. So column sizing in a reactive distillation column is an iterative procedure. A diameter is guessed, tray holdups calculated, and the column is converged. Then, the diameter calculated in *Tray Sizing* is compared with the guessed diameter and the calculations repeated.

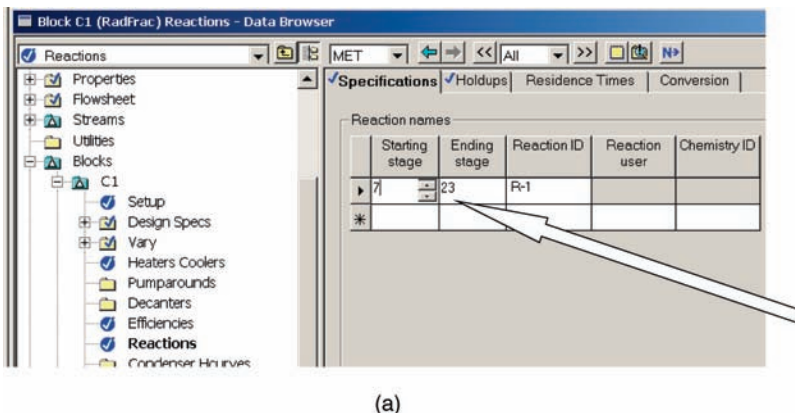
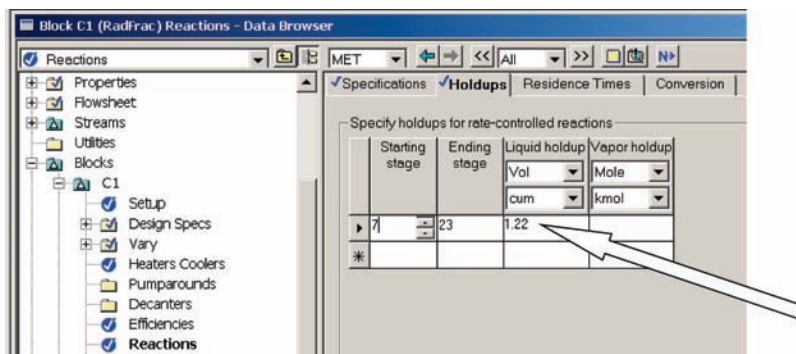


Figure 9.12 (a) Specifying reactive trays and holdups. (b) Tray holdups.



(b)

Figure 9.12 (Continued)

The other important issue is the height of liquid on a tray. Hydraulic limitations prevent the liquid depth from being too large because it would cause large pressure drops. Liquid depths are limited to about 0.1 m. If more liquid holdup is needed, column diameter can be increased beyond the minimum calculated from sizing calculations. Of course, more reactive trays could also be added to the column. However, reactive distillation columns have the interesting feature that there is an optimum number of reactive stages. Having too few reactive stage results in high energy consumption because the reactant concentrations in the reactive zone must be large, and this requires large vapor rates to keep the reactants from leaving in the bottoms or the distillate. Adding more reactive stages reduces the vapor boilup requirements because reactant concentrations in the reactive zone decrease. However, beyond some point, adding more reactive stages begins to increase energy consumption because the reactant concentrations in the reactive zone start to increase due to a larger contribution from the reverse reactions.

Figure 9.13 gives a ternary diagram for the isopentane–methanol–TAME system at 4 bar. The phase equilibrium of this system is complex because of the existence of azeotropes. The UNIFAC physical property package in Aspen Plus is used to model the VLE in all units except the methanol/water column where the van Laar equations are used because of their ability to accurately match the experimental data.

9.5 PLANTWIDE CONTROL STRUCTURE

In preparation for exporting the steady-state flowsheet into Aspen Dynamics, all equipment is sized. Column diameters are calculated by Aspen Tray Sizing. Reflux drums and column bases are sized to provide 5 min of holdup when 50% full, based on the total liquid entering the surge capacity. Pumps and control valves are specified to give adequate dynamic rangeability. Typical valve pressure drops are 2 atm.

When the flowsheet with a tubular reactor was exported into Aspen Dynamics, the program would not run. A liquid-filled plug-flow reactor will not run in Version 12 of Aspen Dynamics. To work around this limitation, the tubular reactor was replaced by two

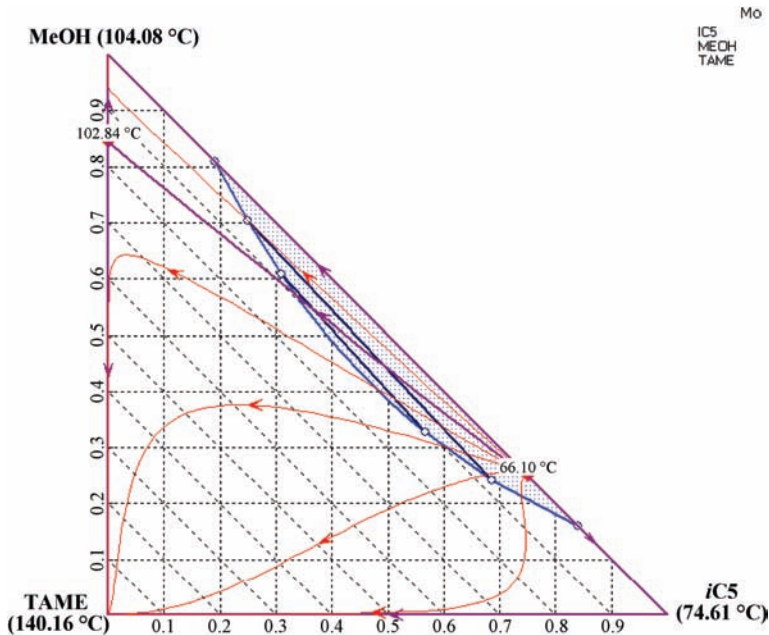


Figure 9.13 *iC5/MeOH/TAME* at 4 bar.

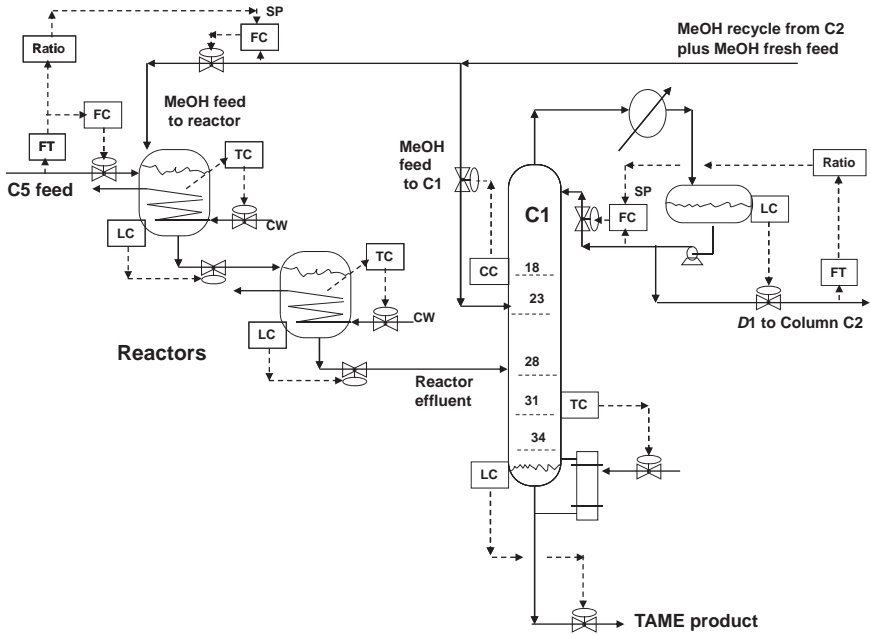
CSTRs in series. Operating temperatures in both reactors were set at 355 K and volume at 10 m^3 . This design gave the same reactor effluent as the tubular reactor.

The plantwide control structure is shown in Figure 9.14. A tray temperature is controlled in each column by manipulating reboiler heat input. The trays are selected by finding the location where the temperature profile is steep: Stage 31 in column C1 (see Fig. 9.8), Stage 7 in column C2, and Stage 7 in column C3. In addition, an internal composition in column C1 is controlled by manipulating the flow rate of methanol to the column. Stage 18 is selected (see Fig. 9.8). The flow rate of methanol to the reactor is ratioed to the feed flow rate.

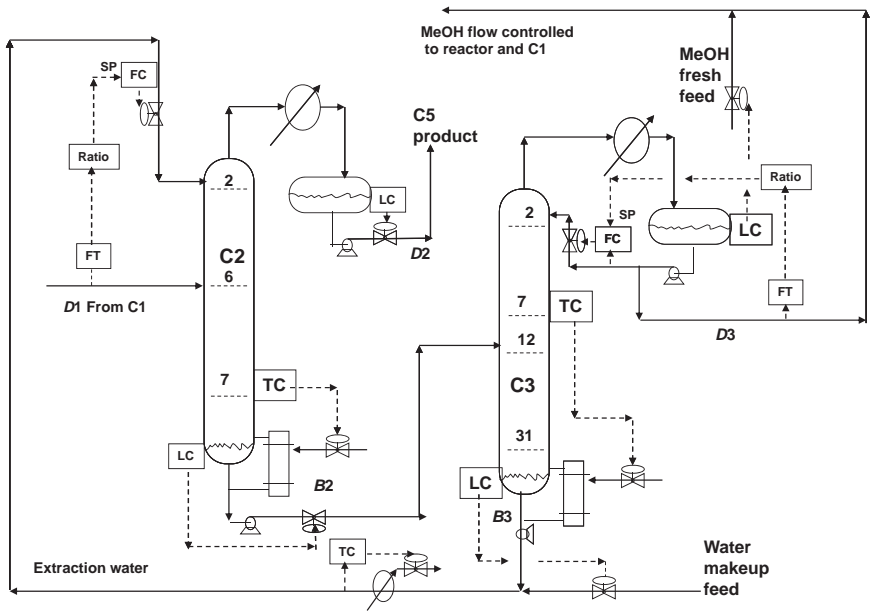
The flow rate of extraction water fed to the top of column C2 is ratioed to the feed to this column D1 by using a multiplier and a remote-set flow controller. The temperature of the extraction water is controlled by manipulating cooling water to the cooler. Base level is controlled by manipulating bottoms, and reflux drum level is controlled by manipulating distillate. The binary methanol/water mixture from the bottom of column C2 is fed to column C3. A constant reflux ratio is maintained in this column by adjusting reflux flow rate.

There are two key plantwide material balance loops associated with column C3. The level in the reflux drum provides a good indication of the inventory of methanol in the system. If this level is going down, more methanol is being consumed in the reaction than is being fed into the process. Therefore, the control structure maintains the reflux drum level in C3 by manipulating the methanol fresh feed.

Note that the flow rate of the total methanol (D3 plus fresh methanol feed) is fixed by the two downstream flow controllers setting the flow rates to the reactor and to column C1. This means there is an immediate effect of fresh feed flow rate on reflux drum level. The



(a)



(b)

Figure 9.14 (a) Control structure for reactors and C1. (b) Control structure for C2 and C3.

distillate flow $D3$ changes inversely with fresh feed flow because the downstream flow rate is fixed. Thus, the reflux drum level sees the change in the methanol fresh feed instantaneously.

At the other end of the column, the base level provides a good indication of the inventory of water in the system. Ideally, there should be no loss of water since it just circulates around between the extractive column and the recovery column. However, there is a small amount of water lost in the overhead from column C2. A water makeup stream is used to control the liquid level in the base of column C3. This makeup flow is very small compared with the water circulation, so the base of the column C3 must be sized to provide enough surge capacity to ride through disturbances.

All temperature and composition controllers have 1 min deadtimes. The PI controllers are tuned by running a relay-feedback test and using the Tyreus–Luyben settings. All liquid levels are controlled by proportional controllers with gains of 2 for all level loops except the two reactors, which have gains of 10. Liquid levels in reflux drums are controlled by manipulating distillate flow rates. The reflux ratios in all columns are controlled by manipulating reflux. Column pressure controllers use default controller settings and manipulate condenser heat removal.

Figure 9.15a gives the responses of the process to 20% changes in feed flow rate. Figure 9.15b gives responses to changes in feed composition. Effective plantwide control is achieved. The control structures provide stable base-level regulatory control for large disturbances. The purity of the TAME product is held quite close to its specification.

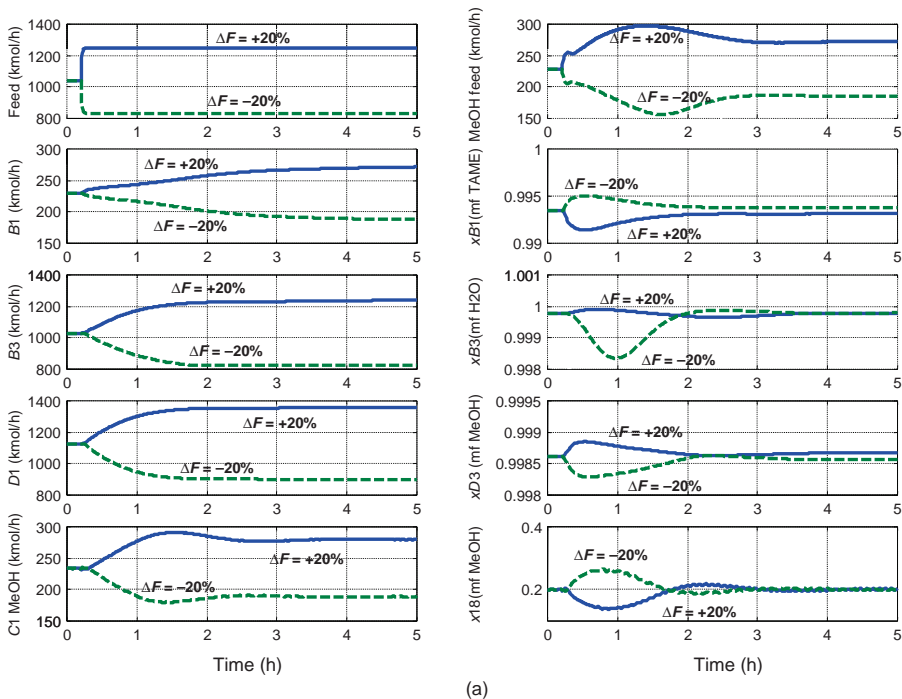


Figure 9.15 (a) Feed rate disturbances. (b) Feed composition disturbances.

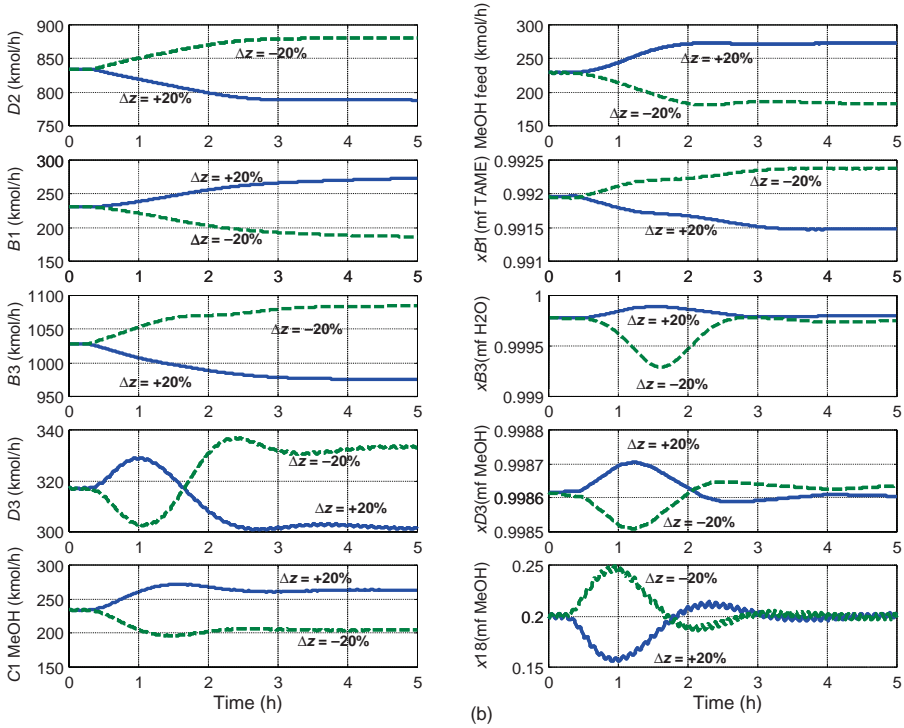


Figure 9.15 (Continued)

9.6 CONCLUSIONS

The design and simulation of reactive distillation systems have been discussed in this chapter. The reactive distillation column is more complex than a plain distillation column because the effects of both phase equilibrium and chemical reaction must be considered simultaneously.

REFERENCES

1. W. L. Luyben and C.-C. Yu, *Reactive Distillation Design and Control*, Wiley, New York, 2008.
2. H. Subawalla and J. R. Fair, Design guidelines for solid-catalyzed reactive distillation systems, *Ind. Eng. Chem. Res.* **38**, 3693 (1999).

CHAPTER 10

CONTROL OF SIDESTREAM COLUMNS

In this chapter, we study distillation columns that have more than the normal two product streams. These more complex configurations provide savings in energy costs and capital investment in some systems. Sidestream columns are used in many ternary separations, and the examples in this chapter illustrate this application. However, a sidestream column can also be used in a binary separation if different purity levels are desired. For example, two grades of propylene products are sometimes produced from a single column. The bottoms stream is propane, the sidestream is medium-purity propylene, and the distillate is high-purity polymer-grade propylene.

The most widespread use of sidestream columns occurs in petroleum fractionators, which have multiple sidestream products that are complex mixtures of many components. The sidestreams have progressively higher boiling point ranges as we move down the column. The top sidestream may be kerosene. The next may be a diesel cut or jet fuel. The next is a light gasoil. The final may be a heavy gasoil. The liquid streams withdrawn from the main column are each fed to a small stripping column. Open steam is fed at the bottom of each sidestream stripper to strip out light components from the liquids withdrawn from the main column. We discuss these types of sidestream columns in Chapter 11.

Sidestream columns come in several flavors. Both liquid and vapor sidestreams are used. Sometimes the sidestream is a final product. Because the purity attainable in a sidestream is limited, the sidestream from the main tower is sometimes fed to a second column (usually a stripper or a rectifier) for further purification with a recycle stream back to the main column. Several examples are studied in this chapter.

10.1 LIQUID SIDESTREAM COLUMN

Liquid sidestream columns are frequently used when the feed stream is a ternary mixture in which the concentration of the lightest component is small. This lightest component is removed in the distillate product. The intermediate component is removed in a sidestream that is withdrawn as a liquid from a tray above the feed tray. A liquid sidestream is used because the concentrations of the lightest component in the *liquid* phase on all the trays above the feed tray are smaller than the concentrations of the lightest component in the *vapor* phase. This indicates a limitation in the application of a liquid sidestream column: the volatility between the lightest and intermediate component must be fairly large. If this volatility is too small, a high-purity sidestream cannot be produced in a single column.

10.1.1 Steady-State Design

The specific numerical case used is a ternary mixture of dimethyl ether (DME), methanol (MeOH), and water. The feed composition is 5 mol% DME, 50 mol% MeOH, and 45 mol% water. The feed flow rate is 100 kmol/h, and the feed is fed on Stage 32 of a 52-stage column. The liquid sidestream is withdrawn from Stage 12. The column pressure is set at 11 atm so that cooling water can be used in the condenser (reflux-drum temperature is 323 K with a distillate composition of 98 mol% DME and 2 mol% MeOH). The NRTL physical property package is used.

The presence of a sidestream provides an additional degree of freedom. Three purities can be set. We use three Design Spec/Vary functions to achieve the following specifications:

1. Distillate impurity is set at 2 mol% MeOH by varying the distillate flow rate.
2. Sidestream impurity is set at 2 mol% water by varying the sidestream flow rate.
3. Bottoms purity is set at 2 mol% MeOH by varying the reflux flow rate.

Note that the other impurity in the sidestream (DME) cannot be specified with a fixed column configuration because there are no remaining degrees of freedom. However, the number of stages and the locations of the feed and the sidestream can be changed to alter the sidestream DME composition.

The key separation in this liquid sidestream column is between DME and MeOH in the section above the feed tray. Because all the DME in the feed must flow up the column past the sidestream drawoff tray, the concentration of DME in the vapor phase is significant. The liquid-phase concentration, however, is smaller if the relative volatility between DME and MeOH is large. The normal boiling points of these two components (DME = 248.4 K and MeOH = 337.7 K) are quite different. This gives a relative volatility at the sidestream drawoff tray of about 24. Thus, the vapor composition of 4.04 mol% DME has a liquid in equilibrium with it that is only 0.16 mol% DME. The column diameter is 0.61 m. The reboiler heat input is 1.346 MW.

Figure 10.1 gives the flowsheet and the steady-state parameters for the process. Note that the distillate flow rate is quite small because of the low concentration of DME in the feed. This gives a very high reflux ratio ($RR = 41$), which means that reflux-drum level will have to be controlled by manipulating reflux flow rate.

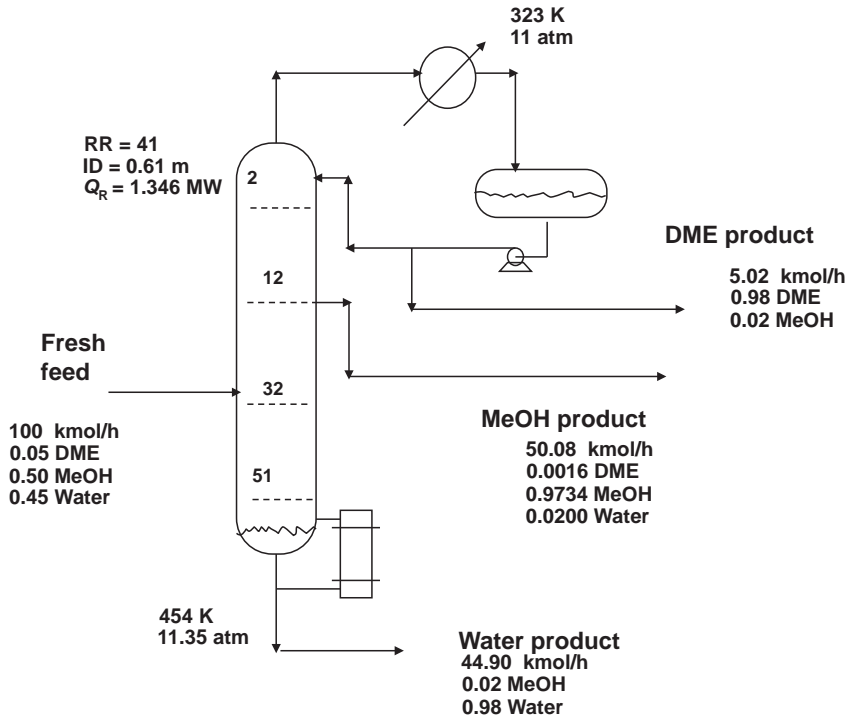


Figure 10.1 Liquid sidestream.

10.1.2 Dynamic Control

The usual sizing calculations are performed, the flowsheet is pressure checked, and the file is exported to Aspen Dynamics. Flow controllers are installed on the feed, distillate, and sidestream. Base level is controlled by manipulating bottoms flow rate. Reflux-drum level is controlled by manipulating reflux flow rate.

The major control structure issues of this sidestream column are how to manipulate the sidestream flow rate and how to manipulate the distillate flow rate. They cannot be fixed or just ratioed to the feed flow rate because changes in feed composition require that the flow rate of the distillate and the sidestream change to achieve the desired purities. Figure 10.2 shows a control structure that provides effective control of this complex column. Figure 10.3 gives the controller faceplates. Note that two of the flow controllers are on “cascade” (remote set points).

The control scheme shown in Figure 10.2 controls the temperature on Stage 3 by manipulating the distillate flow rate and controls the temperature on Stage 51 by manipulating the reboiler heat input. These stages are selected by looking at the temperature and composition profiles shown in Figure 10.4. The two temperature controllers (TC3 and TC51) have 1 min dead times and 100 K temperature transmitter spans. They are tuned by running a relay-feedback test and using the Tyreus–Luyben settings.

Now the remaining issue is how to manipulate the sidestream flow rate. One effective method is to ratio the sidestream flow rate to the reflux flow rate. This lets the sidestream

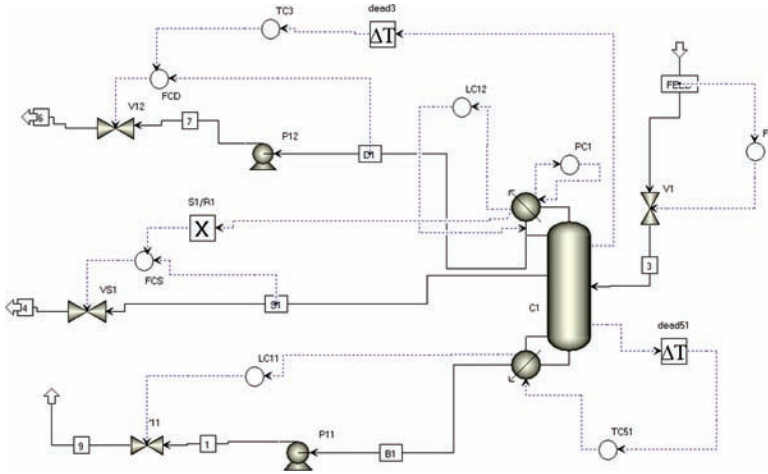


Figure 10.2 Control structure for liquid sidestream column.

flow rate move as disturbances occur. For example, suppose too much MeOH starts to move down the column, this will decrease the temperature on Stage 51, and the TC51 temperature controller will increase the reboiler heat input. This sends more vapor up the column, which increases the reflux-drum level. The level controller increases reflux flow, and the S1/R1 ratio increases the sidestream flow rate, which pulls more MeOH out of the column.

The effectiveness of this control structure is demonstrated in Figures 10.5 and 10.6. The responses of the system to 20% step increases and decreases in feed flow rate are shown in Figure 10.5. The compositions of all three products are returned to their specified values within about 1.5 h. The largest transient deviations occur in the bottoms composition. This could be improved by using a heat-input-to-feed ratio.

Note that the increase in feed flow rate causes the distillate valve to go completely shut for about 20 min, and the decrease in feed flow rate saturates the valve wide open. Remember that the distillate flow rate is very small. Note also in Figure 10.3 that the

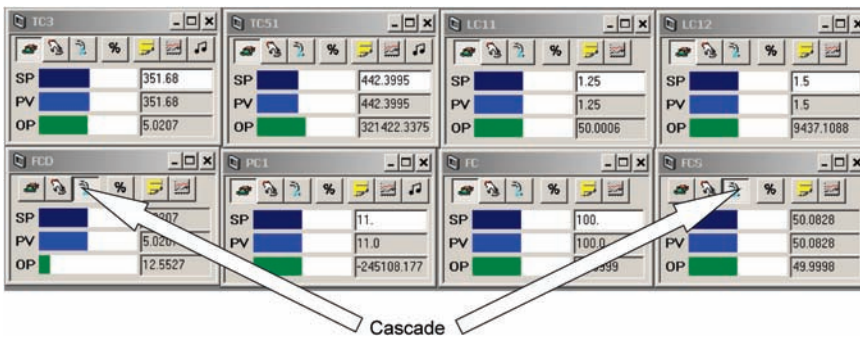


Figure 10.3 Controller faceplates.

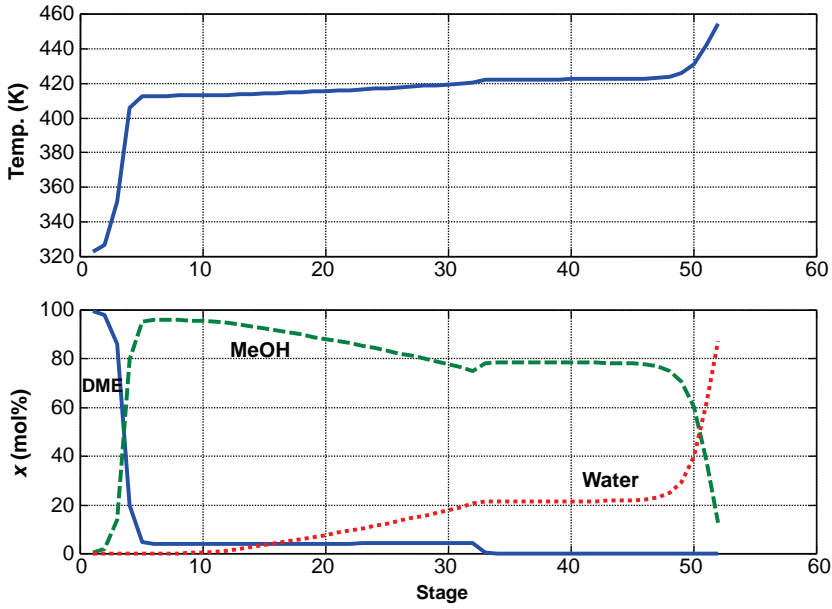


Figure 10.4 Profiles for liquid sidestream column.

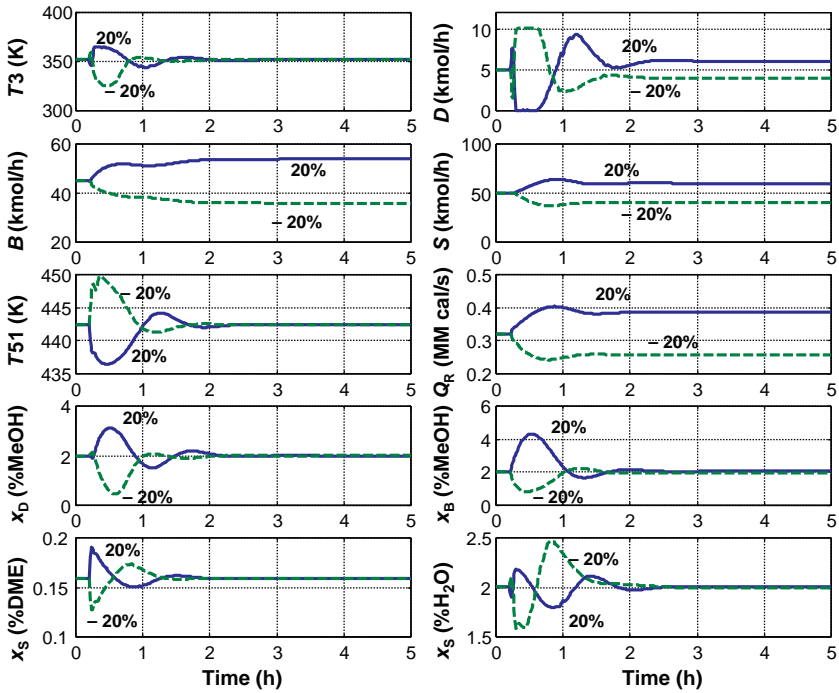
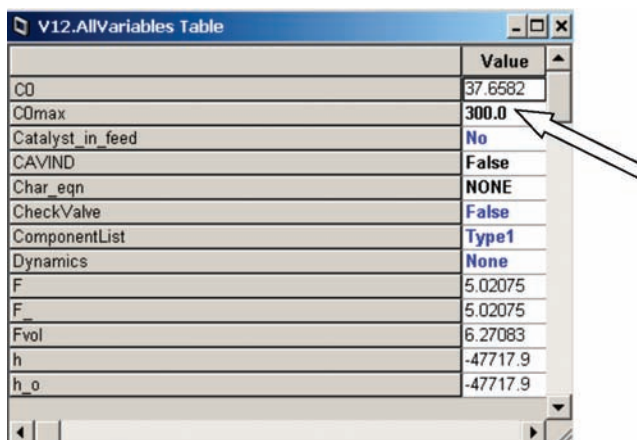


Figure 10.5 Liquid sidestream column: feed rate changes.



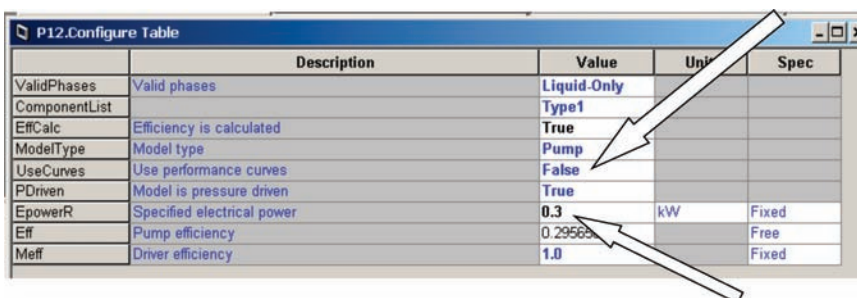
	Value
CO	37.6582
COmax	300.0
Catalyst_in_feed	No
CAVIND	False
Char_eqn	NONE
CheckValve	False
ComponentList	Type1
Dynamics	None
F	5.02075
F _o	5.02075
Fvol	6.27083
h	-47717.9
h _o	-47717.9

Figure 10.6 Increasing valve size.

steady-state controller output signal to the distillate valve (V12) is only 13% instead of the normal 50%. The size of the control valve and the pump work exported from Aspen Plus were both increased to get more rangeability in the distillate flow rate. The valve size is changed by clicking the icon, right clicking, and selecting *Forms* and *All Variables*. Then the value of *COmax* is increased (see Fig. 10.6).

To change the pump power, click the pump P12 icon, right click, and select *Forms* and *Configure* (see Fig. 10.7). Use the drop-down arrow to change *UseCurves* from *True* to *False*, and increase the *EpowerR*.

Figure 10.8 gives responses for three feed composition disturbances. The solid lines show what happens when the DME in the feed is increased from 5 to 7 mol% DME (with MeOH reduced by a corresponding amount). The dashed lines show what happens when the DME in the feed is decreased from 5 to 3 mol% DME. The dotted lines are for an increase in the MeOH concentration in the feed from 50 to 55 mol% (with water reduced by a corresponding amount). Product purities are well maintained.



	Description	Value	Unit	Spec
ValidPhases	Valid phases	Liquid-Only		
ComponentList		Type1		
EffCalc	Efficiency is calculated	True		
ModelType	Model type	Pump		
UseCurves	Use performance curves	False		
PDriven	Model is pressure driven	True		
EpowerR	Specified electrical power	0.3	kW	Fixed
Eff	Pump efficiency	0.29565		Free
Meff	Driver efficiency	1.0		Fixed

Figure 10.7 Increasing pump work.

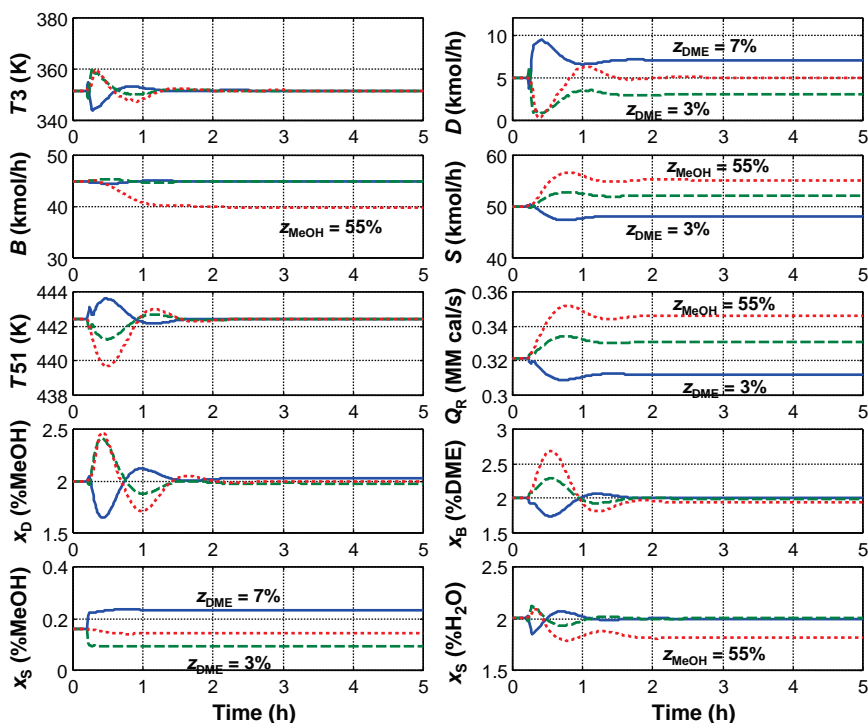


Figure 10.8 Liquid sidestream column: feed composition changes.

10.2 VAPOR SIDESTREAM COLUMN

Vapor sidestream columns are frequently used when the feed stream is a ternary mixture and the concentration of the *heaviest* component is small. The other criterion is that the relative volatility between the intermediate component and the heaviest component must be fairly large.

To illustrate the latter limitation, suppose we take the same ternary mixture considered in Section 10.1. However, now the feed composition is 45 mol% DME, 50 mol% MeOH, and 5 mol% water. Can a vapor sidestream column be effectively used? The normal boiling point of MeOH is 337.7 K. The normal boiling point of water is 373.2 K. This is a much smaller difference than is the case for DME and MeOH (248.4 K vs. 337.7 K). The result is a relative volatility between MeOH and water of about 1.73.

All the water in the feed must flow down past the vapor sidestream drawoff tray. If the liquid composition on this tray is 5.4 mol% water, the vapor composition is 3.2 mol% water. Thus, the purity of the sidestream is low. The only way to reduce the impurity of water in the sidestream is to reduce the water concentration in the liquid by drastically increasing the internal flow rates of the vapor and liquid in the column, that is, increase the RR. This makes the sidestream configuration uneconomical for this chemical separation.

10.2.1 Steady-State Design

In order to consider a reasonable system to illustrate a vapor sidestream column, we change the feed stream to contain *n*-butanol (BuOH) instead of water. The normal boiling point of *n*-butanol is 390.8 K compared with 337.7 K for MeOH. This produces a relative volatility of about 4.4; thus, a *vapor* sidestream product with only 1 mol% BuOH can be produced with an RR of 1.07. The composition of the *liquid* on the sidestream drawoff tray is 4.3 mol% BuOH.

The column has 51 stages, and the feed is introduced on Stage 21. The vapor sidestream is withdrawn from Stage 41. The column operates at 11 atm. Figure 10.9 gives the flowsheet with stream conditions and design parameters for this vapor sidestream column with a ternary feed stream of composition 45 mol% DME, 50 mol% MeOH, and 5 mol% BuOH. The column diameter is 0.635 m. The reboiler heat input is 1.075 MW.

10.2.2 Dynamic Control

Since the RR is 1.07, reflux-drum level can be controlled by either distillate or reflux. We select distillate flow to control level to gain the advantage of proportional-only control smoothing out the disturbances to a downstream process. The reflux is manipulated to control the temperature on Stage 3 at 339.5 K, which maintains the purity of the DME product. Figure 10.10 gives the temperature and composition profiles in the column. Note that the BuOH *vapor* composition y_{BuOH} is smaller than the BuOH *liquid* composition x_{BuOH} on all trays below the feed tray. This illustrates why the sidestream is removed as a vapor instead of a liquid.

The very small bottoms flow rate implies that the base level should be controlled by reboiler heat input and not by bottoms flow rate. The temperature on Stage 50 is controlled

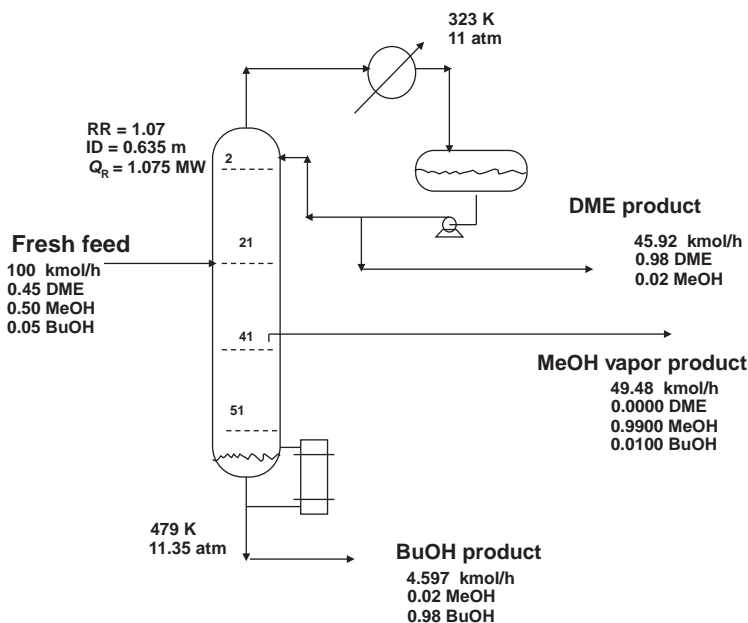


Figure 10.9 Vapor sidestream.

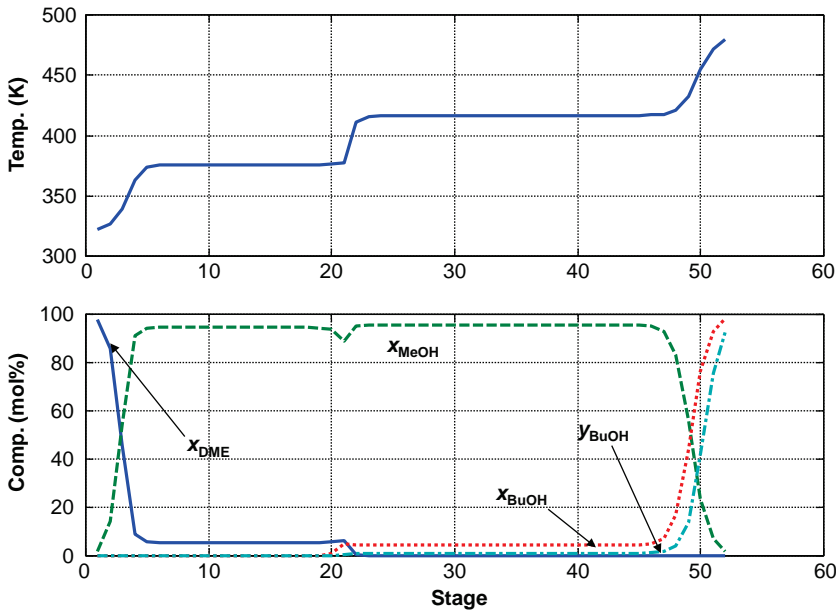


Figure 10.10 Profiles for vapor sidestream column.

by manipulating the bottoms flow rate. It is important to note that the base-level controller must be on automatically for the temperature controller to work because changing the bottoms flow rate has no *direct* effect on Stage 50 temperature. The level loop is “nested” inside the temperature loop.

The key control structure issue is how to set the vapor sidestream flow rate. It certainly must change as disturbances enter the column. One effective way to achieve this is to ratio the sidestream flow rate to the reboiler heat input. This control structure is shown in Figure 10.11. The two temperature controllers (TC3 and TC50) have 1 min dead times and 100 K

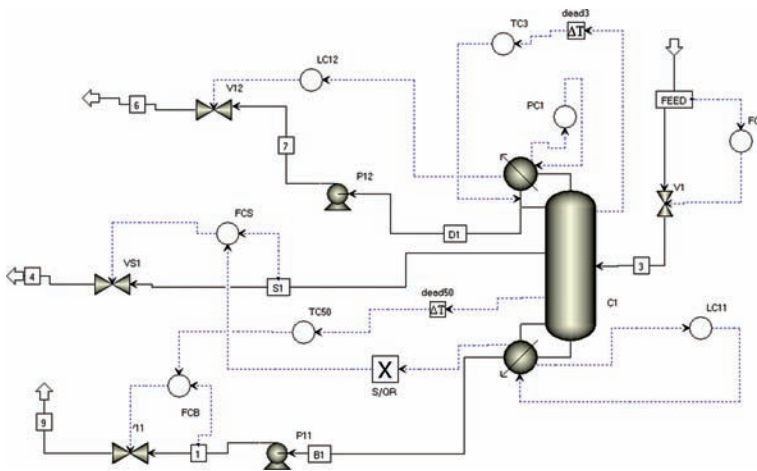


Figure 10.11 Control structure for vapor sidestream column.

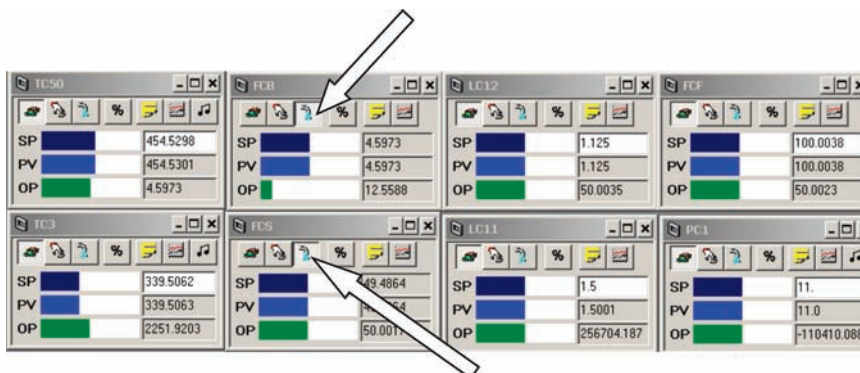


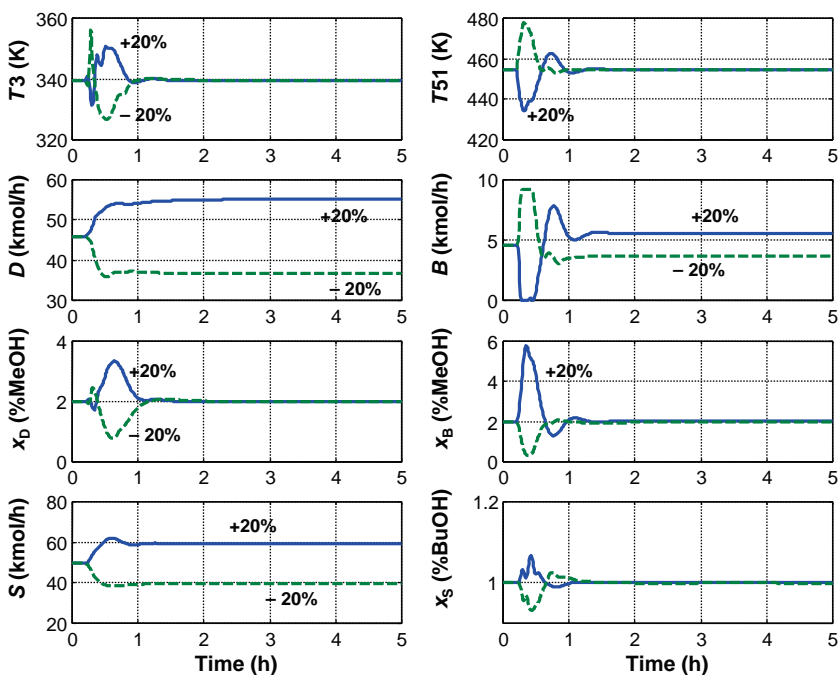
Figure 10.12 Controller faceplates.

temperature transmitter spans. They are tuned by running a relay-feedback test and using the Tyreus–Luyben settings. The TC3 controller manipulating reflux flow rate is tuned first with the TC50 controller on manual. Controller tuning constants are $K_C = 0.46$ and $\tau_I = 9.2$ min. Then, the TC50 controller manipulating bottoms flow rate is tuned with the TC3 controller on automatic (sequential tuning). The tuning constants are $K_C = 3.8$ and $\tau_I = 30$ min. Note that this second loop is slower than the first. Controller faceplates are shown in Figure 10.12. The FCD flow controller is “on cascade” since its setpoint comes from the TC3 temperature controller. The FCS flow controller is also “on cascade” since its setpoint comes from the S/Q_R ratio. Note that the controller output signal for the bottoms flow controller FCB is only 14%. The control valve size and the bottoms pump power were increased to provide more rangeability of the very small bottoms flow rate.

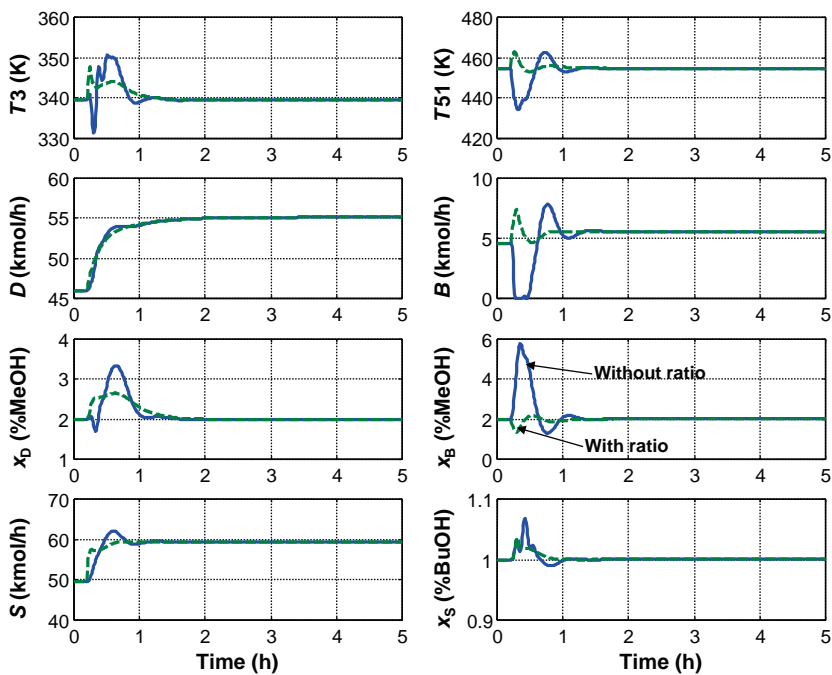
The effectiveness of this control structure is demonstrated in Figures 10.13 and 10.14 for feed rate and feed composition disturbances. Responses to step increases and decreases in feed flow rate of 20% are shown in Figure 10.13a. Stable base-level regulatory control is achieved. Note that the bottoms flow rate saturates wide open or completely closed during these transients because of its small flow rate. Product purities return fairly close to their desired levels, but there is a large transient deviation in the bottoms purity for the +20% step increase.

The use of a steam-to-feed ratio greatly improves this response, as shown in Figure 10.13b. The base-level controller output signal resets the reboiler heat-input-to-feed ratio. The steady-state ratio is 0.038689 (in the required Aspen Dynamic units of “GJ/h” per kmol/h”). The output range of the level controller is changed from 0 to 0.1, and the TC50 controller is retuned ($K_C = 3.2$ and $\tau_I = 29$ min). The deviation in bottoms purity is greatly reduced, and saturation of the bottoms valve is also avoided.

Responses to three feed composition disturbances are given in Figure 10.14. The solid lines are when the BuOH concentration in the feed is increased from 5 to 7 mol%, with the MeOH reduced accordingly. The dashed lines are when the BuOH concentration in the feed is decreased from 5 to 3 mol%, with the MeOH increased accordingly. The dotted lines are when the DME concentration in the feed is decreased from 45 to 40 mol%, with the MeOH increased accordingly. Product purities are held fairly close to their desired values, with the sidestream BuOH composition undergoing the largest changes.



(a)



(b)

Figure 10.13 (a) Vapor sidestream column: feed rate changes. (b) Feed rate +20% change with and without ratio.

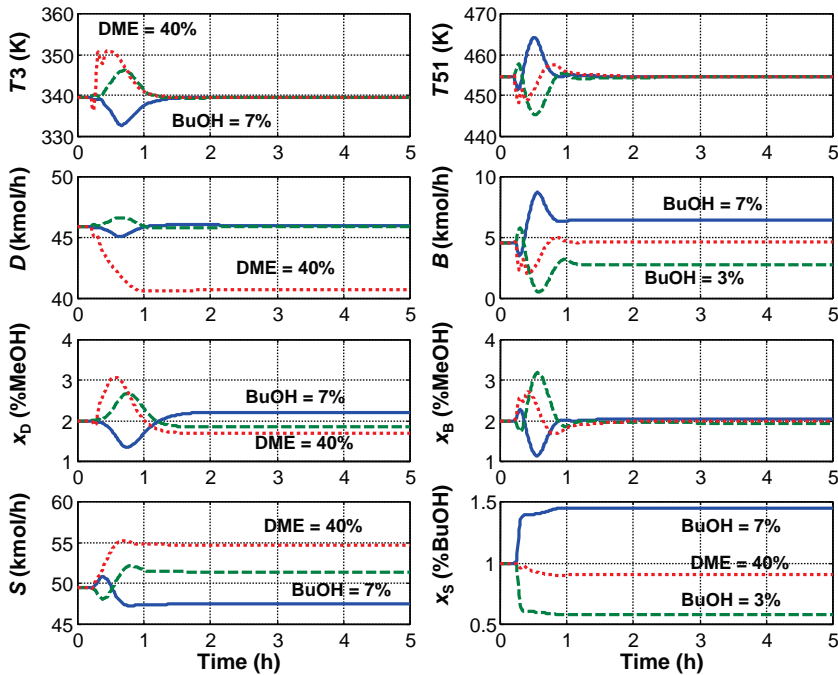


Figure 10.14 Vapor sidestream column: feed composition changes.

10.3 LIQUID SIDESTREAM COLUMN WITH STRIPPER

The flexibility of a sidestream column is greatly increased if additional separation columns are added. This can extend their economic applicability to feeds that have significant amounts of all components and to systems in which relative volatilities are not large. If the sidestream is a liquid, a stripper can be added that removes some of the light impurity in the liquid sidestream coming from the main tower.

To illustrate this configuration, we take the same DME/MeOH/water system studied in Section 10.1, but increase the feed concentration of DME from a small 5 mol% up to a significant 35 mol%.

10.3.1 Steady-State Design

The feed flow rate is 100 kmol/h, and the feed is fed on Stage 32 of a 52-stage column. A liquid sidestream is withdrawn from Stage 12 and is fed into a small 6-stage stripping column. The flowsheet is given in Figure 10.15. The bottoms from the stripper is the MeOH product. The vapor from the stripper is fed back to the main column.

The presence of a stripper provides additional degrees of freedom. In addition to being able to adjust the liquid sidestream drawoff rate from the main column, the heat input to the stripper reboiler can also be adjusted. Of course, the stripper can do nothing to change the amount of the heaviest component (water) that is in the stream that is fed to it. Therefore, the main column must be designed so that the water concentration in the liquid at the sidestream drawoff tray is small. In the design shown in Figure 10.15, the concentration of water is only 0.3 mol% at Stage 12.

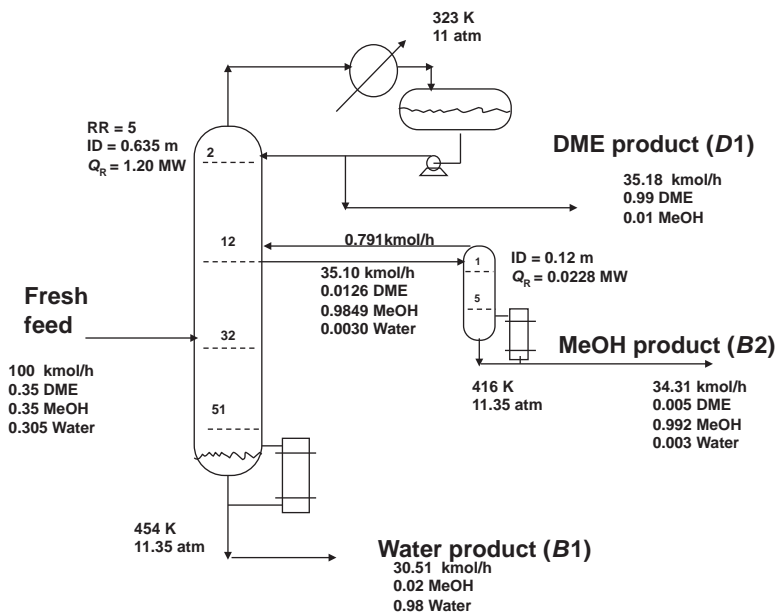


Figure 10.15 Liquid sidestream with stripper.

However, the stripper is able to adjust the amount of the lightest component that leaves as its bottoms product $B2$. Therefore, larger amounts of DME can be present in the liquid at the sidestream tray. This is why the sidestream/stripper configuration can handle larger concentrations of the lightest component in the feed. It is also why this configuration is often economical in systems where the relative volatility between the lightest and intermediate component is not large.

Achieving the steady-state design of this more complex system is not a trivial job. There is a recycle stream and four degrees of freedom. The design was successfully achieved by a sequential approach:

1. Initial guesses were made of the flow rates of the distillate, stripper bottoms and sidestream, and the RR of the main column.
2. A Design Spec/Vary was set up to achieve a distillate impurity $x_{D1(\text{MeOH})}$ of 1 mol% MeOH by adjusting the distillate $D1$ flow rate.
3. A second Design Spec/Vary was set up to achieve a main-column bottoms $B1$ impurity $x_{B1(\text{MeOH})}$ of 0.5 mol% MeOH by adjusting the flow rate of the liquid sidestream $S1$ withdrawn from the main column that is fed to the stripper.
4. A third Design Spec/Vary was set up to achieve a stripper bottoms $B2$ impurity $x_{B2(\text{DME})}$ of 2 mol% DME by adjusting the ratio of the stripper bottoms to the stripper feed ($B2/S1$).

The RR of 5 was held constant during these convergences. This additional degree of freedom could be used to adjust the water concentration in the sidestream fed to the stripper. An RR of 5 gives 0.3 mol% water in the sidestream, which permits a high-purity MeOH product to be produced.

Figure 10.15 gives the steady-state conditions. The energy consumption in the main column is 1.20 MW, and in the stripper it is only 0.0228 MW. The diameter of the main column is 0.635 m and the diameter of the stripper is 0.12 m.

10.3.2 Dynamic Control

The flowsheet shown in Figure 10.15 does not show the plumbing required to run a realistic pressure-driven dynamic simulation. The key feature is that the pressure in the stripper must be greater than that in the main column so that vapor can flow from the top of the stripper back to the main column. Therefore in the simulation, a pump and a control valve are placed in the liquid sidestream. A control valve is also placed in the stripper overhead vapor line. All this plumbing is shown in Figure 10.16. In a real physical setup, it is usually possible to use elevation differences to provide the necessary differential pressure driving force to get the liquid to flow from the main column into the stripper at a higher pressure and avoid the use of a pump.

The usual sizing calculations are performed for both the main column and the stripper (10 min liquid holdups in column bases and reflux drum). The flowsheet is pressure checked and the file is exported to Aspen Dynamics.

A control structure is developed for this more complex system. The various loops are described below. The key issues are how to manipulate the sidestream and how to maintain the compositions of the three product streams:

1. Feed is flow controlled.
2. With an RR of 5, the reflux-drum level is controlled by manipulating reflux flow rate.
3. The temperature on Stage 4 of the main column is controlled by manipulating distillate.
4. Base level is controlled by manipulating bottoms flow rate in both columns.
5. Pressure in the main column is controlled by manipulating condenser heat removal.
6. Pressure in the stripper is controlled by manipulating the valve in the vapor line V22.
7. The temperature on Stage 51 in the main column is controlled by manipulating reboiler heat input to the main column.

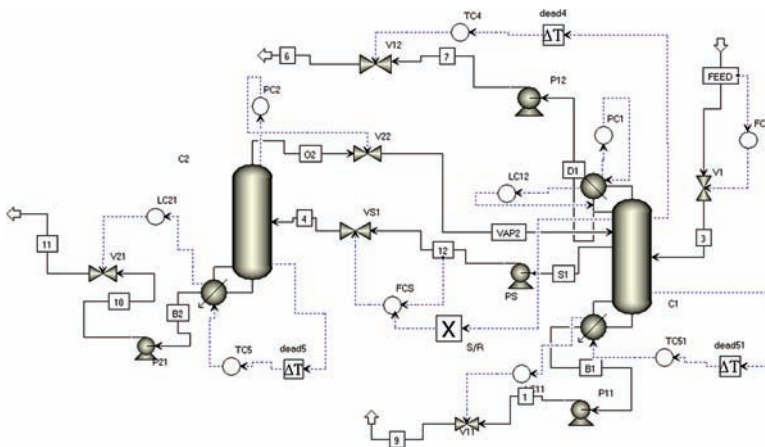


Figure 10.16 Control scheme for liquid sidestream with stripper.

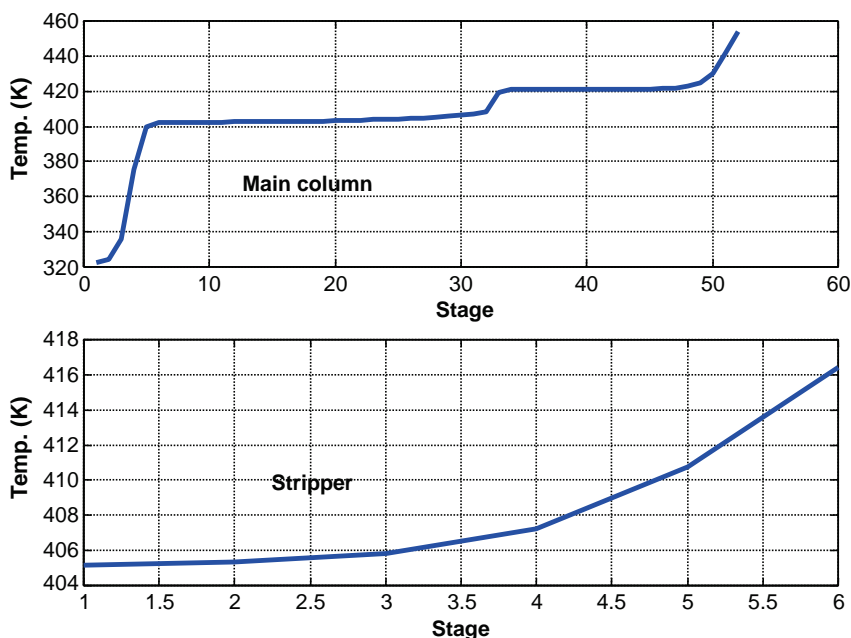


Figure 10.17 Temperature profiles.

8. The temperature on Stage 5 in the stripper is controlled by manipulating stripper reboiler heat input.
9. The sidestream flow rate is ratioed to reflux flow rate.

This last loop is the most important feature of this control structure. It permits the sidestream to change as disturbances enter the system.

The locations of the temperature control trays are selected by looking at the temperature profiles in the two columns, shown in Figure 10.17. The three temperature controllers (TC4 and TC51 in the main column and TC5 in the stripper) have 1 min dead times and 100 K temperature transmitter spans. They are tuned individually by running a relay-feedback test with the other two controllers on manual and using the Tyreus–Luyben settings. The controller tuning constants are given in Table 10.1.

Note that the TC4 temperature control loop is “nested” inside the reflux-drum level controller since a change in distillate flow rate has no *direct* effect on Stage 4 temperature. The tuning of the reflux-drum level controller (LC12) affects the tuning of the TC4 temperature controller, as Table 10.1 shows. Performance is improved by tightening up on the level controller. This is illustrated in Figure 10.18 for a 20% increase in feed flow rate.

TABLE 10.1 Stripper Temperature Controller Parameters

	TC4 with LC12 Gain = 2	TC4 with LC12 Gain = 5	TC51	TC5
K_U	3.67	2.65	2.98	18.0
P_U (min)	11.4	8.4	11.4	3.6
K_C	1.15	0.89	0.93	5.64
τ_1 (min)	25.1	18.5	6.6	7.92

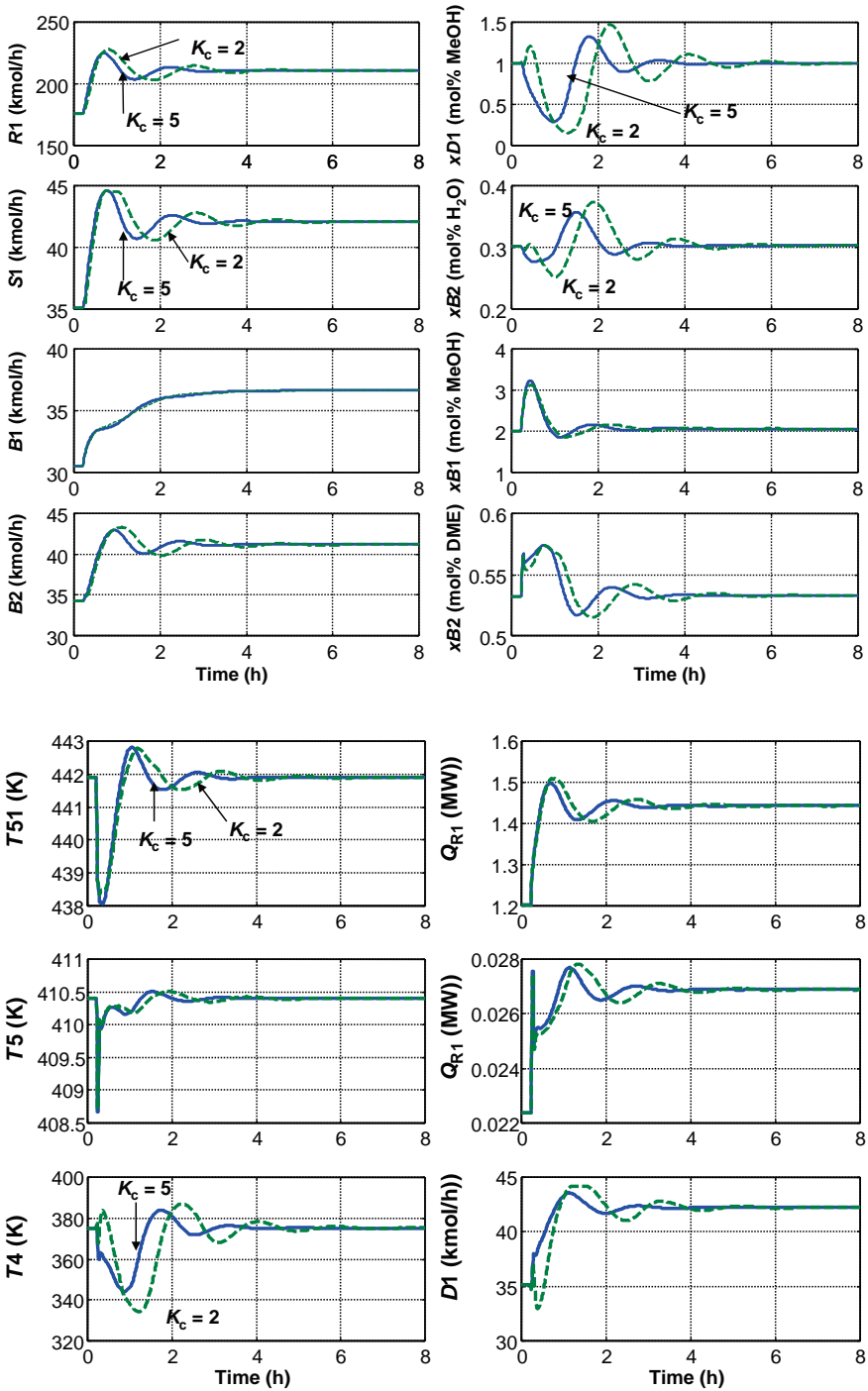
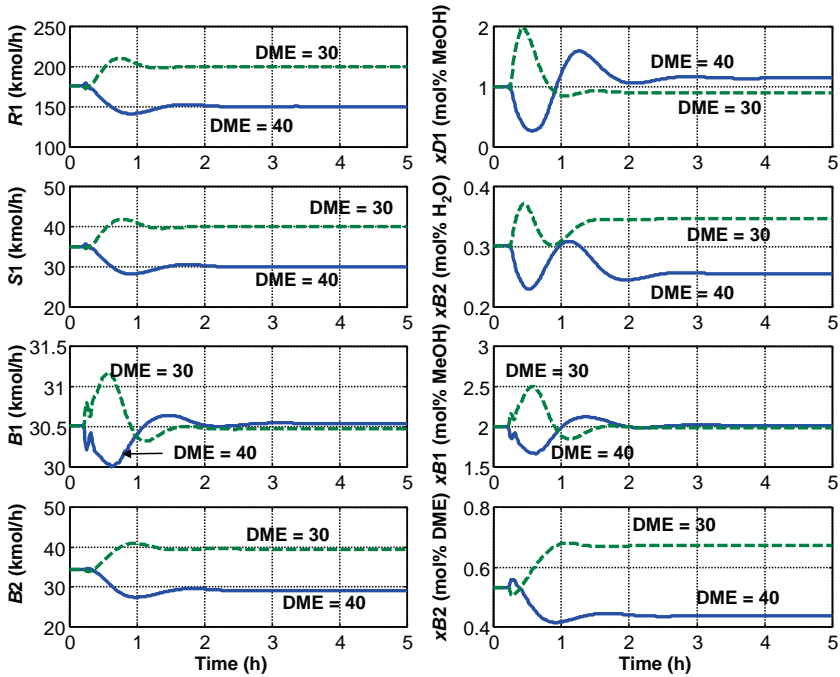
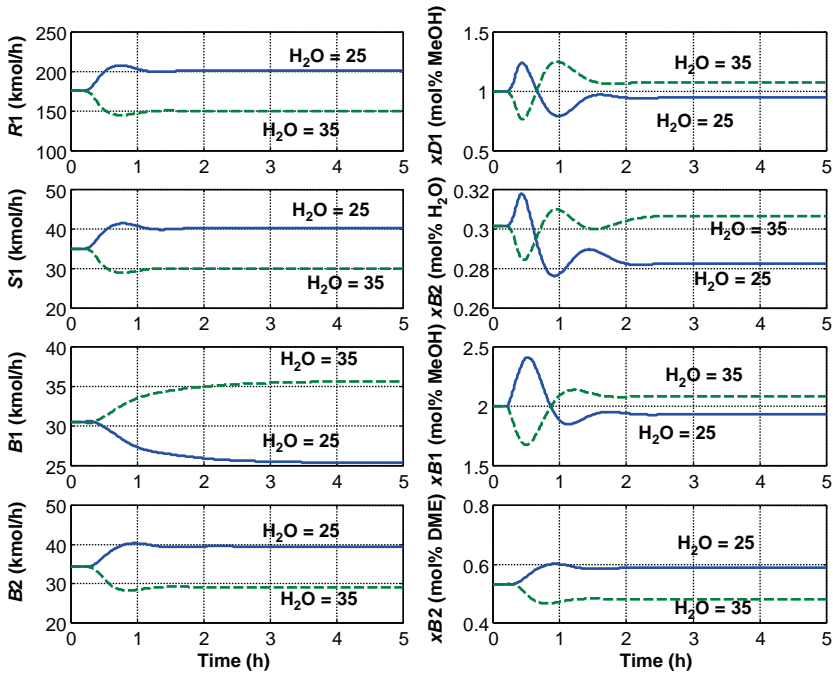


Figure 10.18 The +20% feed rate: level control gains 2 and 5.



(a)



(b)

Figure 10.19 (a) Feed composition change: DME 35 to 40/30. (b) Feed composition change: water 30 to 35/25.

The responses for feed composition disturbances are shown in Figure 10.19. In Figure 10.19a the feed composition is changed from 35 mol% DME to either 40 mol% or 30 mol% DME (with a corresponding change in MeOH). In Figure 10.19b the feed composition is changed from 30 mol% water to either 35 mol% or 25 mol% water (with a corresponding change in MeOH).

The control structure provides stable base-level regulatory control for all these disturbances. Product purities are maintained fairly close to the desired values.

10.4 VAPOR SIDESTREAM COLUMN WITH RECTIFIER

If the sidestream is a vapor, a rectifier can be added that removes some of the heavy impurity in the vapor sidestream coming from the main tower. To illustrate this configuration, we take the same DME/MeOH/water system studied in Section 10.3 but remove a vapor sidestream below the feed stage.

A very important application of this configuration is cryogenic air separation. The ternary mixture is nitrogen/argon/oxygen. A heat-integrated double column is employed with a rectifier attached to the low-pressure column for the production of argon. The overhead vapor is nitrogen and the bottoms is oxygen.

10.4.1 Steady-State Design

The feed flow rate is 100 kmol/h, and the feed is fed on Stage 11 of a 52-stage column. A vapor sidestream is withdrawn from Stage 31 and is fed into a 12-stage rectifier column. The flowsheet is given in Figure 10.20. The distillate $D2$ from the rectifier is the MeOH product. The bottoms liquid stream from the rectifier is pumped back to Stage 32 of the main column.

The rectifier must operate at a lower pressure than the main column so that the vapor sidestream can flow “down hill.” The main column operates at 11 atm. The pressure in the

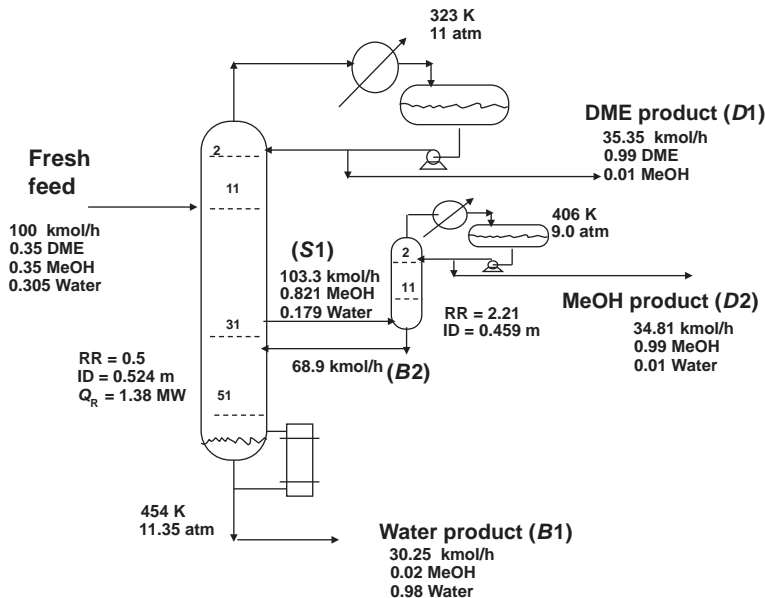


Figure 10.20 Vapor sidestream with rectifier.

rectifier is set at 9 atm to provide some pressure drop over the control valve in the vapor feed line to the rectifier.

The feed composition is 35 mol% DME, 35 mol% MeOH, and 30 mol% H₂O. The distillate from the main column *D1* is the DME product and has an impurity specification of 1 mol% MeOH. The bottoms from the main column *B1* is the water product and has an impurity specification of 2 mol% MeOH. The distillate from the rectifier *D2* is the MeOH product and has an impurity specification of 1 mol% water. The DME concentration in this stream is negligible because there is very little DME in the main column below the feed tray. The feed is fed on Stage 11 near the top. The vapor sidestream is withdrawn down at Stage 31.

The steady-state design of this two-column system with recycle was achieved by a sequential approach. First, the flow rates of the distillates from the two columns were set equal to the molar flow rates of DME and MeOH in the feed. The RR in the main column was set at 2. The flow rate of the vapor sidestream *S1* was set at three times the MeOH product rate, which gives an RR in the rectifier of 2. Note that there is only one degree of freedom in the rectifier, so setting the distillate flow rate completely specifies the column.

Then a guess was made of the composition of the recycle stream $x_{B2,j}$ flowing back to the main column (the bottoms of the rectifier *B2*). The simulation was converged, and the difference between the guessed values of x_{B2} and the calculated values was observed. New guesses were made until there was little difference. Then the recycle loop was closed using a *Tears* specification.

The next step was to adjust the various degrees of freedom to attain the desired purities of the three products. Three Design Spec/Vary functions were used in a sequential manner:

1. The impurity of MeOH in the main column distillate $x_{D1(\text{MeOH})}$ was fixed at 1 mol% MeOH by varying the distillate flow rate *D1*.
2. The impurity of MeOH in the rectifier distillate $x_{D2(\text{MeOH})}$ was fixed at 1 mol% MeOH by varying the distillate flow rate *D2*.
3. The impurity of MeOH in the main column bottoms $x_{B1(\text{MeOH})}$ was fixed at 2 mol% MeOH by varying the flow rate of the vapor sidestream *S1*.

Finally, the RR in the main column was reduced to see the effect on the DME impurity in the sidestream. Since DME is much more volatile than MeOH and is fed above the sidestream drawoff tray, the RR could be reduced to 0.5 without affecting sidestream composition. With an RR of 0.5, the liquid rate in the top section of the main column is quite small (17 kmol/h) compared with the liquid rates lower in the column (180 kmol/h). Therefore, RRs lower than 0.5 were not used.

Figure 10.20 gives design parameters and equipment sizes of this process. The reboiler heat input in the main column is 1.38 MW. It is interesting to compare this with the energy requirements of the sidestream/stripper flowsheet shown in Figure 10.15 ($1.20 + 0.022 = 1.22$ MW). The two processes produce essentially the same three product streams with the same purities. The energy consumptions of the two flowsheets are quite similar.

The diameter of the main column is 0.524 m and the diameter of the rectifier is 0.459 m. Thus, the size of the rectifier is significantly larger than the stripper (0.12 m) in the alternative flowsheet, indicating higher capital cost for the rectifier process. The inherent reason for this is that the MeOH/water separation (which takes place in the rectifier) is more difficult than the DME/MeOH separation (which takes place in the stripper).

10.4.2 Dynamic Control

The flowsheet shown in Figure 10.20 does not show the plumbing required to run a realistic dynamic simulation. The key feature is that the pressure in the rectifier must be less than that in

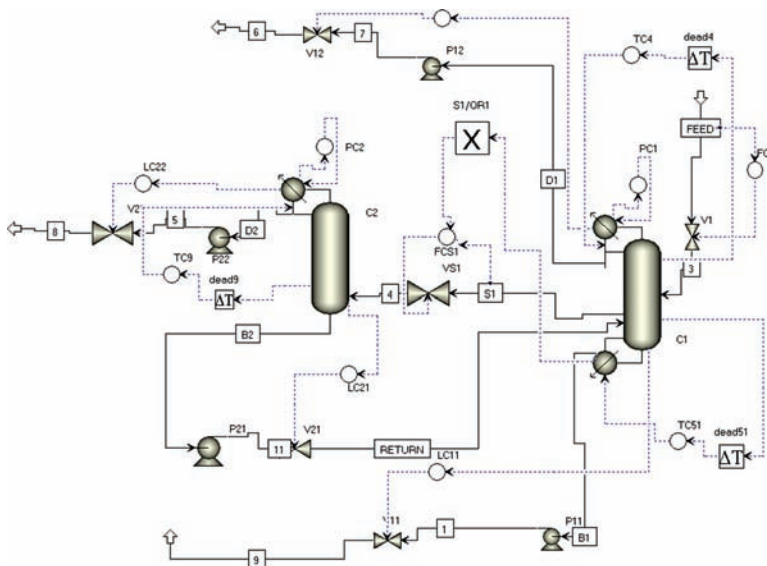


Figure 10.21 Initial control structure.

the main column so that vapor can flow from the main column into the rectifier. Therefore in the simulation, a control valve is placed on the vapor line and a pump and a control valve are placed in the liquid recycle line from the bottom of the rectifier back to the main column. All this plumbing is shown in Figure 10.21. In a real physical setup, it may be possible to use elevation differences to provide the necessary differential pressure driving force to get the liquid to flow from the rectifier into the main column at a higher pressure and avoid the use of a pump.

The usual sizing calculations are performed for both the main column and the rectifier (10 min liquid holdups in column bases and reflux drums). The flowsheet is pressure checked, and the file is exported to Aspen Dynamics.

The development of a control structure for this complex system turned out to be more difficult than for the stripper flowsheet. The initial control scheme evaluated is shown in Figure 10.21. It is a logical extension of the control structure used for the vapor sidestream column in which the vapor sidestream is ratioed to the reboiler heat input. As we will demonstrate below, this structure worked well for some disturbances, but it could not handle decreases in the composition of MeOH in the feed, resulting in a shutdown of the unit.

The various loops of the initial control structure are described below. The key issues are how to manipulate the sidestream and how to maintain the compositions of the three products:

1. Feed is flow controlled.
2. With an RR of 0.5, the reflux-drum level in the main column is controlled by manipulating distillate flow rate.
3. The reflux-drum level in the rectifier is controlled by manipulating its distillate $D2$. The RR is 2.2 in the rectifier.
4. The temperature on Stage 4 of the main column is controlled by manipulating reflux flow rate. Stage 12 is tested as an alternative later.
5. Base levels are controlled by manipulating bottoms flow rates.
6. Pressure in the main column is controlled by manipulating condenser heat removal in the main column condenser.

7. Pressure in the rectifier is controlled by manipulating condenser heat removal in the rectifier condenser.
8. The temperature on Stage 51 in the main column is controlled by manipulating reboiler heat input.
9. The temperature on Stage 9 in the rectifier is controlled by manipulating reflux flow rate in the rectifier.
10. The sidestream flow rate is ratioed to heat input to the reboiler.

The locations of the temperature control trays are selected by looking at the temperature profiles in the two columns, as shown in Figure 10.22. The three temperature controllers (TC4 and TC51 in the main column and TC9 in the rectifier) have 1 min dead times and 100 K temperature transmitter spans. They are tuned individually by running a relay-feedback test with the other two controllers on manual and using the Tyreus–Luyben settings. The controller tuning constants are given in Table 10.2. The only surprising result of this tuning is the very high gain of the TC9 controller.

The response of this control structure for changes in feed flow rate is quite acceptable, as shown in Figure 10.23a. However, when some types of feed composition disturbances are made, the unit shuts down.

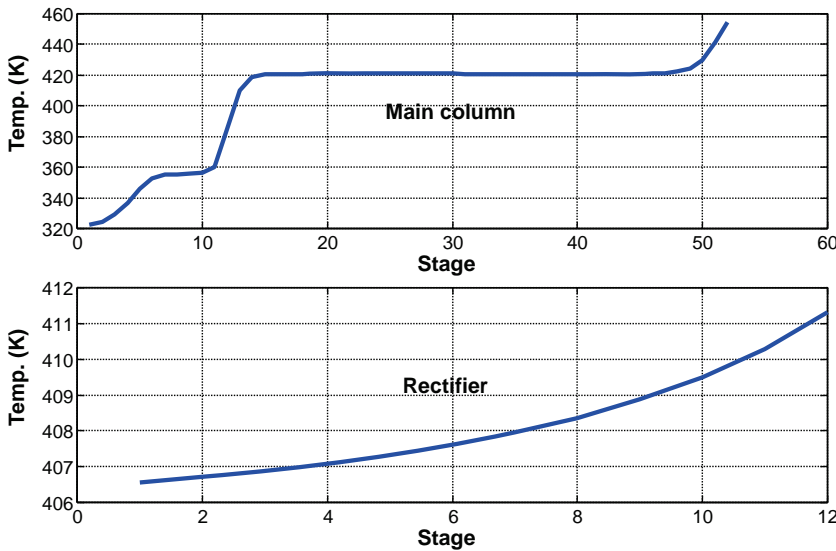
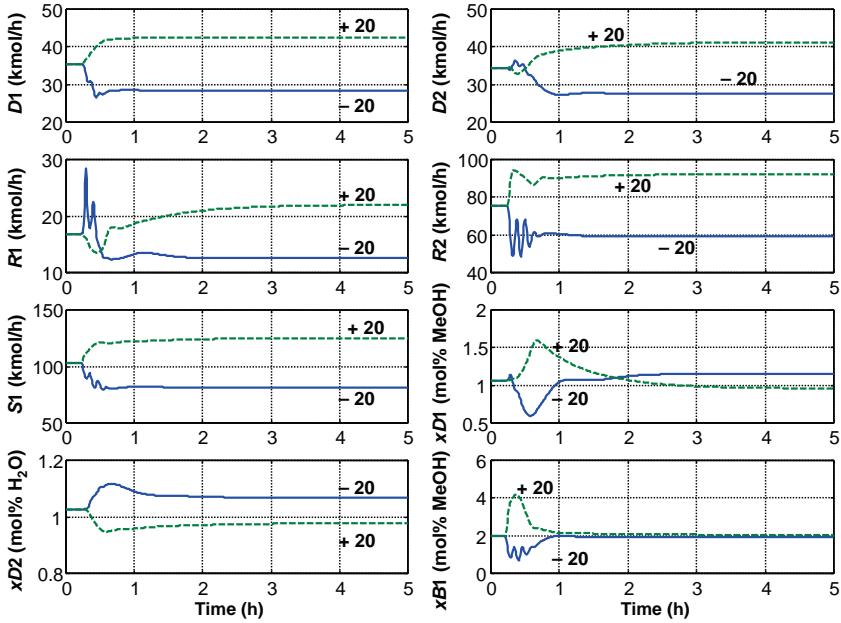


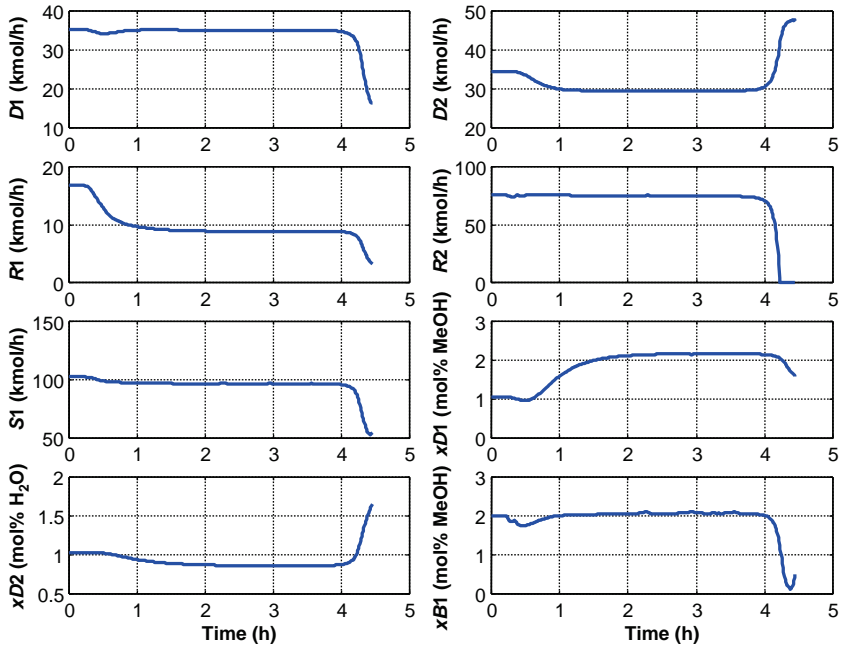
Figure 10.22 Temperature profiles.

TABLE 10.2 Rectifier Temperature Controller Parameters

	TC4	TC51	TC9
K_U	5.54	2.05	190
P_U (min)	4.2	3.6	8.4
K_C	1.73	0.64	59
τ_I (min)	9.24	7.92	18.5



(a)



(b)

Figure 10.23 (a) Initial control structure: feed rate change. (b) Initial control structure: feed composition DME 35–40.

For example, as shown in Figure 10.23b, the process shuts down after about 4 h when the feed composition is changed from 35/35/30 DME/MeOH/H₂O to 40/30/30. The reflux flow rate R_2 in the rectifier goes to zero because the temperature controller responds to lowering temperatures in the rectifier. This occurs because too much DME has worked its way down the column to the vapor sidestream drawoff tray. Once this happens, the rectifier can do nothing about rejecting the light DME. Instead of using Stage 3 for temperature control, Stage 12 was tested, but the results were similar.

To overcome these problems, a new control structure was developed. The flow rate of the reflux in the main column is quite small, so instead of manipulating it to control a temperature, it is held constant for a given feed flow rate (a reflux-to-feed ratio is used). As shown in Figure 10.24, the major change in the control structure is to control the temperature on Stage 12 by manipulating the vapor sidestream flow rate. This is a direct-acting controller: an increase in Stage 12 temperature *increases* the vapor sidestream flow rate to the rectifier to send less vapor up the column. The TC12 temperature controller is tuned by running a relay-feedback test with the other two controllers on manual and using the Tyreus–Luyben settings: $K_C = 0.22$ and $\tau_I = 12$ min.

The modified control structure provides stable regulatory control for both feed flow rate and feed composition. However, as shown in Figure 10.25, the 20% increase in feed flow rate produces a large transient disturbance in the purity of the distillate from the main column with a peak $x_{D1(\text{MeOH})}$ of about 8 mol% MeOH. This can be improved by using feedforward control. Installing a sidestream-to-heat-input ratio, as shown in Figure 10.26, with the ratio reset by the TC12 temperature controller, improves the load response of the system. The temperature controller is retuned ($K_C = 0.10$ and $\tau_I = 12$ min). A maximum controller output of 40 is used since the normal $S1/Q_{R1}$ ratio is 21.

Figure 10.27 compares the responses to a 20% increase in feed flow rate for the two cases, with and without the use of the ratio. The improvement of the purity of the DME product is striking. Figure 10.28a gives results for changes in the DME feed concentration from 35 mol% to either 40 or 30 mol% DME (with corresponding changes in MeOH).

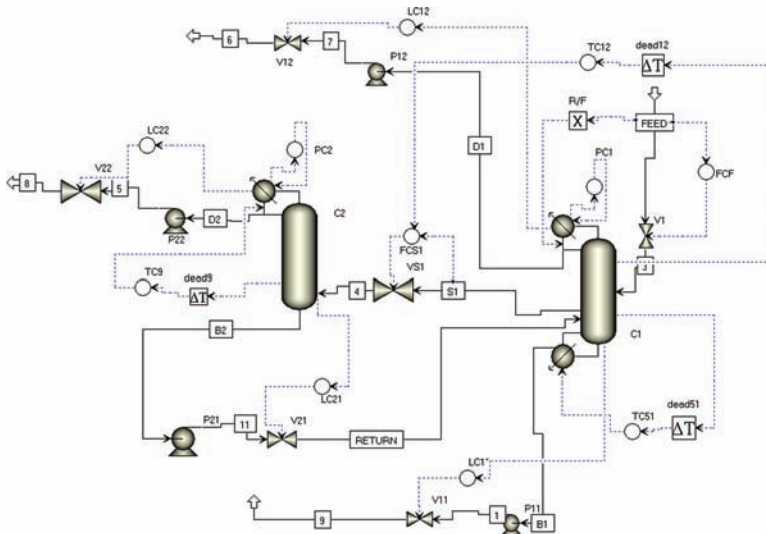


Figure 10.24 Modified control structure.

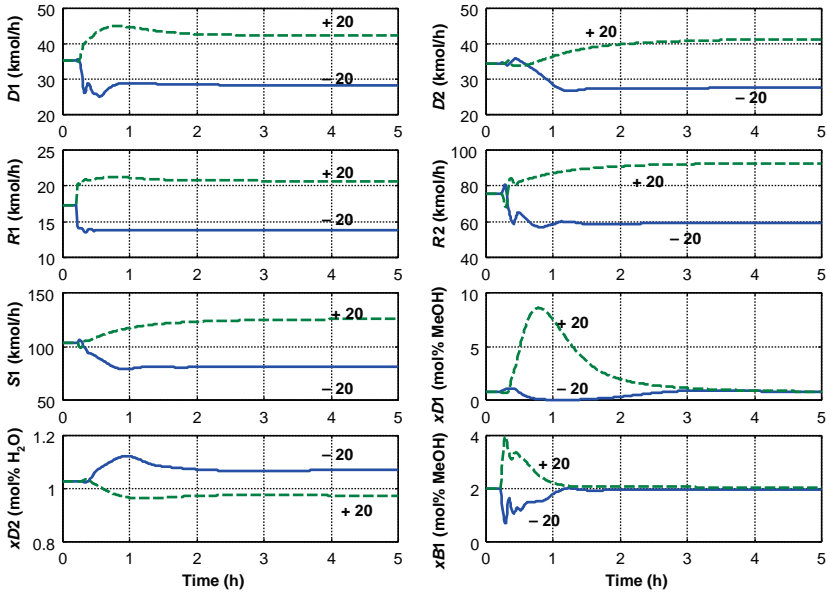


Figure 10.25 Modified control structure: feed rate changes.

Figure 10.28b gives results for changes in the water feed concentration from 30 mol% to either 25 or 35 mol% H₂O (with corresponding changes in MeOH). The control structure handles these many disturbances quite effectively.

Note that the reflux molar flow rate in the main column R1 changes for the changes in feed composition. This occurs because a mass ratio of reflux-to-feed is used and the molar flow rate of the feed is held constant.

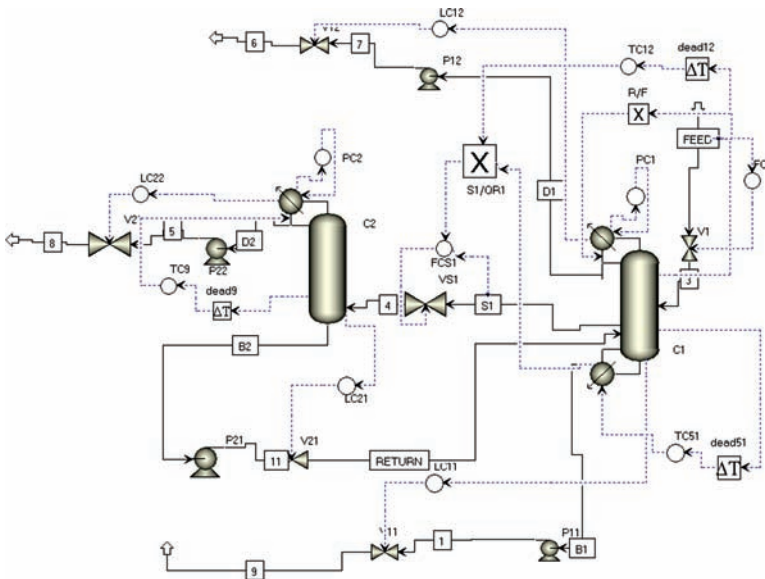


Figure 10.26 Modified control structure with $S1/Q_{R1}$ ratio.

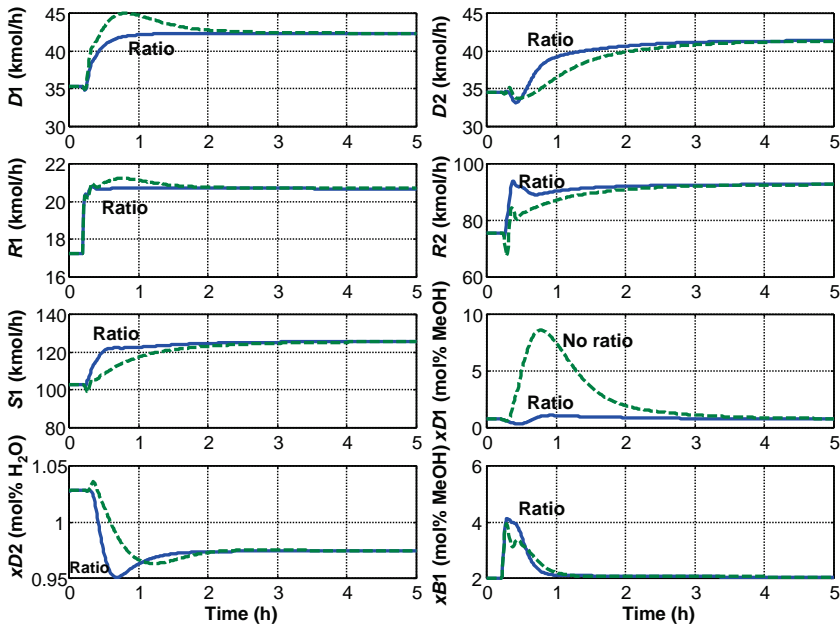
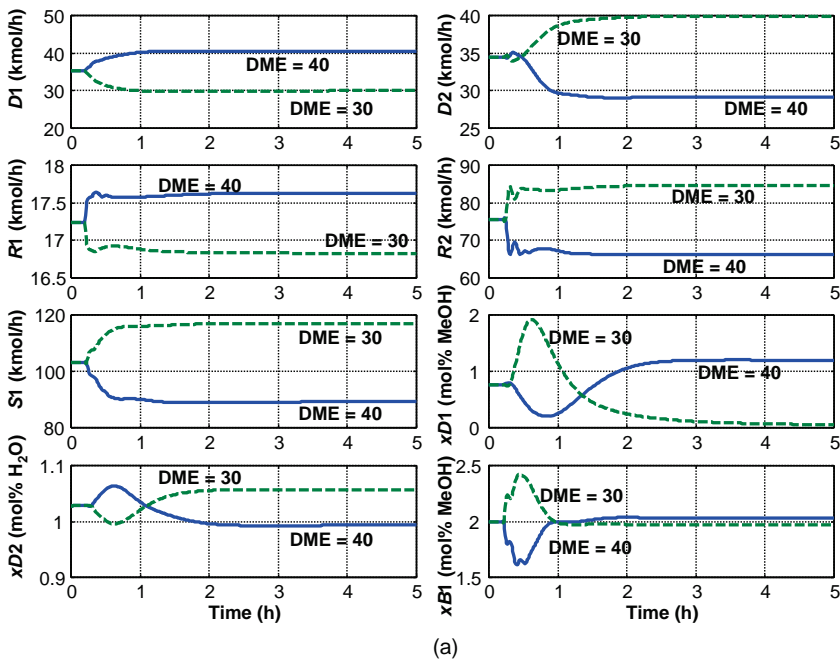


Figure 10.27 The +20% feed rate change with and without $S1/Q_{R1}$ ratio.



(a)

Figure 10.28 (a) Modified control structure: feed composition DME 35 to 30/40. (b) Modified control structure: feed composition H_2O 30 to 25/35.

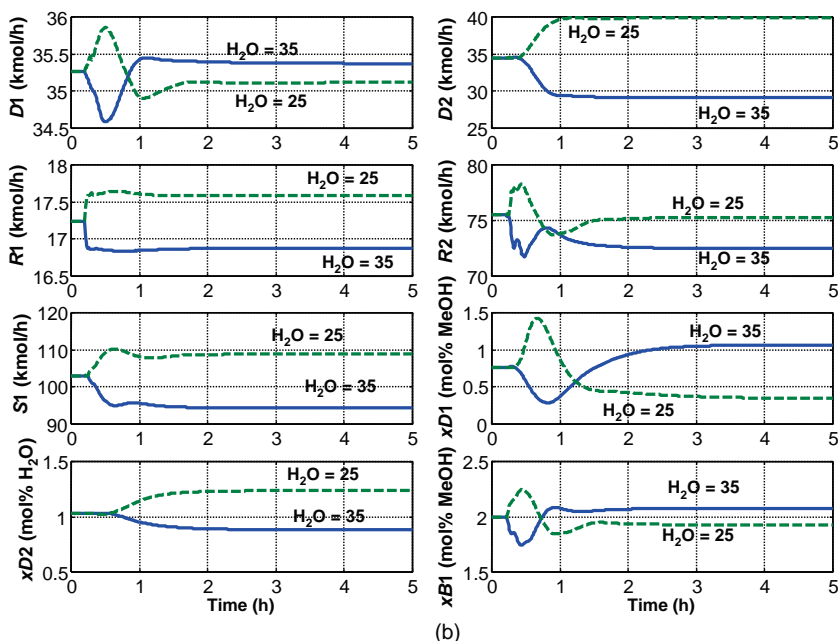


Figure 10.28 (Continued).

10.5 SIDESTREAM PURGE COLUMN

The final sidestream column configuration studied in this chapter is the case where there is a very small amount of the intermediate component in the feed. The lightest component is the distillate product. The heaviest component is the bottoms product. The intermediate component builds up in the middle of the column, forming a composition “bubble.” The objective is to purge off a very small stream from the column at the location where the intermediate composition is fairly large so that there is only a small loss of valuable products. Thus, a high-purity sidestream is not required.

10.5.1 Steady-State Design

The feed flow rate is 100 kmol/h and its composition is 49 mol% DME, 1 mol% MeOH, and 50 mol% water. The feed is fed on Stage 16 of a 31-stage column. A small liquid sidestream is withdrawn from Stage 12 at a flow rate of 1.21 kmol/h with a composition of 17.4 mol% DME, 81.7 mol% MeOH, and 0.9 mol% water. Thus, the purity of the sidestream is low, but this is not a problem because only small amounts of valuable products (the DME and the water) are lost in this small stream.

The purities of the distillate and bottoms products are very high (99.99 mol%). If the specifications for the two product purities were low (e.g., 1 mol% MeOH), the MeOH in the feed could simply be removed in the distillate and bottoms. The column operates at 11 atm with an RR of 0.5 and reboiler heat input of 0.513 MW. Figure 10.29 gives the flowsheet of the process with design parameters.

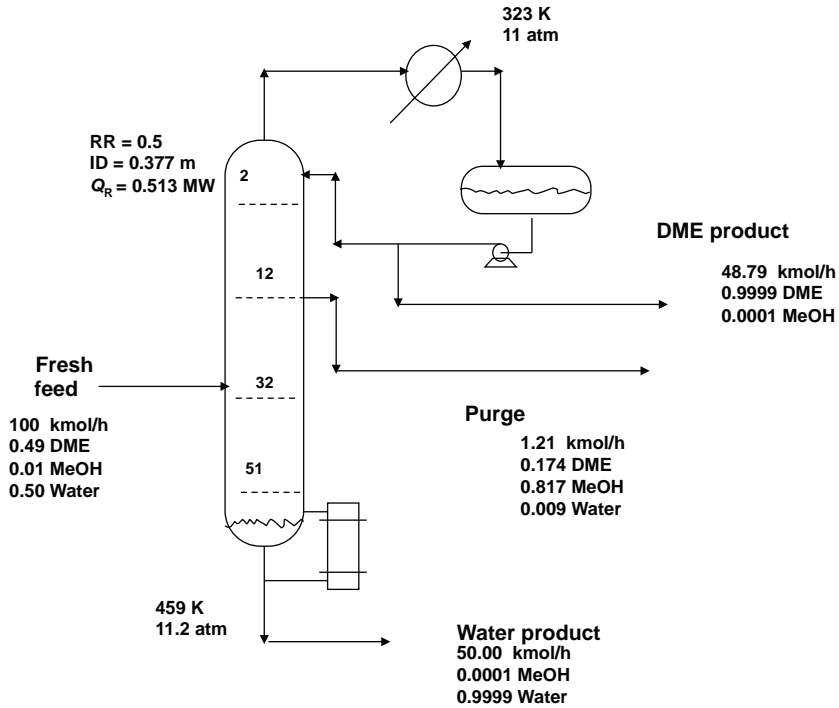


Figure 10.29 Purge sidestream.

The steady-state simulation is converged by first setting the RR equal to 0.5. Then two Design Spec/Vary functions were used: the first adjusted distillate flow rate to achieve 0.01 mol% MeOH in the distillate, and the second adjusted sidestream flow rate to achieve 0.01 mol% MeOH in the bottoms.

The purity of the sidestream and the shape of the composition profiles depend on the RR used. Figure 10.30 gives the composition profiles with an RR of 0.5. Note that there are two

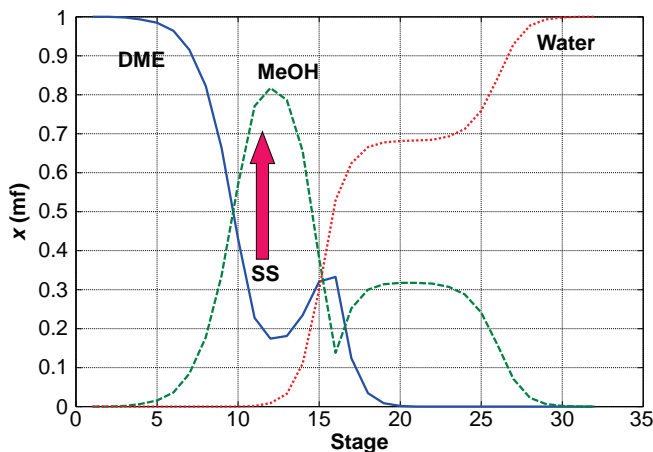


Figure 10.30 Purge sidestream column: RR = 0.5.

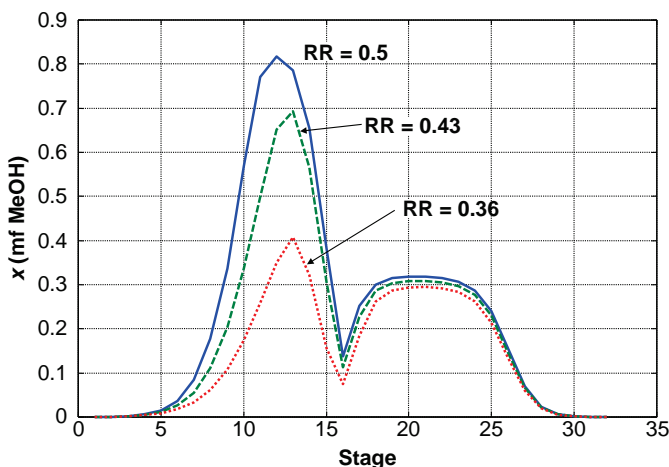


Figure 10.31 Purge sidestream column: effect of RR.

peaks in the MeOH composition profile. The sidestream is withdrawn at Stage 12 where the larger peak occurs. Figure 10.31 shows how the MeOH composition profile changes with RR. The higher the RR, the higher the purity of the sidestream. The RR of 0.5 is selected because it gives a sidestream that is reasonably pure.

10.5.2 Dynamic Control

The control of this purge sidestream column is much more complex than one might expect. Because the sidestream is very small, we might assume that simply flow controlling the sidestream at a rate high enough to remove all the intermediates in the worst case (highest feed concentration) might do the job.

For example, suppose we set the sidestream flow rate at 3 kmol/h instead of the design 1.21 kmol/h, then this reduces the concentration of the MeOH in the sidestream from 81.7 mol% to 33.3 mol% under design conditions where the feed composition is 1 mol% MeOH. Let us consider a control structure in which the temperature on Stage 17 is controlled by manipulating reboiler heat input and reflux flow rate is fixed. Now if the feed composition is increased to 2 mol% MeOH, the sidestream composition only changes to 42 mol% MeOH. This is not enough to remove all the additional MeOH in the feed, so the distillate purity is severely affected (increases to 1.55 mol% MeOH). Thus, a simple control structure with a fixed sidestream flow rate does not provide effective product quality control. The control structure must be able to adjust the sidestream flow rate in some manner so that MeOH cannot drop out of the bottom or go overhead.

An apparently straightforward control structure is to measure the MeOH composition of the sidestream and to control this composition by manipulating sidestream flow rate. As we demonstrate below, this scheme does not work well.

To gain some insight into the problem, singular value decomposition analysis was used. There are three manipulated variables: reflux, reboiler heat input and sidestream flow rate. The steady-state gains between tray temperatures and the three inputs were obtained numerically. The resulting singular values are 119, 15.8, and 2.68. The large condition number indicates that the control of more than one temperature in the column will be

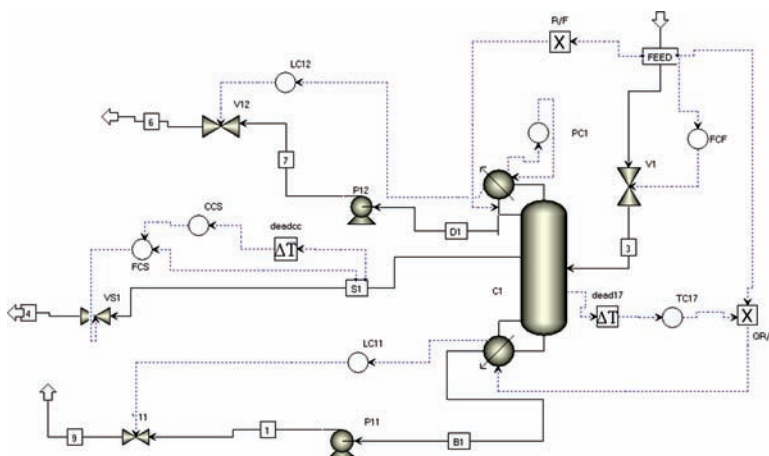


Figure 10.32 Control structure with $x_{S(\text{MeOH})}$ control.

difficult. This was found to be the case. Trying to use two temperature controllers resulted in severe interaction.

Therefore, we assume that an analyzer is available to measure sidestream MeOH composition. A 3 min dead time is used in this loop. Stage 17 temperature is controlled (the location of the steepest part of the temperature profile) by reboiler heat input through a heat-input-to-feed ratio (see Fig. 10.32). The temperature control loop is tuned first ($K_C = 0.159$ and $\tau_1 = 7.9$ min) with the composition loop on manual. Then the composition loop is tuned with the temperature loop on automatic. Note that the flow controller on the sidestream flow is on “cascade” with its setpoint coming from the composition controller. There is also a reflux-to-feed ratio used.

Unfortunately, the relay-feedback test on the composition loop gives very erratic results, as shown in Figure 10.33a, with no symmetrical switches of the controller output and rapid oscillatory response of the process variable (sidestream MeOH composition). The reason for this strange behavior remains a mystery. The resulting controller tuning constants ($K_C = 6.8$ and $\tau_1 = 26$ min) gave unstable responses. Empirical tuning constants of $K_C = 1$ and $\tau_1 = 30$ min give stable response, but poor transient control of product purities. For example, Figure 10.33b gives the response of the system when the MeOH feed composition is increased from 1 to 2 mol%.

Note that there is a huge transient increase in the MeOH impurity in the distillate (upper right graph in Fig. 10.33b), which lasts for over 7 h. Clearly, this performance is unacceptable.

A revised control structure was developed. Instead of controlling the MeOH composition of the sidestream, the MeOH composition of the distillate is controlled by manipulating the sidestream flow rate (see Fig. 10.34). The relay-feedback test of this loop gives reasonable responses ($K_U = 1.16$ and $P_U = 70$ min). If the Tyreus–Luyben settings are used ($K_C = 0.363$ and $\tau_1 = 156$ min), the response is somewhat oscillatory when the MeOH feed composition is increased from 1 to 2 mol%, as shown in Figure 10.35. However, if the Ziegler–Nichols (ZN) settings are used ($K_C = 0.527$ and $\tau_1 = 59$ min), the response is quite good, as shown in Figure 10.36. The transient disturbance in the distillate purity is reduced because the sidestream is increased more quickly due to the higher gain and smaller reset time.

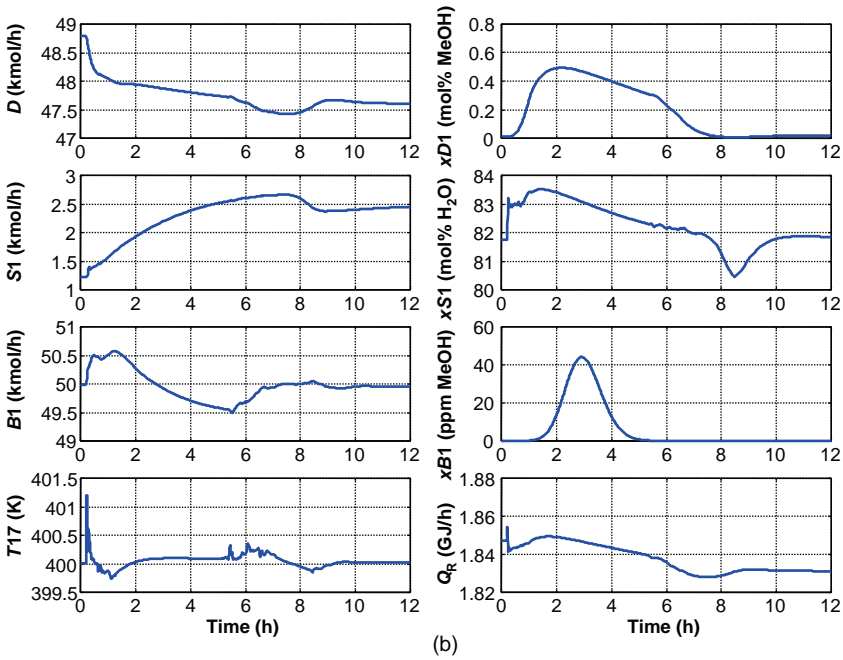
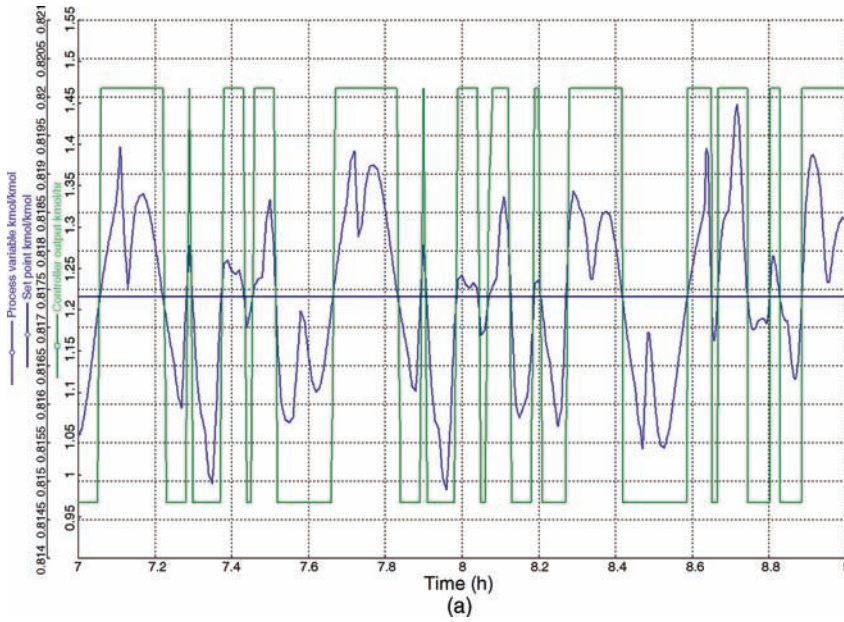


Figure 10.33 (a) Erratic relay-feedback test on CC. (b) Feed 1 to 2 mol% MeOH: CC sidestream with empirical tuning.

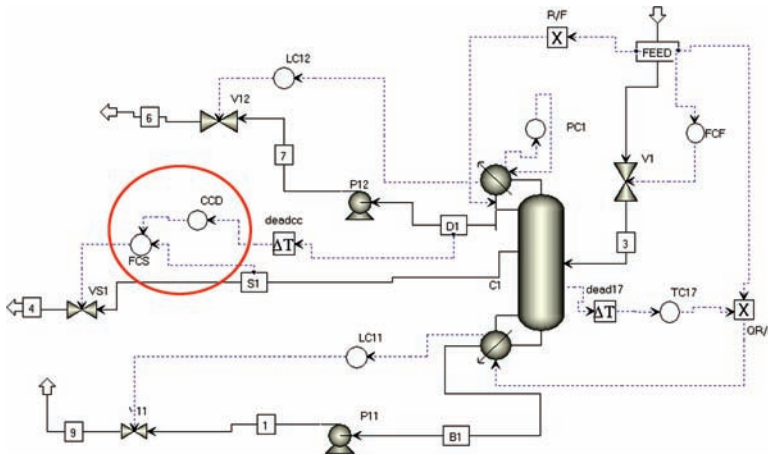


Figure 10.34 CC distillate with sidestream.

Figure 10.37 gives responses for 20% increase and decrease in feed flow rate, using ZN settings in the distillate composition controller. Figure 10.38 gives responses when the DME in the feed is increased from 49 to 54 mol% and when it is decreased from 49 to 44 mol% (with a corresponding change in the water composition). The modified control structure handles all these disturbances quite well.

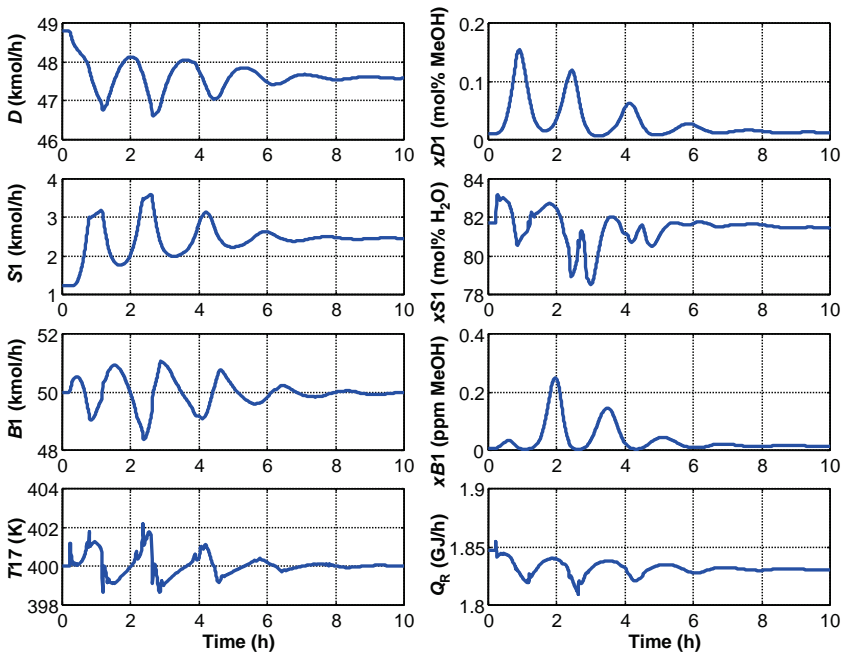


Figure 10.35 Feed 1–2 mol% MeOH: CC distillate; TL settings.

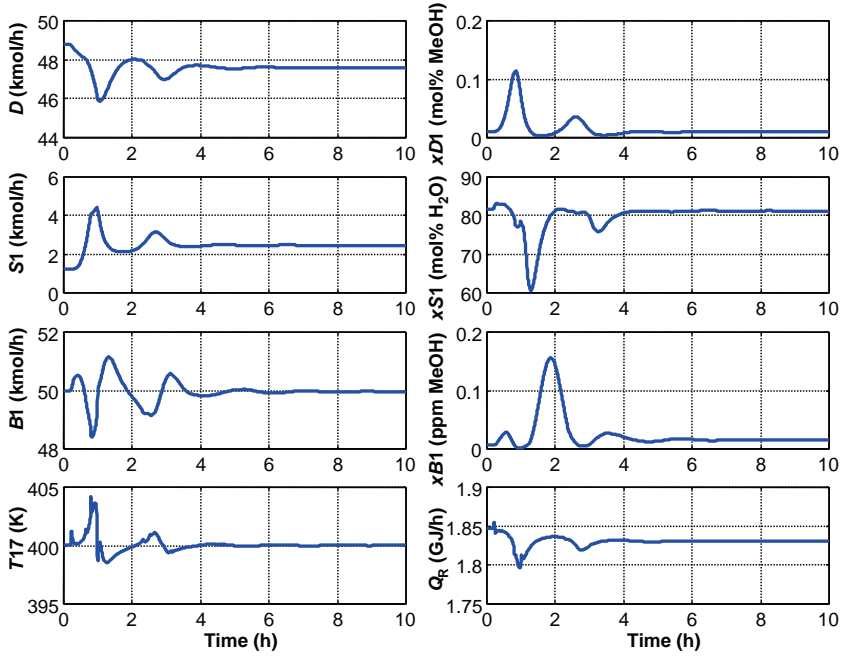


Figure 10.36 Feed 1–2 mol% MeOH: CC distillate; ZN settings.

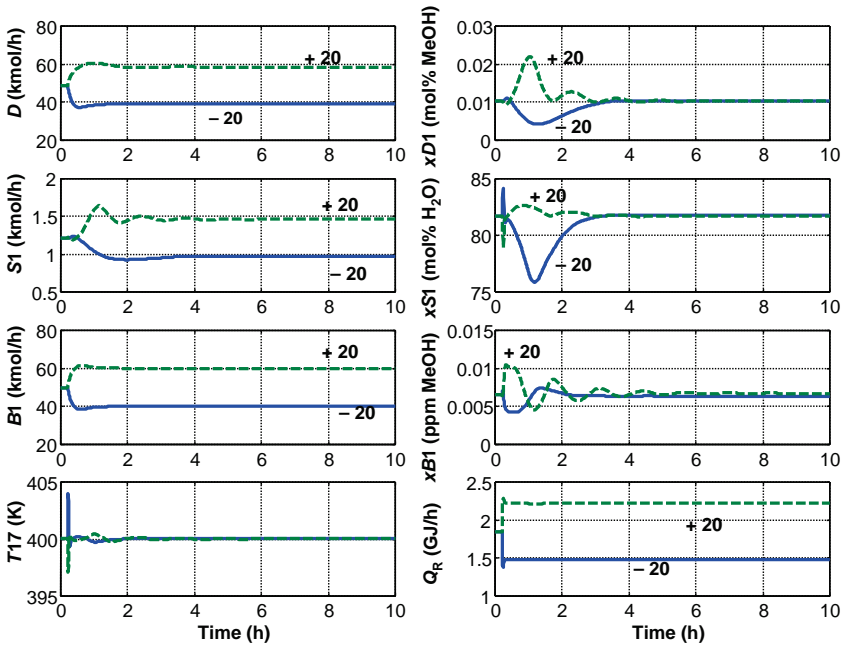


Figure 10.37 Feed rate changes: CC distillate; ZN settings.

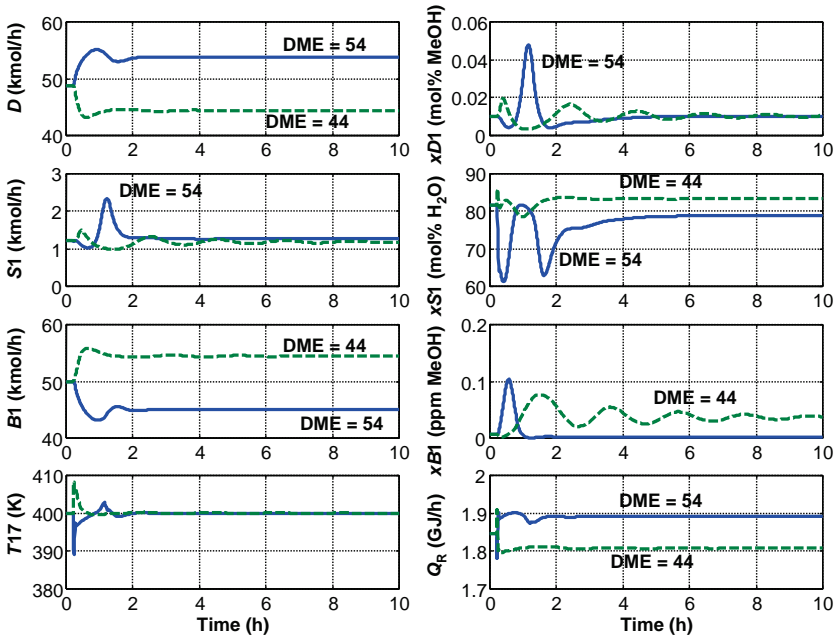


Figure 10.38 Feed composition DME 54/44 changes: CC distillate; ZN settings.

10.6 CONCLUSIONS

Several types of sidestream distillation columns have been considered in this chapter. The additional complexity of using sidestreams, with or without additional columns (strippers or rectifiers), makes the design and control of these processes more difficult.

CONTROL OF PETROLEUM FRACTIONATORS

Up to this point in this book, we have looked at distillation columns that separate specific chemical components. In the refining of crude oil, mixtures of many thousands of components must be handled. These components vary from quite light hydrocarbons (methane, ethane, propane, etc.) to very high-molecular-weight components that boil at extremely high temperatures. Petroleum refineries have units that separate (by distillation) and transform (by a variety of reactions) these mixtures.

Crude oil is produced in hundreds of locations around the world. It is found underground, sometimes under high pressure, and sometimes requiring pumping. A vast system of pipelines and huge supertankers transport the crude oil to refineries in which it is processed to make a large number of important products, such as gasoline, heating oil, jet fuel, asphalt, and wax. Most of the raw feed stocks for the chemical industry are produced in refineries, such as ethylene, propylene, and benzene.

The initial separation of crude oil into several “cuts” is achieved in a very large distillation column called a “pipestill” or “atmospheric crude distillation” unit. These cuts have different boiling point ranges. Low-molecular-weight gas comes off the reflux drum as a vapor product from a partial condenser. The liquid product from the reflux drum is a light low-boiling naphtha. Products of jet fuel, heating oil, and a heavy high-boiling gas oil are removed as sidestreams from the column. The effluent from a catalytic cracking reactor is also a mixture of petroleum fractions, which are separated in a distillation column called a cat fractionator. Many other units in a refinery must deal with these complex mixtures.

Crude oil as it comes from the ground is usually a mixture of saturated hydrocarbons, such as paraffins and naphthenes. The effluent of a cat cracker contains both saturated and unsaturated hydrocarbons, such as aromatics and olefins. These differences in the type of

components affect the density and average molecular weight of the petroleum fraction for the same boiling point range.

As is true with all naturally occurring feed stocks, the composition or boiling range of crude oil varies greatly from production field to production field. This variability results in a very significant dynamic control problem in a refinery that feeds crude oil from a variety of sources, which is often the case.

The book by Nelson¹ provides a thorough discussion of many aspects of the petroleum industry, such as types and sources of crude, characterization of petroleum fraction, and types of refinery operations.

Section 11.1 is a brief introduction to how petroleum fractions are characterized and quantified so that petroleum fractionators can be designed and their control studied. In Section 11.3, we will go through the details of setting up a steady-state simulation using the specified properties of the crude oil to a simple “preflash” column. We then look at the dynamic control of this column in Section 11.4. In Section 11.5, we expand the process considered to include a pipestill (atmospheric crude unit). This large complex column has three sidestreams, which are withdrawn from sidestream strippers using open steam for removing the light hydrocarbons. It also has two “pumparounds” at intermediate locations up the column to remove heat. This complex system presents challenging design problems and challenging control issues.

11.1 PETROLEUM FRACTIONS

In the chemical industry, we deal with compositions (mole fractions). In petroleum refining, we deal with *boiling point ranges*. For example, suppose we take a sample of heating oil and place it in a heated container at atmospheric pressure. The temperature at which the first vapor is formed is called the “initial boiling point (IBP).” This corresponds to the bubblepoint of a mixture of specific chemical components. If we continue to heat the sample, more and more material is vaporized. The “5% point” is the temperature at which 5% of the original sample has vaporized. Liquid volume percents are traditionally used. The “95% point” is the temperature at which 95 liquid volume percent of the original sample has vaporized. The “final boiling point” (FBP) is the temperature at which all of the liquid disappears. This is somewhat similar to the dewpoint of a mixture of specific chemical components. Heating oil has a 5% point of about 460 °F and a 95% point of about 620 °F.

There are three types of boiling point analysis: ASTM D-86 (“Engler”), ASTM D-158 (“Saybolt”), and true boiling point (TBP). The first and second are similar to the boiling of vapor as described in the previous paragraph. In the third, the vapor from the container passes into a packed distillation column and some specified amount is refluxed. Thus, the third analysis has some fractionation, while the first and second are just single stage separations. The ASTM analysis is easier and faster to run. The TBP analysis gives more detailed information about the contents of the crude.

Figure 11.1 gives typical boiling curves for a light naphtha stream. The curve on the left is a TBP curve and that on the right is an ASTM D-86 curve. The abscissa is volume percent distilled. The ordinate is temperature. Note that the initial and final parts of the curves are quite different because of the fractionation that occurs in the TBP distillation. The 50% boiling point is almost the same (249 and 243 °F). Table 11.1 compares the results of these two methods.

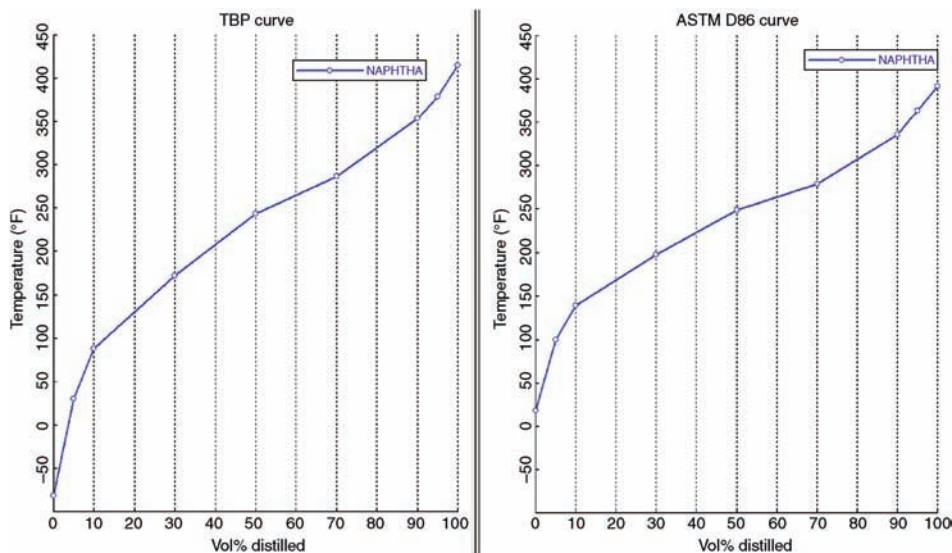


Figure 11.1 Boiling curves for naphtha.

Figure 11.2 gives typical curves for a crude oil. Note the very wide range of the boiling points from -100 to 1600 °F. The TBP curve is wider than the ASTM curve. Table 11.2 gives numerical values of these curves. The 50% points are similar, but both ends of the curves are different.

These curves are obtained by using the Plot Wizard. As we will demonstrate in the next section, after the steady-state program has run, click on *Results Summary* in the *Data Browser*. Then click *Plot* on the top tool bar and select *Plot Wizard*. The window shown at the left in Figure 11.3 opens. Clicking the *Dist Curve* and hitting *Next* open the window shown at the right. The stream of interest and the type of curve are selected. Clicking *Next* and then *Finish* produce a plot.

The TBP plot of the crude gives an estimate of the amount of each petroleum cut in the crude. As shown in Figure 11.4, the boiling point range of each product from the pipe still is shown as the horizontal lines. For example, the boiling point range of the jet fuel in the

TABLE 11.1 Comparison of Boiling Point Methods for Naphtha

Vol% Distilled	ASTM D-86	TBP
IBP	18	-81
5	100	31
10	139	88
30	197	172
50	249	243
70	279	286
90	336	353
95	369	379
FBP	392	415

TABLE 11.2 Comparison of Boiling Point Methods for Crude Oil

Vol% Distilled	ASTM D-86	TBP
IBP	5	-99
5	146	97
10	227	196
30	408	403
50	554	569
70	742	772
90	1021	1143
95	1169	1331
FBP	1317	1563

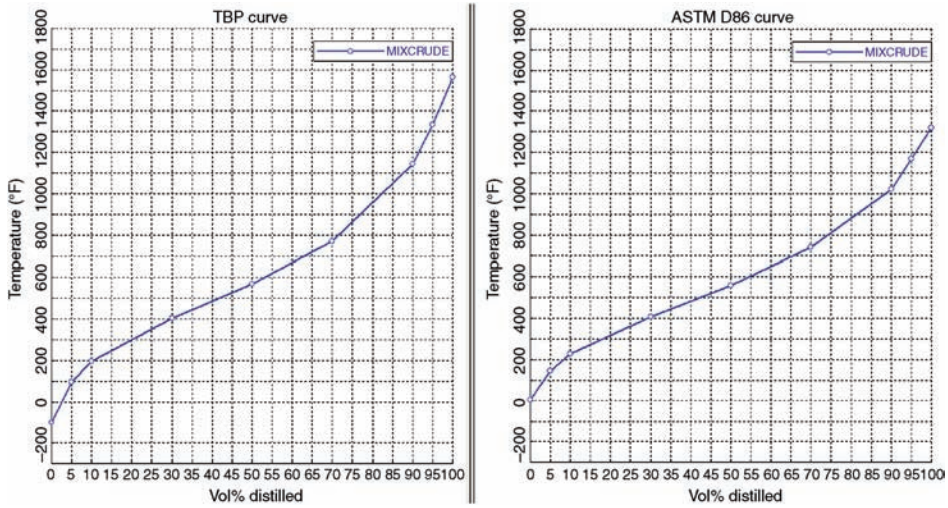


Figure 11.2 Boiling curves for crude oil.

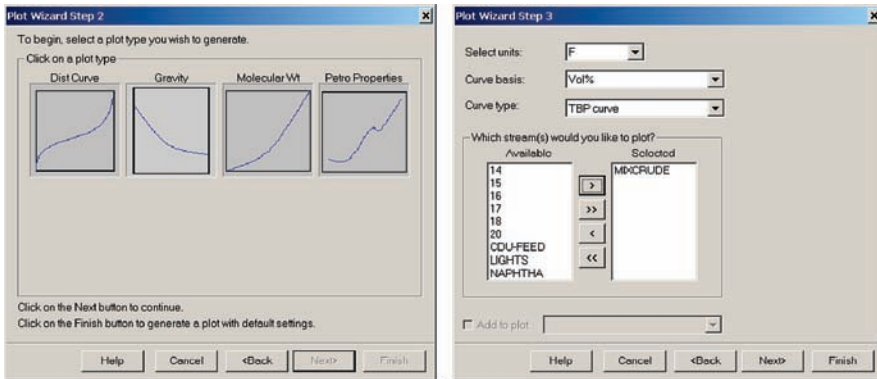


Figure 11.3 Producing boiling curves.

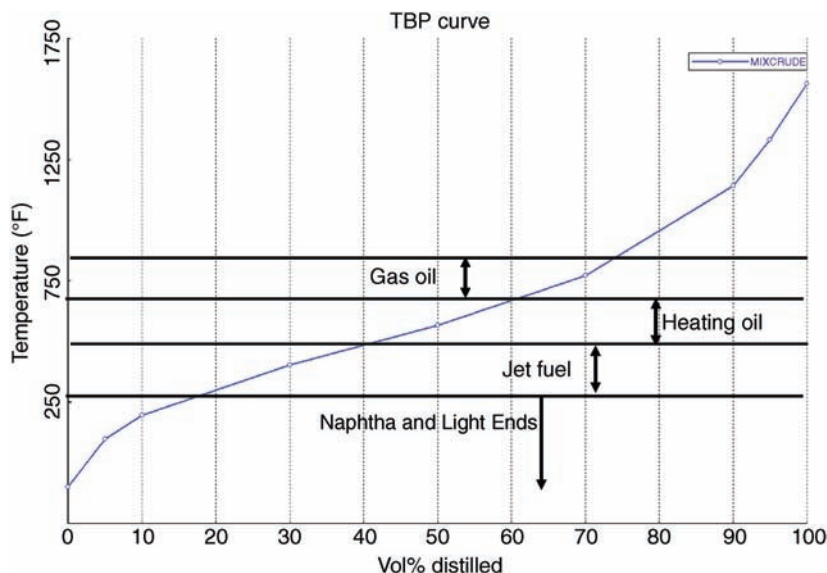


Figure 11.4 Petroleum cuts from TBP curve of crude.

crude is from 280 to 460 °F. By reading off the volume percentages at these temperatures (17 and 40 vol%, respectively), the yield of jet fuel can be estimated to be about 22% of the crude fed to the pipestill. Therefore, a 100,000 B/D (barrels per day) crude unit should produce about 22,000 B/D of jet fuel when fed this type of crude. Of course, the yields will be different for other crudes with different TBP curves.

The properties of a petroleum stream are not specified in terms of compositions. Instead, properties are used, such as 5% point, final boiling point, Reid vapor pressure, flash point, and octane number.

The method for performing quantitative calculations with petroleum fractions is to break them into “pseudocomponents,” with each having an average boiling point, specific gravity, and molecular weight. Aspen Plus generates these pseudocomponents given “assay” information about the crude oil.

Another difference in petroleum refining is how density is defined. In the chemical industry, density is defined as specific gravity or mass per unit volume. The density of a material in petroleum refining is traditionally reported in “degrees API” (°API). Specific gravity and °API are inversely related: the higher the specific gravity, the lower the °API.

$$\text{Degrees API} = \frac{141.5}{\text{specific gravity}} - 131.5$$

For example, the crude considered above has a density of 34.1 °API, which corresponds to a specific gravity of 0.854. The naphtha has a density of 61.7 °API, which corresponds to a specific gravity of 0.732.

The traditional unit used for flow rate in petroleum refining in the United States is B/D. One barrel is 42 U.S. gallons.

11.2 CHARACTERIZATION CRUDE OIL

The information available for a crude oil typically consists of “assay” data. This is a TBP curve, a gravity curve, and a “Light Ends” analysis. These are illustrated below. The material in this section is taken for the very useful and detailed documentation available from Aspen Technology (“Getting Started Modeling Petroleum Processes”), and the example used in this book is based on the example presented in this reference. Petroleum English units are used in the steady-state design because these are used in the above reference. When we move into dynamics, metric units will be used because Aspen Dynamics does not offer Petroleum English units.

We will consider a crude oil called OIL-1. The assay data for OIL-1 are given in Table 11.3. We have already discussed the TBP distillation information. In petroleum refining, the term “Light Ends” refers to specific light hydrocarbons, such as methane and ethane. You can see that there are small amounts of these light component dissolved in the crude oil, even though it is at atmospheric pressure and ambient temperature. The API gravity data give the density of the various cuts as they are produced in the TBP distillation.

A *Template* is set up in Aspen Plus that takes these data and generates pseudocomponents. These will then be used in simulating a simple petroleum distillation column called a preflash unit and a second more complex petroleum pipestill with multiple sidestream products.

The program is started in the normal way by clicking on *Start, Programs, AspenTech, Process Modeling V7.3, and Aspen Plus User Interface*. The window shown at the top of Figure 11.5 opens on which the *Template* option is selected. Clicking *OK* opens the window shown at the bottom of Figure 11.5, with the *Simulation* page tab open. From the list of options on the left, we select *Petroleum with English Units*. At the bottom right of the window, we select *Assay Data Analysis* and click *OK*.

A *Data Browser* window opens and clicking *Setup* and *Specifications* gives the view shown in Figure 11.6. A title can be inserted in the appropriate box. Next, the *Components* item is clicked in the *Data Browse*, and then *Specifications* is clicked, which opens the window shown at the top of Figure 11.7, with the *Selection* page tab selected. The individual components from water to *n*-pentane are typed in the first column (*Component ID*) and the

TABLE 11.3 Crude Oil Assay Data for OIL-1 (31.4°API)

TBP Liq. Vol%	Distillation Temp. (°F)	Light Ends Component	Analysis Liq. Vol. Frac.	API Curve Mid. Vol%	Gravity
6.8	130	Methane	0.001	5	90.0
10	180	Ethane	0.0015	10	68.0
30	418	Propane	0.009	15	59.7
50	650	Isobutane	0.004	20	52.0
62	800	<i>n</i> -Butane	0.016	30	42.0
70	903	2-Methyl-butane	0.012	40	35.0
76	1000	<i>n</i> -Pentane	0.017	45	32.0
90	1255			50	28.5
				60	23.0
				70	18.0
				80	13.5

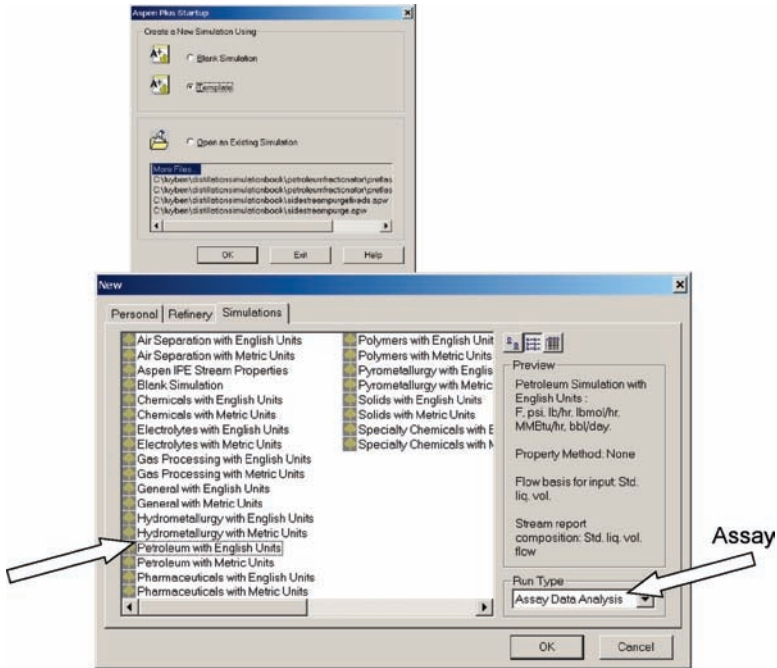


Figure 11.5 Selecting template and petroleum assay.

third column (*Component name*). The *Type* and *Formula* columns are automatically filled in, as shown at the bottom of Figure 11.7.

Now a crude oil is specified. We will use the assay data for OIL-1 given in Table 11.3. On the next line of the *Selection* page tab, we type in *OIL-1* in the first column. Clicking the second column opens a drop-down menu (shown in Fig. 11.8), and *Assay* is selected. Clicking the *Petroleum* page tab and sequentially clicking *Assay/Blend*, *OIL-1*, and *Basic Data* in the *Data Browser* opens the window shown at the top of Figure 11.9. In the

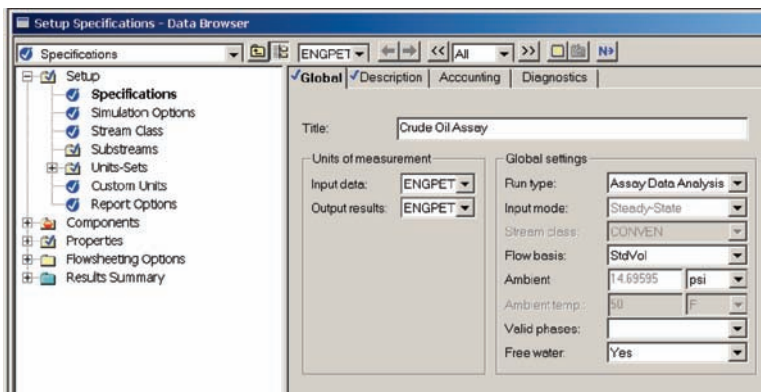


Figure 11.6 Specifications.

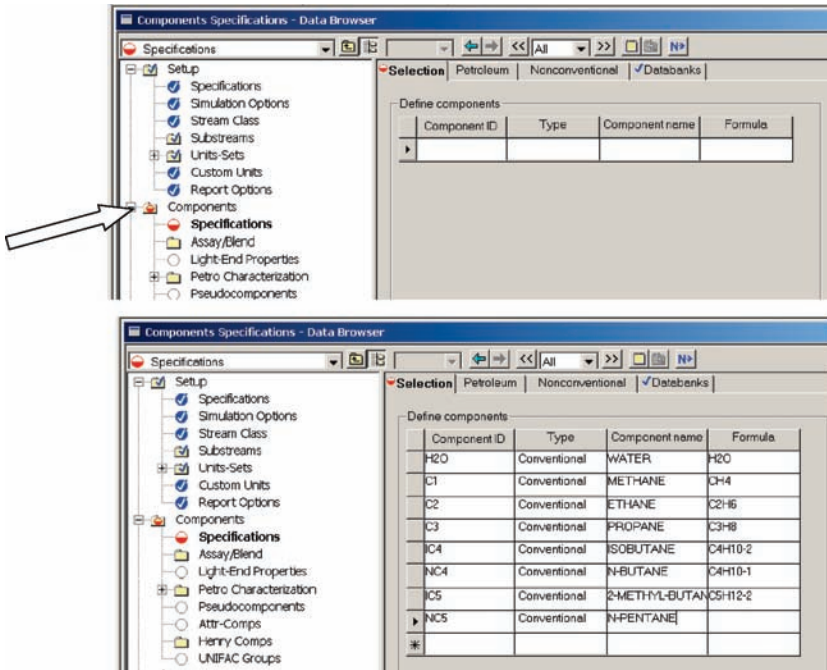


Figure 11.7 Components.

Distillation Curve Type, we use the drop-down menu to select *True boiling point (liquid volume basis)*. In the *Bulk gravity value*, the number 31.4 is entered in the *API gravity* box.

The percent distilled and temperature data for OIL-1 from Table 11.3 are entered, as shown at the bottom of Figure 11.9. The *LightEnds* page tab is clicked and the data from Table 11.3 is entered (see Fig. 11.10). The *Gravity/UOPK* page tab is

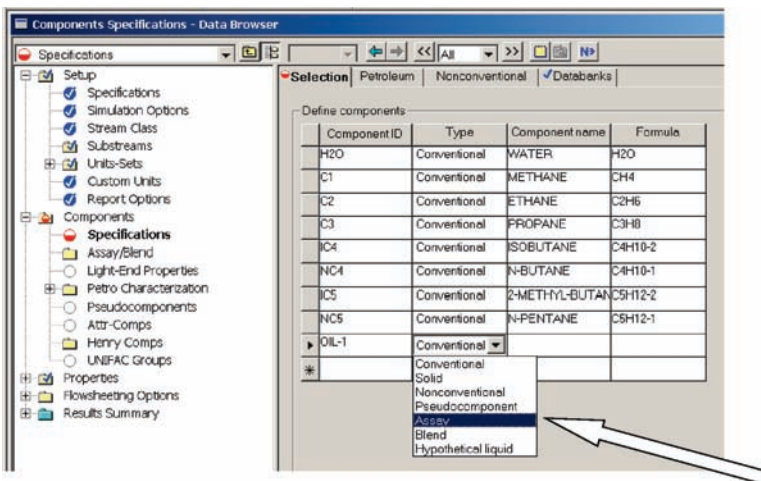


Figure 11.8 Crude oil assay.

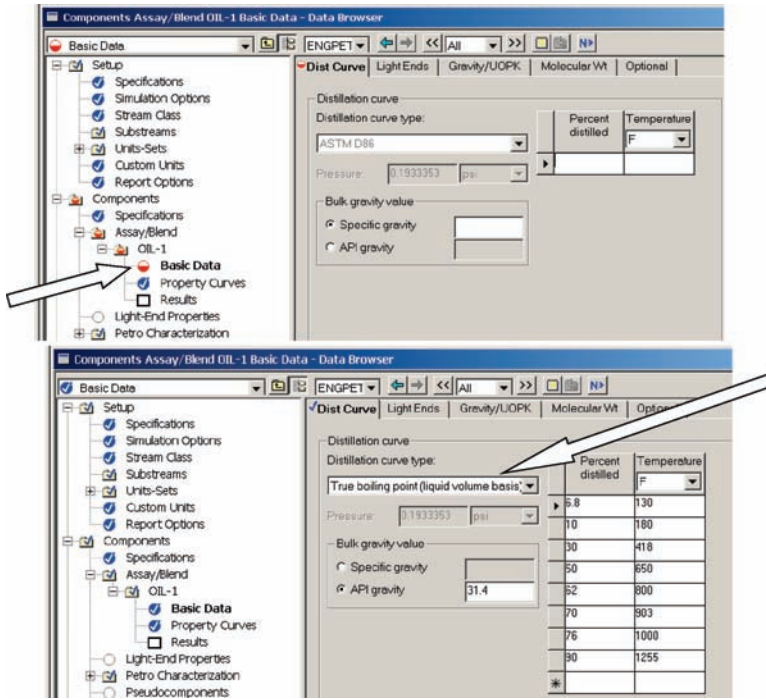


Figure 11.9 Crude oil basic data.

clicked, and the *API gravity* is selected as the type. The data from Table 11.3 is entered (see Fig. 11.11).

All the assay data have been entered, and we are ready to generate pseudocomponents. Clicking the blue *N* button opens the window shown in Figure 11.12a. We select *Specify options for generating pseudocomponents*. A new browser window opens called

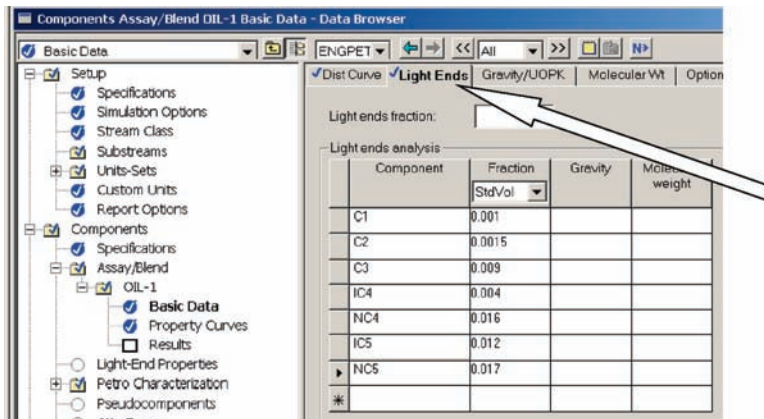


Figure 11.10 Light Ends data.

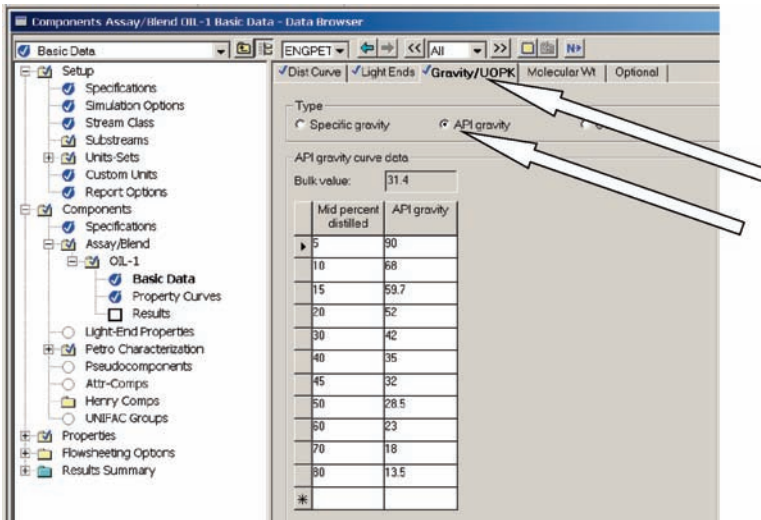
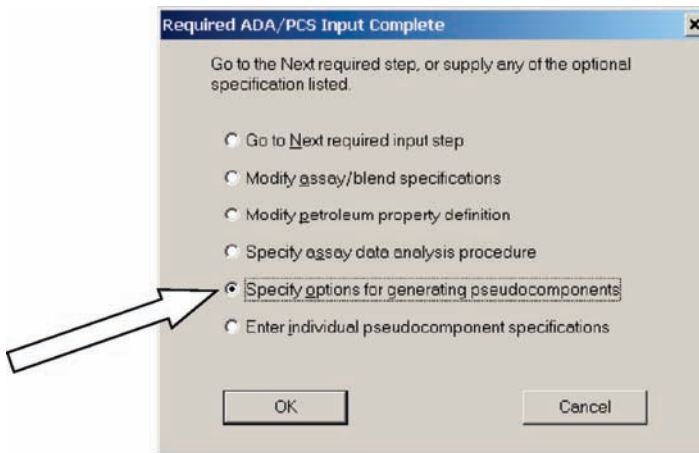


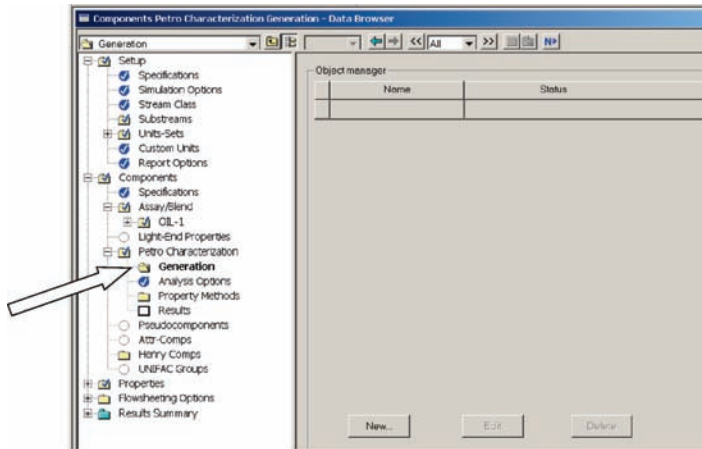
Figure 11.11 Gravity data.

Components Petro Characterization Generation (see Fig. 11.12b). Clicking *New* opens the window shown at the top of Figure 11.13 on which we enter an identification name such as “Crude1.” Clicking *OK* opens window shown at the bottom of Figure 11.13 on which OIL-1 is selected from the drop-down menu to be included. Finally, the blue *N* button is clicked and *OK* is clicked on each of the windows that come up sequentially (shown in Fig. 11.14). This completes the generation of the pseudocomponents, called *Assay Data Analysis*.



(a)

Figure 11.12 (a) Options for pseudocomponents. (b) Generate pseudocomponents.



(b)

Figure 11.12 (Continued)

The results can be seen by going to *Components, Petro Characterization, and Results* on the *Data Browser*. Figure 11.15 gives a partial list of the pseudocomponents. Note that each has a normal boiling point, density, molecular weight, and critical properties.

This same procedure is repeated for a second crude called OIL-2 whose assay data are given in Table 11.4. Note that this crude is somewhat lighter than OIL-1 (API gravity is

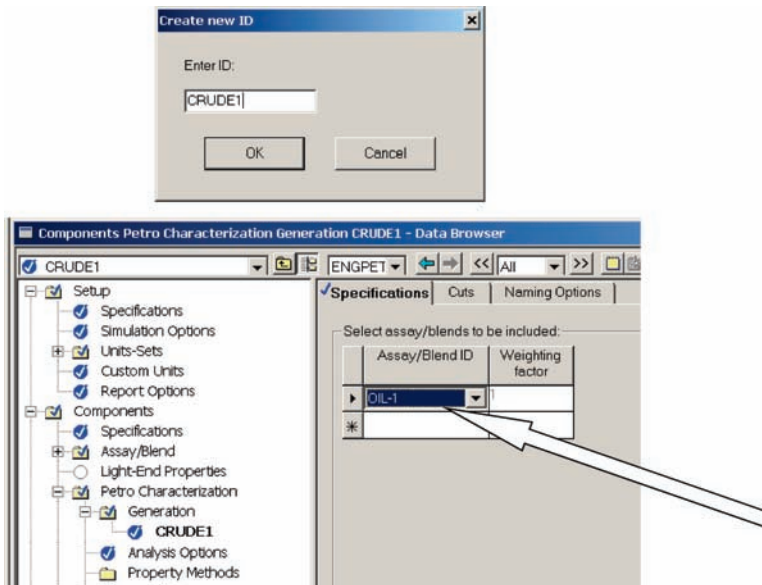


Figure 11.13 Petroleum characterization generation.

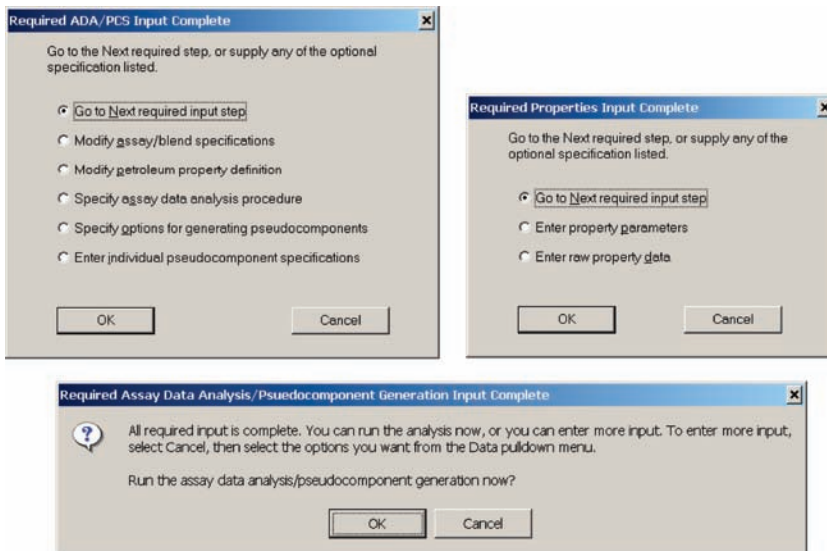


Figure 11.14 Completing petroleum characterization generation.

34.8 compared with 31.4 and 50% point is 450 °F vs. 650 °F for OIL-1). We will feed both of these crude oils to a unit discussed in Section 11.3.

We are now ready to proceed with our simulation. We will start by looking at a simple preflash column that is often used in refineries to remove some of the lightest material from the crude before sending it into the pipestill.

Pseudocomponents	Normal BP	API Gravity	Specific gravity	UOPK	Molecular weight	Critical temperature	Critical Pressure
	F					F	psi
PC11F	120.580086	82.4354147	0.66141457	12.6104718	77.2821166	425.445737	486.533814
PC138F	137.838547	77.7352767	0.67627219	12.4545069	81.2564172	448.067167	478.756565
PC163F	162.58222	71.4238582	0.69730589	12.2433757	87.1109277	480.30865	467.959711
PC188F	187.573076	66.3543473	0.71517256	12.095161	93.3130965	511.127207	453.075698
PC213F	212.642973	63.126997	0.72763172	12.0495409	103.552598	538.970757	431.099426
PC238F	237.636516	60.6568783	0.73637749	12.0422442	110.532407	565.350998	408.120195
PC263F	262.622022	57.5733879	0.74838665	11.9889704	117.457094	592.913284	390.59977
PC288F	287.597411	54.2254507	0.76187727	11.9107842	124.438738	621.10294	376.351497
PC313F	312.582365	51.1002015	0.774917	11.8393404	131.754951	648.95211	362.818377
PC338F	337.518908	48.4018715	0.7865399	11.7887118	139.583821	675.961356	348.83691
PC363F	362.47192	46.0636946	0.79689718	11.7556506	147.949416	702.200114	334.945818
PC387F	387.429089	44.0032562	0.80625285	11.7355416	156.817986	727.801568	321.14537
PC412F	412.428766	42.1315177	0.81494421	11.7235823	166.201568	752.967794	307.818868
PC438F	437.530229	40.3858957	0.82322054	11.716025	176.094323	777.876119	295.105981
PC463F	462.517943	38.7898433	0.83093623	11.7140071	186.448245	802.270605	283.002071
PC488F	487.508744	37.2970441	0.83828085	11.7153294	197.295885	826.347795	271.520594
PC512F	512.499292	35.8760117	0.84540191	11.7179265	208.615436	850.18649	260.716476
PC537F	537.490025	34.494369	0.85243855	11.7193358	220.379454	873.866839	250.63011
PC562F	562.481128	33.2134093	0.85906788	11.7258477	232.890101	897.209134	240.978906

Figure 11.15 Partial list of pseudocomponents.

TABLE 11.4 Crude Oil Assay Data for OIL-2 (34.8 °API)

TBP Liq. Vol%	Distillation Temp. (°F)	Light Ends Component	Analysis Liq. Vol. Frac.	API Curve Mid. Vol%	Gravity
6.5	120	Methane	0.001	2	150.0
10	200	Ethane	0.002	5	95.0
20	300	Propane	0.005	10	65.0
30	400	Isobutane	0.01	20	45.0
40	470	<i>n</i> -Butane	0.01	30	40.0
50	450	2-Methyl-butane	0.005	40	38.0
60	650	<i>n</i> -Pentane	0.025	50	33.0
70	750			60	30.0
80	850			70	25.0
90	1100			80	20.0
95	1300			90	15.0
98	1475			95	10.0
100	1670			100	5.0

11.3 STEADY-STATE DESIGN OF PREFLASH COLUMN

The first petroleum fractionator simulated is a simple distillation column that removes some of the light material in the crude. Figure 11.16 gives the Aspen Plus flowsheet of this unit. There are two crude feed streams that are combined and heated in a furnace in which the feed is partially vaporized before entering the bottom of the column. There is no reboiler. Live steam is introduced in the bottom of the column to strip out some of the light components in the bottoms stream, which is fed to a pipestill to be considered in Section 11.4.

The valves and pumps are standard equipment, but the column is different than the typical *RadFrac* used when specific chemical components are used. A petroleum fractionator is selected from the model library menu on the bottom of the Aspen Plus window by clicking *Columns* and then *PetroFrac*. Figure 11.17 shows the palette of possible configurations. We choose fourth from the left on the top row, which is a rectifier with a furnace.

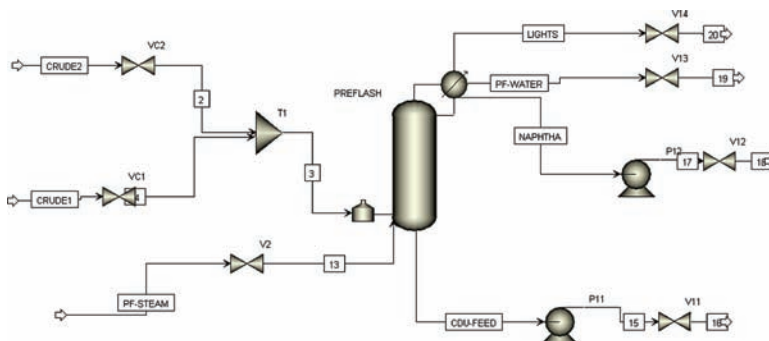


Figure 11.16 Preflash column.

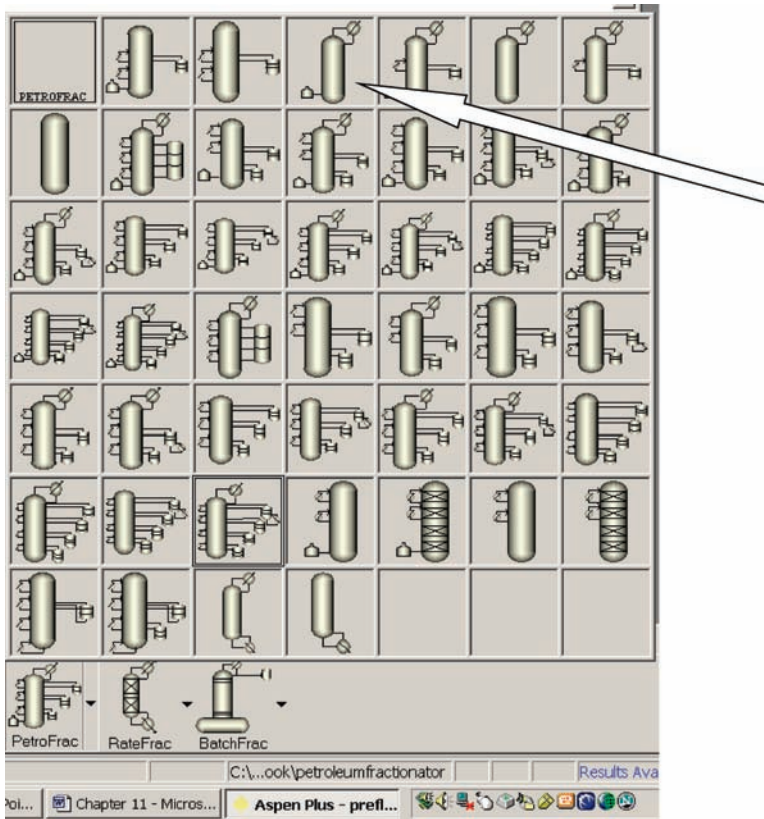


Figure 11.17 Types of petroleum (PetroFrac) columns.

It is a little tricky to attach the stream from the tee where the two crudes are mixed to the furnace. When a material stream is selected at the bottom of the Aspen Plus window and the cursor is moved to the flowsheet, a red input arrow appears at the bottom of the column, as shown in the left picture in Figure 11.18. Place the cursor over the red arrow and drag it to

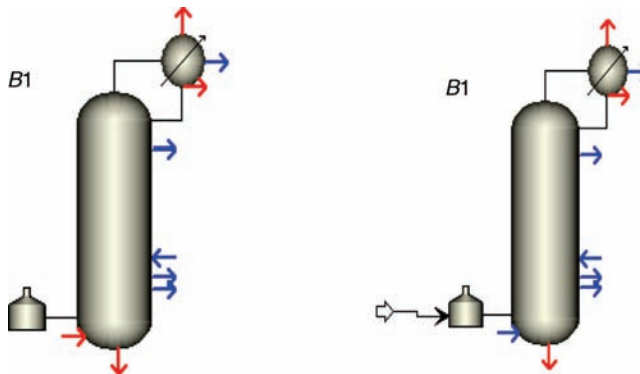


Figure 11.18 Attaching feed to furnace.

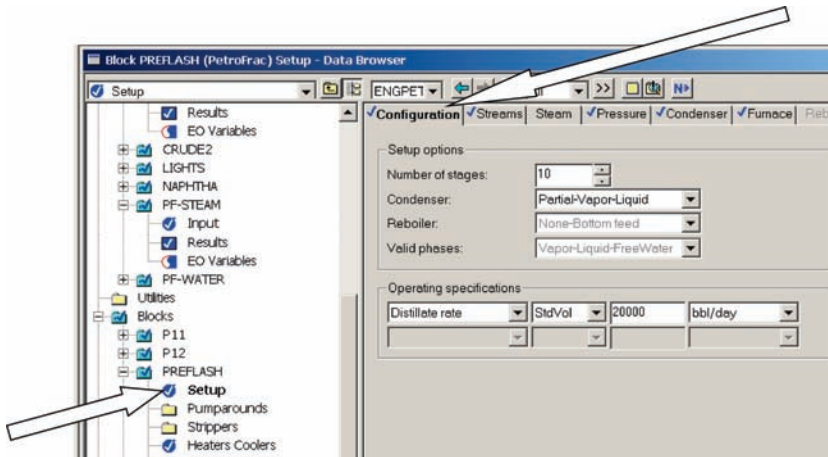


Figure 11.19 Column setup.

the left until it points to the furnace. Then click this arrow, which attaches the stream (see the right picture in Fig. 11.18).

The total crude feed to the preflash column is 100,000 B/D, with each of the two crudes (OIL-1 and OIL-2) set at 50,000 B/D. Their temperatures are 200 °F. The furnace outlet temperature is specified to be 450 °F, which requires a heat input of 203 MMBtu/h (203×10^6 Btu/h). The crude is about 30 wt% vaporized in the furnace.

Selecting *Setup* under the column block (*PREFLASH*) opens the window shown in Figure 11.19. There are page tabs of *Configuration*, *Streams*, *Pressure*, *Condenser*, and *Furnace*. The column is set up to have 10 stages, no reboiler and a partial condenser.

Both a gas stream and a liquid distillate are removed from the reflux drum. In addition, since live steam is fed into the bottom of the column and separates into an aqueous phase in the reflux drum, a water stream is removed from a small “boot” at the bottom of this drum that serves as a decanter. The stripping steam flow rate is 5000 lb/h and its temperature is 400 °F. Both the gas and the liquid products contain some water. The water decanted is 244 lb/h.

The distillate rate is set at 20,000 B/D. This will be adjusted later to obtain a desired ASTM 95% point of 375 °F for the liquid distillate product, which is a light naphtha stream. Note that there is only one degree of freedom in this rectifying column since there is no reboiler. All of the vapor coming up the column comes from the partially vaporized furnace effluent.

Clicking the *Stream* page tab opens the window shown in Figure 11.20 on which the combined crude feed stream is specified to be fed to the furnace by using the drop-down menu. The stripping steam is fed on Stage 10.

Opening the *Pressure* page tab (shown at the top of Fig. 11.21) permits setting pressures in the column. The pressure in the reflux drum is specified to be 39.7 psia. The condenser pressure drop is 2 psi, so the pressure on Stage 2 is set at 41.7 psia. The pressure at the bottom of the column is specified to be 44.7 psia.

Clicking the *Condenser* page tab opens the window shown at the bottom of Figure 11.21 on which the condenser temperature is specified to be 170 °F. This is high enough to permit the use of air-cooled condensers, which conserves the use of cooling water.

Clicking the *Furnace* page tab opens the window shown in Figure 11.22 on which the temperature is set at 450 °F and the pressure is set at 44.7 psia. This is the same pressure as the

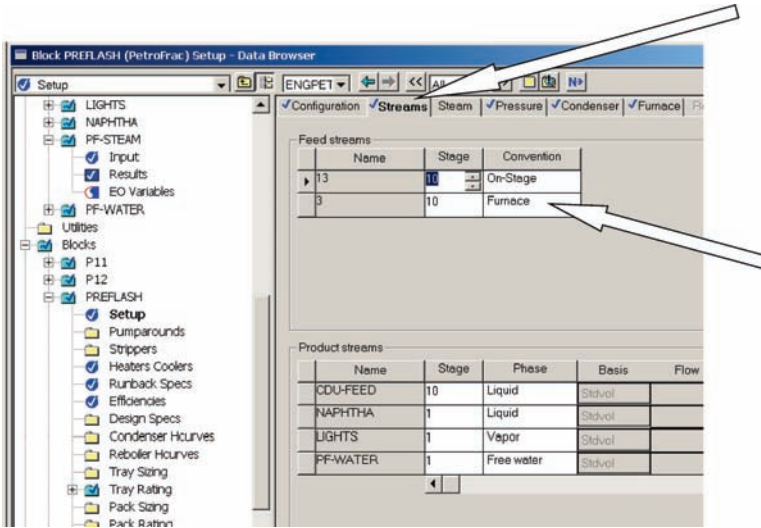


Figure 11.20 Stream locations.

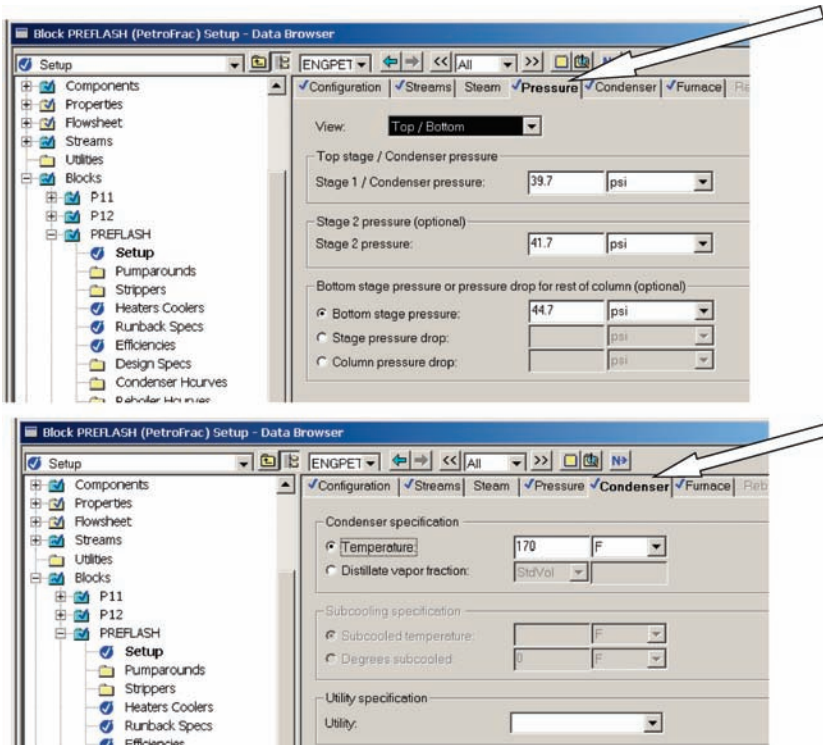


Figure 11.21 Setting pressures.

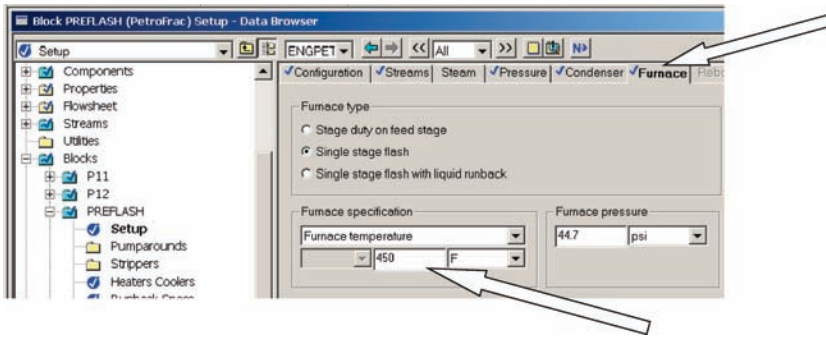


Figure 11.22 Setting furnace conditions.

bottom of the column. If the pressure is set at a higher pressure, the steady-state simulation will run, but an error occurs when exporting a pressure-driven dynamic simulation file.

The final job in the steady-state design is to achieve the desired specification of an ASTM 95% point of 375 °F (ASTM D-86). An initial guess of 20,000 B/D for the liquid distillate flow rate gives an ASTM 95% point of 353 °F. This is lower than the specification, which indicates that more material can be taken overhead. Increasing the flow rate carries more higher-boiling material into the naphtha product. To display the TBP and ASTM boiling point values for the process streams, go to *Setup, Report Options, Stream, Property Sets* and select *Petro*.

A “Design Specs” function can be used to achieve the specification. Clicking *Design Specs* under the *PREFLASH* column block, clicking *New* and giving an identification label open the window shown at the top of Figure 11.23. The *Type* is specified at *ASTM D86 temperature (dry, liquid volume basis)*. The *Target* is 375 °F at a *Liquid %* of 95%. Click the *Feed/Product Streams* and select *NAPHTHA* as the *Selected Stream* (see the bottom of

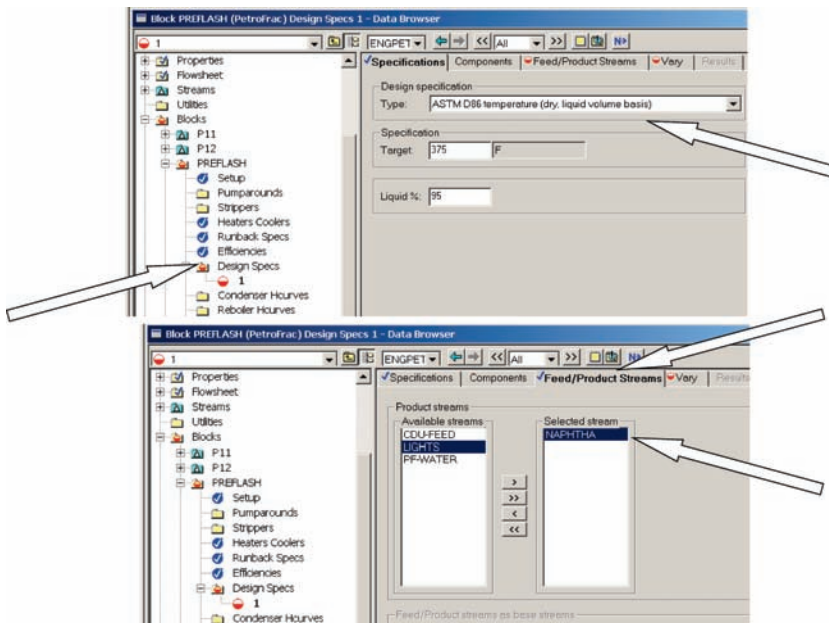


Figure 11.23 Design Specs.

TABLE 11.5 LIGHTS Composition

	Mole Fraction	lb mol/h	lb/h
H ₂ O	0.150	86.3	1,554
C1	0.0697	39.5	634
C2	0.0854	49.1	1,478
C3	0.144	82.8	3,652
<i>i</i> C4	0.0918	52.8	3,069
<i>n</i> C4	0.154	88.3	5,131
<i>i</i> C5	0.0555	31.9	2,302
<i>n</i> C5	0.115	66.2	4,777
Total	1.00	575	29,726

Fig. 11.23). Finally, the *Vary* page tab is clicked and *Distillate flow rate* is selected as the *Type* (see Fig. 11.24). Run the simulation by clicking the blue *N* button produces at NAPHTHA flow rate of 21,040 B/D to achieve the 375 °F target.

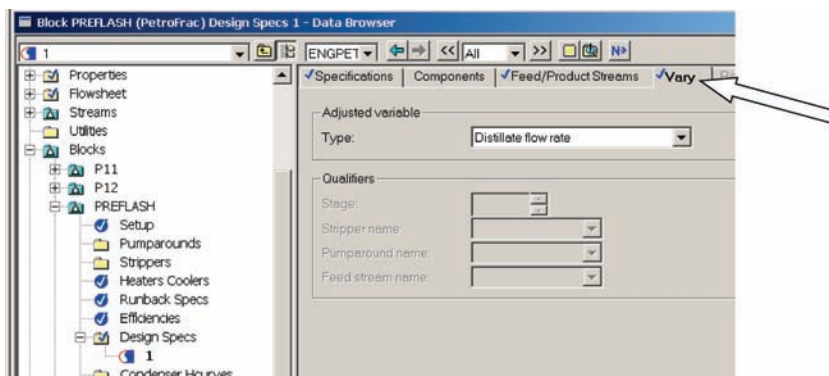
One source of confusion is a difference between the B/D flow rates specified in the original *Setup* and the *Liq. vol. 60F bbl/day* reported in the *Stream Results*. The specified 20,000 B/D is at the actual flow conditions (temperature and pressure). The results given in the *Stream Results* are at standard conditions (60 °F and 1 atm).

The diameter of the column is calculated in the normal way by using the *Tray Sizing* feature. The result is a diameter of 11.1 ft. The composition of the LIGHTS vapor stream from reflux drum is given in Table 11.5. Most of the light hydrocarbons that are in the crude oil feed streams are removed in this vapor steam. They are sent to downstream units for separation into individual components.

The steady-state design is now complete. Figure 11.25a gives the flowsheet of the PREFLASH column with conditions and properties of the various streams. All of the flow rates are given in B/D at standard conditions.

Because Petroleum English units are not available in Aspen Dynamics, we will switch to metric units when we look at dynamic control. Figure 11.25b gives the flowsheet of the PREFLASH column in metric units ($T = 1000$ kg).

It should be noted that there is no claim that the design of the preflash column presented above is the economic optimum. It is presented for purposes of illustration. A modified

**Figure 11.24** Set vary in Design Specs.

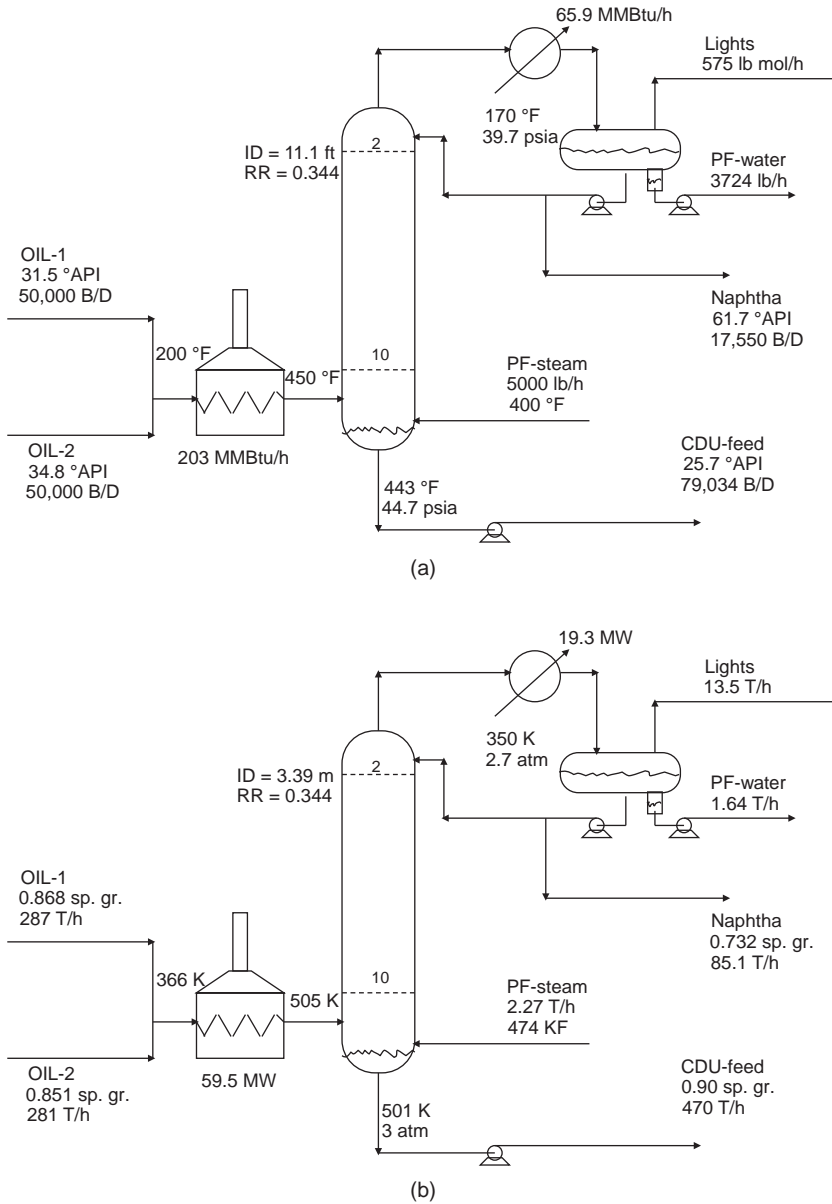


Figure 11.25 (a) PREFLASH flowsheet (engineering units). (b) PREFLASH flowsheet (metric units).

design was developed in a recent paper,² which optimized the column. Changes from the original design included

1. Reducing reflux-drum temperature from 170 to 130 °F and raising pressure from 39.7 to 42 psia.
2. Reducing furnace outlet temperature from 450 to 400 °F.

These resulting in a significant reduction in the vapor distillate from the reflux drum (575 decreases to 251 lb mol/h), which reduces the compression costs of recovering the valuable components in this stream.

11.4 CONTROL OF PREFLASH COLUMN

The reflux drum and column base are sized to provide 5 min of liquid holdup when half full. The file is pressure checked and exported to Aspen Dynamics. The initial control scheme that opens is shown in Figure 11.26. Note that there is a level controller (LCW1) that pulls off free water from the reflux drum. The other level controller (LC12) manipulates reflux flow rate to hold the liquid level of the organic phase in the reflux drum. Since the reflux ratio is only 0.344 in this column, we change the control structure to hold reflux-drum level with the NAPHTHA flow rate (valve V12). Pressure controller PC1 manipulates the valve V14 in the vapor line.

Flow controllers are added to the two crude feeds and the stripping steam. A base-level controller is added that manipulates bottoms flow rate. A temperature controller is added that holds the furnace outlet temperature by manipulating furnace heat input.

The only remain loop is a controller that manipulates the flow rate of the NAPHTHA to maintain a 95% point at 375 °F (191 °C in the metric units used in Aspen Dynamics). The default properties available in Aspen Dynamics for any stream do not include boiling point information. To obtain these data, we must turn on the “Stream Sensor.” Select the NAPHTHA stream, right click, select *Forms*, and select *Configure Sensor*. The view shown at the left in Figure 11.27 shows the window that opens on which we click the *Sensor On* and *Calculate Phase Properties* boxes, specify the *Valid Phases* to be *Liquid-Only* and select the additional properties we wish to have available. In our case, the *ASTM D86 temperature* is the item of interest, so it is moved to the right column under *Selected Properties*. The number “95” is entered in the *Liquid Volume % Distilled* box. Now this property is reported in the stream results for the NAPHTHA stream (see the right side of Fig. 11.27). This property is also available to be selected as an input to a controller (“95% boiling point”), which will manipulate reflux flow rate to maintain the desired ASTM 95% boiling point of the naphtha.

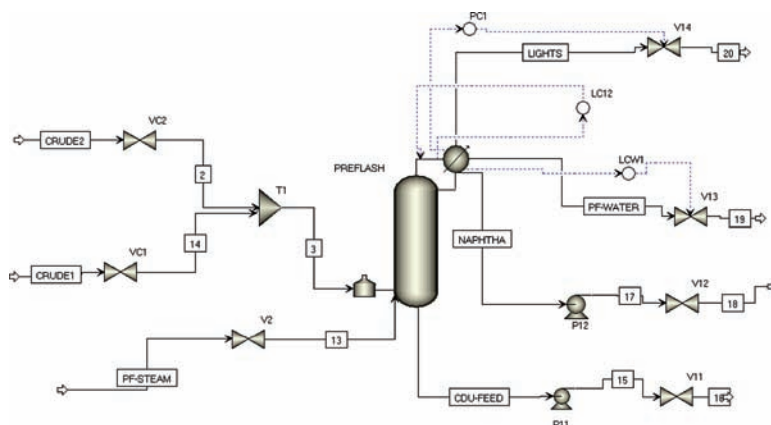


Figure 11.26 Initial control scheme.

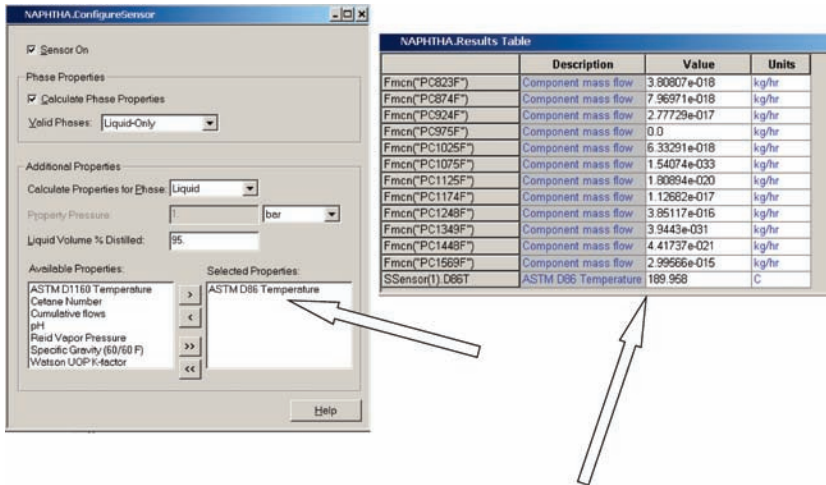


Figure 11.27 Setting up Stream Sensor.

Figure 11.28 shows the control structure. All level controllers are proportional with gains of 2. The furnace temperature loop has a deadtime of 3 min instead of the normal 1 min deadtime used in temperature loops because the dynamics of a fired furnace are usually slower than a steam-heated reboiler. Relay-feedback testing and Tyreus–Luyben settings give controller tuning constants of $K_C = 0.465$ and $\tau_I = 13$ min (with a temperature transmitter range 100–500 °C and a maximum heat input of 428 GJ/h). The 95% boiling point controller has a deadtime of 3 min and is tuned in the same way as the temperature controller ($K_C = 0.821$ and $\tau_I = 26$ min) with a boiling point temperature transmitter range 150–250 °C and a maximum reflux flow rate of 70,000 kg/h.

The effectiveness of this control structure is demonstrated in Figure 11.29a for a 20% increase and a 20% decrease in the flow rates of both crude feeds and steam to the base of the column. The peak dynamic deviations in the 95% boiling point of the

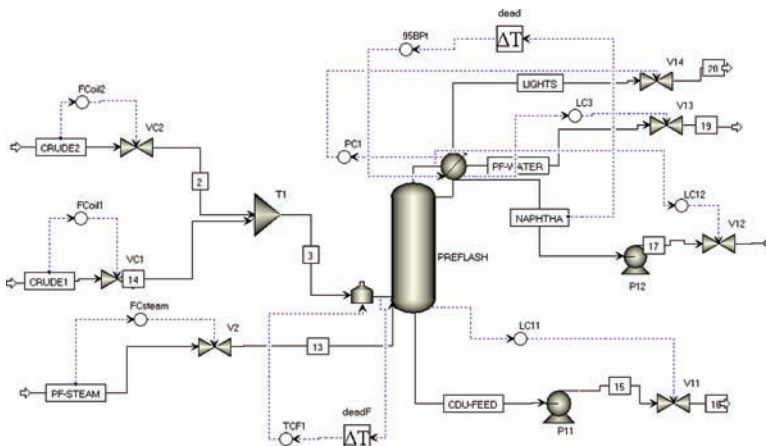
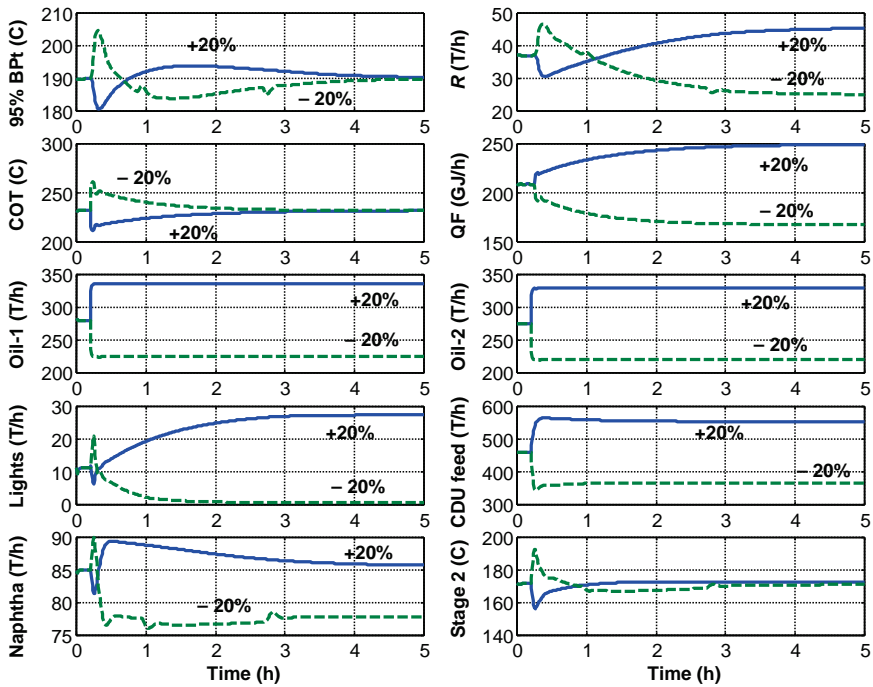
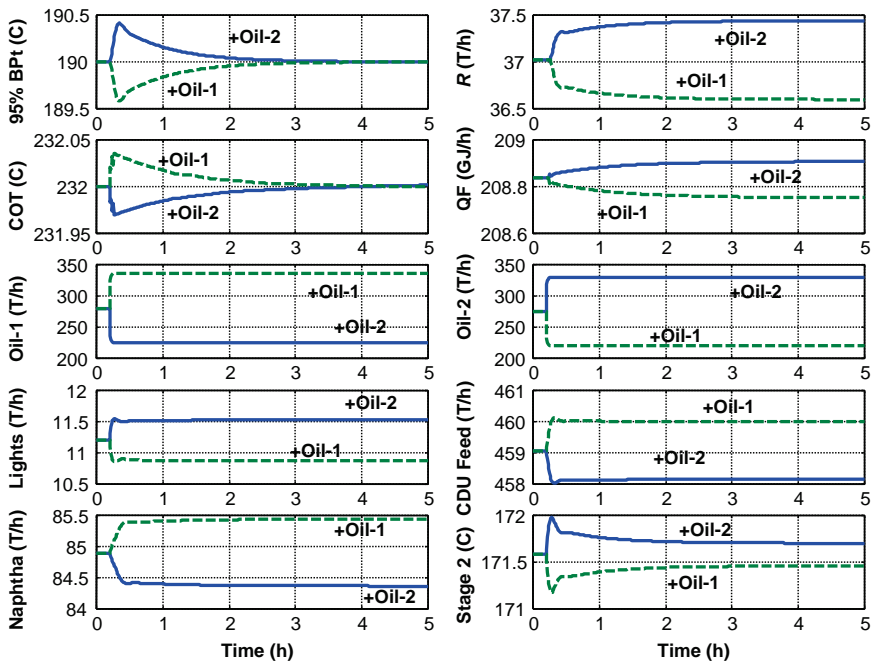


Figure 11.28 Control structure with 95% boiling point control.



(a)



(b)

Figure 11.29 (a) Feed rate changes. (b) Switching crudes.

naphtha are about 12°C . The new steady state for an increase in feed has higher flow rates of reflux, lights, and bottoms (CDU Feed), but only a small increase in the flow rate of the naphtha. The new steady state for a decrease in feed has lower flow rates of reflux, naphtha, and bottoms (CDU Feed), but the reduction in lights is smaller than is the increase for the positive change in feed. Increasing the load on the column reduces the yield of naphtha at the expense of lights for the same naphtha with 95% boiling point at 191°C (375°F).

Figure 11.29b gives results when there is a change in the ratio of the two crude oils. The solid lines are for a decrease in Crude1 from 280 to 224 T/h, while Crude2 is increased from 275 to 329 T/h. Since Crude2 is lighter than Crude1, there is an increase in the flow rate of the Lights and a decrease in the flow rate of the bottoms. Unexpectedly, the naphtha decreases slightly. The dashed lines are for an increase in Crude1 from 280 to 336 T/h, while Crude2 is decreased from 275 to 221 T/h. Responses are almost the mirror image of the reverse disturbance.

Note that it takes about 3 to 4 h for the 95% boiling point loop to settle out. Note also that the temperature on Stage 2, which is given in the bottom right graph in these figures, does not change much at the new steady-state conditions for these disturbances. This suggests that the use of temperature control instead of boiling point control might work pretty well.

To test this, the control structure is modified to manipulate reflux to hold Stage 2 at 171.6°C , as shown in Figure 11.30. The TC2 temperature controller has a deadtime of 1 min and is tuned in the usual way, yielding tuning constants $K_C = 0.90$ and $\tau_1 = 5.3$ min (with a temperature transmitter range $150\text{--}250^{\circ}\text{C}$ and a maximum reflux flow rate of 70,000 kg/h). Note that this reset time is much smaller than that of the 95% boiling point controller, so faster closed-loop dynamics can be expected.

Figure 11.31 shows that this is indeed true. The responses with temperature control are represented by solid lines. The responses with 95% boiling point control are represented by dashed lines. The disturbance is a swing in crude oils to less OIL-1 and more OIL-2. The process steadies out in about 90 min with temperature control. The naphtha boiling point is not held exactly at 191°C , but ends up at about 189.3°C . The naphtha yield is somewhat smaller, with more bottoms.

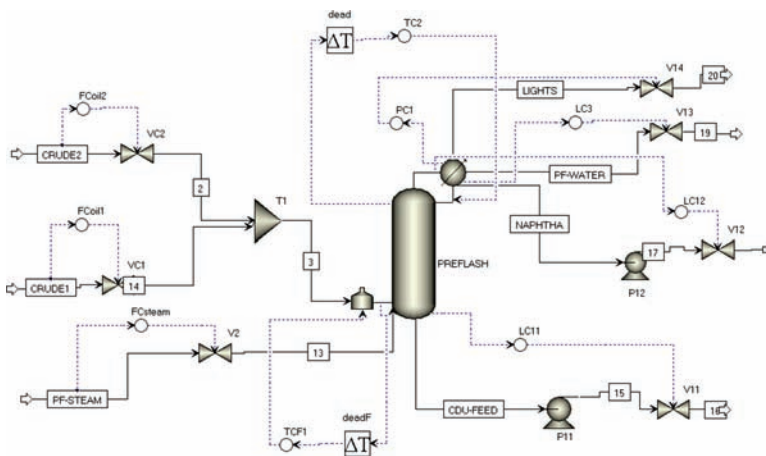


Figure 11.30 Stage 2 temperature control.

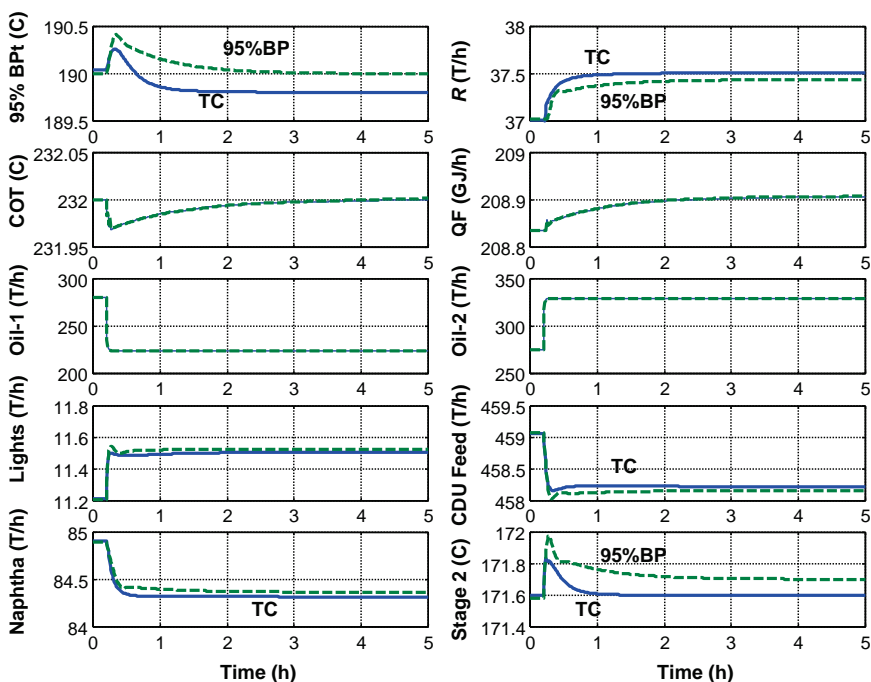


Figure 11.31 Swinging crudes with Stage 2 temperature control.

11.5 STEADY-STATE DESIGN OF PIPESTILL

Now that we have learned the fundamentals of working with petroleum fractionators by looking at a simple preflash column, we are ready to tackle the next downstream unit, a pipestill. The preflash column has removed the light hydrocarbons from the crude feed as a vapor product and produced a light naphtha product as a distillate overhead product. The bottoms from the preflash column is pumped through a furnace in which about 70% of the material is vaporized (depending on the assay of the crude) and fed into a very large column. This column produces an overhead distillate product (heavy naphtha) and three sidestreams: kerosene, diesel, and atmospheric gas oil (AGO). The bottoms is called “reduced crude” and is fed to another downstream pipestill operating under vacuum so that more gas oil can be recovered.

Two “pumparounds” are used to recover some of the high-temperature energy in the vapor stream flowing up the column. A pumparound takes hot liquid from a tray and pumps it through a heat exchanger that cools the liquid. The cooled liquid is returned back to a tray higher in the column. These pumparound trays are direct-contact heat exchangers. Typically, the heat is used to preheat the crude feed to the unit with the objective of reducing furnace fuel consumption. The design of a pipestill incorporates an interesting trade-off between energy consumption and product purity and yield. If no pumparounds were used, all of the vapor in the stream from the furnace would pass up the column and be condensed in the water- or air-cooled condenser. No heat would be recovered, so furnace firing would be much larger. A large amount of reflux would be required, which would give higher L/V ratios in the column and therefore better fractionation. This improves the

separation between the sidestream products. Therefore, the trade-off is between energy consumption and separation.

11.5.1 Overview of Steady-State Design

The flowsheet of the pipestill is shown in Figure 11.32. The column is very large in diameter (20.3 ft), operates with a top pressure of 15.7 psia, and has a total of 25 stages. The

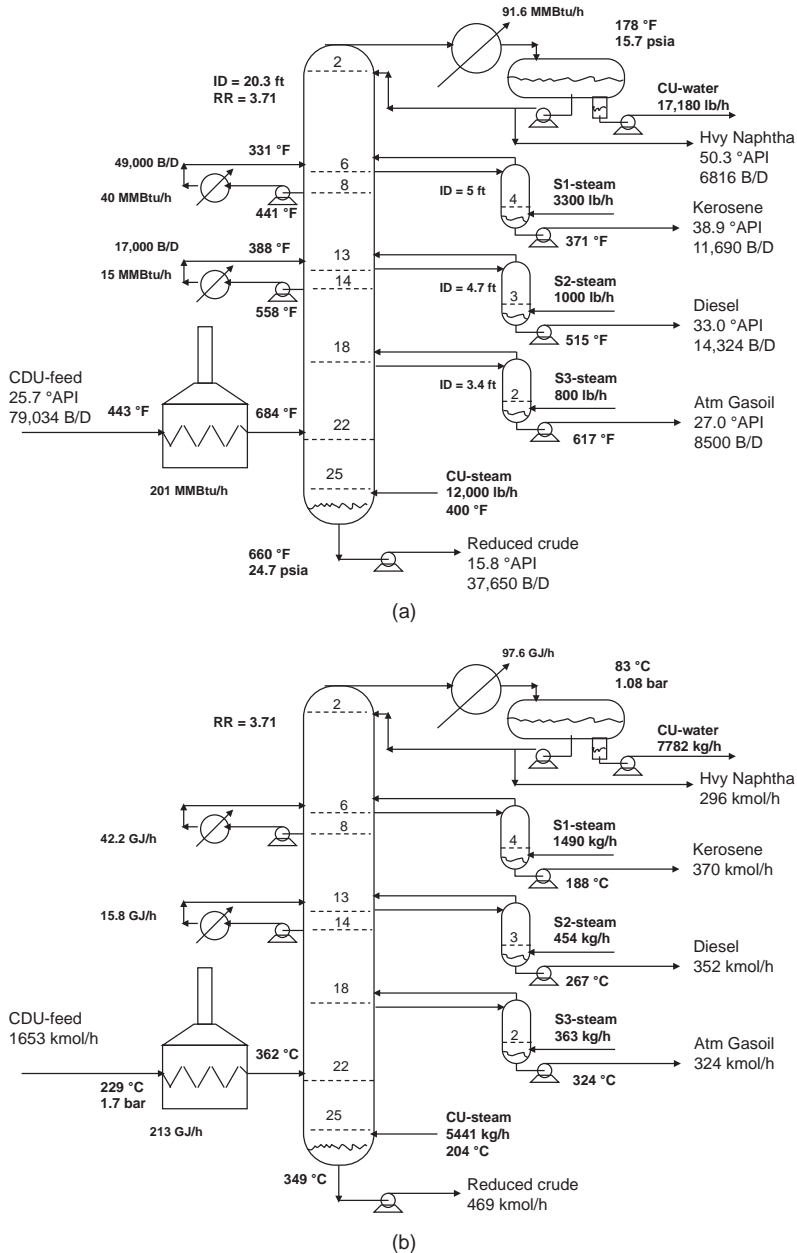


Figure 11.32 (a) Pipestill flowsheet (engineering units). (b) Pipestill flowsheet (metric units).

bottoms stream from the preflash column (see Fig. 11.25) is pumped to a furnace that heats the stream to 684 °F. The higher the temperature of the furnace exit (coil outlet temperature), the more of the stream is vaporized and the more gas oil can be recovered. However, there is a limit to the furnace temperature due to excessive thermal decomposition (“cracking”) of the crude in the furnace. If the furnace tube wall temperatures are too high, coke will be formed. This interferes with heat transfer and eventually requires a shutdown of the unit to remove the coke. The heat duty in the furnace is 201 MMBtu/h.

The feed is partially vaporized: 2278 lb mol/h of vapor with a feed of 3644 lb mol/h. It is introduced into the flash zone on Stage 22. There are three stages below the flash zone that are used to strip out any light material that is in the liquid leaving the flash zone. Open steam is fed to the bottom of the column at a rate of 12,000 lb/h. The bottoms stream from the pipestill (“reduced crude”) goes to a downstream vacuum pipestill in which more gas oil is recovered. The low pressure in the vacuum furnace produces more vapor for the same furnace temperature.

The vapor from the pipestill flash zone flows up the column. At Stage 14, a pumparound removes 15 MMBtu/h, which reduces the vapor flowing up the column and increases the liquid flowing down the column. This high-temperature heat (558 °F) is used for feed preheating. At Stage 8, a second pumparound removes 40 MMBtu/h, which further reduces the vapor flow rate and increases the liquid flow rate. This high-temperature heat (441 °F) is also used for feed preheating.

The vapor leaving the top of the column is condensed in a water- or air-cooled condenser. The liquid distillate is a heavy naphtha stream, which is used for the production of gasoline. It has ASTM 5% and 95% boiling points of 195 and 375 °F, respectively. In some refineries, it is sent to a reforming unit to produce aromatics (benzene, toluene, and xylenes) and hydrogen. The condensed water is decanted off the reflux drum. Note that this water stream is quite large (17,180 lb/h) because of all the open stripping steam that is used in the column base and sidestream strippers.

The reflux ratio is 3.71. At Stage 6, some liquid is withdrawn and fed to a 4-stage stripper. Open steam (3300 lb/h) is used to strip light material from the liquid leaving the main column. A kerosene product is produced from the bottom of the stripper. It has ASTM 5% and 95% boiling points of 396 and 502 °F, respectively.

In the distillation of distinct chemical components, we talk about separation in terms of the compositions of the impurities in the product streams. In the distillation of petroleum fraction, separation is expressed in terms of “gaps” and “overlaps.” These terms refer to the difference between the 95% boiling point of a lighter product and the 5% boiling point of the adjacent next heavier product. If there were perfect separation of the petroleum cuts, the final boiling point of a lighter product would be equal to the initial boiling point of the next heavier product. But separation is not perfect. The 95–5% difference is used as a measure of fractionation. It can be improved by using more trays or by increasing the liquid-to-vapor ratio in the section of the column in which the separation between the two cuts is occurring. For example, there is a *gap* of 21 °F between the heavy naphtha (95% point of 375 °F) and the kerosene (5% point of 396 °F). This fairly good separation is achieved because of the 3.71 reflux ratio and the five trays between these two products. As we will see, the separations between the other products have overlaps instead of gaps because of the smaller liquid-to-vapor ratios in the lower sections of the column.

Liquid from Stage 13 is withdrawn and fed to a 3-stage stripper. Open steam (1000 lb/h) is fed to the bottom of the stripper. A diesel product is produced from the bottom of the stripper. It has ASTM 5% and 95% boiling points of 489 and 640 °F, respectively. Note that there is a 13 °F *overlap* between the 95% point of the kerosene (502 °F) and the 5% point of the diesel (489 °F).

A 2-stage stripper at Stage 18, using 800 lb/h of open steam, produces AGO with ASTM 5% and 95% boiling points of 589 and 782 °F, respectively. There is a 51 °F *overlap* between the 95% point of the diesel (640 °F) and the 5% point of the AGO (589 °F). This sloppy separation between petroleum cuts is typical of petroleum separation. The values of the different products are usually not drastically different and improved fractionation can seldom be justified.

11.5.2 Configuring the Pipestill in Aspen Plus

Installing all the equipment and setting up all the conditions discussed above is a fairly involved procedure. We will go through the details step by step. The pipestill is installed on the flowsheet by clicking *Columns* and *PetroFrac* on the *Model Library* tool bar at the bottom of the Aspen Plus window. As shown in Figure 11.33, the “CDU10F” icon is selected (third row, middle column) and pasted on the flowsheet. This configuration has a furnace, multiple sidestream strippers, and multiple pumparounds. Figure 11.34 shows the final flowsheet with all the equipment installed, including the pumps and valves required for dynamic control.

The first step is to connect the bottoms from the preflash column to the furnace of the pipestill. As we did with the preflash furnace, the red input arrow that appears at the bottom of the column (shown at the top of Fig. 11.35) must be dragged over to the furnace (shown at the bottom of Fig. 11.35).

A similar procedure of clicking an arrow and dragging it to the desired location must be performed on the strippers to connect the steam lines and the product withdrawal lines at

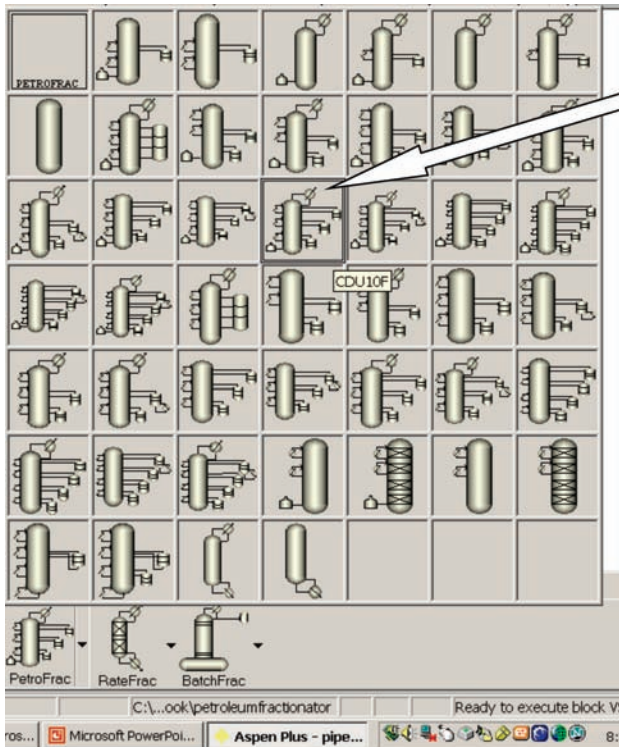


Figure 11.33 PetroFrac palette.

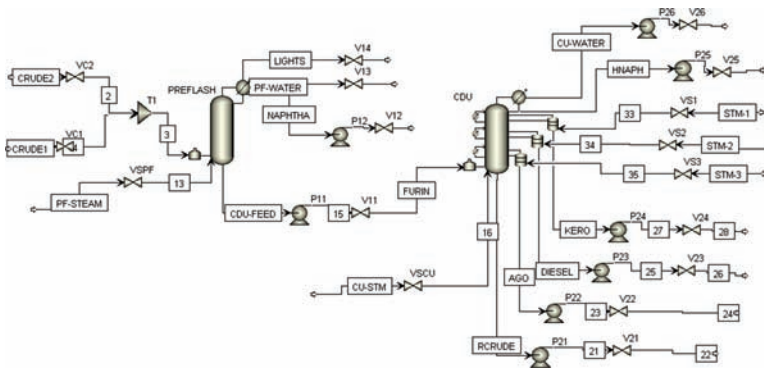


Figure 11.34 Preflash and pipestill.

the base of the stripper. Figure 11.36 gives an example in which a material stream is selected to be installed as steam to the third stripper. The top picture shows that blue arrows appear at the *top* stripper. We click on the input arrow pointing to the side of the stripper and drag it to the side of the *third* stripper. When the blue arrow is in the desired location (see the bottom picture in Fig. 11.36), the mouse button is released and the connection is made. This is repeated for the steam inputs of the other strippers and for the product streams leaving the bottom of each stripper.

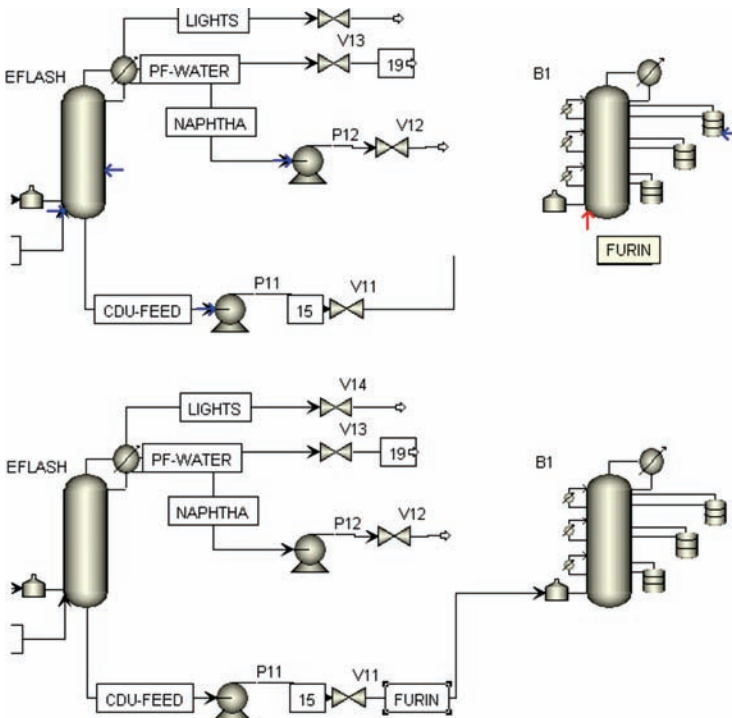


Figure 11.35 Connecting feed to furnace.

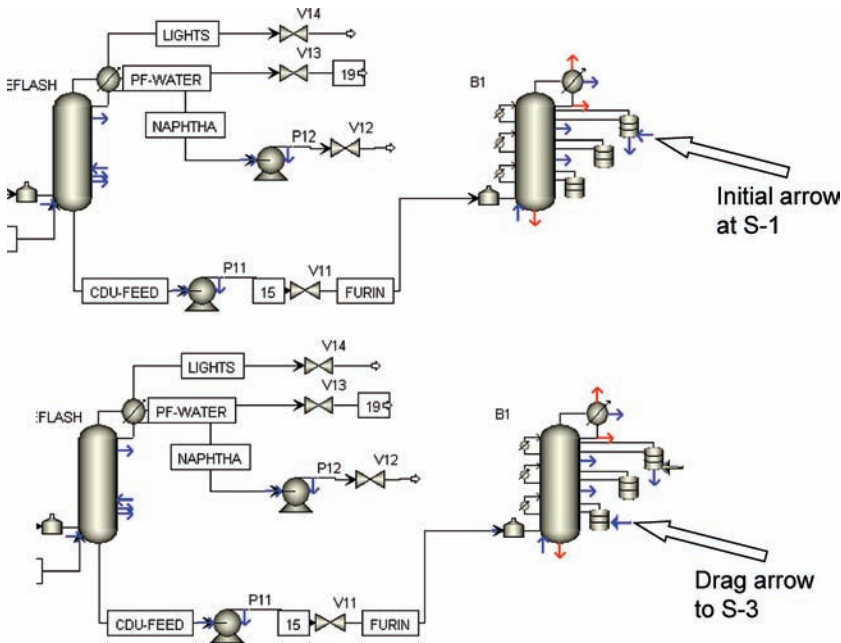


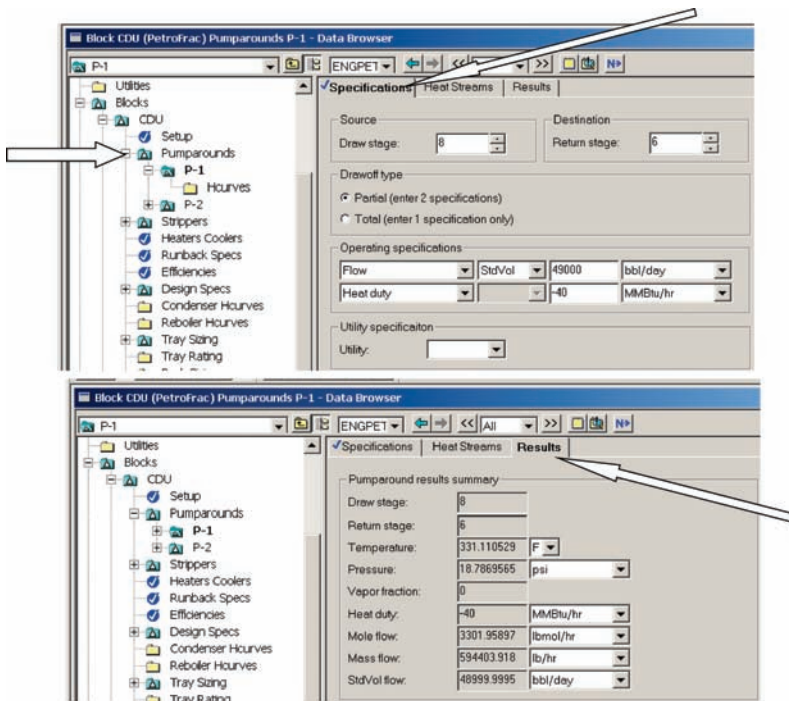
Figure 11.36 Making connections to the strippers.

Material streams for the heavy naphtha distillate (HNAPH), water from the reflux-drum decanter (CU-WATER), steam to the column base (CU-STM), and the bottoms (RCRUDE) are made in the normal way.

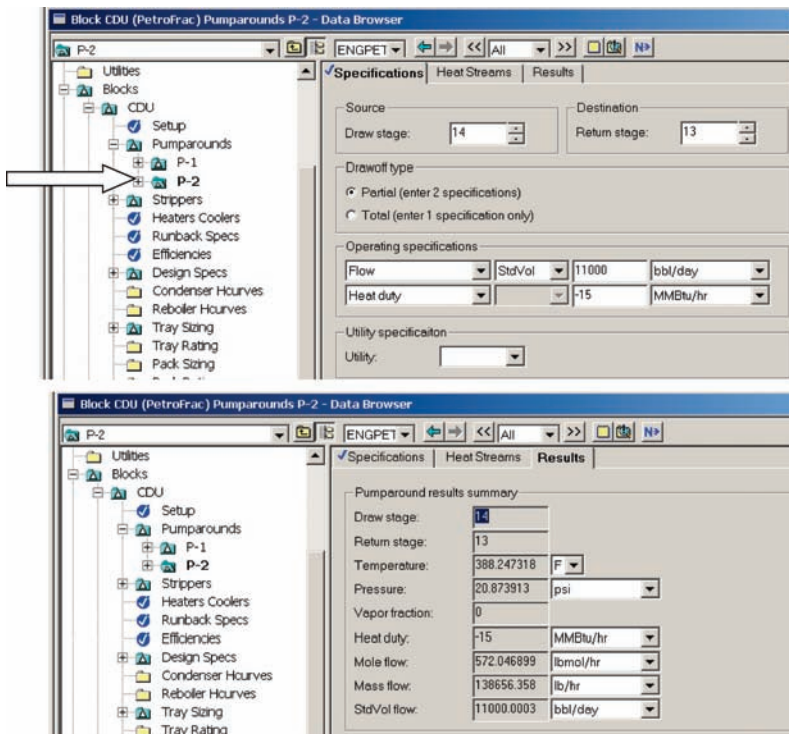
Now we must set up the pumparounds and the strippers. On the Aspen Plus *Data Browser* under the CDU block, there are items for pumparounds and strippers. Clicking the *Pumparounds* item opens a window on which *New* is clicked, an identification label is selected and the window shown at the top of Figure 11.37a opens. On the *Specifications* page tab, a number of items are specified. For pumparound P-1, the stage from which the hot liquid is removed is Stage 8. The stage to which the cool liquid is returned is higher in the column at Stage 6. The flow rate is specified to be 49,000 B/D, and the heat removed is set at 40 MMBtu/h. Clicking the *Results* page tab (after the simulation has been run) gives useful information about pumparound P-1, as shown in the bottom window of Figure 11.37a. Note that the temperature of the return pumparound liquid is 331 °F.

The setup and results for the second pumparound P-2 are shown in Figure 11.37b. The stage from which the hot liquid is removed is Stage 14. The stage to which the cool liquid is returned is Stage 13. The flow rate is specified to be 11,000 B/D, and the heat removed is set at 15 MMBtu/h.

The three strippers are installed in a similar manner. The *Stripper* item under the CDU block is clicked, the *New* button is clicked, the new stripper is identified, and the window shown at the top of Figure 11.38 opens. With the *Configuration* page tab clicked, a number of parameters of the stripper are specified. For the top stripper S-1, the number of stages is 4, the product is *KERO*, the liquid draw stage from the main stripping column is Stage 6, and the vapor from the stripper is returned to Stage 5. The steam stripping is done by the stream labeled “33.” The flow rate of the bottoms product from the stripper is specified to be 11,700 B/D. Clicking the *Pressure* page tab opens the window shown at the bottom of Figure 11.38 on which the Stage 1 pressure and the pressure drop per stage are set.



(a)



(b)

Figure 11.37 (a) Specifying pumparound P-1. (b) Specifying pumparound P-2.

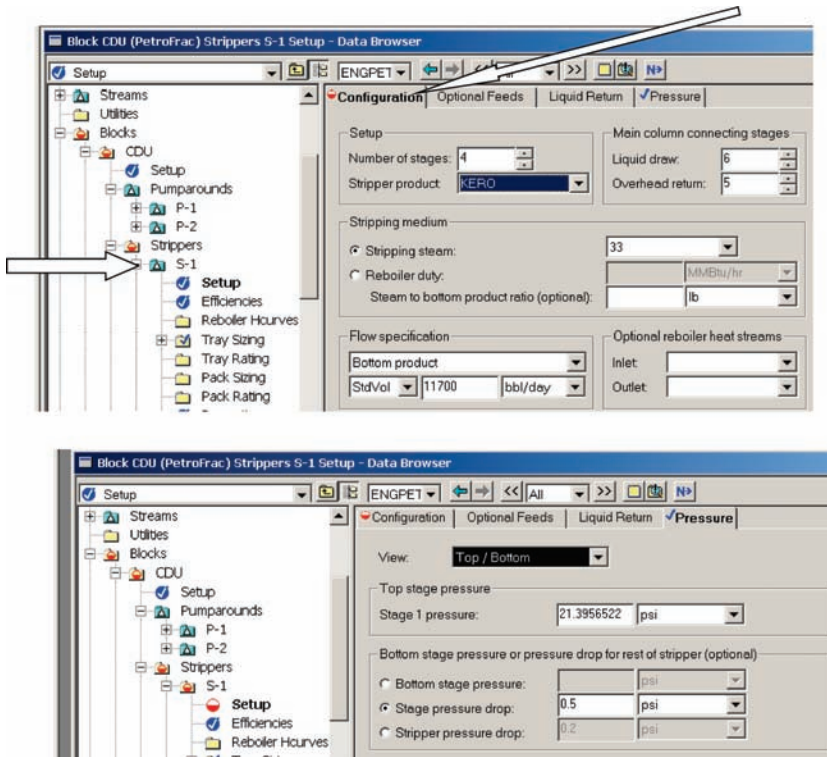


Figure 11.38 Specifying stripper S-1.

The pumps on the pipestill are specified in the normal way with 100 psi pressure rises. The valves are specified to have 50 psi pressure drops. The diameter of the main column and the diameters of each of the strippers are calculated using the *Tray Sizing* functions. The *Specifications* page tab is shown in Figure 11.39 for the top stripper (S-1).

Setting up the main column starts with clicking the *CDU* item under *Blocks* in the *Data Browser*. Then *Setup* is clicked and the *Configuration* page tab, which opens the window shown at the top of Figure 11.40a. The number of stages, a total condenser, and an estimate of the

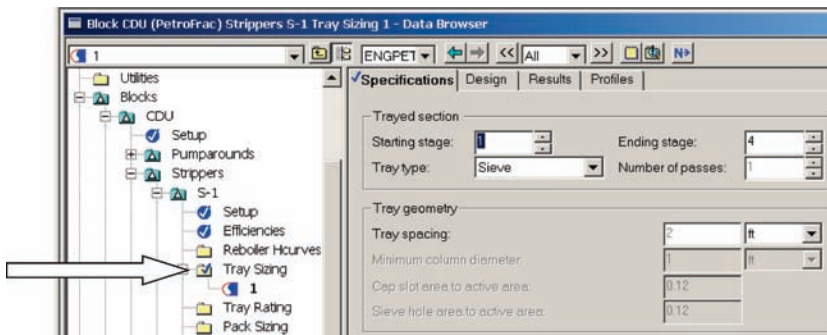
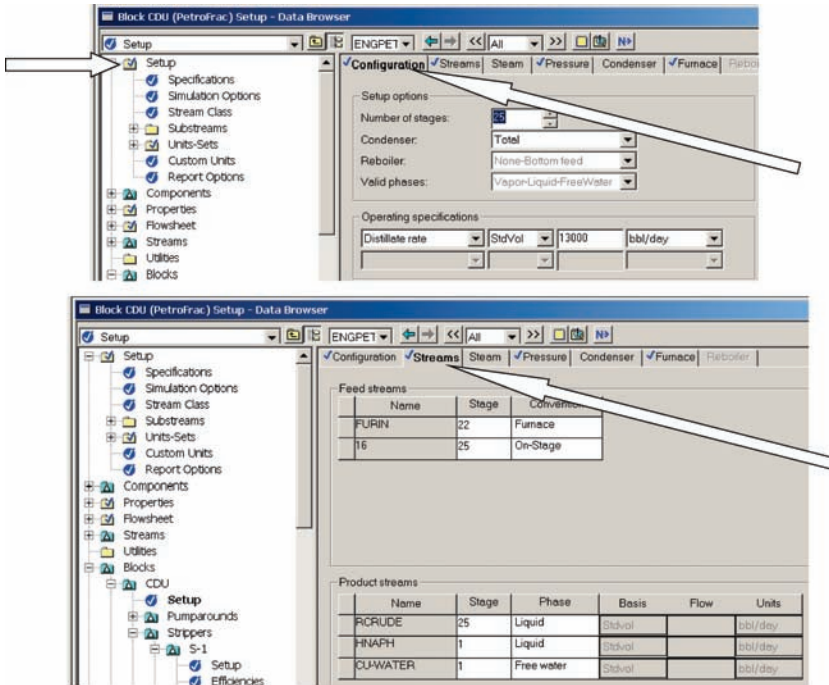
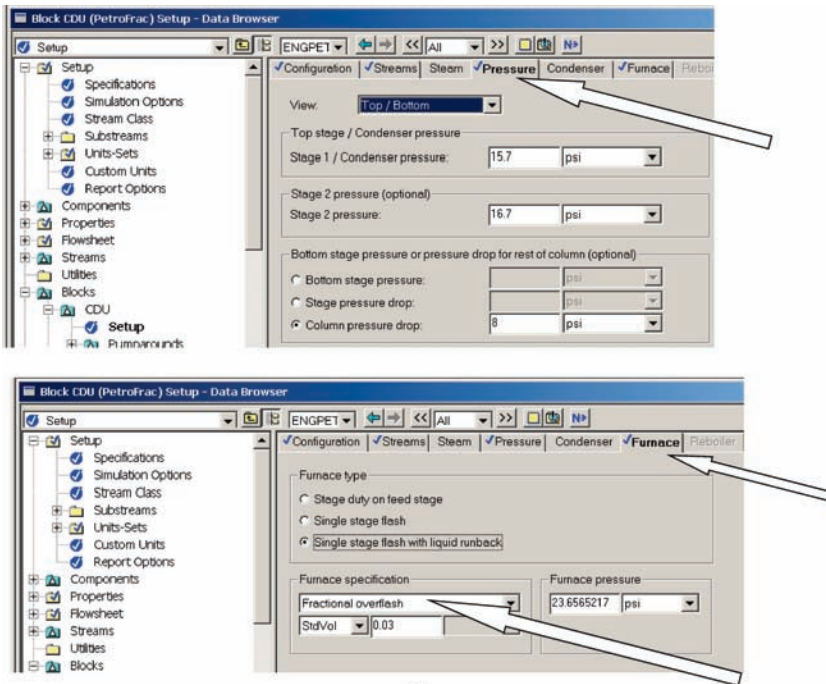


Figure 11.39 Tray sizing for stripper S-1.



(a)



(b)

Figure 11.40 (a) Setup for main column: configuration and streams. (b) Setup for main column: pressure and furnace.

distillate flow rate are specified. Clicking the *Streams* page tab opens the window shown at the bottom of Figure 11.40a on which the locations of the various input and output streams are specified. Note that the feed to the furnace is specified to enter on Stage 22, and the stripping steam enters three trays lower (Stage 25). Clicking the *Pressure* page tab gives the window shown at the top of Figure 11.40b and the appropriate pressure information is entered.

Clicking the *Furnace* page tab opens the window shown at the bottom of Figure 11.40b. There are several options for setting up the furnace. For *Furnace type*, we select the *Single stage flash with liquid runback*. For *Furnace Specification*, we select *Fractional overflash* and specify it to be 0.03. The term “overflash” refers to the fraction of the vapor that is produced in the flash zone of the column that is returned as liquid to the flash zone from the tray above the flash zone. Most of the liquid coming down the column is withdrawn as sidestreams, but some liquid is needed on the trays below the lowest sidestream and above the flash zone to prevent entrainment of heavy liquid up the column with the vapor. Entrainment could drive the color of the gas oil off-specification. It could also increase the concentration of metal contaminants in the gas oil because some crude oils contain small amounts of metals. The gas oil is usually fed to a catalytic cracking unit, and the catalyst in this unit is deactivated by metals. Therefore, a small “wash” or “overflash” stream is needed.

The final part of the steady-state design is to set up two *Design Specs*. The first varies the flow rate of the heavy naphtha to achieve an ASTM 95% boiling point of 375 °F. The second varies the flow rate of the diesel to achieve an ASTM 95% boiling point of 640 °F. The setups for these are shown in Figure 11.41. The top picture in Figure 11.41a gives the

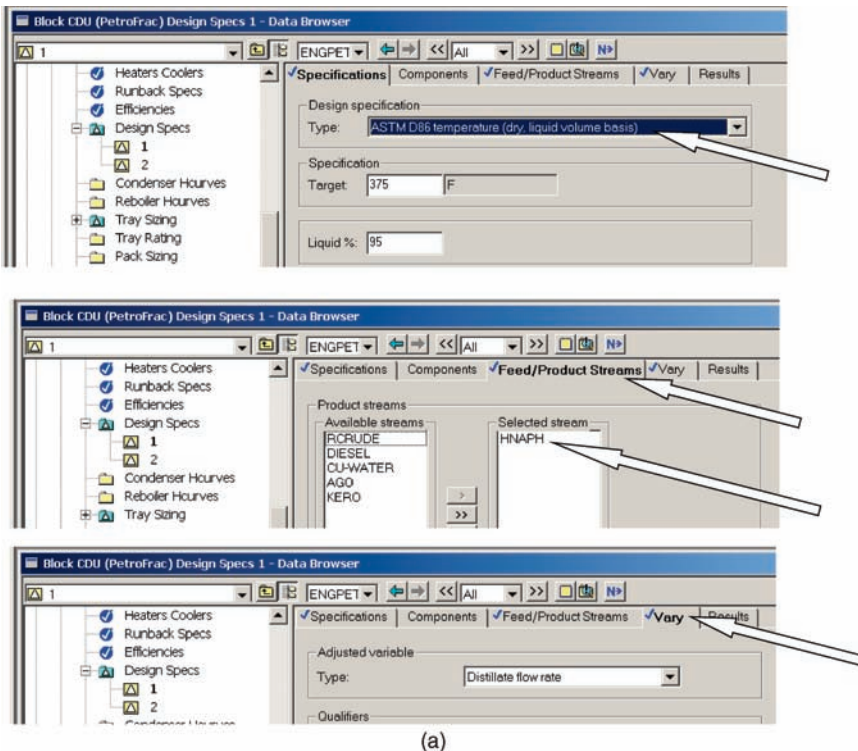


Figure 11.41 (a) Design Spec for heavy naphtha. (b) Design Spec for diesel.

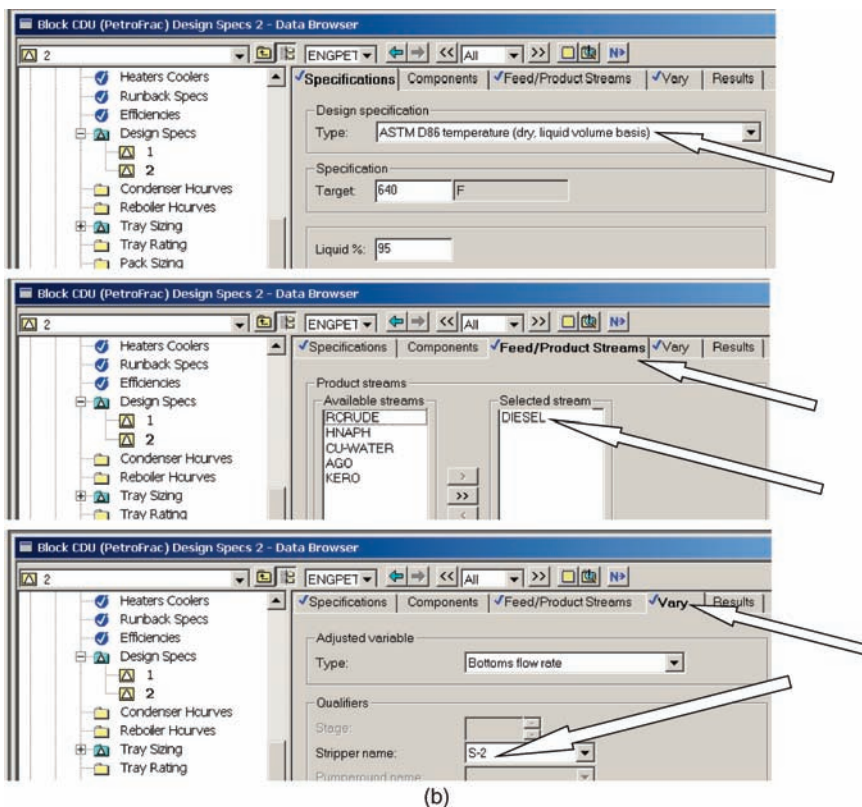


Figure 11.41 (Continued)

Specification page tab for the heavy naphtha Design Spec. The middle picture gives the *Feed/Product Streams* page tab. The bottom picture gives the *Vary* page tab. Note that *Distillate flow rate* is selected.

Figure 11.41b gives the same information for the diesel design specification. Note that the stream selected to vary is *Bottoms flow rate* from the S-2 stripper.

The ASTM curves for all the products from the pipestill are generated by going to *Results Summary* on the *Data Browser* window, clicking *Streams*, selecting the *Vol.% Curves* page tab, and selecting the *ASTM D86 curve* in the *Curve view* window, as shown in Figure 11.42.

Next, left click the top of the *Vol%* column, which highlights this column. Go to the toolbar at the top of the Aspen Plus window, click *Plot* and click *X-Axis Variable*. Highlight each of the columns for the products that you want to plot by holding down the *Ctrl* key and clicking the top of each column. Then go to the toolbar, click *Plot* and click *Y-Axis Variable*. Finally go to the toolbar, click *Plot* and click *Display Plot*. Results are shown in Figure 11.43.

Two of the unique features of a petroleum fractionator are the large changes in temperature and flow rates from the bottom to the column. Figure 11.44 gives these profiles for the pipestill.

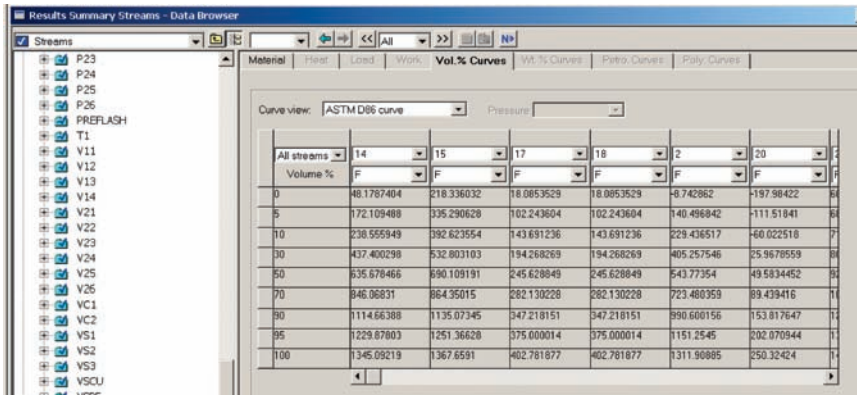


Figure 11.42 Generating ASTM curves for all products.

The temperature range is from near 180 °F at the top to over 650 °F at the flash zone. Note that the temperature decreases slightly in the bottom three trays due to the stripping with 400 °F steam.

The molar flow rates of the liquid and vapor increase as we move up the column from the flash zone. At the pumparounds the vapor rate decreases.

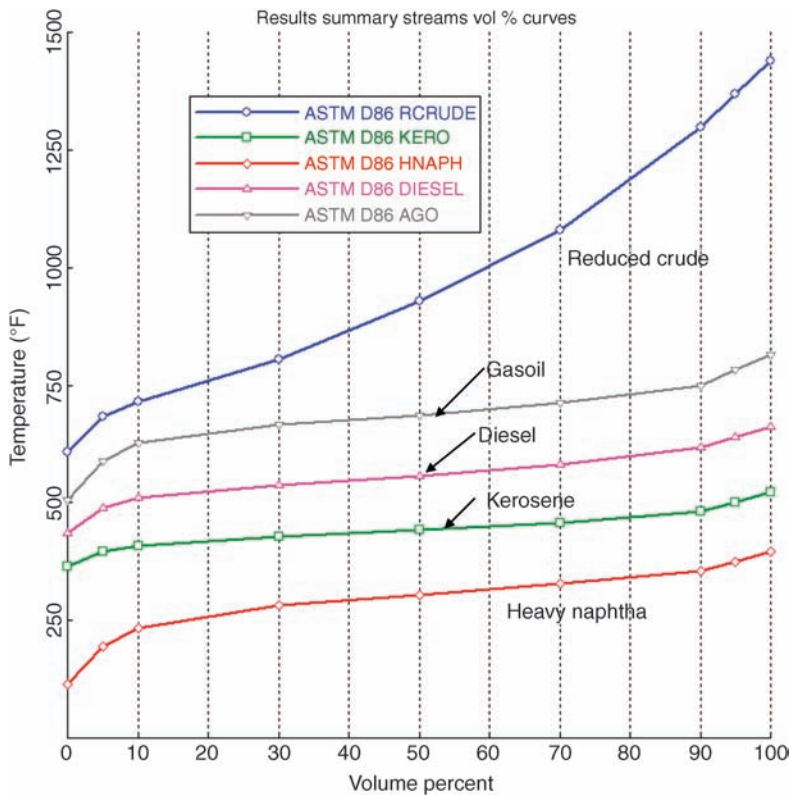


Figure 11.43 ASTM curves for cuts.

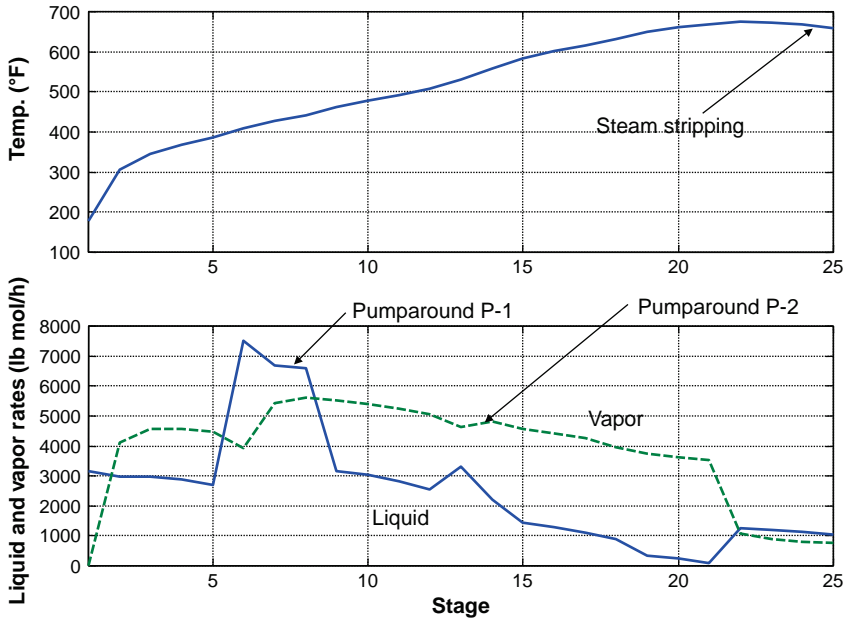


Figure 11.44 Pipestill profiles.

11.5.3 Effects of Design Parameters

Before we move on to dynamics and control, it may be useful to explore briefly the impact of some of the design parameters on the yields and the boiling points of the various products. This insight will be used when a control structure is developed to maintain the several specifications in the face of disturbances.

In setting up the steady-state design, we have specified all of the equipment parameters (the number of stages and locations of feeds and withdrawal points). In addition, we have specified 10 operating variables, that is, there are 10 operating degrees of freedom in this pipestill process.

1. The 95% boiling point specification on the heavy naphtha stream is 350 °F.
2. The diesel 95% boiling point specification is 640 °F.
3. The flow rate of AGO is 8500 B/D.
4. The fractional overflash specification is 0.03.
5. The four stripping steam flow rates are fixed (one to the base of the column and one to each of the three strippers).
6. The heat removals in the two pumparounds.

Let us explore what the steady-state effects are of changing some of these variables and establish some principles of operating a petroleum fractionator.

Effect of Changing a 95% Specification. Suppose we change the 95% boiling point specification on the heavy naphtha stream from 375 to 350 °F, with the other degrees of freedom unchanged. The result is a decrease in the heavy naphtha flow rate from 6830 to

5425 B/D. The lower 95% boiling point means that a lower fraction of the crude is taken off as heavy naphtha. There is a corresponding reduction in the 5% boiling point of the kerosene, which changes from 395 to 380 °F. This illustrates an important principle in the operation of sidestream petroleum fractionators.

Principle 1

*The 95% and 5% boiling point of adjacent cuts cannot be **independently** set. For example, a decrease in the draw rate of a product results in a **decrease** in its 95% boiling point and a **decrease** in the 5% boiling point of the next heavier product stream.*

The reflux flow rate also increases (from 2517 to 2884 lb mol/h). This and the lower distillate flow rate produce a higher reflux ratio (increases from 3.875 to 5.41), which has the effect of providing more fractionation between the heavy naphtha and the kerosene. The “gap” between these cuts increases from $395 - 375 = 20$ to $380 - 350 = 30$ °F.

In a similar way, suppose the specification on the 95% boiling point of the diesel is reduced from 640 to 620 °F. The flow rate of the diesel decreases from 14,363 to 12,112 B/D. This drops more light material into the lower AGO stream, so its 5% point drops from 589 to 500 °F and its 95% point from 782 to 765 °F. The flow rate of the bottoms increases from 37,647 to 39,953 B/D, and its 5% point changes from 692 to 665 °F.

Effect of Changing a Pumparound. Changing a pumparound heat removal affects the vapor traffic in the column above the pumparound and the liquid traffic below the pumparound. Of course, it also affects the furnace firing rate because the temperature of the feed to the furnace changes. For example, suppose we change the heat removal in top pumparound (P-1) from 40 to 30 MMBtu/h. More vapor flows up through the top part of the column, which increases the reflux ratio from 3.875 to 4.466 and increases the condenser heat removal from 92 to 102 MMBtu/h. The higher liquid/vapor ratio provides better fractionation above the pumparound. The gap between the heavy naphtha and the kerosene increases from $395 - 375 = 20$ to $398 - 375 = 23$ °F. Thus, there is a slight improvement in this separation.

The downside of this change is that more heat is rejected to cooling water in the condenser instead of being recovered by feed preheating. The effect on furnace firing depends on the configuration of the heat exchanger network used, which is not modeled in the simulation considered in this chapter.

Principle 2

Pumparounds affect separation between cuts and furnace firing in opposite ways. Reducing a pumparound heat removal improves separation between cuts above the pumparound, but increases furnace energy consumption.

Effect of Changing Stripping Steam. Open steam is used in the strippers to remove the light material that is in the liquid withdrawn from the main column. Changing stripping steam flow rate affects the initial part of the boiling point curve, but has less of an effect on 5% point and essentially no effect on the 95% point and product flow rates. Of course, using more steam increases steam consumption and increases the load on water purification facilities required to handle the water decanted off the reflux drum.

For example, suppose the stripping steam to the top (kerosene) stripper is increased from 3300 to 5000 lb/h. All other degrees of freedom remain unchanged. The initial *TBP* boiling point of the kerosene changes from 311 to 321 °F. The initial *ASTM* boiling point of the kerosene changes from 366 to 374 °F. The *ASTM* 5% point only changes from 395 to 399 °F. The *ASTM* 95% point only changes from 502 to 503 °F.

Principle 3

The flow rate of stripping steam affects the initial boiling point or the flash point of the cut.

The steady-state design is now complete. We are ready to investigate dynamics and control of this complex system.

11.6 CONTROL OF PIPESTILL

A petroleum fractionator, such as a pipestill or a cat fractionator, is almost overwhelmingly complex. In addition to the main column, there are strippers that have vapor and liquid streams going back to and coming from the main column. There are a very large number of control loops to set up. Let us enumerate the loops that we will set up, considering both the preflash column and the pipestill.

1. *Temperature loops*: Temperatures of both furnaces (two loops).
2. *Flow loops*: Two crude feeds, steam to two column bases, steam to three strippers, and Stage 19 liquid in the pipestill (eight loops)
3. *Pressure loops*: Condenser in both columns and three strippers (five loops)
4. *Level loops*: Base level of two columns, water level in two reflux drums, organic level in two reflux drums, and base levels in three stripper bases (nine loops)
5. *ASTM boiling points*: 95% boiling point of light naphtha, 95% boiling point of heavy naphtha, 5% boiling point of diesel, and 95% boiling point of diesel (four loops)

There are 28 controllers to set up on these two columns.

The equipment associated with the preflash column has already been sized. The diameters of the pipestill column and the three strippers are sized using the *Tray Sizing* feature of Aspen Plus for each vessel. The results are

Pipestill diameter = 20.3 ft

Stripper S-1 diameter = 5.0 ft

Stripper S-2 diameter = 4.7 ft

Stripper S-3 diameter = 3.4 ft

The reflux drum, the column base, and the bases of the three strippers are sized to give 5 min of holdup at a 50% level.

The file is pressure checked and exported into Aspen Dynamics.

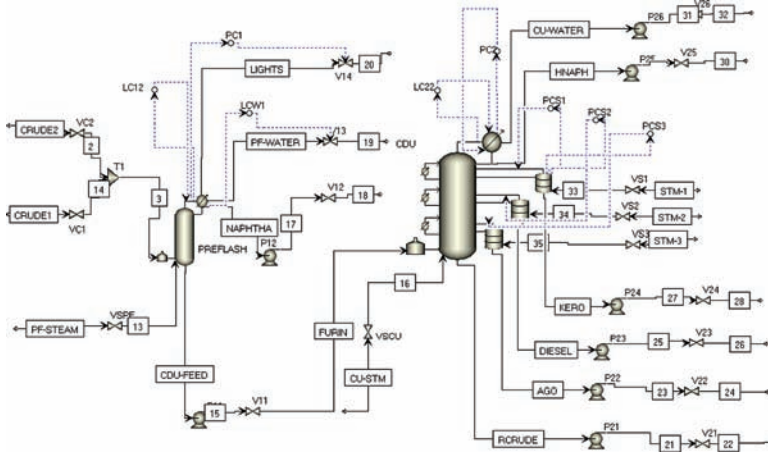


Figure 11.45 Initial control structure.

The initial control structure set up by Aspen Dynamics is shown in Figure 11.45. The flowsheet is quite congested with many process lines, control lines, and equipment. It takes a fair amount of art work to rearrange the drawing to make it readable.

The two condenser pressure controllers, two organic-phase level controllers, and the water-phase level controller in the preflash column have been installed. In addition, pressure controllers on the three strippers are set up. Note that the vapor flows from the strippers back to the main column are manipulated. No control valve is shown in the vapor line, indicating that a “flow-driven” assumption is made in this flow. Note also that the three stripper pressure signals all appear to come from the first stripper. These will be moved in the final flowsheet to start from the appropriate stripper for each pressure controller. This is done by clicking the control signal, clicking the blue arrow at the point of origin, and dragging it to the correct location when the arrow turns red. The original flowsheet showed the three pressure controller output signals all going to the vapor line of the top stripper. These lines have been relocated to show them going to the correct vapor line of each stripper.

Installing the level controller to hold the levels in the base of each column and the two levels in each reflux drum is straightforward. Note that the organic level is controlled by manipulating the reflux flow rate in both columns because the reflux ratios are large. When selecting the *PV* signal for the levels in the reflux drums, the organic phase is *Level 1* and the water phase is *Level 2*. Proportional controllers with gains of 2 are used on all levels. The two furnace temperature controllers are installed in the conventional way. Deadtimes of 1 min are used in these loops, and temperature transmitter ranges are 100–500 °C. Relay-feedback testing and Tyreus–Luyben tuning give controller gains of 0.6 and integral times of 4 min in both controllers.

Flow controllers are installed on the steam to the base of the two columns. These flow rates are ratioed to the feed flows to the respective column by using multipliers. The molar steam-to-feed ratio in the preflash column is $125.9/2722 = 0.04625$. The total crude feed is used (after the summer). The molar steam-to-feed ratio in the pipestill is $302.1/1654 = 0.1827$.

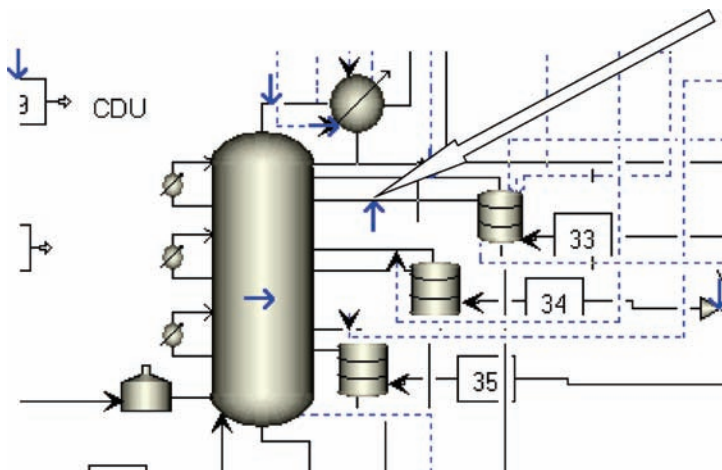


Figure 11.46 Selecting draw rate to stripper.

The two steam flow controllers are “on cascade” with their set points coming from multipliers set up with the appropriate constant and with the appropriate flow signal input.

Setting up the stripper base level controllers requires a little graphical skill. All the input and output arrows appear on the top stripper and must be moved to the correct location. For example, Figure 11.46 shows an arrow pointing to the liquid line between the main column and the top stripper. This is the correct location for the *Stripper Draw (S-1)* when the output signal for the stripper S-1 level controller is being set up. For the other strippers, the arrow must be moved to the correct location. Figure 11.47 shows the selection of the manipulated variable (level controller *OP* signal). In Aspen Dynamics, the *OP* signal is called the *Control Variable* instead of the less confusing terminology of calling it the manipulated variable. In this book the “controlled” variable is the *PV* signal.

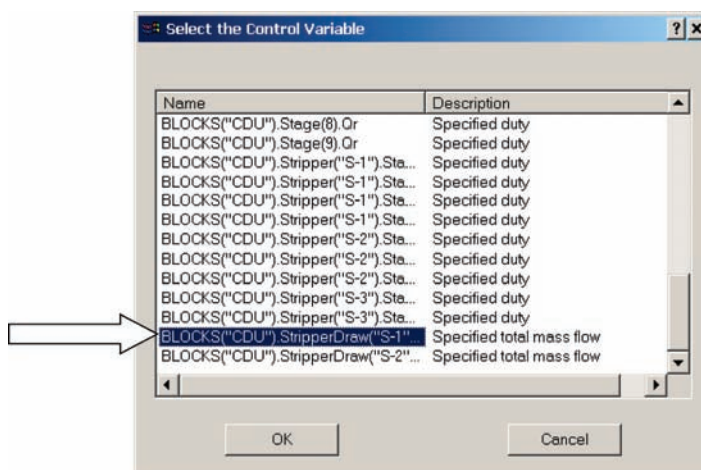


Figure 11.47 Selecting draw rate to stripper S-1.

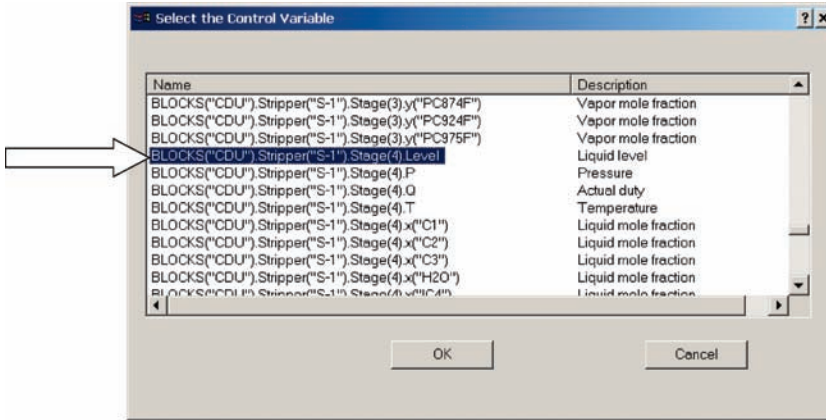


Figure 11.48 Selecting Stage 4 level in stripper S-1.

Specifying the *PV* signal to the stripper S-1 level controller is shown in Figure 11.48. The stripper has four stages, so the level on Stage 4 is selected. Each of the three stripper level controller is set up in the same way. The diagram is quite congested. Figure 11.49 gives an enlarged view of the stripper section of the flowsheet showing the three pressure and three level controllers with the *PV* and *OP* signals coming from the correct locations on the appropriate stripper vessels. Note that the level controllers are “reverse” acting since they control level by changing the flows of material *into* the strippers.

A flow controller is installed to control the “overflow” flow of liquid below the AGO draw off tray. This is achieved by manipulating the control valve V22 in the AGO line. Remember that the

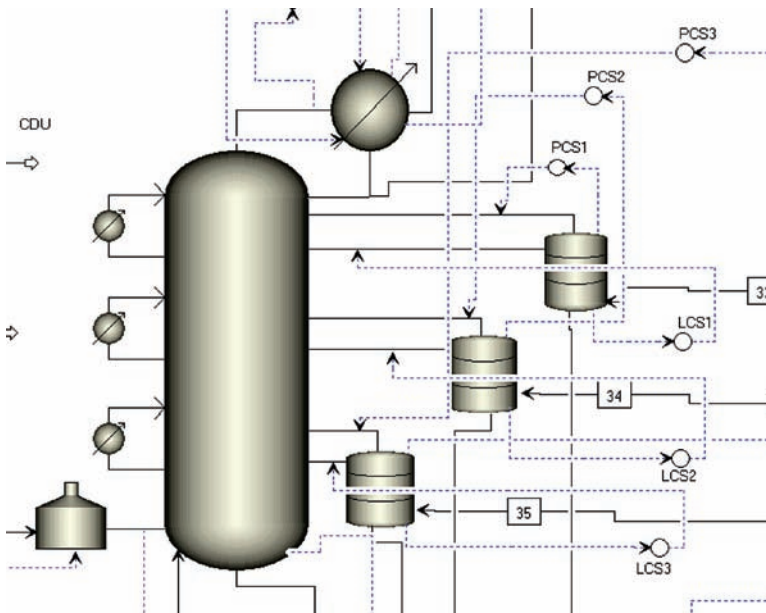


Figure 11.49 Pressure and level control setup of strippers.

```

Text Editor - Editing Flowsheet
CONSTRAINTS
// Flowsheet variables and equations...

Blocks("FCwash").PV=Blocks("CDU").Stage(19).Fml_out;
END

```

Figure 11.50 Flowsheet equation for controlling wash flow rate.

liquid draw from the column to the stripper controls the liquid level in the base of the stripper. Manipulating the AGO flow changes the liquid draw rate and therefore the amount of liquid that is *not* drawn off and, as a result, flows down the column. The FCwash flow controller must be “direct” acting, that is, if there is too much Stage 19 liquid, the AGO flow should be increased.

The internal liquid and vapor flow rates are not listed in the possible output variables to be controlled, so a *Flowsheet Equation* is used. Figure 11.50 shows the equation used. The mass flow rate of liquid leaving Stage 19 (“Fml_out”) of the main column (“CDU”) is defined as the *PV* signal to a flow controller (“FCwash”). When this equation is compiled, the red light at the bottom of the window indicates that the system is overspecified. This is corrected by changing the *PV* variable in the FCwash controller from “fixed” to “free.” The appropriate ranges of the variables are inserted in the controller. The steady-state flow rate of Stage 19 liquid is 48,800 kg/h.

The final controllers to install are the ASTM boiling point controllers. The appropriate boiling points are selected as discussed earlier in this chapter by using the *Configure Sensor* feature for each stream. The light naphtha flow in the preflash column is manipulated to control its 95% boiling point at 190.6°C. The heavy naphtha flow in the pipestill is manipulated to control its 95% boiling point at 190.6°C. The diesel flow is manipulated to control its 95% boiling point at 338°C. All of these controllers are reverse acting.

We also want to control the 5% boiling point of the diesel. This is achieved by manipulating flow rate of the kerosene. To get this 5% boiling point, another *Configure Sensor* is used, looking at Stream 25 of the flowsheet, which has the same composition as the diesel. Note that this controller is reverse acting. If the 5% boiling point of the diesel is too high, more light material needs to be dropped down into this sidestream. This means the kerosene flow should be decreased.

Relay-feedback tests are performed on each loop individually with the other boiling point controllers on manual. Tuning results are given in Table 11.6.

TABLE 11.6 Boiling Point Controllers Tuning

	SP (°C)	TT (°C)	<i>D</i> (min)	<i>K_U</i>	<i>P_U</i> (min)	<i>K_C</i>	τ_1 (min)
Naphtha 95%	190.6	150–250	3	1.49	6	0.46	13
HNAPH 95%	190.6	150–250	3	6.63	21	2.1	46
Diesel 5%	254	200–300	3	7.03	23	2.0	51
Diesel 95%	338	300–400	3	4.06	23	1.2	51

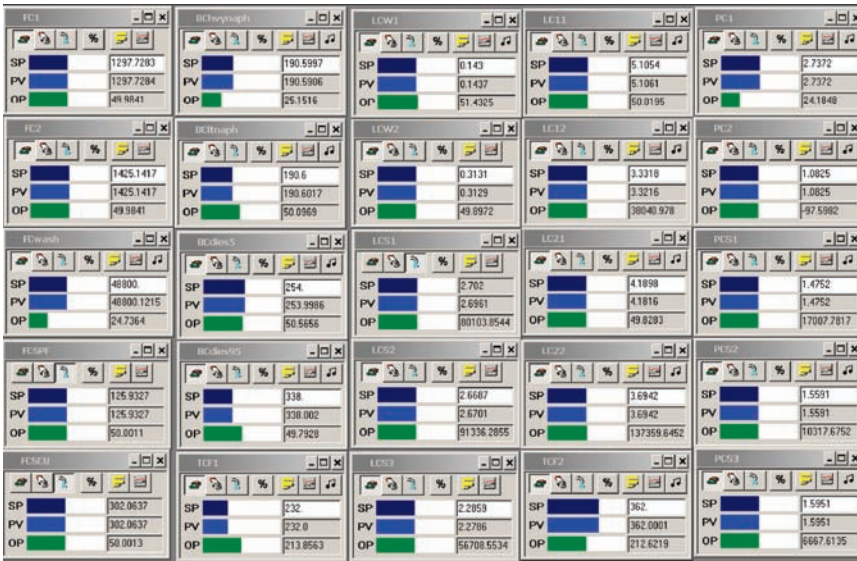


Figure 11.51 Controller faceplates.

All of the controller faceplates are shown in Figure 11.51. There are 25 controllers. There should be three more flow controllers, one on each of the steam to the strippers. The final flowsheet is given in Figure 11.52. Not installed or shown are the steam flow controllers on the strippers because they add more congestion to an already cluttered picture.

The effectiveness of this control scheme is demonstrated in Figure 11.53. The disturbances are step changes in the set points of the two crude oil flow controllers at time equal 0.2 h. The responses to both positive and negative 20% changes are shown. The maximum deviations in the 95% boiling points of the light and heavy naphtha products are about 6 °C.

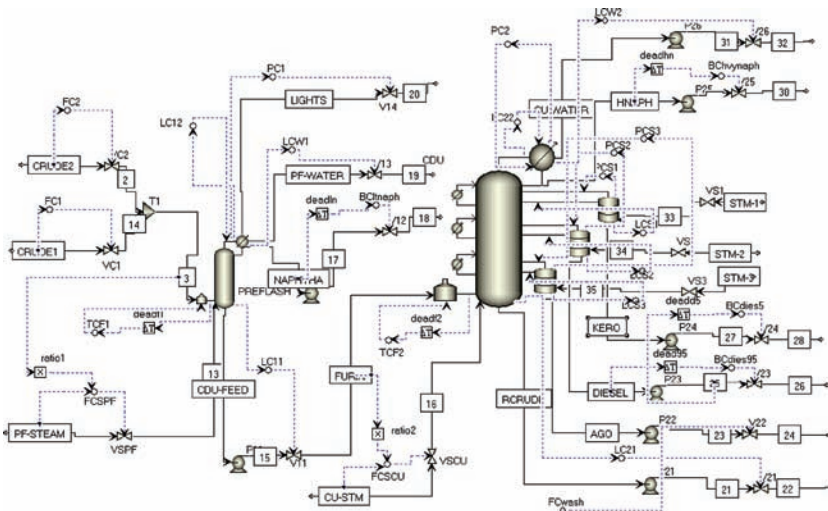
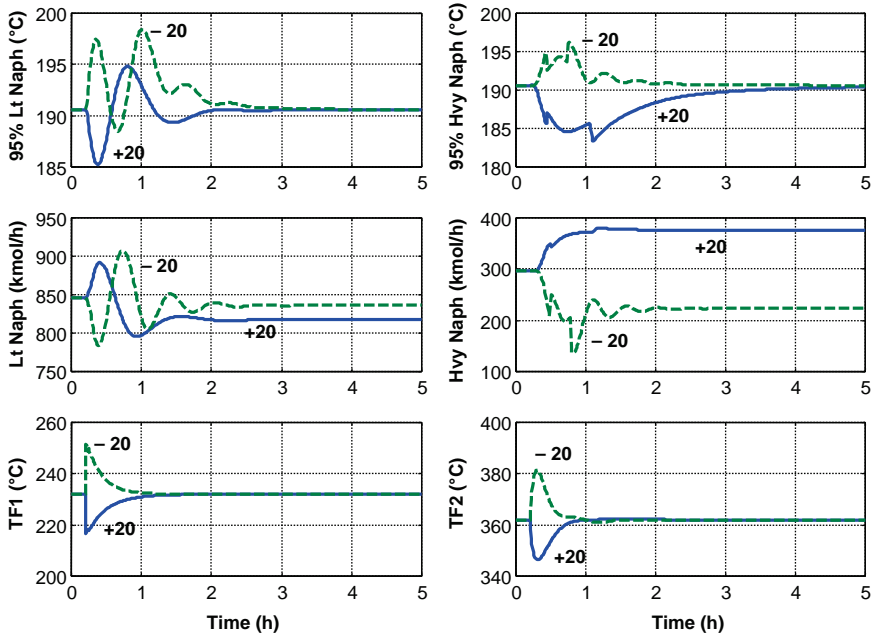
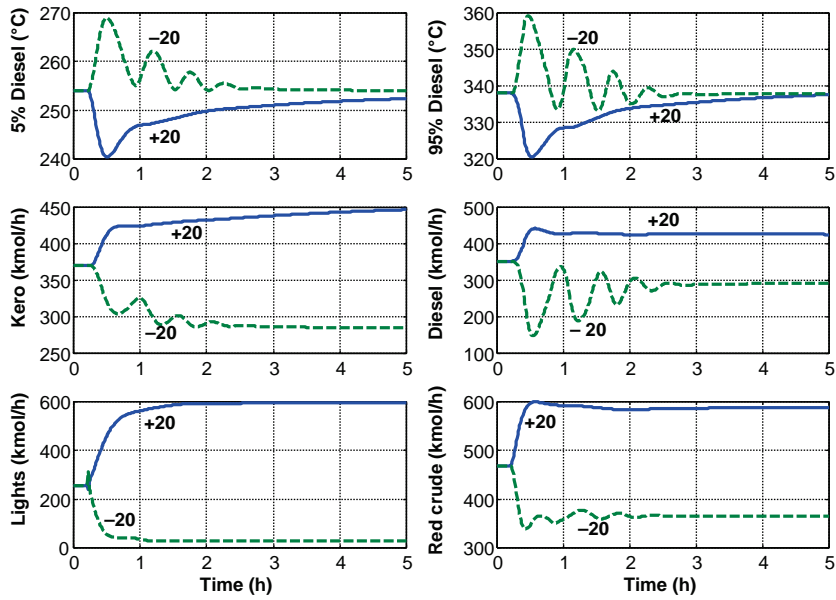


Figure 11.52 Control structure.



(a)



(b)

Figure 11.53 (a) Feed flow rate disturbances of both crudes. (b) Increasing Crude 1 and decreasing Crude 2.

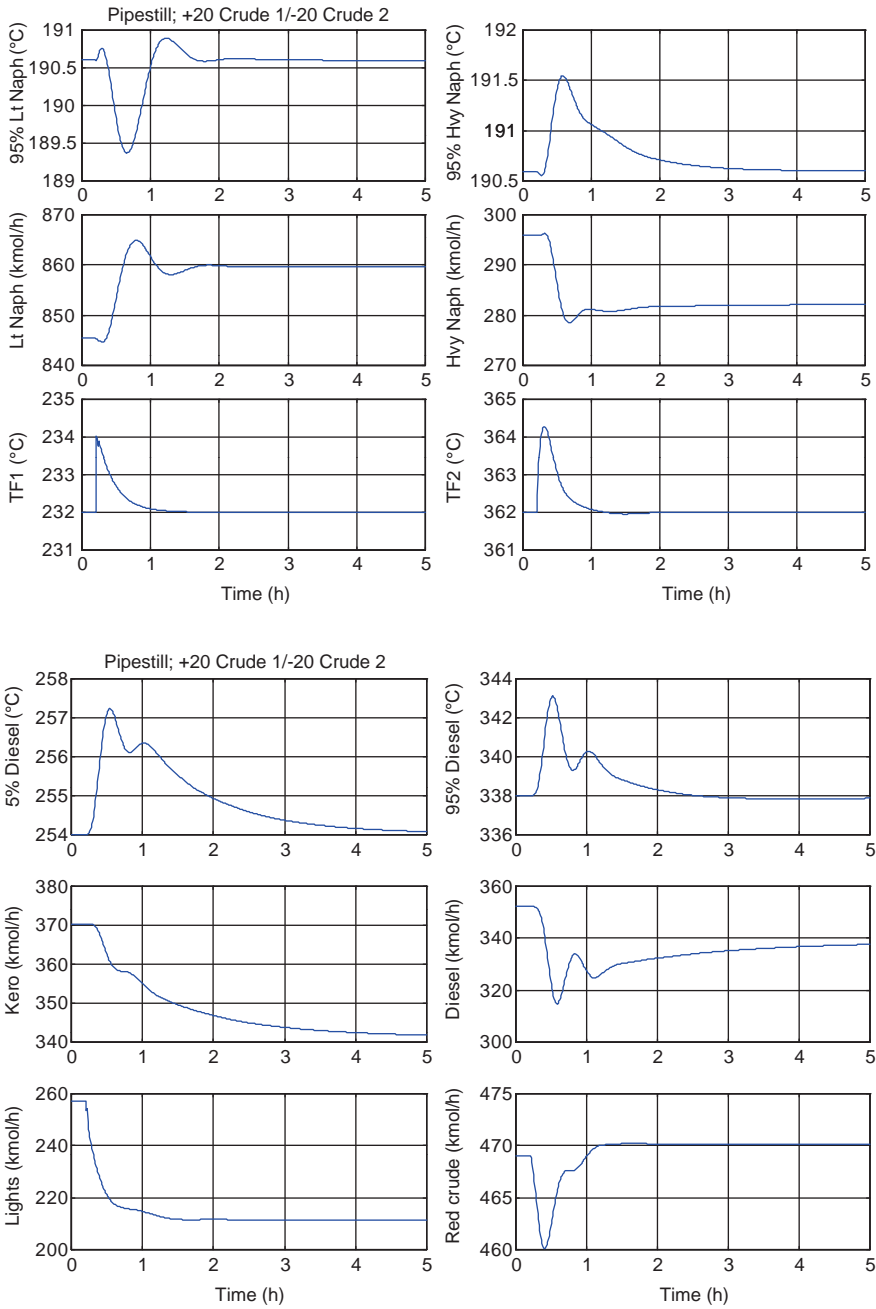


Figure 11.53 (Continued)

The deviations in the 5% and 95% boiling points of the diesel product are about 20 °C for these quite large disturbances.

The 20% increase in feed flow resulted in the saturation of several control valves when the original design size was used (valves 50% open). The valve sizes were doubled to remove these limitations. The valves modified were V14 (LIGHTS from the preflash column), V25 (HNAPH), and V22 (AGO). The steady-state positions of these three valves are now about 25% open, as can be seen on the faceplates of the “BChvynaph” 95% boiling point controller, the “PC1” pressure controller in the preflash column, and the “FCwash” flow controller, which manipulates the AGO to hold constant the Stage 19 liquid flow rate (see Fig. 11.51).

11.7 CONCLUSIONS

We have studied an example of a petroleum fractionator in this chapter. The handling of petroleum cuts by looking at boiling points has been reviewed. The control problem is to maintain the desired boiling point specifications.

The pipestill is a very complex column with multiple sidestreams, which come from stripping columns attached to the main column. In addition to the normal base and reflux-drum levels and column pressures, the levels and pressures in these strippers must also be controlled.

REFERENCES

1. W. L. Nelson, *Petroleum Refinery Engineering*, 4th ed., McGraw-Hill, New York, 1958.
2. W. L. Luyben, Design of a petroleum preflash column, *Energy Fuels* **26**, 1268–1274 (2012).

CHAPTER 12

DIVIDED-WALL (PETLYUK) COLUMNS

12.1 INTRODUCTION

The conventional “direct” separation sequence with two columns is typically used for separating ternary mixtures. However, other two-column configurations have been shown to have lower energy and capital costs for some systems. These alternatives feature a main column and a second column (stripper, rectifier, or prefractionator). The prefractionator configuration can have separate reboilers and condensers in the two columns, or it can split the vapor and liquid streams between the two columns using a single reboiler and a single condenser. The latter type is called a Petlyuk column configuration. Instead of using two separate vessels, a practical implementation of the Petlyuk configuration is to use a single vessel with an internal wall that separates the feed and sidestream sides of the vessel. This is called a divided-wall column (DWC).

Energy reductions of up to 30% have been reported in some systems for Petlyuk and divided-wall column configurations compared with the direct-separation sequence. Figure 12.1 gives the flowsheet of a divided-wall column for the numerical benzene/toluene/xylene separation example considered later in this chapter. The material presented in this chapter is based on the paper that studied the control of divided-wall columns.¹

The divided-wall column splits the middle section of a single vessel into two areas by inserting a vertical wall in the vessel at an appropriate position, not necessarily at the diameter. Feed is introduced into the prefractionator side of the wall. A sidestream is removed from the other side. The sidestream is mostly the intermediate boiling component of the ternary mixture. The lightest component goes overhead in the distillate product, and the heaviest component goes out in the bottoms product.

At the bottom of the divided-wall section, the vapor is split between the two sides in proportion to the cross-sectional area of each side, which is fixed by the physical location of

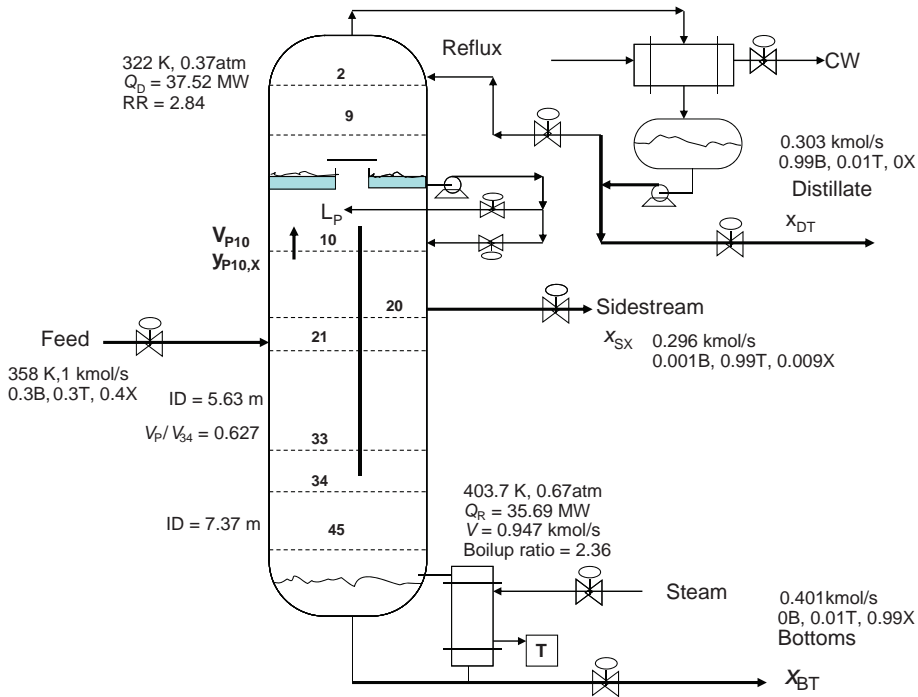


Figure 12.1 Divided-wall column flowsheet using *RadFrac* models.

the wall. This is set at the design stage and cannot be changed during operation. At the top of the divided-wall section, the liquid coming down from the rectifying section can be split between the two sides of the wall by using a total liquid trap-out tray and sending part of the total liquid to the prefractionator side (L_P) and the rest to the sidestream side. Thus, this internal liquid split is available for control purposes.

The divided-wall column has many degrees of freedom at the steady-state design stage. The number of stages in the four different sections of the column, the locations of the feed and sidestream withdrawal points, and the location of the wall are seven of the parameters that must be specified and are all fixed by the physical equipment at the time of construction. They cannot be changed during operation. The location of the wall fixes how the vapor splits between the two sides of the wall, so the vapor split is not adjustable during operation for control purposes.

In addition, there are four degrees of freedom that are adjustable during design and are also adjustable during operation of the column: reflux flow rate (R), vapor boilup (V), sidestream flow rate (S), and the liquid split ratio ($\beta_L = L_P/L_R$). The variable L_P is the liquid flow rate fed to the prefractionator side of the wall, and L_R is the total liquid leaving the bottom tray in the rectifying section. Of course, the rest of the liquid coming from the bottom of the rectification section is fed to the sidestream side of the column. Distillate and bottoms flow rates are used to maintain liquid levels in the reflux drum and column base, respectively.

These four control degrees of freedom can be used to control four variables. Ideally the purities (or impurities) of all three product streams should be controlled. The fourth degree of freedom can be used to achieve some other objective. In the control structure discussed later in this chapter, it is used to achieve implicitly minimum energy consumption as feed

compositions change. Feed flow rate changes do not require a change in the liquid split since all flows simply scale up and down with throughput, assuming pressures and tray efficiencies do not vary significantly with vapor and liquid rates.

The divided-wall column is an example of a complex column configuration whose industrial applications for separating ternary mixtures have expanded in recent years. Since there is only one column, one reboiler, and one condenser, capital costs are reduced compared with a conventional two-column configuration. An increasing number of industrial applications of the divided-wall column have been reported in recent years with about 100 columns reported to be in service. The divided-wall column is a practical way to implement the topology of the Petlyuk column.

Many papers discuss the steady-state design issues and propose heuristic and rigorous design optimization methods. Design of a divided-wall column is more difficult than a simple conventional column because of the interaction between the many design optimization variables: number of total trays, number of trays in the wall section, feed and sidestream locations, vapor split, and liquid split. In addition, the purity (or impurity) specifications of the three product streams must be satisfied simultaneously.

The dynamic control of the divided-wall column has been explored in a relatively small number of papers. Control is more difficult than with a conventional two-column separation sequence because there is more interaction among controlled and manipulated variables since the four sections of the column are coupled. The vapor split is fixed at the design stage and cannot be changed during operation, but the liquid split can be manipulated to achieve some control objective.

In this chapter, we discuss both the steady-state design and the dynamic control of divided-wall columns. Aspen simulation tools are used. The industrially important ternary separation of benzene, toluene, and *o*-xylene (BTX) is used as a numerical example. The normal boiling points of these three components are 353, 385, and 419 K, respectively, so the separation is a fairly easy one with relative volatilities $\alpha_B/\alpha_T/\alpha_X$ of about 7.1/2.2/1. The feed conditions are a flow rate of 3600 kmol/h, a composition of 30/30/40 mol% B/T/X, and a temperature of 358 K. Chao–Seader physical properties are used in the Aspen simulations. Product purities are 99 mol%. All simulations use rigorous distillation column models in Aspen Plus.

12.2 STEADY-STATE DESIGN

There are two approaches to using Aspen Plus for the simulation of a DWC. A model can be developed using four *RadFrac* vessels: a rectifier with only a condenser, two absorbers with neither a condenser nor a reboiler, and a stripper with only a reboiler. Interconnecting vapor and liquid streams and splitters are used to model the streams feeding and leaving all vessels. Alternatively, a model can be developed using a *MultiFrac* model that inherently contains all the vessels and connections. In the following sections, we discuss the use of both approaches.

12.2.1 *MultiFrac* Model

In designing a conventional single column, the *RadFrac* model in Aspen Plus is used. To use a *MultiFrac* model with a Petlyuk configuration, select the appropriate icon and drop it onto the process flow diagram as shown in Figure 12.2. Then feed, distillate, and bottoms material streams are added as shown in Figure 12.3. The model block is labeled *DWC*.

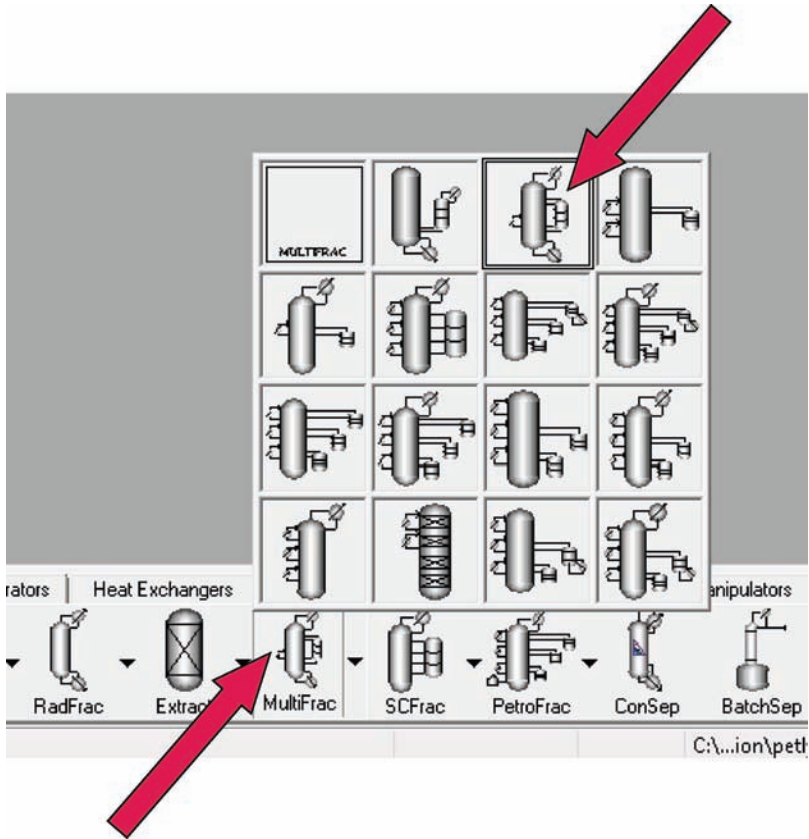


Figure 12.2 MultiFrac selection of Petlyuk column.

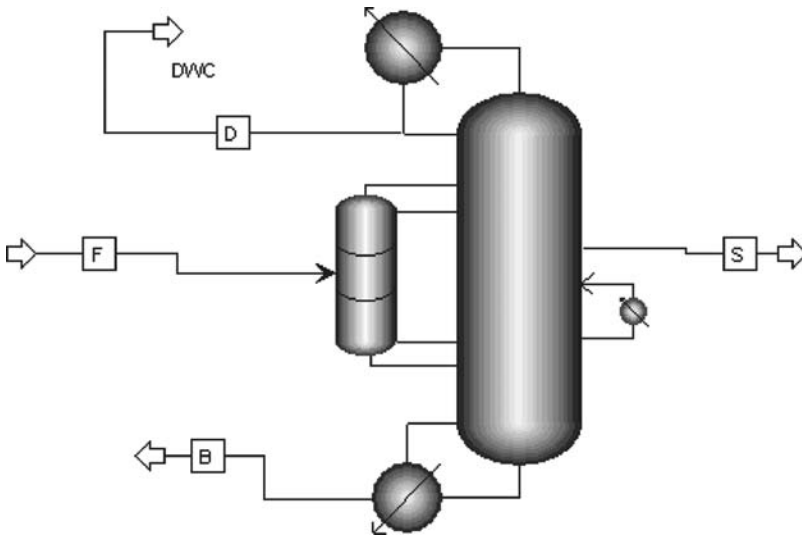


Figure 12.3 Petlyuk column.

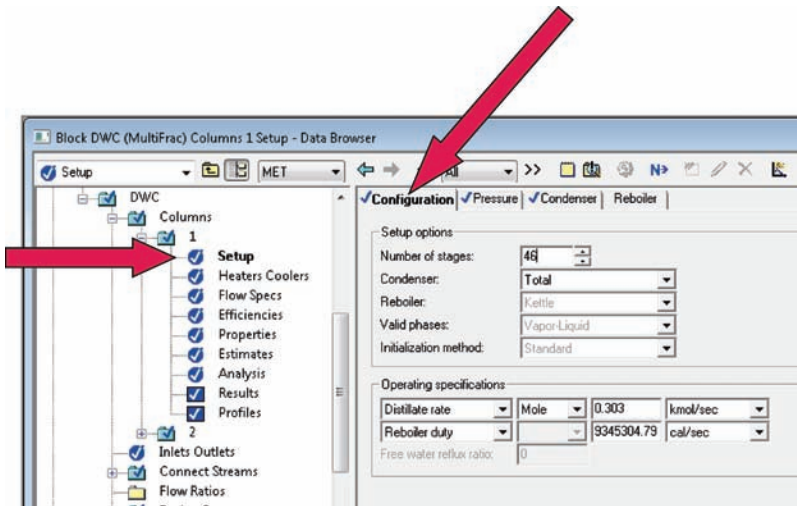


Figure 12.4 Column 1 (main column with sidestream side of wall).

Columns. Open the *DWC* block on the *Data Browser* window and add two columns by right clicking and selecting *New*. We will call the main column C1 (labeled “1”) and the prefractionator C2 (labeled “2”). Figure 12.4 gives the view when the *Setup* item is clicked for column C1 in which we can specify the configuration, pressure, and two operating specifications. A 46-stage column is specified with a total condenser and a partial (kettle) reboiler. Preliminary estimates of the distillate flow rate and reboiler duty are made. These variables will be changed later to achieve the desired product purities. Reflux-drum pressure is set at 0.37 atm, which gives a reflux-drum temperature of 322 K so cooling water can be used in the condenser. Tray pressure drop is set at 0.0068 atm per stage.

Figure 12.5 shows the *Setup Configuration* view for column C2 on which a 24-stage column is specified that has neither a condenser nor a reboiler. The top pressure is set at 0.43 atm because (as discussed later) there are nine stages between the top of the column and the top of the wall (the location where some liquid is sent to C2 and the vapor from the top of C2 goes back into C1).

Inlet and Outlet Streams. Clicking on the *Inlets Outlets* item in the *DWC* block opens the view shown in Figure 12.6. The column into which the feed is fed is specified to be column C2 and the feed location is set at Stage 12. The three product streams are specified to leave from column C1: the distillate from Stage 1 (reflux drum), the sidestream from Stage 30, and the bottoms from Stage 46 (column base). Note that the flow rate of the sidestream is also specified. This is an initial guess that will be changed later by one of the *Design Spec/Vary* adjustments defined below. The flow rates of the other two product streams are *not* specified on the page because we have already used up the two remaining degrees of freedom by specifying the distillate flow rate and reboiler heat input in the column C1 setup (see Fig. 12.4).

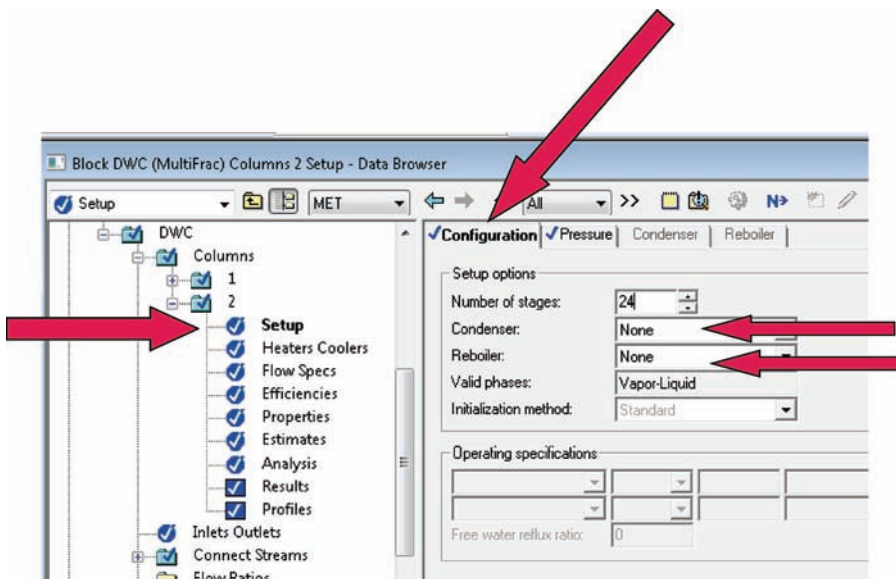


Figure 12.5 Column 2 (prefractionator column with feed side of wall).

Connect Streams. Probably the most important (and perhaps the most confusing) issue in setting up a *MultiFrac* Petlyuk column in Aspen Plus is the definition of where the four interconnecting streams (two liquids and two vapors) leave and enter the two columns. There are four *Connect Streams*. The flow rates of the two streams entering column C2 (one liquid at the top and one vapor at the bottom of the prefractionator) will be specified. The other two streams are dependent variables and will be calculated in the model.

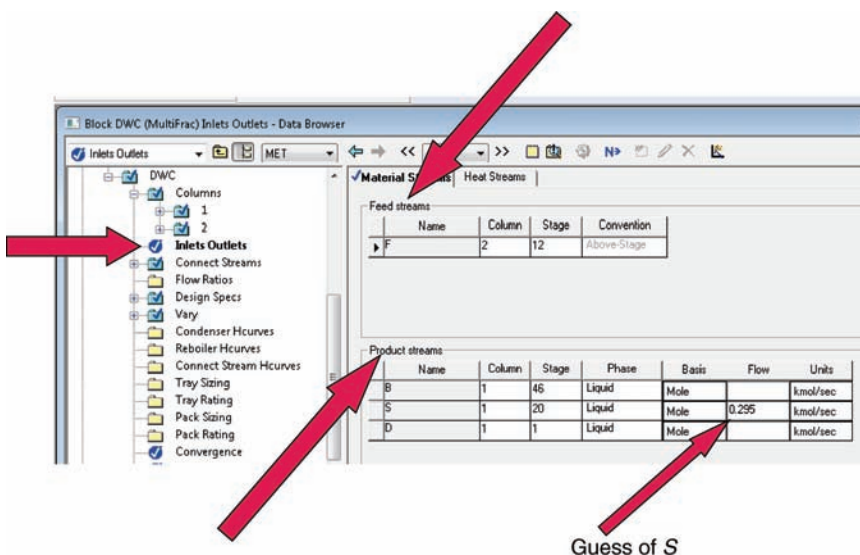


Figure 12.6 Inlet and outlet stream locations.

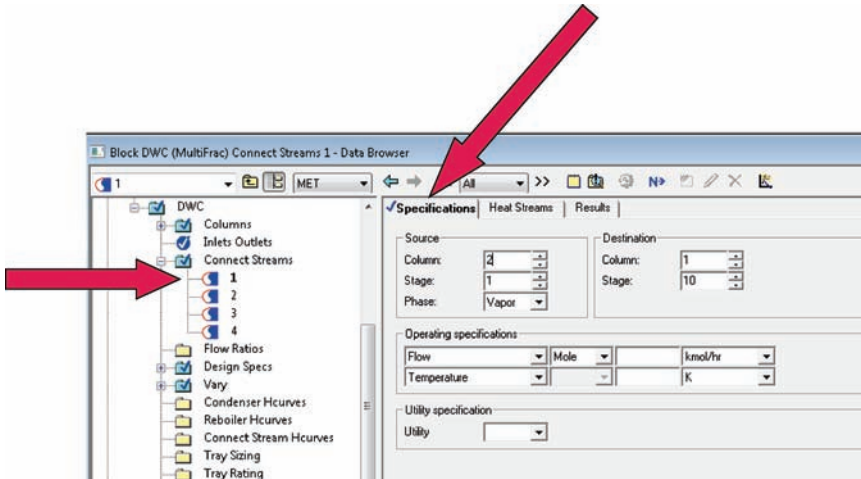


Figure 12.7 Connect stream 1 (vapor from top of prefractionator).

Figure 12.7 shows that *Connect Stream 1* is specified to be a vapor stream leaving column 2 at Stage 1 (the top of the vessel) and going into Stage 10 of column C1 (at the top of the wall). Its flow rate is *not* specified.

Figure 12.8 shows that *Connect Stream 2* is specified to be a liquid stream leaving column 1 at Stage 9 (tray above the wall) and going into Stage 1 of column C2 (top of the prefractionator). Its flow rate is *specified* to be 740 kmol/h. This flow rate will be changed later as a design optimization variable whose optimum value will minimize reboiler energy consumption for the set column configuration (trays and stream locations fixed).

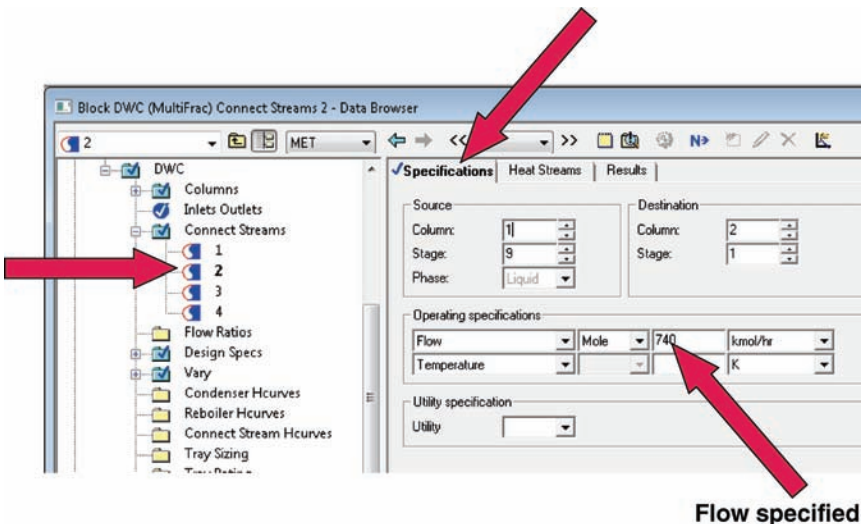


Figure 12.8 Connect stream 2 (liquid to top of prefractionator).

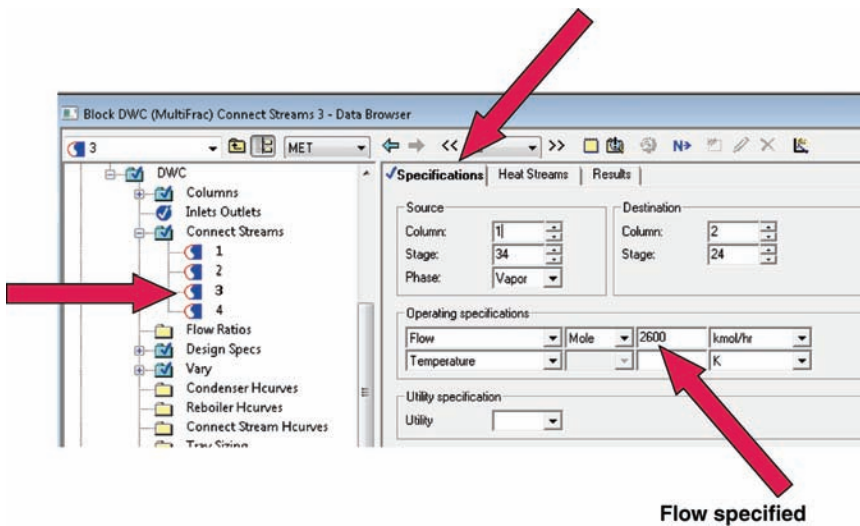


Figure 12.9 Connect stream 3 (vapor to bottom of prefractionator).

Figure 12.9 shows that *Connect Stream 3* is specified to be a vapor stream leaving column 1 at Stage 34 (tray below the wall) and going into Stage 24 of column C2 (bottom of the prefractionator). Its flow rate *is specified* to be 2600 kmol/h. This flow rate will be changed later by a *Design Spec/Vary* adjustment to attain one of the four desired product compositions discussed below.

Figure 12.10 shows that *Connect Stream 4* is specified to be a liquid stream leaving column 2 at Stage 24 (the bottom of the prefractionator) and going into Stage 24 of column C1 (tray below the wall). Its flow rate is *not* specified.

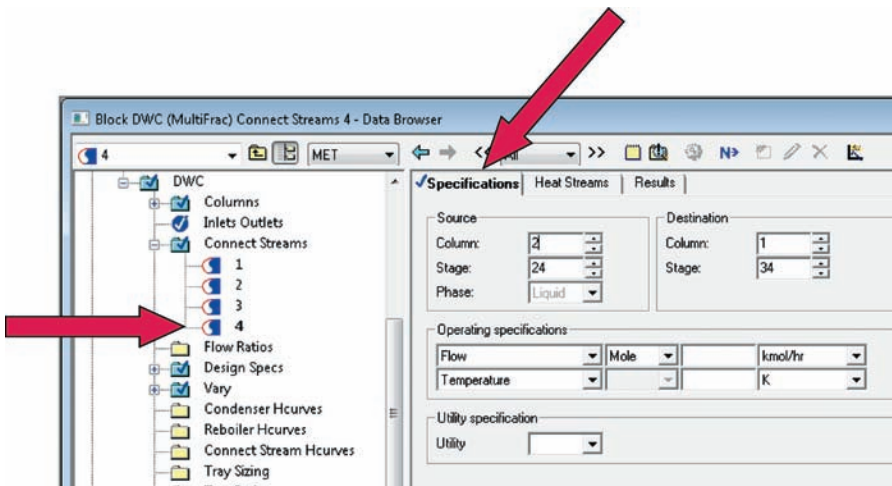


Figure 12.10 Connect stream 4 (liquid from bottom of prefractionator).

Design Specifications. The desired product purities in this numerical BTX example are all 99 mol%. The distillate should be 99 mol% benzene with only toluene as the impurity at 1 mol% since there is negligible xylene impurity in the distillate. The bottoms should be 99 mol% xylene with only toluene as the impurity at 1 mol% since there is negligible benzene impurity in the bottoms.

The sidestream is less straightforward because it by necessity contains small amounts of both benzene and xylene. The composition of toluene should be 99 mol%. But what should the individual impurity levels of the other two components be? We know they have to add up to 1 mol%. We might assume that making each impurity equal to 0.5 mol% would be optimum. But this is not the case in the BTX system. The compositions used in this study are 0.2 mol% benzene and 0.8 mol% xylene. These values are found to give the minimum reboiler energy consumption. The reason for these nonequal compositions is that it is easier to keep the benzene out of the toluene (relative volatility = 3.2) than it is to keep xylene out of the toluene (relative volatility = 2.2).

Therefore, we have four compositions to achieve (four *Design Specs*) that required four variables to vary. The design specifications with their corresponding manipulated variables are

- DS 1: Distillate toluene impurity $x_{D(T)} = 0.01$ varying distillate flow rate D .
- DS 2: Bottoms toluene impurity $x_{B(T)} = 0.01$ varying sidestream flow rate S .
- DS 3: Sidestream xylene impurity $x_{S(X)} = 0.008$ varying reboiler duty Q_R .
- DS 4: Sidestream benzene impurity $x_{S(B)} = 0.002$ varying flow rate of vapor to the bottom of the prefractionator V_p (this is *Connect Stream 3* shown in Fig. 12.9).

The first three *Design Spec/Vary* setups are straightforward. The fourth is somewhat different than the conventional. Figure 12.11 shows how the benzene impurity in the sidestream is specified. Figure 12.12 shows how the fourth *Vary* is defined to be the vapor

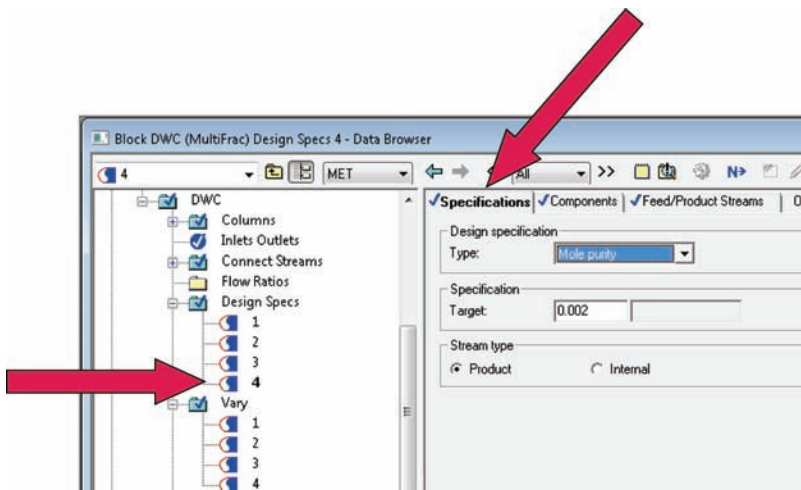


Figure 12.11 Design Spec for sidestream benzene impurity $x_{S(B)}$ varying flow of vapor to prefractionator (column 2).

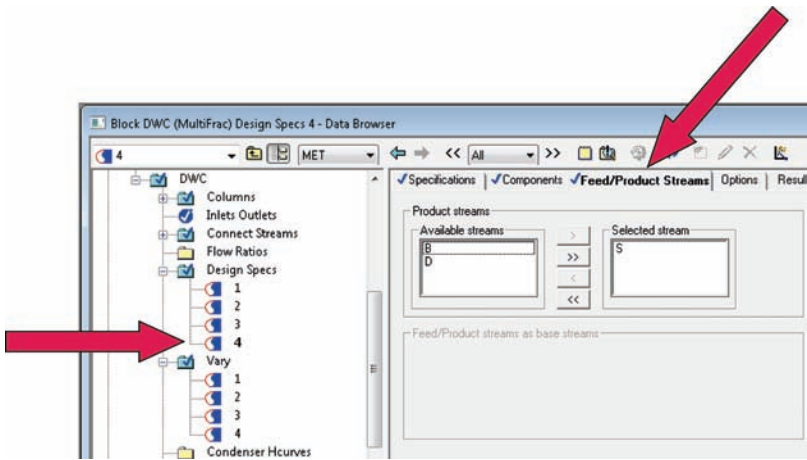
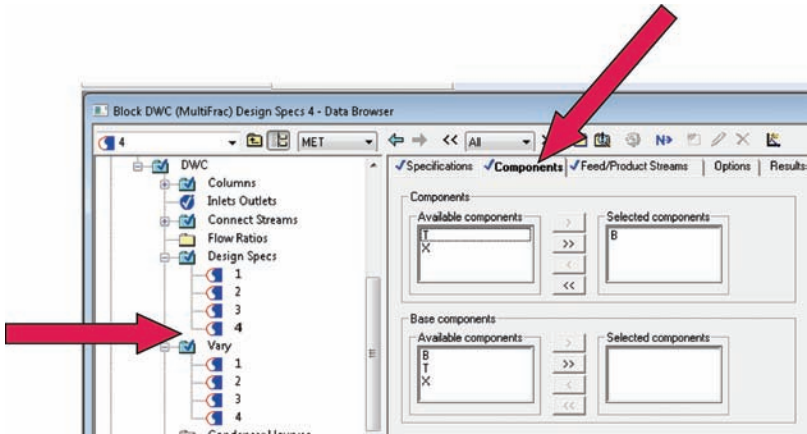


Figure 12.11 (Continued).

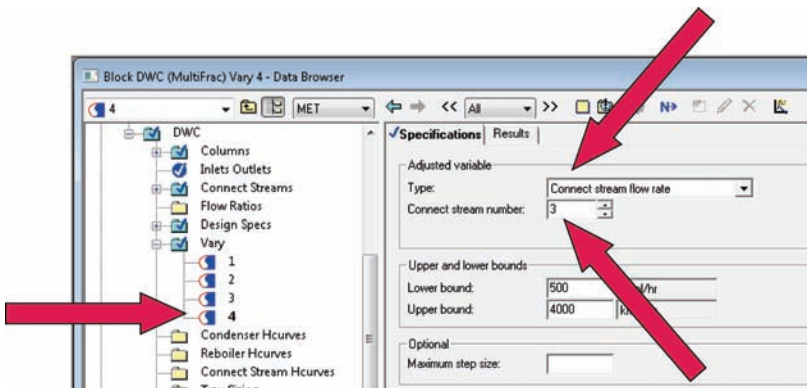


Figure 12.12 Varying flow of vapor (connect stream 3) to prefractionator (column 2).

fed to the bottom of the prefractionator. The *Type* is *Connect Stream flow rate* and *Connect Stream number* is 3.

It is important to remember that we have specified four variables (the impurity of toluene in the distillate, the impurity of toluene in the bottoms, the impurity of benzene in the sidestream, and the impurity of xylene in the sidestream). To achieve these four specifications, we have varied four variables (distillate flow rate, sidestream flow rate, vapor flow rate to the prefractionator, and reboiler duty). The one remaining design degree of freedom is the flow rate of liquid to the top of the prefractionator L_P (stream 2).

Optimization. Now that the column configuration has been established and the product purities have been attained, the one remaining design degree of freedom L_P (stream 2) can be varied to find the value of this variable that minimizes energy consumption (reboiler duty). This is the optimum design condition for the selected column configuration (total trays in each column, location of the wall, location of the feed, and location of the sidestream withdrawal). All of these column configuration parameters affect only the capital cost of the vessel.

Figure 12.13 shows how reboiler duty changes as L_P is varied over the range 700–800 kmol/h. The minimum energy point corresponds to 750 kmol/h. Figure 12.14 gives the Petlyuk column flowsheet with the tray numbering convention and the optimum design conditions. Figure 12.15 shows the reboiler duty in column C1 that is found in the *Results* item in the block list. Figures 12.16 and 12.17 give temperature and composition profiles found in the *Profiles* item in the two blocks.

The *MultiFrac* model is somewhat easier to set up and converge than the *RadFrac* model discussed in the next section. However, the *MultiFrac* model cannot be exported

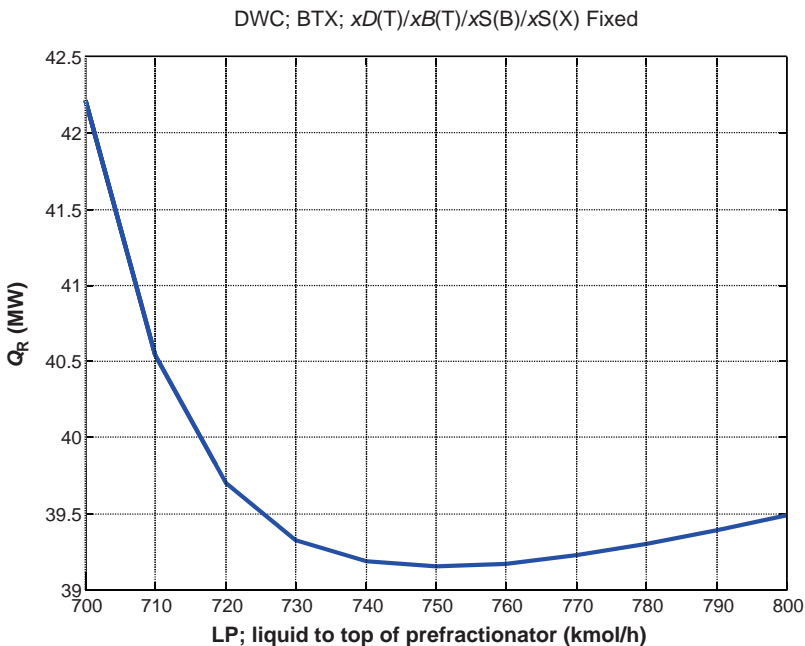


Figure 12.13 Optimum liquid split (stream 2) to prefractionator.

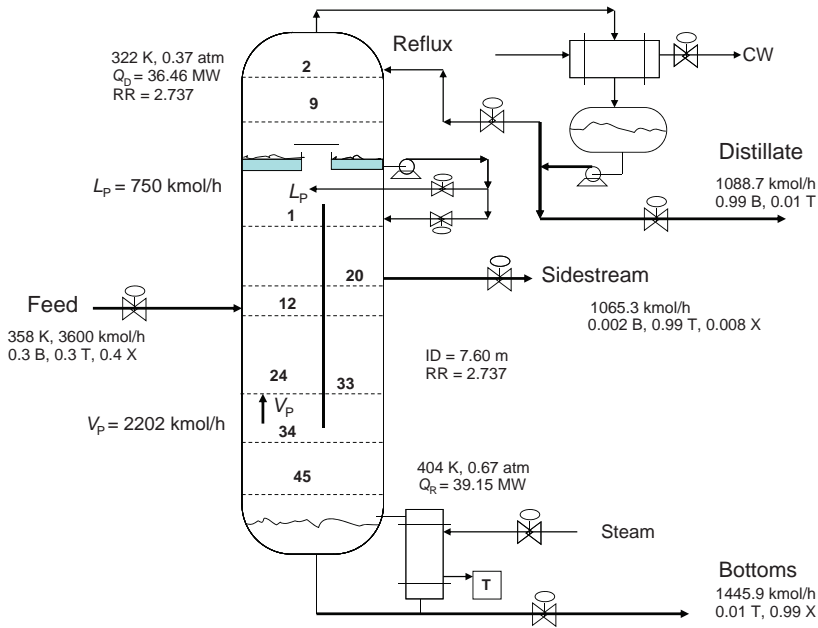


Figure 12.14 Petlyuk column flowsheet.

into Aspen Dynamics, so the important issue of dynamic controllability cannot be studied. Dynamics can be studied if a model is generated using four *RadFrac* units with appropriately interconnecting vapor and liquid streams.

12.2.2 *RadFrac* Model

Figure 12.1 gives the optimum economic design of the divided-wall column developed by Ling and Luyben using four *RadFrac* vessels. The optimum is based on minimizing total annual cost (TAC), which includes both energy and capital costs. The number of trays in

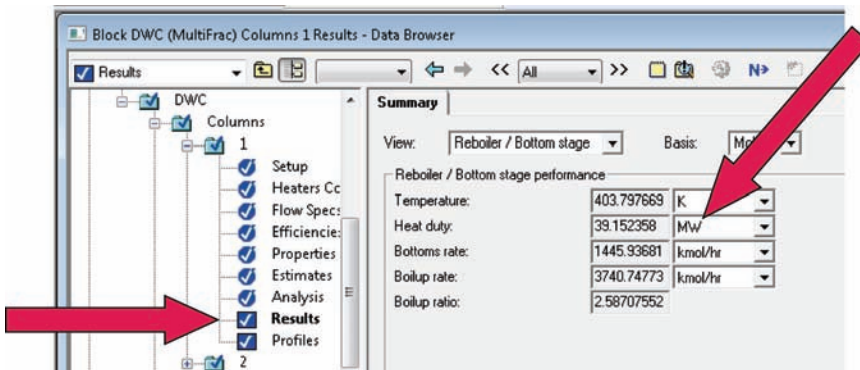


Figure 12.15 Column 1 results (reboiler duty).

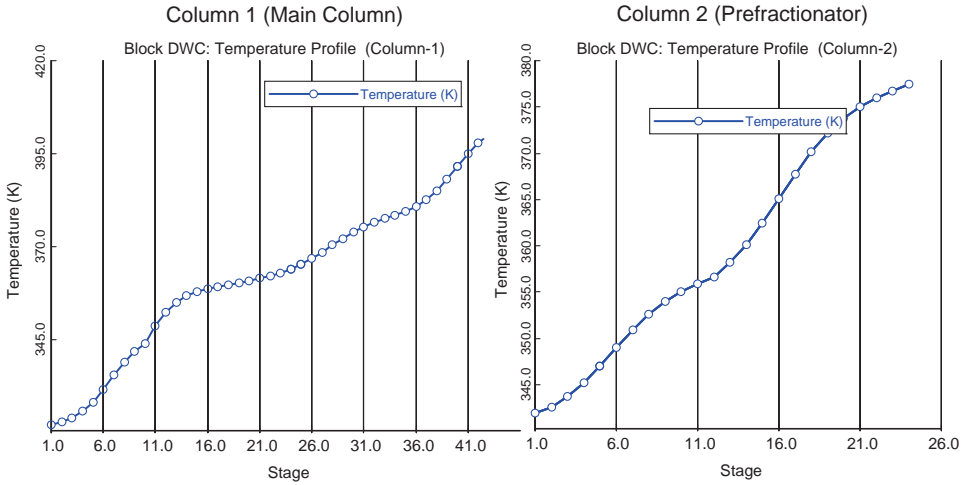


Figure 12.16 Temperature profiles.

the four-column sections, the location of the feed inlet and sidestream withdrawal, the vapor split, and the liquid split were all varied to find the minimum TAC design that produces the specified product purities. The same number of trays is used in the column sections on both sides of the wall since the tray spacing is assumed to be identical.

A comparison of Figure 12.1 (the *RadFrac* design) and Figure 12.14 (the *MultiFrac* Petlyuk design) shows that they are almost the same with only slight differences in the reboiler duties, reflux ratios, liquid splits, and vapor splits.

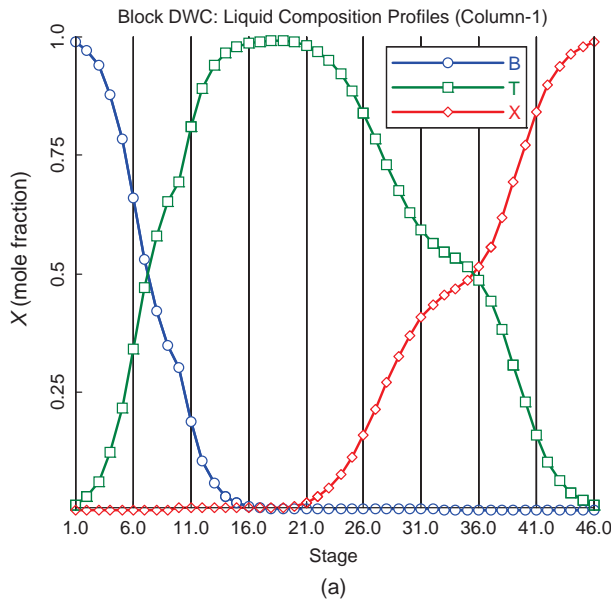


Figure 12.17 Composition profiles. (a) Column 1 (main column). (b) Column 2 (prefractionator).

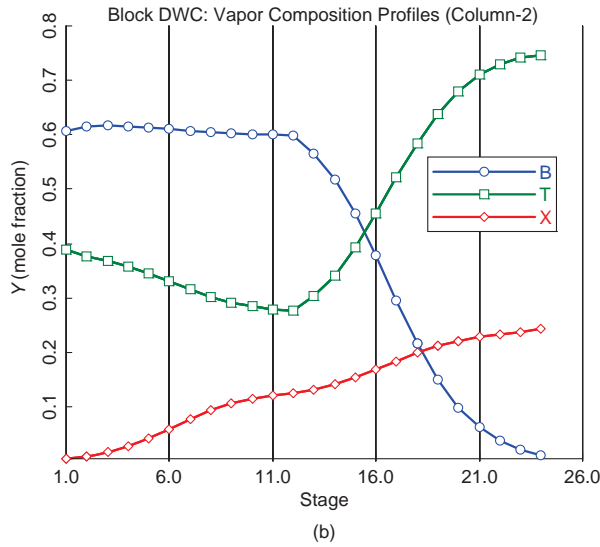


Figure 12.17 (Continued)

Table 12.1 gives detailed information of the equipment sizing and economics for the *RadFrac* divided-wall column and the conventional direct-separation sequence. The economic gain is about 30%.

The optimum economic steady-state design of a two-column direct-separation sequence is shown in Figure 12.18. The number of trays, feed tray locations, and reflux ratios were varied in each column to find the configuration giving the minimum TAC. An additional

TABLE 12.1 Comparison of Divided-Wall and Conventional Flowsheet Optimum Designs for BTX System

	Divided-Wall Column	Conventional Arrangement			Relative Gain ^a
		Column 1	Column 2	Total	
Stages					
N_F	46	30	28	58	
N_S	21	14	14		
Diameter of column (m)	7.32	6.19	8.22		
Q_C (MW)	37.52	27.88	27.81	55.69	0.33
RR	2.84	1.87	1.53		
Q_R (MW)	35.69	25.04	24.53	49.57	0.28
A_C (m ²)	3162	2349.95	2344.05	4693.99	0.33
A_R (m ²)	1802	1264.52	1238.77	2503.29	0.28
Shell (10 ⁶ \$)	2.38	1.39	1.77	3.16	0.25
HX (10 ⁶ \$)	2.33	1.89	1.88	3.77	0.38
Energy (10 ⁶ \$/year)	5.29	3.71	3.64	7.35	0.28
Capital	4.71	3.28	3.65	6.93	0.32
TAC (10 ⁶ \$/year)	6.86	4.80	4.85	9.66	0.29

^aRelative gain = 1 – (divided-wall column value/conventional value).

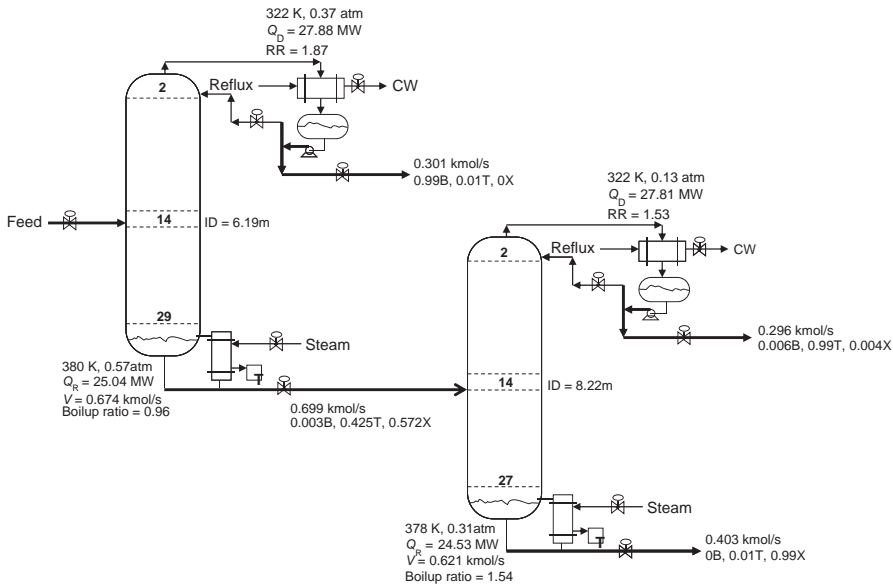


Figure 12.18 Conventional direct-separation flowsheet.

design degree of freedom is the benzene impurity in the bottoms of the first column. Benzene is removed overhead in the first column. The bottoms stream from this column is a mixture of toluene and *o*-xylene that is separated in the second column. The first column has 30 stages and is fed on Stage 14. The reflux drum operates at 0.37 atm, giving a reflux-drum temperature of 322 K. Base pressure is 0.57 atm, which gives a base temperature of 380 K with the toluene/xylene mixture in the bottoms. The reflux ratio is 1.87, and the reboiler heat input is 25.04 MW. The column diameter is 6.19 m.

The second column has 28 stages and is fed on stage 14. The reflux drum operates at 0.13 atm, giving a reflux-drum temperature of 322 K. Base pressure is 0.31 atm, which gives a base temperature of 378 K. The reflux ratio is 1.53, and the reboiler heat input is 24.53 MW. The column diameter is fairly large (8.22 m) because of the vacuum operation.

Table 12.1 compares the two alternative flowsheets. The divided-wall column has both capital and energy advantages. The reduction in TAC is about 29%. These results are similar to those reported by many others for a number of component separations.

12.3 CONTROL OF THE DIVIDED-WALL COLUMN

12.3.1 Control Structure

The control objectives are to maintain stable on-specification operation in the face of disturbances in throughput and feed composition and to minimize energy consumption. We limit our study to conventional PID control structures.

Conventional distillation control wisdom says that it is usually more effective to control *impurity* levels than to control *purity* levels. The use of impurity instead of purity is a

standard process control principle because you want to control a variable that is sensitive to the manipulated variable. A change in impurity from 1 to 1.5 mol% is much greater (on a relative basis) than the corresponding change in purity from 99 to 89.5 mol%. The principle is particularly important in distillation control where changes in trace amounts of other nonkey components can make it impossible to maintain a key-component purity, but maintaining an impurity of the other key component is still possible.

Therefore, we will control the toluene impurity in the distillate at $x_{D(T)} = 0.01$ and the toluene impurity in the bottoms at $x_{B(T)} = 0.01$. The sidestream has two impurities, both benzene and xylene, but the xylene impurity is much larger than the benzene impurity. Therefore, xylene impurity $x_{S(X)} = 0.009$ is controlled.

These three controlled variables require three manipulated variables. There are four available: reflux flow rate, sidestream flow rate, vapor boilup, and liquid split. Vapor boilup has an immediate and strong effect on all compositions throughout the system, and therefore, in theory, could be used to control any of the three product compositions or a composition in the prefractionator. Reflux affects all compositions, but the only composition that it affects *quickly* is the distillate composition. Its effect on products lower in the column can take considerable time because of the liquid hydraulic lags. Therefore, it seems logical to control distillate composition with reflux. Reflux-drum level is then controlled by manipulating distillate. This choice is for situations in which the reflux ratio is not high. If the reflux ratio is greater than about 3, conventional distillation control wisdom says to control composition with distillate and control the reflux-drum level with reflux.

In a sidestream column, changing the flow rates of liquid streams above or at a product withdrawal location affects the composition of that product and all other products *below* it. Changing the flow rate of the sidestream has little effect on the products *above* it. Therefore, sidestream composition can be controlled by vapor boilup, reflux flow rate, liquid split, or sidestream flow rate. As discussed later, we want to control a composition near the top of the prefractionator, and the logical manipulated variable to achieve this control is the liquid split. If reflux is used for distillate control, we are left with using either sidestream flow rate or vapor boilup for the control of the sidestream composition.

The bottoms composition can be controlled most quickly with vapor boilup. However, the flow rate of the sidestream could be used if there are not too many trays between the bottom and the sidestream withdrawal stage. In the numerical case studied, there are 25 trays between the sidestream and the bottom of the column. Therefore, we will control sidestream impurity with sidestream flow rate and bottoms impurity with vapor boilup.

The fourth control loop in the proposed control structure is one in which the concentration of the heaviest component xylene at the top of the prefractionator is controlled. As discussed earlier, the main function of the prefractionator is to keep xylene from going out the top of the wall. Any xylene that does get up this far must be rejected in the rectifying section, and this means that xylene is present in the liquid flowing down into the sidestream side of the wall. The liquid split ratio is 0.353, so 65.7% of the liquid from the rectifying section enters the sidestream side of the wall. The concentration of the xylene will be higher in the liquid phase than in the vapor phase. Since a liquid sidestream is being withdrawn, the xylene impurity will show up in the sidestream product. Therefore, it is vital to prevent xylene from getting to the top of the wall in the prefractionator.

On the other hand, the prefractionator's other job is to keep the lightest component benzene from dropping out the bottom of the wall. Any benzene that does get down this far must be rejected in the stripping section and this means that benzene will be present in the vapor flowing up into the sidestream side of the wall. However, this is less of a problem

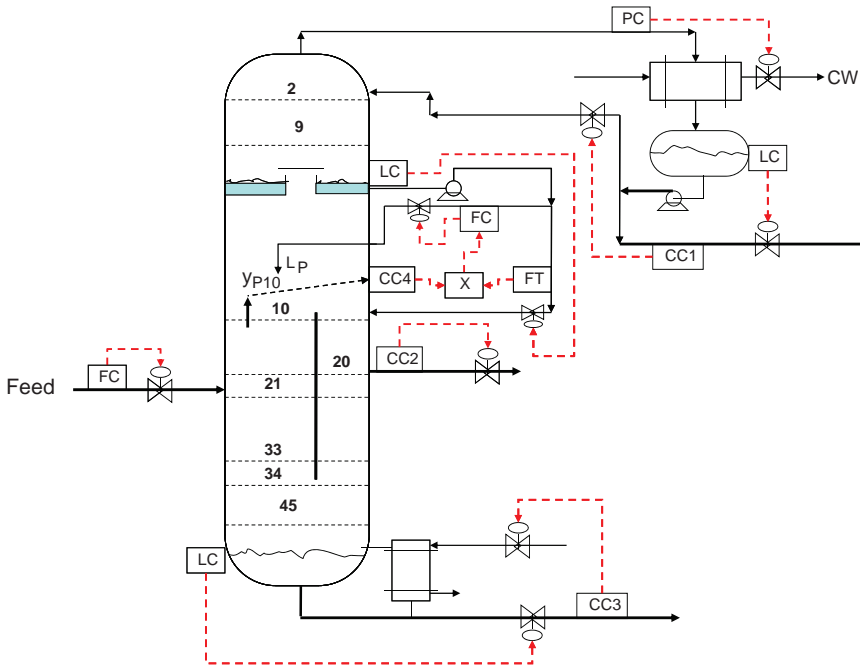


Figure 12.19 Control structure for divided-wall column.

because the sidestream is a liquid in which the benzene concentration will be lower than in the vapor phase where most of the benzene is present. A divided-wall column with a liquid sidestream is more sensitive to the heaviest component getting over the wall than to the lightest component getting under the wall. Therefore, we use a control structure in which the xylene concentration near the top of the wall in the prefractionator is controlled by the liquid split. Figure 12.19 gives the proposed control structure. Note that direct composition control is used in all four loops.

The importance of manipulating the liquid split was discussed in detail by Wolff and Skogestad² in terms of its effect on energy consumption at steady-state conditions. Figure 12.20 gives results for the system studied in this chapter that demonstrate that holding a xylene composition at the top of the prefractionator ($y_{P10(X)}$) has the potential of achieving the objective of minimizing energy consumption for changes in feed composition. These results are for the case when the vapor split is constant at the optimum design value. All three product purities are fixed at 99 mol% purities in these steady-state results.

It should be emphasized that the liquid split ratio does not change for feed flow rate changes, but Figure 12.20 clearly shows that it should change for feed composition changes if energy is to be minimized.

The top graph in Figure 12.20a shows how reboiler duty Q_R varies with liquid split for changes in the amount of benzene in the feed. The base conditions are a feed composition of 30 mol% benzene, 30 mol% toluene, and 40 mol% *o*-xylene. Several different benzene compositions are shown. Results for a 10% change mean that the benzene in the feed is changed from 30 to 33 mol%. A 20% change means that the benzene is changed from 30 to 36 mol%. The other two feed compositions are changed and kept in the same ratio of 30/40 to make the total add to one.

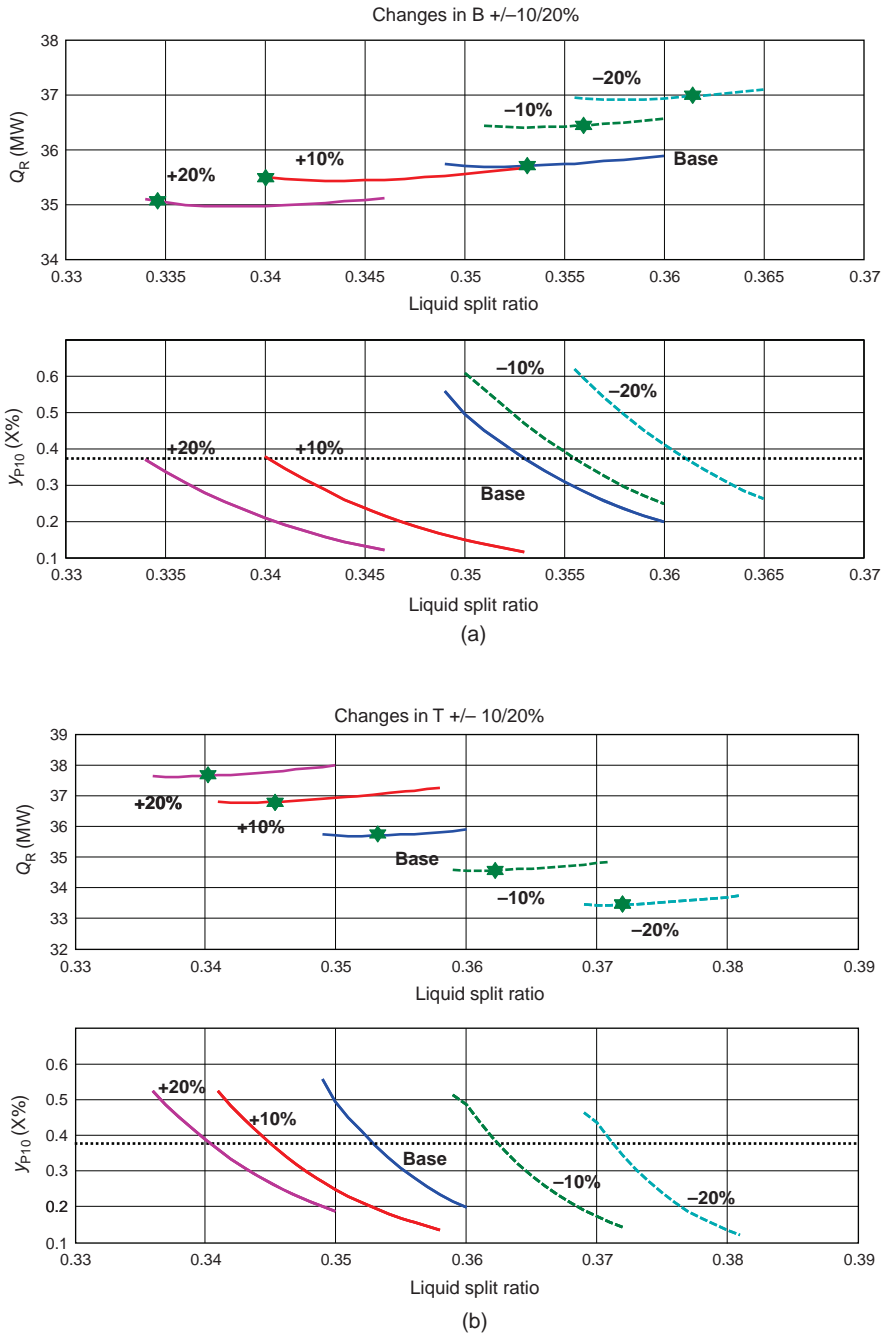


Figure 12.20 (a) Effect of liquid split ratio on energy consumption and prefractionator vapor composition for changes in benzene feed composition. (b) Effect of liquid split ratio on energy consumption and prefractionator vapor composition for changes in toluene feed composition. (c) Effect of liquid split ratio on energy consumption and prefractionator vapor composition for changes in xylene feed composition.

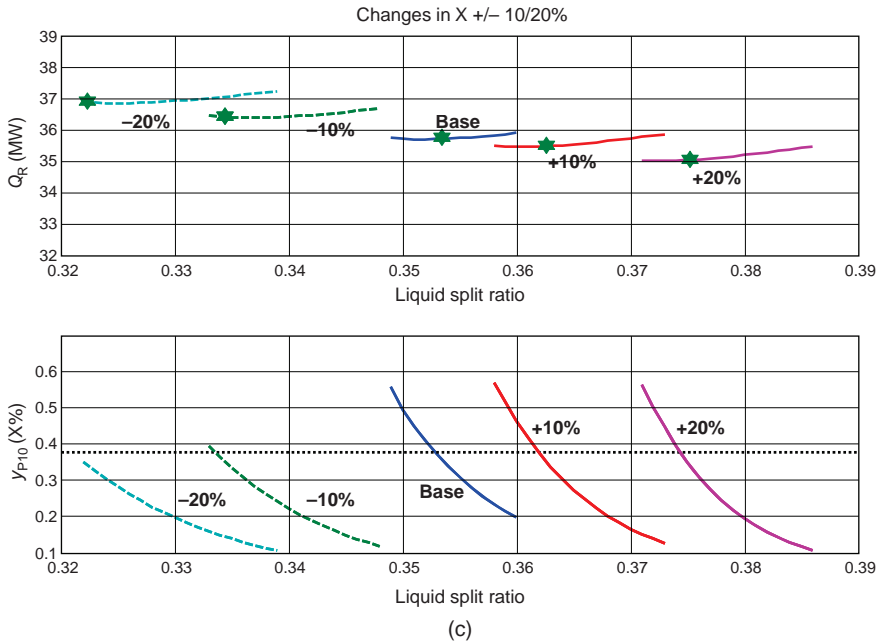


Figure 12.20 (Continued)

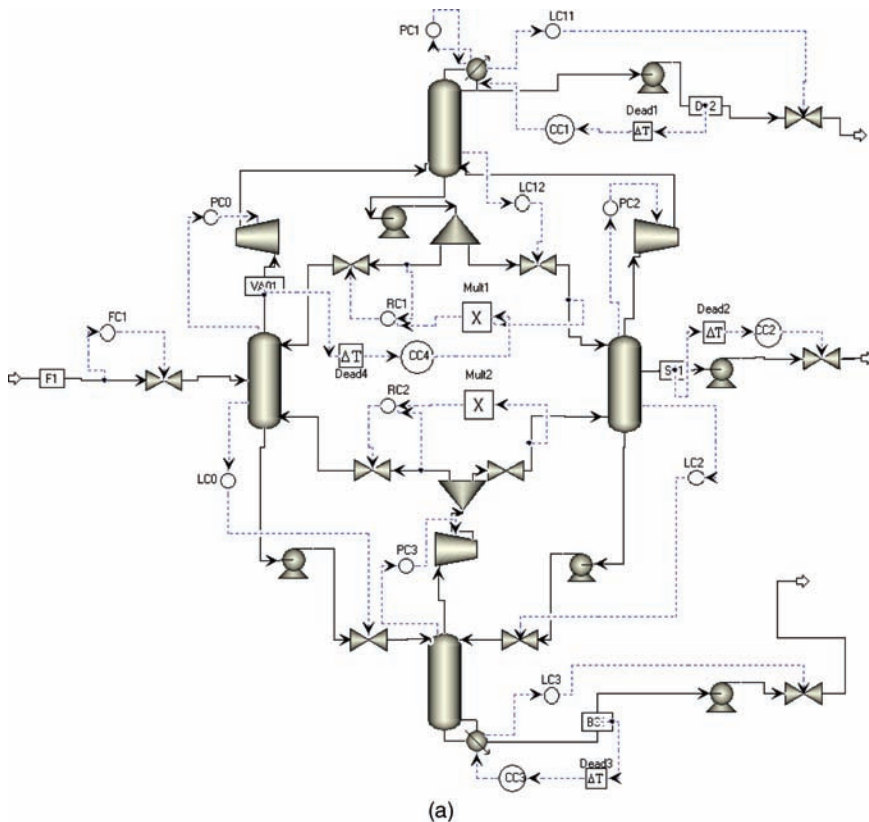
There is an optimum liquid split that minimizes energy, but this optimum changes with feed composition. The optimum values are marked with a star. The lower graph in Figure 12.20a shows how the vapor composition of xylene on Stage 10 at the top of the prefractionator ($y_{P10(X)}$) varies with the liquid split for the same values of feed composition. Note that the values of the liquid split corresponding to $y_{P10(X)} = 0.0039$ are almost the same as the values that minimize energy consumption for the five feed composition cases.

Figure 12.20b gives results for changes in the toluene feed composition. Figure 12.20c gives results for changes in *o*-xylene feed composition. The obvious conclusion is that controlling xylene composition at the top of the prefractionator is an *implicit* and practical way to minimize energy consumption in the face of feed composition disturbances.

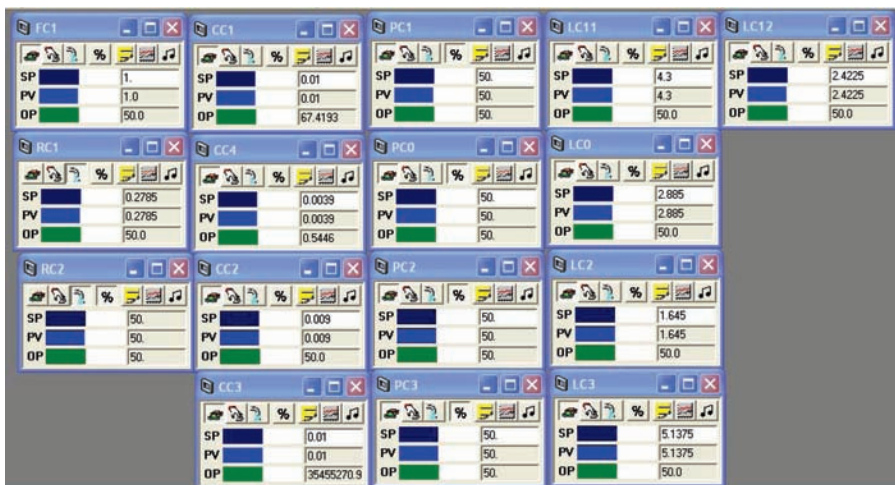
12.3.2 Implementation in Aspen Dynamics

The steady-state *RadFrac* model in Aspen Plus consisted of four-column sections: one stripper, two parallel absorbers, and a rectifier. In reality, there is only one column, but these four “fictitious” vessels are used in the simulation to model the real physical equipment. Before exporting the file into Aspen Dynamics, a number of important changes had to be made in order to obtain a pressure-driven dynamic simulation. Figure 12.21a gives the Aspen Dynamics process flow diagram with all the real and “fictitious” elements shown. The lower part of Figure 12.21b shows the controller faceplates. Note that the two controllers with remote set points (RC1 and RC2) are on cascade.

Vapor Flows. Pressures and pressure drops in the various sections of the steady model can be specified, and no valves are required between the “fictitious” vessels. However,



(a)



(b)

Figure 12.21 (a) Aspen Dynamics implementation. (b) Controller faceplates.

Aspen Dynamics requires that valves be inserted between the vessels, and these valves must have some pressure drop. To compensate for this additional pressure drop, three “fictitious” compressors are installed on the vapor lines coming out the top of the stripper and the tops of the two sides of the wall. Three pressure controllers are installed to hold the back pressure in each of these three vessels by manipulating the work to the compressors. At the top of the rectifier, pressure is controlled in the conventional way by manipulating condenser heat removal.

After the compressor in the stripper vapor line, the vapor line splits into two lines, one going to the prefractionator and the other going to the sidestream side of the wall. Control valves were inserted in both lines. A ratio control system is used to keep the vapor split constant. The total vapor from the stripper is determined by the compressor (to hold pressure in the stripper) and is measured. This flow signal is sent to a multiplier, whose other input is the desired ratio of vapor to the prefractionator to total vapor (the vapor split ratio). The output of the multiplier is the set point signal of a flow controller that controls the flow of vapor to the prefractionator by changing the position of the control valve in the line.

Liquid Flows. The liquid levels in the base of all three “fictitious” columns must be controlled. Fictitious pumps and control valves are installed at the base of each column. The base level in the stripper is controlled in the conventional way by manipulating bottoms flow rate. The liquid level in the base of each of the absorber columns (the prefractionator and sidestream side of the wall) are controlled by their corresponding control valves.

The liquid level in the base of the rectifier corresponds physically to the total liquid trap-out tray. A pump and two parallel lines with control valves in each are installed. Since the flow rate to the sidestream side of the wall is the larger of the two, the level on the trap-out tray is controlled by manipulating the control valve in the liquid line to that side of the wall. A ratio scheme then adjusts the other control valve to maintain the desired liquid split. The liquid flow rate to the sidestream section is measured, and this signal is sent to a multiplier whose other input is adjusted to give the desired liquid split. The output of the multiplier is the set point signal to a flow controller that manipulates the valve in the liquid line to the prefractionator to achieve the specified flow rate. Note that this ratio is changed by the composition controller in the prefractionator.

12.3.3 Dynamic Results

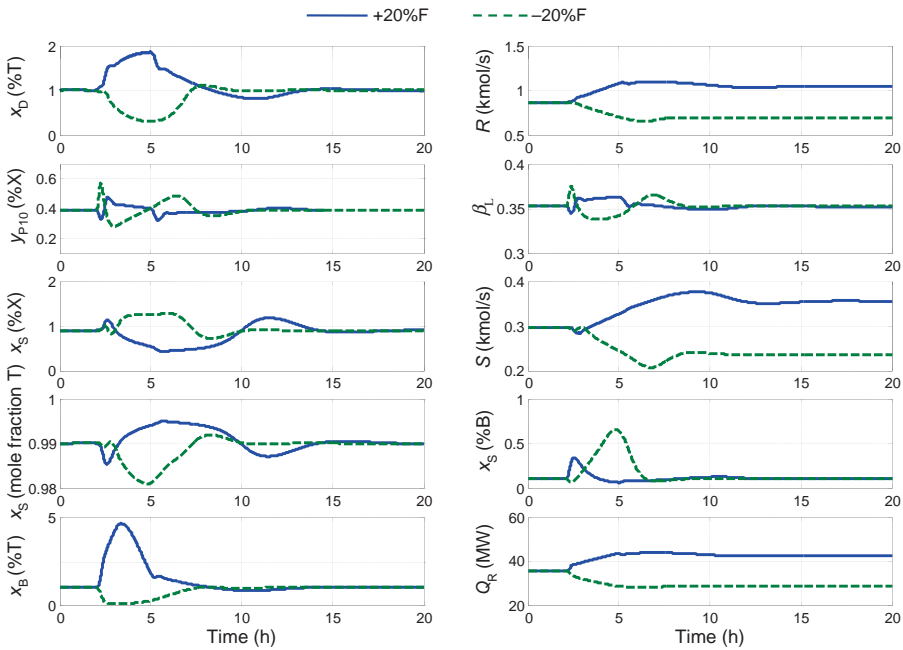
The four composition control loops each have a 5 min deadtime. They were tuned using a sequential method. Because reboiler heat input affects all of the controlled variables fairly quickly, the $x_{B(T)}/Q_R$ loop was tuned first with the other three controllers on manual. Relay-feedback testing was used to find the ultimate gain and period. Tyreus–Luyben tuning rules were used. Next, since reflux affects all compositions, the $x_{D(T)}/R$ loop was tuned using the same procedure with the $x_{B(T)}/Q_R$ loop on automatic. Then the $x_{S(X)}$ loop was tuned with the two loops on automatic. Finally, the $y_{P10(X)}$ loop was tuned with the other three loops on automatic. Table 12.2 gives controller tuning results for all four loops.

Figures 12.22–12.25 give the responses of the divided-wall process in the face of throughput and feed composition disturbances. In Figure 12.22, increases and decreases of

TABLE 12.2 Controller Tuning Parameters

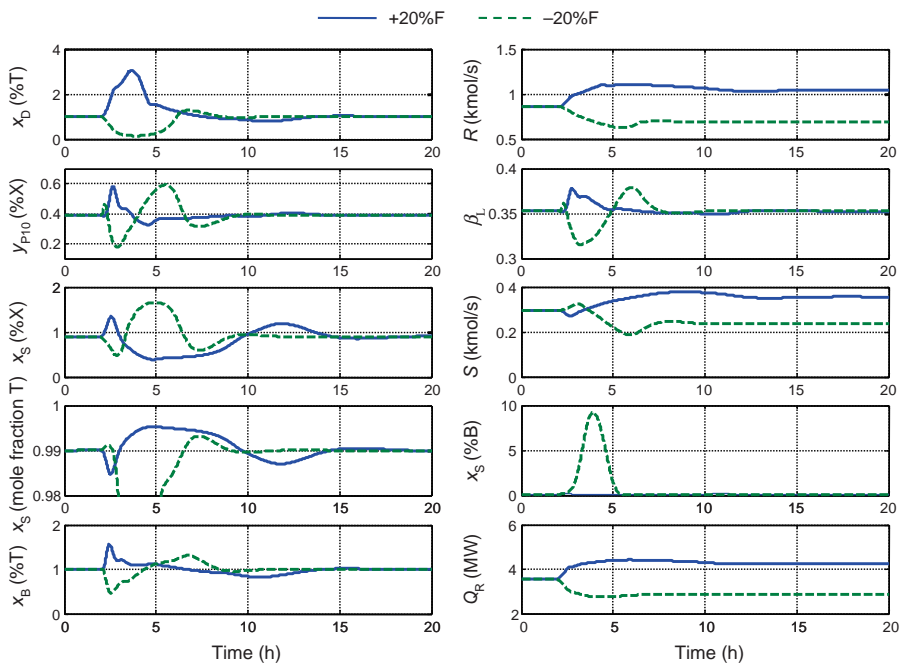
	Controlled Variable	Manipulated Variable	Controller Gain K_C	Controller Integral Time τ_I (min)
Divided-wall column				
CC1	$x_{D(T)}$	R	0.11	71
CC2	$x_{S(X)}$	S	0.19	55
CC3	$x_{B(T)}$	Q_R	0.07	71
CC4	$y_{P10(X)}$	β_L	0.19	51
Conventional				
CC11	$x_{D1(T)}$	$R1$	0.073	103
CC12	$x_{B1(B)}$	Q_{R1}	0.060	74
CC21	$x_{D2(X)}$	$R2$	0.056	110
CC22	$x_{B2(T)}$	Q_{R2}	0.069	82

5 min deadtime in all composition loops. Level controllers—proportional only with gain of 2. Flow controllers— $K_C = 0.5$, $\tau_I = 0.3$ min.

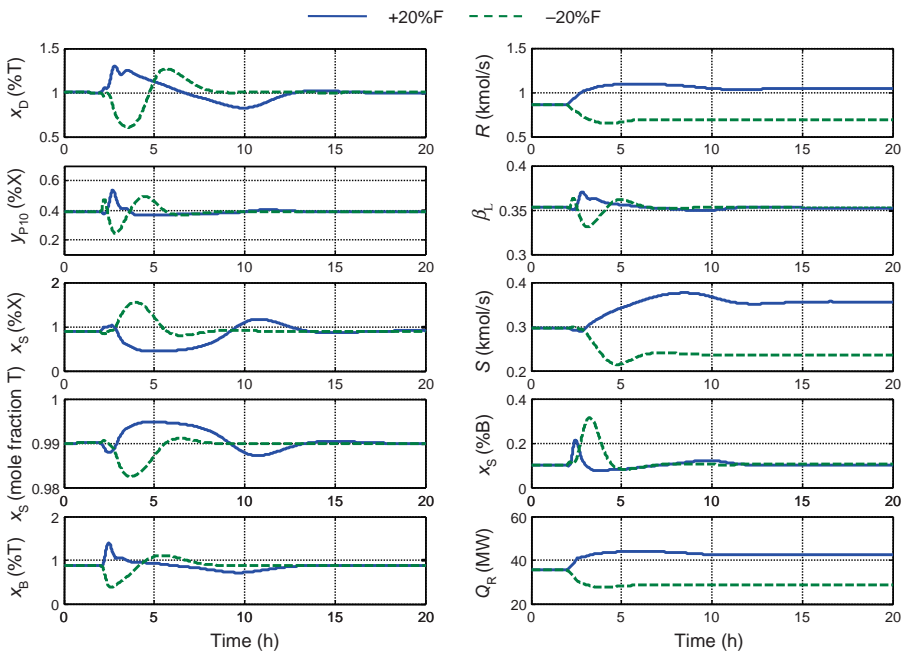


(a)

Figure 12.22 (a) 20% feed flow rate disturbances for divided-wall column. (b) 20% feed flow rate disturbances with Q_R/F ratio control. (c) 20% feed flow rate disturbances with Q_R/F ratio and R/F control.



(b)



(c)

Figure 12.22 (Continued)

20% in the feed flow rate are made at time equal to 2 h. Stable regulatory control is achieved with product purities returned to their specifications in about 8 h. In Figure 12.22a, the purity of the bottoms shows a large increase in the toluene impurity for the 20% increase and a moderate increase in the benzene impurity in the sidestream for the 20% decrease in feed flow rate. Figure 12.22b shows that the use of a feedforward ratio scheme (Q_R/F ratio) greatly reduces the transient deviation in bottoms purity. However, the maximum deviation in sidestream purity is increased for a reduction in feed flow rate. Figure 12.22c shows that the use of both the Q_R/F ratio and an R/F ratio provides improved control for both the sidestream and the bottoms. In addition, the deviations in the distillate purity are also reduced. Note that the final steady-state values of the liquid split β_L are the same as the initial steady-state value.

Figure 12.23 gives results when the feed composition is changed by increasing or decreasing the benzene concentration, with the other two components remaining in the initial ratio to each other. The purities of all three products are well controlled. Note that the liquid split changes for these changes in feed composition. The second graph from the top on the right side of Figure 12.23 shows that the liquid split β_L decreases when the benzene concentration in feed increases. This occurs because there is less xylene going up the prefractionator side, so less liquid is required to maintain the specified xylene composition at the top of this section.

Figures 12.24 and 12.25 show results for changes in the concentrations of toluene or xylene. Note that increasing xylene directly or indirectly (by decreasing benzene or toluene) causes the liquid split β_L to increase.

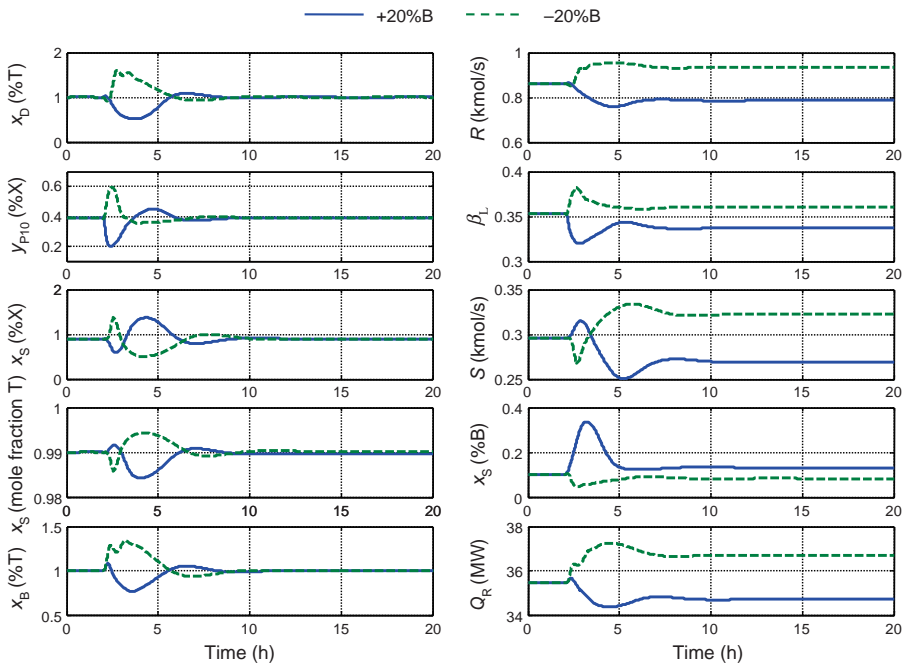


Figure 12.23 20% benzene disturbances of divided-wall column.

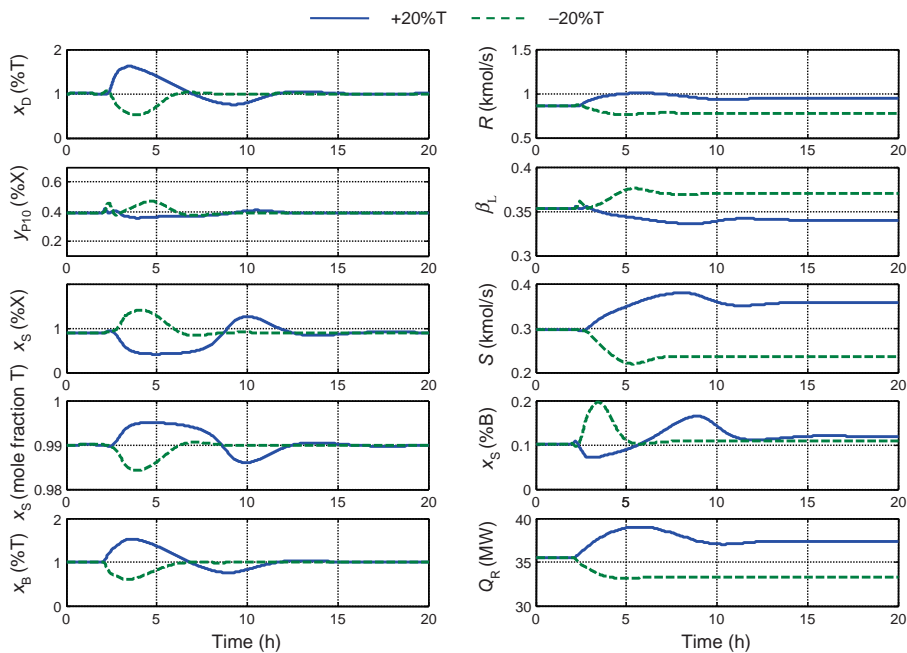


Figure 12.24 20% toluene disturbances of divided-wall column.

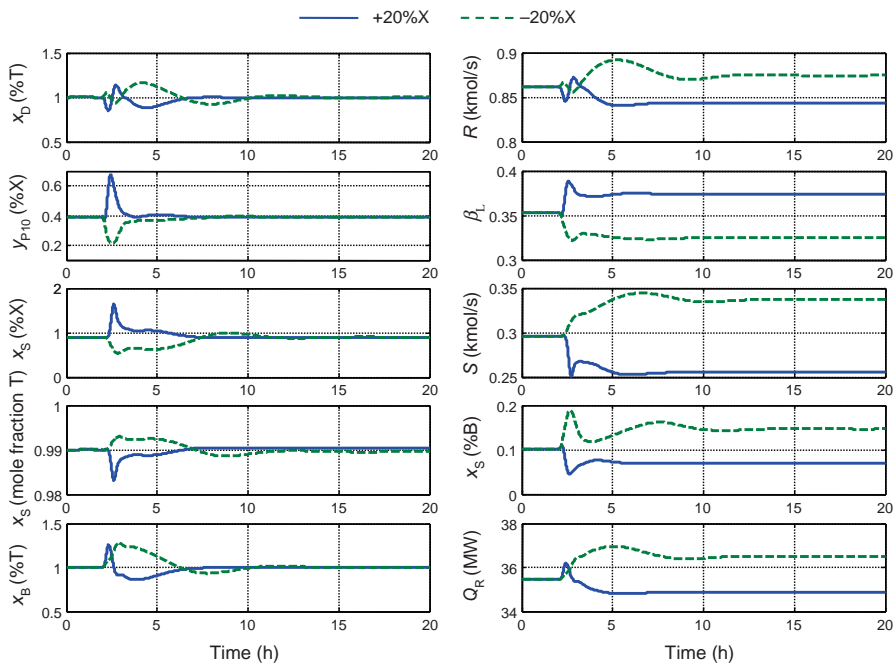


Figure 12.25 20% xylene disturbances of divided-wall column.

These simulation results demonstrate that the proposed control structure provides effective control for a variety of quite large disturbances. Energy consumption is also implicitly held very close to its minimum for large disturbances in feed composition.

12.4 CONTROL OF THE CONVENTIONAL COLUMN PROCESS

12.4.1 Control Structure

The control objectives for the conventional direct-separation sequence are quite similar to those of the divided wall. Each column has two manipulated variable: reflux and reboiler heat input. Therefore, two variables can be controlled in each column. Figure 12.26 gives the proposed control structure for this conventional two-column process.

In the first column, the toluene impurity in the distillate benzene product is controlled by manipulating reflux, and the benzene impurity in the bottoms is controlled by manipulating reboiler heat input. Any benzene that drops out of the bottom of the first column ends up as an impurity in the distillate of the second column, and nothing can be done in the second column to affect this situation. The distillate specification is 1 mol% toluene. The bottoms specification is 0.3 mol% benzene, which gives a distillate impurity in the second column of 0.6 mol% benzene.

In the second column, the impurity of xylene in the distillate toluene product is controlled at 0.4 mol% by manipulating reflux. The toluene impurity in the bottoms xylene product is controlled at 1 mol% by manipulating reboiler heat input.

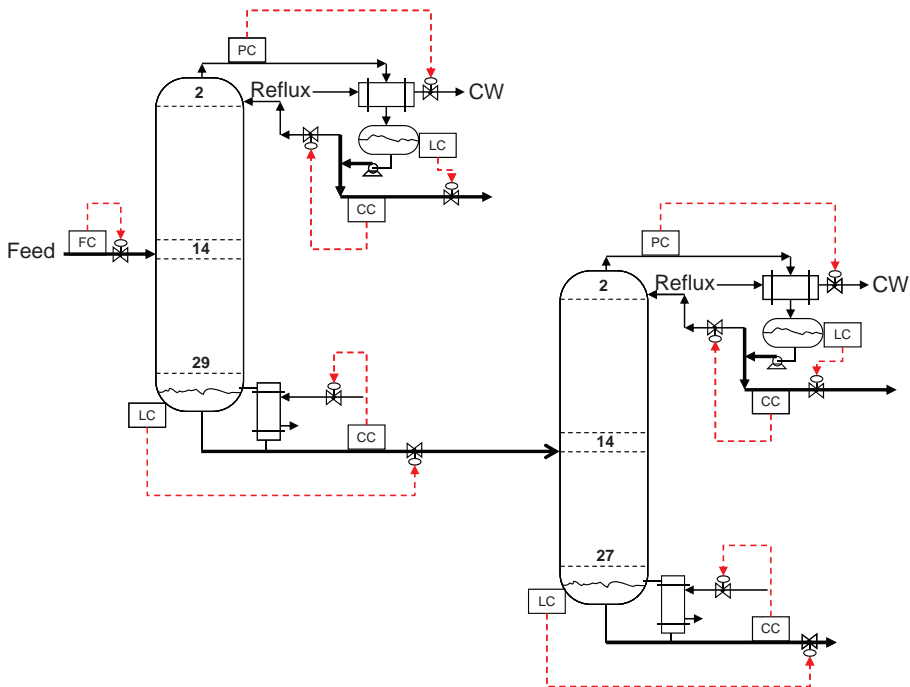


Figure 12.26 Control structure for conventional two-column process.

All four loops contain 5 min deadtimes. The loops in each column were tuned sequentially with the reboiler heat input loop closed first with the reflux loop on manual. Relay-feedback and Tyreus–Luyben tuning were used. Then, with the reboiler heat input loop on automatic, the reflux loop was tuned. Table 12.2 gives the tuning parameters.

12.4.2 Dynamic Results and Comparisons

The control structure discussed above was evaluated using the same disturbances imposed on the divided-wall column. Stable regulatory control was obtained with all four products held close to the specifications.

Figures 12.27–12.30 give direct comparisons between the dynamic responses of the divided-wall column and the conventional process. The purities of the three product streams are plotted for the two flowsheets.

In Figure 12.27, the left three graphs give results for 20% increases in feed flow rate. The right three graphs are for 20% decreases. The middle graph on the left side of Figure 12.27 shows a large drop in the purity of the toluene product in the conventional process for the 20% increase in feed flow rate. This occurs because benzene drops down the first column quickly with an increase in the liquid feed. The ratio schemes are not used in these simulations, but control performance for feed flow rate disturbances could be improved in both systems by their use, as Figure 12.22 illustrates for the divided-wall column.

Figures 12.28–12.30 give results for the three feed composition disturbances. The control effectiveness is about the same in the two systems.

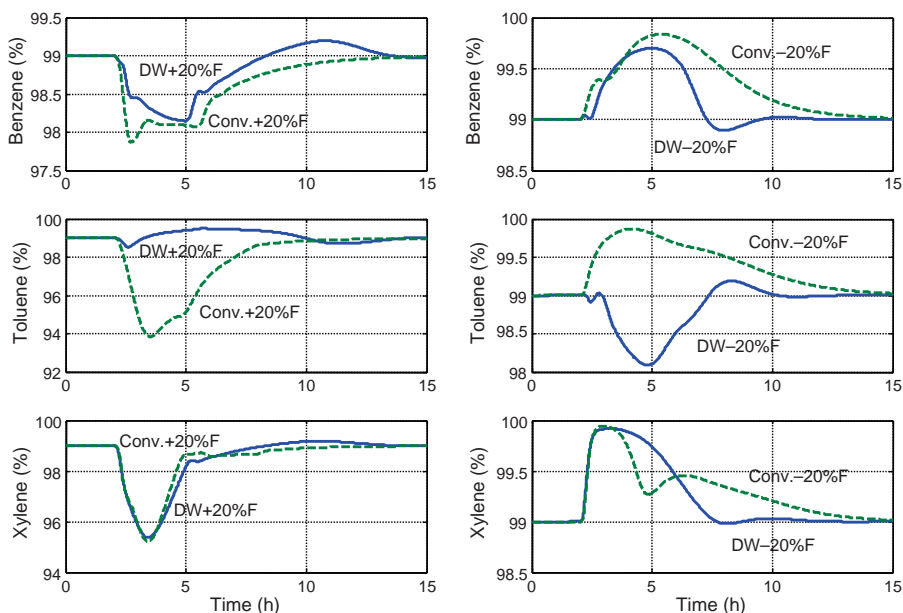


Figure 12.27 Comparison of DW and conventional: feed flow rate disturbances.

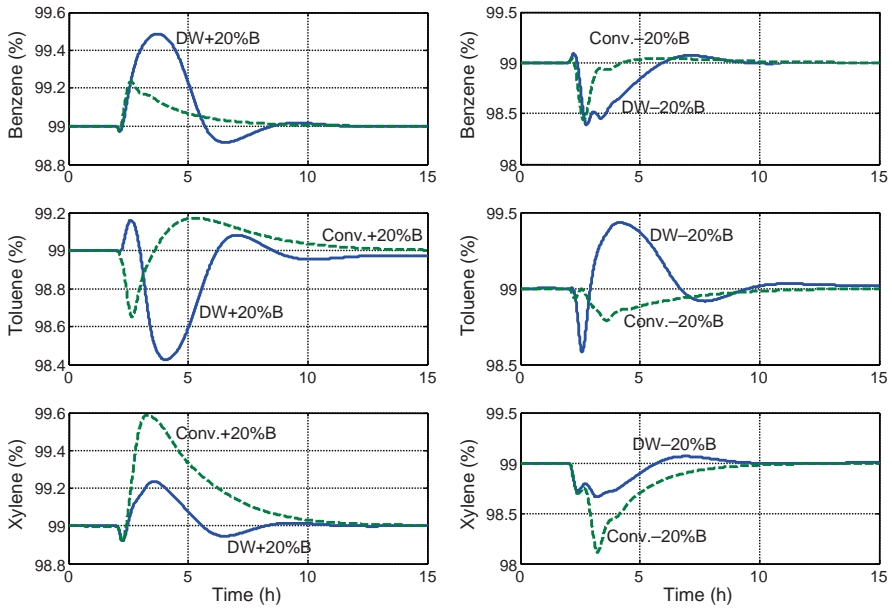


Figure 12.28 Comparison of DW and conventional: benzene feed composition disturbances.

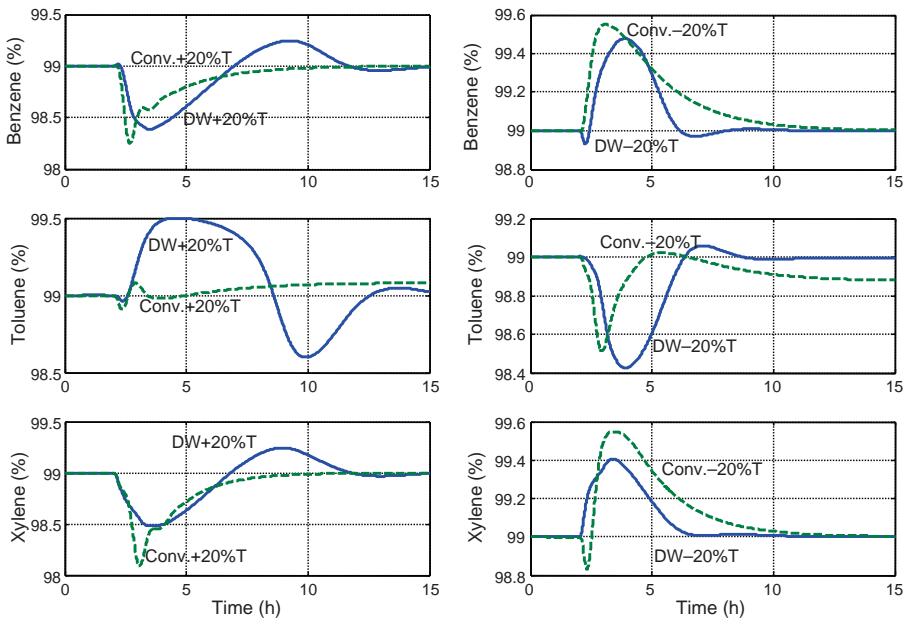


Figure 12.29 Comparison of DW and conventional: toluene feed composition disturbances.

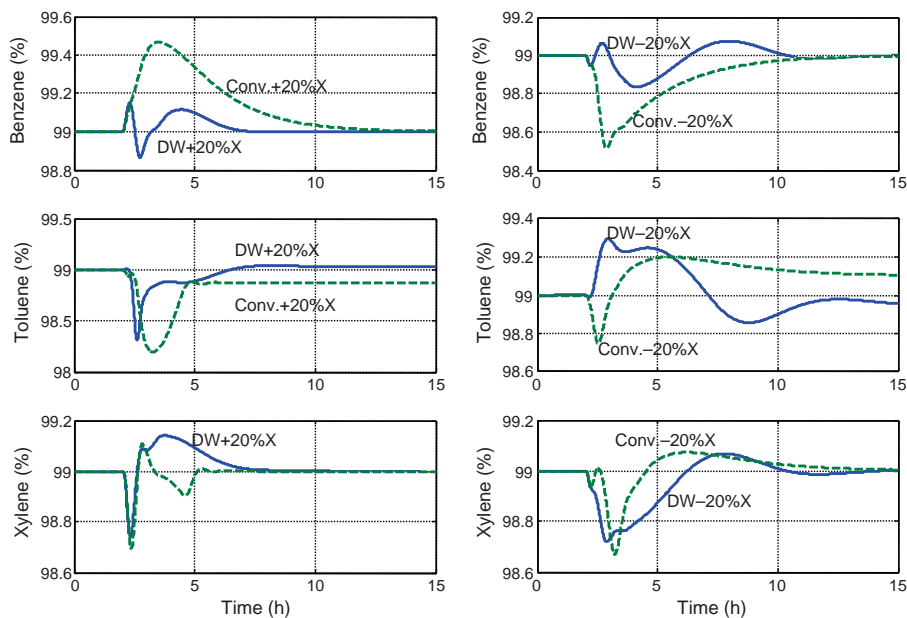


Figure 12.30 Comparison of DW and conventional: xylene feed composition disturbances.

12.5 CONCLUSIONS AND DISCUSSION

This chapter has discussed the modeling and control of a divided-wall column. A control structure for divided-wall distillation columns has been developed that is capable of simultaneously controlling product compositions and minimizing energy consumption in a practical way. The essential idea is to control a xylene composition at the top of the prefractionator side of the wall by manipulating the liquid split. Steady-state relationships show that maintaining this composition produces energy consumptions that are very close to the minimum values as feed compositions change. Thus, the method implicitly minimizes energy consumption.

One important issue is the question of general applicability. We have examined in this chapter one chemical system (BTX). The relative volatilities in this system are $B/T = 2.51$ and $T/X = 2.54$ at the bottom of the column (68.374 N/m^2). At the top of the column ($37,369 \text{ N/m}^2$), they are $B/T = 2.72$ and $T/X = 2.76$. We have also studied another chemical system (methanol/ethanol/propanol (MEP)) and found that the proposed control structure works well. In the MEP system, the relative volatilities are $M/E = 1.79$ and $E/P = 2.04$. Therefore, we feel that the structure can be applied in a number of systems.

The basic reason why the heavy impurity at the top of the prefractionator should be controlled is the fact that the sidestream withdrawn from the main column is a liquid. Heavy component going out the top of the wall will appear in the liquid flowing down in the main column and strongly affect sidestream purity. On the other hand, any light impurity that drops out the bottom of the wall will appear in the vapor flowing up in the main column. As the sidestream is liquid, small amounts of light impurity in the vapor will not

greatly affect its composition. If the sidestream were withdrawn as a vapor, we would probably have to control the light impurity at the base of the prefractionator.

REFERENCES

1. H. Ling and W. L. Luyben, New control structure for divided-wall columns, *Ind. Eng. Chem. Res.* **48**, 6034–6049 (2009).
2. E. A. Wolff and S. Skogestad, Operation of integrated three-product (Petlyuk) distillation columns, *Ind. Eng. Chem. Res.* **34**, 2094–2103 (1995).

CHAPTER 13

DYNAMIC SAFETY ANALYSIS

13.1 INTRODUCTION

The many examples given in this book have illustrated that dynamic simulations of distillation columns can be used to develop effective control structures for a wide variety of individual columns and multiple-column systems. However, there is another use of dynamic simulations that is very important for the safe operation when process and equipment emergencies occur. The most common example is a cooling water failure, which can lead to very rapid increases in column pressure.

The normal distillation models assume instantaneous heat transfer in the condenser and reboiler, and the normal default heat-transfer option is “Direct Q.” The basic model does not accurately represent the short-term rapid dynamic response under severe conditions because the capacitance (holdup) of material and mass of equipment metal in the reboiler and condenser heat exchangers are not considered.

Accurate response times are essential in the design of safety systems for the column. Rapid increases in pressures and temperatures can occur in seconds, and accurately determining the rates of increase in these important variables and the time period to reach critical limits (*safety response time*) permits the engineer to quantitatively design effective safety systems.

This chapter illustrates how rigorous condenser and reboiler models can be developed in Aspen Plus and their dynamics evaluated in Aspen Dynamics.

13.2 SAFETY SCENARIOS

When an emergency arises, the time it takes to approach a high limit in some critical variables (temperature, pressure, or composition) is important because it determines how

fast the safety protection equipment (sensors and valves) must be able to respond to the detected event. A common example is a loss of coolant, which could be refrigerant (low-temperature operation), cooling water (medium-temperature operation) or boiler feed water (if cooling is achieved by generating steam). This type of loss can be detected in several ways. The most obvious is a measurement of the flow rate of the coolant. But flow sensors are often noisy due to turbulent flow conditions and have limited reliability. Impulse lines and orifice plates can plug and foul. Shutting down a whole plant due to faulty measurement signal is very undesirable. Therefore, other more reliable sensors (temperature or pressure) are often used to infer a loss of coolant. Multiple sensors based on different physical principles are used to improve fault detection reliability.

There are several levels of action to be taken as the critical variable moves away from its normal value. As sketched in Figure 13.1, at some percentage of departure from normal pressure, perhaps 10%, an alarm will be activated to alert the operator. At a larger percentage (20%), an override system will begin to adjust other manipulated variables not normally used to maintain the pressure in an attempt to ride through the disturbance without necessitating a complete plant shutdown. For example, the feed flow rate and/or the reboiler heat input could be reduced as the column pressure approaches this “override” limit. If conditions worsen and the pressure continues to rise up to perhaps 30% above normal, an interlock system will be activated that shuts down the process. If these actions are unable to prevent a further rise in pressure, the last line of defense to protect the physical integrity of the vessels is opening of safety valves or blowing of rupture disks at perhaps 40% above normal. Of course, the vent/scrubbing/flaring systems into which these discharges empty must be sized adequately to handle the dynamic loads that occur during the event.

A discussion of the safety responses of several chemical reactor systems has been presented.¹ Reactors often present critical safety issues, and the wide variety of different

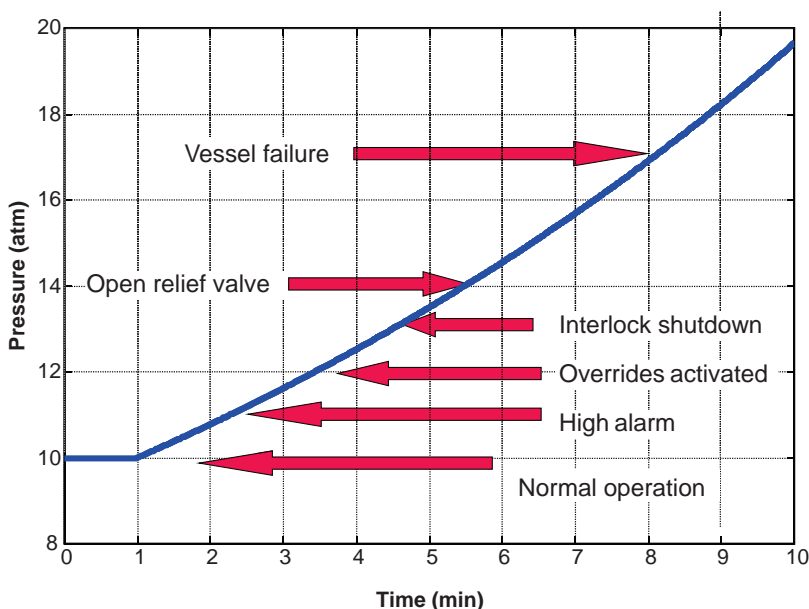


Figure 13.1 Safety constraints and actions: pressure limitations.

reactor and reaction types and conditions yield a wide range of safety reaction times. This chapter addresses dynamic simulations for the safety analysis of a typical distillation column. Columns are usually more benign than chemical reactors, and there are fewer types of configurations and ranges of operating variables. A typical numerical example is considered.

13.3 PROCESS STUDIED

The binary separation of methanol and water is used as an example column. A feed of 82 mol% methanol and 18 mol% water is fed to a column with 40 trays (42 stages in Aspen terminology with feed on Stage 27 and the condenser labeled as Stage 1). Condenser pressure is 1 bar, condenser pressure drop is 0.1 bar, and tray pressure drop is 0.01 bar per tray (giving a base pressure of 1.5 bar). Product purities are 99.9 mol% methanol in the distillate and 99.9 mol% water in the bottoms. The required reflux ratio is 0.8569. Column diameter is 5.61 m. Reboiler heat input is 64.1 MW. Condenser heat removal is 60.0 MW. The NRTL physical property package is used.

13.4 BASIC RADFRAC MODELS

The basic Aspen *RadFrac* model incorporates *implicitly* a condenser and a reboiler. The process flow diagram of this base model is shown in Figure 13.2. The dynamics of the system depend on the column diameter, the tray weir height, and the holdups in the column base (reboiler) and reflux drum (condenser).

This basic model has several options for handling the dynamics of the heat exchangers.

13.4.1 Constant Duty Model

The default mode is *Constant duty* in which heat-transfer rates (Q_C in the condenser and Q_R in the reboiler) are set immediately with no dynamic lags. These heat-transfer rates are directly manipulated in the dynamic model and their effects are immediately felt by

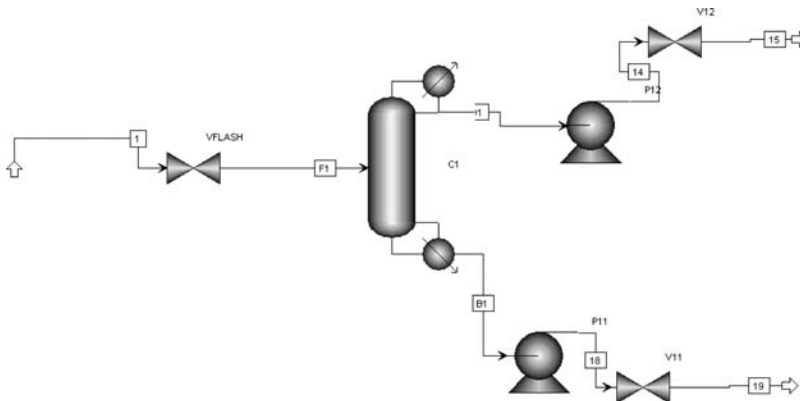


Figure 13.2 Base Aspen distillation column model.

column. There is no consideration of heat-transfer area, temperature driving forces, or heat-transfer coefficient. The holdup of material on the utility-side of the heat exchanger and the mass of the metal of the heat exchangers are not considered.

In normal control studies, these assumptions are reasonable because the composition dynamics of the column trays, column base, and reflux drum are typically much slower than the dynamics of the heat exchangers. However, for predicting rapid responses to safety scenarios, the dynamics of the heat exchangers should not be neglected.

13.4.2 Constant Temperature Model

The temperature of the cooling medium in the condenser or the temperature of the heating medium in the reboiler are set, and then Aspen calculates the required UA product (overall heat-transfer coefficient U and heat-transfer area A) from the known heat-transfer rate and temperature differential driving force. This temperature is manipulated in the dynamic simulations. No heat-exchanger dynamics are considered.

13.4.3 LMTD Model

If the condenser uses the flow rate of a cooling medium (typically cooling water) or if the reboiler uses the flow rate of a heating medium (hot oil), a model, using a log-mean temperature differential driving force (temperature differentials at outlet and inlet ends), can be used. The inlet medium temperature and the minimum approach temperature difference between the process and the medium are specified. Then Aspen calculates the required UA product (overall heat-transfer coefficient U and heat-transfer area A) and the required flow rate of the medium from the known heat-transfer rate.

The flow rate of the medium is manipulated in the Aspen Dynamic simulations, not Q_C or Q_R directly. However, this model contains no dynamics. The holdup of medium in the heat exchanger is not considered. Medium flow rate changes produce instantaneous changes in temperature driving forces and subsequent heat-transfer rates.

13.4.4 Condensing or Evaporating Medium Models

An *Evaporating* model can be used in the condenser, and a *Condensing* model can be used in the reboiler if the cooling/heating medium undergoes a phase change. If the reboiler is heated by a condensing vapor (typically steam), the difference in temperature between the condensing steam at a specified temperature and the column base temperature is used to calculate the UA and the flow rate of the steam from the known reboiler duty Q_R . The flow rate of the steam is manipulated in the Aspen Dynamics simulations, not Q_R directly.

If the condenser is cooled by a vaporizing liquid (boiler feed water in high-temperature columns or liquid refrigerant in low-temperature columns), the difference in temperature between the specified temperature of the vaporizing liquid and the temperature of the process in the condenser is used to calculate the UA and the flow rate of the coolant from the known condenser duty Q_C . The flow rate of the coolant is manipulated in the Aspen Dynamics simulations, not Q_C directly.

13.4.5 Dynamic Model for Reboiler

There is one heat-exchanger model in the standard model that considers heat-exchanger dynamics, but is only available for the reboiler. The *Dynamic* model uses the holdup of the

heating medium in the reboiler. The medium is assumed to be at a single temperature (perfectly mixed). The inlet medium temperature and the approach temperature to the process are specified. Then Aspen calculates the required UA and the medium flow rate from the known heat-transfer rate Q_R . The larger the medium holdup, the more slowly the perfectly mixed medium temperature changes for a change in medium flow rate. So this model is the only built-in model that considers dynamic lags in the heat exchanger equipment associated with the column.

However, this model can only be realistically used when the reboiler heating medium is a hot liquid stream, and the holdup of this liquid on the shell or tube side is significant. If the reboiler is heated with a condensing vapor, which is much more frequently the case, this dynamic model is not applicable.

13.5 RADFRAC MODEL WITH EXPLICIT HEAT-EXCHANGER DYNAMICS

Figure 13.3 gives a process flow diagram of a more rigorous Aspen simulation that explicitly incorporates separate units for the condenser and the reboiler. Figure 13.4 gives a detailed flowsheet of operating conditions and equipment sizes. The column itself is a *RadFrac* column, but it has neither a reboiler nor a condenser. These are added externally as standard Aspen *HeatX* models. In addition, a separate reflux drum and a liquid circulation from the base of the column through the reboiler are explicitly added as new units.

13.5.1 Column

The top tray is now labeled as Stage 1 in this absorber model. So the feed stage and the bottom stage must be decreased by one to make this column equivalent to the basic column. The feed and reflux are fed to column along with a partially vaporized stream from the

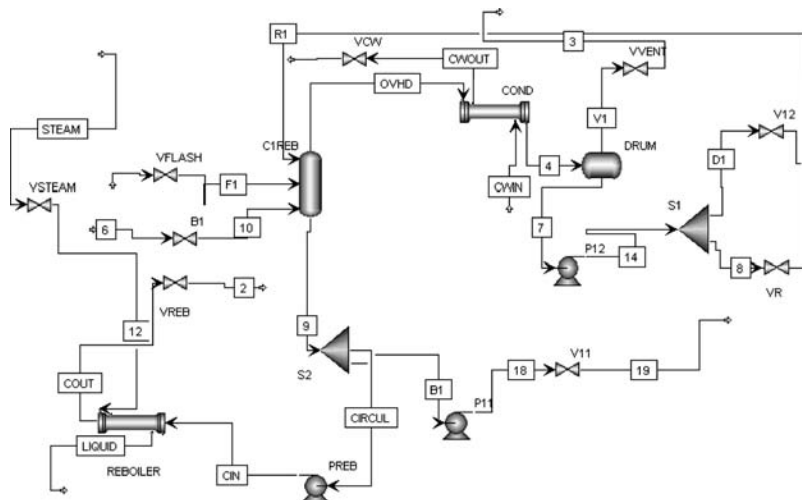


Figure 13.3 Rigorous Aspen distillation column model: steady state.

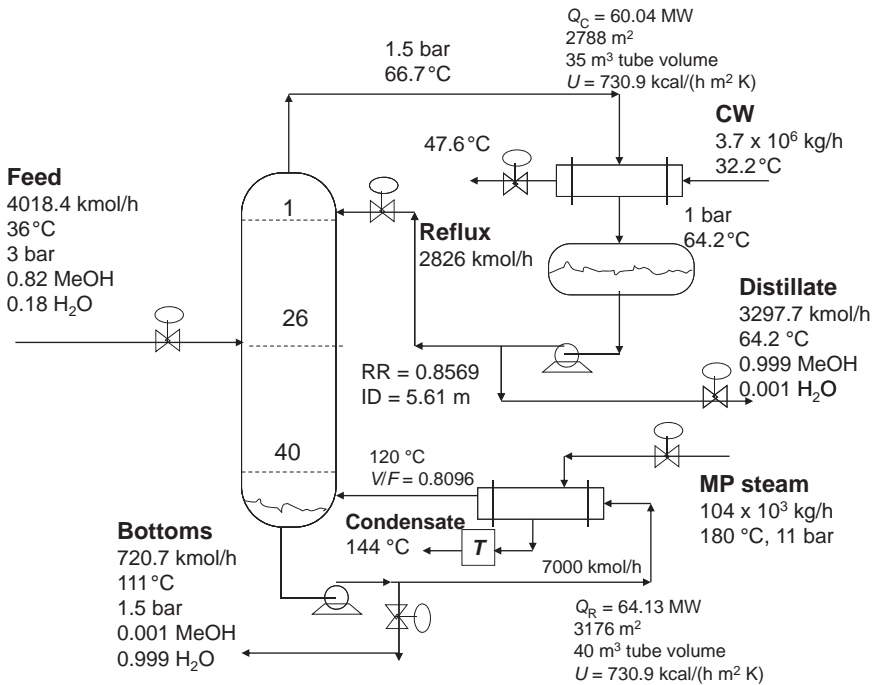


Figure 13.4 Column flowsheet.

reboiler. This vessel has no design specifications. Top pressure is 1.1 bar. Base pressure is 1.5 bar.

13.5.2 Condenser

The overhead vapor from the column is condensed in a water-cooled heat exchanger. The design specification for this *HeatX* model is the exit temperature of the hot stream at 64.2°C (the bubblepoint temperature of the distillate at 1 bar). Cooling water flows through the condenser (3.7×10^6 kg/h), entering at 32.2°C and exiting at 47.6°C. With a heat-transfer rate of 60.06 MW and an overall heat-transfer coefficient of 730.9 kcal/(h m² K), the required area is 2788 m².

The volume of the tubes is estimated by assuming tubes 0.05 m in diameter and 5 m in length. The number of tubes required to give the necessary heat-transfer area is calculated and the inside volume of these tubes (35 m³) is used to give dynamics in the *HeatX* model. Shell volume is set equal to tube volume. In the *Dynamics* section of the *HeatX* block, the default is *Instantaneous*. Use the drop-down arrow to select *Dynamics*, and enter the inlet and outlet volumes on both hot and cold sides of the heat exchanger.

The dynamic capacitance of the tube metal in the condenser can also be included if it is significant compared to that of the cooling water in the tubes. The mass of cooling water times its heat capacity is $(35 \text{ m}^3)(1000 \text{ kg/m}^3)(4.184 \text{ kJ/(kg K)}) = 145,600 \text{ kJ/K}$. Assuming a metal tube wall thickness of 0.00127 m, the volume of the tube metal is 3.54 m³. Then using a metal density of 7750 kg/m³ and a heat capacity of 0.836 kJ/(kg K), the product of metal mass times heat capacity can be calculated:

$(3.53 \text{ m}^3)(7750 \text{ kg/m}^3)(0.836 \text{ kJ/(kg K)}) = 22,940 \text{ kJ/K}$. Thus, the metal heat capacitance is only 15% of the water capacitance.

13.5.3 Reflux Drum

An Aspen *Flash2* model is used for the reflux drum with pressure set at 1 bar and design specification of a vapor fraction of 10^{-5} , which makes the drum essentially adiabatic. A small vapor flow rate is necessary so that the control valve in this vent line can be sized. In the Aspen Dynamics simulation, the valve is completely closed. The liquid holdup in the drum is set to give 5 min at 50% full (diameter 3 m and length 6 m).

13.5.4 Liquid Split

Liquid from the drum is pumped up to 4 bar and split into a reflux stream (set at exactly the value used in the base case, 2826 kmol/h) and the distillate (see Fig. 13.3 (*Splitter S1*)). As discussed below, the conditions in the reboiler will be adjusted to drive the distillate to be the same as in the base case (3297.7 kmol/h).

13.5.5 Reboiler

Liquid from the column base is split (*Splitter S2* in Fig. 13.3) between the bottoms and a circulating stream that flows through a *HeatX* model used for the reboiler. The bottoms flow rate is set equal to that found in the base case (720.7 kmol/h). Note that the feed and bottoms flow rates are set to same values as the base case. Therefore, the distillate flow rate must also be the same. Using the same reflux flow rate should yield exactly the same tray and product compositions, which is indeed true (99.9 mol% purities of both product streams).

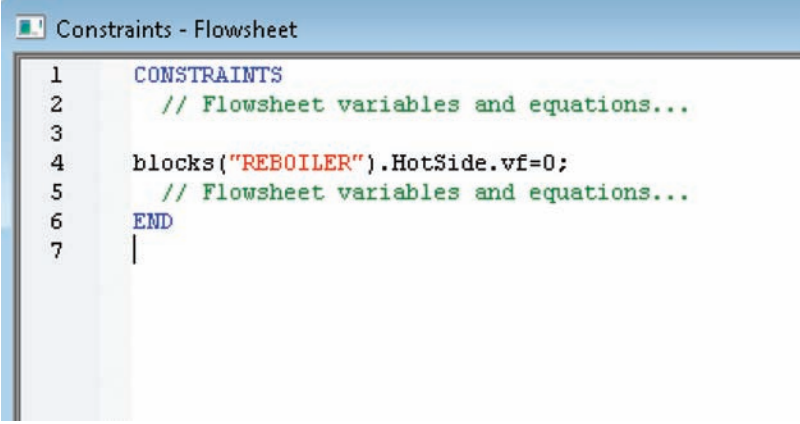
The circulating stream is pumped to 2.5 bar and enters the reboiler at a high flow rate (7000 kmol/h) and 111 °C. The circulating loop mimics the flow rate found in a thermosiphon reboiler. The heat duty in the reboiler is 64.13 MW, which produces a partially vaporize process exit stream (vapor fraction = 0.8096) at a temperature of 120 °C.

Setting up this circulating loop is not trivial. The circulating stream was “torn” and a guessed value for the flow rate of a stream entering the base of the column is assumed. The composition of the stream is known (same as bottoms). The vapor fraction of this stream was varied using an Aspen *Flowsheet design spec* to drive the distillate flow rate to the desired value. Then another *Flowsheet design spec* was used to change the flow rate of the steam to produce this vapor fraction.

When the recycle loop was closed in Aspen Plus, it would *not* converge. However, after exporting into Aspen Dynamics, the loop was successfully closed and converged to the steady state. In Aspen Dynamics, the streams “6” and “2” are deleted, as is block “B1” (see Fig. 13.3). Then the source of stream “10” is reconnected to block “VREB”.

The steam used in the reboiler is medium-pressure steam at 11 bar and 180 °C with a flow rate of $104.5 \times 10^3 \text{ kg/h}$. The steam temperature in the reboiler shell is 144 °C, which provide the necessary driving force to transfer 64.13 MW in the 3176 m^2 heat exchanger using an overall heat-transfer coefficient of $730.9 \text{ kcal/(h m}^2 \text{ K)}$.

The specification of the reboiler *HeatX* model in Aspen Plus is a hot stream outlet vapor fraction of zero (liquid condensate leaving from the stream trap). When the file is exported into Aspen Dynamics, the default condition in the reboiler is a fixed steam-side pressure.



```

1  CONSTRAINTS
2  // Flowsheet variables and equations...
3
4  blocks("REBOILER").HotSide.vf=0;
5  // Flowsheet variables and equations...
6  END
7  |

```

Figure 13.5 Flowsheet equation.

This, of course, is not what we want since the pressure (and temperature) must vary to change the heat-transfer rate and the steam flow rate. It is necessary to use *Flowsheet Equations* in Aspen Dynamics to change the specification to have an exit hot stream with a vapor fraction of zero. Figure 13.5 shows the equation used. It is also necessary to change the pressure of the hot exit stream from *fixed* to *free* so that the system is not over specified.

13.6 DYNAMIC SIMULATIONS

Both the base case column and the rigorous column/heat-exchanger process were exported into Aspen Dynamics. A standard conventional distillation control structure was installed on both processes. Three of the loops are identical in both systems.

1. Reflux-drum level is controlled by manipulating the flow rate of distillate using a proportional control with $K_C = 2$.
2. Column base level is controlled by manipulating the flow rate of bottoms using a proportional control with $K_C = 2$.
3. The reflux flow rate is ratioed to the feed flow rate.

The other two loops, a tray temperature controller (TC) and a pressure controller, are different in the two cases.

13.6.1 Base Case Control Structure

For the base case, condenser pressure is controlled by condenser heat removal (direct Q_C). The Aspen Dynamics default tuning parameters are used ($K_C = 20$ and $\tau_1 = 12$ min). A temperature on Stage 40 is controlled by manipulating reboiler duty (direct Q_R). Stage 40 is selected because it is near the bottom but still in the region in which changes in the temperature profile are large, as shown in Figure 13.6. A 1 min deadtime is installed in this loop, and a relay-feedback test gives an ultimate gain $K_U = 2.8$ and an ultimate period $P_U = 3.6$ min. The Tyreus–Luyben tuning rules give the TC tuning constants $K_C = 0.88$ and $\tau_1 = 8$ min.

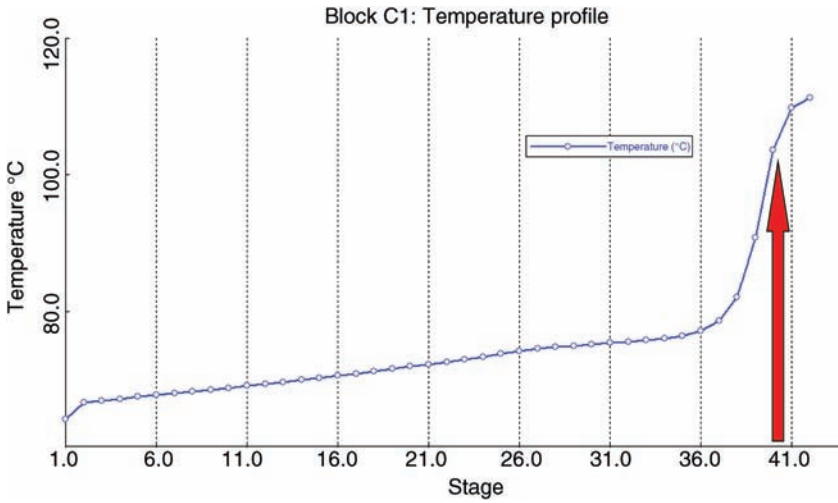


Figure 13.6 Temperature profile.

13.6.2 Rigorous Case Control Structure

For the simulation with external heat exchangers for the reboiler and condenser, the temperature and pressure loops have the same controlled variables but different manipulated variables than those used in the base case.

Reflux drum pressure is controlled by manipulating the control valve in the cooling water line as shown in Figure 13.7. The Aspen Dynamics default tuning parameters are used ($K_C = 20$ and $\tau_1 = 12$ min).

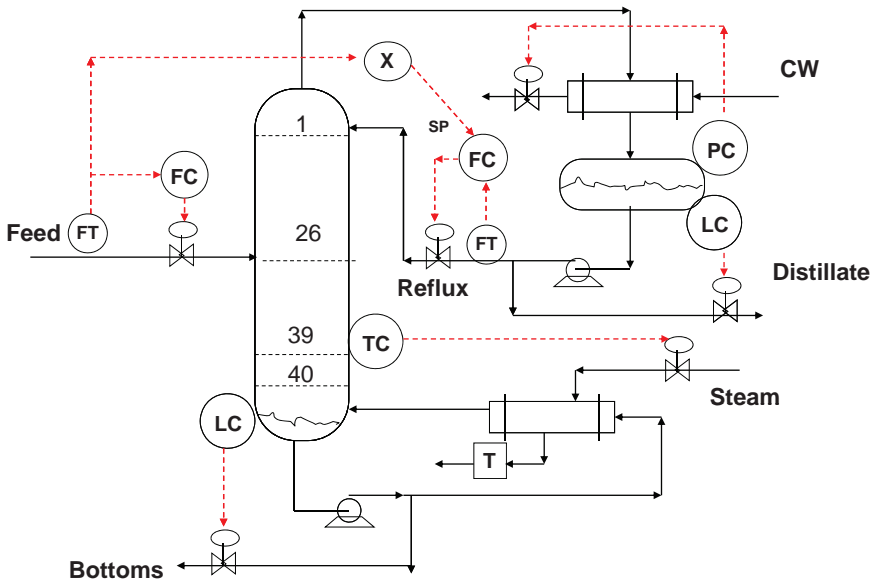


Figure 13.7 Control structure for rigorous case.

The tray temperature controller now controls Stage 39 instead of Stage 40 because of the difference in stage numbering in a stripping column (top tray is Stage 1). The temperature and composition profiles are identical in both columns. The temperature controller manipulates the control valve in the steam line, not Q_R directly. A 1 min deadtime is installed in this loop, and a relay-feedback test gives an ultimate gain $K_U = 17$ and an ultimate period $P_U = 4.8$ min. The Tyreus–Luyben tuning rules give the temperature controller tuning constants $K_C = 5.5$ and $\tau_I = 11$ min.

13.7 COMPARISON OF DYNAMIC RESPONSES

Two types of safety events are explored. In the first, there is a failure in the supply of cooling water to the condenser. In the second, a large surge in steam to the reboiler occurs.

13.7.1 Condenser Cooling Failure

With the basic model, this failure is simulated by running at steady state for 10 s, putting the pressure controller on manual and setting controller output signal (which is Q_C directly) to zero. The dashed line in Figure 13.8 shows the response of reflux-drum pressure. There is an immediate rapid rise in pressure from the operating level of 1 bar. It takes only 10 s for the pressure to climb to 1.2 bar.

For the rigorous model, the failure is simulated by running at steady state for 10 s, putting the pressure controller on manual and setting controller output signal (which is signal to the air-to-close valve) to 100% (valve completely closed). The solid line in Figure 13.8 shows the response of reflux-drum pressure. The rise in pressure is less rapid, taking about 20 s to reach a pressure of 1.2 bar.

Figure 13.9 shows how several other variables change for the two models. The middle graph on the left shows how the reboiler heat input is unchanged with the base model

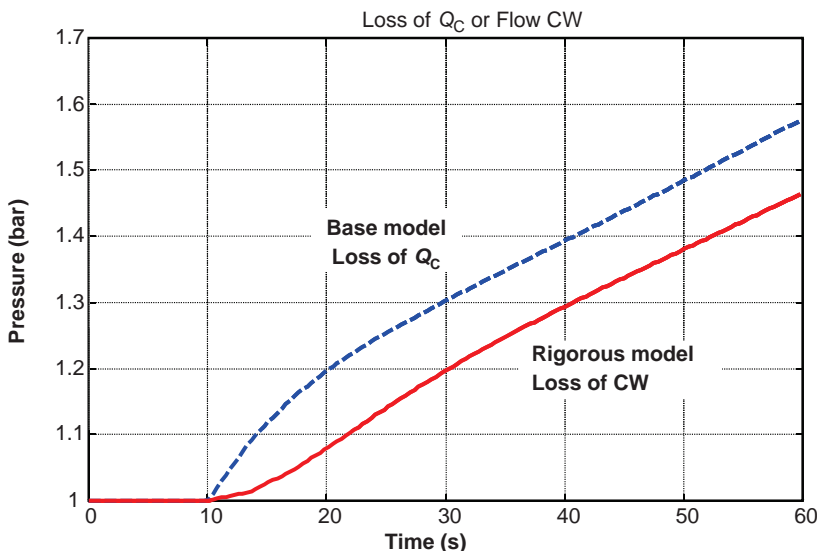


Figure 13.8 Pressure responses: loss of Q_C or loss of CW.

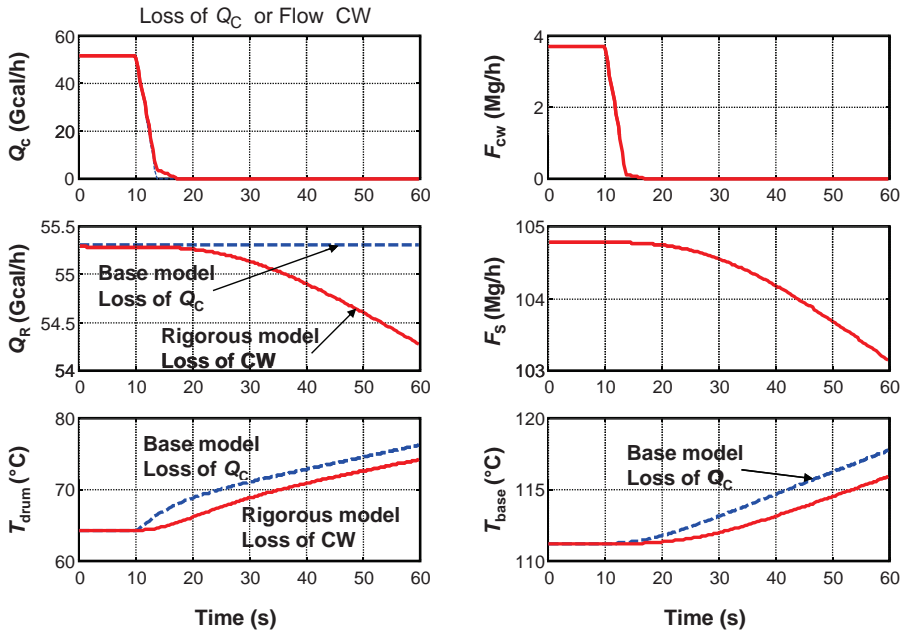


Figure 13.9 Other variables with loss of Q_C or loss of CW.

(dashed lines). However, with the rigorous model, the steam flow rate drops off (middle graph on right). This occurs because the base temperature rises as column pressure rises, which reduce the temperature differential in the reboiler and lowers the heat-transfer rate (solid line in middle graph on left).

Thus, the dynamic response of pressure is slowed down by both the thermal capacitance of the condenser and the rigorous handling of heat transfer in the reboiler.

13.7.2 Heat-Input Surge

A second event that could result in over-pressuring the column would be a sudden increase in heat input. This could be caused by an operator mistakenly putting the temperature controller on manual and opening the steam valve.

With the basic model, this failure is simulated by running at steady state for 0.5 min (note the change in the time scale), putting the temperature controller on manual and setting the controller output signal (the reboiler duty) equal to twice the steady-state value. The dashed lines in Figure 13.10 show the response of reflux-drum pressure to this disturbance. The pressure rise is much slower and much smaller in magnitude than for a condenser cooling failure. It takes about 1 min for the pressure to rise up to 1.037 bar.

For the rigorous model, the failure is simulated by running at steady state for 0.5 min, putting the temperature controller on manual and setting controller output signal (which is signal to the air-to-open valve) to 100% (valve completely open). The solid line in Figure 13.10 shows that the response of reflux-drum pressure is slower, taking about 1.4 min to reach 1.037 bar.

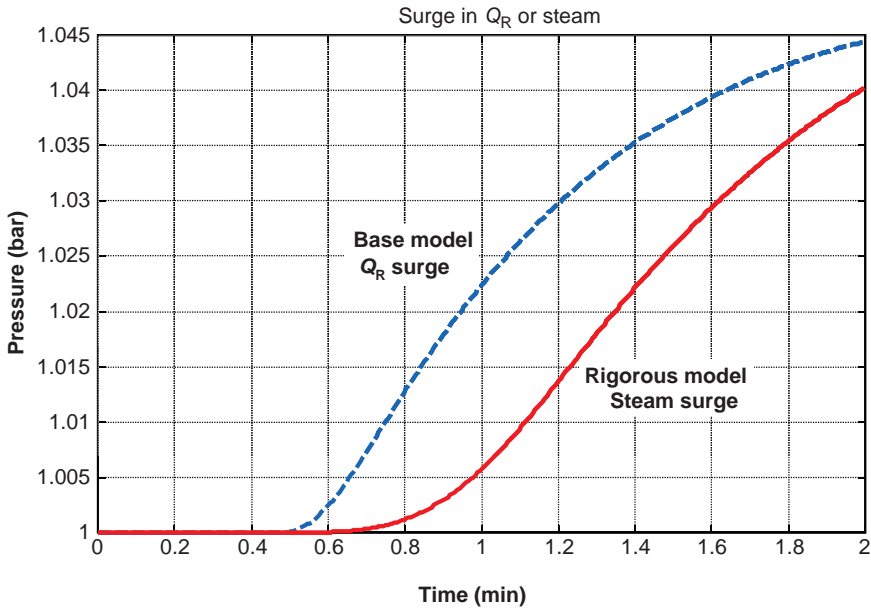


Figure 13.10 Pressure responses: surge in steam or Q_R .

Figure 13.11 compares the responses of the two models for several other variables. The middle left graph shows that there is an immediate large rise in reboiler duty for the base model, but in the rigorous model, the change in reboiler duty is fairly small. This occurs because doubling the control valve opening does not double the steam flow rate

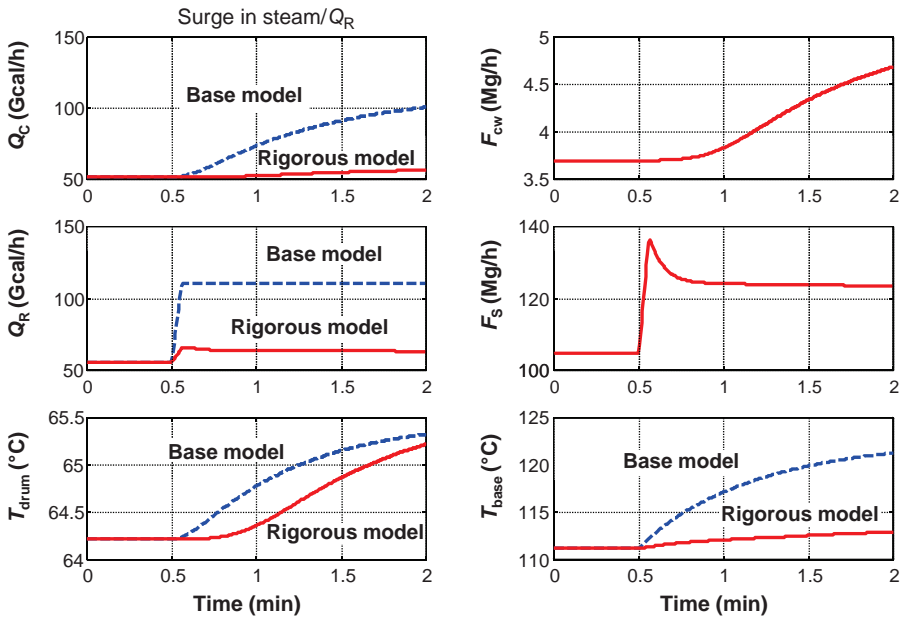


Figure 13.11 Other variables with surge in Q_R or steam.

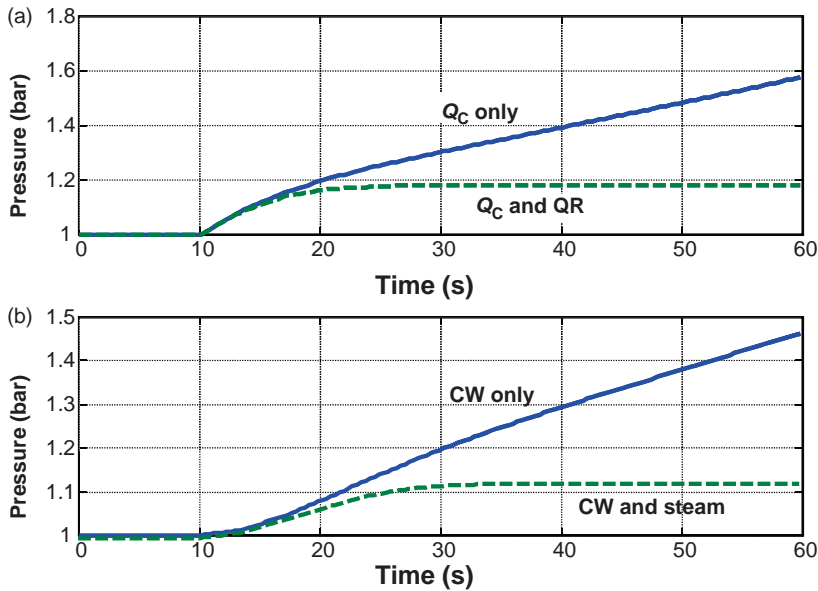


Figure 13.12 Simultaneous loss of condenser cooling and reboiler heating. (a) Base model: loss of Q_C and Q_R . (b) Rigorous model: loss of CW and steam.

(see middle right graph). The steam flow rate is set by the heat-transfer rate as determined by the temperature differential between the steam and column base.

Note that the pressure controller is on automatic during this disturbance, so the condenser heat removal is increased in the base model (dashed line in top left graph in Fig. 13.11) and condenser cooling water flow rate is increased in the rigorous model (top right graph).

It is interesting to see what the effect on pressure dynamics would be if an immediate change in the reboiler duty is made when condenser cooling is lost. Responses for this scenario are shown in Figure 13.12 for the two models. The rise in pressure is limited to only 1.18 bar in the base model and 1.12 in the rigorous model. Of course the column temperatures would drop and product quality would quickly go off-specification (methanol would drop out the bottom). But over pressuring could be prevented by interlocking the reboiler steam.

13.8 OTHER ISSUES

The numerical example used in this study has a large column (5.61 m in diameter) with large reboiler and condenser duties. Are these results applicable with smaller columns? The answer is yes. All the vessel volumes and heat-transfer areas scale directly with flow rates, so the dynamics should be the same. The only exception is tray liquid hydraulics because weir lengths scale directly with column diameter, not cross-sectional area. So, liquid height of the weir is different for different capacities. However, the short-term pressure responses should not be affected by liquid flow rates.

13.9 CONCLUSIONS

The standard basic *RadFrac* model in Aspen simulations does not accurately predict the rapid pressure changes during emergency situations because the default heat-exchanger models do not account for heat-exchanger dynamics (condenser and reboiler). Simulations can be developed that include external heat exchangers whose dynamics can be incorporated with the model of the column vessel.

REFERENCE

1. W. L. Luyben, Use of dynamic simulation for reactor safety analysis, *Comput. Chem. Eng.* **40**, 97–109 (2012).

CARBON DIOXIDE CAPTURE

Environmental concerns about global warming have increased interest in reducing the emissions of carbon dioxide into the atmosphere. The man-made sources of carbon dioxide are primarily from fossil fuels, with the combustion of coal for the production of electric power being a major contributor. Power plants are usually very large and centrally located, so capturing the carbon dioxide they generate is technically possible. Whether this is economically or politically possible remains an open question.

Transportation fuels (gasoline and diesel) are also major sources, but the possibility of capturing carbon dioxide from these widely distributed and mobile sources is remote. The electric car could reduce this problem since the power would be centrally generated.

The vast majority of current power plants use coal or natural gas as the fuel source and air as the source of oxygen. In these plants, the stack gas is at essentially atmospheric pressure and contains a large concentration of nitrogen (76 mol%). A small amount of excess air is used, which gives a stack composition of 4.8 mol% O₂. The carbon dioxide concentration is only 13.2 mol%. The principal proven method for carbon dioxide removal from a low-concentration, low-pressure gas uses amine absorption, which involves chemical reaction of carbon dioxide with an amine, such as monoethanolamine (MEA).

However, in the future, power plants may be considerably different. Instead of combustion of a hydrocarbon source (coal, biomass, natural gas) using air in a low-pressure furnace, a high-pressure gasification vessel may become more attractive that uses oxygen for partial combustion of the biomass. The synthesis gas generated in the gasifier is a mixture of hydrogen, carbon monoxide, and carbon dioxide. A water-gas shift reactor converts most of the carbon monoxide to carbon dioxide, generating more hydrogen. The resulting gas is mostly hydrogen and carbon dioxide. So the absorber has a much higher carbon dioxide concentration and is at high pressure, making carbon dioxide removal much easier.

In this process, the gas stream from which carbon dioxide is to be removed is at high pressure and a physical solvent can be used. A mixture of the dimethyl ethers of polyethylene glycol is used to physically absorb the carbon dioxide. The off-gas from the high-pressure absorber is a hydrogen-rich stream (90 mol% H₂) that is fed to a combustion turbine that drives a generator for direct generation of electricity. The hot gas leaving the turbine can be used to generate steam to drive a steam turbine for additional power generation. This type of system is called integrated gasification combined cycle (IGCC).

These two types of processes both use absorber/stripper systems but with different characteristics. Both are discussed in detail in this chapter.

Feed gas is fed to the bottom of the absorber and the “lean” solvent is fed to the top. The amount of carbon dioxide removed from the gas depends on the flow rate and concentration of the solvent fed. The “fat” solvent leaving the bottom of the absorber is fed to a distillation column in which it is heated, driving off the carbon dioxide and regenerating the solvent for circulation back to the top of the absorber. The heat input to the reboiler is the major energy consumption of the process.

A considerable amount of water is lost in both the absorber and the stripper gas product streams. Some solvent is also lost in these two streams. So the management of the water and solvent fresh makeup streams is one of the essential features of the plantwide control structure.

14.1 CARBON DIOXIDE REMOVAL IN LOW-PRESSURE AIR COMBUSTION POWER PLANTS

The numerical example considered in this chapter is based on the informative paper by Desideri and Paolucci.¹ The plant is designed for a 320 MW steam power plant using coal as fuel. The aqueous amine considered is MEA in the range of about 30 wt%.

14.1.1 Process Design

The stack gas flow rates in a 320 MW power plant are so huge that *four* parallel absorber/stripper trains are required because of vessel size limitations. Figure 14.1 gives the flowsheet of *one* of these two-column processes. Notice that the diameters of the two columns are very large (absorber 9.05 m and stripper 5.16 m).

The stream conditions shown in Figure 14.1 are from the dynamic simulation of the process at steady-state conditions with the recycle of solvent loop closed. This loop did not converge in the steady-state Aspen Plus simulation. Other simulation issues are discussed in the next section.

Absorber. A column with 11 stages operates at 1 atm pressure at the top. A tray pressure drop of 0.2 psi is specified in order to satisfy the requirement that the specified pressure drop is greater than the pressure drop calculate from the hydraulics when exporting to Aspen Dynamics. The design feed gas is 13,100 kmol/h and is compressed to 1.136 atm and fed at the bottom of the absorber. The specified recovery of carbon dioxide is 90%, which corresponds to an absorber exit gas composition of 1.3 mol% CO₂.

The required flow rate of the lean solvent to the top of the absorber to achieve this recovery is 32,860 kmol/h. This flow rate is after the makeup water and makeup

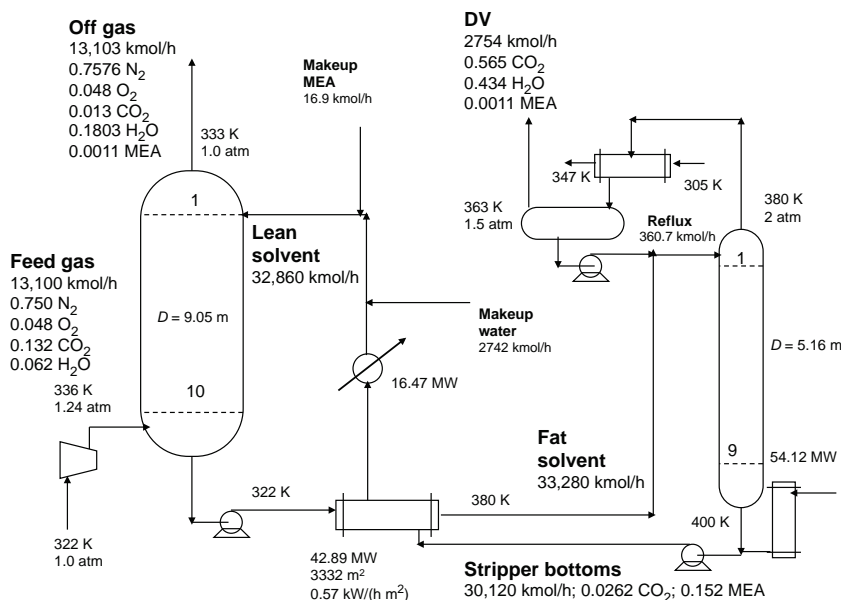


Figure 14.1 Amine absorber/stripper flowsheet.

MEA have been added. The bottoms from the stripper has a concentration of 15.2 mol% MEA. The concentration of carbon dioxide in the stripper bottoms is not negligible (2.62 mol% CO₂).

Both fresh water and fresh MEA are necessary because of losses in the off-gas from the absorber and the vapor product stream from the reflux drum of the stripper. Small amounts of MEA are lost in the absorber off-gas (13.9 kmol/h) and in the vapor from the stripper reflux drum (3.17 kmol/h). The water losses are quite significant in the off-gas (2347 kmol/h) and in the vapor from the stripper reflux drum (1192 kmol/h). The water in the feed gas is 824.3 kmol/h.

Stripper. Absorber bottoms at 322 K is preheated to 380 K in a heat exchanger using the hot stripper bottoms at 400 K and fed to the top of a stripping column with 10 stages and operating at 2 atm in the column and 1.5 atm in the reflux drum. Reboiler heat input is 54.12 MW to maintain a reflux-drum temperature of 363 K, as suggested by Desideri and Paolucci as a balance between stripper reboiler energy and water losses in the vapor from the reflux drum.

All the liquid that condenses at this pressure and temperature is refluxed to the top of the column (360.7 kmol/h). The bottoms stream is 30,120 kmol/h at 400 K and has a composition of 2.62 mol% CO₂ and 15.2 mol% MEA.

14.1.2 Simulation Issues

Several important issues arose in attempting to put together both the steady-state and the dynamic simulations. The *AMINES* physical property package was used in both simulations and gave reasonable results in Aspen Plus. The only simulation issue in Aspen Plus was failure of the solvent recycle loop to converge. This was solved by exporting the file

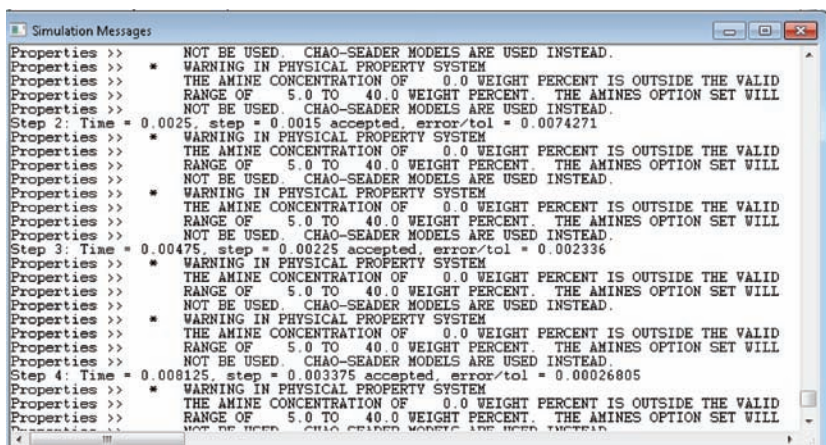


Figure 14.2 Amine messages in Aspen Dynamics.

into Aspen Dynamics, closing the recycle loop in the dynamic simulation and running out to a steady-state condition.

The absorber was modeled using a *RadFrac* column with no condenser and no reboiler. When the absorber by itself was exported to Aspen Dynamics, it ran but messages about switching from *Amines* to *Chao-Seader* were displayed, as shown in Figure 14.2. However, the calculated results all appear to be reasonable. Aspen Support was contacted and reported that there is a bug in Aspen Dynamics that gives these messages, but they can be ignored.

In the original simulation, the stripper was modeled using a normal *RadFrac* column with a partial condenser and a total reboiler. Serious simulation issues arose when the stripper was exported to Aspen Dynamics. When a normal *RadFrac* model with condenser and reboiler was used (see Fig. 14.3a), the file could not be initialized in Aspen Dynamics.

Eventually, a work-around was discovered that produced a running file. In Aspen Plus, the normal *RadFrac* model with both a condenser and a reboiler was replaced with a model that had only a reboiler. Then an external heat exchanger, a reflux drum, and a reflux pump were added to the flowsheet (see Fig. 14.3b). The heat exchanger *HeatX* model was used with cooling water as the cooling medium (5000 kmol/h entering at 305 K and exiting 347 K). The drum used the *Flash2* model. This file could be initialized and run in Aspen Dynamics.

Another simulation issue was the type of integrator used. The default “Implicit Euler” with a variable step size gave very erratic and oscillatory behavior of the pressure in the stripper reflux drum. Switching to the “Gear” algorithm and specifying a very small and “fixed” integration step size (0.0001 h) reduced this numerical problem but slowed down the simulation. It took about 30 min of real time to run a simulation out to 10 h. Figure 14.4 illustrates the numerical problem, showing stripper pressure. For the first 60 min, the Gear algorithm is used with a fixed step size. Then the algorithm is switched to Implicit Euler with a variable step size until time equal 90 min, at which time Gear was again used.

Figure 14.5 shows the Aspen Plus flowsheet with the solvent recycle loop *open*. The makeup flow rates of water and MEA were estimated from the losses of these components. After exporting to Aspen Dynamics, the block “VDUM” and the streams “CALC” and “SOLVENT” are deleted. Then stream “LEAN” is connected to mixer “M1.”

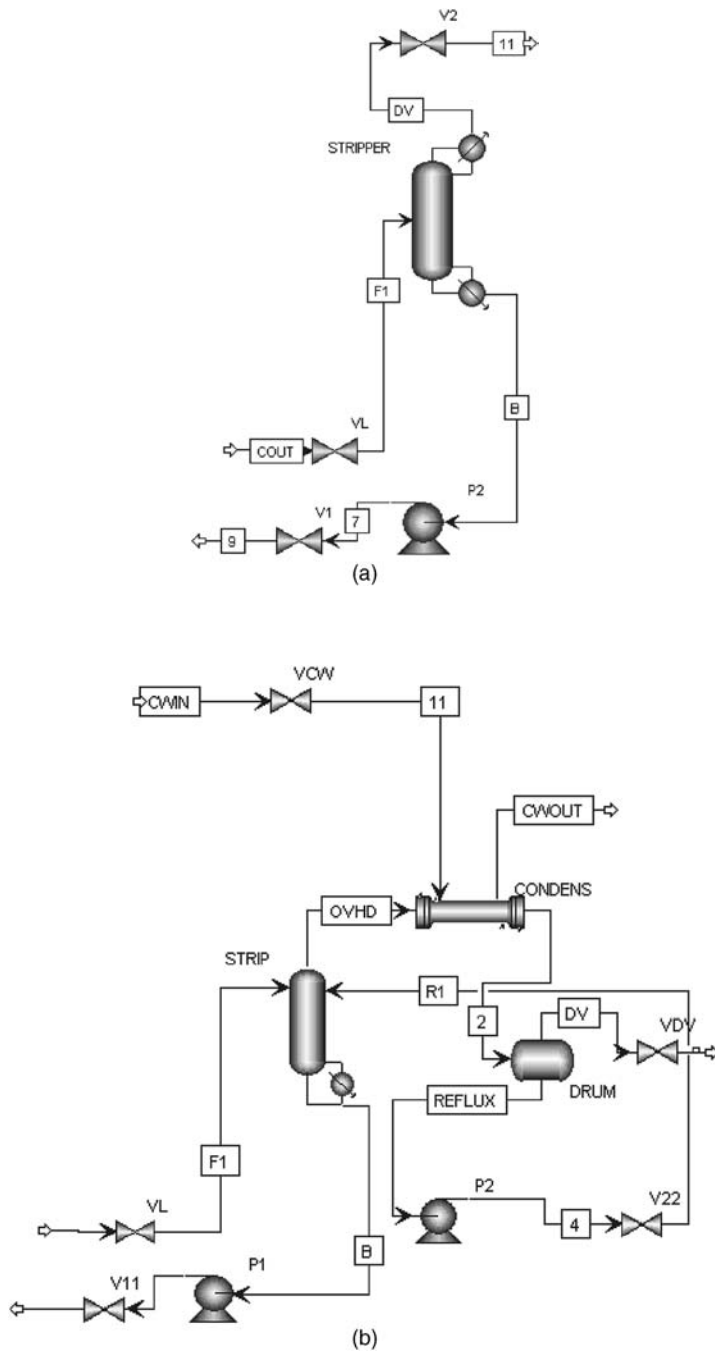


Figure 14.3 (a) Column with normal model. (b) Column with external condenser and reflux drum.

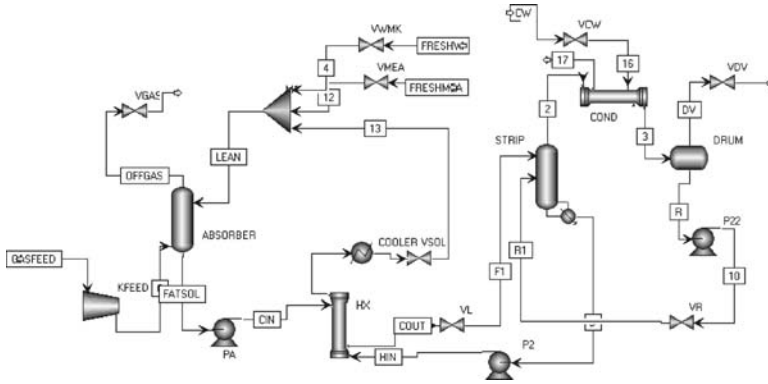


Figure 14.6 Absorber/stripper flowsheet with recycle closed.

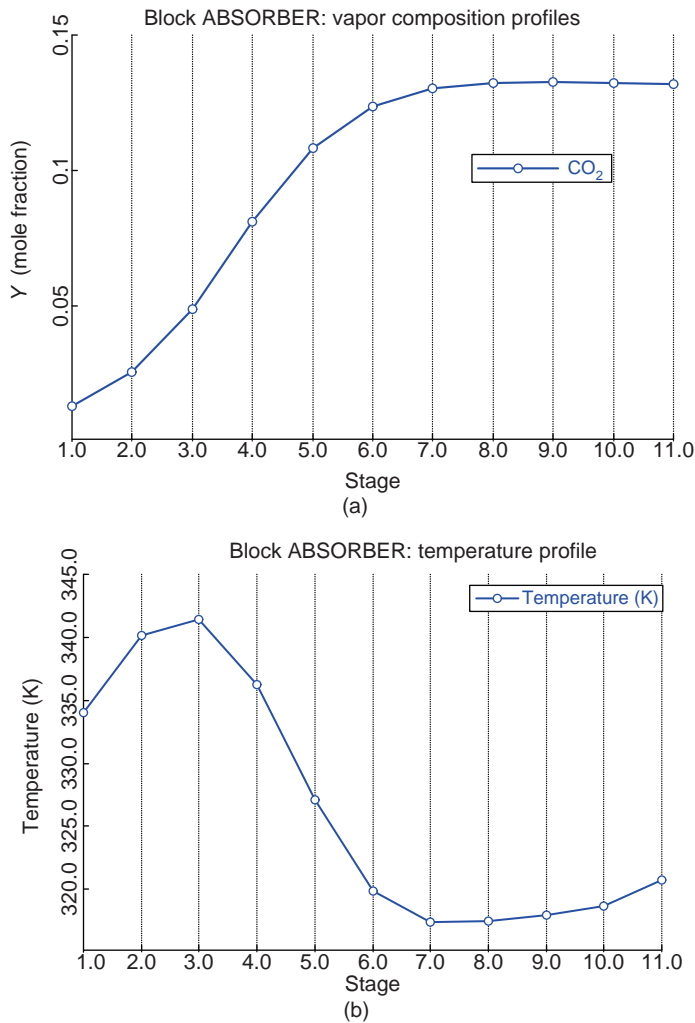


Figure 14.7 (a) Absorber CO₂ vapor composition profile. (b) Absorber temperature profile.

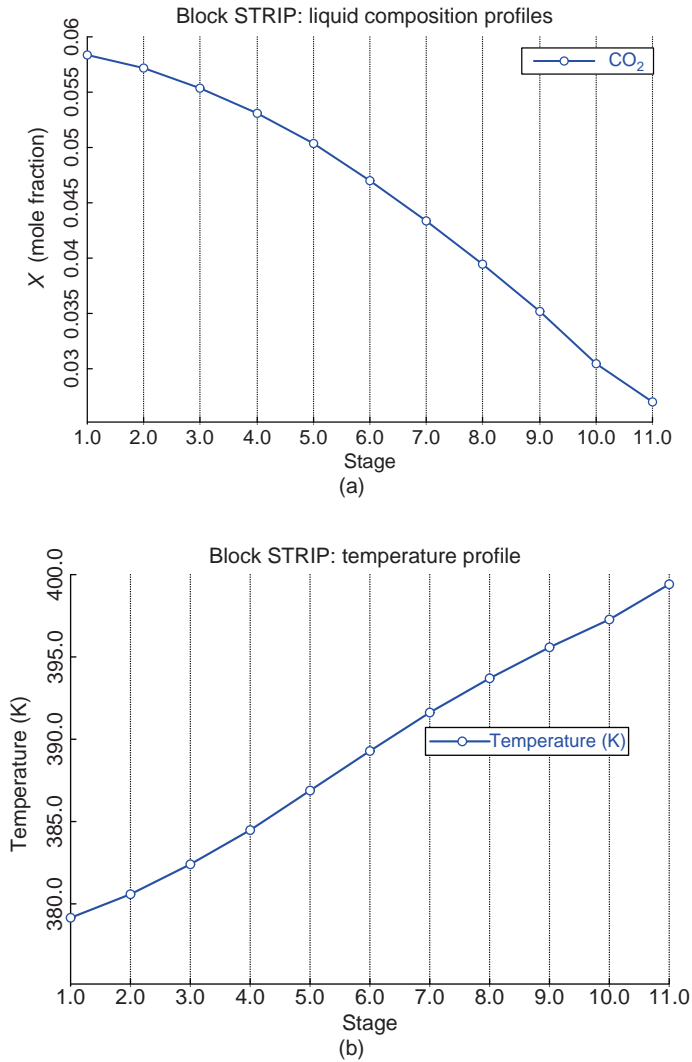


Figure 14.8 (a) Stripper CO₂ liquid composition profile. (b) Stripper temperature profile.

The two other important loops are setting the flow rates of the fresh makeup streams of water and MEA to account for the losses of these components in the off-gas from the absorber and the vapor from the stripper reflux drum.

Several alternative control structures were evaluated. The final recommended plantwide structure is shown in Figure 14.9 and all loops are described in the following

1. Feed gas is flow controlled by adjusting power to the feed compressor.
2. Absorber pressure is controlled by manipulating the valve in the off-gas line.
3. The flow rate of lean solvent to the top of the absorber is ratioed to the feed gas flow rate.

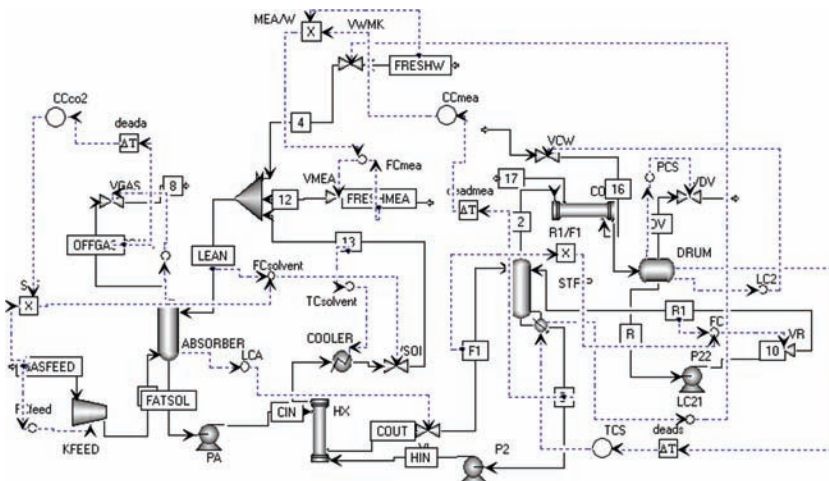


Figure 14.9 Plantwide control structure.

- Carbon dioxide concentration in the off gas is controlled by manipulating the ratio of the lean solvent to the feed gas. A 3 min deadtime is inserted in the loop, and relay-feedback testing and Tyreus–Luyben tuning give $K_C = 0.20$ and $\tau_1 = 26$ min. Note that controller faceplates shown in Figure 14.10 indicate that the lean solvent flow controller “FCsolvent” is “on cascade” with its set point signal coming from a multiplier whose one input is the feed gas flow rate and the other input is the output signal from the CO₂ composition controller “CCco2”.
- Absorber base level is controlled by manipulating the valve in the bottoms line using a proportional $K_C = 2$ controller.

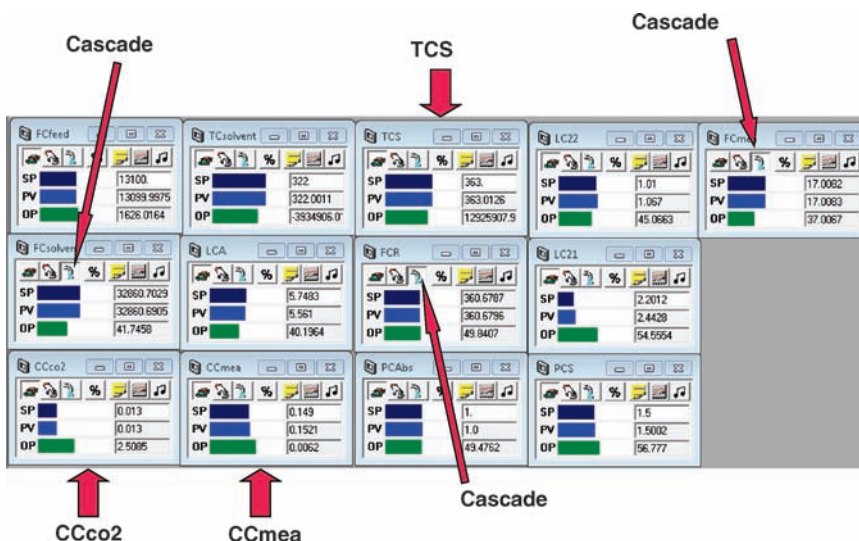


Figure 14.10 Controller faceplates.

6. Pressure in the reflux drum of the stripper is controlled by manipulating the valve in the vapor line from the drum.
7. Liquid level in the stripper reflux drum is controlled by manipulating the valve in the cooling water line to the condenser using a proportional $K_C = 2$ controller.
8. Stripper reflux flow rate is ratioed to stripper feed flow rate using molar flow rates. The reflux flow controller is on cascade with its set point coming from a multiplier whose one input is the stripper feed flow rate and the other is a constant 0.01097 (the steady-state design ratio).
9. Reflux-drum temperature in the stripper is controlled by manipulating stripper reboiler duty (temperature controller “TCS” in Fig. 14.10). A 1 min deadtime is inserted in the loop, and relay-feedback testing and Tyreus–Luyben tuning give $K_C = 2.65$ and $\tau_I = 13.2$ min.
10. The temperature of the lean solvent leaving the cooler is controlled by heat removal.
11. Stripper base level is controlled by manipulating the water makeup flow rate using a proportional $K_C = 2$ reverse-acting controller.
12. The flow rate of the MEA makeup stream is ratioed to the flow rate of the makeup water.
13. The MEA concentration in the lean solvent is controlled by manipulating this ratio (composition controller “CCmea” in Fig. 14.10). Note that controller faceplates shown in Figure 14.10 indicate that the makeup MEA flow controller is “on cascade” with its set point signal coming from the multiplier whose one input is the makeup water flow rate and the other input is the output signal of the MEA composition controller. A 3 min deadtime is inserted in the loop, and relay-feedback testing and Tyreus–Luyben tuning give $K_C = 110$ and $\tau_I = 124$ min.

This last loop is obviously very slow because of the very small MEA makeup flow rate compared to the total amount of MEA in the solvent system. The response using a PI controller displayed a slow long period oscillation. The process behaves almost like a pure integrator in terms of MEA, and using integral action in the controller places two integrators in series, which can lead to oscillatory behavior. This problem was solved by using a proportional controller with $K_C = 50$, which kept the MEA concentration very close to the desired value.

14.1.4 Dynamic Performance

The first issue to examine is the responses of the solvent flow rates throughout the system, the level in the base of the stripper and the flow rate of the makeup water into the system. The base of the stripper is sized to provide 5 min of holdup when half full, based on the large total volumetric flow rate of liquid entering the base ($14.3 \text{ m}^3/\text{min}$). The size of the sump is 5 m in diameter by 10 m in length.

Figure 14.11a gives results for a 20% step increase in the flow rate of feed gas. The solvent-to-feed ratio immediately increases the lean solvent flow rate to the absorber, which rapidly drops the level in the stripper base from 2.4 m down to a minimum level of 1.2 m before coming back up to a steady-state level of 1.8 m. Remember this level controller is proportional only. Makeup water is increased by the base level controller, lining out at a higher flow rate since more makeup water is required at the higher feed flow

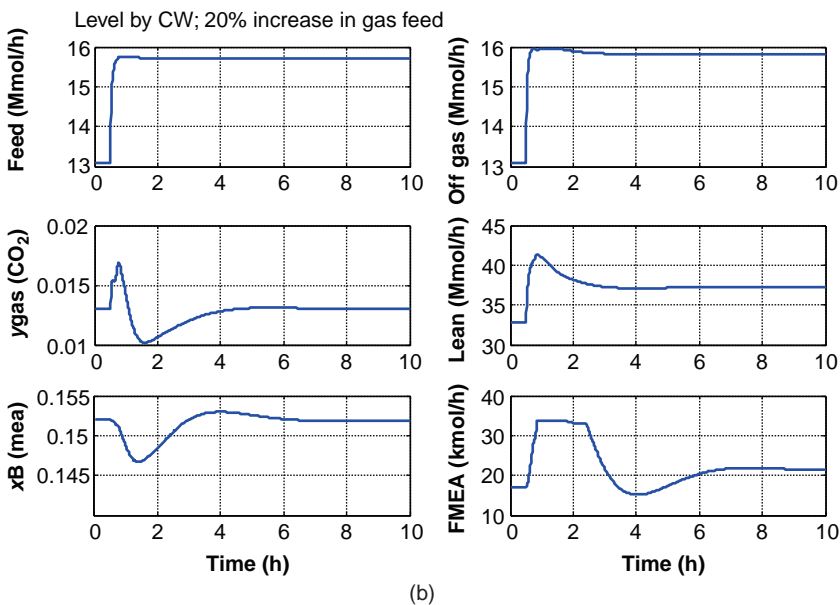
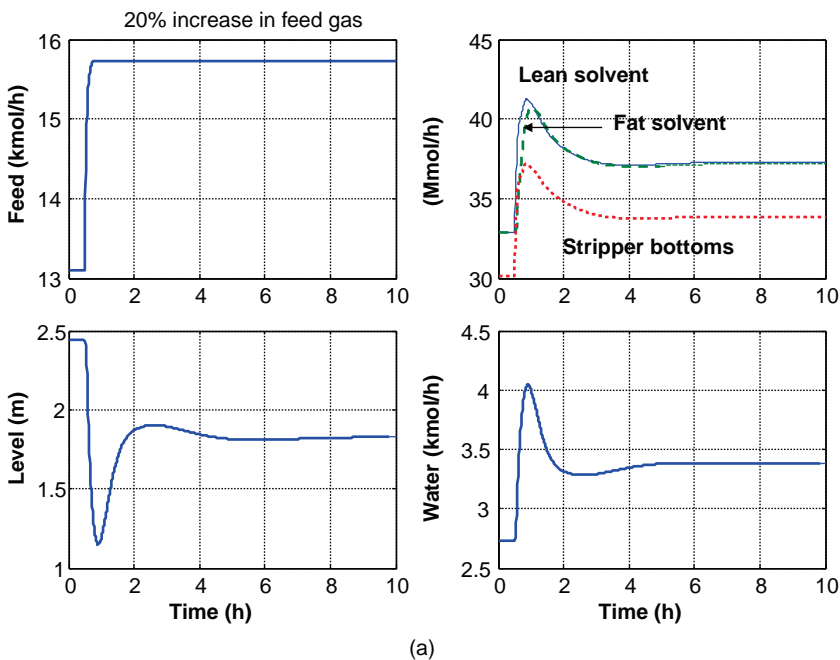


Figure 14.11 (a) 20% increase in feed: solvent loop variables. (b) 20% increase in feed: absorber/stripper variables.

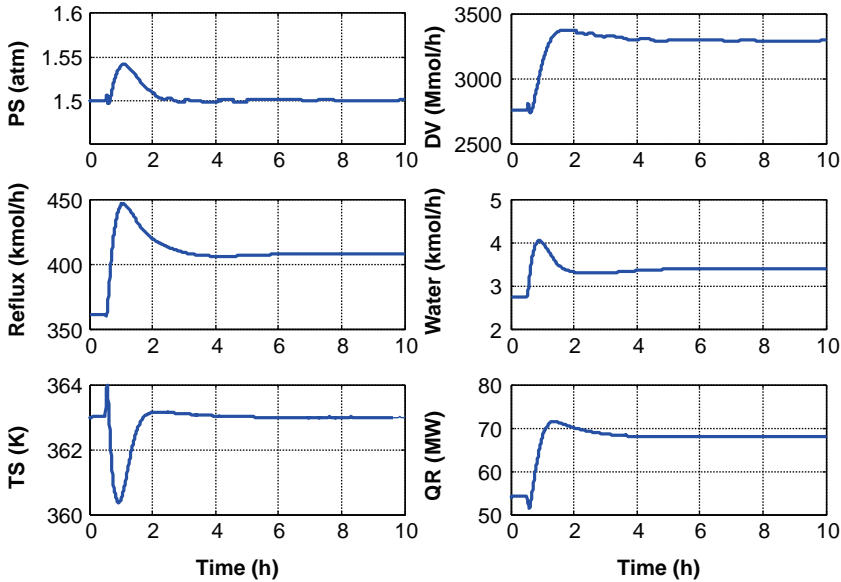


Figure 14.11 (Continued)

rate. These hydraulic results demonstrate that a 5 min design holdup can handle a 20% feed increase without losing the liquid level in the stripper base.

Figure 14.11b gives the responses of other variables. The off-gas product stream from the absorber increases immediately as expected. The carbon dioxide concentration in the off-gas (y_{gas}) goes through a transient, hitting a peak of 1.7 mol% CO_2 , but the composition controller trims up the solvent-to-feed ratio to drive the concentration back to the specification of 1.3 mol% after about 3 h.

As more fresh water is added, more fresh MEA is added due to the ratio. The MEA concentration of the stripper bottoms (x_B) drops slightly, but the MEA concentration controller adjusts the ratio of fresh MEA to fresh water and drives the concentration close to its specification of 15.2 mol% MEA. Stripper vapor product and reflux both increase as expected with increasing feed. The stripper temperature controller shows a peak transient error of about 3 K.

Figure 14.12 gives results for a 20% step decrease in the flow rate of feed gas. The solvent-to-feed ratio immediately decreases the solvent flow rate, which rapidly raises the level in the stripper base up to transient peak of 3.4 m. Makeup water is decreased by the base level controller. So the hydraulics can successfully handle large changes in throughput without violating stripper base level constraints.

Figure 14.13 gives responses of the process when the composition of the feed gas changes. The solid lines are when the CO_2 composition increases (changing from 13.2 to 15.2 mol%) with an appropriate change in the water composition. The dashed lines are when less CO_2 is in the feed (from 13.2 to 11.2 mol%) with an appropriate change in the water composition. More solvent is required as more CO_2 enters the absorber. The vapor product from the stripper naturally increases, as does the stripper reflux.

These results demonstrate that the plantwide control structure developed provides effective regulatory-level control for large disturbances.

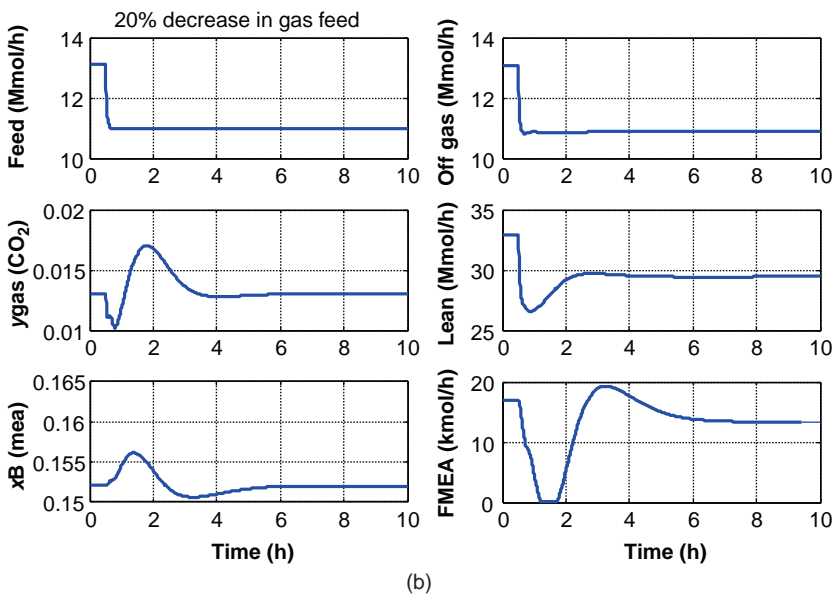
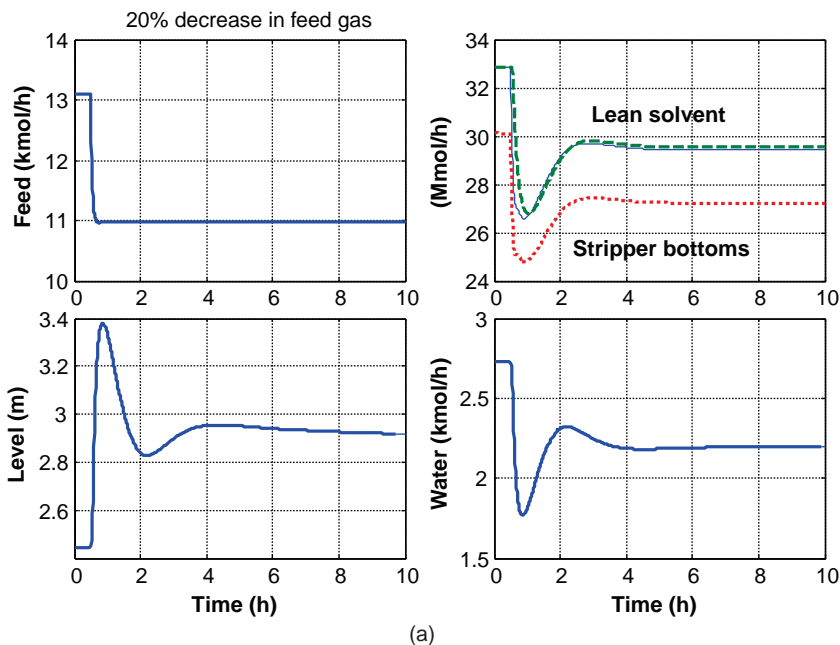


Figure 14.12 (a) 20% decrease in feed: solvent loop variables. (b) 20% decrease in feed: absorber/stripper variables.

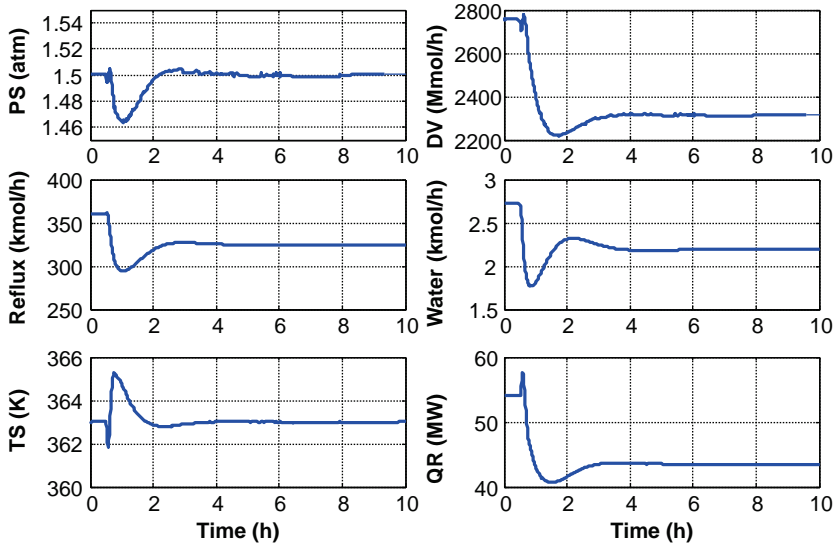


Figure 14.12 (Continued)

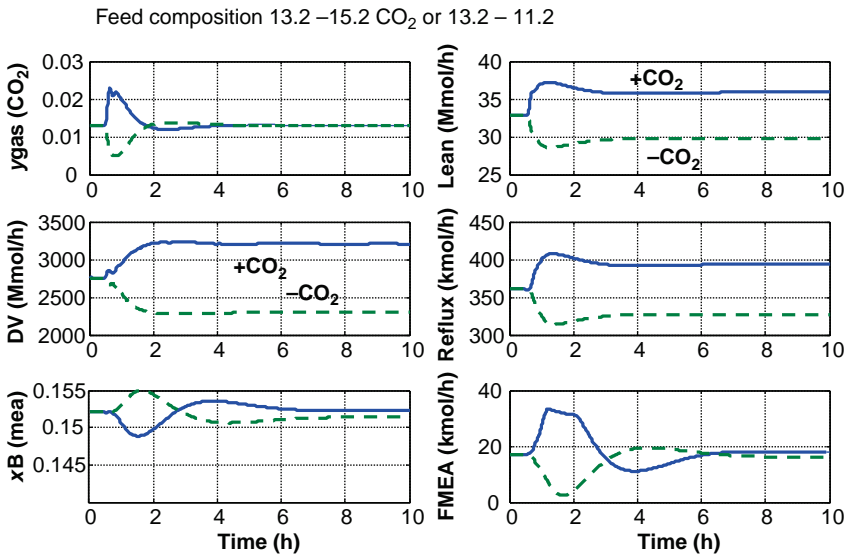


Figure 14.13 Feed composition disturbances.

14.2 CARBON DIOXIDE REMOVAL IN HIGH-PRESSURE IGCC POWER PLANTS

In the previous section, we studied the absorption of carbon dioxide in a low-pressure system in which a reactive amine was used. Now we want to consider a significantly different situation in which the absorber pressure is quite high, in fact high enough so that physical absorption in a suitable solvent is effective.

The numerical example considered is an IGCC power plant that generates 773 MW of total electric power. The system is based on a paper by Robinson and Luyben.²

The process has two parallel high-temperature and high-pressure gasifier vessels. A coal/water slurry is pumped into the partial oxidation zone in the vessels along with a high-purity oxygen stream. The gasifiers operate at 800 psia and 2500 °F in the combustion zone. The synthesis gas produced is a mixture of mostly carbon monoxide, carbon dioxide, and hydrogen. After cooling by generating high-pressure steam and quenching with water, most of the carbon monoxide is “shifted” to carbon dioxide and more hydrogen in two adiabatic water-gas shift reactors in series that operate at different inlet temperatures. The gas leaving these reactors is about 36 mol% carbon dioxide and 60 mol% hydrogen, with very little nitrogen to dilute the gas and make carbon capture difficult.

Figure 14.14 gives the flowsheet of the absorber/stripper unit. The absorber off-gas is rich in hydrogen and is fed to a combustion turbine to generate electrical power.

The physical absorption solvent consists of a mixture of dimethyl ethers of polyethylene glycol of the formula $\text{CH}_3\text{O}(\text{C}_2\text{H}_4\text{O})_x\text{CH}_3$ where x is between 3 and 9. In the Aspen Plus component library, the heaviest dimethyl ether of polyethylene glycol is triethylene glycol (TEG). Although in reality the solvent is a mixture of many different polyethylene glycols with very little water, a reasonable mixture of 89 wt% TEG and the rest water is used as the solvent for these simulations. We label this compound “DME–DEG.” It can be found by specifying the formula $\text{C}_{12}\text{H}_{26}\text{O}_6$ (pentaethylene glycol dimethyl ether: Chemical Abstract Number 1191-87-3). It has a molecular weight of 266.2 and a normal boiling point of 647 °F.

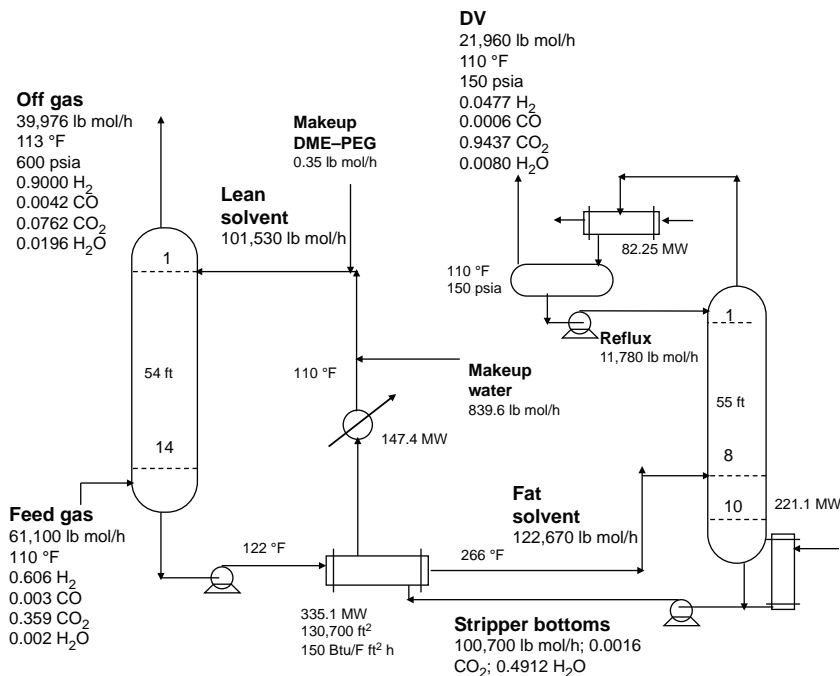


Figure 14.14 Flowsheet of high-pressure CO₂ absorber/stripper process.

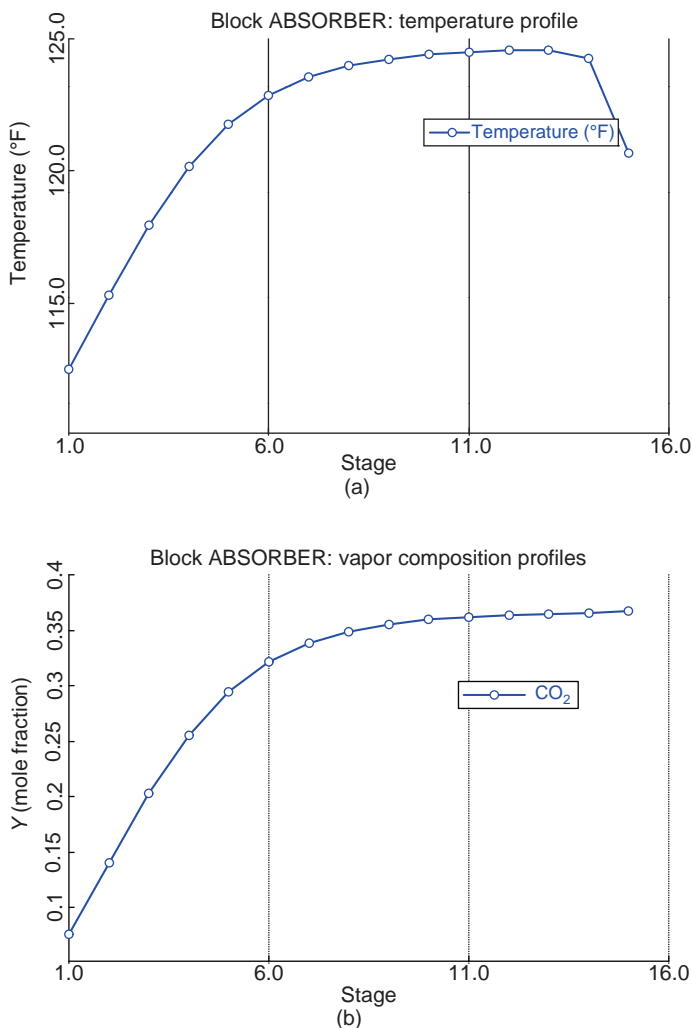


Figure 14.16 (a) Absorber temperature profile. (b) Absorber CO₂ vapor composition profile.

that it would take days or weeks for the solvent makeup flow rate to affect the solvent (DME-PEG) concentration in the system.

On the other hand, the flow rate of water makeup does affect the solvent concentration. If the water coming into the system is larger than the water being lost by the system, the solvent concentration slowly decreases over a several hour period. The change in solvent concentration can affect the rate of CO₂ absorption. Therefore, the water balance cannot be too far off. This is achieved by using a proportional level controller on the base of the stripper that manipulates the flow rate of the fresh makeup water. The gain of this controller, set at the usual $K_C = 2$ used for smooth average level control, is effective in not letting the solvent composition change too much.

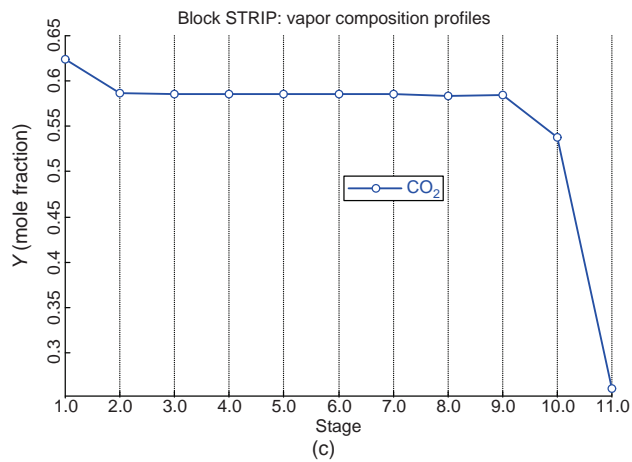
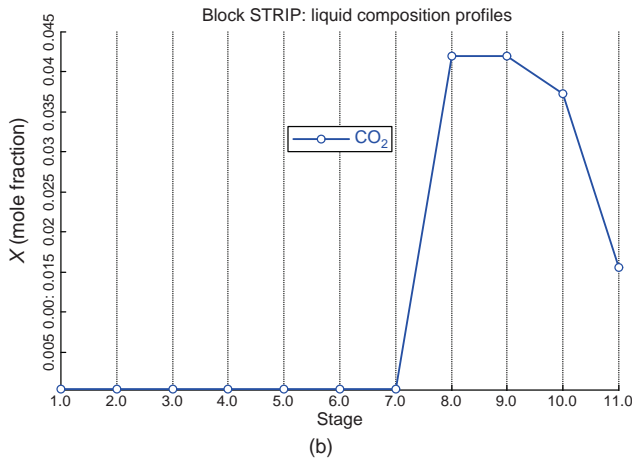
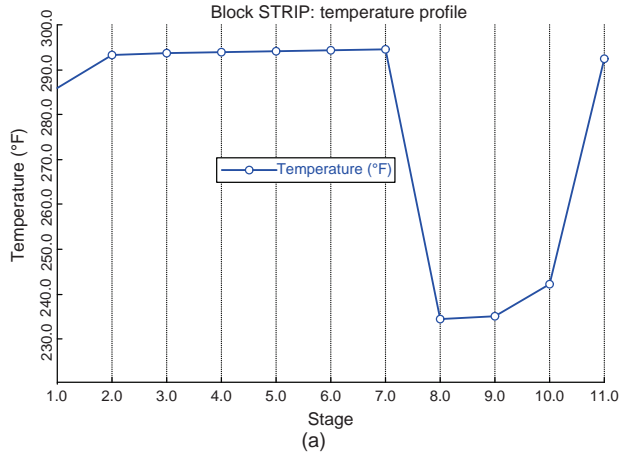


Figure 14.17 (a) Stripper temperature profile. (b) Stripper CO₂ liquid composition profile. (c) Stripper CO₂ vapor composition profile.

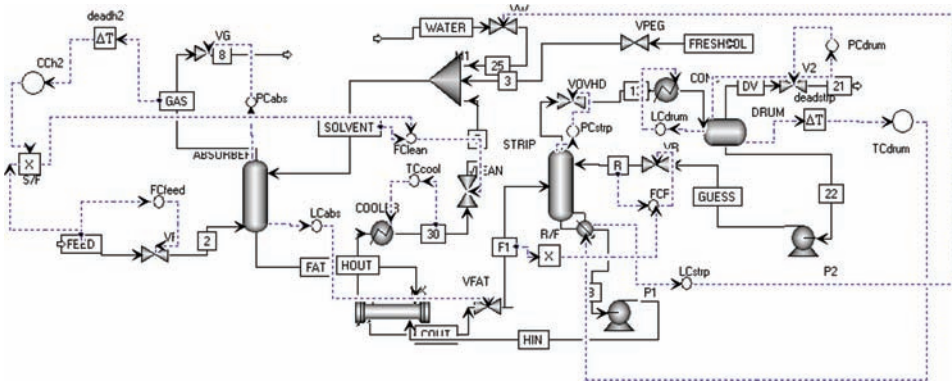


Figure 14.18 Plantwide control structure for high-pressure CO₂ capture.

Each loop in the plantwide control structure is listed and described below. Figure 14.18 shows the Aspen Dynamics implementation of the control structure. Figure 14.19 shows the controller faceplates.

1. Feed gas is flow controlled.
2. Absorber pressure is controlled by manipulating the valve in the off-gas line.
3. The flow rate of lean solvent to the top of the absorber is ratioed to the feed gas flow rate.
4. Hydrogen concentration in the off-gas is controlled by manipulating the ratio of the lean solvent the feed gas. A 3 min deadtime is inserted in the loop, and relay-feedback testing and Tyreus–Luyben tuning give $K_C = 0.14$ and $\tau_1 = 63$ min. Note that controller faceplates shown in Figure 14.19 indicate that the lean solvent flow

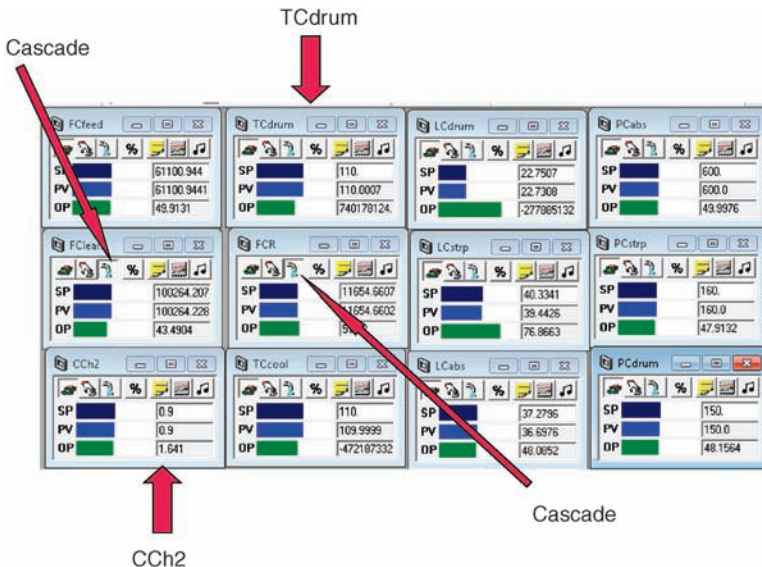


Figure 14.19 Controller faceplates.

controller “FClean” is “on cascade” with its set point signal coming a multiplier whose one input is the feed gas flow rate and the other input is the output signal from the CO₂ composition controller “CCh2”.

5. Absorber base level is controlled by manipulating the valve in the bottoms line using a proportional $K_C = 2$ controller.
6. Pressure in the reflux drum of the stripper is controlled by manipulating the valve in the vapor line from the drum.
7. Liquid level in the stripper reflux drum is controlled by manipulating the heat removal in the condenser using a proportional $K_C = 2$ controller.
8. Stripper reflux flow rate is ratioed to stripper feed flow rate using molar flow rates. The reflux flow controller is on cascade with its set point coming from a multiplier whose one input is the stripper feed flow rate and the other is a constant 0.09603 (the steady-state design ratio).
9. Reflux-drum temperature in the stripper is controlled by manipulating stripper reboiler duty (temperature controller “TCdrum” in Fig. 14.19). A 1 min deadtime is inserted in the loop, and relay-feedback testing and Tyreus–Luyben tuning give $K_C = 0.26$ and $\tau_1 = 66$ min. The set point of this temperature controller is 110 °F. This should be compared to the 363 K (193 °F) used in the low-pressure amine process.
10. The temperature of the lean solvent leaving the cooler is controlled by heat removal.
11. Stripper base level is controlled by manipulating the water makeup flow rate using a proportional $K_C = 2$ reverse-acting controller.
12. A very small constant flow rate of 0.35 lb mol/h of makeup DME–PEG solvent is fed into the process.

There were no dynamic simulation issues experienced in this system. The default Implicit Euler numerical integration algorithm worked well, giving quite short simulation times (1 min of real time to simulate 10 h of process time).

14.2.3 Dynamic Performance

The control effectiveness of the control structure is tested by imposing large disturbances on the process. Figure 14.20 gives results for 20% changes in the flow rate of the feed gas. The solid lines are for 20% increases; the dashed lines are for 20% decreases.

The hydrogen purity of the off-gas is controlled quite close to its specification of 90 mol%. Increasing feed flow rate results in increases in the flow rates of solvent (Lean), makeup water, stripper vapor (DV), stripper reflux, and off-gas. The level in the base of the stripper decreases somewhat.

The temperature of the stripper reflux drum shows very large deviations, particularly for feed decreases. The reboiler heat input is manipulated and eventually brings the temperature back to its specified 110 °F. The CO₂ composition takes a big drop due to the high temperature driving more water overhead. The use of some feed forward control should significantly reduce these dynamic transients. In the current structure, the reflux is ratioed instantaneously to the feed. Inserting a dynamic lags would prevent the reflux from dropping so quickly and help to keep the reflux-drum temperature from rising. In addition,

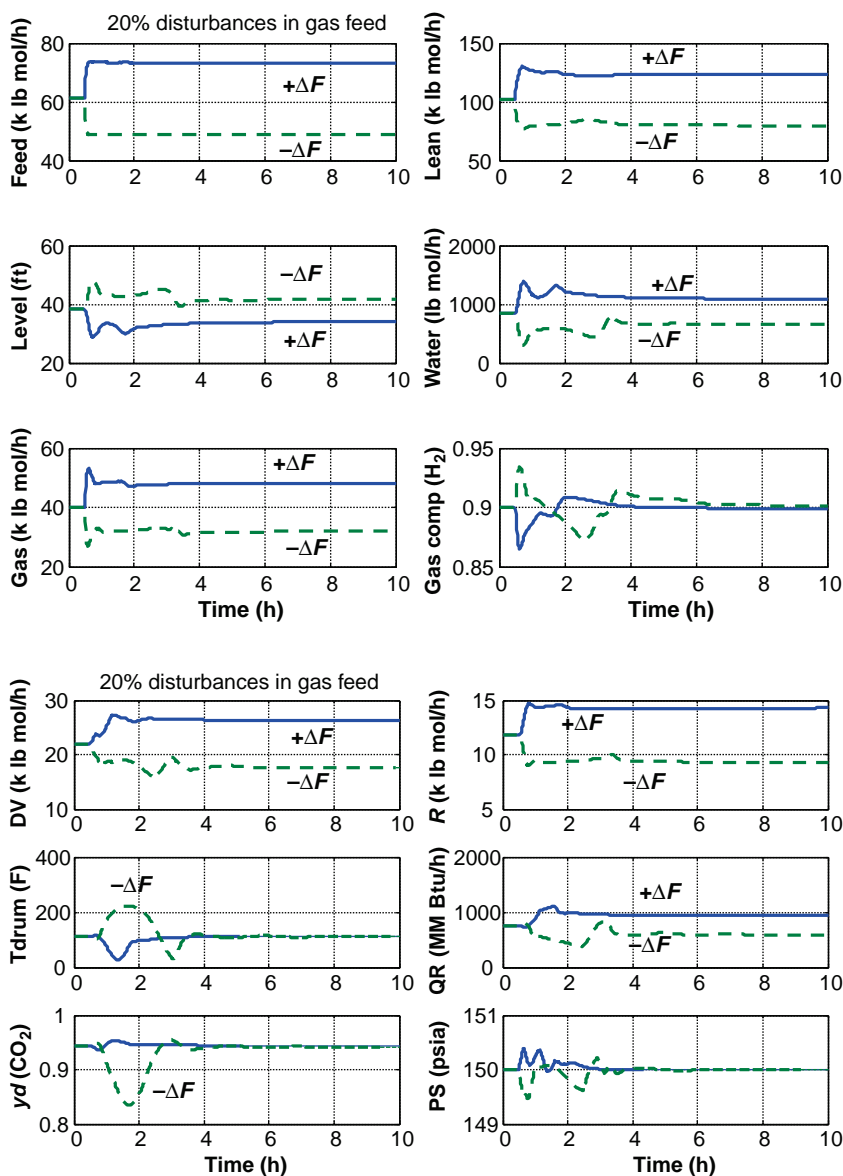


Figure 14.20 20% disturbances in feed flow rate.

the use of a steam-to-feed ratio in the stripper should help to reduce these transient disturbances.

Responses to feed composition disturbances are shown in Figure 14.21. The solid lines are when the feed gas composition is change from 38.9 to 42.9 mol% CO_2 with a corresponding reduction in hydrogen composition. The dashed lines are when the feed gas composition is change from 38.9 to 34.9 mol% CO_2 with a corresponding increase in hydrogen composition. Putting more CO_2 into the process requires an increase in the solvent flow rate. There is less off-gas but more vapor product from the stripper.

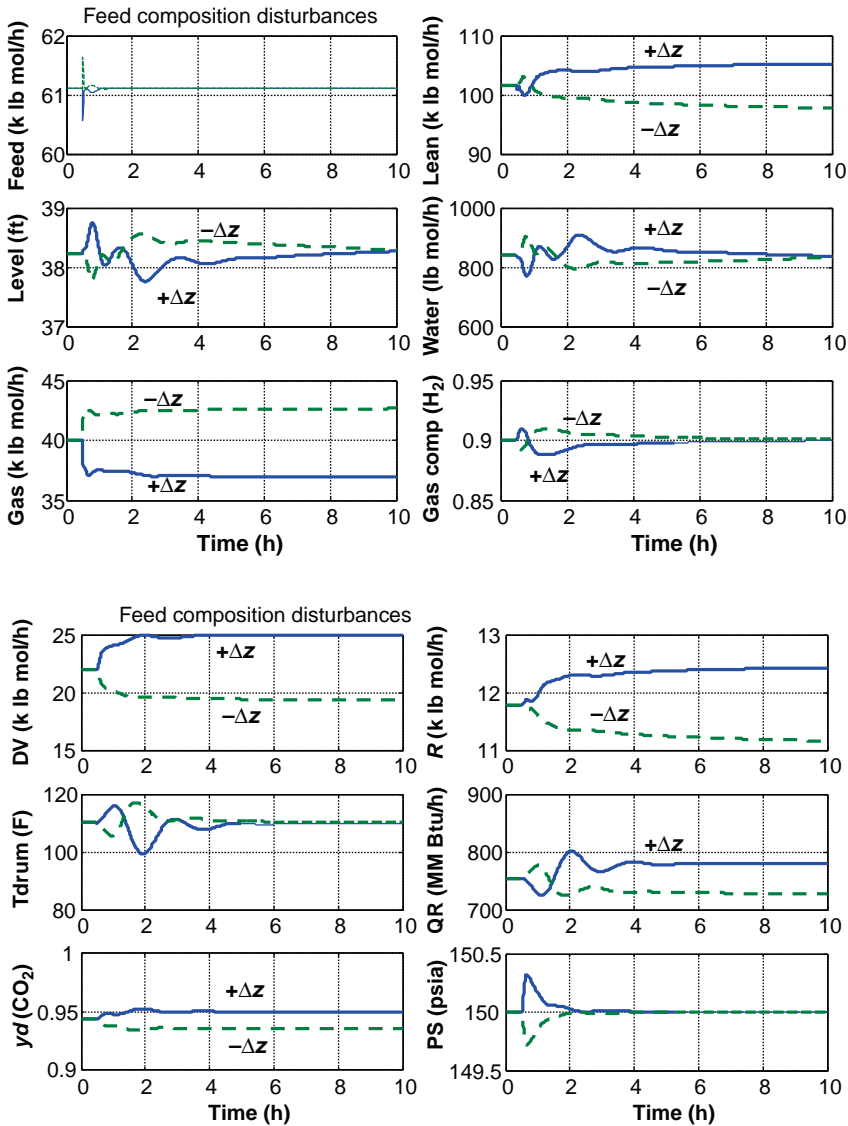


Figure 14.21 Feed composition disturbances.

Notice that the reflux-drum temperature is disturbed much less for these composition disturbances because the feed flow rates to the stripper change much less rapidly.

14.3 CONCLUSIONS

Two carbon-capture processes have been studied in this chapter. Both use a two-column absorber/stripper flowsheet. The low-pressure amine system presents more problems in dynamic simulation than does the high-pressure physical absorption system. The plantwide control structures that are effective for the two systems are quite similar.

REFERENCES

1. U. Desideri and A. Paolucci, Performance modeling of a carbon dioxide removal system for power plants, *Energy Convers. Manage.* **40**, 1899–1915 (1999).
2. P. J. Robinson and W. L. Luyben, Integrated gasification combined cycle dynamic model: H₂S absorption/stripping, water-gas-shift reactors and CO₂ absorption/stripping, *Ind. Eng. Chem. Res.* **49**, 4766–4781 (2010).

DISTILLATION TURNDOWN

Future chemical plants may be required to have much higher flexibility and agility than existing processes in order to be able to handle new hybrid combinations of power and chemical units. An important example is a gasification process producing synthesis gas that can either feed a combustion turbine for the generation of electricity or, during periods of lower power demand, feed a chemical plant. The chemical plant would be designed for the maximum capacity that is associated with periods of minimum electric power demand. But the plant would have to be able to turn down to low throughputs during periods of maximum electric power demand. The 24 h power demand swings in many locations can be a factor of two or more from day to night.

The separations required in many chemical processes are achieved using distillation columns. If the process must operate over a wide range of throughputs, the columns must also have wide rangeability. There are several low-throughput limitations in distillation columns, usually involving hydraulic constraints. The most common is a low limit on vapor flow rate below which weeping can adversely affect tray efficiency and separation. The vapor limit depends on tray design, with valve trays being the most rangeable. Even valve trays lose performance below about 50% of design vapor rates. If the plant throughput must be reduced to 25% of design capacity and the column vapor can only be reduced to 50% of design, a control structure that effectively handles this situation is required. The purpose of this chapter is to explore three alternative control structures for columns with significant turndown requirements.

15.1 INTRODUCTION

Chemical plants developed in the 1900s traditionally operated at fairly fixed capacities. Large tanks for feed material and products were used to handle swings in supply and

demand. Each process in a plant operated essentially independent of other units. Cheap energy meant the design and control complexities of energy integration could not be economically justified.

Rapid increases in energy prices and concerns about carbon dioxide production have resulted in modern chemical flowsheets that are much more complex and interconnected. The future may hold even more need for complex, hybrid processes. A recent paper¹ discusses a flowsheet with a coal gasification plant producing synthesis gas, which is converted into hydrogen for consumption in either a combustion turbine for generation of electric power or in a chemical plant. The gasifier operates at a constant throughput because of its sensitivity to dynamic upsets. The power demand varies from hour-to-hour, so the hydrogen fed to the combustion turbine varies directly with power. The amount of hydrogen and synthesis gas fed to the chemical plant making methanol varies inversely with that fed to the combustion turbine. A chemical plant that can handle large changes in throughput results in a smaller plant for the same swings in power demand. Some of the economics of this type of system have been presented by Cooper.²

Some other future flowsheets are discussed by Forsberg³ who predicted that coupling power and chemical plants may offer significant energy-consumption and carbon-footprint advantages. His vision is a chemical plant capable of converting essentially all of the carbon in its feed (coal or biomass) into liquid transportation fuels by using nuclear power to generate the hydrogen needed to convert coal (hydrogen-to-carbon ratio of 1) into liquid fuel (hydrogen-to-carbon ratio of 2). Forsberg states that “this will imply major changes in process flowsheets.”

If the chemical plant must operate over a wide range of throughputs, the distillation columns in the plant must be able to turn down to low throughputs. Hydraulic limitations will be unavoidably encountered, so the control structure must be able to avoid these limitations. In this chapter, we assume that the *minimum* vapor rate is the limitation.

The inverse problem was studied by Kanodi and Kaistha⁴ where the objective was to maximize throughput. In this situation, the limitation is a *maximum* vapor flow rate. Several strategies were explored for adjusting the feed flow rate to the column so as to operate at the maximum vapor limitation.

The objective in this chapter is to avoid minimum vapor flow rate limitations. If feed rates to a distillation column are reduced due to a reduction in plant throughput or a diversion of the feed stream to a more economical product (i.e., hydrogen gas to combustion turbine during peak power demand instead of methanol), the distillation control structure needs to be robust enough to handle these disturbances while maintaining product specifications. Three alternative control structures are explored to obtain this objective.

15.2 CONTROL PROBLEM

Many distillation column use reboiler heat input as a primary manipulated variable, usually to control a temperature on an appropriate tray. This means that reboiler heat input is not constrained during normal operation with normal feed flow rates. However, as the feed flow rate to the column is decreased, less vapor boilup is required to achieve the same separation. If the feed drops to the point where the low vapor-boilup limit is encountered, the control structure must change. Three alternative control structures for achieving stable operation at minimum vapor flow rates are discussed in the following.

In the numerical example presented later in this chapter, the normal control structure features standard distillation column control methods.

1. Tray temperature is controlled by reboiler heat input.
2. Reflux is ratioed to feed.
3. Pressure is controlled by condenser heat removal.
4. Reflux-drum level is controlled by distillate flow rate.
5. Base level is controlled by bottoms flow rate.

15.2.1 Two-Temperature Control

Figure 15.1 shows a control structure that uses two temperature controllers operating in parallel. The temperature controller TC1 is the one that manipulates steam to the reboiler under normal operating conditions. The output signal from TC1 is normally the set point signal to the steam flow controller. Note that reboiler duties (GJ/h) are shown in the figure instead of steam flow rates.

A high-selector (HS1) with two inputs is used to prevent the steam flow from dropping below the minimum. One input to the high-selector comes from TC1. The second high-selector input is a fixed signal corresponding to the minimum steam flow rate. So as feed flow rate is reduced and the required steam flow rate decreases, at some point the steam flow controller set point will be limited to its minimum. The TC1 temperature controller will no longer be controlling the tray temperature.

The second temperature controller TC2 manipulates the flow rate of reflux during those periods when steam cannot be used. The TC2 controller has a slightly higher set point than TC1, so during periods of normal operation, it will call for less reflux (since the

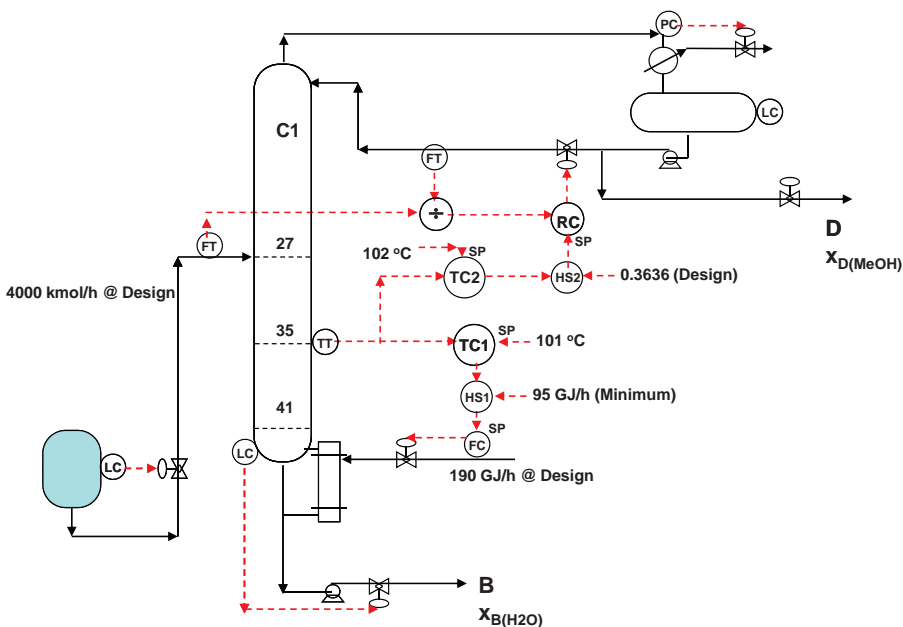


Figure 15.1 Two temperature control.

temperature is lower than its set point), and its output signal will decrease. This output signal is one input to a second high selector HS2. The other input to HS2 is a fixed signal that corresponds to the design reflux-to-feed ratio. During normal operation the output of HS2 is the normal R/F ratio. It is the set point signal of a ratio controller RC whose process variable signal is the actual measured ratio of reflux to feed. A divider block with inputs of measured reflux and feed flow rates is used to generate this ratio.

Thus, this two-temperature control structures uses steam flow rate to control temperature during normal operation but switches to using reflux to control temperature when the minimum steam flow rate limitation is reached.

The dynamic response between steam and a tray temperature is usually fairly fast. The dynamic response between reflux and a tray temperature depends on the number of trays between the top of the column where the reflux enters and the control tray. The further down the column, the slower the dynamics are. The example presented in a later section illustrates that the reflux-to-temperature dynamics are usually much slower than the steam-to-temperature dynamics. This means that tighter temperature control can be attained using steam than using reflux.

So when the minimum steam limit is reached, there may be some deterioration in performance of the temperature loop. But the steam flow rate will never drop below its minimum.

15.2.2 Valve-Position Control

Figure 15.2 shows an alternative control structure in which there is only one temperature controller TC that always manipulates the set point of the steam flow controller. Fairly tight control of temperature is maintained under all feed flow rate conditions.

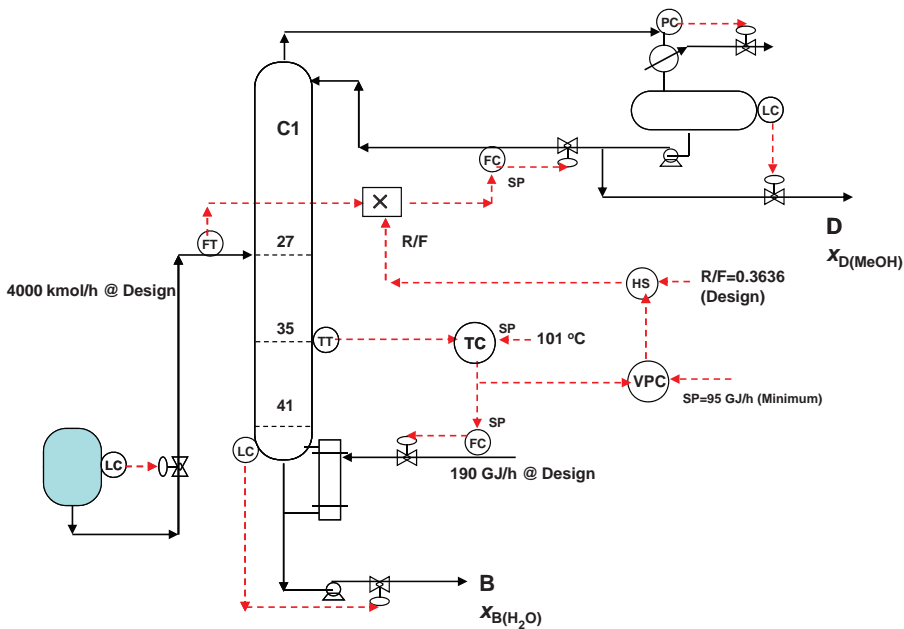


Figure 15.2 VPC control.

However, the steam flow set point signal coming from the TC is also sent as the process variable signal to a “valve-position controller” (VPC) whose set point signal is the minimum steam flow rate. Valve-position control is a type of optimizing control suggested over three decades ago by Shinsky⁵ who used it to achieve floating pressure control in distillation columns. Many other practical applications have been described.⁶

The VPC controller’s job is to change the reflux-to-feed ratio when the steam flow approaches or goes below its minimum flow rate. In normal operation, the set point signal of the VPC controller is lower than the actual steam flow rate, so its output signal is low and is not selected by the high selector HS. The other input to the high selector is the design R/F value. The output of the high selector is sent to a multiplier whose other input is the measured feed flow rate. The output signal from the multiplier is the set point signal of the reflux flow controller. In normal operation the reflux-to-feed ratio is maintained at its design value as feed flow rates change. However, when reboiler duty drops to its minimum, the VPC increases the R/F ratio to try to keep the reboiler duty near its minimum value.

Thus, this control structure will always control temperature with steam and provide good temperature control. However, there is no absolute guarantee that the steam flow rate will never drop below its minimum limitation.

15.2.3 Recycle Control

Figure 15.3 shows a third alternative that avoids the problems of the two control structures discussed above. The steam flow rate can never be less than the minimum, and fairly tight temperature control can be maintained. The basic idea is to use the flow rate of feed to the column to control temperature during periods when plant throughput rates are low. This is achieved by recycling some of the distillate and bottoms streams back to the feed to the column so that the total feed (fresh plus recycles) to the column can be adjusted and is independent of the net feed coming from the upstream unit.

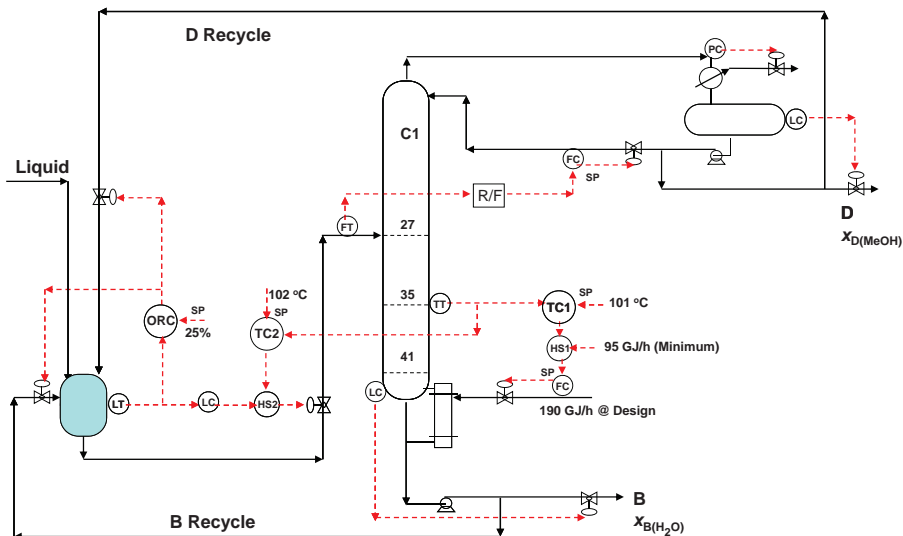


Figure 15.3 Recycle control.

Controlling a temperature in the lower section of the column using reflux results in less tight temperature control than using steam because the effect of reflux flow takes some time to be felt on the lower trays due to inherent hydraulic lags. However, the hydraulic lags between the liquid feed and these lower trays are smaller. Therefore, we would expect better temperature using feed than using reflux. The numerical example presented in the next section demonstrates that this is indeed true.

It should be recognized that implementing this control structure will require some piping changes, and pump heads may need to be modified. However, the improvement in dynamic performance may well justify these modifications.

As shown in Figure 15.3, there are two temperature controllers operating in parallel with TC1 manipulating steam during normal operation and having a low limit on the steam set point using the high selector HS1. The second temperature controller TC2 can manipulate the feed flow rate to the column using the high selector HS2. This selector has two inputs. One is the output signal from the upstream level controller, which normally positions the control valve in the feed line. The other input to HS2 is output signal from TC2, which sends out a signal that increases as the tray temperature increases (direct acting) so that more feed is introduced to the column when the steam flow rate is fixed at its minimum and TC1 can no longer maintain temperature.

During these periods of low throughput when the feed valve is controlling temperature, the liquid level in the upstream tank must be controlled using some other manipulated variables. The tank level transmitter output signal is fed to an override controller (ORC). The set point of this proportional controller is fixed at 25% of tank level, so that its output signal begins to increase (reverse action) when the level gets low. The output of ORC positions control valves in the two recycle lines (distillate and bottoms) that send liquid back to the upstream tank.

The dynamic responses of these three control structures are compared using a numerical example discussed in the next section. Dynamic simulations are performed using Aspen Dynamics.

15.3 PROCESS STUDIED

The numerical example is taken from a paper⁷ that studied the design and control of a methanol process. The distillation column in this process separates methanol and water. The flowsheet of the entire process is shown in Figure 15.4. Feed to the column comes from a flash drum operating at 2 bar. The column operates at 1 bar and has 42 stages. Aspen notation is used with the reflux drum being Stage 1. A reflux ratio of 0.407 gives high-purity distillate (98.9 mol% methanol) and bottoms (99.99 mol% water). The design feed flow rate to the column is 4000 kmol/h. Feed stage is 27. Reflux and feed are saturated liquids at their corresponding pressures and compositions. A small vent stream from the top of the reflux drum removes the small amount of inert present in the feed from the flash drum.

The design value of reboiler heat input is 190 GJ/h when the feed flow rate is at the design value of 4000 kmol/h. A minimum reboiler duty of 95 GJ/h is assumed in this study.

Figure 15.5 gives the temperature profile in the column at design feed flow rate conditions. Stage 35 is selected as the temperature control tray. Note that the reflux must come down 34 trays to affect this temperature. Column feed has to come down only 8 trays, so we expect the dynamics between feed and Stage 35 temperature to be faster than the dynamics between reflux and Stage 35 temperature.

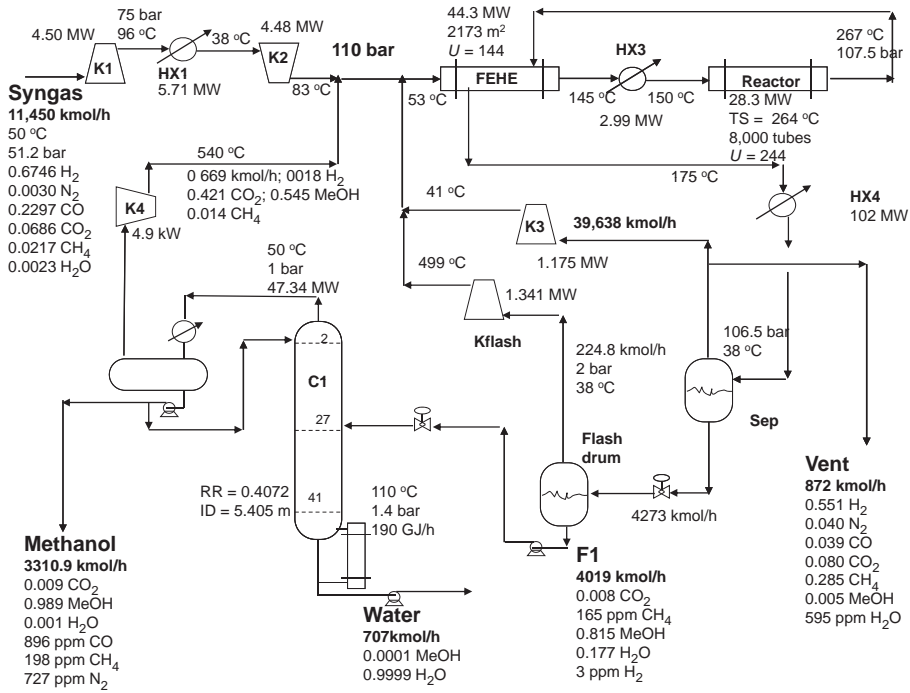


Figure 15.4 Methanol flowsheet.

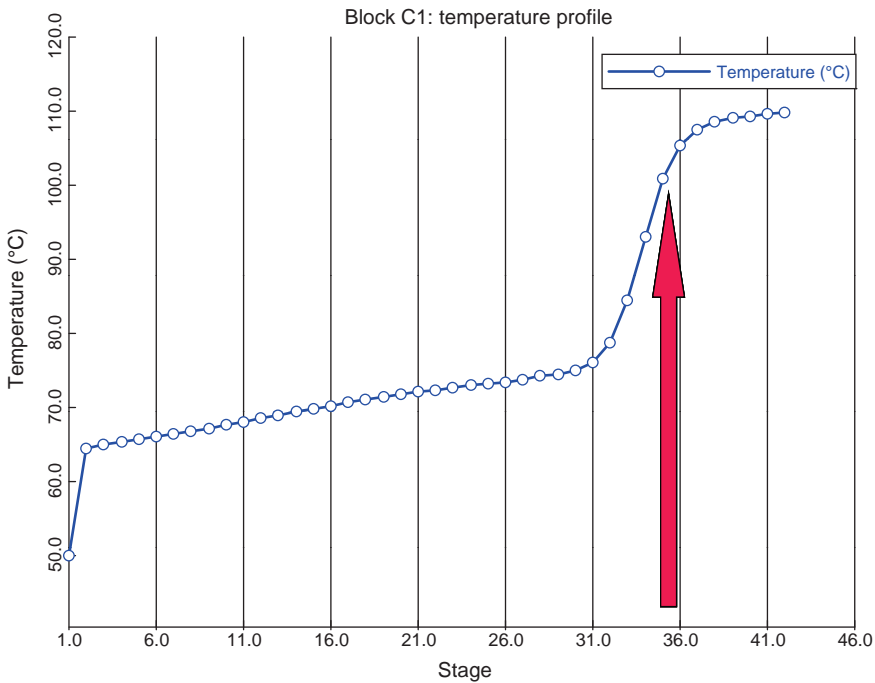


Figure 15.5 Column temperature profile.

The disturbances imposed on the column are ramp and step functions up and down from the design feed flow rate of 4000 kmol/h. For the ramp disturbances, starting from the normal feed flow rate at time equal zero, the feed is ramped down over a 6 h period to 1500 kmol/h, which is a turndown to 37% of design. This feed flow rate is held constant until time equal 12 h. Then the feed flow rate is ramped up over a 6 h period to 4000 kmol/h and held constant for 6 h. This disturbance is intended to approximate the summertime hour-to-hour swings in electric power demand that inversely affect the amounts of hydrogen and synthesis gas that are fed to the methanol process. Time zero in these disturbances represents the beginning of the increase in power demand, perhaps 9 in the morning. Power demand increases for 6 h and holds steady until 9 in the evening. Feed to the column is at its lowest level during this high-ambient temperature period. Then power demand begins to drop off as air conditioning loads drop. By 3:00 am the power demand is at its lowest level and the throughput of the methanol plant is at its highest level and remains there until 9:00 am.

Ramp functions can be implemented in Aspen Dynamics by setting up a “task” that changes a variable over a period of time. The variable must be a “fixed” variable (in the notation of Aspen Dynamics). We want to ramp the set point of the feed flow controller, so the controller must be placed on “cascade” and the variable that is ramped is “FC.SPRemote.” Figure 15.6 gives the two Aspen Dynamics tasks used to ramp up and then ramp down the flow controller set point. Both tasks are edited, compiled, and activated.

(a) Ramp down task (run at time = 0.1)

```

Text Editor - Editing rampdown *
Task rampdown
Runs At 0.1
Ramp {FC.SPRemote,1500,6};
End

```

(b) Ramp up task (run at time = 12)

```

Text Editor - Editing rampup *
Task rampup // <Trigger>
Runs At 12
Ramp {FC.SPRemote,4000,6};
End

```

Figure 15.6 Tasks for ramping set point of flow controller. (a) Ramp down task (run at time = 0.1). (b) Ramp up task (run at time = 12).

15.4 DYNAMIC PERFORMANCE FOR RAMP DISTURBANCES

The ramp disturbances are imposed on the process using each of the three control structures. The temperature and valve-position controllers are tuned by running relay-feedback tests. Deadtimes of 1 min are used in these loops. Temperature controller TC1 is tuned at the normal design feed flow rate (4000 kmol/h), and Tyreus–Luyben tuning give $K_C = 1.37$ and $\tau_I = 9.2$ min.

The TC2 temperature controller is tuned at the low-flow conditions since this is where it is active. Ziegler–Nichols tuning is used so that the tightest possible temperature control is achieved. Base and reflux-drum level controllers are proportional with $K_C = 2$.

15.4.1 Two-Temperature Control

At low feed flow rates, reflux is manipulated to control temperature in this control structure through the R/F ratio controller. The tuning of the TC2 temperature controller gives $K_C = 1.53$ and $\tau_I = 31$ min. Notice that the integral time is much larger, even using Ziegler–Nichols tuning, than the integral time found in the reboiler-temperature loop. The dynamic hydraulic lag between reflux fed to Stage 2 and temperature on Stage 35 is quite significant.

Figure 15.7a gives the response of the process with the two-temperature control structure. The upper left graph shows how the feed flow rate ramps up and down over the 24 h period. The upper right shows how the reflux changes. For the first 5 h, the RC controller reduces the reflux to maintain the design R/F ratio of 0.3636 kg/kg. At time equal 5 h, the reboiler heat input limitation is encountered (95 GJ/h), which is set at 50% of the design value. The middle left graph shows that the temperature T35 begins to rise above the 101 °C set point of TC1, so the TC2 controller starts to increase the R/F ratio. It takes about 4 h for the reflux to climb from 21 to 50 mg/h, and the temperature is above the TC2 set point of 102 °C for almost 3 h before the temperature is driven to the desired value. This is due to the large integral time in the TC2 controller (31 min). The distillate methanol purity undergoes a dynamic drop to about 98.7 mol% methanol. This fairly small disturbance may be adequate, but as we demonstrate later, it is somewhat larger than the product purity disturbances produced by the other control structures. Bottoms purity is high throughout the period. Figure 15.7b shows the various control signals from the controllers and selectors. The units of reflux flow rate are “mg/h” (10^6 g/h).

Notice that the TC1 controller does not hold the T35 temperature at 101 °C during the period when the feed is ramping down or up. A PI controller will produce offset when subjected to a ramp disturbance. This offset occurs in all control structures during the ramp load disturbances. This offset problem could be reduced by using a lag-compensated PI controller⁸ for TC1.

In this numerical example, the temperature control tray is located in the lower section of the column, which results in slow dynamics between temperature and reflux. In other columns where the temperature control tray is high in the column, the use of reflux for temperature control should work better than in this example. The phase of the feed stream would also affect the dynamics between feed flow rate and tray temperature. A liquid feed is used in the numerical example, so it affects temperature below the feed tray fairly quickly. If the feed were vapor, it would not affect temperatures below the feed tray as quickly, but would affect temperatures above the feed tray very quickly.

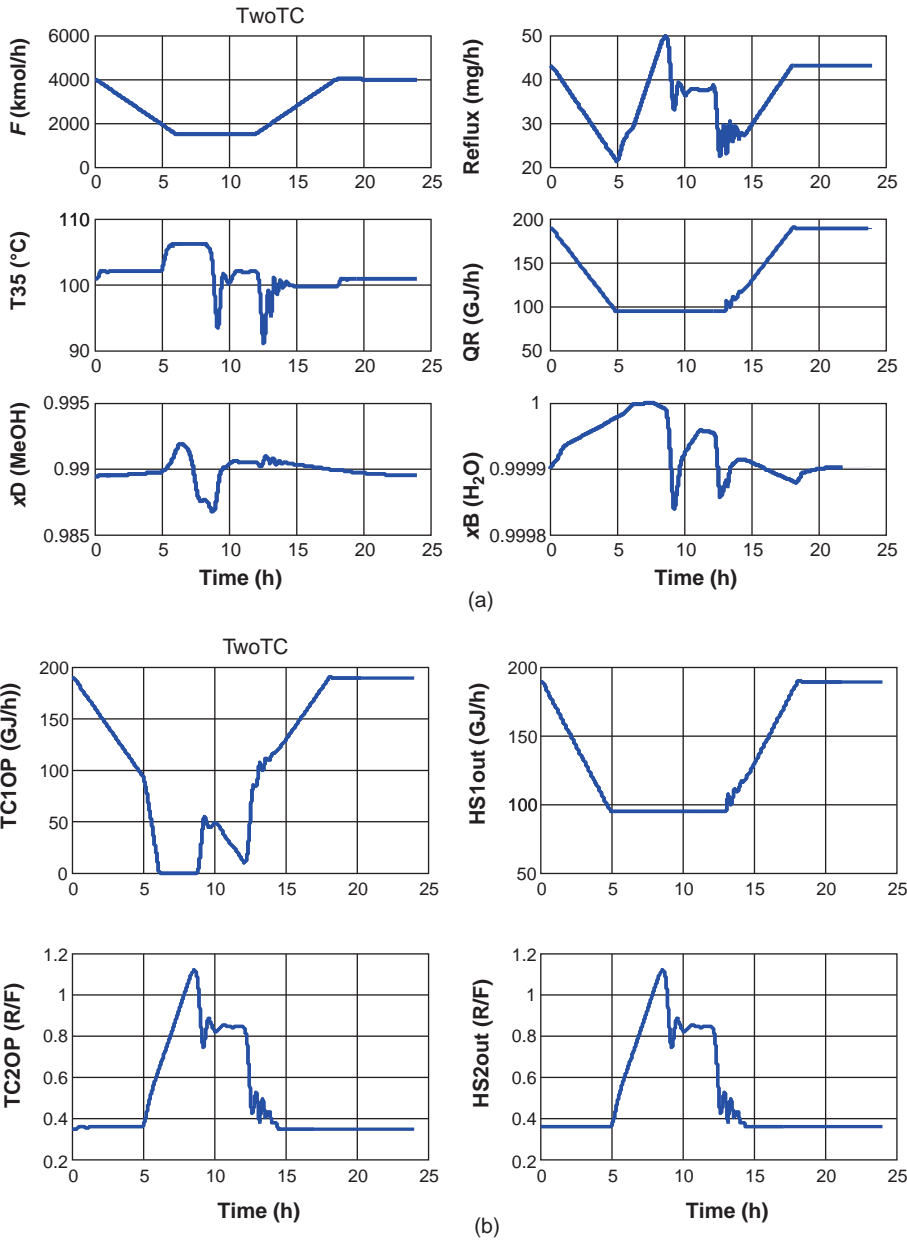


Figure 15.7 (a) Two-temperature ramp results. (b) Two temperature control signals.

15.4.2 VPC Control

Temperature is controlled by manipulating reboiler duty at all times with this structure, so tight temperature control is expected. Figure 15.8 confirms this expectation. The second graph on the left shows how the temperature on Stage 35 (T35) varies as the ramp disturbances in feed flow rate enter the system. A comparison with Figure 15.7a shows that the dynamic deviations in T35 are smaller using the VPC structure than those observed in

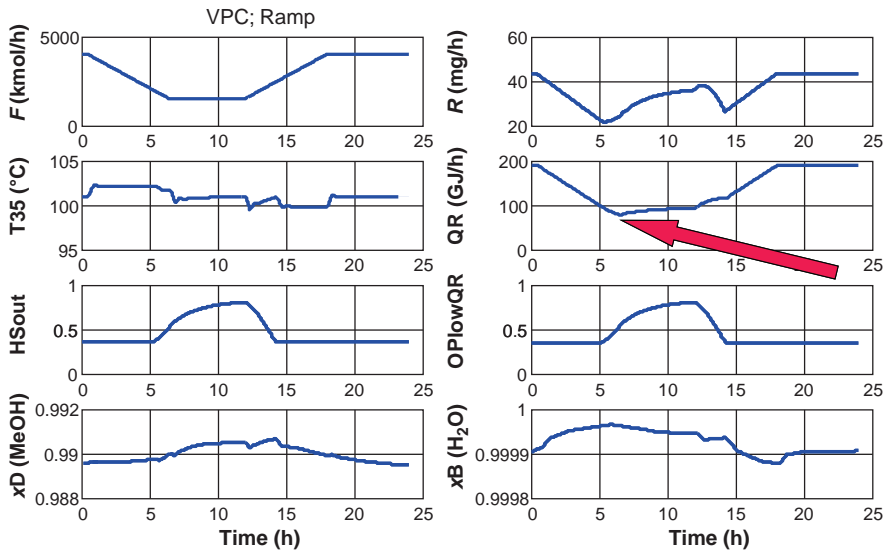


Figure 15.8 VPC control ramp disturbances.

the two-temperature control structure. In the VPC structure the TC1 controller has an integral time of 9.2 min, using conservative Tyreus–Luyben tuning. In the two-temperature control structure, the TC2 controller has an integral time of 20 min, using the aggressive Ziegler–Nichols tuning.

However, notice in the second graph on the right in Figure 15.8 that the reboiler heat input QR is not exactly limited to the 95 GJ/h constraint. It dips slightly below at about 6 h, but is gradually brought back up as the VPC controller increases reflux flow rate (top right graph). To guarantee that the constraint is not violated, the set point of the VPC controller could be raised, but this would mean that reboiler heat input would not be at its minimum during low-throughput operation and some energy would be wasted.

15.4.3 Recycle Control

Temperature is controlled by manipulating column feed during periods of low throughput with this structure. The TC2 controller has an integral time of 6.5 min, which is much smaller than that used in the two-temperature control structure (20 min). Temperature control should be tighter.

Figure 15.9 gives result for the ramp disturbance with the recycle control structure in service. The ramp disturbances are imposed on the stream (Liq in top left graph) entering the upstream flash drum, not on the feed to the column. The column feed (third left graph) ramps down for a little over 5 h until the minimum reboiler duty limitation is reached. Thereafter, the TC2 controller uses the feed flow rate to control temperature. The feed to the column only drops to 2045 kmol/h, not to 1500 kmol/h because recycle of some of the distillate and bottoms is coming back to the flash drum. As shown in Figure 15.9b, these two recycle flows (Drecycle and Brecycle) are normally zero but are brought up by the ORC controller to hold the liquid level in the upstream flash drum when the feed to the column is being used by TC2 to control temperature. Tight temperature control is achieved throughout the whole period of the ramp disturbances.

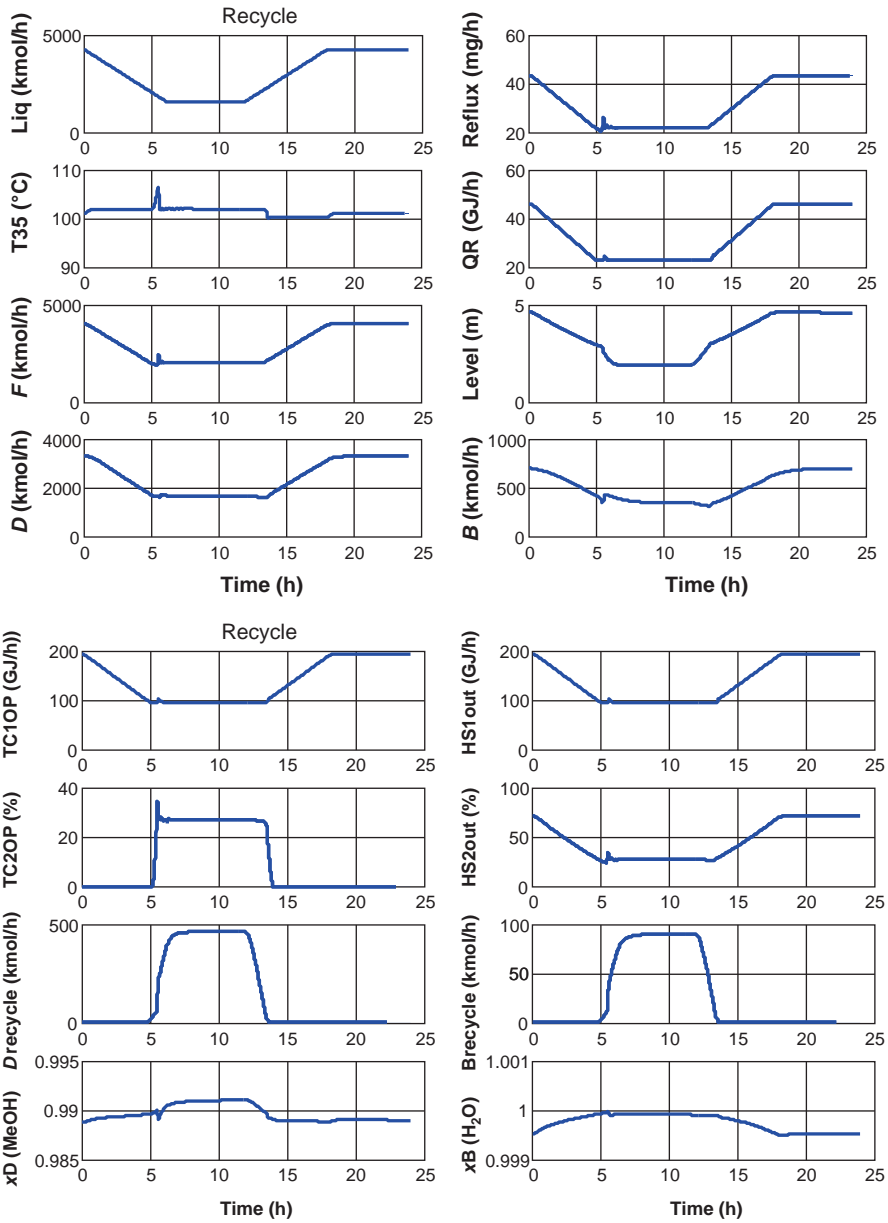


Figure 15.9 Recycle ramp results.

15.4.4 Comparison

Figure 15.10 gives a direct comparison of the performances of the three control structures for the same ramp disturbances. The dashed lines are for the two-temperature control structure. The dotted lines are for the VPC control structure. The solid lines are for the recycle control structure.

The worst temperature control and the largest deviations in methanol product purity (x_D) occur with the two-temperature control structure. The VPC control structure does not

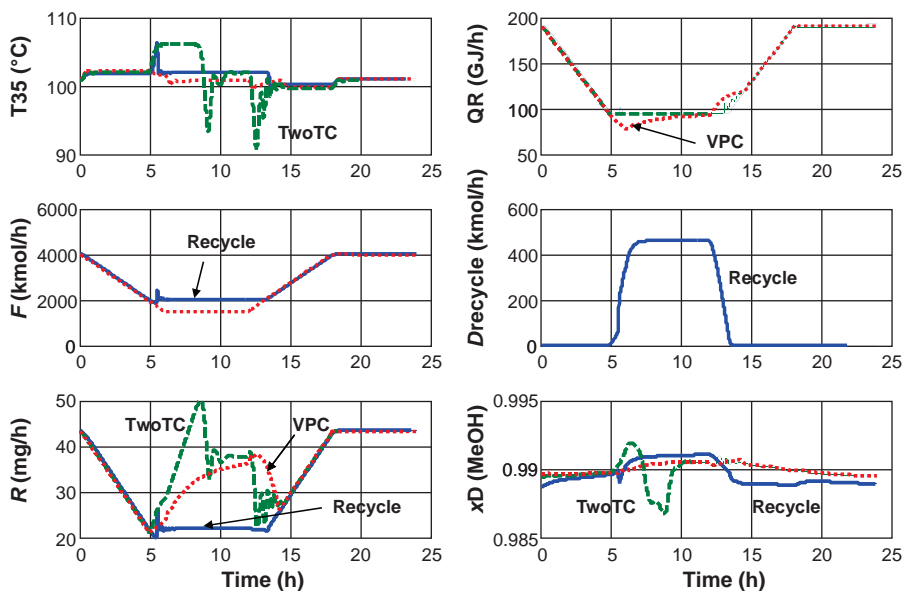


Figure 15.10 Comparison of alternative control structures: ramp disturbances.

keep the reboiler duty from dipping below the minimum limitation. The recycle control structure provides the best control of temperature and product compositions.

15.5 DYNAMIC PERFORMANCE FOR STEP DISTURBANCES

The ramp disturbances used in the previous section are gradual, and therefore do not test the performance of the control structure as severely as step disturbances. Figures 15.11–15.15 give results for a series of step changes in throughput for the three control structures. Feed flow rates are dropped from 4000 to 3000 kmol/h at time equal 0.5 h, then to 2000 kmol/h at 4 h, and finally to 1500 kmol/h at 8 h.

15.5.1 Two-Temperature Control

Figure 15.11 gives results for the two-temperature control structure. When feed flow rate is dropped to 3000 kmol/h, temperature rises up to 105 °C, and the TC1 controller decreases reboiler heat input. At the same time, the R/F ratio controller produces an immediate drop in reflux flow rate. However, the rise in temperature causes the TC2 controller to increase reflux temporarily until the temperature is returned to the TC1 set point of 101 °C.

A similar sequence of events occurs at 4 h when feed is dropped to 2000 kmol/h. The reboiler duty is just at its lower limit, so reflux is beginning to be used to control temperature. At 8 h when the feed is dropped to 1500 kmol/h, reboiler duty is fixed, so temperature is controlled only by the TC2 controller with reflux. The temperature jumps to 107 °C, but the large integral time in TC2 results in a long ramping up of its output signal to bring up reflux and drive temperature back to its set point. This ramp is about 5 h in duration

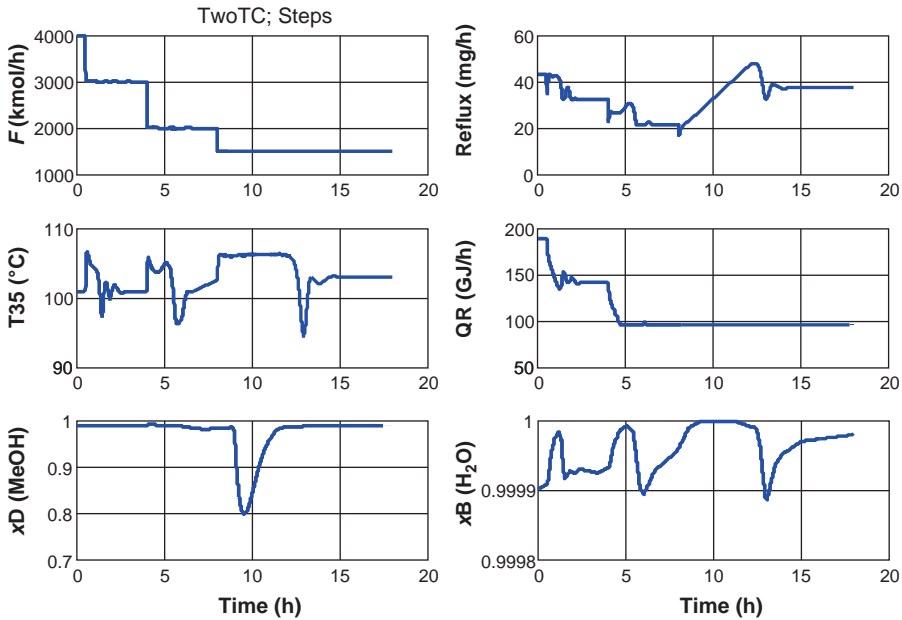


Figure 15.11 Two-temperature control step disturbances.

during which there is a drastic drop in distillate purity all the way down to 80 mol% methanol. This is a clear demonstration that the two-temperature control structure does not provide tight temperature control for large rapid disturbances.

15.5.2 VPC Control

Figure 15.12 gives results for the VPC control structure. Tight temperature control is maintained throughout the 18 h period of large step disturbances, but there are brief periods when reboiler duty drops somewhat below its minimum limitation.

Notice that there is a small drop in distillate purity about 2 h after the first step decrease in feed. This is due to the temperature controller TC1 taking about 1 h to bring the temperature back to its set point after the large step disturbance. This illustrates the inherent slow dynamics of compositions at the fairly high-purity levels occurring in this process.

The second step from 3000 to 2000 kmol/h produces a similar but larger transient drop in distillate purity all the way down to 91 mol% methanol, which occurs about 1.5 h after the disturbance. By the time the third drop in feed occurs, the VPC controller has increased reflux flow rate enough to filter the effects on distillate purity.

So the VPC control structure is better than the two-temperature control structure but has some performance issues.

15.5.3 Recycle Control

Figure 15.13 gives results for the recycle control structure. The top left graph shows the series of step changes in the liquid feed to the upstream flash tank. The third left graph

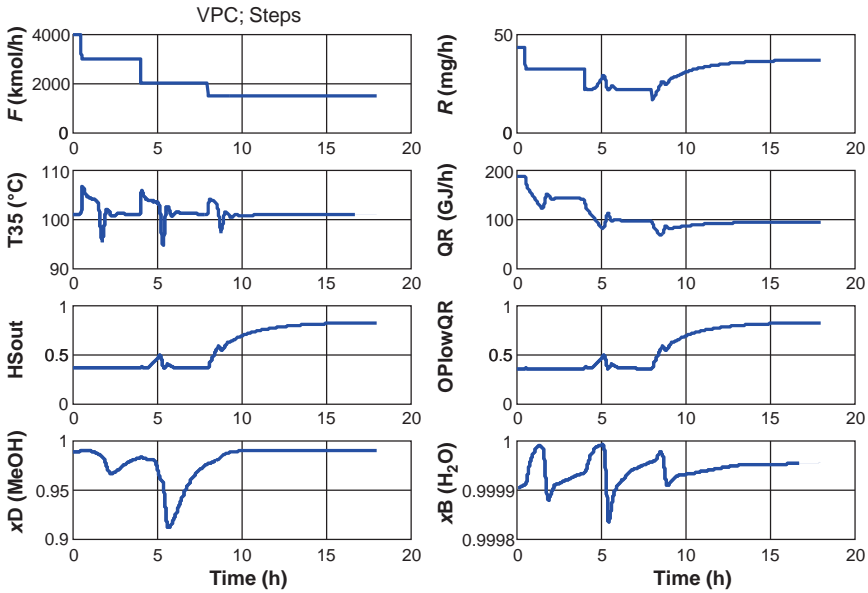


Figure 15.12 VPC control step disturbances.

shows the feed flow rate to the column that directly follows the liquid disturbance for the first two steps. Shortly, after the second step, reboiler duty reaches its minimum, and the TC2 controller takes over temperature control by manipulating feed to the column. Liquid level in the flash drum has dropped to the set point of the ORC. When the third step decrease occurs, the level drops further so recycles of distillate and bottoms begin so as to

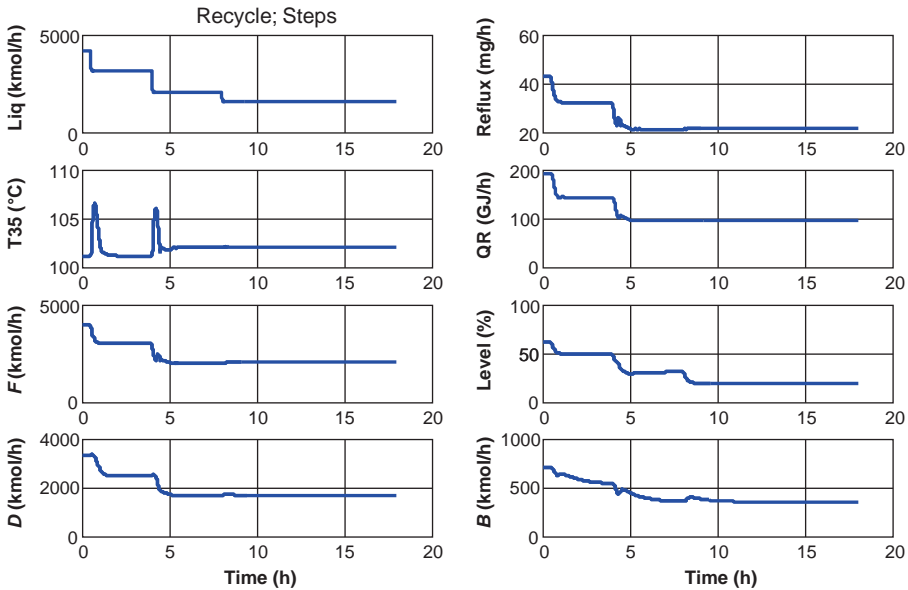


Figure 15.13 Recycle control step disturbances.

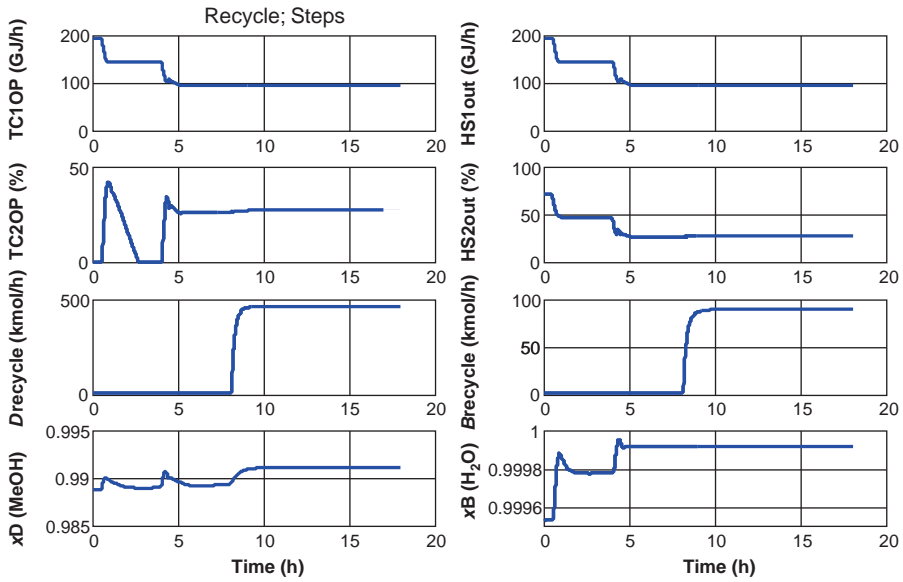


Figure 15.13 (Continued)

hold the level. Stage 35 temperature is hardly disturbed at all because the feed to the column does not change. Distillate and bottoms purities are held very close to or above their specifications.

Figure 15.14 provides a direct comparison among the three control structures. The superiority of the recycle control structure is clearly demonstrated. Notice that the other

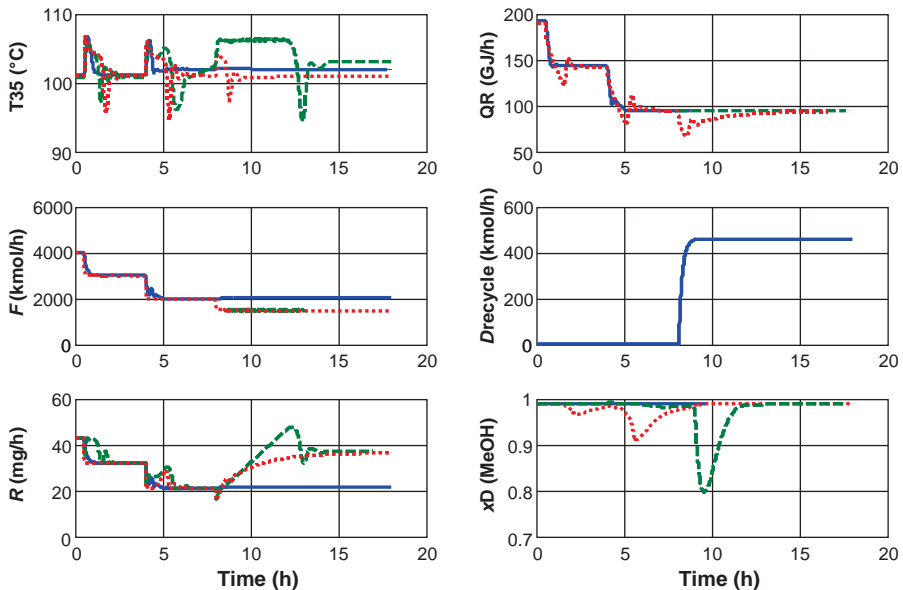


Figure 15.14 Comparison of alternative control structure: step disturbances.

two control structures require large changes in reflux flow rate to control temperature for the fixed reboiler duty and fixed (low) feed flow rate. The recycle control structure changes the feed to control temperature, so the reflux flow rate is much smaller and only changes as a ratio to the feed to the column, which does not decrease as much as the process throughput because of the recycles.

15.6 OTHER CONTROL STRUCTURES

There are other control structures that one might think would work, but the two discussed below are shown to not handle the turndown problem.

15.6.1 No Temperature Control

We might simply low-limit the steam and use no temperature control, erroneously expecting that this would provide overpurification at low loads. This structure is fatally flawed.

Simply putting a low limiter on the reboiler steam flow rate and using *no* temperature control will *not* result overpurification. Remember that the control structure in use has a reflux-to-feed ratio. As the feed flow rate drops below 50% of design, the reflux also will drop below 50% of design. If the reboiler heat input is fixed at the 50% level, the lower reflux and the same vapor boilup will produce an increase in distillate. This will drive water up the column and send the distillate off-spec.

To demonstrate this problem, steady-state runs are made under conditions where the feed flow rate and the reflux flow rate are 49% of design, but the reboiler duty is varied from 49% to 50% of design. At 49% reboiler duty, the distillate water impurity is the specified 0.1 mol%. If reboiler duty is raised to 49.5%, distillate composition is 1.3 mol% water. At the set low-limit of 50% reboiler duty, distillate composition is 2.6 mol% water. These results demonstrate the strong effect of changes in the distillate flow rate that occur when the reflux is 49% of design while the reboiler duty is 50% of design. Simply low-limiting the steam will *not* work.

Some other modification of the control structure would also be necessary. We might think of also limiting the reflux flow rate or switching to a reflux ratio scheme. However, neither of these will work in the face of feed composition disturbances. Control of some temperature or composition in the column *must* be included in any workable control structure (Second Law of Distillation Control).

To demonstrate this problem, steady-state runs are made at the 100% design level. Feed and reflux flow rate and reboiler duty are fixed at their 100% levels. There is no temperature control. Then very small changes are made in feed composition. Table 15.1 gives results when methanol feed composition is decreased from its design value of 81.53 mol% methanol with corresponding increases in water concentration. There is no temperature control. The effect on bottoms impurity is striking.

Notice that both Stage 35 and Stage 10 temperatures are higher at the lower feed methanol concentrations than at design conditions. We would expect more water to come overhead and adversely affect distillate purity. However, Table 15.1 shows that distillate unexpectedly gets more pure, and bottoms purity gets worse. Methanol impurity in the bottoms increases from 0.01 to 2.1 mol%. This counter-intuitive result can be explained by looking at the distillate flow rate. It is decreasing more than the molar flow rate of methanol

TABLE 15.1 Effect of Feed Composition on Bottoms Purity with Fixed Reflux and Reboiler Duty

Feed Composition (mol% Methanol)	Distillate (kmol/h ⁻¹)	Bottoms Composition (mol% Methanol)	Distillate Composition (ppm Water)	Temperature Stage 35 (°C)	Temperature Stage 10 (°C)
81.53 (Design)	3311.5	0.0001	1000	101	67.72
81.33	3309.5	0.300	3	109.06	69.16
81.13	3308.1	0.500	2	109.15	70.11
80.57	3304.5	1.10	0.001	108.20	71.81
79.57	3297.6	2.10	Trace	108.26	73.08

entering the column is decreasing. This means that more methanol must drop out the bottom of the column. Remember that reboiler heat input is fixed. Since the latent heat of vaporization of water is larger than that of methanol, less vapor goes overhead. Since reflux flow rate is fixed, distillate flow rate decreases.

These quantitative examples demonstrate that the strategy of simply low-limiting the steam flow rate will *not* provide effective control during column turndown operation. Control of some temperature or composition in the column *must* be included in any workable control structure. The three control structures considered in this paper all control Stage 35 temperature with either reboiler duty or reflux. Not controlling temperature does *not* work.

15.6.2 Dual Temperature Control

The control structure used in this chapter uses single-end temperature with a reflux-to-feed ratio. If the column were using a dual-temperature control structure, would the turndown problem be inherently solved?

There are two questions associated with this possibility. First, how widely is dual temperature control used? Second, does it really solve the turndown problem?

Concerning the first question, there are many more distillation columns that use single-end temperature control than use dual-temperature control. This is the standard control structure in the methanol/water separation. Using the reflux-to-feed ratio scheme and a single temperature result in energy consumption that is almost the minimum possible by using dual-composition control in the methanol/water system. Instrumentation complexity and loop interaction are avoided. So the structure used in this paper is widely applied in industrial columns.

Concerning the second question, the dual-temperature control structure was tested on this methanol/water column and found to not work.

The basic problem is that there is only one break in the temperature profile (see Fig. 15.5). SVD analysis shows only one stage with a significant U (see Fig. 15.15). There is a very small hump in the U curve at Stage 10, so this stage is selected to be controlled by manipulating the reflux-to-feed ratio.

The two interacting temperature loops are tuned using conventional sequential tuning. The faster of the two loops (Stage 35-to-reboiler duty) is tuned first with the other loop on manual. Then the Stage 10-to-R/F loop is tuned with the first loop on automatic. Relay-feedback tests of this loop show the “shark’s tooth” shape associated

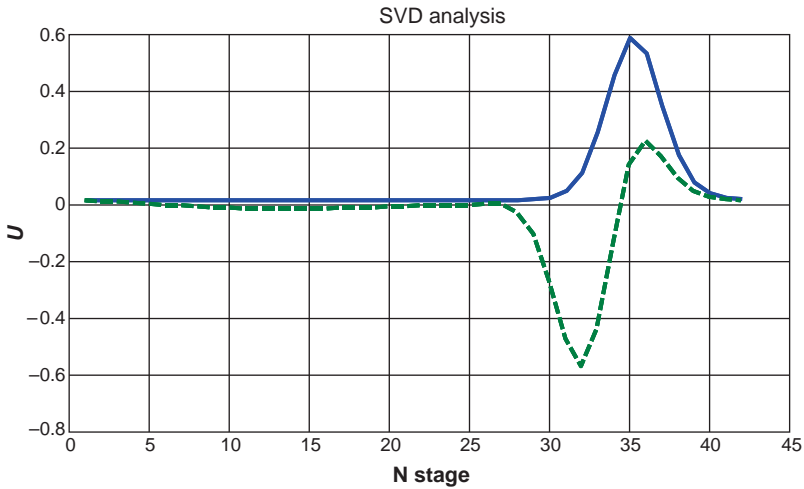


Figure 15.15 Singular-value decomposition results.

with inverse response, which leads to a low gain ($K_C = 0.5$) and a huge integral time ($\tau_I = 195$ min).

The performance of the dual-temperature control structure is shown in Figure 15.16 for the same sequence of step disturbances imposed on the other structures. The distillate purity x_D drops drastically when the reboiler low limit is reached because the reflux cannot be increased quickly enough.

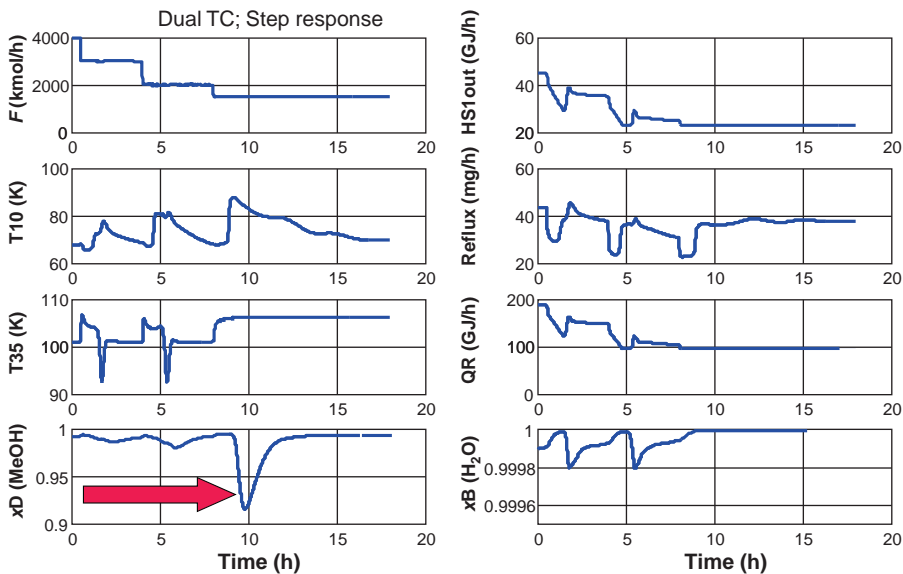


Figure 15.16 Dual temperature control: step responses.

15.7 CONCLUSIONS

Three control structures for handling large turndowns of distillation columns have been studied. The agility requirements of future chemical plants may require large variations in throughputs, which will challenge the control structures used in the process. Since distillation columns must operate inside numerous constraints, most of which are hydraulic, control of distillation columns will present significant challenges under these conditions.

The most effective control structure is one in which the column feed is used to control temperature while recycling products back to the upstream feed unit. This strategy can be applied to multiple column sequences in a plantwide environment.

REFERENCES

1. P. J. Robinson and W. L. Luyben, Integrated gasification combined cycle dynamic model: H₂S absorption/stripping water–gas shift reactors and CO₂ absorption/stripping, *Ind. Eng. Chem. Res.* **49**, 4766–4781 (2010).
2. H. W. Cooper, Producing electricity and chemicals simultaneously, *Chem. Eng. Progr.* **106**, (2), 24–32 (2010).
3. C. Forsberg, Nuclear power: Energy to produce liquid fuels and chemical, *Chem. Eng. Progr.* **106**, (7), 41–44, 50 (2010).
4. R. Kanodi and N. Kaistha, Plantwide control for throughput maximization: A case study, *Ind. Eng. Chem. Res.* **49**, 210–221 (2010).
5. F. G. Shinskey, *Chem. Eng. Progr.* **72**, 73 (1976), and *Chem. Eng. Progr.* **74**, 43 (1978).
6. M. L. Luyben and W. L. Luyben, *Essentials of Process Control*, McGraw-Hill, 1997, p. 126.
7. W. L. Luyben, Design and control of a methanol reactor/column process, *Ind. Eng. Chem. Res.* **49**, 6150–6163 (2010).
8. W. L. Luyben, Fed-batch reactor control using lag compensation and gain scheduling, *Ind. Eng. Chem. Res.* **43**, 4243–4252 (2004).

CHAPTER 16

PRESSURE-COMPENSATED TEMPERATURE CONTROL IN DISTILLATION COLUMNS

Tray temperature control is used in most distillation columns to infer product composition, but changes in pressure on the control tray can adversely affect the estimation of composition. Pressure is typically controlled in the condenser, not on the control tray, so changes in vapor flow rates will change tray pressure due to changes in tray pressure drops. “Pressure-compensated” temperature control was proposed over four decades ago to solve this problem. Measurements of both temperature and pressure on the control tray are used to estimate composition. The method has been qualitatively described in many practical distillation control books, but the author is not aware of any quantitative evaluation of its effectiveness that has appeared in the open literature.

In this chapter, we present a numerical example to illustrate quantitatively the performance of pressure-compensated temperature control. In addition, a simple but accurate method for finding temperature/pressure/composition relationships is described, and the techniques for implementing pressure compensation in Aspen Dynamics are presented.

16.1 INTRODUCTION

The distillation column is probably the most extensively studied unit operation in terms of control. An extensive literature of hundreds of papers and dozens of books has appeared over the last half century discussing methods for controlling distillation columns.

Although the “ideal” control scheme would control the compositions of both products (dual-composition control), in practice most distillation column use temperature control

because composition measurements are expensive and can degrade control due to large deadtimes. In addition, loop interaction issues can arise when two controllers are employed. In the commonly used simple single-end temperature control structure, an appropriate tray is selected whose temperature is maintained by manipulating a suitable input variable. Several methods have been proposed to find the best location of the control tray, but the most frequently used is to select a tray where the temperature changes from tray to tray are large. Temperature is used to infer composition so that the composition profile can be held in the column and product purities maintained close to their specified values in the face of disturbances in feed flow rate and feed composition.

However, a constant temperature of a binary system is not indicative of a constant composition if the pressure varies. If the pressure on the tray where the temperature is being measured changes, the estimation of composition will be incorrect. This pressure will change if the condenser pressure changes or if the pressure drops through the trays change. The former is controlled in most columns, but there are important exceptions where column pressure is variable. Changes in tray pressure drops occur in all columns and with all types of internals when vapor flow rates change, as they must with changes in throughput (and to a lesser extent with changes in feed composition). The problem becomes worse as the location of the control tray moves lower and lower in the column (more trays for pressure drops to change).

The problem was recognized many years ago and solutions were proposed and applied. One solution discussed by Shinsky¹ is to use a differential vapor-pressure transmitter. This device is a differential-pressure cell with one side of the diaphragm open to pressure of the column at the control tray and the other side connected to a bulb inserted on the same tray. The bulb contains liquid with a composition the same as the desired composition on the tray. A zero differential pressure means that the composition on the tray is equal to the desired composition.

A more flexible approach² was documented in 1973 and used measurements of both pressure and temperature to calculate a "pressure-compensated" temperature signal to be controlled. Equation (16.1) shows the relationships among the measured variables (temperature and pressure) and the calculated composition on the tray.

$$\Delta x = \left(\frac{\partial x}{\partial P} \right)_T \Delta P + \left(\frac{\partial x}{\partial T} \right)_P \Delta T \quad (16.1)$$

where the Δ s are changes from design conditions. The first partial derivative is the slope at the desired composition of the saturated liquid line of the plot of composition on the ordinate axis versus pressure on the abscissa at constant temperature (reciprocal of the conventional P_{xy} diagram). The second partial derivative is the slope at the desired composition of the saturated liquid line of the plot of composition on the ordinate axis versus temperature on the abscissa at constant pressure (reciprocal of the conventional T_{xy} diagram). Several other discussions of pressure-compensated temperature control have appeared (Tolliver,³ Rhiel⁴).

The need for pressure compensation becomes very important in systems where pressures can change significantly due to the mode of operation (in addition to pressure drop effects). An important example is when it is desirable to operate the column at minimum pressure to conserve energy by using maximum cooling water flow rate. Column pressure then floats up and down with changes in the cooling-water supply temperature,

which is affected by day-to-night and ambient conditions. Another important application is in heat-integrated columns in which the pressure in the high-pressure column changes to provide the required temperature differential driving force in the condenser/reboiler.⁵

All of these discussions in the literature have been qualitative and descriptive in nature with no quantitative evaluation of the performance of pressure compensation. This chapter attempts to provide such information.

16.2 NUMERICAL EXAMPLE STUDIED

A debutanizer column is considered as a typical case. A mixture of 50 mol% *n*-butane (*n*C4) and 50 mol% *n*-pentane (*n*C5) is separated in a column with 61 stages. The feed flow rate is 100 kmol/h and the feed is introduced on Stage 23 (using the Aspen notation that the condenser is Stage 1). The design specifications are 1 mol% *n*C5 impurity in the distillate and 1 mol% *n*C4 impurity in the bottoms. The reflux-drum pressure is set at 4.5 atm to give a 322 K reflux-drum temperature so that cooling water can be used in the condenser. Figure 16.1 gives the flowsheet with design conditions. The column diameter is 0.7145 m, the reflux ratio is 1.323, and reboiler duty is 0.758 MW.

The tray pressure drop is specified to be 0.1 psi per stage. With a reflux-drum pressure of 4.5 atm and 60 trays in the column, the base pressure is 4.9 atm.

Steady-state simulations are performed in Aspen Plus using Choa–Seader physical properties. Dynamic simulations are performed in Aspen Dynamic using the rigorous *RadFrac* distillation column model.

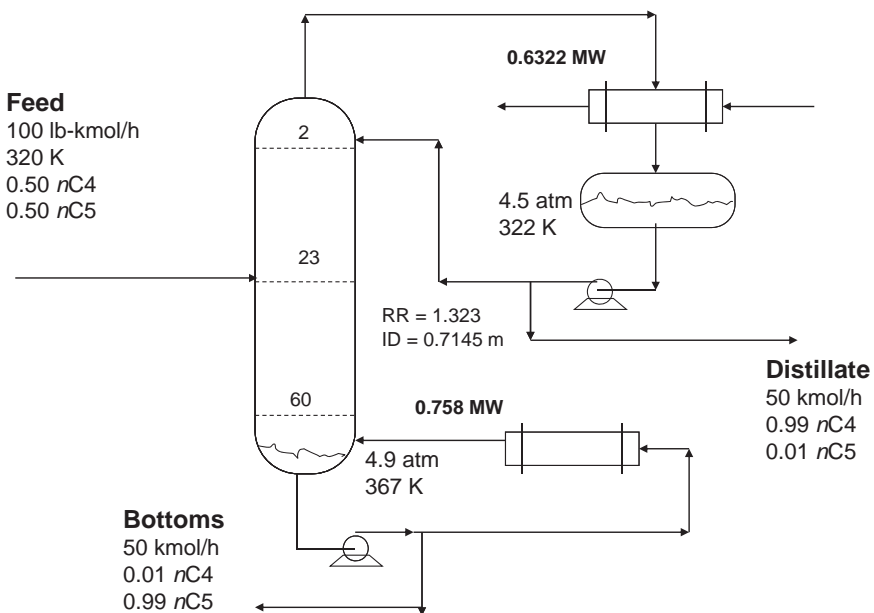


Figure 16.1 Column flowsheet: *n*C4/*n*C5 at 4.5 atm.

16.3 CONVENTIONAL CONTROL STRUCTURE SELECTION

A conventional control system is applied to the column. Feed is flow-controlled. Pressure in the reflux drum is controlled by condenser heat removal. Reflux-drum level is control by manipulating distillate flow rate. Base level is controlled by manipulating bottoms flow rate.

There are two remaining control degrees of freedom. The “ideal” dual-composition control structure would control $nC5$ impurity in the distillate by manipulating reflux flow rate and $nC4$ impurity in the bottoms by manipulating reboiler duty. However, this ideal control structure is the exception not the rule in industrial applications. We usually try to find a more simple control structure in which a “single-end” control scheme provides adequate regulatory control using a suitable tray temperature.

First, we need to recognize that in theory everything scales up and down with throughput. In designing the column, all compositions, temperatures, and pressures throughout the column are exactly the same for any feed flow rate since we normally specify the design pressure drop per tray. Therefore, in theory, any control structure that establishes a flow ratio and holds a single temperature constant will drive the column to a steady state that has the desired product purities for any feed flow rate. The two most commonly applied ratio schemes are holding a constant reflux ratio or holding a constant reflux-to-feed ratio.

However, these ratios do not stay constant when feed composition changes occur. Many of the tray compositions must change also. So the critical disturbance that the control structure must be able to handle is feed composition changes. In some columns, dual-composition control may be needed. In others a more simple structure may be adequate.

To find out if such a simplified structure has any chance of working, we can use the steady-state design simulation to see how reflux flow rate and reflux ratio must change as feed composition change while still achieving the two desired product purities. Two *Design Spec/Vary* functions are used in the Aspen Plus simulation to drive the compositions of the two product streams to their specified values by varying distillate flow rate and reflux ratio.

Table 16.1 illustrates this procedure for the debutanizer example. The design feed composition is 0.5 mole fraction $nC4$ and 0.5 mole fraction $nC5$. The reflux ratio is 1.323 and the reflux-to-feed ratio is 0.6616 (on a molar basis). These values give the desired distillate and bottoms purities (achieved by using two *Design Spec/Vary* functions in Aspen Plus).

Then the feed composition is changed to 0.6 mole fraction $nC4$ and 0.4 mole fraction $nC5$ with the product specification held constant. The required reflux ratio and reflux-to-feed ratio are 1.075 and 0.6471, respectively. Next the feed composition is changed to 0.4 mole fraction $nC4$ and 0.6 mole fraction $nC5$ with the product specification held constant. The required reflux ratio and reflux-to-feed ratio change to 1.665 and 0.6626, respectively. The third and fifth columns in Table 16.1 show the percent changes in the two variables from the design values. Since the changes in the reflux-to-feed ratio are quite small, a single-end control structure may be able to handle feed composition disturbances fairly well.

TABLE 16.1 Feed-Composition Sensitivity

Feed Composition (mol% $nC4$)	Reflux Ratio	Percent Change from Design	Reflux-to-Feed Ratio	Percent Change from Design
40	1.665	+25.8	0.6626	0.20
50 (Design)	1.323	0	0.6616	0
60	1.075	-18.7	0.6471	2.2

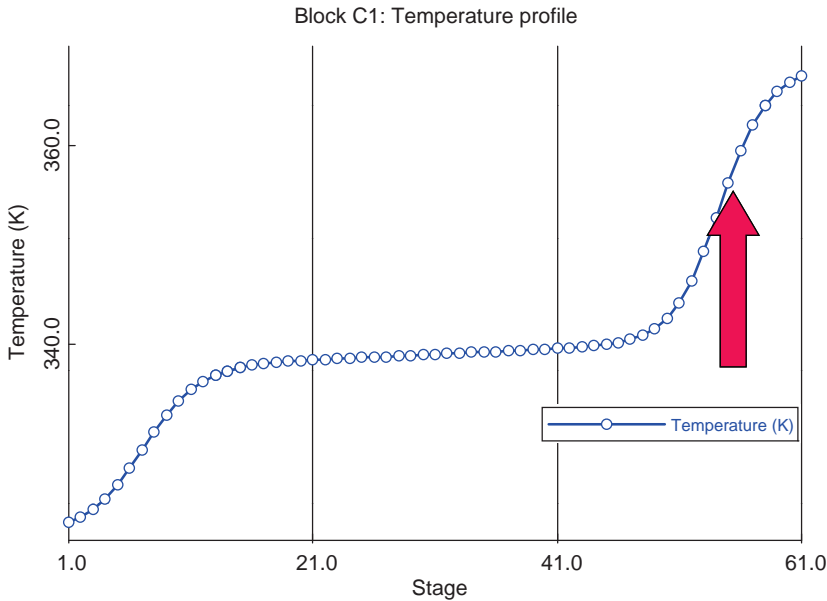


Figure 16.2 Temperature profile.

So the basic conventional control structure selected has reflux-to-feed ratio. This is implemented in Aspen Dynamics using a multiplier block (R/F) with one input being the molar flow rate of feed and the other input the specified reflux-to-feed molar ratio. Since Aspen Dynamics has the rather odd limitation of only being able to directly specify the mass flow rate of the reflux, a flow controller must be installed whose process variable signal is the reflux molar flow rate, and whose output signal is the reflux mass flow rate. This flow controller is put onto “cascade” with its set point signal coming from the R/F multiplier.

Finally, a suitable tray must be selected for temperature control. Figure 16.2 shows the steady-state temperature profile. Stage 55 is in the middle of a section where temperatures are changing rapidly from tray to tray, so the temperature on Stage 55 (356.2 K) is controlled by manipulating reboiler heat input.

Figure 16.3 gives the pressure profile in the column predicted by the dynamic model at different throughputs where tray pressure drop changes with vapor rate. The design case is for a feed flow rate of 100 kmol/h (the middle curve), which is established in Aspen Plus using a 0.1 psi pressure drop per tray. The other curves come from the dynamic model when feed flow rate is changed. The curves clearly show how the pressure on Stage 55 will increase or decrease as vapor flow rates up the column increase or decrease. Therefore, in this column, pressure-compensated temperature control should improve performance.

Figure 16.4 shows the Aspen Dynamics flowsheet with controllers installed. A steam-to-feed ratio is used with the ratio changed by the temperature controller. The need for this ratio to improve load performance is illustrated in Figure 16.5. A 50% increase in feed flow rate is the disturbance. The solid lines show responses without the QR/F ratio. There are very large drops in Stage 55 temperature that result in large transient increases in the nC_4 impurity in the bottoms (x_B). The units of the multiplier must be metric in the Aspen Dynamics simulation (GJ/kmol).

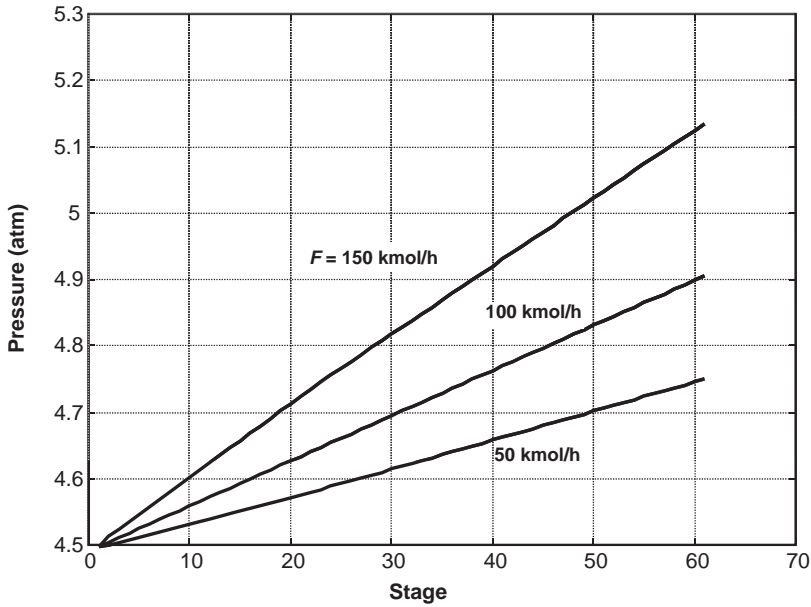


Figure 16.3 Pressure profiles in Aspen Dynamics.

Notice that the increase in feed flow rate produces an instantaneous increase in reboiler duty when the QR/F ratio is installed, which actually causes the Stage 55 temperature to initially increase. Inserting a lag in the feed flow measurement signal sent to the multiplier can reduce the initial responses, as shown in Figure 16.6 where a 0.5 min first-order lag is

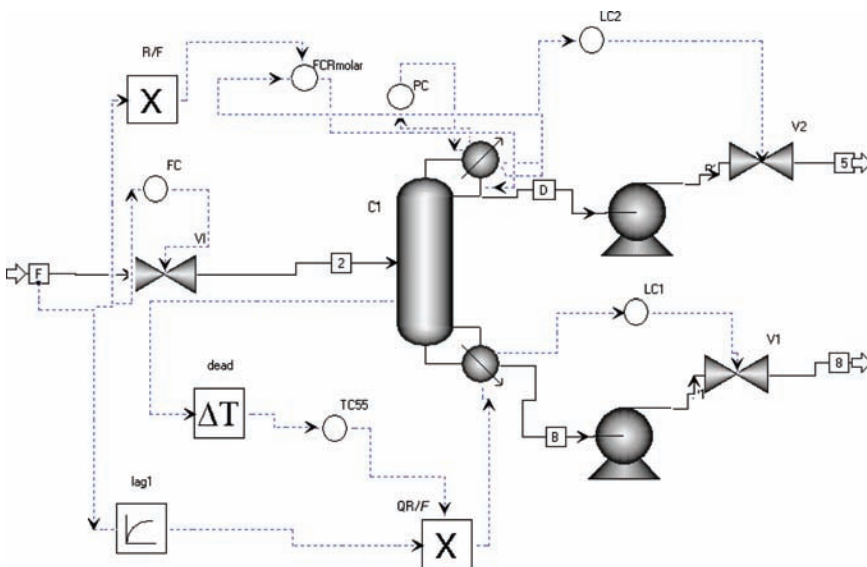


Figure 16.4 Temperature control structure with QR/F ratio and lag.

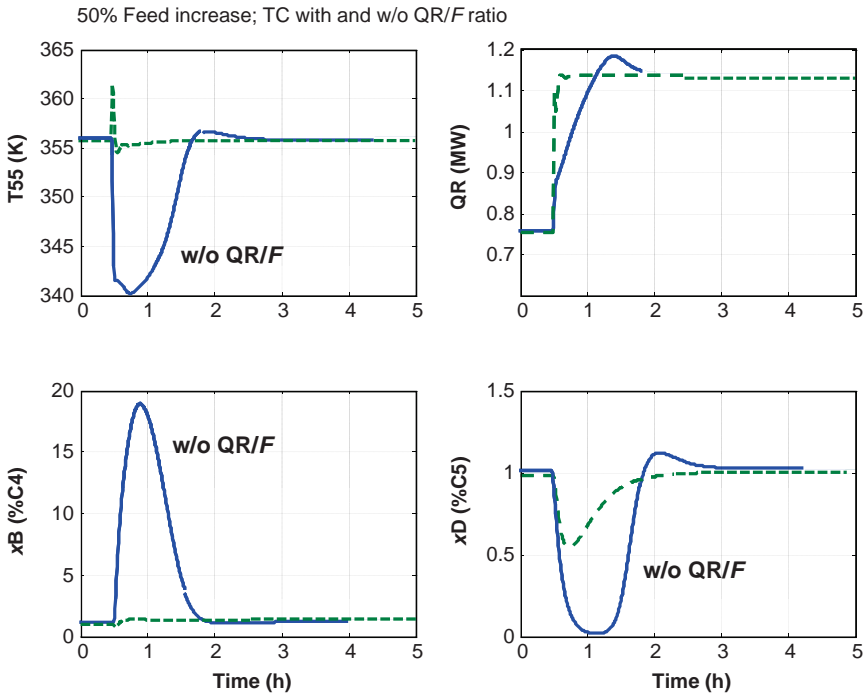


Figure 16.5 Effect of QR/F ratio: 50% feed increase.

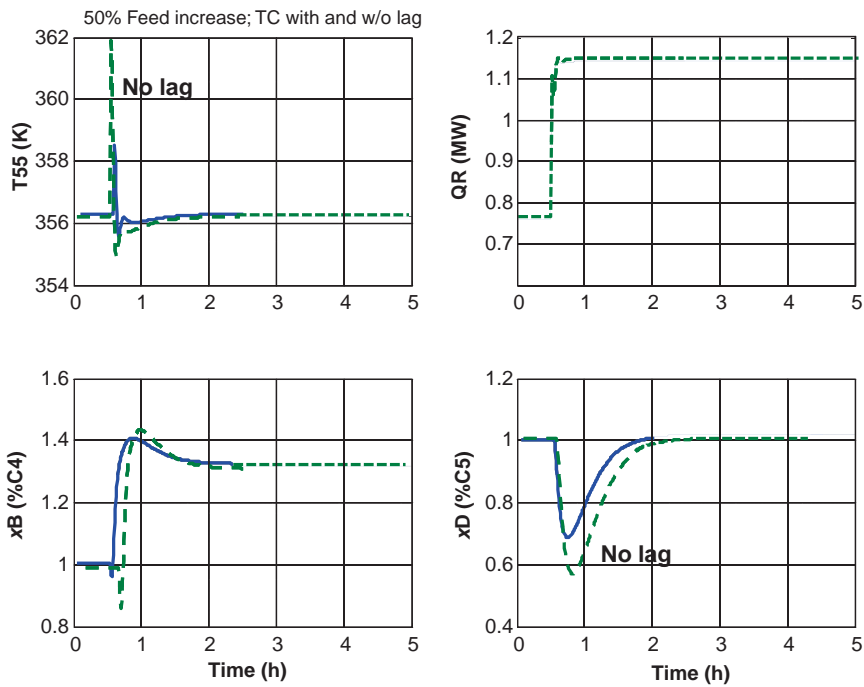


Figure 16.6 Effect of lag: 50% feed increase.

used. The deviation in Stage 55 temperature is reduced, as are the transient peaks in the product impurity compositions.

The tuning of the temperature controller is different with and without the QR/F ratio since in the former case the controller output is reboiler duty while in the latter case it is the QR/F ratio. A 1 min deadtime is inserted in the temperature measurement. Relay-feedback testing and Tyreus–Luyben tuning give $K_C = 0.636$ and $\tau_I = 14.5$ min using a temperature transmitter range of 300–400 K and a controller output range of 0–0.05 ratio.

16.4 TEMPERATURE/PRESSURE/COMPOSITION RELATIONSHIPS

The temperature on Stage 55 is 356.2 K. The pressure on Stage 55 at design conditions is 4.867 atm. The liquid composition on Stage 55 at design conditions is 0.1902 mole fraction nC_4 (light impurity). We need to develop a relationship that permits us to calculate the composition on the tray from the measured temperature and pressure.

$$x_{nC_4} = f_{(T,P)} \quad (16.2)$$

An accurate but simple way to quantify the vapor–liquid equilibrium relationships is to generate T_{xy} diagrams at two different pressures. Over a fairly small composition range at a constant pressure, a linear dependence of composition on temperature should provide sufficiently accurate predictions.

$$x_{nC_4} = m_{(P)}T + b_{(P)} \quad (16.3)$$

where the slope m and the intercept b are functions of pressure, as shown in Eq. (16.4).

$$\begin{aligned} m_{(P)} &= c_1P + c_2 \\ b_{(P)} &= c_3P + c_4 \end{aligned} \quad (16.4)$$

Table 16.2 gives the VLE data used at pressures of 4.5 and 5 atm for compositions of 0.15 and 0.25 mole fraction nC_4 . The data are generated in Aspen Plus from T_{xy} diagrams. Note that metric units are provided because Aspen Dynamics uses metric units in all its calculations. The parameters m , b , and c_k must be generated using metric units. The resulting parameters are given in Eq. (16.5).

TABLE 16.2 Pressure/Temperature/Composition Data

	Liquid Composition (mol% nC_4)	Temperature (K)	Temperature ($^{\circ}C$)
4.5 atm (4.56 bar)	15	355.09	81.94
	25	349.8	76.65
5.0 atm (5.066 bar)	15	359.54	86.387
	25	354.23	81.081

$$\begin{aligned}
 c_1 &= 0.000113 \\
 c_2 &= -0.019417 \\
 c_3 &= 0.1564 \\
 c_4 &= 0.98576
 \end{aligned}
 \tag{16.5}$$

Note that we are calculating an estimate of the light-key nC_4 composition on Stage 55, not an adjusted temperature signal. This composition signal is fed as the process variable into a composition controller whose output signal changes the QR/F ratio and whose set point signal is 0.19 mole fraction nC_4 .

The conventional temperature controller is “Reverse” acting since an increase in temperature should result in a reduction of reboiler heat input. The “pressure-compensated” composition controller is “Direct” acting since an increase in the light component composition on Stage 55 should result in an increase in reboiler heat input so that the light impurity is driven up the column. The composition controller is tuned by using a relay-feedback test and Tyreus–Luyben tuning to give $K_C = 0.139$ and $\tau_I = 14.5$ min using a composition transmitter range of 0–0.4517 and a controller output range of 0–0.05 ratio.

The problem has been viewed in this chapter as one of estimating the composition of the light-key component on a tray by measuring both the temperature and the pressure. The resulting controller is a “light-key” composition controller and has “Direct” action. We could alternatively choose to estimate the heavy-key composition, in which case the composition controller would have “Reverse” action.

In implementing this structure in a plant environment, it may improve operator acceptance by reporting the estimated composition in terms of a “pseudo temperature” that is equivalent to a heavy-key composition.

16.5 IMPLEMENTATION IN ASPEN DYNAMICS

The equations derived above are implemented in Aspen Dynamics using *Flowsheet Equations*. Figure 16.7 shows the syntax required to use the measured pressure and temperature on Stage 55 to estimate the nC_4 composition on Stage 55. This calculated variable is the input signal to the deadtime block. The control signal line from the column icon to the deadtime block is deleted on the process flowsheet diagram.

```

1  CONSTRAINTS
2  // Flowsheet variables and equations...
3  // xC4 = m T + b T in C and P in bar
4  // h = c1 P + c2
5  // m = c3 P + c4
6
7  blocks("dead").input_ = (0.000113*(blocks("C1").stage(55).P) - 0.019417)
8  |* (blocks("C1").stage(55).T )
9  + 0.1564*(blocks("C1").stage(55).P ) + 0.98576;
10 END
11

```

Figure 16.7 Flowsheet equations for pressure-compensated temperatures.

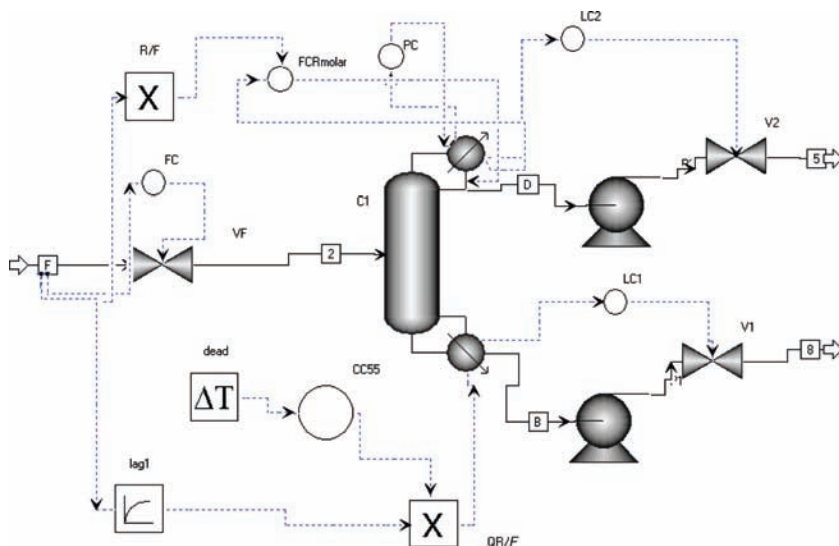


Figure 16.8 Aspen Dynamics process control diagram with pressure-compensated temperature control.

When this script is “*compiled*” in Aspen Dynamics a message appears stating that the flowsheet is overspecified. The input signal to the dead time block must be changed from “*fixed*” to “*free*” for the dynamic simulation to run. Figure 16.8 shows the modified Aspen Dynamics flowsheet.

16.6 COMPARISON OF DYNAMIC RESULTS

Two types of disturbances are imposed on the process, and the performance of conventional temperature control is compared with that of pressure-compensated temperature control.

16.6.1 Feed Flow Rate Disturbances

Results for a 50% increase in feed flow rate are given in Figure 16.9. The solid lines (TC) are for the conventional control structure with the QR/F ratio and a 0.5 min lag. The set point of the feed flow controller is increased from 100 to 150 kmol/h at 0.5 h. The temperature controller drives the temperature on Stage 55 back to its set point value. The vapor rates in the column increase, which increases tray pressure drop. The result is a higher pressure on Stage 55 (see Fig. 16.3). With the same temperature and a higher pressure, the composition of the lighter *n*C4 component increases. This results in a higher concentration of the *n*C4 impurity in the bottoms stream (x_B shown in the lower left graph in Fig. 16.9), which increases from 1 to 1.3 mol%. The impurity of *n*C5 in the distillate is affected only slightly (x_D shown in the lower right graph in Fig. 16.9).

The dashed lines (PTC) in Figure 16.9 are for the pressure-compensated temperature (composition) control. It should be remembered that we are estimating the *n*C4 composition on Stage 55 and controlling this calculated *n*C4 composition by manipulating the QR/F ratio. The set point of the composition controller is 19 mol% *n*C4. The increasing

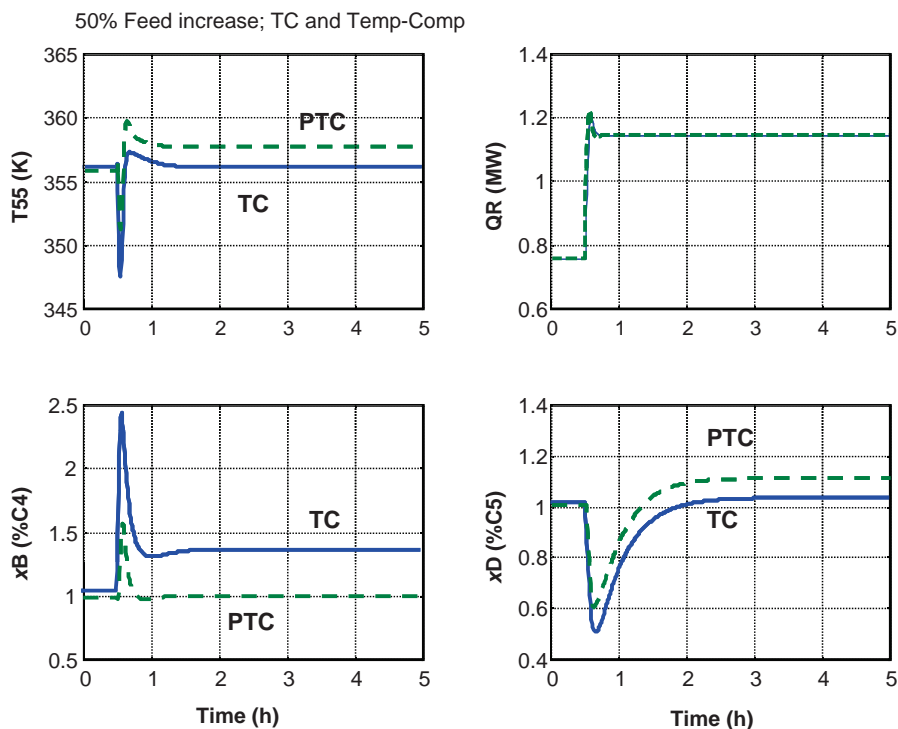


Figure 16.9 Conventional and pressure-compensated: 50% feed increase.

pressure on Stage 55 leads to a prediction of higher nC_4 impurity, so the composition controller (CC55 in Fig. 16.8) increases the reboiler heat input. The temperature on Stage 55 does not stay constant but is driven to a higher value (upper left graph in Fig. 16.9). The result is that the nC_4 impurity in the bottoms changes very little from its specification of 1 mol%.

Results for a 50% decrease are given in Figure 16.10. The set point of the feed flow controller is decreased from 100 to 50 kmol/h at 0.5 h. In the conventional structure, the temperature controller drives the temperature on Stage 55 back to its set point value. The vapor rates in the column decrease, which decreases tray pressure drop. The result is a lower pressure on Stage 55 (see Fig. 16.3). With the same temperature and a lower pressure, the composition of the lighter nC_4 component decreases. This results in a lower concentration of the nC_4 impurity in the bottoms stream (x_B shown in the lower left graph in Fig. 6.10). Thus, the bottoms is overpurified. The impurity of nC_5 in the distillate is affected only slightly (x_D shown in the lower right graph in Fig. 16.10).

16.6.2 Pressure Disturbances

Disturbances in the reflux-drum pressure are imposed on the column. These could occur if we are trying to minimize the pressure in the column to conserve energy and cooling water temperatures change due to ambient conditions.

Figure 16.11 gives results when the set point of the pressure controller is increased from 4.5 to 5.0 atm at 0.5 h. Solid lines are conventional temperature control and dashed lines are

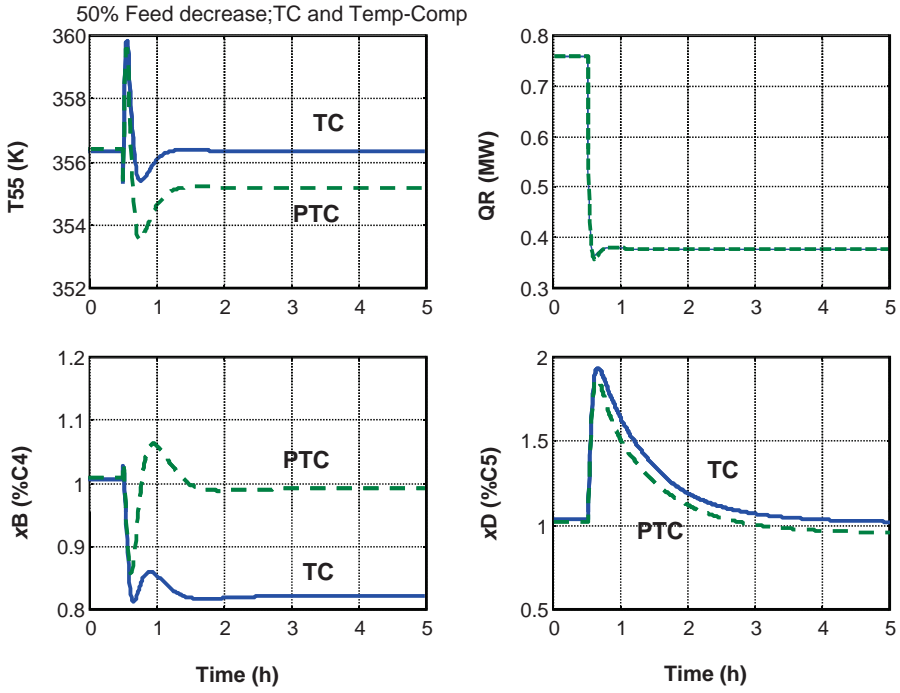


Figure 16.10 Conventional and pressure-compensated: 50% feed decrease.

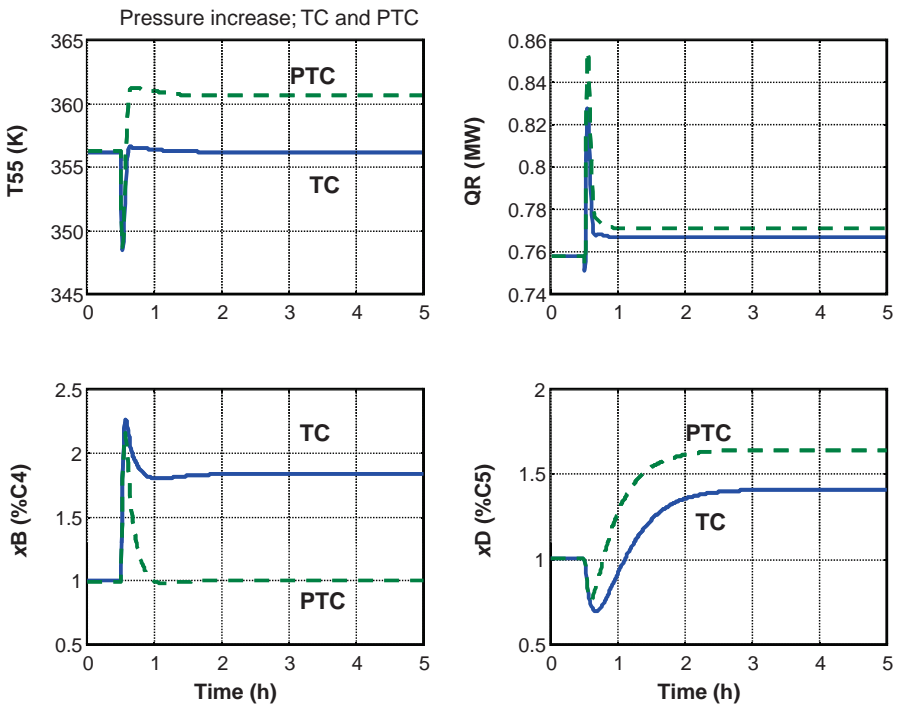


Figure 16.11 Conventional and pressure-compensated: pressure increase.

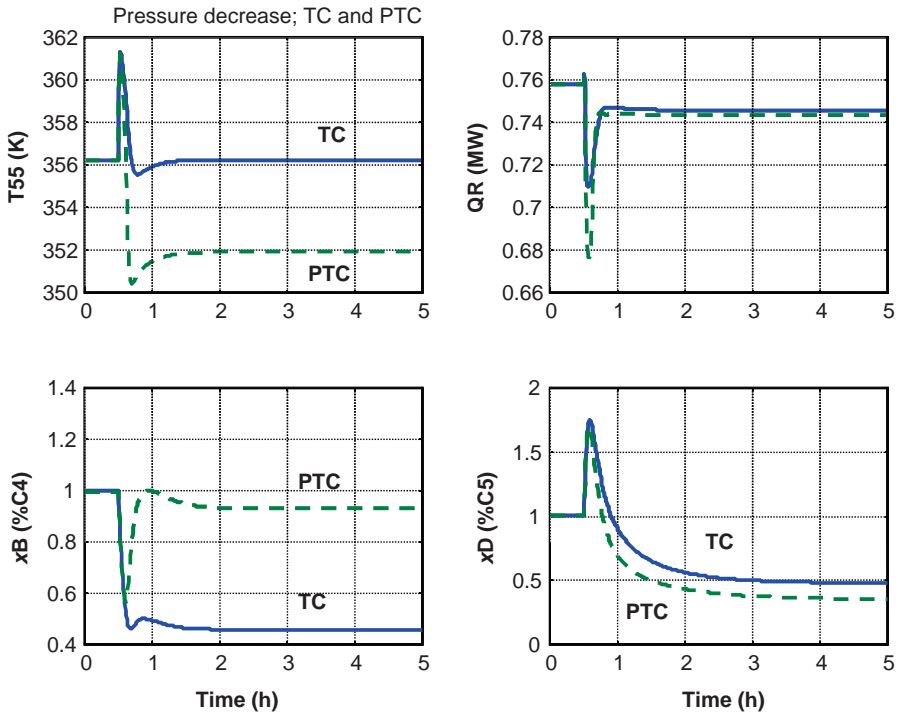


Figure 16.12 Conventional and pressure-compensated: pressure decrease.

pressure compensation. Very large changes in the bottoms composition result without pressure compensation. The temperature on Stage 55 must be significantly increased to keep the bottoms on specification. Figure 16.12 gives results for a decrease in pressure from 4.5 to 4.0 atm. The performance of the pressure-compensated control structure is better than conventional temperature control.

These simulation results demonstrate the effectiveness of the pressure-compensation approach. Many columns do not need pressure compensation because pressure disturbances and pressure drop changes are negligible. But there are several important cases in which pressure compensation provides significant improvements in product quality control.

16.7 CONCLUSIONS

The improvement in control by the use of pressure compensation has been quantitatively demonstrated. The implementation of this type of structure in Aspen Dynamics has been outlined. A simple procedure for deriving the relationships between temperature, pressure, and composition has been illustrated. Pressure compensation should be considered in distillation columns where pressure changes at the control tray are significant.

REFERENCES

1. F. G. Shinskey, *Distillation Control for Productivity and Energy Conservation*, McGraw-Hill, 1977, p. 26, 254.
2. W. L. Luyben, *Modeling, Simulation and Control for Chemical Engineers*, McGraw-Hill, 1973, p. 339.
3. T. L. Tolliver, Control of distillation columns via distributed control systems, in *Practical Distillation Control*, van Nostrand-Reinhold, 1992, p. 351.
4. F. F. Rhiel, Model-based control, in *Practical Distillation Control*, van Nostrand-Reinhold, 1992, p. 441.
5. W. L. Luyben, Heat-integrated columns, in *Practical Distillation Control*, van Nostrand-Reinhold, 1992, p. 492.

ETHANOL DEHYDRATION

Several processes are available for the important operation of dehydrating ethanol/water mixtures to concentrations above the azeotrope (90 mol%). Heterogeneous azeotropic distillation has been studied using several entrainers: benzene, cyclohexane, isooctane, ethylene glycol, and so on. A pioneering paper by Ryan and Doherty¹ explored several alternative process configurations and concluded that the three-column flowsheet with a preconcentrator (beer still), an azeotropic column, and a recovery column was the economic optimum. They used approximate ternary diagram methods. It appears that they arbitrarily assumed a beer still distillate composition with an ethanol concentration of about 88 mol%, which is quite close to the azeotropic composition of 90 mol%.

Energy consumption in the beer still increases as its distillate composition gets closer to the azeotrope. On the other hand, energy consumption in the azeotropic-recovery column section of the process decreases as the feed to this section becomes richer in ethanol. It appears that this fundamental trade-off has not been studied in the literature.

This chapter examines quantitatively, using rigorous simulations, how this design parameter affects the energy and capital investment of the entire system. The focus is the distillate composition trade-off. The example used is the heterogeneous azeotropic distillation process, but the same issue applies in any of the other methods (e.g., extractive distillation) in which a preconcentrator column is used.

17.1 INTRODUCTION

The production of high-purity ethanol from the ethanol/water mixture coming from batch fermenters in biorefineries is complicated by the occurrence of an azeotrope with a composition of 90 mol% ethanol at atmospheric pressure. Typical ethanol concentration in

the fermenter broth is 5 mol% ethanol. The concentration needed for blending into gasoline is 99.5 mol% ethanol.

One method for ethanol dehydration is heterogeneous azeotropic distillation, which has been used for many decades.² A suitable light entrainer component (benzene, cyclohexane, isooctane, ethylene glycol, and so on) is added to modify the relative volatilities. The water is driven overhead with the entrainer and a high-purity ethanol bottoms stream is produced in the azeotropic column. The overhead vapor is condensed and fed to a decanter. The organic phase is refluxed back to the column. The aqueous phase is fed to another column that produces a bottoms product of high-purity water and a distillate that is recycled back to the azeotropic column. A third column in the front end of the process is used to preconcentrate the low-concentration stream from the fermenter up to a concentration closer to the azeotrope before feeding this into the azeotropic column.

In addition to heterogeneous azeotropic distillation, several alternative methods are available for ethanol dehydration such as extractive distillation, adsorption, and pervaporation. A comprehensive review of the subject, including 302 references, has been presented by Vane.³ A recent paper⁴ by Kiss and Paul claims that the heterogeneous azeotropic distillation process is more economical than adsorptive drying because of the large amount of energy required to regenerate the adsorbent.

A pioneering paper by Ryan and Doherty¹ explored several alternative heterogeneous azeotropic configurations using benzene as the entrainer. They examined two- and three-column flowsheets and concluded that the three-column flowsheet with a preconcentrator (beer still), an azeotropic column, and a recovery column was the economic optimum. They used approximate ternary diagram methods of analysis.

Figure 6 in the Ryan–Doherty paper shows a binary feed composition to the azeotropic column of about 88 mol% ethanol. There is no discussion in the paper of the impact of this parameter on the optimum design. Fairly detailed information is given for the azeotropic column and the recovery column, but essentially nothing is provided about the beer still.

The 88 mol% ethanol concentration is quite close to the azeotropic composition of 90 mol%. Energy consumption in the beer still could be reduced by designing for ethanol concentrations further away from the azeotropic composition. However, lower ethanol concentrations in the feed to the azeotropic column will increase energy consumption in the azeotropic column. Clearly, there is an optimum beer still distillate composition.

Other papers have also arbitrarily assumed beer still distillate compositions. For example, Martinez et al.⁵ specify a beer still feed flow rate of 45.36 kmol/h with 10 mol% ethanol. Then they set the beer still distillate flow rate at 5.41 kmol/h. With negligible losses of ethanol in the bottoms, the distillate composition is $4.536/5.41 = 0.838$, which is about 6 mol% away from the azeotropic composition. Li and Bai⁶ select an 85 mol% distillate.

In this chapter, we explore this interesting trade-off. In addition, each of the distillation columns is optimized in terms of the number of stages, which leads to columns that are significantly different from those given by Ryan and Doherty. It should be emphasized that this composition trade-off exists in any other process, such as extractive distillation, that uses a preconcentrator. An additional contribution of this chapter is to demonstrate an effective homotopic method for converging the two recycle loops that occur in this very nonlinear system.

17.2 OPTIMIZATION OF THE BEER STILL (PRECONCENTRATOR)

Three different distillate compositions are considered, and the optimum beer still configuration for each is determined using total annual cost (TAC) as the economic objective. For all cases, the operating pressure is set at 1 atm in the reflux drum. Tray pressure drop is assumed to be 0.1 psi per tray, so base pressure varies as the number of trays is changed. Base pressure affects the base temperature for a fixed composition, which impacts the required reboiler heat-transfer area and resulting capital investment. Low-pressure steam (433 K and \$7.78 per GJ) is used since the base temperature is never greater than 382.3 K in all cases. Cooling water inlet and outlet temperatures are assumed to be 305 and 315 K, respectively. Reflux-drum temperature varies slightly with distillate composition. Overall heat-transfer coefficients in the condenser and reboiler are 0.852 and 0.582 kW/m² K, respectively. Column vessel and heat-exchanger capital costs are given by the equations given in Chapter 4.

Aspen Plus UNIQUAC physical properties are used. A total condenser, partial reboiler and theoretical trays are assumed. The optimum feed tray location is determined for each selected number of total trays by finding the feed location that minimizes reboiler duty.

The feed of fermentation broth is assumed to be 1000 kmol/h with a composition of 5 mol% ethanol and 95 mol% water. The two design specifications in the beer still are a bottoms ethanol concentration of 50 ppm (molar) and a distillate ethanol concentration that is set for the three cases: 75, 80, and 85 mol% ethanol. The variables that are manipulated to achieve these two specifications are the distillate flow rate and the reflux ratio.

Table 17.1 gives results for the 85 mol% distillate composition case for a range of total stages. Energy costs and column diameters decrease as more stages are used. The capital cost of the column vessel increases as more stages are used, but the capital cost of the heat exchangers (condenser and reboiler) decrease. The 46-stage column has the minimum TAC for the 85 mol% case.

Tables 17.2 and 17.3 give results for the 80 and 75 mol% cases. Since the beer still distillate composition is moved further from the azeotropic composition, energy and capital costs decrease, as does the optimum number of stages. It is clear that lower beer still distillate compositions reduce costs in the beer still. In the next section, we see what the effect is in the azeotropic and recovery columns.

TABLE 17.1 Beer Still Optimization: 85 mol% Case

NTI	36	46	56
NF1opt	29	39	48
QR1 (MW)	3.422	3.326	3.302
QC1 (MW)	2.124	1.996	1.538
ID1 (m)	1.084	1.050	1.047
TB1 (K)	379.3	380.8	382.3
Capital (10 ⁶ \$)			
HX	0.2122	0.2037	0.1728
Column	0.2590	0.3062	0.3586
Total	0.4712	0.5099	0.5313
Energy (10 ⁶ \$/y)	0.8396	0.8160	0.8100
TAC (10 ⁶ \$/y)	0.9966	0.9860	0.9872

Reflux drum = 351.3 K.

TABLE 17.2 Beer Still Optimization: 80 mol% Case

NT1	21	26	36
NF1opt	13	16	22
QR1 (MW)	3.067	2.906	2.853
QC1 (MW)	1.823	1.644	1.538
ID1 (m)	1.056	1.030	1.047
TB1 (K)	376.5	377.6	379.3
Capital (10 ⁶ \$)			
HX	0.1922	0.1797	0.1734
Column	0.1611	0.1878	0.2409
Total	0.3532	0.3675	0.4143
Energy (10 ⁶ \$/y)	0.7525	0.7130	0.7000
TAC (10 ⁶ \$/y)	0.8702	0.8355	0.8381

Reflux drum = 351.4 K.

TABLE 17.3 Beer Still Optimization: 75 mol% Case

NT1	16	21	26
NF1opt	8	10	13
QR1 (MW)	3.047	2.906	2.853
QC1 (MW)	1.821	1.996	1.538
ID1 (m)	1.029	1.050	1.047
TB1 (K)	375.9	376.5	377.6
Capital (10 ⁶ \$)			
HX	0.1916	0.1755	0.1729
Column	0.1286	0.1564	0.1853
Total	0.3202	0.3318	0.3582
Energy (10 ⁶ \$/y)	0.7476	0.6938	0.6898
TAC (10 ⁶ \$/y)	0.8543	0.8045	0.8092

Reflux drum = 351.6 K.

17.3 OPTIMIZATION OF THE AZEOTROPIC AND RECOVERY COLUMNS

The beer still considered in the previous section can be optimized in isolation given a specified distillate composition. The downstream columns do not affect the beer still since there is no recycle back to it. However, the other two columns must be optimized together because of the recycle of the recovery column distillate back to the azeotropic column and the recycle of the organic phase from the decanter back to the azeotropic column.

In the Ryan–Doherty paper, the number of stages in the azeotropic column is given as 36, and the number of stages in the recovery column is given as 30. A similar flowsheet was used in a control study⁷ of these two columns. No consideration of the steady-state economic optimum design was considered in that study. The feed stage locations assumed in that study (using Aspen notation) were

1. Beer still distillate (*D1*) was fed on Stage 15 of a 32-stage azeotropic column.
2. Recycle of recovery column distillate (*D3*) was fed on Stage 10 of the azeotropic column.

3. The organic phase from the decanter plus a very small benzene makeup was fed at the top of the azeotropic column.
4. The aqueous phase was fed on Stage 11 of the 32-stage recovery column.

The azeotropic column feed flow rate was adjusted from that used in the previous study (216 kmol/h) to correspond to the 1000 kmol/h of fermenter broth fed to the beer still used in the present study. With a distillate composition of 85 mol% ethanol, this feed flow rate is 62.44 kmol/h. With this flow rate and with the number of trays and feed locations stated above, the reboiler duty (QR2) in the azeotropic column is 1.597 MW and the reboiler duty in the recovery column is 0.7122 MW.

These results are based on designing the azeotropic column for 0.02 mol% benzene and 0.026 mol% water in the bottoms, giving an ethanol product with 99.54 mol% ethanol. The two variables adjusted to achieve these specifications were organic reflux (R2) and bottoms flow rate (B2). The organic reflux for this design is 82.7 kmol/h.

The design specification in the recovery column is a bottoms purity of 99.9 mol% water. The separation is quite easy, so the reflux ratio is set at a very small value (RR = 0.1). An Aspen *Flash3* model is used for the decanter, so a small vapor stream is required. The decanter is adiabatic, and the heat duty in the overhead condenser is adjusted to give a very small flow rate of gas with the decanter temperature of 322 K and pressure of 0.56 atm.

The column labeled “Base” in Table 17.4 gives the economic results for this base-case design. Note that the TAC of the two columns (not including the beer still) is \$820,500 per year.

17.3.1 Optimum Feed Locations

The first issue is to find the optimum feed locations, which were not optimized in the original control study. Changing feed stage locations from Stage 15 and Stage 10 in the azeotropic column to Stage 12 and Stage 1 (top tray in the Aspen stripping *RadFrac* column) lowered the reboiler duty from 1.597 to 1.456 MW. The flow rate of organic reflux dropped from 82.70 to 69.89 kmol/h.

TABLE 17.4 Azeotropic Column Optimization: 85 mol% Case; NT3 = 32

	Base			
NF2	32	52	62	72
NF2	12	20	24	28
Organic reflux R2 (kmol/h)	82.70	62.12	60.91	60.29
QR2 (MW)	1.597	1.280	1.255	1.243
QC2 (MW)	1.595	1.270	1.241	1.227
ID2 (m)	0.868	0.7643	0.7643	0.7443
TB2 (K)	373.0	374.5	375.2	376.4
QR3 (MW)	0.7122	0.5944	0.5773	0.5692
Capital (10 ⁶ \$)				
Azeotropic column	0.4236	0.4468	0.4762	0.5068
Recovery column	0.3381	0.3248	0.3228	0.3218
Energy (10 ⁶ \$/y)				
Azeotropic column	0.3918	0.3140	0.3079	0.3050
Recovery column	0.1747	0.1458	0.1416	0.1396
TAC ^a (10 ⁶ \$/y)	0.8205	0.7170	0.7158	0.7208

^aAzeotropic and recovery columns: decanter, 322 K, 0.56 atm; azeotropic column, 2 atm; recovery column, 32 stages, 1.1 atm.

Then the feed stage location in the recovery column was changed from Stage 11 to Stage 4, which lowered its reboiler duty from 0.7122 to 0.7033 MW and lowered the organic reflux further to 68.86 kmol/h.

17.3.2 Optimum Number of Stages

The next issue is to find the economic optimum number of stages in each column. The locations of the feeds were scaled up or down directly with the total number of stages using the results for the 32-stage columns. Note that the distillate of the recovery column (*D3*) is fed to the top of the azeotropic column in all cases.

The right three columns in Table 17.4 give results for the azeotropic column with varying number of stages. The number of stages in the recovery column is fixed at 32. Adding more stages reduces the amount of organic reflux required to meet the specification, which reduces energy consumption. A 62-stage azeotropic column gives the minimum TAC of the two-column portion of the process. Note that this is almost twice the number of stages recommended by Ryan and Doherty.

Then the number of stages in the recovery column is varied with the number of stages in the azeotropic column fixed at 62. Table 17.5 shows that the optimum number of stages (12 is selected as the minimum practical number) is much smaller than recommended in the Ryan–Doherty design.

Remember that these results are for an 85 mol% ethanol beer still distillate. Combining all three columns is considered in the next section. We assume that the optimum numbers of stages in the azeotropic and recovery columns do not change significantly as the beer still distillate composition varies over the range of 75–85 mol% ethanol.

17.4 OPTIMIZATION OF THE ENTIRE PROCESS

The optimum beer still designs with their associated capital and energy costs are now combined with the azeotropic and recovery column designs for the three values of beer

TABLE 17.5 Recovery Column Optimization: 85 mol% Case; NT2 = 62

NF3	12	22	32
NF3	3	3	4
NF2	62	62	62
Organic reflux R2 (kmol/h)	60.99	60.98	60.91
QR2 (MW)	1.255	1.255	1.255
QC2 (MW)	1.242	1.242	1.241
ID2 (m)	0.7523	0.7523	0.7523
TB3 (K)	381.0	379.2	375.2
QR3 (MW)	0.5771	0.5775	0.5773
Capital (10 ⁶ \$)			
Azeotropic column	0.4764		
Recovery column	0.1986		
Energy (10 ⁶ \$/y)			
Azeotropic column	0.3079		
Recovery column	0.1416		
TAC ^a (10 ⁶ \$/y)	0.6745		

^aAzeotropic and recovery columns: decanter, 322 K, 0.56 atm; azeotropic column, 62 stages; 2 atm; recovery column, 1.1 atm.

TABLE 17.6 Overall Optimization: NT2 = 62; NT3 = 12

x_{D1} (mol% Ethanol)	75	80	85
$D1$ (kmol/h)	66.60	62.44	58.76
Organic reflux $R2$ (kmol/h)	72.86	65.69	60.11
Aqueous phase (kmol/h)	60.11	55.61	53.34
$B3$ (kmol/h)	16.60	12.36	8.733
$D3$ (kmol/h)	43.51	43.25	40.32
NT1	21	26	46
QR1 (MW)	2.828	2.906	3.326
QR2 (MW)	1.450	1.333	1.255
QR3 (MW)	0.5826	0.5699	0.5771
Capital (10^6 \$)			
Beer still	0.3318	0.3675	0.5099
Azeotropic column	0.5300	0.4851	0.4764
Recovery column	0.1936	0.1970	0.1986
Total capital	1.0454	1.0496	1.1849
Energy (10^6 \$/y)			
Beer still	0.6938	0.7130	0.8160
Azeotropic column	0.3559	0.3270	0.3079
Recovery column	0.1429	0.1398	0.1416
Total energy	1.1926	1.1799	1.2655
TAC (10^6 \$/y)	1.541	1.5297	1.6605

Decanter, 322 K, 0.56 atm; beer still, 1 atm; azeotropic column, 62 stages; 2 atm; recovery column, 12 stages; 1.1 atm.

still distillate composition. Table 17.6 summarizes the results using the previously found optimum designs of the beer still for each distillate composition (x_{D1}) and finding the required organic reflux and reboiler duties in the other two columns for each value of x_{D1} .

The beer still distillate flow rate decreases slightly as distillate composition is increased but less organic reflux ($R2$) is required. This reduces reboiler duty in the azeotropic column (QR2). However, the reboiler duty in the beer still (QR1) increases as distillate composition is increased, as does the optimum number of stages in the beer still (NT1). So, beer still capital and energy costs increase while those costs in the azeotropic column decrease.

The energy and capital costs in the recovery column are less affected by the beer still distillate composition. The flow rate of the feed to the recovery column (*Aqueous*) decreases since less water needs to be removed from the bottom of the column ($B3$ decreases as x_{D1} increases). The recovery column distillate ($D3$), which is recycled back to the azeotropic column, decreases slightly.

The net result of all these effects on the total capital cost is an increase with increasing beer still composition. The net result of all these effects on the total energy cost is a minimum at a beer still composition of 80 mol% ethanol. Total annual cost also is minimized at 80 mol% ethanol.

Figure 17.1 gives the flowsheet for this case with details of the equipment sizes, stream conditions, and operating conditions. Figure 17.2 shows the ternary diagram at 2 atm. The overhead vapor from the azeotropic column is located in the narrow wedge at the bottom of the upper region. The bottoms of the azeotropic column is located at the ethanol corner. Figure 17.3 gives the temperature and composition profiles in the azeotropic column.

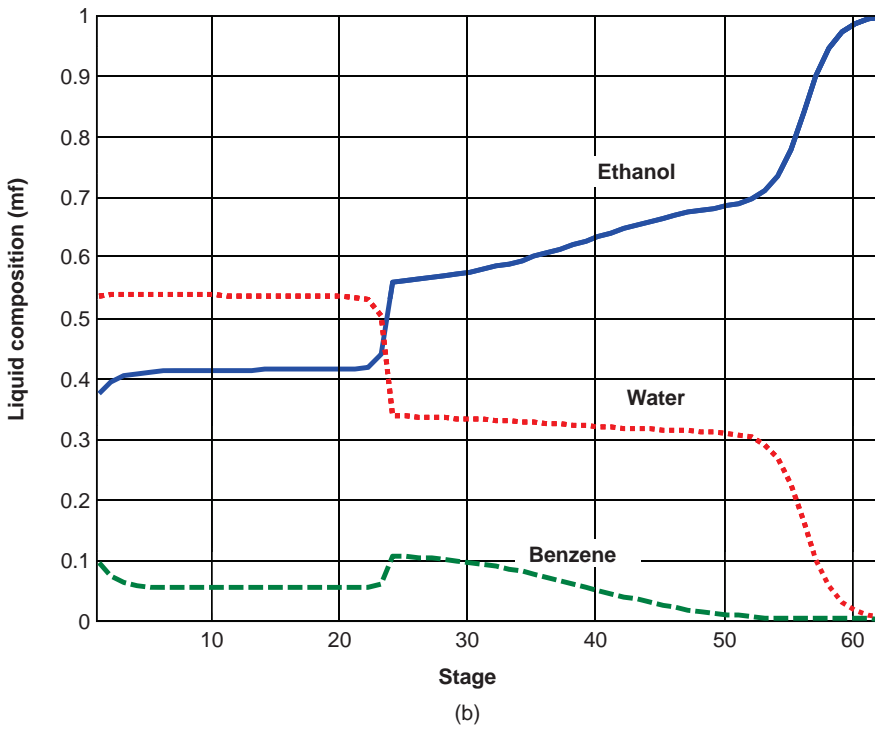
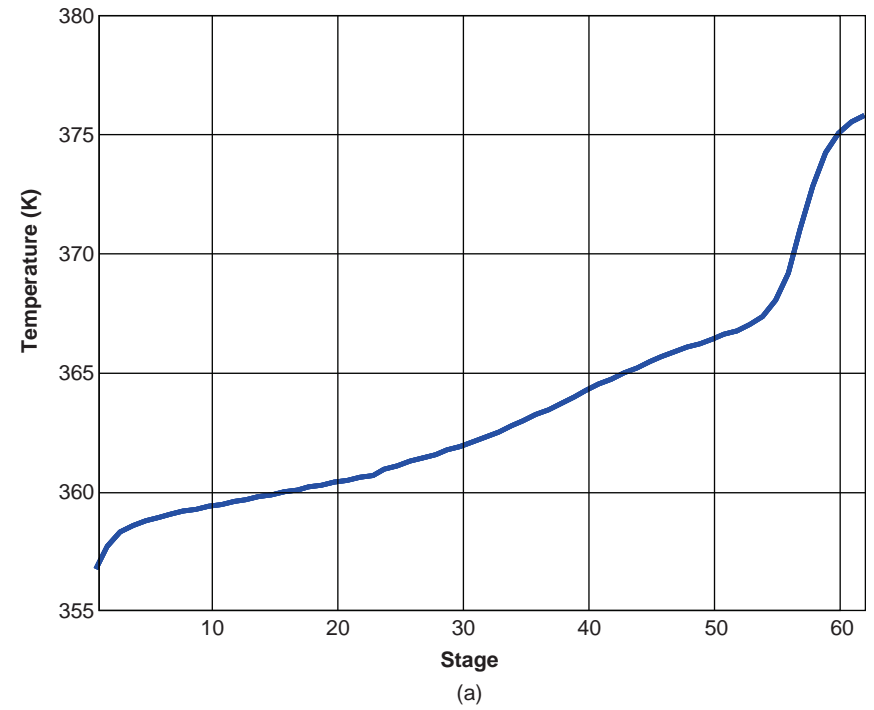


Figure 17.3 (a) Temperature profile in azeotropic column. (b) Liquid composition profiles in azeotropic column.

It should be noted that the total energy consumption in the proposed design is 7500 kJ/kg of ethanol product. The Ryan–Doherty flowsheet was stated as 8200 kJ/kg. No comparison of capital investment can be made since insufficient information was provided in their paper.

17.5 CYCLOHEXANE ENTRAINER

Benzene has been used in the cases studied in the previous sections. To see the effect of entrainer choice, the same basic process configuration was examined with cyclohexane substituted for benzene. The beer still is not affected. The number of stages and feed locations in the other two columns are kept the same as those used for benzene. The specifications are the same except that the 0.2 mol% impurity in the ethanol product stream is now cyclohexane.

The simulation was easily converted to the different solvent. Table 17.7 gives a comparison of the benzene and the cyclohexane processes. The latter uses less total energy than the former (1.658 MW vs. 1.903 MW) in the reboilers of the azeotropic and recovery columns. The organic phase has a higher entrainer concentration than it does in the benzene case (92.95 mol% cyclohexane vs. 81.85 mol% benzene). The aqueous phase has a lower entrainer concentration than it does in the benzene case (2.82 mol% cyclohexane vs. 7.94 mol% benzene). This reduces the required flow rate of the organic solvent from 65.69 kmol/h in the benzene process to 51.71 kmol/h in the cyclohexane process. Of course, cyclohexane has the additional advantage over benzene of avoiding the problem of carcinogenic properties.

17.6 FLOWSHEET RECYCLE CONVERGENCE

Recycle streams can present problems in process simulations. The process studied in this paper has two recycles and is very nonlinear, both of which complicate the convergence of the flowsheet simulation. Up to this point, the only successful solution of the problem discussed in the literature⁵ for this process used the approach of converting the simulation into a dynamic one and then closing the recycle loops with a plantwide control structure in place to drive the process to the desired steady state.

During the course of the present study, a different approach was used, which proved quite effective and avoided the conversion to a dynamic simulation. The method uses “homotopy”

TABLE 17.7 Comparison of Benzene and Cyclohexane Entrainer Processes: 80 mol% Case

	Benzene	Cyclohexane
Organic reflux R2 (kmol/h)	65.69	51.71
QR2 (MW)	1.333	1.137
QR3 (MW)	0.5699	0.5215
Total (MW)	1.903	1.658
Organic phase (mol%)	81.85 mol% benzene	92.95 mol% cyclohexane
Aqueous phase (mol%)	7.94 mol% benzene	2.83 mol% cyclohexane

Beer still distillate composition, 80 mol% ethanol; azeotropic column, 62 stages; 2 atm; recovery column, 12 stages; 1.1 atm; decanter, 322 K; 0.56 atm.

to slowly converge each recycle loop. For example, in the recycle of recovery column distillate back to the azeotropic column, a temporary flow splitter is installed in the line with the loop closed. A fraction of the total stream ($\sim 5\%$) is initially specified to be purged out of the process. This makes the closing of the loop less difficult because the numerical convergence algorithm does not have to find the solution where the process equations are perfectly balanced so as to precisely match the feed streams fed into the system and all the other fixed variables. Once this initial solution is found, the fraction of the stream split is slowly reduced getting closer and closer to no purge. In the limit as the specified split fraction is made negligibly small, the solution is the desired one. This method was directly and successfully applied to the recovery column distillate recycle loop.

The same basic approach was used for the organic recycle loop with some modification. One of the Aspen *Design spec/vary* functions used in the azeotropic column manipulated the flow rate of the organic reflux (R2) to attain the specified composition of benzene in the bottoms (0.2 mol% benzene). So, the flow rate of this stream could not be independently set. It was also necessary to make a guess of the composition of this stream.

To get around this problem, a second flow splitter was inserted in the line after the organic phase from the decanter and the very small benzene makeup stream had been mixed. The loop was not closed. A small fraction of this total stream was purged off. What remains is compared with the R2 flow rate (determined by the *Design spec/(vary)* function) and the guessed composition of R2. The fraction split is adjusted to make the two flow rates the same and the composition of R2 is adjusted with each iteration to match that calculated. When the loop has converged, there is nothing purged and the guessed and calculated compositions of R2 are identical.

17.7 CONCLUSIONS

This chapter has explored the important design optimization variable of beer still distillate composition in ethanol dehydration processes. The trade-off between the beer still and the azeotropic columns has been neglected in many papers, both those considering heterogeneous azeotropic distillation and extractive distillation for ethanol dehydration. The economic optimum flowsheet has been developed for the benzene entrainer system. The three-column configuration proposed by Ryan and Doherty is used. The number of stages in the columns and the feed locations are adjusted to arrive at the most economical design in terms of total annual cost.

The composition of the distillate from the beer still is demonstrated to be a key design optimization variable. Ryan and Doherty assume a composition (88 mol% ethanol) quite close to the azeotropic composition. Other authors select compositions around 85 mol%.

This chapter demonstrates that the optimum is much lower (80 mol%) so that the capital and energy costs of the two sections of the process are economically balanced.

REFERENCES

1. P. J. Ryan and M. F. Doherty, Design optimization of ternary heterogeneous azeotropic distillation sequences, *AIChE J.* **35**, 1592–1601 (1989).
2. C. Black, Distillation modeling of ethanol recovery and dehydration processes for ethanol and gasohol, *Chem. Eng. Prog.* **76** (9), 78 (1980).

3. L. M. Vane, Separation technologies for the recovery and dehydration of alcohols from fermentation broths, *Biofuels Bioprod. Bioref.* **2**, 553–588 (2008).
4. A. A. Kiss and D. Suszwalak, Enhanced bioethanol dehydration by extractive and azeotropic distillation in dividing-wall columns, *Sep. Purif. Technol.* **86**, 70 (2012).
5. A. A. Martinez, J. Saucedo-Luna, J. G. Sequovia-Hernandez, S. Hernandez, F. I. Comez-Castro, and A. J. Castro-Monteya, Dehydration of bioethanol by hybrid process liquid–liquid extraction/extractive distillation, *Ind. Eng. Chem. Res.* **51**, 5847–5855 (2012).
6. G. Li and P. Bai, New operation strategy for separation of ethanol–water by extractive distillation, *Ind. Eng. Chem. Res.* **51**, 2723–2729 (2012).
7. W. L. Luyben, Control of a multi-unit heterogeneous azeotropic distillation process, *AIChE Journal* **52**, 115–134 (2006).

CHAPTER 18

EXTERNAL RESET FEEDBACK TO PREVENT RESET WINDUP

Reset windup problems can occur in override control structures when controllers have integral action. Large swings (bumps) in control valve position can result as control is transferred from one controller to another. One method for achieving “bumpless transfer” is the use of the Shinskey/Buckley control structure called “external reset feedback.” Unfortunately, this type of controller is not available in commercial dynamic simulators.

In this chapter, we illustrate how external reset feedback can be implemented in Aspen Dynamics and demonstrate the improved dynamic performance using two process examples.

18.1 INTRODUCTION

Reset windup occurs when a feedback controller with integral action cannot drive the process variable to the setpoint. This problem is experienced in override control structures where a manipulated variable can be set by two controllers, depending on conditions in the process. High or low selectors are used to choose which controller is positioning the control valve. The controller whose output signal is not selected will continue to integrate the error signal and drive its output signal to a high or low limit. When conditions change and this controller should start positioning the control valve, a large bump in the control valve position can occur because the integral component of the controller output will not start to change until the sign of the error changes (i.e., until the process variable signal crosses the setpoint signal). The controller output already has significant unwinding momentum when it “takes up” the valve manipulation. In addition, it may take a long time to return the controlled variable to its desired setpoint.

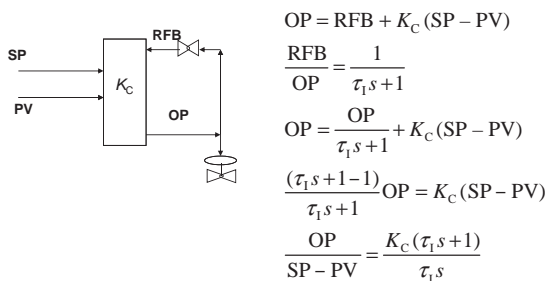


Figure 18.1 Internal reset feedback circuit for PI controller.

Windup problems can be significantly reduced by applying “external reset feedback” as suggested by Shinskey¹ over 45 years ago and extensively applied by Buckley² to a variety of process applications, particularly distillation columns.

The method evolved from how integral action was achieved in some of the original pneumatic controllers. A proportional controller multiplies the difference between the process variable signal PV and the setpoint signal SP by a gain K_C and adds a constant bias pressure to produce a controller output signal OP. To convert the device to provide integral action, a positive feedback of the output signal was used. The output pressure signal is fed back through a needle valve into the reset chamber where the original bias pressure was set. Thus, the controller output signal will continue to change until there is no error (SP equal to PV).

This unity-feedback circuit was normally done through internal piping. However, the signal to the reset chamber can come from an external source. Figure 18.1 illustrates how the external reset circuit is set up and how it works.³ Other digital methods have also been explored.⁴ The pneumatic controller output signal OP is fed back through a needle valve into the reset chamber where the pressure is RFB. This RFB pressure is related to the output pressure OP by a first order lag due to the volume in the reset chamber and the flow restriction of the needle valve. The needle valve position determines the integral time constant in the controller. Figure 18.1 shows that the resulting input/output relationship of this device is that of a proportional-integral controller.

Figure 18.2 shows the modified circuit in which the reset input signal can come from an external source. In this example, the control valve is direct acting (air-to-open) so that it

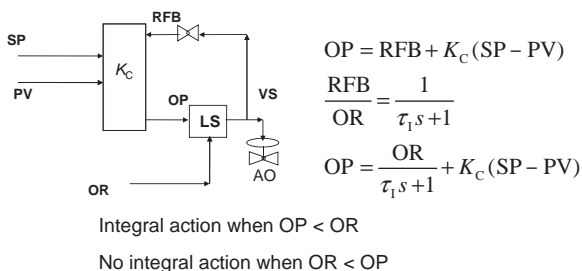


Figure 18.2 External reset feedback circuit for PI controller.

will fail in the safe position of completely closed. Therefore, a low selector is used to choose whether the controller output signal OP or the override signal OR from a second controller (the override controller) goes to the control valve. When the override signal is *higher* than the controller output signal, the controller performs as a normal PI controller. However, when the override signal is *lower* than the controller output signal, the integral action no longer occurs. The OP signal simply lags behind the OR signal with an added error times gain component. The unselected controller output remains close to the implemented control signal, differing only by the K_C times error component. When control is taken up, one has to unwind only by the K_C times error component instead of all the way from 100% or 0%. External reset thus facilitates quick taking up and giving up of valve manipulation by a PI controller.

Two examples are presented later in this chapter that demonstrate the windup problem when external reset feedback is not used and the improvement in control when it is used.

First, we will show how external reset feedback is implemented in the widely used commercial dynamic simulator Aspen Dynamics. Developing effective control structures for processes often require the use of override controllers to handle operating up against constraints. Unfortunately, Aspen Dynamics does not have a module for an external reset feedback controller. The following section shows how one can be implemented using the available control element blocks and points out some of the problems in getting the simulation to initialize and run.

18.2 EXTERNAL RESET FEEDBACK CIRCUIT IMPLEMENTATION

There are several mathematical operations that are required to achieve the setup of the external reset controller shown in Figure 18.2. The Aspen Dynamics blocks are shown in Figure 18.3.

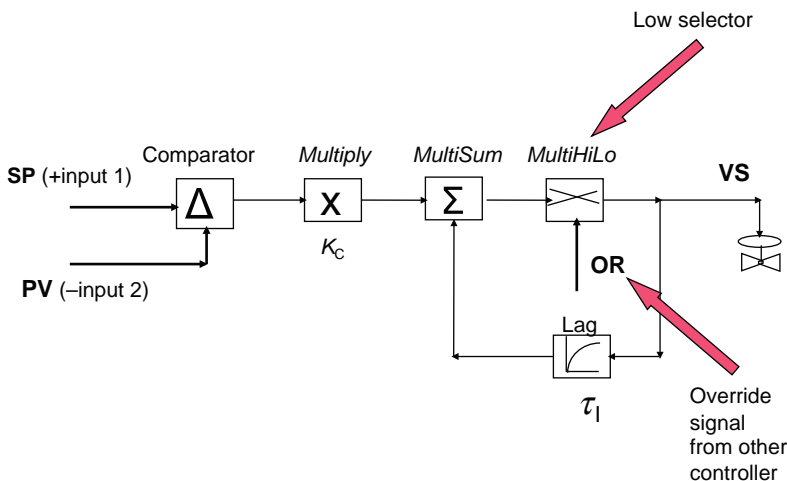


Figure 18.3 External reset feedback in Aspen Dynamics.

18.2.1 Generate the Error Signal

The process variable signal PV from the transmitter of the controlled variable must be subtracted from the setpoint signal SP to generate an error signal. The simplest way to implement this operation is to use a *Comparator* block in Aspen Dynamics. The *Input2* signal is subtracted from the *Input1* signal. Of course a more complex setup could be used in which the PV signal is fed into a *Multiply* block with constant of negative one as the other input, and then the output of the *Multiply* block fed into a *MultiSum* block whose other input is the SP signal.

18.2.2 Multiply by Controller Gain

The output of the *Comparator* block is fed to *Multiply* block whose other fixed input is the controller gain (as determined by an appropriate tuning method such as relay-feedback testing). The sign of the gain is determined by the correct action of the controller. A positive gain corresponds to a “reverse acting” controller: when the PV signal goes up, the controller output signal OP goes down.

18.2.3 Add the Output of Lag

The output of the *Multiply* block is added to a signal coming from a *Lag* block to be discussed later. A *MultiSum* block is used.

18.2.4 Select Lower Signal

The output of the *MultiSum* block and the signal OR from the override controller are the two inputs to a *MultiHiLoSelect* block, which can be configured to select either the higher or the lower of the two input signals. In the example, a low selector is required. The output signal VS of the low selector goes to the control valve (the manipulate variable), and it also goes to a lag to provide integral action when the override controller does not have control of the valve (normal operation).

18.2.5 Setting up the Lag Block

The time constant of the lag is the appropriate integral time tuning constant τ_I for the controller. A *Lag* block is used with a gain of unity and a time constant of τ_I . Getting this part of the circuit to initialize and run correctly is the most difficult aspect of the implementation.

A procedure that works is to not close the feedback loop but to feed a fixed control signal into the lag block that corresponds to expected signal from the low selector. For example, if the control valve is designed to be half open at normal conditions, the valve signal will be 50% and the low selector output signal is 50%. So insert a control signal onto the Aspen Dynamics process flow diagram, specify its value to be 50 and make it a “fixed” variable type. Then open up the “all variables” view of the lag block and specify the output variable to be an “initial” variable type. Make an initialization run. The output of the lag block should show 50%.

Finally, reconnect the source of the input signal to the lag block to be the output of the low selector. At this point the “run” button at the bottom of the screen will be red, indicating

that the system of equations is over-specified. The inlet signal to the lag must be changed to a “free” variable type. The red light should turn green and the simulation should run properly.

Another useful element is the *Scale* block that converts one type of signal into another set of units. For example, if the process variable is temperature and we want to generate a “percent of scale” signal (or an electronic or pneumatic signal) that would come from a temperature transmitter, a *Scale* block provides this conversion. On the other end of the control loop, the output signal from the controller (% , ma or psig) can be converted into the appropriate manipulated variable units (GJ/h, lb/h, etc.) by the use of a *Multiply* block. The use of the *Scale* block will be illustrated in the second example, which is more complex than the first example discussed below.

18.3 FLASH TANK EXAMPLE

We start with a simple process example to illustrate the procedure and demonstrate the improvement in performance provided by the use of external reset feedback. Only the normal controller has integral action in this example. The override controller is a proportional-only controller, so it does not need reset-windup protection.

18.3.1 Process and Normal Control Structure

Figure 18.4 gives the flowsheet of a simple flash tank. A mixture of light hydrocarbons at 300 psia is flashed through a valve into a tank at 75 psia. The ratio of the vapor product to the feed is specified to be 0.8, so the 100 lb mol/h of feed produces 80 lb mol/h of vapor from the top of the tank and 20 lb mol/h of liquid from the bottom. The heat input required (to the jacket or internal coil) is 0.113×10^6 Btu/h. The resulting temperature in the tank is 137.9 °F.

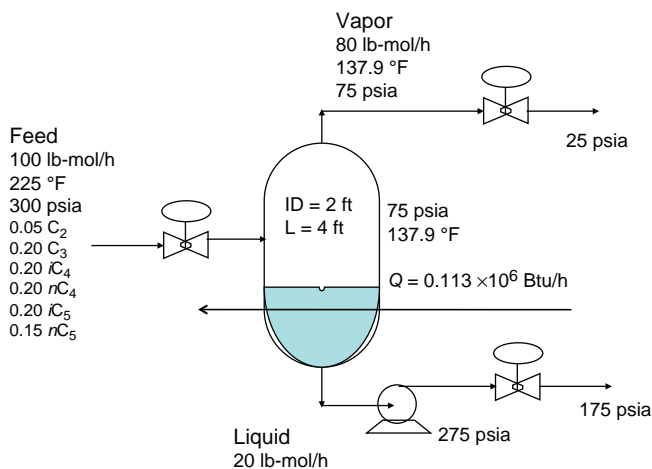


Figure 18.4 Flash tank.

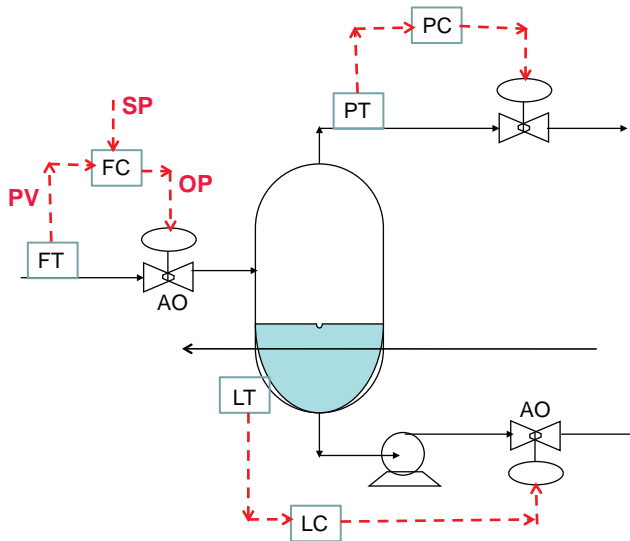


Figure 18.5 Flash tank PT structure.

Figure 18.5 shows the normal control structure. Feed is flow controlled with a reverse-acting PI controller manipulating the control valve in the feed line. Pressure is controlled using a direct-acting PI controller manipulating the valve in the vapor line. Tank liquid level is controlled using a simple direct-acting P-only controller ($K_C = 2$) by setting the position of the valve in the liquid line after the pump. All valves are air-to-open and are 50% open at design conditions. For simplicity, the heat input is assumed constant.

Note, in Figure 18.4 the design pressure drop over the liquid control valve is 100 psi, which may seem quite large. However, the simulation results given below demonstrate that an increase in the feed flow rate of 22% drives the liquid valve wide open, which means that larger increases in feed flow rate will flood the tank.

18.3.2 Override Control Structure Without External Reset Feedback

The control objective is to prevent the liquid level in the tank from climbing too high by having a high-level override controller take over the feed control valve. Since the feed flow controller has integral action, it will windup when overridden. Of course, the rate of windup (and unwinding) depends on the integral time constant. If the normal fast controller tuning constant for a flow controller is used ($\tau_I = 0.3$ min), the unwinding is so fast that the bump is of short duration. In the simulations presented below, we show the effect of this parameter.

Figure 18.6 shows the Aspen Dynamics flowsheet with a standard PI flow controller (no external reset feedback) and a high-level override controller. Liquid level is normally controlled by the liquid valve. The normal level is at 2 ft, so the setpoint of the normal level controller is 2 ft. The level transmitter span is 4 ft. A simple P-only high-level override controller is set up to come into action when the level gets too high. The setpoint of the

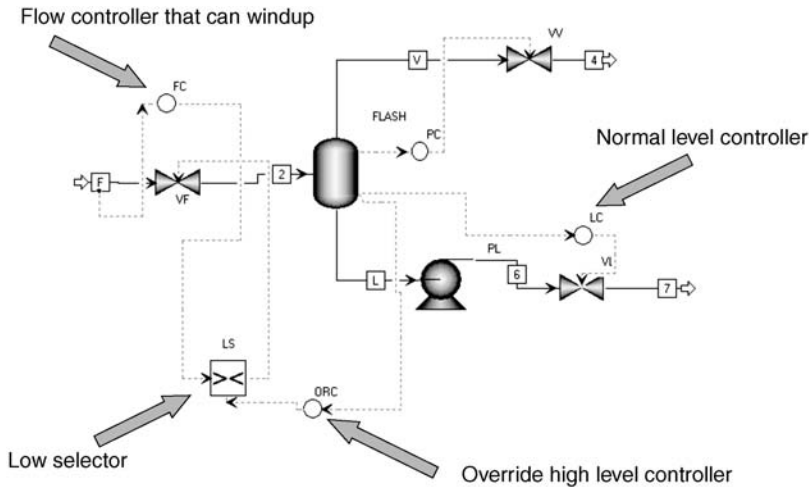


Figure 18.6 High-level override controller: plain feed flow controller.

override controller is set at 3.75 ft. The normal output of the override controller is 100%. It is reverse-acting and its gain is 2.

Figure 18.7 gives results for a 30% increase in the setpoint of the feed flow controller at 0.5 h. The flow controller output signal (OP FC) increases. The integral time of the feed flow controller in this simulation is 5 min. The level increases, which opens the liquid

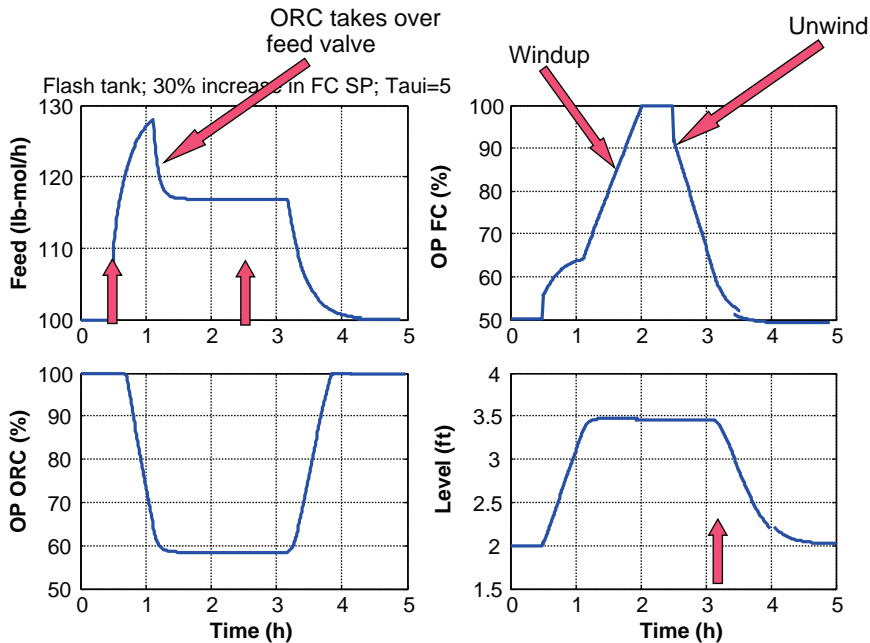


Figure 18.7 30% feed disturbances: high-level override controller; plain feed flow controller.

control valve. When the level reaches 3 ft, the level transmitter output has changed by 25%. Since the controller gain is 2, the output of the level controller has changed by 50%, which means the liquid valve is wide open.

But the level continues to increase, so the output signal of the override controller (OP ORC) drops. At about 1.1 h, the override controller output becomes less than the flow controller output. The low selector then sends the lower signal to the feed control valve, which cuts back the feed flow rate, limiting it to about 117 lb mol/h although the setpoint is 130 lb mol/h. The level stops climbing, leveling out at about 3.5 ft. The flow controller output signal winds up to 100% in about 0.9 h.

At 2.5 h, the setpoint of the feed flow controller is dropped back to 100 lb mol/h. There is an immediate proportional drop in flow controller output, but it takes until about 3.1 h for the integral action to slowing ramp the output down to the point where it is lower than the output of the override controller. So there is an extended period of about 1 h when the feed flow rate is higher than desired.

18.3.3 Override Control Structure with External Reset Feedback

The external reset feedback control structure discussed in Figure 18.3 is inserted in the Aspen Dynamics flowsheet for the flash tank process as shown in Figure 18.8. The feed flow controller has its output signal OP_{FC} sent to a low selector. The other input to the low selector is the output signal OP_{ORC} of the high-level override controller. The override controller is proportional-only, so it does not need anti-reset windup protection.

Figure 18.9 gives the “AllVariables” views of the individual blocks in the feed flow controller with external reset feedback. The setpoint of the flow controller SP_{FC} is set by a fixed-variable stream. The low selector inputs are the output signals from the two controllers (OP FC and OP ORC). The level transmitter for the override controller is simulated by using a *Multiply* block in which the liquid level (with units of “ft”) is

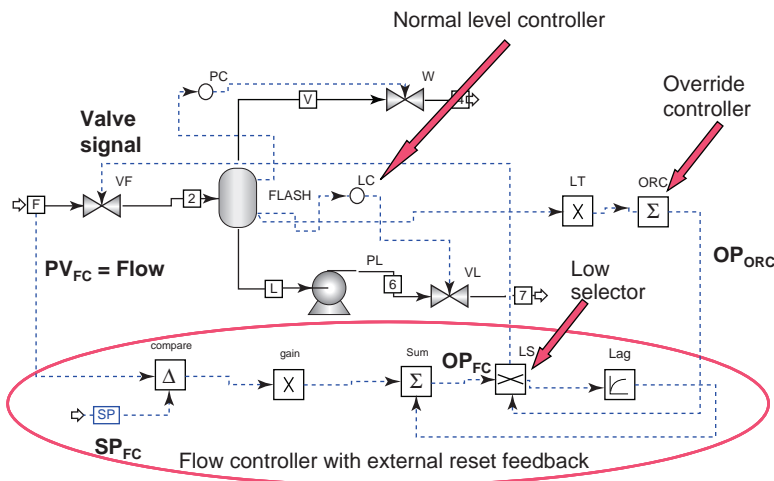


Figure 18.8 External reset feed flow controller: Aspen Dynamics implementation.

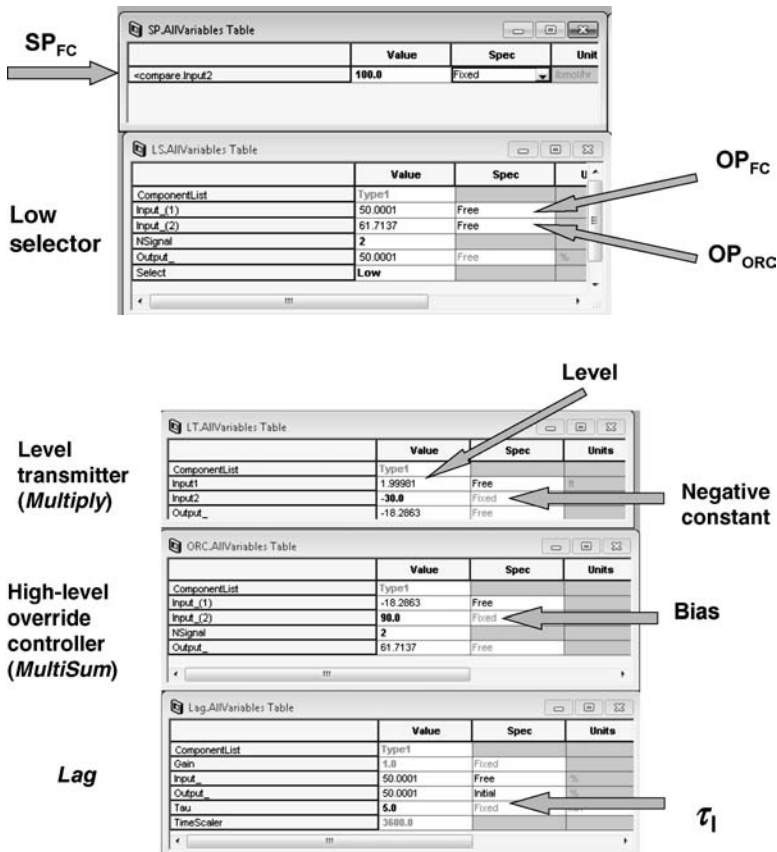


Figure 18.9 External reset feedback elements.

multiplied by a negative constant (-30) to get a signal that decreases as level increases. The output of this block goes to a *MultiSum* block in which a fixed signal of 90 is added to give an output signal of 61.7% at normal conditions. When the level goes up, this signal goes down. It is fed to the low selector. The gain of the lag is unity and its time constant (the integral time of the feed flow controller) is set at 5 min for this run.

Figure 18.10 gives a direct comparison between the feed flow controller with and without external reset feedback. The upper right graph shows that the output signal of the flow controller does not ramp up when external reset is used. It stays at 62% . The level rises up to 3.5 ft. The override controller output is controlling the feed valve since its output signal is 59% and is the output signal of the low selector. When the flow controller setpoint is reduced to 100 lb mol/h at 2.5 h, the feed flow rate is returned to the desired value in about half the time it takes when external reset is not used.

In Figure 18.10, the feed flow controller integral time was $\tau_I = 5$ min and the gain was $K_C = 0.5$. Reducing the integral time tuning parameter to $\tau_I = 2$ min produces the results

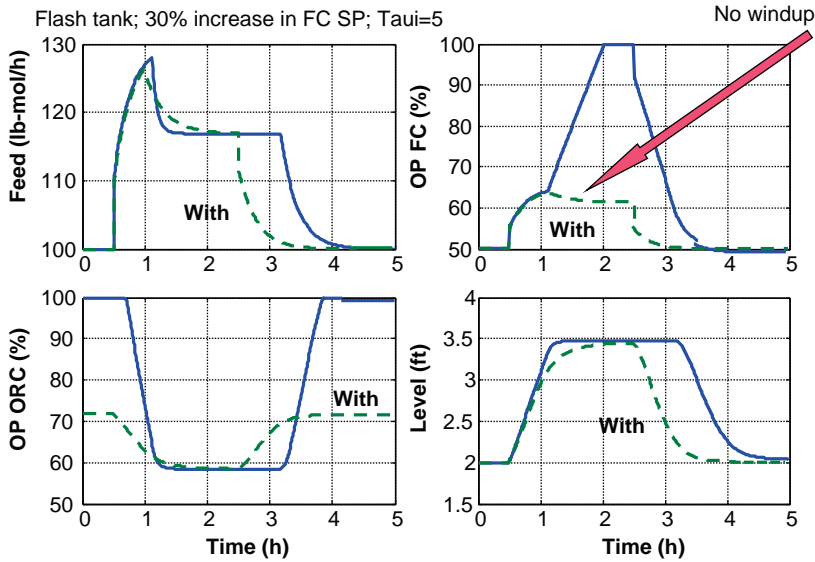


Figure 18.10 Comparison with and without external reset feedback: $\tau_1=5$.

shown in Figure 18.11. The unwinding speeds up. So if the normal tuning of a flow controller ($K_C=0.5$ and $\tau_1=0.3$ min) were used, reset windup presents little problem.

In the second example discussed in the next section, a more complex process is considered in which reset action is needed in both the normal and the override controller, and the integral tuning constants are fairly large.

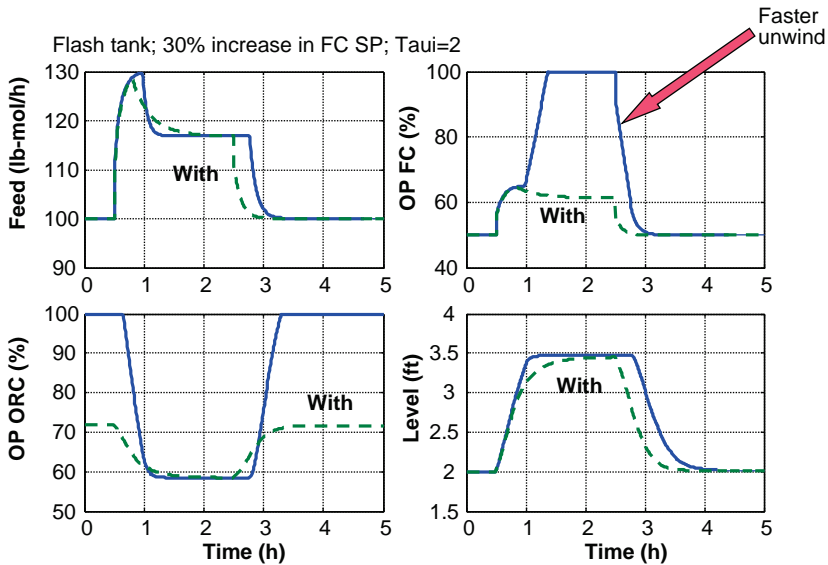


Figure 18.11 Comparison with and without external reset feedback: $\tau_1=2$.

18.4 DISTILLATION COLUMN EXAMPLE

A 42-stage distillation column separating methanol and water in a methanol-from-syngas process is used as an example of a more typically complex process. In the normal control structure, the temperature of a tray in the column is controlled by manipulating reboiler duty. However, there is a high column pressure-drop override controller to prevent flooding the column. Both of these controllers are PI and both can exhibit reset windup.

The feed flow rate is 4018 kmol/h of a mixture of mostly methanol (81.5 mol%) and water (17.7 mol%) with 0.8 mol% carbon dioxide and trace amounts of other light inert components (methane, carbon monoxide, and nitrogen). The column operates at 1 bar pressure and is fed on Stage 27. The tray pressure drop at design is specified to be 0.01 bar per tray, so the total pressure drop over the 40 trays is 0.4 bar.

The two design specifications are 0.1 mol% water in the distillate and 0.01 mol% methanol in the bottoms. The required reflux ratio is 0.4072 and the reboiler duty is 45.38 MMkcal/h (190.8 GJ/h). Figure 18.12 gives the flowsheet at design conditions. Figure 18.13 gives the temperature profile in the column.

18.4.1 Normal Control Structure

Figure 18.14 gives the normal control structure. Reflux is ratioed to feed (mass ratio = 0.3637). The temperature on Stage 34 is controlled at 93 °C by manipulating reboiler. It is important to note that the manipulated variable is not a percent of a control valve opening in this Aspen Dynamics simulation. So, scaling of variables becomes more important than in the simple flash tank process. Another complicating factor is the use of metric units by Aspen Dynamics for all calculations. The units used in the simulation for heat duties are MMkcal/h. However in Aspen Dynamics calculation blocks, energy units are GJ/h. This causes some of the blocks to display heat duty as MMkcal/h and others as GJ/h, which can be quite confusing.

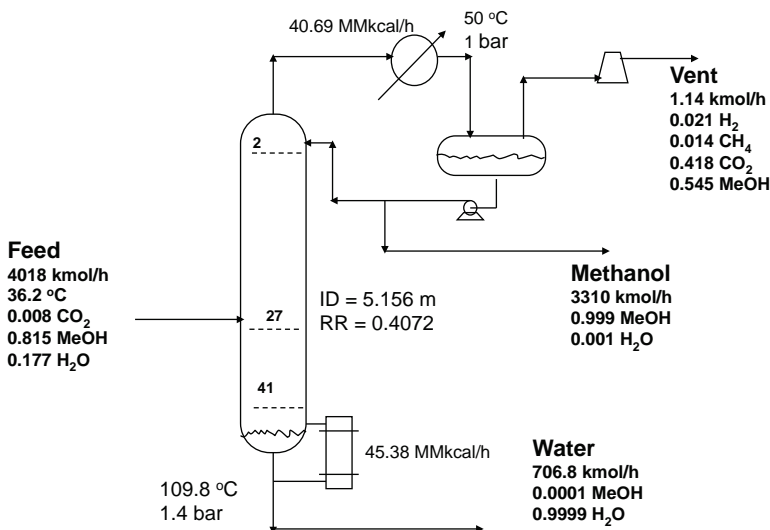


Figure 18.12 Column flowsheet.

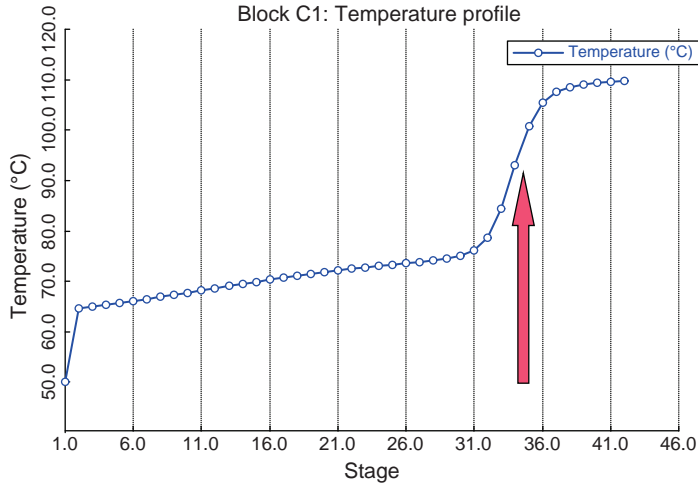


Figure 18.13 Column temperature profile.

Reflux-drum level is controlled by manipulating distillate flow rate and base level is controlled by manipulating bottoms flow rate using proportional controllers ($K_C = 2$). Pressure is controlled by manipulating condenser cooling ($K_C = 1$ and $\tau_I = 20$ min). Reflux-drum temperature is controlled by manipulating compressor work, which removes the small amount of light inert components coming into the column in the feed.

The *Dead_time* block is used to place a 1 min deadtime in the temperature control loop to account for temperature-measurement delays. The controller is tuned by running a

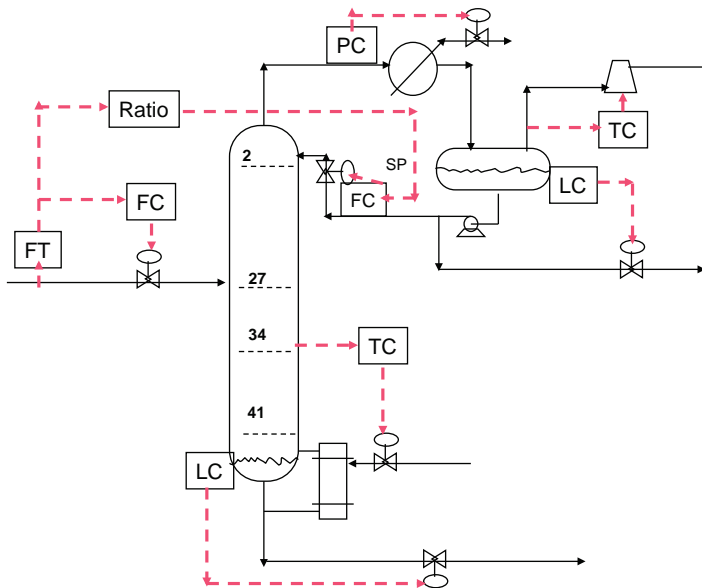


Figure 18.14 Normal control structure.

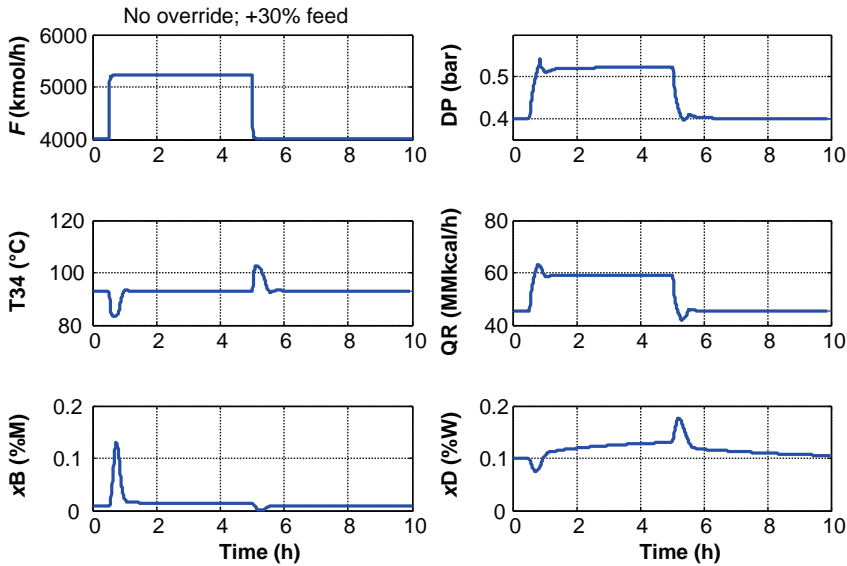


Figure 18.15 Response to 30% disturbances in feed flow rate with no constraints.

relay-feedback test. With a temperature transmitter range of 50–150 °C and an output range of 0–380 GJ/h, the Tyreus–Luyben tuning rules give $K_C = 0.97$ and $\tau_I = 12$ min.

The responses of the column for 30% disturbances in feed flow rate when there are no constraints are shown in Figure 18.15. At 0.5 h, the setpoint of the feed flow controller is increased by 30%. At 5 h, it is decreased back to the design value. The system handles these disturbances fairly well except for the large transient spike in the bottoms methanol impurity x_B . The large step change in feed causes a 10 °C drop in the temperature on Stage 34. Of course, the dynamic response could be significantly improved by using a feedforward structure in which reboiler duty is ratioed to feed flow rate. The required value of reboiler duty to keep Stage 34 temperature at its setpoint for the 30% increase in feed flow rate is 59.08 MMkcal/h.

Notice that the column pressure drop (upper right graph in Figure 18.15) increases to over 0.5 bar at the high feed flow rate because of the increase in column vapor and liquid flow rates. In the following section, we assume that there is a 0.5 bar constraint on the allowable pressure drop, so a high pressure-drop override controller is required.

18.4.2 Normal and Override Controllers Without External Reset

Configuring a control structure with a normal controller and an override controller is quite straightforward *if we ignore the reset windup issue*. Two conventional PI controllers are installed on the Aspen Dynamics flowsheet using the *PIDinc* control block. As shown in Figure 18.16, the normal temperature controller is called “TC” and the override controller is called “ORC.” The output signals of these controllers, which are both reboiler duty signals, are fed into a *MultiHiLoSelect* block. The reboiler duty is set by the smaller of the two signals.

Transmitter ranges and output ranges are set up in the normal way using the *Configure* button on the controller faceplate. Note that the ΔP process variable in the high pressure-

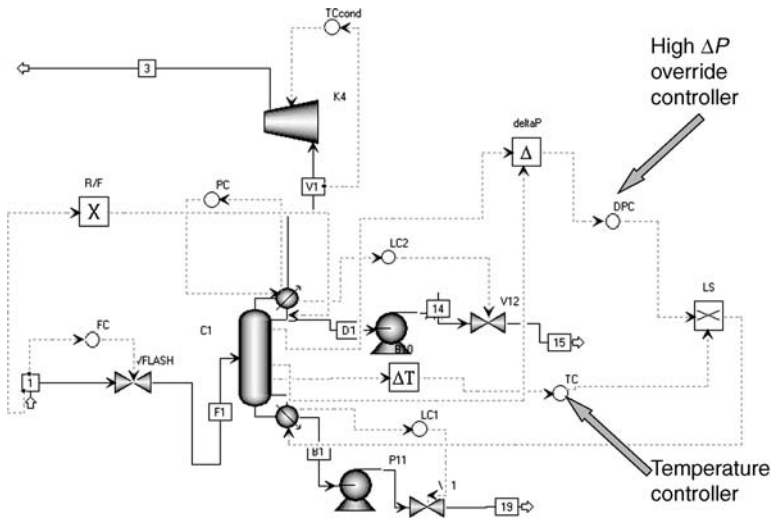


Figure 18.16 Override controller without external reset feedback.

drop override controller is generated by using a *Comparator* block to subtract the pressure on Stage 2 from the pressure on Stage 42. The override controller is tuned by running a relay-feedback test when it has taken control of the reboiler duty. Tyreus–Luyben tuning constants are $K_C = 0.74$ and $\tau_I = 3.96$ min when a transmitter range of 0.3–0.6 bar and an output range of 0–400 GJ/h are used. The tuning of the temperature controller is the same as that found in the normal control structure.

Figure 18.17 gives the responses of the process to the 30% disturbances in the setpoint of the feed flow controller for this system with no anti-reset-windup protection. The column pressure drop increases when feed flow rate increases as the temperature controller calls for a higher reboiler duty. When the pressure drop gets to 0.5 bar, the

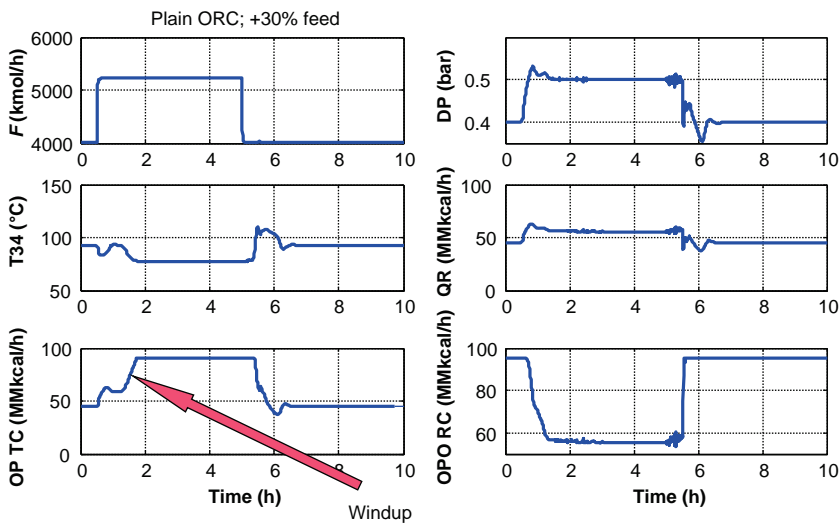


Figure 18.17 30% feed disturbances: no external reset feedback.

override controller takes over control of the reboiler duty and limits it to 55.63 MMkcal/h. This is lower than the 59.08 MMkcal/h required to keep Stage 34 temperature at its setpoint, so it drops to 77 °C, which means the bottoms impurity of methanol has increased drastically to over 31 mol%. This could be prevented by using a second override controller that would cut back the feed flow rate to maintain Stage 34 temperature much nearer to its setpoint value.

The output signal of the temperature controller windups up to the maximum of its range (90 MMkcal/h, 380 GJ/h). When the step reduction in feed flow rate is made at 5 h, the temperature controller output takes some time to ramp down once the temperature crosses the setpoint. The result is a significant bump in Stage 34 temperature, which overshoots its setpoint by 17 °C and takes 1.5 h from the time the feed was reduced to return to the desired 93 °C setpoint.

18.4.3 Normal and Override Controllers with External Reset Feedback

Both controllers can windup since they both have integral action. Therefore, two external reset feedback controllers were configured in Aspen Dynamics. Figure 18.18 gives the elements of the control structure. The process variables and the setpoints of both controllers use *Scale* blocks to convert the values from process units (°C or bar) to percent-of-scale units. At the other end of the loops, *Multiply* blocks are used to convert percent-of-scale units to reboiler duty units (MMkcal/h but are shown as GJ/h in some of the blocks).

The *AllVariables* view of several of the important blocks are shown in Figure 18.19 with their functions, the type of control block used and signals (input and output). The top window illustrates how the temperature signal is converted into a percent-of-scale signal using a *Scale* block, which is found in the *Controls2* page tab in the model library. The input is Stage 34 temperature in °C. The scale maximum and minimum are specified to be 50–150 °C. The output signal is 43% since the temperature is 93 °C. An identical *Scale* block is used to convert the setpoint signal into percentage.

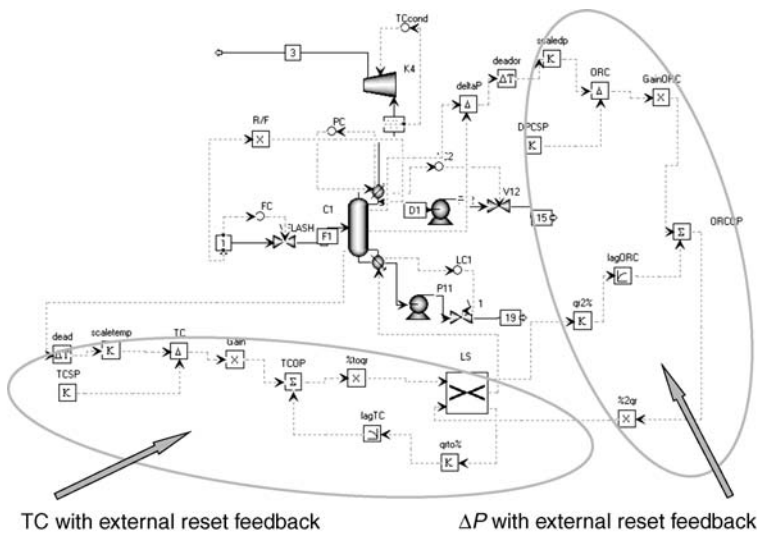


Figure 18.18 External reset feedback on both TC and ORC.

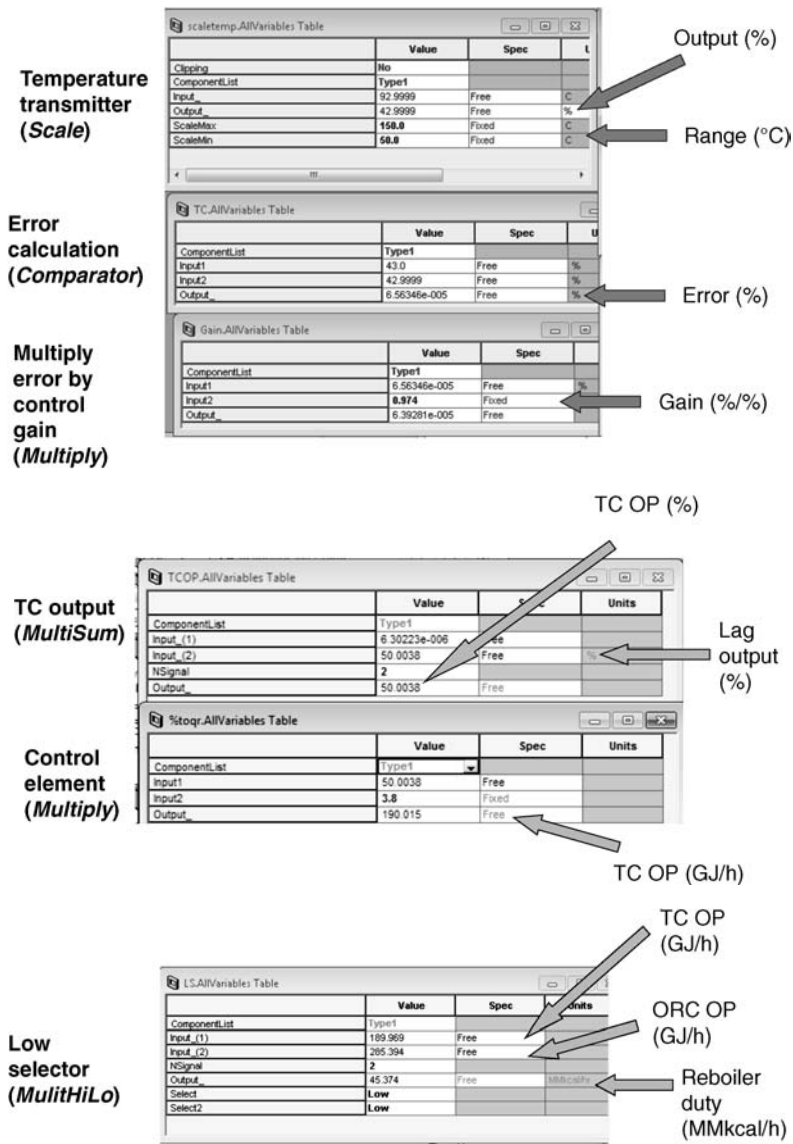


Figure 18.19 Block parameters.

The next window shows that a *Comparator* block subtracts the process variable (%) from the setpoint (%). The third window shows that a *Multiply* block generates the product of the controller gain and the error. The fourth window generates the temperature controller output by adding the output of the previous block to the output of the *Lag_1* block. The next window shows that a *Multiply* block converts the percent-of-scale signal to a reboiler duty (shown in GJ/h). The final window gives the low selector. Note that the reboiler duties of the two inputs from the two controllers are in GJ/h while the output has units of MMkcal/h. Input1 comes from the normal temperature controller, and it is the lower of the two at design conditions.

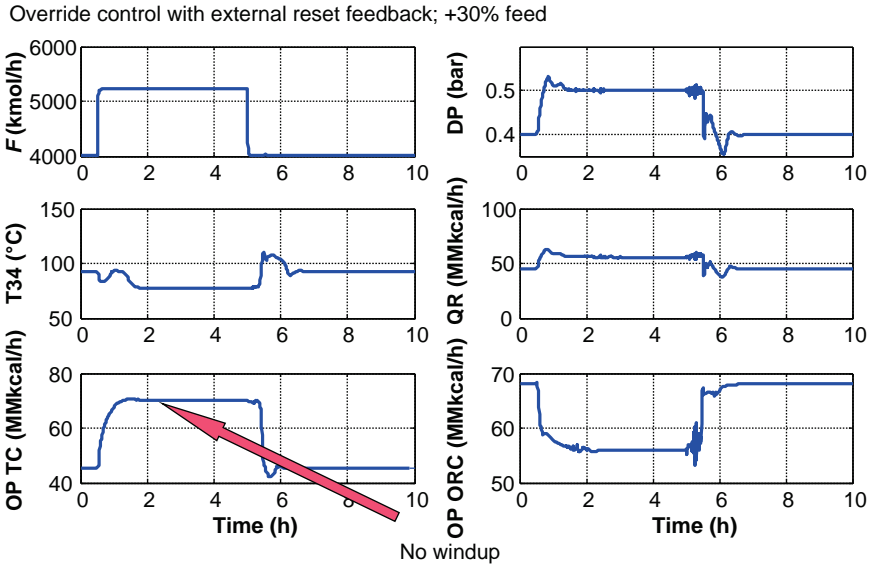


Figure 18.20 External reset feedback results.

The responses of the system to the feed flow rate disturbances are shown in Figure 18.20. The column pressure drop is controlled at 0.5 bar during the period at the high feed flow rates. But the temperature controller output signal OP TC (bottom left graph) does not windup.

Figures 18.21 and 18.22 provide direct comparisons between the override control structures with and without external reset feedback. The bump in temperature when the

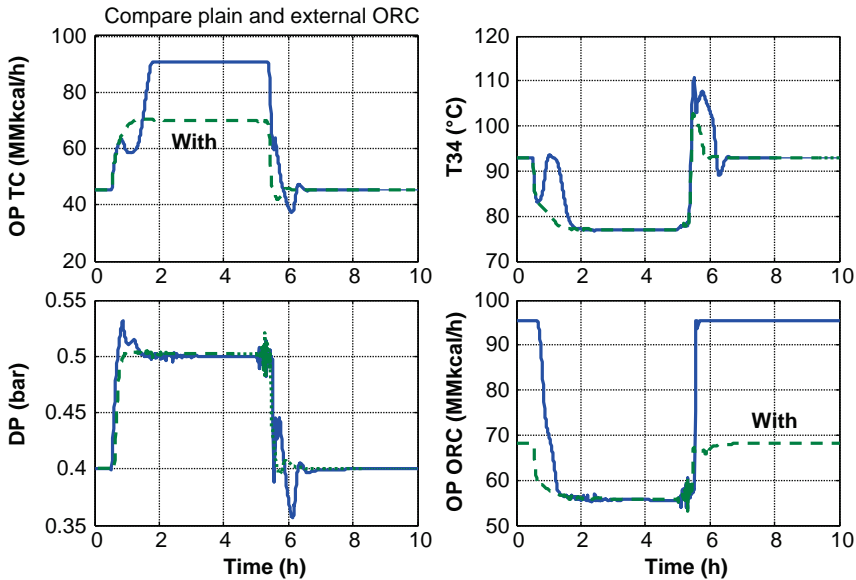


Figure 18.21 Comparison: plain and external ORC.

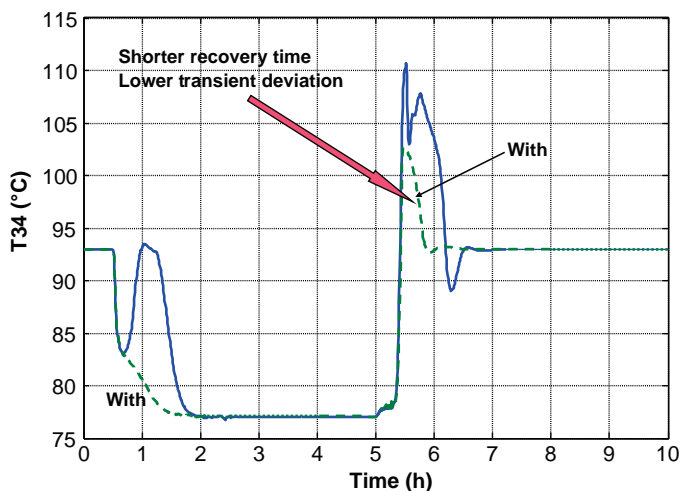


Figure 18.22 Comparison of Stage 34 temperature responses.

feed flow rate decreases is reduced from a peak of 110 °C without external reset feedback to about 103 °C with reset windup protection. The period it takes to get back to the temperature setpoint is reduced from about 1.5 h without external reset feedback to about 1 h with reset windup protection.

These dynamic results clearly demonstrate the improvement in control that the use of external reset feedback provides in override systems.

18.5 CONCLUSIONS

The implementation of external reset feedback in Aspen Dynamics has been presented. The available Aspen Dynamics control blocks can be configured to simulate external reset feedback. Getting the simulation to run requires that the lag elements used for integral action must first be initialized with fixed signals and then connected to the rest of the blocks.

Two process examples have been presented that demonstrate the improvement in performance when coming out of an override situation. The magnitude of the transient disturbance is reduced and the period of time to return to the setpoint is also shortened.

Override controllers have a wide area of application since the optimum operation of most processes involves operating at constraints. Therefore, the ability to model external reset controllers should be of considerable industrial and academic importance.

REFERENCES

1. F. G. Shinskey, *Process Control Systems*, McGraw-Hill, 1967.
2. P. S. Buckley, W. L. Luyben, and J. P. Shunta, *Design of Distillation Control Systems*, Instrument Society of America, 1985.
3. W. L. Luyben, *Process Modeling, Simulation and Control for Chemical Engineers*, McGraw-Hill, p. 341, 1973.
4. J. Khanderia and W. L. Luyben, Experimental evaluation of digital algorithms for antireset windup, *Ind. Eng. Chem. Proc. Des. Dev.* **15**, 278–285 (1976).

INDEX

- Activity coefficient, 9
- Agility, 423
- Adsorption, 458
- Alarms, 386
- Amine absorption, 399, 401
- API, degrees, 313
- Assay, crude oil, 313, 314
- ASTM boiling point control, 350
- ASTM D-86 (Engler), 310
- ASTM D-158 (Saybolt), 310
- Atmospheric crude unit, 309
- Azeotrope, 13, 115
 - heterogeneous, 13, 226
 - homogeneous, 13
 - maximum boiling, 13
 - minimum boiling, 13
- Beer still, 459
- Biorefinery, 457
- Bubblepoint, 8
- Bumpless transfer, 469
- Capture screen layout, 164
- Carbon dioxide capture, 399
- Cascade control, 170, 181, 430
- Chemical potential, 8, 74
- Closed-loop multiplicity, 143
- Closed-loop unstable system, 251
- Coil outlet temperature, 334
- Composition control, 170
 - Conceptual design, 17
 - Condenser cooling failure, 394
 - Controller faceplate, 153
 - Cyclohexane entrainer, 466
- Deadtime, 162
- Decanter, 105, 227, 231
- Degrees of freedom, 29, 356
- Design problem, 87
- Design spec/vary function, 58
- Differential vapor pressure cell, 444
- Dimethyl sulfoxide (DMSO), 96
- Direct separation, 355
- Distillation boundary, 13, 22, 106
- Distillation, first law, 238
- Divided-wall column, 355
- DME-DEG (dimethyl ether of polyethylene glycol), 413
- Dual composition control, 127, 206, 440
- Economics, 81, 84
- Energy costs, 84, 85
- Entrainers, 457
- Equimolar overflow, 30
- ETBE, 262
- Ethanol dehydration, 105, 457

- Excess reactant in reactive distillation, 260
- Exporting to Aspen Dynamics, 148
- External reset feedback, 469
- Extractive distillation, 95, 185, 458

- Feed composition sensitivity analysis, 128
- Fermenter, 457
- F-Factor, 73
- Fenske equation, 37, 81
- Fictitious vessel, compressor, pump, valve, 373
- Flash3 decanter model, 227, 233
- Flexibility, 423
- Flowsheet equations in Aspen dynamics, 219, 392, 451
- Flowsheeting options, 122
- Fugacity coefficient, 9

- Gaps in petroleum cuts, 334
- Gasifier, 399, 413, 424
- Gear integration algorithm, 402
- Global warming, 399

- Heat input surge, 395
- Heat-integrated columns, 121, 217
- Heat-transfer options
 - constant duty, 212, 387
 - constant temperature, 212, 388
 - dynamic, 388
 - LMTD, 212, 388
- Heterogeneous azeotropic distillation, 226, 457
- Heuristic optimization, 81
- Homotopy, 466

- IGCC (integrated gasifier combined cycle), 400, 412
- Integration, numerical, 237, 402
- Interlocks, 386

- Light ends analysis, 314
- Limiting conditions, 36
- Liquid split, 356

- Matlab, 174
- McCabe–Thiele diagram, 30
- Minimum number of trays, 37, 71, 81
- Minimum reflux ratio, 37, 71, 83
- Multieffect distillation, 95
- MultiFrac model, 357
- Multiple steady states, 113

- Neat operation, 121, 217, 260
- Nonlinear programming, 89

- Open steam, 334
- Operating lines, 32
- Optimization, 81
 - operating, 87
- Optimum feed tray, 70, 461
- Optimum number trays, 462
- Optimum pressure, 92
- Overflash, 341
- Overlaps in petroleum cuts, 334
- Override control, 386, 469

- Partial condensers, 191
- Performance evaluation, 172
- Pervaporation, 458
- Petlyuk column, 355, 357
- Petroleum fractionator, 309
- Pinch, 36
- Pipestill, 309, 332
- Plot wizard, 67
- Plots, 172
- Powerpoint, 175
- Preconcentrator, 105, 459
- Preflash column, 321
- Preractionator, 355
- Prereactor, 263
- Pressure-compensated temperature, 443
- Pressure-swing azeotropic distillation, 115
- Pseudo components, 313
- Pumparound, 332, 337, 345
- Pumps, 55
- Purge column, 300

- q-line, 33

- RadFrac model, 366
- Rating problem, 87
- Reactive distillation, 257
- Reboiler heat input to feed ratio, 176, 208, 448
- Recovery column, 460
- Recycle control, 427, 433, 436
- Recycle convergence, 466
- Reflux, 156
- Reflux-to-feed ratio, 167
- Reflux ratio, 168
- Relative volatility, 7, 81
 - geometric average, 81
- Relay-feedback test, 162, 165
- Reset windup, 469
- Residue curves, 15
- Rewind, 159
- Rupture disk, 386

- Safety, dynamic analysis, 385
- Safety response time, scenario, 385
- Safety valve, 386
- Saturated liquid, 3
- Saturated vapor, 3
- Sidestream column, 275
 - liquid sidestream, 275, 286
 - vapor sidestream, 281, 292
- Silebi's first law of simulation, 157
- Single-end control, 127
- Sizing, column, 72, 146
- Solvent recycle, 401
- Stripper, 337
- Stripping steam, 345
- Subcooled liquid, 3
- Superheated vapor, 3

- TAME, 262
- Task function in Aspen Dynamics, 430
- Temperature control tray selection, 129
 - invariant temperature criterion, 131
 - location, 162
 - minimum product variability criterion, 131
 - sensitivity criterion, 130
 - singular value decomposition (SVD), 130
 - slope criterion, 130
- Temperature differential, 85
- Ternary diagram, 9, 17
- Ternary mixing rule, 9
- Thermodynamics, first law, 125
- Throughput, low limitations, 423
- Total annual cost, 85
- Total reflux, 21
- True boiling point (TBP), 310
- Two-end control, 128
- Txy diagram, 3
- Tyreus–Luyben tuning, 162, 167

- Underwood equations, 37, 83

- Valve position control, 252, 426, 432, 436
- Valves, 55
- Vapor–liquid–liquid phase equilibrium, 1, 106
- Vapor–liquid phase equilibrium, 1
- Vapor pressure, 1
- Vapor split, 355
- VLE nonideality, 11

- xy diagrams, 3

